Molecular Mechanism behind Stay Green Trait in Bread Wheat (*Triticum aestivum* L.)

By

SADIA LATIF

Registration No. 03041311003

Department of Plant Sciences

Faculty of Biological Sciences

Quaid-i-Azam University

Islamabad, Pakistan

2022

Molecular Mechanism behind Stay Green Trait in Bread Wheat (*Triticum aestivum* L.)

A Thesis Submitted to the Quaid-i-Azam University in Partial Fulfillment of the Requirements for the Degree of

DOCTOR OF PHILOSOPHY

in

Plant Sciences

By

SADIA LATIF

Registration No. 03041311003

Department of Plant Sciences
Faculty of Biological Sciences
Quaid-i-Azam University
Islamabad, Pakistan
2022

APPROVAL CERTIFICATE

This is to certify that the research work presented in this thesis, entitled as **"Molecular Mechanism behind Stay Green Trait in Bread Wheat (*Triticum aestivum* L.)"** was conducted by **Ms. Sadia Latif** (Registration No. 03041311003) under the supervision of **Dr. Umar Masood Quraishi**, Associate Professor, Department of Plant Sciences, Quaid-i-Azam University, Islamabad, Pakistan. No part of this thesis has been submitted anywhere else for any other degree. This thesis is submitted to Department of Plant Sciences, Faculty of Biological Sciences, Quaid-i-Azam University, Islamabad, Pakistan in the partial fulfillment of the requirements for the degree of Doctor of Philosophy in the field of **Plant Sciences**.

Sadia Latif (Ph.D. Scholar) Signature: _____

Examination Committee

External Examiner 1

Prof. Dr. Fayyaz-ul-Hassan
Dean, Faculty of Crop and Food Sciences
PMAS, Arid Agriculture University, Rawalpindi

Signature: _____

External Examiner 2

Dr. Muhammad Ibrar Shinwari
Associate Professor
Department of Environmental Sciences
International Islamic University, Islamabad

Signature: _____

Supervisor

Dr. Umar Masood Quraishi
Associate Professor
Department of Plant Sciences
Quaid-i-Azam University, Islamabad

Signature: _____

Chairman

Prof. Dr. Mushtaq Ahmad
Department of Plant Sciences
Quaid-i-Azam University, Islamabad

Signature: _____

Dated: **March 4, 2022**

FOREIGN EXAMINERS

1. **Prof. Dr. Meral Yucel**
   Middle East Technical University
   Department of Biological Sciences
   Dumlupinar Bulvari 06800 Cankaya/ Ankara/ Turkey
   Tel: +90(0312)2105159, Fax: +90(0312)2107976
   Email: meraly@metu.edu.tr

2. **Prof. Dr. Kulvinder S. Gill**
   Washington State University
   640 SW Sundance Ct
   Pullman, WA 99163, USA
   Tel: 509-335-4666, Fax: 509-335-8674
   Email: ksgill@wsu.edu

SIMILARITY INDEX

This is to certify that this thesis entitled as **"Molecular Mechanism behind Stay Green Trait in Bread Wheat (*Triticum aestivum* L.)"** submitted by **Ms. Sadia Latif** (Registration No. 03041311003) has been checked on Turnitin for Originality. The similarity index was **18%** that lies within the limit provided by HEC (19%).

Supervisor:

Dr. Umar Masood Quraishi
Associate Professor
Department of Plant Sciences
Quaid-i-Azam University
Islamabad

Dated: **March 4, 2022**

Turnitin Originality Report

Molecular Mechanism behind Stay Green Trait in Bread Wheat (Triticum aestivum L.) by Sadia Latif .

From CL QAU (DRSML)

- Processed on 17-Mar-2022 10:25 PKT
- ID: 1786150496
- Word Count: 58722

Similarity Index
18%
Similarity by Source

Internet Sources:
15%
Publications:
8%
Student Papers:
3%

Verified

Focal Person (Turnitin)
Quaid-i-Azam University
Islamabad

sources:

1 3% match (Internet from 13-Jul-2020)
https://www.mdpi.com/journal/agronomy

2 2% match (Internet from 14-Jan-2013)
http://www.boe.cuyahogacounty.us/pdf_boe/en-US/CuyahogaPrecincts.pdf

3 1% match (Internet from 19-Dec-2015)
http://wheatatlas.org/(X(1)S(qwjivz0qmlo4qe3poi1r5ibp))/country/varieties/PAK/0?AspxAutoDetectCookieSupport=1

4 < 1% match (Internet from 21-Jul-2020)
https://www.mdpi.com/2073-4395/10/7/1001/review_report

5 < 1% match (Internet from 15-Oct-2021)
https://www.mdpi.com/2073-4395/11/1/27

6 < 1% match (Internet from 13-Jan-2022)
https://www.mdpi.com/2223-7747/9/3/363/htm

7 < 1% match (Internet from 12-Jan-2020)
https://www.mdpi.com/2223-7747/8/9/303/html

8 < 1% match (student papers from 03-Nov-2017)
Submitted to Higher Education Commission Pakistan on 2017-11-03

AUTHOR'S DECLARATION

I, Sadia Latif hereby affirm that the thesis entitled as **"Molecular Mechanism behind Stay Green Trait in Bread Wheat (*Triticum aestivum* L.)"** is my own work and that the material in this thesis is original. Where other sources of information are used, they have been acknowledged.

The thesis has not been submitted previously by me for taking any degree from Department of Plant Sciences, Quaid-i-Azam University or any other university nationwide or worldwide.

At any time if my statement is found to be incorrect even after my graduate, the university has the right to withdraw my Ph.D. degree.

Sadia Latif

PLAGIARISM UNDERTAKING

I, Sadia Latif solemnly declare that the research work presented in the thesis entitled as **"Molecular Mechanism behind Stay Green Trait in Bread Wheat (*Triticum aestivum* L.)"** is solely my research work with no significant contribution from any other person. Small contribution/help wherever taken has been duly acknowledge and that the complete thesis has been written by me.

I understand the zero-tolerance policy of HEC and Quaid-i-Azam University, Islamabad towards plagiarism. Therefore, I as an author of the above titled thesis declare that no portion of my thesis has been plagiarized and any material used as reference is properly cited.

I undertake that if I am found guilty of any formal plagiarism in the above titled thesis even after award of Ph.D. degree, Quaid-i-Azam University, Islamabad reserves the right to withdraw/revoke my Ph.D. degree and that HEC and Quaid-i-Azam University, Islamabad has the right to publish my name on the HEC/University website on which names of students are placed who submitted plagiarized thesis.

Student/Author Signature: _____

Sadia Latif

Dated: **March 4, 2022**

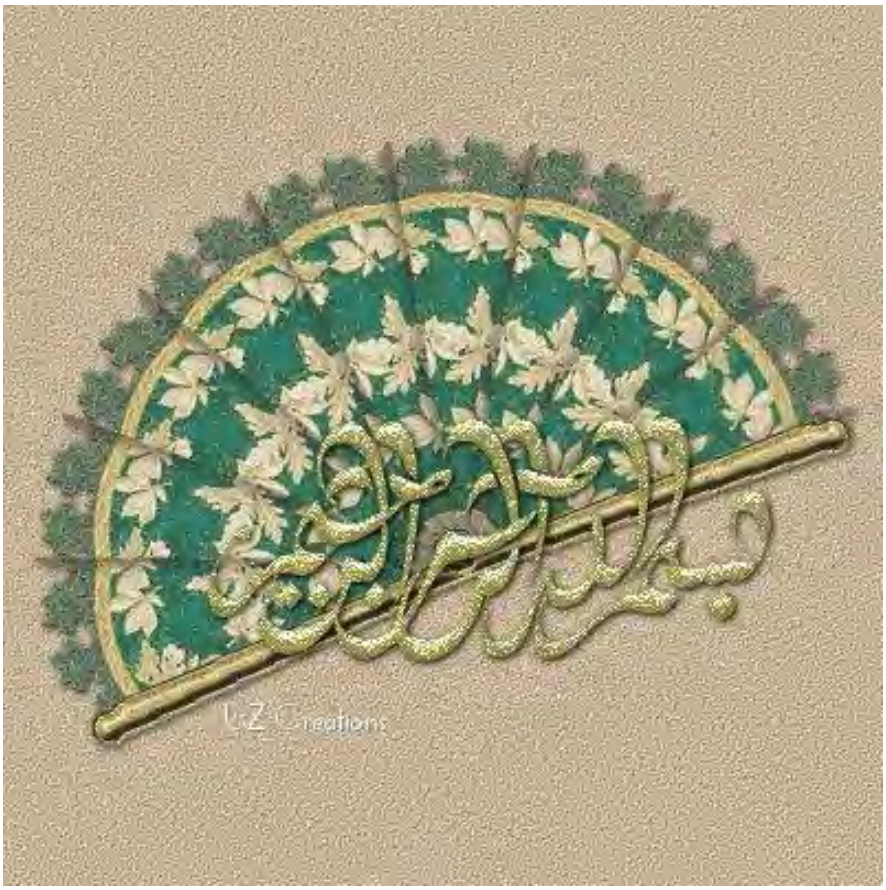

He who issues forth in search of knowledge is busy in the cause of Allah till he returns from his quest.

Dedicated to

my grandfather

Muhammad Shabbir (Late)

my father

Muhammad Latif

and my mother

Hafeeza Khatoon

for instilling the importance of hard work and higher education

Sadia Latif

TABLE OF CONTENTS

LIST OF TABLES

LIST OF FIGURES

ANNEXURE

LIST OF ABBREVIATIONS

GLM	General linear model
MLM	Mixed linear model
FarmCPU	Fixed and random model circulating probability unification
GWAS	genome-wide association study
rMVP	Memory-efficient Visualization-enhanced Parallel-accelerated
QTL	Quantitative trait loci
ANOVA	Analysis of variance
CHL_T	Chlorophyll content at tillering
CHL_B	Chlorophyll content at booting
CHL_H	Chlorophyll content at heading
CHL_A	Chlorophyll content at anthesis
CHL_10DAA	Chlorophyll content at 10 days after anthesis
CHL_20DAA	Chlorophyll content at 20 days after anthesis
CHL_30DAA	Chlorophyll content at 30 days after anthesis
fv/fm	Maximum quantum yield of photosystem II
fv/fm_H	Photosynthetic efficiency at heading
fv/fm_A	Photosynthetic efficiency at anthesis
fv/fm_14DAA	Photosynthetic efficiency at 14 days after anthesis
fv/fm_21DAA	Photosynthetic efficiency at 21 days after anthesis
SPAD	Soil plant analysis development
NDVI	Normalized difference vegetative index
NDVI_H	Normalized difference vegetative index at heading
NDVI_A	Normalized difference vegetative index at anthesis
NDVI_14DAA	Normalized difference vegetative index at 14 days after anthesis
NDVI_21DAA	Normalized difference vegetative index at 21 days after anthesis
CSF	Cumulative SPAD flag leaf
ADSF	Absolute difference in SPAD flag leaf
RDSF	Relative difference in SPAD flag leaf
CN	Cumulative Normalized difference vegetative index
ADN	Absolute difference in normalized difference vegetative index
RDN	Relative difference in normalized difference vegetative index
PH	Plant height
TN	Tiller number
SL	Splike length
SPS	Splikelet per spike
TKW	Thousand kernal weight
GY	Grain yield
BY	Biological yield
g	Grams

cm	Centimeter
SNP	Single nucleotide polymorphism
LD	Linkage disequilibrium
MTAs	Marker trait associations
TASSEL	Trait Analysis by aSSociation Evolution and Linkage
DNA	Deoxyribonucleic acid
IWGSC	International Wheat Genome Sequencing Consortium
BLUPs	Best linear unbiased predictions
CIMMYT	International Maize and Wheat Improvement Center
NSG	Non-stay-green
MNSG	Moderately non-stay-green
MSG	Moderately stay-green
SG	Stay-green
FSG	Functional stay-green
NFSG	Non-functional stay-green
CaO	Chlorophyllide a oxygenase
Cab	Light-harvesting complex
SGR	Stay-green
RCCR	Red chlorophyll catabolite reductase
RNA	Ribonucleic acid
cDNA	Complementary DNA
dNTPs	Deoxyribonucleotide triphosphates
DDT	Dithiothreitol
PCR	Polymerase chain reaction
RT-qPCR	Reverse Transcription Quantitative PCR
°C	Degree Celsius
min	Minute
sec	Seconds
CT	Threshold cycle
HSD	Honest significant difference
UHPLC-HRMS	Ultra-high performance liquid chromatography high resolution mass spectrometry
PLSDA	Partial Least Squares Discriminant Analysis
SAM	Significant Analysis of Metabolites
cADPR	Cyclic ADP Ribose
MSI	Membrane stability index
C	Conductivity
ΦPSII	Effective quantum yield of photosystem II

ACKNOWLEDGEMENT

*All the praises, thanks and acknowledgements are for the creator **Allah Almighty**, the most beneficent, the most merciful, who gave me strength and enabled me to undertake and execute this research task. Countless salutations upon the Holy Prophet **Hazrat Muhammad (S.A.W)**, source of knowledge for enlightening with the essence of faith in Allah and guiding the mankind, the true path of life. In obeisance of Almighty Allah's order his creature must also be acknowledged.*

*I would like to express my gratitude to all those who gave me the possibility to do the necessary research work to accomplish this thesis. I express my thanks to **Prof. Dr. Safia Ahmed,** Dean, Faculty of Biological Sciences, Quaid-I-Azam University, Islamabad, for providing research facilities.*

*I am obliged to **Prof. Dr. Mushtaq Ahmad,** Chairman and **Prof. Dr. Abdul Samad Mumtaz**, Ex-Chairman, Department of Plant Sciences, Faculty of Biological Sciences, Quaid-i-Azam University, Islamabad, for providing the necessary support and guidance; I have needed to complete my thesis.*

*I offer my sincerest gratitude to my supervisor, **Dr. Umar Masood Quraishi**, Associate Professor, Department of Plant Sciences, Faculty of Biological Sciences, Quaid-i-Azam University, Islamabad, who has supported me throughout my thesis with his patience and knowledge whilst allowing me to work in my own way.*

*I am deeply indebted to **Dr. Md Ali Babar**, Associate Professor, Department of Agronomy, Institute of Food and Agriculture Science (IFAS), University of Florida, USA. Dr. Md Ali Babar great expertise in wheat metabolomics made me accomplish my research work. His meticulous approach and analytical mind has always inspired me in dealing with problems instantly with logical reasoning.*

*I pay special gratitude to **Dr. Sunish Kumar Sehgal**, Associate Professor, Department of Agronomy, Horticulture & Plant Science, South Dakota State University, USA, for his continued valuable guidance, encouragement, support and critical suggestions in the research work.*

*I would like to express my very special appreciation and deep gratitude to **Dr. Jianping Wang**, Associate Professor, Department of Agronomy, University of Florida, Gainesville for her valuable guidance and unreserved devotion throughout the course of my research at University of Florida.*

*I would like to acknowledge the **Higher Education Commission Pakistan** for providing me **International Research Support Initiative Program** fellowship to carry out my Ph.D. research work at **Institute of Food and Agriculture Science (IFAS), University of Florida, USA**. I also want to acknowledge **National Agricultural Research Centre, Islamabad** for enabling me to perform field experiments and **Pakistan Meteorological Department** for providing daily climate data, pertaining to Pakistan Meteorological Department weather observing station located at **Islamabad** from*

November, 2014 to May, 2016 under Pakistan Meteorological Department (PMD) support program for academic research purpose.

I especially want to thank ***Dr. Abdul Mujeeb Qazi (****CIMMYT Distinguished Scientist, HEC Foreign Faculty Professor and Program Leader of Wheat Wide Crosses and Cytogenetics Program (WWCCP)****, Dr. Jalal*** *(PSO)****, Dr. Liping Wang, Dr. Muhammad Sohail*** *(PSO)****, Dr. Zeshan Ali*** *(SSO)****, Dr. Naeem Khan, Dr. Zahid Mahmood*** *(SSO)****,*** *and* ***Luqman Bin Safdar*** *for their support during my research. They were alway accessible and willing to help me during research work and thesis write-up. I acknowledge their assistance and thank them for their belief in me.*

I express sincere thanks to my colleagues at Allama Iqbal Open University, Islamabad ***Dr. Hina Fatimah, Dr. Rizwana Kousar, Samar Naseer, Dr. Saba Farooq, Dr. Muhammad Waseem and Dr. Zahid Ullah*** *for their continued encouragement, moral support, and necessary guidance. I am grateful to my lab/batch mates at Quaid-i-Azam University, University of Florida, and South Dakota State University.* ***Sehrish Talib, Dr. Jahangir Khan, Tayaba Andleeb, Siraj Uddin, Dr. Muhammad Adeel, Dr. Muhammad Jawad, Dr. Shazia Rehman*** *and* ***Navjot Kaur;*** *their presence was perpetually revitalizing, helpful, and memorable****.***

My Grandfather ***Muhammad Shabbir*** *deserves a special mention for his inseparable support and prayers. My Father* ***Muhammad Latif****, in the first place is the person who showed me the joy of intellectual pursuit ever since I was a child. My Mother* ***Hafeeza Khatoon****, is the one who sincerely raised me with her gentle love. Moreover, I am indebted to my brothers* ***Saqib Latif*** *and* ***Salik Latif****, sisters* ***Uzma Latif****,* ***Marfua Latif, Samia Bano,*** *and* ***Ismah Ali*** *for providing essential support during my research work and my nephew* ***Abdul Moiz*** *and my niece* ***Abeeha, Areeha*** *and* ***Meeral*** *for their prayers and love.*

In an effort to avoid the inadvertent omission of any individual, I would like to acknowledge the numerous individuals who have directly or indirectly affected my educational experience at Quaid-e-Azam University, including but not limited to the faculty members who have served us, the employees in the laboratory and Plant Sciences Office and other post graduate students. The scientific research could not be achieved without the cooperation of all the aforementioned people.

Sadia Latif

Molecular Mechanism behind Stay Green Trait in Bread Wheat (*Triticum aestivum* L.)

Abstract

Stay-green refers to ―heritable delayed foliar senescence during grain filling", is associated with retention of chlorophyll and improved photosynthesis together with the maintenance of assimilated carbon supply during grain filling stage. Consequently, confirming maximum mass per grain. Stay-green trait has received substantial attention from crop breeders owing to crop improvement under abiotic and biotic stresses. The stay-green trait needs to be further explored at morpho-physiological, biochemical, and, molecular levels for introgression in the future breeding programs. Our first study aimed to unraveled the genetic composition of the stay-green trait in a diverse germplasm consisting of landraces, green revolution, post green revolution, elite cultivars, and CIMMYT advance cultivars using 90K SNP array by employing general linear model, mixed linear model, and fixed and random model circulating probability unification based genome-wide association mapping. Forty eight loci were detected for chlorophyll content, chlorophyll fluorescence, NDVI, stay-green indices, plant height, and tiller number. Annotation of thirty six putative genes extracted from identified loci revealed their role in plant development, defense responses under stress, flowering time control, chloroplast development, and damage tissues regeneration.

The second study aimed to demonstrate the impact of the stay-green trait in bread wheat under terminal heat stress. Field experiments (2014-2015 & 2015-2016) were conducted to investigate the influence of terminal heat stress on the morpho-physiological traits in different stay-green types. In addition, the greenhouse experiment was performed to dissect the stay-green trait in functional stay-green, non-functional stay-green, and non-stay-green genotypes. Field experiments confirmed that genotypes exhibiting the stay-green trait have significantly high chlorophyll content, normalized difference vegetative index, grain yield, biological yield, kernel weight, and low canopy temperature under control and heat stress conditions. In the greenhouse experiment, functional stay-green and non-functional stay-green genotypes showed a high chlorophyll

content and photochemical efficiency, whereas biological yield and grain yield showed a significant relation with the functional stay-green genotype. The sequencing and expression analysis of chlorophyllide a oxygenase (CaO), light-harvesting complex (Cab), stay-green (SGR), and red chlorophyll catabolite reductase (RCCR) in functional stay-green, non-functional stay-green, and non-stay-green genotypes revealed variations in the exons of CaO and RCCR; and significant difference in the regulation of CaO and Cab at 7 days after anthesis under terminal heat stress.

The third study aimed to demonstrate the metabolic regulation of the secondary stay-green trait using stay-green and non-stay-green genotypes under control and heat stress treatments by employing Ultra-High-Performance Liquid Chromatography High-Resolution Mass Spectrometry (UHPLC-HRMS). Analysis of Variance, Partial Least Squares Discriminant Analysis, and Significant Analysis of Metabolites identified 166 significant known metabolites. The predominant metabolites that showed significant high accumulation in non-stay-green genotype were deoxyuridine, deoxycytidine, 5'-deoxyadenosine, glycyl-L-leucine, leucyl-proline, cytidine, uridine, isocytosine and adenine, whereas the dominant metabolites that showed high accumulation in stay-green genotype were ADP, phosphocholine, glutathione, 2-phosphoglyceric acid, cADPR, allantoin, trigonelline, syringic acid, spermine, and hexanesulfonic acid sulfate under control and heat stress treatments. The variation in the levels of metabolites in non-stay-green and stay-green genotypes highlighted variable metabolic adjustment in stay-green genotype that reduces heat impacts.

Chapter #1

Introduction and Review of Literature

Chapter #1

Introduction and Review of Literature

The dawn of agriculture has led to the evolution of human civilization from the prehistoric era to the modern era. In the modern era, 7.8 billion people directly and indirectly are fed by agriculture. Domestication and continuous selections of agronomic traits of interest has led to yield increase enabling us to withstand food security (Salamini *et al.*, 2002; Eckardt, 2010). Domestication, a colossal evolutionary step has guided the acclimatization and speciation, ultimately creating novel species (Darwin, 1905). The domestication of cereal crops has played a major role in the development of human civilization. Since the beginning of Agriculture, humans have selected crops against visual agronomic traits. This selection continued till the early 19th century (Brown, 2010). Beginning of 20th century marked the rediscovery of Mendel‘s laws and their utilization in crops (Smýkal *et al*., 2016). However, most agronomic traits are quantitative in nature and do not follow Mendel‘s law of inheritance. Quantitative agronomic traits are governed by the interaction and additive effect of multiple genes. Each locus contributes relatively weak individual effects. Environment also influences these traits (Doust *et al*., 2014). Though, crop evolution and improvement were based on selections rather than prior knowledge of genes involved lead to persistent increase in crop yield. In addition to selection, improvement in agronomic practices e.g., fertilizers, pesticide, and farm practices also played a dividend role in improvement of agricultural crops (FAO, 2011). Green revolution and deployment of short statured wheat and rice has been marked as most important milestones in the agricultural era. Since 1960, cereals grain yield has significantly improved (Figure 1.1).

1.1. Socioeconomic importance of wheat

Species of *Poaceae* family which are consumed as staple food are called cereals. The major cereal crops included Maize, Wheat, Rice, Sorghum, Millets, Oat, and Rye. Cereals are the backbone of food security, as they provide approximately 60% of daily nutrients to the world population (Varshney, 2006).

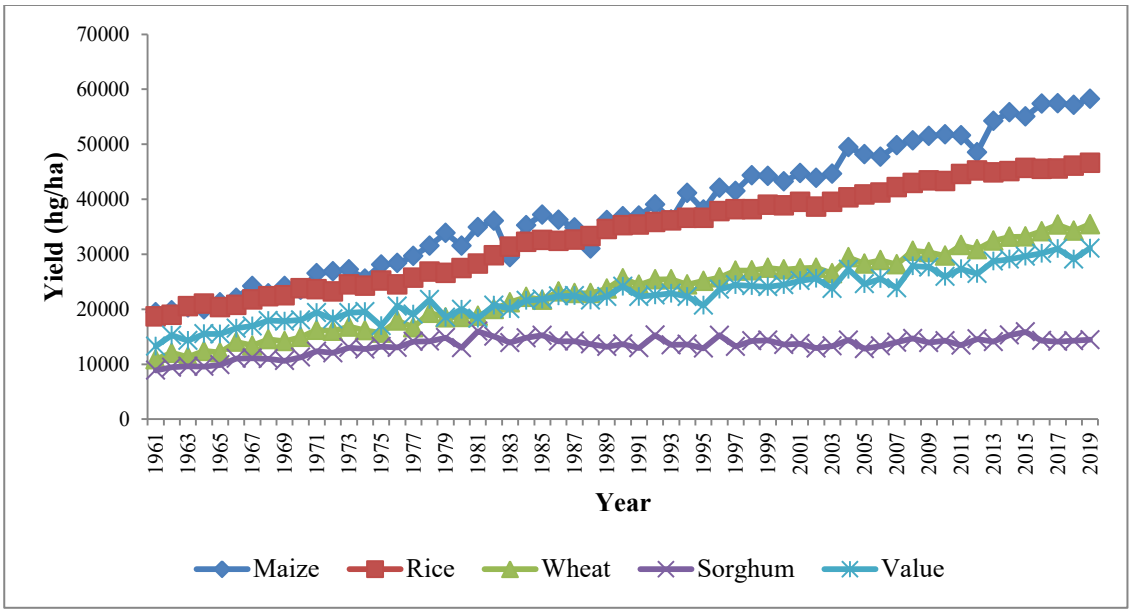

Figure 1.1. Trends in worldwide major cereal crops production since the green revolution [On the x axis are the years since the green revolution, whereas the y axis represents world yield (hectogram/hectare)] (Source: http://www.fao.org/faostat).

The golden ear of wheat has been the symbol of food security. It provides nearly 20% of the total calories and proteins and is a staple food of around 40% of the world population (Curtis, 2019; Giraldo *et al*., 2019). Wheat is the youngest polyploid crop and first domesticated crop of the world (Hanson *et al.,* 1982; Charmet *et al*., 2011). Hexaploid wheat (*Triticum aestivum*) is cultivated around the globe for bread, chapati, cakes, and noodles. Tetraploid durum wheat (*Triticum durum)*, is used for making pasta, biscuits, and noodles (Peña, 2019; Giraldo *et al*., 2019).

Wheat can be adapted to variable agro-climatic zones that include tropical and temperate climatic conditions. This ability has enabled farmers in every continent to cultivate wheat. Unlike other crops, the presence of gluten protein makes wheat loaf visco-elastic, suitable for variable human consumption. Wheat is also nutritionally rich and provides carbohydrates, minerals, protein and dietary fibers (Curtis *et al*., 2002) to humans as well as animals. The socio-economic importance plus industrial applications makes wheat the most important commodity from farm via market to table.

1.2. Wheat production and consumption

Globally, wheat is cultivated on 218 million hectares versus 162 million hectares for rice and 177 million for maize. America, Australia, Canada, China, France, Germany, India, Pakistan, Russia, and Ukraine are the leading wheat producers of the world (Figure 1.2).

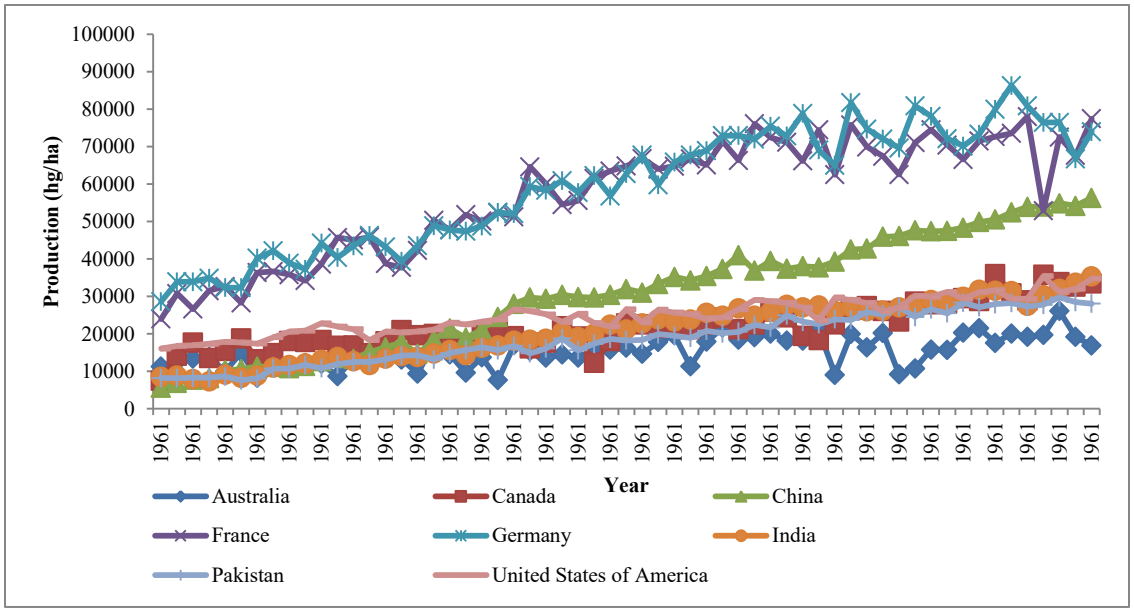

Figure 1.2. Wheat Production in the major world wheat producting nations since 1961. (Source: **http://www.fao.org/faostat*). x-axis represents years since green revolution and y-axis represents wheat yield.***

Pakistan is ranked 8th in terms of wheat production, with annual wheat yield approximately 25.5 million metric tons (MMT) in 2020. Approximately, 80% of Rabi cultivation is wheat in Pakistan (9 million hectare). The export value of wheat is 41.1 billion US dollars, highest among all cereals, (*http://faostat.fao.org*). The average per capita consumption of wheat and its products in 2019 was 67.8kg, which is 47% of total cereal consumption. In Pakistan, per capita consumption of wheat is highest in the world (115kg). This makes wheat the highest consumed product as well as has a great impact on the economy of Pakistan. Wheat crop contributes 10% to the agriculture sector and 2.1% to the national GDP (Source: Economic Survey of Pakistan 2017-18).

1.3. Future outlook of wheat

Worldwide population is growing at an alarming rate; it is projected to increase to 9.7 billion from the current 7.9 billion people by 2050. This makes food security a daunting task for agriculturists in general and wheat breeders specifically. Approximately, a 2% annual increase in wheat production will ensure our food security in 2050. Reduction in land resources, water resources and variable climatic conditions has made food security one of the biggest challenges of this decade (FAO, 2017).

1.4. Wheat genome and evolution

Among cereals, wheat has the largest genome ~17 giga base-pairs. Wheat is an allohexaploid and has 21 pairs of chromosomes belonging to three sub-genomes (A, B, and D). The three genomes each consisting of 14 chromosomes are evoluted from different diploid species (Sakamura, 1918; Kihara, 1919; Sax, 1922; Kihara, 1924; Sears, 1952). Wheat genome has approximately eighty percent of repetitive elements (Mayer *et al*., 2014). Comparative studies have estimated that all cereals have evolved from a common ancestor about 50 to 70 million years back (Bolot *et al.*, 2009; Alaux *et al*., 2018). The A-genome ancestor *Triticum urartu* (genome A^uA^u) was naturally crossed with B-genome ancestor *Aegilops speltoides* (genome SS) and resulted in an amphi-tetraploid *Triticum turgidum* (genome A^uA^uBB). This species is the progenitor of durum wheat. The next event of polyploidization occurred around 10,000 years ago. The tetraploid *Triticum turgidum* was naturally crossed with D-genome *Aegilops tauschii* to produce allohexploid *Triticum aestivum L.* (Figure 1.3). Continuous selection and natural mutations have assisted in creation of actual free thrashing, soft bread wheat.

1.5. Wheat growth and development

Wheat yield is dependent on intricate interactions between biological, economical, technological, and ecological factors. Till date, breeders and farmers are working on devising strategies and methodologies to improve crop yield. The key solution to this problem is to reduce pre- and post-harvest losses. Researchers have

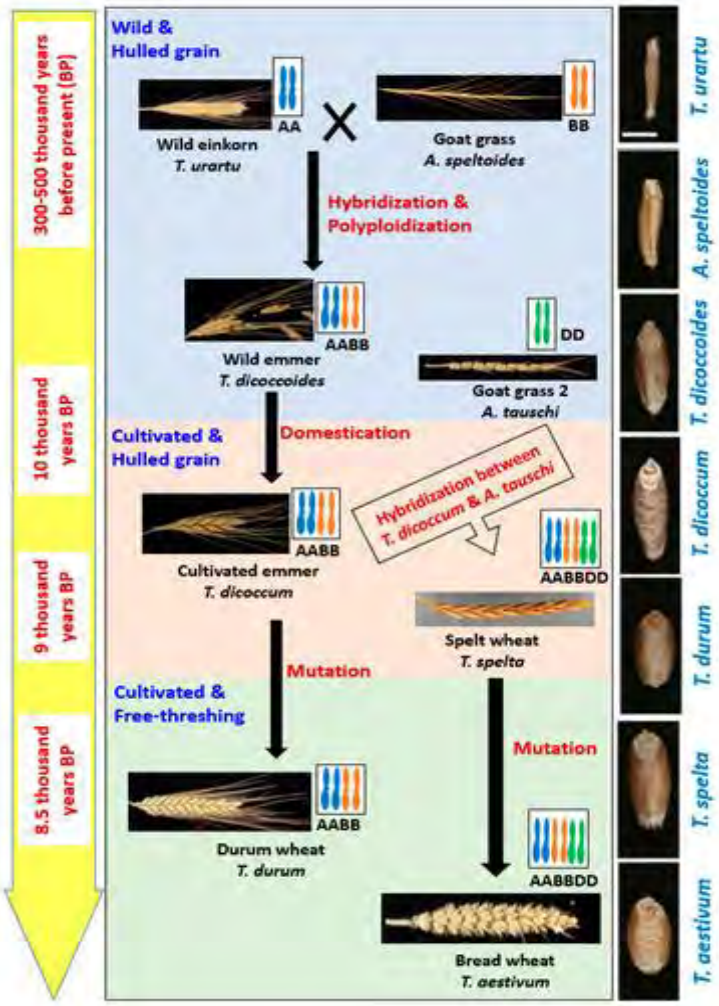

Figure 1.3. Evolution of wheat from diploid Triticum urartu, Aegilops speltoides, and Aegilops tauschii to allo-hexaploid Triticum aestivum (Source: Rahman et al., 2020)

broaden the scope of identification of strategies and methodologies from farming practices, utilization of chemical fertilizers, to exploring the genetic diversity, to use of wild relatives, to hybrid wheat, and even to transgenic approaches to find solutions for this problem. Basics of all future development depend upon our understanding on plant growth and development.

As discussed earlier, wheat is the best adapted crop of the world. It is planted in both tropic and temperate climatic conditions. Due to complex genome, wheat is to adapt to various osmotic conditions from littoral to xerophytic water availability (Curtis *et al*., 2002). This in addition to different utility makes wheat one of the most diverse cereal

crop. The classification of wheat is done based on its cropping pattern (winter or spring wheat), based on its grain softness (soft, medium hard or hard), based on its grain color (red, amber, white). Spring wheat is cultivated in early winters (November) and harvested in summers (April-May) in Asia, Africa, and lower latitudes. As compared to spring wheat, winter wheat which is cultivated in October and harvested in May-June in Europe, North America, China, and higher latitudes.

Wheat is a C-3 plant and needs a cool environment to initiate vegetative growth. It is planted in Rabi season, as compared to other cereal crops (maize and rice) which are planted in kharif season. The development of wheat plants is divided into different growth stages. Physiology and morphology of these stages have significant positive impact on eventual grain yield. The brief description of these morphological stages is described below.

1.5.1. Wheat growth stages

Hanft and Wych, (1982) grouped wheat growth into four stages that are growth stage E (germination to emergence), growth stage 1 (tillering, stem elongation), growth stage 2 (stem elongation to booting to heading), and growth stage 3 (anthesis to grain filling to physiological maturity). The duration of these stages are dependent upon the genotype as well as environmental conditions.

The life of a wheat plant starts with the imbibition of seeds. After imbibition, the seed is sprouted with the emergence of radicle and coleoptile. Seminal roots develop from radicle, while coleoptile elongates to form first leaf. The emergence of first leaf determines the start of the seedling stage. The second crown tiller emerges from the auxiliary bud of the primary tiller. Tiller formation marks the end of seedling stage and start of growth stage 1. Tiller formation is one of the most important yield determining stages of wheat developmental phases, as it has a significant impact on plant yield. Tiller formation in general lasts for 10-20 days after emergence. Production of new leaves in addition to halt in production of new tillers marks the end of tillering stage. Now the plant enters into growth stage 2 in which development of sexual organs occurs for eventual reproductive stage. Internode of each tiller is elongated to form a stem. Booting

is initiated with the development of the head inside the sheath of the flag leaf. The head emerges from the flag leaf after 10-20 days of booting. Just after the heading (2-5 days), anthesis is initiated. Wheat plants are often self-pollinated. After fertilization and initial cellular divisions, endosperm cells and amyloplasts are formed. The initial phase just after fertilization is called as the lag phase. After the lag phase grain filling is initiated and lasts for about 20-30 days. The first phase of filling is known as milky or water ripe phase. In this phase endosperm is developed and storage of starch and protein is initiated. Then comes dough developmental phase, linear grain growth and starch deposition in the endosperm is continued (Jones *et al.,* 1985). This is the stage of grain development where it gains most of its weight and all the food/vitamins stored during vegetative phase are translocated to seeds. At physiological maturity, the seed dough loses the water and gets hardened and final grain weight is achieved. This phase is called the ripening phase, which has a direct impact on eventual yield of the crop.

Table 1.1. Life cycle of spring wheat in Pakistan

Development stage	Months	Time
Emergence	November, 1 to 15	0
Three leaf stage	December, 1 to 7	20
Terminal spikelet	December, 25 to 30	45
First node	January, 1 to 15	60
Booting	February, 15 to 28	90
Heading	March, 1 to 15	100
Anthesis	March, 15 to 30	100
Physiological maturity	April, 15 to May, 5	140

1.5.2. Wheat yield and related traits

Wheat crop is preferred over other Rabi crops due to its high agronomic adaptability, crop yield, and production of palatable foods adapted to different cultures of the world. Stable increase in wheat production to meet our global food demands, is one of the major goals of wheat breeders in this century. Crop yield is the annual rate of return of the crop. Breeders have tried to increase the grain yield per unit area since the origin of

agriculture. To date, yield is the target of all breeding programs. Crop yield is a quantitative trait which is significantly influenced by environmental factors. Combinations of different morphological, physiological, anatomical, and genetic traits influence the eventual yield. To improve crop yield we should understand and dissect these traits (Gupta *et al*., 2008). The extent of divergence of grain yield is explained by the following equation.

$$GY(unit\ area) = No.of\ plants\ (per\ unit\ area)\ X\ Tiller\ Number\ X\ SPS\ X\ KW$$

Where, *GY*= grain yield; SpS=spikelet per spike; KW= kernel weight.

Each phase of plant growth has an eventual impact on different component of grain yield (Figure 1.4).

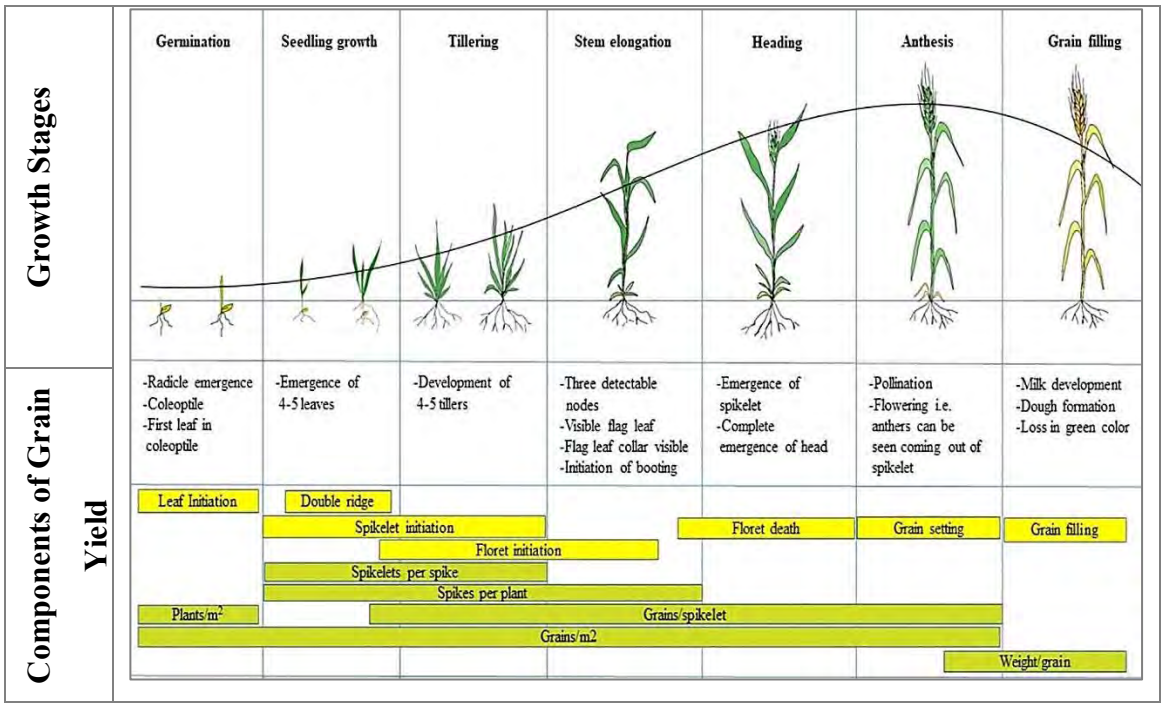

Figure 1.4. Wheat development stages along with the associated yield components at each developmental stage (Khadka et al., 2020).

1.6. Factors affecting wheat yield

Wheat, the largest cultivated cereal in different agro-ecological zones, is affected by numerous biotic and abiotic stresses during its life cycle.

1.6.1. Biotic factors

The biotic factors that influence crop yield include microbes (bacteria, fungi, and viruses), pests (insects and birds), and weeds. In the recent decade, crop breeders and researchers are exploring genetic resources for stress resistance. This approach is more effective in a way that it is environmental friendly and economical compared to the conservation agriculture approach that uses pesticides which have more input cost and deteriorate the environment (Table 1.2).

Table 1.2. List of biotic factors and causal agents that influences wheat yield

Diseases/pathogens	**Causal agent**
Leaf rust	*Puccinia triticina*
Stem rust	*Puccinia graminis*
Yellow rust	*Puccinia striiformis*
Loose smut	*Ustilago tritici*
Powdery mildew	*Blumeria graminis*
Fusarium head blight	*Fusarium graminearum,*
Karnal bunt	*Tilletia indica*
Tanspot	*Pyrenophora tritici-*
Cereal yellow dwarf	*Luteovirus*
Septoria tritici blotch	*Mycosphaerella graminicola*
Stagonospora nodorum blotch	*Phaeosphaeria nodorum*
Eyespot strawbreaker/footrot	*Tapesia yallundae*
Bacterial leaf streak	*Xanthomonas translucens*
Wheat curl mite	*wheat streak mosaic virus*
Green bug	*Schizaphis graminum*
Hessian fly	*Mayetiola destructor*
Diuraphis noxia	*Diuraphis noxia*

1.6.2. Abiotic factors

Abiotic factors that affects crop yield includes resources (water, light, carbondioxide, nitrogen (N), phosphorus (P), and potassium (K), stressor (salinity, soil PH, temperature and flood), and xenobiotic factors (air pollutants, organic and inorganic toxins) (Figure 1.5). Water is a major limiting factor; approximately 25% of the total agriculture land is affected by water deficit due to irregular patterns in rainfall. Drought stress limits crop production more than any other abiotic factor by influencing growth and development of plants (Shao *et al*., 2009; Rad *et al.*, 2012). Water deficit induces early senescence, resulting in yield losses (Farooq *et al*., 2009; Praba *et al.*, 2009; Ji *et al*., 2010; Sarto *et al.,* 2017). The prolonged exposure to high light intensity can also decline wheat yield by reducing grain filling duration (Abhinandan *et al.*, 2018). The macronutrients that include NPK frequently applied as fertilizers play a vital role in plant growth and development (Kulcheski *et al*., 2015). Approximately, 40% of the irrigated area under wheat cultivation is affected by heat stress (Reynolds *et al*., 2001). Wheat yield declined by 6% with 1℃ rise in temperature above 15℃ (Asseng *et al.,* 2013). High temperature stress results in oxidative damage, which results in early leaf senescence and decrease in crop yield (Sairam *et al*., 2000; Wilkinson and Davies, 2002; Dias and Lidon, 2009). Due to anthropogenic activities, almost 20% of the agricultural land has been affected by salinity stress (Shrivastava and Kumar, 2015). The rapid industrialization has resulted in an increase in xenobiotics including air pollutants, organic, and inorganic toxins, which negatively influences quality and quantity of grain harvest. Grain yield improvement under reduced land and water resources and adverse environmental conditions is a daunting task.

1.7. Mechanisms of biotic and abiotic stress tolerance

Plants have evolved different intricate morphological, physiological, and anatomical mechanisms to manage the harmful effects of environmental stresses. Some

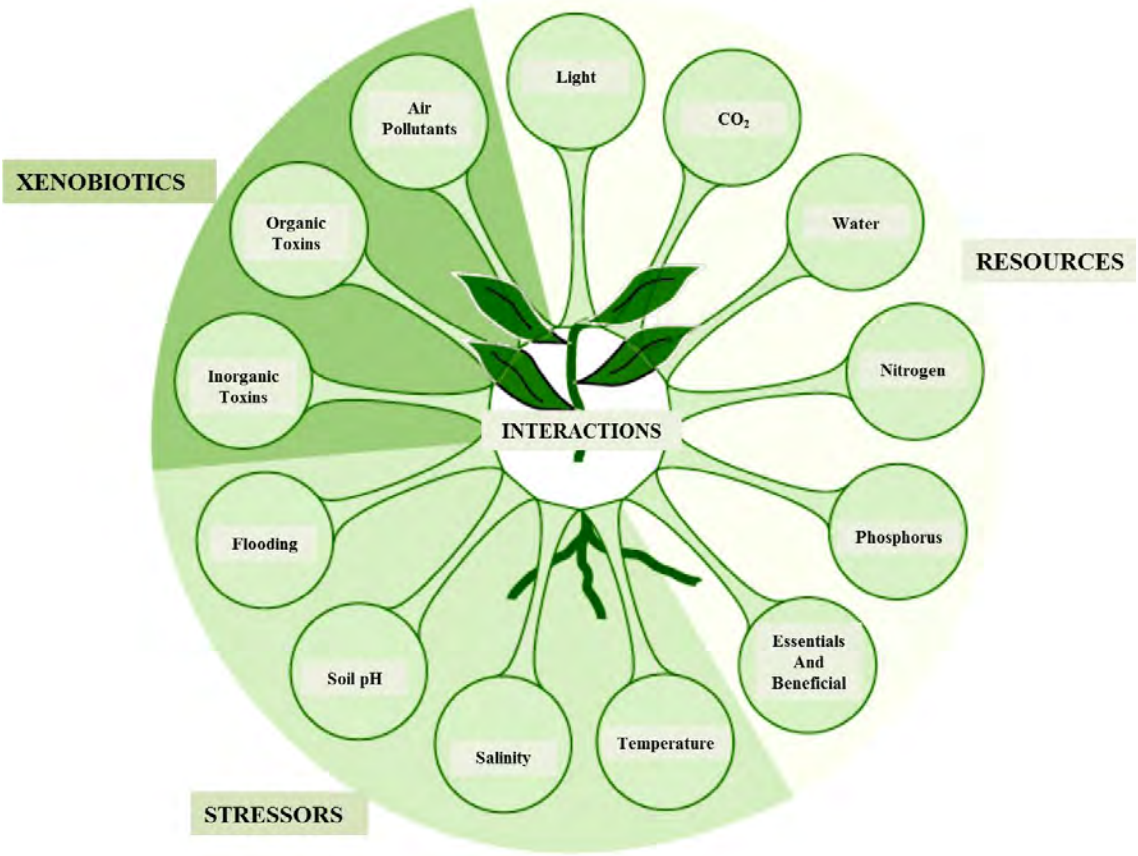

Figure 1.5. Abiotic factors influencing growth and development of wheat (Source: Willey, 2015)

plants exhibit stress tolerance, whereas others display avoidance mechanism (Peleg and Blumwald, 2011; Mickelbart *et al*., 2015). The plant‘s stress responses are regulated at different organization levels. Cellular level responses include membrane system adjustments, cell wall structural modifications, cell cycle alteration, and low molecular weight molecules like abscisic acid, jasmonic acid, salicylic acid, and ethylene synthesis (Fujita *et al*., 2006; Onaga and Wydra, 2016). Genomic level plant responses included altered expression of stress induced genes, which are involved in protecting plants against stresses. These genes can be divided into two categories, first group consist of genes encoding membrane osmolyte synthesis enzymes, antioxidant enzyme (superoxide dismutase, glutathione transferases, dehydrins), membrane proteins, and macromolecular protection proteins such as chaperons and LEA protein and second group included genes that encodes transcription factors, signal-transduction proteinases, protein kinases, and

receptor and ribosomal protein kinases (Dos Reis *et al*., 2012). The altered accumulation of phenolic compounds, terpenoids, flavonoids, alkaloids, and isoflavonoids are also involved in stress responses (Akula and Ravishankar, 2011). At the morphological level, evolution of stress avoidance mechanism allowed plants to escape the negative impacts of environmental stresses by reducing plant vegetative growth, early heading, and premature senescence (Cramer *et al*., 2011; Maggio *et al*., 2018). However, premature senescence results in significant yield losses. During the last decade, plant breeding and genetic engineering approaches have been deployed to overcome yield reduction caused by stresses, only a few studies have been successful. One of the novel attributes that grabbed the attention of crop breeders is delayed senescence. Genotypes displaying delayed senescence/ stay-green phenotype can tolerate biotic as well as abiotic stresses and can be used as a potential source of genetic improvement in important cereal crops (Kassahun *et al*., 2010; Luche *et al*., 2015; Abdelrehman *et al*., 2017). Stay-green trait has been linked with better performance in sorghum, rice, maize, and wheat under heat, drought, and spot blotch infection (Joshi *et al*., 2007; Borrell *et al*., 2014; Kumari *et al*., 2007).

1.8. Stay-green

The term stay-green is relatively new in origin, the first record found in a publication ―Investigation into the cultivation and processing of 5 broad bean varieties" by Steinbuch and coworkers in 1962 (Thomas and Ougham, 2014). Stay-green referred to cultivars, mutants, or transgenic plants with a trait of heritable prolonged foliar greenness during terminal grain filling duration or delayed senescence compared with wild type or reference genotypes (Thomas and Ougham, 2014; Thomas and Smart, 1993). They can be classified into functional stay-green type or non-functional stay-green type (Thomas and Smart, 1993; Park *et al*., 2007; Thomas and Ougham, 2014). In the functional stay-green, retention of chlorophyll is associated with increased photosynthesis and the supply of assimilated carbon is maintained during the grain filling stage, thus confirming the maximum mass per grain. Senescence syndrome progresses unhurriedly by delaying canopy development from carbon capture to nitrogen mobilization. There are two types of functional stay-green, type A and type B. In type A plants, senescence is initiated late, whereas in type B senescence initiation is on time but the progression of senescence is

delayed. In non-functional stay-green retention of chlorophyll does not couple with increase in the photosynthetic capacity of the plant, thus has no impact on yield improvement. Non-functional stay-green plants can be divided into type C, type D, and type E. Type C refers to a cosmetic type, in which the chlorophyll degradation pathway is impaired, whereas the rest of the senescence event proceeds at normal rate. Type D also called as pseudo-stay green, dies before the completion of senescence and appears green. Type E called hyper green has higher accumulation of chlorophyll, so during senescence it will take longer to degrade chlorophyll (Hortensteiner, 2009; Thomas and Howarth, 2000) (Figure 1.6). The features that determine stay-green include duration of senescence, rate of senescence, and chlorophyll content at anthesis (Harris *et al*., 2007).

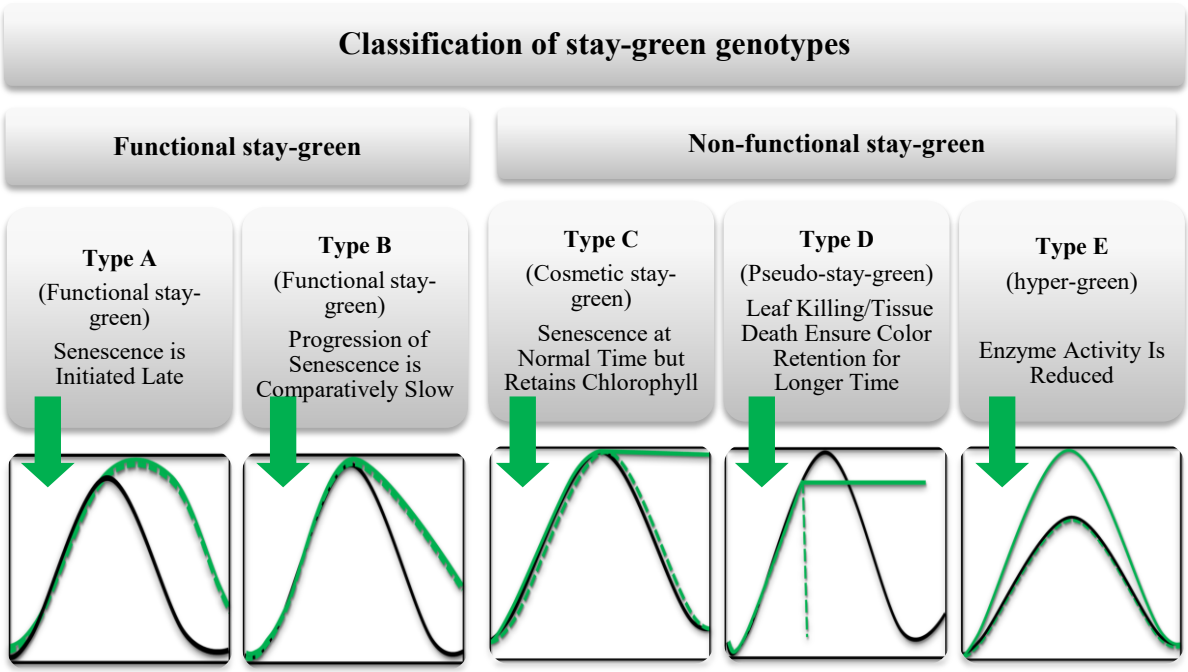

Figure 1.6. Classification of stay-green genotypes (Source: Thomas and Howarth, 2000, Ho¨rtensteiner, 2009).

Senescence is the programmed final developmental stage of a plant that results in progressive loss of green leaf area (Nood´en, 1988). Senescence initiates during development in response to abiotic factors (drought, inadequate nutrition, high or low temperature, oxidative stress, shade and ozone) and biotic factors (like pathogen attack). Senescence is regulated by different pathways. Under stress different hormones are

regulated in plants. The hormones involved in the senescence process include cytokinin, ethylene, abscisic acid, jasmonic acid, brassinosteroids, and gibberellins. Ethylene, abscisic acid, and jasmonic acid are linked to a common pathway during senescence. A transcription factor ORE9 is up-regulated by the hormones and ORE9 disrupts an unknown protein that results in leaf senescence. The *Arabidopsis* mutant ORE9 showed delayed senescence when treated with ethylene, abscisic acid and jasmonic acid (Woo *et al*., 2001). High cytokinin levels delays the phenomena of senescence, whereas low cytokinin levels lead to early senescence (Masferrer *et al*., 2002). A homeobox gene Knotted 1 controlled by a promoter of the senescence-associated gene SAG12, expression in plants can increase chlorophyll and cytokinin levels that delays senescence (Buchanan-Wollaston *et al*., 2003). A senescent leaf when treated with cytokinin can reactivates proteins and chlorophyll synthesis, and retains photosynthesis (Howarth, 2000; Zavaleta-Mancera *et al*., 1999). Cytokinin delays leaf senescence by inducing the expression of extracellular invertase that synthesizes hexose monomers from sucrose in the apoplastic pathway which are then supplied to sink tissues (Lara *et al*., 2004). Gibberellins also delay leaf senescence (Gibson, 2005). Brassinosteroid enhances the process senescence (Yin *et al*., 2002). Over expression of an acyl hydrolase encoding SAG101 gene induces leaf senescence (Yoshida, 2003) (Figure 1.7).

The key events that occur during senescence are the degradation of chlorophyll and disruption of photosynthetic apparatus that results in decrease in photosynthetic efficiency (Weng *et al*., 2005; Zhang *et al*., 2006). Chlorophyll catabolism is a multistep process that converts chlorophyll to non-fluorescent chlorophyll catabolites (NFCC). The process involves six chlorophyll catabolic enzymes, metal chelator, and transport system that delivers chlorophyll catabolic product to vacuole. The steps involved in chlorophyll degradation includes: conversion of chlorophyll b (Chl b) to 7-hydroxymethyl chlorophyll *a* (HMChl a) in the presence of Chl b reductase. HMChl a is then converted to chlorophyll a (Chl a) by HMChl a reductase. Chlorophyll a degrades to pheophorbide *a* (Pheide *a*) by pheophytinase, which breaks phytol side chain by removing the central magnesium atom. Pheide *a is* catalyse to form the primary fluorescent chlorophyll catabolite (PFCC) by pheide *a* oxygenase and red chlorophyll catabolite reductase. PFCC present in chloroplast is then transferred to vacuole, where it

is converted to NFCC because of the vacuolar acidic pH (Hortensteiner and Krautler, 2011) (Figure 1.8).

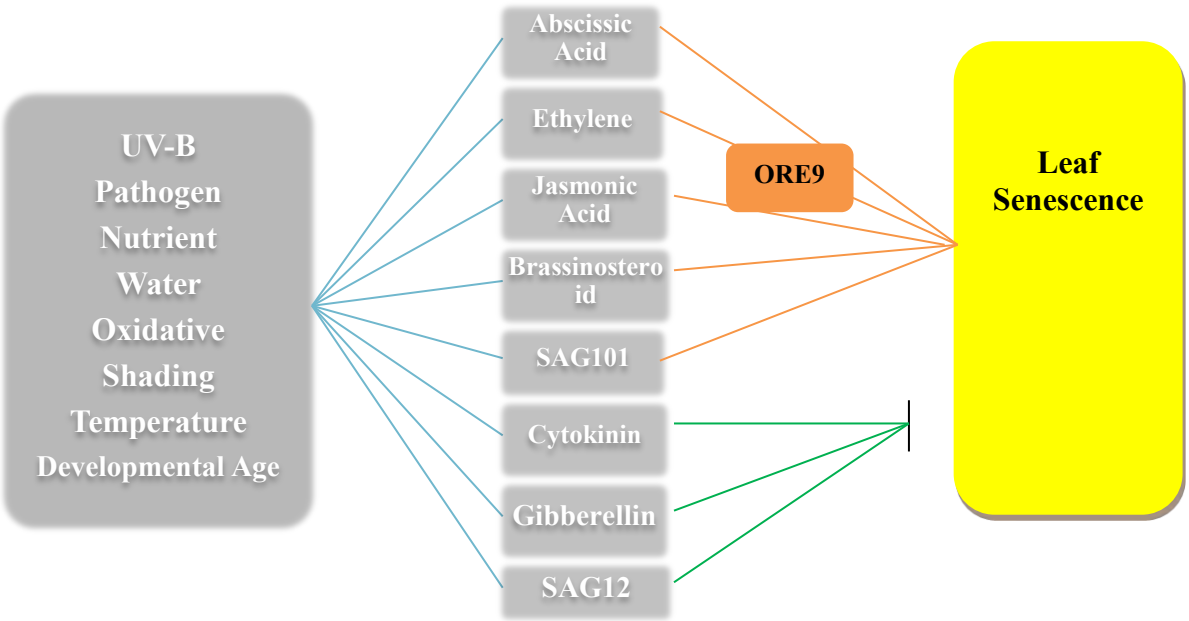

Figure 1.7. Leaf senescence pathway

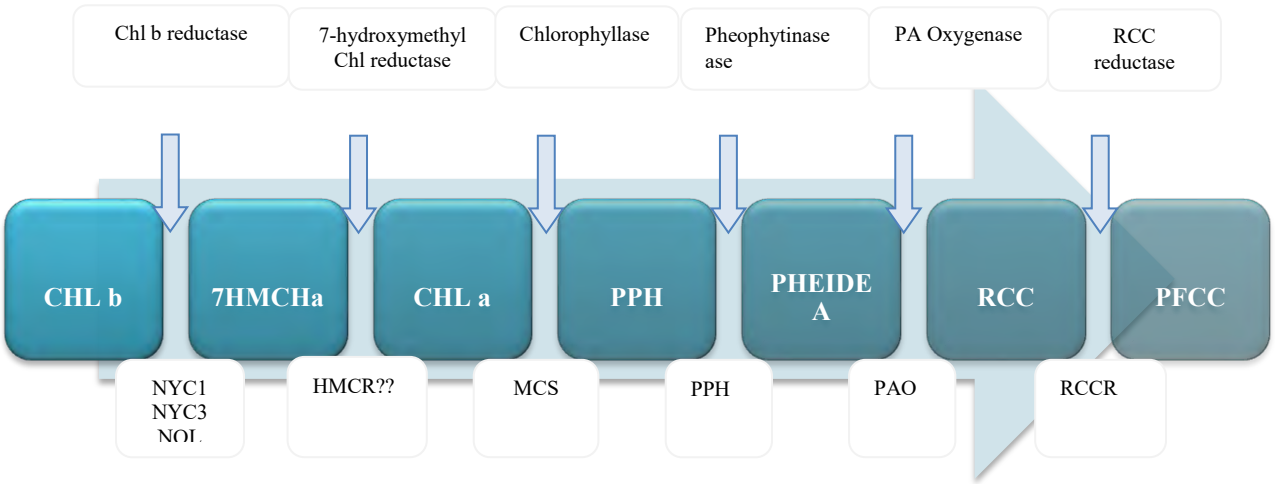

Figure 1.8. Chlorophyll degradation pathway

1.8.1. Phenomics of the stay-green trait

Variability in the duration and progression of senescence during terminal grain filling period can be used to measure the stay-green trait. Historically, phenotyping of the

stay-green trait relied on visual scoring (Thomas and Smart, 1993). Stay-green trait scored on 1 to 5 scale (Reddy *et al*., 2007), 0 to 9 scale (Joshi *et al*., 2007) or 1 to 10 scale (Silva *et al*., 2001) for both flag leaf and spike on the basis of visual greenness at the late grain filling stage. The difference between the flag leaf score and spike score was used to characterize the genotypes into different groups, stay-green (3-6), moderately stay-green (2-3), moderately non-stay-green (1-2), and non-stay-green (0-1). Till 2010, most of the studies refer stay-green for leaf greenness despite the fact that other organs such as stem and spike also contribute to plant total photosynthesis. Spike captures approximately 20% of carbon dioxide absorbed by flag leaf in wheat (Teare *et al*., 1972). Spikes contribute to grain yield improvement and the yield can be increased up to 70% in wheat and barley under stress conditions (Thorne, 1963; Biscoe *et al*., 1973; Araus *et al*., 1993; Maydup *et al*., 2010). Accurate non-destructive method periodic Normalized Difference Vegetation Index (NDVI) measurements by Greenseeker proposed by Christopher and colleagues to study the stay-green trait under field conditions estimate stay-green from the entire plant canopy. The information was used to calculate time from anthesis to senescence onset , mid senescence, near complete senescence, maximum NDVI level, rate of senescence, and green leaf area duration (Christopher *et al*., 2014). Recently, a High Resolution Plant Phenomics Centre at Commonwealth Scientific and Industrial Research Organization has developed a portable Phenomobile consisting of Greenseeker to measure NDVI together with Light Detection and Ranging (LiDAR) to detect the canopy green biomass and leaf area (Deery *et al*., 2014). Satellite based remote spectral imaging has been deployed in modeling vegetation indices (Bauerle *et al*., 2012) that can be used to identify or design the genotypes better adapted to changing environments. Agronomics evaluation of the stay-green trait showed its positive correlation with yield (Duvick *et al*., 2004; Pinto *et al*., 2016).

1.8.2. Physiology behind the stay-green trait

The physiology behind the stay-green phenotype is not yet clear. Thomas and Smart consider plants as stay-green, if they have higher water and chlorophyll content at maturity (Thomas and Smart, 1993). It is hypothesized that nitrogen and water management are associated with the stay-green trait. It has been elucidated that a balance

between nitrogen demand by the grain and nitrogen supply during grain filling leads to the expression of stay-green trait (Borrell *et al*., 2001; Borrell and Hammer, 2000). In sorghum, the stay-green trait was found to be associated with higher leaf nitrogen (Borrell *et al*., 2001). Addition of nitrogen fertilizer can delay leaf senescence and maintain the rate of photosynthesis (Zhang *et al*., 1997; Mi *et al*., 2007). Stay-green phenotype can be the result of improved water management by plant (Hammer, 2006). The plant having an active green leaf during terminal development phases requires access to water. So, the stay-green genotypes minimize or optimize the water use (Kholová *et al*., 2010b) or have a deeper root system to extract maximum water (Vadez *et al*., 2007). Plants can retain more water by reducing leaf area or conductance of the canopy (Kholová *et al*., 2010a; Kholová *et al*., 2010b). Reduced leaf area at anthesis results in stay-green phenotype by reducing the water losses (Hammer, 2006). It has been suggested that the stay-green can be the result of high water use efficiency (Van Oosterom *et al*., 2006).

1.8.3. Genomics of the stay-green trait

Stay-green genotype results by the disruption in the normal phenomena of senescence. Genes which are regulated during senescence are called senescence associated genes (SAGs) (Lim *et al*., 2003). Microarray studies elucidated large changes in gene expression in adult *Arabidopsis thaliana* during senescence (Buchanan-Wollaston *et al*., 2005; van der Graaff *et al*., 2006; Wagstaff *et al*., 2009). Gepstein and coworkers confirmed the differential expression of 130 non-redundant genes by Northern blot analysis (Gepstein *et al*., 2003). Buchanan-Wollaston in 2005 revealed around 800 SAGs concomitant with the dramatic change in physiology accompanying the program cell death (PCD) process (Buchanan-Wollaston *et al*., 2005). The Leaf Senescence Database (LSD) was developed that initially included 1145 SAGs from 21 species (Liu *et al*., 2010). More recently, Leaf Senescence Database 2 (LSD2), an extension of LSD contains 5356 SAGs from 44 species (Li *et al*., 2014). Genes involved in the chlorophyll degradation pathway have been studied extensively to demonstrate their role in the stay-green trait. Chlorophyll degradation begins with the conversion of chlorophyll b to 7-hydroxymethyl chlorophyll a, the gene involved is non-yellow color 1 or non-yellow

color one like (NOL). Non yellow coloring 1 (NYC1) mutants retain their chlorophyll content during senescence induced by dark (Kusaba *et al*., 2007). Non yellow coloring 3 (NYC3) mutant in rice also retains higher chlorophyll a and chlorophyll b concentration, but other senescence parameters proceed at normal rate suggesting it a non-functional stay-green mutant (Morita *et al*., 2009). 7-hydroxymethyl chlorophyll a is converted to chlorophyll a using 7-hydroxymethyl chlorophyll a reductase (HMCR) (Meguro *et al*., 2011). A complex stay-green gene, chlorophyll catabolic enzyme gene and light harvesting complex (SGR-CCE-LHCII) is formed by interaction between SGR and CCEs in LHCII. It is a dilemma whether HMCR is a component of SGR-CCE-LHCII. Stay-green rice gene (SGR) mutants were used to identify SGR gene in rice that encodes a unique chloroplast protein that is responsible for foliar greenness during senescence. The SGR mutants maintain a stay-green trait because of non-disruption of light-harvesting chlorophyll binding protein (LHCP) complexes. The SGR interacts with LHCPII, forming SGR-LHCPII complexes in the thylakoid membrane. Over expression of SGR regulates chlorophyll degradation by inducing LHCPII disassembly (Park *et al*., 2007). Chlorophyll a is converted to pheophorbide a oxygenase via chlorophyllide and pheophytin using chlorophyllide a oxygenase (CaO), and pheophytinase (PPH) or accelerated cell death 1 (ACD1) genes. Overexpressing the CaO gene has been reported to photosynthesize for a longer duration and retain a larger biomass (Biswal *et al*., 2012). Mutants deficient with PPH exhibit a stay-green phenotype and ACD1 inhibition led to photo-oxidative damage of the cell (Tanaka *et al*., 2003). *Arabidopsis* mutant deficient in PPH exhibits stay-green phenotype because of non-disruption of chlorophyll during senescence (Schelbert *et al*., 2009). Pheophorbide converts to red chlorophyll catabolite; the gene involved is pheophorbide a oxygenase (PaO). The gene SGR like PaO was up-regulated during dark-induced senescence. The expression of SGR and PaO was enhanced by abscisic acid (ABA) and inhibited by cytokinin. SGR over expression resulted in decrease in the number of lamellae in the grana thylakoids that caused decline in chlorophyll content. In the SGR mutants, Pheophorbide a was also detected that propose a possible role of SGR in the regulation of PaO. In *Pisum sativum* and *Festuca pratensis*, the stay-green phenotype was induced by the disruption of PaO (Vicentini *et al*., 1995). Red chlorophyll catabolite converts to primary fluorescence chlorophyll

catabolite (pfCC), the gene involved is accelerated cell death 2 (ACD2) (Wüthrich *et al*., 2000). A cytoplasmic gene (cytG), two recessive alleles d1 and d2 and a dominant G is responsible for greenness in foliages, pod walls, seed coats and embryos (Guiamét *et al*., 1990). CytG is responsible for stability of chlorophyll b by hindering its conversion to chlorophyll a (Guiamet *et al*., 1991). During senescence, d1d2 homozygote delays soluble protein degradation (Guiamet and Giannibelli, 1996). The marker genes for senescence RuBisCO (RBCS) and Chlorophyll a/b binding protein (CAB) can elucidate the stay-green trait by detecting whether photosynthetic machinery is intact or disrupted (Rampino *et al*., 2006). Genes associated with the stay-green trait are listed in the Table 1.3

1.8.4. Quantitative trait loci studies for the stay-green trait

The genetic basis behind the stay-green trait has been explored in numerous plant species by employing Quantitative Trait Loci (QTL) mapping approach. In *Festuca pratensis*, genetic analysis of the non-yellow mutant using Amplified Fragment Length Polymorphism (AFLP) markers revealed that stay-green trait was control by a single recessive nuclear allele referred to as Senescence-Induced-Deficiency (SID) (Thomas, 1987; Thomas *et al*., 1997). In the Lolium population, leaf senescence was associated with six QTLs (Thorogood *et al*., 1999). Early senescence gene was mapped on chromosome number 4 in *Arabidopsis* (Nakamura *et al*., 2000).

In sorghum, three QTLs stg1, stg2, and stg3 were detected using Restriction Fragment Length Polymorphism (RFLP) markers. These regions included genes for key photosynthetic enzymes, heat shock protein, and abscisic acid responsive gene (Xu *et al.*, 2000). Successful introgression of the stay-green QTLs stg1, stg3, stg4, and SZtgb via marker-assisted backcrossing from B35 sorghum line to R16 synchronized line raised drought stress tolerance capacity in the introgression lines produced (Kassahun *et al*., 2010).

Table 1.3. List of genes identified for stay-green trait

	Name of Gene	Species	Function	Reference
PSAG	Premature Senescence-Associated Gene	*Oryza sativa*	ARM-like	Li *et al*., 2004
Ipt	tRNA Isopentenyltransferase	*Oryza sativa*	tRNA Isopentenyltransferase	Sakamoto *et al*., 2006
DHS	Deoxyhypusine synthase	*Oryza sativa*	Deoxyhypusine synthase	Ohyanagi *et al*., 2006
ATG6	Beclin 1 like	*Triticum aestivum*	Autophagy	Botti *et al*., 2005
ACD1	Accelerated cell death 1	*Arabidopsis thaliana*	non heme oxygenase	Gary *et al*., 2002
ACD2	Accelerated cell death 2	*Arabidopsis thaliana*	red chlorophyll catabolite reductase	Mach *et al*., 2001
SAG12	Senescence associated gene 12	*Arabidopsis thaliana*	Cysteine peptidase	Swarbreck *et al*., 2011
RCCR	Red chlorophyll catabolite reductase	*Hordeum vulgare*	catabolism of chlorophyll	Wuthrich., 2000
SGR	Senescence inducible chloroplast stay green protein	*Hordeum vulgare*	catabolism of chlorophyll	Park *et al*., 2007
UDPGP	UDP-glucose pyrophosphorylase	*Oryza sativa*	UDP-glucose pyrophosphorylase	Eimert *et al*., 1995
COR1	Coronatine-induced protein	*Oryza sativa*	Chlorophyllase	Thorpe *et al*., 2002
EIF5a2	Eukaryotic translation initiation factor 5A2	*Triticum aestivum*	Elongation factor	Zhou *et al*., 2005
NYC3	Non Yellow Coloring 3	*Oryza sativa*	Chlorophyll degradation during senescence	Morita *et al*., 2009
SGR	Senescence inducible chloroplast stay green protein	*Oryza sativa*	Chlorophyll degradation	Zhou *et al*., 2011
CAO	Chlorophyllide A Oxygenase	*Nicotiana tabacum*	Overexpressing the CAO gene have been reported to photosynthesize for a longer duration and retain a larger biomass	Biswal *et al*., 2012

In maize, QTL mapping revealed 14 loci concomitant with stay-green and kernel yield traits (Zheng *et al*., 2009).

Cha and co-workers mapped a gene sgr between RG662 and C985 markers on chromosome 9 using RFLP markers in glutinous *japonica* rice Hwacheong-*wx* mutant. The mutant showed delayed yellowing but photosynthetic activity was similar to that of the non-stay-green plants. Thus, the mutation only affects the chlorophyll degradation pathway (Cha *et al*., 2002). A functional stay-green japonica rice ―SNU-SG1" was crossed with two regular lines (M23 and Ilpum) to develop F2 and RIL populations for the identification of QTLs responsible for stay green trait. Three QTLs, dcfs7, dcf9, and dcfs9 were detected on chromosome number 7 and 9 in both populations for the stay-green trait (Yoo *et al*., 2007). In rice, four QTLs tcs4, csfl6, csfl9 and csfl12 linked with the stay-green trait were identified on chromosome 4, 6, 9, and 12 respectively in two RIL populations by a cross between Suweon490 and SNU-SG1 and Andabyeo and SNU-SG1. The stay-green QTLs that include *Csfl6* and *Tcs9* co-localized with grain yield QTLs (*Yld6* and *Yld9*), thus strengthening the link between stay-green attribute and high productivity (Fu *et al.*, 2011).

In barley, the stay-green trait was associated with nine QTLs. Of the nine QTLs one QTL was found consistent in all environments, indicative of a simple genetic mechanism controlling the stay-green trait (Emebiri, 2013).

In wheat stay-green ―Chirya" and non-stay-green ―Sonalika" derived population used for QTL mapping identified three QTLs on chromosome number 1AS, 3BS, and 7DS associated with the stay-green trait (Kumar *et al*., 2010). Another QTL study for the stay-green trait in wheat detected 44 loci associated with stay-green and related traits. The stable QTLs with more repeatable effect were detected on chromosome 2A, 4A, 1B, 2B, 4B, and 7D. Co-location of the stay-green trait QTLs and performance traits QTLs confirmed that the stay-green attribute is an important adaptive trait under non-stress and heat stress environments (Pinto *et al*., 2016).

1.8.5. Transcriptomics studies for senescence and stay-green trait

Approximately, 200 transcription factors that differentially express during leaf senescence includes APETALA2, basic-leucine zipper, WRKY, NAC, two MYB transcription factors (MYBa and MYBb), PTF1 (Pi starvation-induced transcription factor 1), GLK1 (Golden-like 1) and an F-box protein, zinc finger, and GRAS families (Buchanan-Wollaston *et al*., 2005). Over expression of WRKY6 transcription factor results in necrosis. It activates the promoter of Senescence-Induced Receptor Kinase1in senescent leaves (Robatzek and Somssich, 2002). High expression of WRKY53 also results in premature senescence, however the WRKY53 mutants revealed stay-green phenotype (Miao *et al*., 2004). Expressed sequence tags (EST) database revealed the role of 20 NAC transcription factors during senescence (Guo *et al*., 2004). ORESARA1 (ORE1 or ANAC092) is a NAC transcription factor that triggers age regulated cell death. The accumulation of ORE1 is prevented by miRNA164 in young leaves but during aging the down regulation of miRNA164 results in up-regulation of ORE1 expression (Kim *et al*., 2009). NAP (activated by AP3/PI), NAC family transcription factor promotes premature senescence (Guo and Gan, 2006). ORE1 SISTER1/ANAC059 is a NAC transcription factor that positively regulates leaf senescence (Balazadeh *et al*., 2011). ORE9 is an F-box protein and it is suggested that over expression of ORE9 promotes leaf senescence as mutants that lack ORE9 delays leaf senescence (Woo *et al*., 2001). F box proteins are components of SCF-type E3 complexes that function as ubiquitin ligase (Lechner *et al*., 2006). ORE9 interacts with core SCF subunits (Stirnberg *et al*., 2007). The ATE1 (arginyl- tRNA:protein arginyltransferase) part of the ubiquitin-dependent proteolytic system, is a positive regulator of senescence (Yoshida *et al*., 2002). The ring type ubiquitin ligase and the plant U-box E3 ubiquitin ligase Senescence-Associated Ubiquitin Ligase1 (SAUL1) negatively regulates leaf senescence (Peng *et al*., 2007). SAUL1 mutant that lacks the expression of SAUL1 gene positively regulates senescence under low light conditions (Raab *et al*., 2009). NLA mutation results in early senescence under nitrogen limiting conditions (Peng *et al*., 2007) (Table 1.4).

Table 1.4. List of Transcription factors (TF) associated with the stay-green trait

TF family	Gene	Effect	Reference
WRKY	WRKY6	NSG	Robatzek and Somssich., 2002
	WRKY30	NSG	Besseau *et al*., 2012
	WRKY53	NSG	Miao *et al*., 2004
	WRKY54	SG	Besseau *et al*., 2012
	WRKY57	SG	Jiang *et al*., 2014
	WRKY70	SG	Besseau *et al*., 2012
NAC	ORE1 SISTER1	NSG	Balazadeh et al., 2011
	NAM-B1	NSG	Uauy *et al*., 2006
	ANAC019	NSG	Hickman *et al*., 2013
	ANAC055	NSG	Hickman *et al*., 2013
	OsNAP	NSG	Zhou *et al*., 2013; Liang *et al*., 2014
	VNI2	SG	Yang *et al*., 2011
	JUB1a	SG	Wu *et al*., 2012
homeodomain	KNAT2	SG	Hamant *et al*., 2002
GARP	GLK2	SG	Rauf *et al*., 2013
GBF	GBF1	NSG	Smykowski *et al*., 2010
AP2/ERF	NtERF3	NSG	Koyama *et al*., 2013
	AtERF4	NSG	Koyama *et al*., 2013
	AtERF8	NSG	Koyama *et al*., 2013
	SlERF36	NSG	Upadhyay *et al*., 2013
	RAV1	NSG	Woo *et al*., 2010
	GmRAV	NSG	Zhao *et al*., 2008
	EDF1	SG	Chen *et al*., 2011
	EDF2	SG	Chen *et al*., 2011
	SUB1A	SG	Fukao *et al*., 2012
	CBF2	SG	Sharabi-Schwager *et al*., 2010
	CBF3	SG	Sharabi-Schwager *et al*., 2010
	CRF6	SG	Zwack *et al*., 2013
TCP	TCP2	NSG	Schommer *et al*., 2008
	TCP3	NSG	Schommer *et al*., 2008; Koyama *et al*., 2013
	TCP4	NSG	Schommer *et al*., 2008
	TCP5	NSG	Koyama *et al*., 2013
	TCP10	NSG	Schommer *et al*., 2008; Koyama *et al*., 2013
	TCP13	NSG	Koyama *et al*., 2013
	TCP19	SG	Danisman *et al*., 2012

	TCP20	SG	Danisman *et al*., 2012
	TCP24	NSG	Schommer *et al*., 2008
Zn finger	SlZF2	SG	Hichri *et al*., 2014
MADS	FYF	SG	Chen *et al*., 2011
MYB	MYBR1/MYB44	SG	Jaradat *et al*., 2013
ARF	ARF2a	NSG	Ellis *et al*., 2005; Lim *et al*., 2010
bHLH	CIB	NSG	Meng *et al*., 2013
EIN3	EIN3	NSG	Li *et al*., 2013; Kim *et al*., 2014
GBF	GBF1	NSG	Smykowski *et al*., 2010
GRAS	GAIa	SG	Chen *et al*., 2014
GRF	GRF3	SG	Debernardi *et al*., 2014

SG: Stay-green, NSG: Non-stay-green

1.8.6. Proteomics studies for senescence and stay-green trait

More than 9000 different proteins were identified in barley in early and late senescence lines. Proteins that were up-regulated in early senescent line were related to pathogenesis, intracellular receptors or co-receptors, membrane receptors or co-receptors, pathogen cell walls attacking enzymes (glucanases), cuticle modifying enzyme and DNA repair enzymes (Mason *et al*., 2016). The F box protein coronatine-insensitive 1 is a key regulator in jasmonic acid dependent pathways. In *Arabidopsis*, 35 coronatine-insensitive 1 dependent proteins regulated by jasmonic acid were identified. Rubisco activase, a COI1-dependent JA-repressed protein is down-regulated during leaf senescence (Shan *et al*., 2011). Senescence progression is accompanied by disruption of chlorophyll and decrease in photosynthesis related proteins (Bate *et al*., 1991). In chloroplast the proteolysis begins during early senescence. Plastidial peptide hydrolases are involved in degradation of rubisco and stromal enzymes in chloroplast. Cysteine proteases are also expressed during senescence but their role in chloroplast degradation is not clear yet (Hörtensteiner and Feller, 2002).

1.8.7. Metabolomics studies of the stay-green trait

Till date, stay-green trait has not been explored at metabolic level. The mutants showed that impairing chlorophyll synthesis can result in early senescence because of the accumulation of phototoxic intermediates (Tanaka and Tanaka, 2007, Mochizuki *et al*.,

2010). The biosynthetic pathways of plant secondary metabolites can abet in elucidating the complex metabolic reactions occurring during chlorophyll degradation (Jørgensen *et al*., 2005), which might contribute towards our understanding of the metabolic pathways underlining the stay-green trait.

1.8.8. Phytohormones studies of the stay-green trait

Alteration in the phytohormone metabolism and signaling can result in stay green phenotype, particularly networks involving cytokinins and ethylene (Woo *et al*., 2001; Yan *et al*., 2007). Cytokinin prevents leaf senescence but once senescence is initiated it can‘t halt the process (Weaver *et al*., 1998). Cytokinin biosynthesis gene Isopentyl transferase (IPT) under the control of SAG12 promotor was expressed in *Agrobacterium* and tobacco plants were produce with delayed leaf senescence (Gan and Amasino, 1995). It is found in transgenic tobacco that the over expression of isopentenyl transferase, an enzyme for cytokinin biosynthesis, results in increase in chlorophyll and cytokinin levels and delay leaf senescence (Ori *et al*., 1999). In wheat the expression of *pSAG12-IPT* slows the process of senescence but grain yield was not enhanced (Sykorova *et al.*, 2008). When senescence-associated receptor-like kinase (SARK) promoter was used, IPT expression in tobacco increased cytokinin in leaves. There was no effect on the phenotype of plants under normal conditions but leaf senescence was prevented in the plant under drought stress with dramatic grain yield improvement (Rivero *et al*., 2007). Mutations in cytokinin receptors such as AKH3 can cause reduced chlorophyll content in the leaf (Riefler *et al*., 2006). Many genes associated with ethylene biosynthesis are up-regulated during senescence (van der Graaff *et al*., 2006). The MKK9-MPK3/MPK6 signaling cascade has a role in ethylene signaling. Therefore it is possible that it regulates ethylene dependent leaf senescence (Zhou *et al*., 2009). A mutant *ore9-1* showed delayed senescence in response to downstream signaling of MeJA, ethylene and abscissic acid (ABA) (Woo *et al*., 2001). ABA dependent receptor kinase (RPK1) overexpression results in early senescence whereas mutation in these RKP1 delays senescence (Lee *et al*., 2011). ABA effects age dependent senescence, it make the senescence process faster once it has been started. ABA cannot induce senescence in premature plants (Lee *et al*., 2011; Weaver *et al*., 1998). ABA under low nitrogen condition can promote biosynthesis

of chlorophyll and inhabit chlorophyll degradation (Oka *et al*., 2012). E3 ubiquitin ligase SAUL1 mutant showed early senescence and resulted in increased ABA levels under low light conditions (Raab *et al*., 2009). This increase in ABA was due to the over expression of ABA biosynthesis gene AAO3. Mutation in *auxin response factor 2(arf2)* results in delayed senescence (Ellis *et al*., 2005). Over expression of YUCCA6, an auxin biosynthesis gene delayed the phenomena of senescence (van der Graaff *et al*., 2006). Jasmonic acid (JA) biosynthesis genes up regulate in response to age dependent senescence (van der Graaff *et al*., 2006). A transcription factor OsDOS in rice is a JA related negative regulator of leaf senescence (Kong *et al*., 2006). JA dependent Rubisco activase in *Arabidopsis* also found to be negative regulator of senescence (Shan *et al*., 2011). Mutation in histone deacetylase gene (*HDA6),* the gene involves in the expression of JA response genes results in delayed senescence (Wu *et al*., 2008). Mutants deficient in Salicyclic acid (SA) degraded chlorophyll at a normal rate but the photosystem II remain functional thus maintain photosynthesis for longer duration (Abreu and Munne-Bosch, 2009). The genes associated with SA and senescence are specific for natural senescence (Buchanan-Wollaston *et al*., 2005; van der Graaff *et al*., 2006).

1.8.9. Stay-green trait under abiotic stresses

Increase temperature and irradiance promotes the production of reactive oxygen species (ROS). This results in cell damage and hasten the loss of foliar greenness (Christiansen, 1978; McDonald and Vanlerberghe, 2004). In stay-green genotypes, the negative impact of heat stress is coped by minimized the generation of ROS. The plant pigments such as xanthophylls and carotenes protect the chloroplast and photosynthetic apparatus by dissipating excessive radiant energy (Zhao and Tan, 2005; Suzuki and Mittler, 2006). The detail mechanism behind the stay-green trait under stress has not yet been explored. However, the stay-green has been associated with yield improvement under abiotic stresses.

1.9. Conclusion and Future Perspectives

Stay-green trait has been studied in monocots very extensively. A functional type stay-green in sorghum, rice, maize, and wheat revealed a direct relationship of stay-green trait with grain yield (Borrell and Hammer, 2000; Spano, 2003; Yoo *et al*., 2007; Fu and Lee, 2008; Echarte *et al*., 2008). In wheat stay-green trait was found to influence the grain yield and biomass up to 25.7% under field conditions (Chen *et al*., 2010; Luo *et al*., 2006). A stay-green hybrid winter wheat XN901 also showed a positive significant correlation with grain yield, grain yield improves by 15% with six days increase in grain filling duration (Gong *et al*., 2005).

Stay-green occupies central position under changing climate by showing tolerance to heat and drought stress. In cereal crops such as sorghum, rice and wheat, the QTLs studies under high temperature and drought stress unveil QTLs for stay-green trait and performance traits at the same location confirming that the stay-green phenotype is associated with productivity augmentation.

Understanding the mechanism behind functional stay-green trait that is associated with improved photosynthetic efficiency can be a key component to boost yield particularly under adverse environmental conditions. The trait needs to be explored in different crops under different environmental conditions to harness the advantage in grain yield, quality, and tolerance to biotic and abiotic stresses. The stay-green trait may provide the breeder with a solution to major stresses and yield improvement.

1.10. Aims and objectives of the study

The general aim of the present study was to evaluate the stay-green trait in historical bread wheat panel, identify quantitative trait loci associated with the stay-green trait, access the stay-green trait under terminal heat stress, determine expression profiles of the stay-green trait related genes, and reveal comprehensive array of metabolites associated with stay-green trait.

Specific aims of each chapter were:

- ***Chapter#2:*** The objective of the study was to unravel the genetic basis behind the stay-green trait using 90K SNP array by GLM, MLM, and FarmCPU based Genome Wide Association Mapping in a diverse panel comprising landraces, green revolution, post green revolution, elite cultivars, and CIMMYT advance cultivars.

- ***Chapter#3:*** The study aimed to examine the association of the stay-green trait with the chlorophyll content, photochemical efficiency, normalized difference vegetative index (NDVI), canopy temperature, grain yield, biological yield, kernel weight, expression profile of chlorophyll catabolism pathway genes (CaO, SGR, and RCCR), and the photosynthetic responsive gene (Cab) in bread wheat under terminal heat stress.

- ***Chapter#4:*** The objective of the study was to demonstrate the differential accumulation of metabolites in the leaf tissues of non-stay-green and stay-green genotypes in control and heat stressed plants during grain filling duration using UHPLC-HRMS based untargeted global metabolomics to unveil the mechanism behind stay-green trait in relation to heat stress tolerance.

Chapter #2

Genome-Wide Association Study of Stay-green Trait in Triticum aestivum L.

Chapter #2

Genome-Wide Association Study of Stay-green Trait in *Triticum aestivum* L.

2.1. Abstract

The global climate extremes with diminishing quality and quantity of arable land are projected to significantly reduce the global cereal production. The crop yield needs to be enhanced by 70% to meet the food requirement of the increasing global population of 9 billion by 2050. To cope with yield losses due to climatic extremes and increasing crop yield to meet future food demand, there is an urgent need for exploring sustainable strategies for yield improvement. The functional stay-green trait seems to be a significant adaptive mechanism that confirms maximum mass per grain by maintaining chlorophyll content, photosynthetic capacity, and supply of assimilated carbon during the terminal stages of development under adverse conditions. The genetic basis behind stay-green trait is complex and has not been fully explored in wheat. The present study aimed to parse the genetic composition of the stay-green trait in a diverse germplasm consisting of landraces, green revolution, post green revolution, elite cultivars, and CIMMYT advance cultivars using 90K SNP array by GLM, MLM, and FarmCPU based genome-wide association study (GWAS). The morpho-physiological traits including chlorophyll content, chlorophyll fluorescence, normalized difference vegetative index (NDVI), plant height, tiller number, spike length, spikelet per spike, thousand kernel weight, grain yield, and biological yield were evaluated during field experiments from 2012-2016. The stay-green indices: SPAD chlorophyll content at heading, absolute difference in the SPAD chlorophyll content, relative difference in the SPAD chlorophyll content, cumulative SPAD chlorophyll content, NDVI at heading, absolute difference in NDVI, relative difference in NDVI, cumulative NDVI were determined from chlorophyll content and NDVI measured at different time points. Analysis of variance revealed significant difference between genotypes for chlorophyll content, chlorophyll fluorescence, NDVI, plant height, tiller number, spike length, spikelet per spike, grain yield, and biological yield. Heritability of the measured traits varied between 0.427-0.73. Chlorophyll content, chlorophyll fluorescence, NDVI, and stay-green indices showed positive correlation with

thousand kernel weight, grain yield, and biological yield. GWAS identified 83 highly significant marker trait associations at –log10(p) ≥4.3, scattered over 48 loci in wheat genome, for chlorophyll content, chlorophyll fluorescence, NDVI, stay-green indices, plant height, and tiller number. Of these, 20 loci identified by multiple GWAS methods were selected for gene identification to list the potential candidate genes for future studies. These 20 loci had 342 high confidence protein coding genes based on the International Wheat Genome Sequence Consortium reference assembly RefSeq v1.0. Only 36 out of 342 genes had descriptors in the reference assembly which were involved in primary mechanisms of plant growth, development, stress tolerance, flowering time control, chloroplast development, and damage tissues regeneration. The identified loci from a genetically diverse germplasm through rigorous GWAS methods provide basis for future studies to search for candidate genes underlying the stay-green trait in wheat.

2.2. Introduction

Stay-green refers to mutants, transgenic plants, or cultivars with the trait of heritable extended foliar greenness during late grain filling duration compared with wild type or reference genotype (Thomas and Stoddart, 1975; Thomas and Smart, 1993; Thomas and Howarth, 2000; Thomas and Ougham, 2014). The stay-green genotypes are classified into functional stay-green and non-functional stay-green. The functional stay-green plants are the target of plant breeders as they have the potential to delay chlorophyll degradation, retain photosynthetic activity, and increase plant productivity. The functional stay-green genotypes either delay senescence (Type-A) or delay progression of senescence (Type-B). The non-functional stay-green plants maintain chlorophyll content, but maintenance of chlorophyll content is not coupled with increase in photosynthetic activity and plant productivity. In the non-functional stay-green genotypes, chlorophyll degradation impairs with rest of the senescence events (Type-C), or plant dies before or at the mid of senescence (Type-D), or chlorophyll accumulation is higher in some genotypes compared with wild type, so chlorophyll degradation will take longer but the genotypes possess normal photosynthetic capacity (Thomas and Howarth, 2000; Jiang *et al*., 2004; Ho¨rtensteiner, 2009; Sato *et al*., 2009; Schelbert *et al*., 2009; Thomas and Ougham, 2014; Shimoda *et al*., 2016; Zhao *et al*., 2019). The functional type

stay-green maize, rice, wheat, and sorghum reveal a direct relationship of the stay-green trait with grain yield (Borrell and Hammer, 2000; Spano *et al*., 2003; Yoo *et al*., 2007; Fu and Lee, 2008; Echarte *et al*., 2008). In wheat stay-green trait was found to influence the grain yield up to 25.7% under field conditions (Luo *et al*., 2006). A stay-green hybrid winter wheat XN901 showed an increase in grain yield by 15% with 6 days increase in grain filling duration (Gong *et al*., 2005). Stay-green trait has been considered as a mechanism of tolerance to abiotic and biotic stresses (Kumari *et al*. 2007; Joshi *et al*., 2007; Borrell *et al*., 2014; Pinto *et al*., 2016; Adeyanju *et al*., 2016; George-Jaegglia *et al*., 2017; Kamal *et al*., 2018). For decades, the stay-green trait has been considered as a selection criterion for improving crop yield, as extended greenness during post-anthesis ensures maximum mass per grain. Despite of the importance of the stay-green trait in yield improvement, the genetic basis behind the stay-green trait is not yet well understood.

Historically, the phenotyping of the stay-green trait relied on a subjective visual scoring approach. The stay-green trait was scored on 1-5 scale (Reddy *et al*., 2007), 0-9 scale (Joshi *et al*., 2007; Kumar *et al*., 2010), and 1-10 scale (Silva *et al*., 2001) for both flag leaf and spike on the basis of visual greenness at the late grain filling stage. The difference between the flag leaf score and spike score and leaf area under greenness were used to characterize the genotypes into different groups, stay-green, moderately stay-green, moderately non-stay-green, and non-stay-green (Joshi *et al*., 2007). Later, the handheld SPAD meter was used for the quantification of the stay-green trait as it offers an accurate measurement of the individual flag leaf greenness. The SPAD chlorophyll values were used to calculate stay-green indexes that included rate of senescence and green leaf area at maturity (Harris *et al*., 2007). The GreenSeeker, a precise non-destructive high throughput approach has been used to measure total canopy greenness. The periodic normalized difference vegetation index (NDVI) measurements from GreenSeeker were used to calculate stay-green indices that included time from anthesis to senescence onset, mid senescence, near complete senescence, maximum NDVI level, rate of senescence, and green leaf area duration (Lopes & Reynolds, 2012; Christopher *et al*., 2014; Pinto *et al*., 2016; Christopher *et al*., 2018). These approaches enabled the quantification of the stay-green trait in large number of samples used in Quantitative trait

loci (QTL) mapping. In the present study both SPAD chlorophyll and NDVI values were used to calculate the stay-green indices that were flag leaf score at heading, canopy score at heading, absolute difference in the flag leaf score at heading and 30 days after heading, absolute difference in the canopy score at heading and 30 days after heading, relative difference in the flag leaf score at heading and 30 days after heading, relative difference in the canopy score at heading and 30 days after heading, cumulative SPAD score, and cumulative NDVI score (Zhao *et al*., 2019). The assessment of the stay-green trait allows identification of the loci controlling the stay-green trait which can be used as tools for marker assisted selection in plant breeding.

With the advent of high throughput phenotyping and genotyping, the molecular basis of complex trait can be elucidated by the quantitative trait loci (QTL) mapping (Langridge and Reynolds, 2015). Among QTL mapping approaches, genome-wide association study (GWAS) has a greater advantage; as GWAS offers higher QTL mapping resolution and explores all the evolutionary recombination events (Buckler and Thornsberry, 2002; Flint-Garcia *et al*., 2003; Yu and Buckler, 2006). For QTL mapping, simple sequence repeats, expressed sequence tags, restriction fragment length polymorphism, amplified fragment length polymorphism, random amplified polymorphic DNA, diversity array technique, and single nucleotide polymorphism markers have been employed. The high density single nucleotide polymorphisms (SNPs) have been widely used (Ibrahim *et al*., 2020). General Linear Model (GLM), Mixed Linear Model (MLM), and Fixed and random model Circulating Probability Unification (FarmCPU) using PLINK, TASSEL, GAPIT, GenABEL, EMMAX, GEMMA, GCTA, and FarmCPU_pkg packages have been used in GWAS (Purcell *et al*., 2007; Bradbury *et al*., 2007; Aulchenko *et al*., 2007; Kang *et al*., 2010; Yang *et al*., 2011; Lipka *et al*., 2012; Zhou and Stephens, 2012; Tang *et al*., 2016; Yin et al., 2021). With the increase in number of samples and SNPs in GWAS, the computational analysis using these packages has become more challenging. To improve the computational efficiency, the Memory-efficient Visualization-enhanced Parallel-accelerated (rMVP) package has been developed that effectively processes the large data-sets, efficiently estimates population structure, rapidly evaluates variance components, and implements GLM, MLM, and FarmCPU analysis methods for marker trait association (Yin *et al*., 2021).

Genetic variability for the stay-green trait has been exploited in maize, rice, wheat, soybean, oat, pea, fescue, and other plant species (Thomas and Stoddart, 1975; Thomas and Smart, 1993; Duvick *et al*., 2004; Armstead *et al*., 2006; Barry *et al*., 2008). In wheat, the QTL mapping of the stay-green trait using a recombinant inbred lines population between the stay-green Chirya-3 and the non-stay-green Sonalika under field conditions identified three QTLs (*QSg.bhu-1A*, *QSg.bhu-3B* and *QSg.bhu-7D)* on chromosome 1AS, 3BS and 7DS. The three stay-green QTLs explained 38.7% of the phenotypic variation (Kumar *et al.*, 2010). Shi *et al*., (2017) identified 28 QTLs for the chlorophyll content and 43 QTLs for NDVI using a high density genetic map comprising 2,575 markers under altered water regimes. Remarkably in several studies, stay-green QTLs co-localized with QTLs of other agronomics traits, this can allow the simultaneous selection of important agronomics traits in breeding. Huang *et al*., (2004) detected QTL for the stay-green trait and QTL for grains per spike on the similar region of the chromosome 3BS (Huang *et al*., 2004). Pinto *et al*., (2016) identified 44 QTLs for the stay-green trait and other important agronomic traits, some of the genomic regions associated with stay-green trait were found to have an effect on NDVI, canopy temperature, length and rate of grain filling, grain number, grain weight, and yield. Christopher *et al*., (2018a) detected the stay-green QTL co-localized with QTLs for the root number of seedlings and Rht height genes. The co-localization of the stay-green loci and performance trait loci confirmed that the stay-green phenotype is useful for yield improvement in hot and water limited environments (Pinto *et al*., 2016; Christopher *et al*., 2018a).

Deeper understanding of physiological and molecular basis of the stay-green trait is crucial to reduce the negative effects of the changing climate. So far few bi-parental QTL mapping studies demonstrated the genetic basis of the stay-green trait in wheat (Huang *et al*., 2004; Kumar *et al.*, 2010; Pinto *et al*., 2016; Shi *et al*., 2017; Christopher *et al*., 2018a). Therefore, the present study aimed to explore QTLs associated with the stay-green trait by GWAS using historical spring wheat cultivars of Pakistan and advance cultivars of CIMMYT. GWAS using GLM, MLM, and FarmCPU models was performed to identify QTL associated with chlorophyll content, NDVI, stay-green indexes, and yield parameters in wheat historical panel of Pakistan.

2.3. Materials and methods

2.3.1. Plant material

A diverse historical panel of 125 Pakistani bread wheat cultivars including landraces, green revolution, post green revolution, and elite cultivars adapted to different climatic zones (irrigated, semi-arid, and arid) and 25 CIMMYT advance varieties were selected for field trials (Annexure 2.1). The seeds of the selected cultivars were obtained from Wheat Wide Crosses Laboratory, National Agricultural Research Centre, Islamabad, Pakistan.

2.3.2. Field experiment

The selected association panel was subjected to field trials for five consecutive cropping seasons from 2012 to 2016 at National Agricultural Research Centre, Islamabad, Pakistan located between 33°40‘28”N latitude and 73°7‘28”E longitude. Plantation was done on November 15 each year in an alpha lattice design. Each plot consisted of four 1 m rows with a sowing density of 20 seeds per row and spaced 20 cm apart from adjoining plots. The field trials were managed by standard agronomic management practices.

2.3.3. Phenotyping

The traits evaluated were chlorophyll content, photosynthetic efficiency, normalize difference vegetative index, plant height, tiller number, spike length, spikelet per spike, thousand kernel weight, biological yield, and grain yield. All the traits were measured according to the procedures described by Pask *et al*., 2012.

The chlorophyll content was determined at booting, heading, anthesis, 10 days after anthesis (DAA), 20 DAA, and 30 DAA using SPAD 502 PLUS chlorophyll meter (Konica Minolta). Chlorophyll content was measured from 1/3 of the distance, 1/2 of the distance, and 2/3 of the distance from base of the flag leaves of three central plants for each genotype during mid-day between 11am and 3pm. The average of nine readings from three replicates at each time point was used for further analysis. To evaluate the

stay-green trait four indices were used; the SPAD chlorophyll content of flag leaf at heading (SFH), absolute difference in the SPAD chlorophyll content at heading and the SPAD chlorophyll content at 30 DAA (ADSF= SPAD chlorophyll content at heading - SPAD chlorophyll content at 30 DAA), relative difference in the SPAD chlorophyll content at heading and the SPAD chlorophyll content at 30 DAA (RDSF= ADSF/SFH), and cumulative SPAD chlorophyll content at booting, heading, anthesis, 10 DAA, 20 DAA, and 30 DAA (CSF= Sum of SPAD chlorophyll content at booting, heading, anthesis, 10 DAA, 20 DAA, and 30 DAA).

Chlorophyll fluorescence parameter fv/fm (maximum quantum yield of PSII) was measured at booting, heading, anthesis, 14 DAA (mid grain filling duration), and 21 DAA (near complete physiological maturity) from the flag leaves using Pocket PEA chlorophyll fluorimeter (Hansatech) during mid-day between 11 am and 2 pm. The chlorophyll fluorimeter relied on leafclips system that pre-conditions (dark adaption) the flag leaf. The dark treatment using leafclips was applied for 20 minutes prior to measuring the chlorophyll fluorescence parameters.

Normalize Difference Vegetative Index (NDVI) was recorded at heading, anthesis, 14 DAA (mid grain filling duration), and 21 DAA (near complete physiological maturity) between 11 am and 2 pm by measuring the canopy reflectance at 660 nm and 770 nm [(R770-R660)/(R770+R660)] with a handheld GreenSeeker crop sensor (Trimble). The distance between the canopy and the NDVI meter was kept around 50 cm. The stay-green trait was calculated by using four indices: 1. NDVI at heading (NH), 2. Absolute difference in the NDVI values at heading and NDVI values at 21 DAA (ADN= NDVI at heading - NDVI at 21 DAA), 3. Relative difference in the NDVI values at heading and NDVI values at 21 DAA (RDN= AND/NH), and 4. Cumulative NDVI values at heading, anthesis, 14 DAA, and 21 DAA (CN= Sum of NDVI at heading, anthesis, 14 DAA, and 21 DAA).

Plant height (PH) was assessed by measuring the plant from base to tip of the spike excluding awn using a measuring rod at physiological maturity. Tillers per plant (TN) were recorded by counting the total number of fertile tillers in individual plant at

anthesis. Spike length (SL) was determined by measuring the spike from base of the rachis to tip of the upper spikelet, excluding awns at physiological maturity. Spikelet per spike (SPS) was recorded by counting the spikelet number from base (sterile spikelet) to tip (fertile spikelet) of the spike. The average values from three biological replicates for PH, TN, SL, and SPS were used for statistical analysis. The above ground biomass excluding row edges was harvested, dried, and weighed using an electronic balance to determine biological yield (BY). The harvested above ground biomass was threshed and grain harvest obtained after threshing was weighed using an electronic balance to measure grain yield (GY).

2.3.4. Statistical analysis

Phenotypic data was subjected to best linear unbiased predictions (BLUPs) analysis using lme4 package in R version 3.5.1 (Bates *et al*., 2015). BLUPs estimate the real breeding value of a trait by eliminating environmental anomalies (Robinson, 1991; Viana *et al*., 2010; Mi *et al*., 2011). BLUPs data for each trait was used for descriptive statistics, and correlation analysis. Analysis of variance (ANOVA) was performed on primary five years field data for each trait. Descriptive statistics and ANOVA were performed by XLSTAT version 2014.5.03. Trait correlations were analyzed and visualized using GGally package in R version 3.5.1.

2.3.5. Genotyping

The genomic DNA was extracted from fresh leaves of 25 days old wheat seedlings according to the CIMMYT Molecular Genetics Manual (Dreisigacker *et al*., 2012). The DNA with 50-100 ng/µL concentration per sample was sent to CapitalBio® genotyping facility in Beijing for genotyping via high-density Illumina 90K Infinium SNP array consisting of 81,587 markers (Akhunov *et al*., 2009; Wang *et al*., 2014). Genome Studio program version 2011.1 was used for genotype calling. Genetic similarities were estimated by PowerMarker v.3.0 with Dice coefficient based on ratio of shared alleles (Liu *et al*., 2005). Polymorphism information content was employed to determine genetic diversity at each chromosomal locus. Monomorphic markers, markers having missing values more than 20% or allele frequency less than 5% or an unclear SNP

calling were removed. The effective 20,853 SNP markers were used for estimation of population structure analysis, principal component analysis, kinship analysis, and genome wide association mapping. The International Wheat Genome Sequence Consortium reference assembly (IWGSC) RefSeq-v.1.0 was used to determine physical positions of SNP markers along chromosomes.

2.3.6. Population structure

Population structure was determined using STRUCTURE software 2.3.3, which uses model-based Bayesian cluster analysis. A total of 1000 unlinked SNP markers, 100,000 burns in iterations followed by 500,000 Markov- Chain iteration were used to give a putative number of subpopulation between k= 1 to 15 (Pritchard *et al*., 2000). Sampling variance was estimated by 10 independent runs for each k. The rate of change of log probability between the successive values basis for ΔK was used to estimate K (Evanno *et al*., 2005; Quraishi *et al*., 2011).

2.3.7. Linkage disequilibrium, genome wide association analysis and gene annotation

The observed allele frequency and expected allele frequency were used to calculate linkage disequilibrium (LD) in TASSEL v.5.0. The Memory efficient Visualization enhanced and Parallel accelerated (rMVP) R package with default setting was used for Genome Wide Association Study (GWAS). The rMVP employed three models i.e., General Linear Model (GLM), Mixed Linear Model (MLM), and Fixed and random model Circulating Probability Unification (FarmCPU) to estimate the marker trait associations (MTA). For multiple testing correction, the bonferroni correction (bonferroni correction= 1/ total number of markers) was applied to calculate the threshold. The association between marker and trait was considered significant if the –log10 (p) value was greater than the threshold of –log10 (p) $\geq$4.3 ($p < 0.000047$). Finally, genes associated with the locus were extracted from *Triticum aestivum* genes (IWGSC) dataset at Ensembl Plants using BioMart function.

2.4. Results

2.4.1. Descriptive statistics, analysis of variance, and heritability

The minimum, maximum, mean, standard deviation, variance, and heritability of the morph-physiological traits evaluated under the field trials from 2012-2016 are presented in Table 2.1. The analysis of variance revealed significant difference between genotypes for CHL_20DAA, CHL_30DAA, fv/fm_14DAA, CSF, ADSF, RDSF, PH, TN, SL, SPS, GY, and BY. The heritability of the morpho-physiological traits varied between 0.427 - 0.73 (Table 2.1), which indicated that the traits were significantly influenced by genetic factors and thus suitable for genetic association study.

Table 2.1. Descriptive statistics, analysis of variance, and heritability of the morphological traits evaluated under field trials

Trait	Year	Range	Mean±std. Deviation	ANOVA (p value)	Heritability
CHL_T	2016-2017	31.27~54.27	45.71±3.97	0.06	0.55
	2015-2016	38.44~55.30	47.04±3.61		
	2014-2015	30.90~57.57	39.88±4.43		
	2013-2014	31.13~49.27	40.45±4.02		
	2012-2013	35.97~56.60	44.76±3.93		
	BLUPs	41.3~46.39	43.59±0.98		
CHL_B	2016-2017	32.33~53.87	44.26±4.32	0.188	0.53
	2015-2016	27.08~51.00	39.13±4.48		
	2014-2015	28.87~50.57	36.27±4.04		
	2013-2014	28.22~51.55	42.09±4.40		
	2012-2013	36.47~52.95	43.71±3.26		
	BLUPs	37.92~44.87	41.11±1.19		
CHL_H	2016-2017	29.57~55.13	43.96±4.52	0.187	0.5
	2015-2016	34.50~50.19	43.28±2.85		
	2014-2015	23.37~45.53	34.89±4.28		
	2013-2014	23.33~58.20	43.73±6.99		
	2012-2013	29.10~54.87	42.60±5.41		
	BLUPs	37.00~45.57	41.69±1.32		
CHL_A	2016-2017	35.47~56.30	46.52±4.26	0.282	0.52
	2015-2016	21.20~52.90	35.60±5.83		
	2014-2015	25.33~45.87	34.78±3.81		
	2013-2014	25.63~57.30	40.34±5.77		
	2012-2013	29.97~51.27	38.58±4.73		
	BLUPs	34.64~44.39	39.27±1.72		

CHL_10DAA	2016-2017	26.40~56.90	42.02±5.69	0.955	0.44
	2015-2016	11.40~44.15	27.01±6.89		
	2014-2015	21.87~47.37	34.46±3.98		
	2013-2014	22.17~57.10	36.96±6.79		
	2012-2013	20.13~48.63	34.54±5.64		
	BLUPs	32.41~38.77	35.00±1.31		
CHL_20DAA	2016-2017	19.27~55.43	35.53±7.59	**0.0053****	0.58
	2015-2016	5.70~43.53	22.72±8.81		
	2014-2015	14.58~39.25	23.58±4.39		
	2013-2014	13.50~55.77	32.82±8.42		
	2012-2013	16.33~54.13	32.10±7.50		
	BLUPs	21.93~36.29	29.35±2.93		
CHL_30DAA	2015-2016	0.00~43.50	18.42±11.09	**0.000367*****	0.61
	2014-2015	1.80~37.30	12.69±7.30		
	2013-2014	11.80~27.87	18.97±3.69		
	2012-2013	12.90~25.83	18.28±2.48		
	BLUPs	14.56~20.21	17.34±1.20		
fv/fm_H	2015-2016	0.39~0.73	0.56±0.06	0.68	0.482
	2014-2015	0.41~0.72	0.52±0.06		
	2013-2014	0.40~0.83	0.63±0.09		
	BLUPs	0.58~0.66	0.61±0.014		
fv/fm_A	2015-2016	0.49~0.72	0.62±0.04	0.974	0.427
	2014-2015	0.36~0.66	0.49±0.05		
	2013-2014	0.26~0.70	0.51±0.09		
	BLUPs	0.55~0.60	0.57±0.01		
fv/fm_14DAA	2015-2016	0.30~0.76	0.51±0.08	**< 0.0001*****	0.642
	2014-2015	0.31~0.68	0.49±0.06		
	2013-2014	0.19~0.80	0.47±0.09		
	BLUPs	0.41~0.58	0..49±0.02		
fv/fm_21DAA	2015-2016	0.12~6.62	0.32±0.11	0.69	0.481
	2014-2015	0.03~0.53	0.18±0.1		
	2013-2014	0.17~0.40	0.27±0.05		
	BLUPs	0.25~0.27	0.25±0.004		
NDVI_H	2015-2016	0.61~0.84	0.75±0.05		
NDVI_A	2015-2016	0.41~0.79	0.65±0.07		
NDVI_14	2015-2016	0.29~0.62	0.47±0.06		
NDVI_21	2015-2016	0.15~0.57	0.35±0.09		

SFH	2016-2017	29.57~55.13	43.96±4.52	0.187	0.501
	2015-2016	34.50~50.19	43.28±2.85		
	2014-2015	23.37~45.53	34.89±4.28		
	2013-2014	23.33~58.20	43.73±6.99		
	2012-2013	29.10~54.87	42.60±5.41		
	BLUPs	37.00~45.57	41.69±1.32		
CSF	2016-2017	123.70~214.90	168.3±17.23	**0.00054*** **	0.601
	2015-2016	83.00~217.90	147.6±30.09		
	2014-2015	104.00~193.30	140.4±16.47		
	2013-2014	109.5~240	172.8±23.09		
	2012-2013	123.1~220.9	166.1±19.28		
	BLUPs	144.5~180.7	159.3±7.60		
ADSF	2015-2016	2.47~49.31	25.14±10.90	**0.00071*** **	0.605
	2014-2015	3.60~38.23	23.20±7.01		
	2013-2014	2.33~45.10	24.76±7.79		
	2012-2013	7.40~38.67	24.32±5.71		
	BLUPs	21.92~27.30	24.16±1.02		
RDSF	2015-2016	0.06~1.00	0.58±0.25	**0.00244** **	0.593
	2014-2015	0.09~0.95	0.66±0.17		
	2013-2014	0.09~0.78	0.55±0.12		
	2012-2013	0.25~0.74	0.56±0.08		
	BLUPs	0.54~0.62	0.58±0.02		
NH	2015-2016	0.61~0.84	0.75±0.05		
CN	2015-2016	1.60~2.64	2.23±0.22		
ADN	2015-2016	0.20~0.61	0.39±0.08		
RDN	2015-2016	0.26~0.79	0.528±0.11		
PH	2016-2017	84.3~131.2	101.4±8.6	**< 0.0001*** **	0.73
	2015-2016	74.0~134.8	99.9±11.9		
	2014-2015	58.0~123.5	90.1±10.7		
	2013-2014	79.4~133.7	99.3±9.9		
	2012-2013	59.0~104.7	87.2±7.9		
	BLUPs	78.28~114.62	95.44±6.00		
TN	2016-2017	3.0~10	5.4±1.2	**< 0.0001*** **	0.64
	2015-2016	3.0~9.0	5.3±1.2		
	2014-2015	2.0~8.0	4.4±1.2		
	2013-2014	3.3~10	5.8±1.2		
	2012-2013	2.3~9.3	4.8±1.4		

	BLUPs	4.08~6.44	5.13±0.43		
SL	2016-2017	5.6~14.3	9.8±1.5	**< 0.0001*** **	0.73
	2015-2016	8.2~14.8	11.0±1.2		
	2014-2015	6.6~13.1	9.5±1.16		
	2013-2014	7.3~14.3	10.1±1.3		
	2012-2013	6.2~13.3	10.3±1.2		
	BLUPs	8.41~12.44	10.15±0.65		
SPS	2016-2017	12.3~24.3	17.8±2.4	**< 0.0001*** **	0.68
	2015-2016	11.0~26.0	19.5±2.2		
	2014-2015	12.7~22.7	17.3±1.9		
	2013-2014	14.0~21.7	18.1±1.5		
	2012-2013	14.0~24.7	18.9±1.9		
	BLUPs	15.54~20.57	18.34±0.84		
TKW	2016-2017	23.9~56.6	41.7±5.9	0.843	0.46
	2015-2016	18.5~46.1	29.3±5.3		
	2014-2015	22.0~44.0	30.8±4.8		
	2013-2014	18.3~49.2	32.8±5.4		
	2012-2013	18.9~47.6	33.8±5.2		
	BLUPs	30.98~36.44	33.75±1.19		
GY	2016-2017	42.9~270.0	141.9±47.2	**< 0.0001*** **	0.64
	2015-2016	17.4~422.7	151.2±64.9		
	2014-2015	31.6~212.2	119.5±41.3		
	2013-2014	6.0~244.0	84.7±53.9		
	2012-2013	3.27~276.21	107.5±48.3		
	BLUPs	86.8~171.2	121.6±16.04		
BY	2016-2017	158.6~980.3	599.1±177.1	**0.0115***	0.57
	2015-2016	220.0~837.5	503.1±114.5		
	2014-2015	112.0~652.0	339.7±124.8		
	2013-2014	24.0~1025.0	405.5±164.0		
	2012-2013	90.0~1028.0	457.7±171.8		
	BLUPs	342.3~590.3	460.2±44.28		

Standard deviation (Std. deviation), Chlorophyll content at tillering (CHL_T), Chlorophyll content at booting (CHL_B), Chlorophyll content at heading (CHL_H), Chlorophyll content at anthesis (CHL_A), Chlorophyll content at 10 days after anthesis (CHL_10DAA), Chlorophyll content at 20 days after anthesis (CHL_20DAA), Chlorophyll content at 30 days after anthesis (CHL_30DAA), photosynthetic efficiency at heading (fv/fm_H), photosynthetic efficiency at anthesis (fv/fm_A), photosynthetic efficiency at 14 days after anthesis (fv/fm_14DAA), photosynthetic efficiency at 21 days after anthesis (fv/fm_21DAA), NDVI at heading (NDVI_H), NDVI at anthesis (NDVI_A), NDVI at 14 days after anthesis (NDVI_14DAA), NDVI at 21 days after anthesis (NDVI_21DAA), Plant height (PH), Tiller number (TN), Spike length (SL), Spikelet per spike (SPS), Thousand kernel weight (TKW), Grain yield (GY), Biological yield (BY), Best linear unbiased predictions (BLUPs)

2.4.2. Correlation analysis

The BLUPs for all the morpho-physiological traits were subjected to correlation analysis. Correlation analysis revealed positive correlation between chlorophyll content at tillering, booting, heading, anthesis, 10 DAA, 20 DAA, and 30 DAA with thousand kernel weight (0.346***, 0.276**, 0.163, 0.073, 0.199, 0.177, 0.241*), grain yield (0.125, 0.388**, 0.077, 0.234*, 0.470***, 0.317**, 0.313**), and biological yield (0.096, 0.247**, 0.004, 0.267*, 0.281**, 0.194, 0.234*) (Figure 2.1). The photosynthetic efficiency (fv/fm) at heading, anthesis, 14 DAA, and 21 DAA displayed significant positive correlation with thousand kernel weight (0.243**, 0.225**, 0.270**, 0.238**) and grain yield (0.195**, 0.299***, 0.409***, 0.238**), whereas photosynthetic efficiency at anthesis and 14DAA showed significant positive correlation with biological yield (0.222**, 0.262**) (Figure 2.2). NDVI at heading and anthesis displayed significant positive correlation with thousand kernel weight (0.183*, 0.173*). NDVI at heading, anthesis, 14 DAA, and 21 DAA showed significant positive correlation with grain yield (0.289***, 0.310***, 0.193*, 0.234**) and NDVI at heading, anthesis, and 21 DAA exhibited significant positive correlation with grain yield (0.352***, 0.287***, 0.204*) (Figure 2.3). Stay-green indices SHF, CSF, ND, and CN showed positive correlation with thousand kernel weight (0.163, 0.317**, 0.183*, 0.320**), grain yield (0.077, 0.449***, 0.289**, 0.398**), and biological yield (0.004, 0.293**, 0.352***, 0.266*), whereas ADSF, RDSF, ADN and RFN showed negative correlation or slight positive correlation with thousand kernel weight (-0.009, -0.098, 0.033, 0.028), grain yield (-0.128, -0.247*, 0.009, -0.285**), and biological yield (-0.140, -0.226*, -0.007, -0.382***). TN, SL, and SPS showed slight positive correlation with grain yield (0.115, 0.147, 0.189) and biological yield (0.058, 0.150, 0.199) (Figure 2.4).

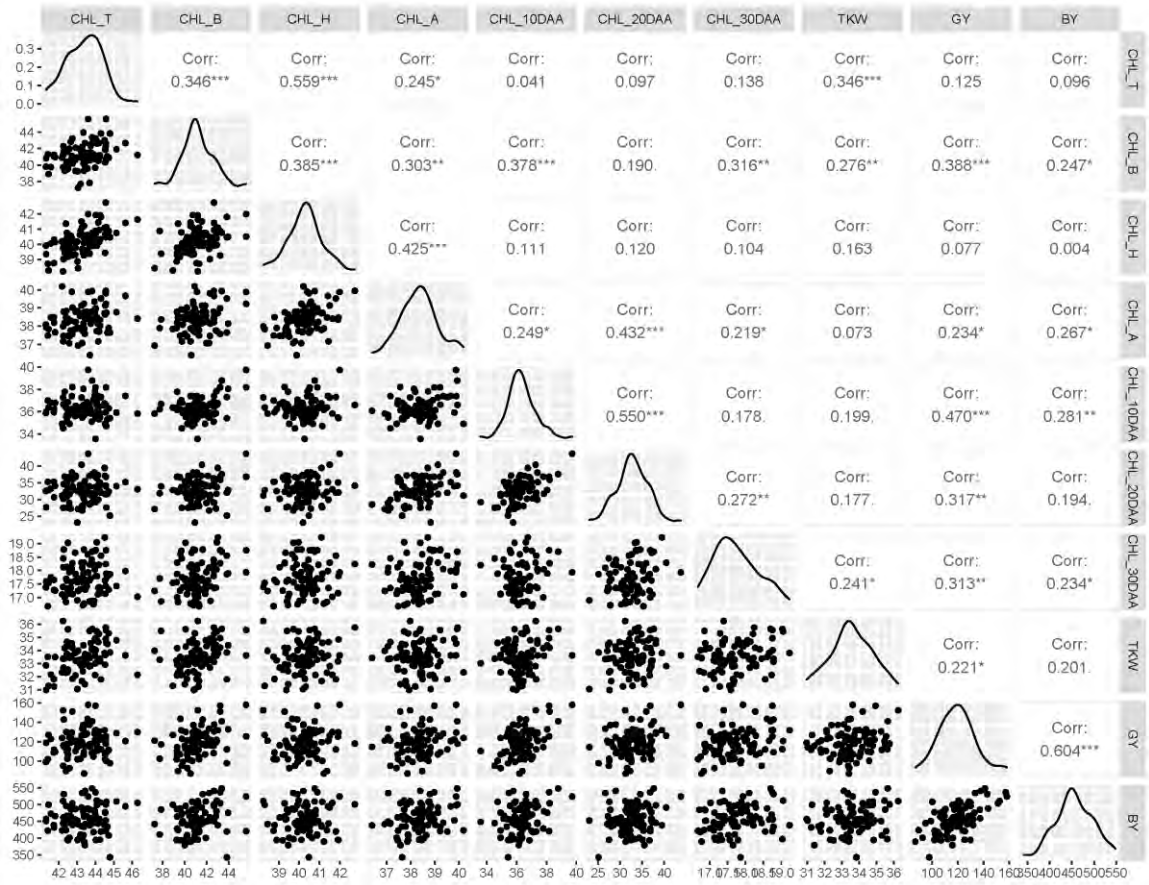

Figure 2.1. Correlation analysis between chlorophyll content at tillering (CHL_T), booting (CHL_B), heading (CHL_H), anthesis (CHL_A), 10 days after anthesis (CHL_10DAA), 20 days after anthesis (CHL_20DAA), 30 days after anthesis (CHL_30DAA), thousand kernel weight (TKW), grain yield (GY), and biological yield (BY).

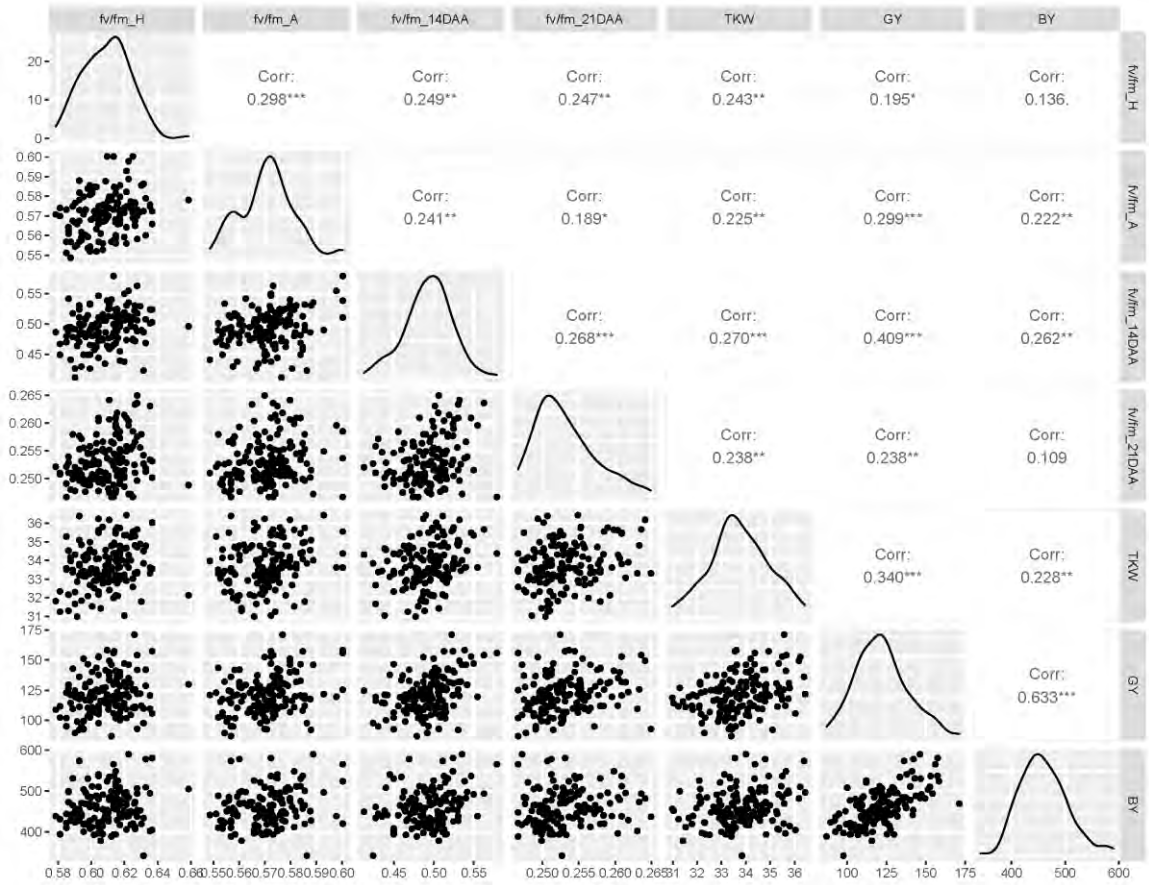

Figure 2.2. Correlation analysis between photosynthetic efficiency (fv/fm) at heading (fv/fm_H), anthesis (fv/fm_A), 14 days after anthesis (fv/fm_14DAA), 21 days after anthesis (fv/fm_21DAA), thousand kernel weight (TKW), grain yield (GY), and biological yield (BY).

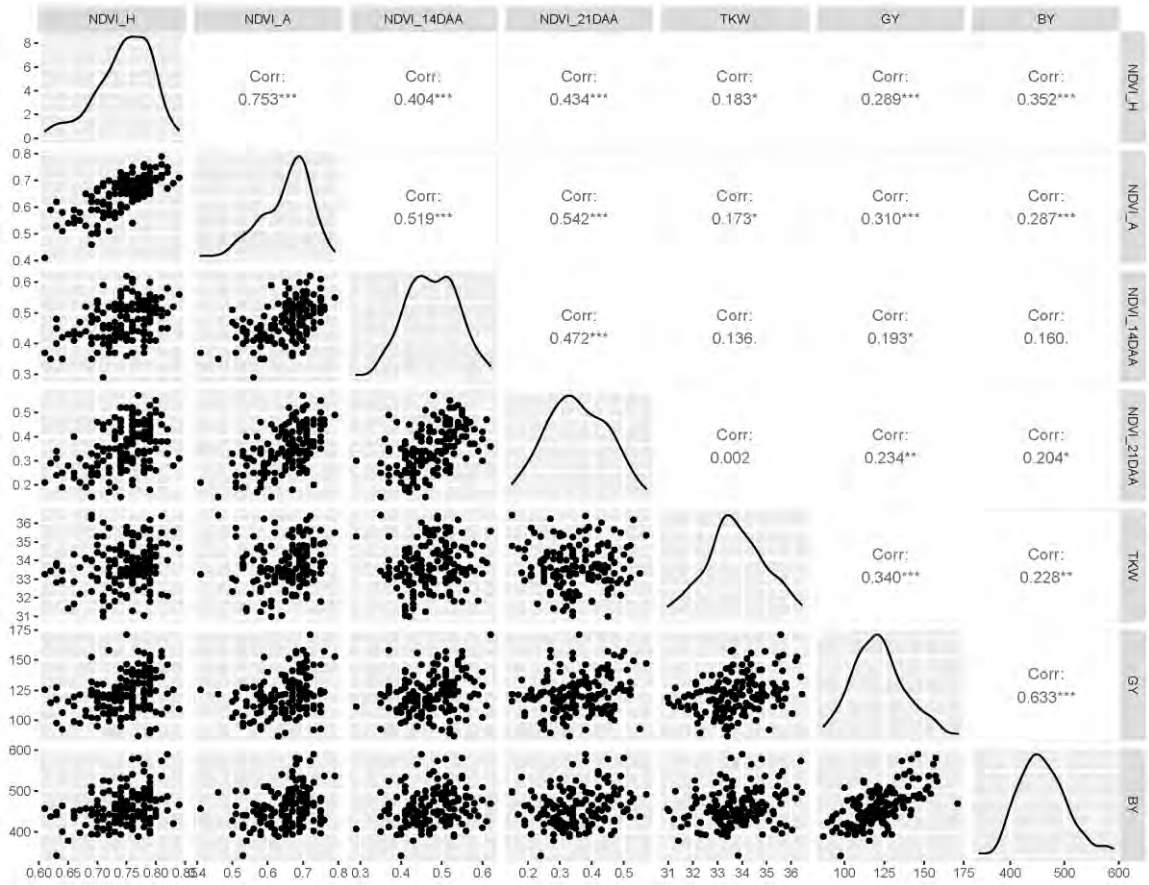

Figure 2.3. Correlation analysis between NDVI at heading (NDVI_H), anthesis (NDVI_A), 14 days after anthesis (NDVI_14DAA), 21 days after anthesis (NDVI_21DAA), thousand kernel weight (TKW), grain yield (GY), and biological yield (BY).

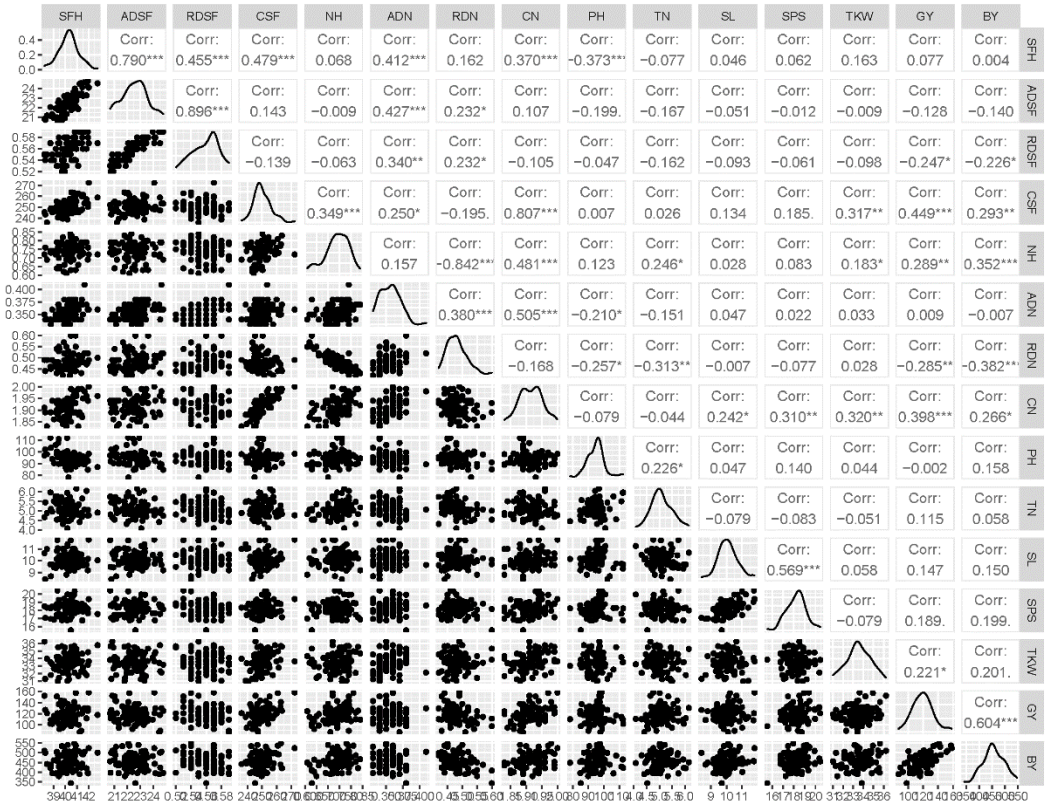

Figure 2.4. Correlation analysis between stay-green indices including SPAD chlorophyll of the flag leaf at heading (SFH), absolute difference in SPAD chlorophyll of the flag leaf (ADSF), relative difference in SPAD chlorophyll of the flag leaf (RDSF), cumulative SPAD chlorophyll of the flag leaf (CSF), NDVI at heading (ND), absolute differences in NDVI (ADN), relative difference in NDVI (RDN), cumulative NDVI (CN) and agronomic traits including plant height(PH), tiller number (TN), spike length (SL), spikelet per spike (SPS), thousand kernel weight (TKW), grain yield (GY), and biological yield (BY).

2.4.3. Population structure and linkage disequilibrium

Population structure was determined using the rate of change in log probability between K values. The graph of K against ΔK showed a break in slop at K= 7 which indicated that cultivars were divided into seven sub-groups. Group-1 consisted of post green revolution cultivars adapted to irrigated areas, Group-2 included post green revolution cultivars adapted to rainfed areas, Group-3 included landraces and their derivatives, Group-4 comprised of green revolution cultivars and their derivatives, Group-5 included green revolution cultivars adapted from CIMMYT, Group-6 included post green revolution cultivars adapted from CIMMYT and Group-7 composed of elite cultivars having Inqalab-91 genetic background. The population structure revealed that about 65% of the cultivars had admixture and 35% of the population had single genetic background (Figure 2.5). LD was estimated in TASSEL standalone 5.0 for each of the three wheat sub-genomes (A, B & D). The distance at which LD decayed to half of its maximum value (r^2 value) was considered as LD decay distance. This was 300, 800 and 500 Kb for A, B and D sub-genomes, respectively.

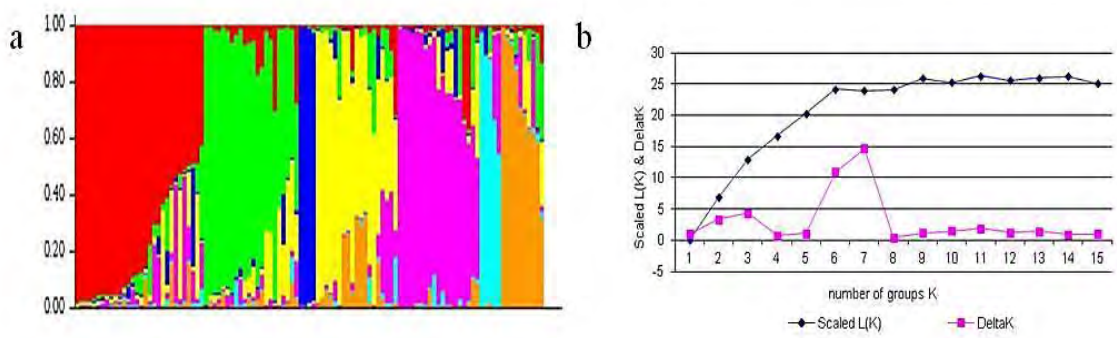

Figure 2.5. Population structure of the mapping panel. (a) The average logarithm of probability of likelihood and delta K, where K =7, (b) Membership co-efficient showing whole population is partitioned into seven sub-populations.

2.4.4. Marker trait association analysis

rMVP detected a total of 1786 MTAs [FarmCPU (881), GLM (660), and MLM(245)] associated with chlorophyll content, chlorophyll indices, chlorophyll fluorescence, NDVI, NDVI indices, PH, TN, SL, SPS, TKW, GY, and BY at -log10(p)

≥3 (Annexure 2.2). Of the 1786 MTAs, 83 [FarmCPU (54), GLM (29)] linked with chlorophyll content, chlorophyll indices, chlorophyll fluorescence, NDVI, NDVI indices, PH, and TN were statistically significant with -log10(p) ≥4.3 (the threshold calculated via Bonferroni correction). The highly significant markers were scattered over 48 loci on wheat genome (A genome= 24, B genome= 20, D genome= 4) on the basis of LD decay distance. Eight loci were associated with chlorophyll content on chromosomes 1B, 3B, 4A, 4D, 5A, 5B, and 7A. For photosynthetic efficiency (fv/fm), two loci were identified on chromosomes 2B and 5A. For NDVI, 23 loci were detected on chromosomes 1A, 1D, 2B, 3A, 4A, 5A, 6A, 6B, 7A, and 7B. For stay-green indices, six loci were detected on chromosomes 1B, 1D, 2B, 3A, and 6A. For PH, eight loci were detected on chromosomes 2A, 2B, 3A, and 6B. Two loci for TN were detected on chromosome 1B and 6D (Table 2.2).

Chlorophyll content at tillering was associated with locus q7A-1 (tag SNP: BS00109911_51) found on chromosome 7A. Chlorophyll content at heading was associated with two loci, q5A-2 (tag SNP: BS00078076_51) and q5A-3 (tag SNP: BS00066127_51) found on chromosome 5A. Chlorophyll content at anthesis was linked with loci q3B-1 (tag SNP: BS00085434_51), q4A-2 (tag SNP: Excalibur_c55561_127), and q4D-1 (tag SNP: BobWhite_c4264_325) present on chromosomes 3B, 4A, and 4D, respectively. Chlorophyll content at 10DAA was associated with locus q5B-1 (tag SNP: BS00110064_51) located on chromosome 5B. Chlorophyll content at 20DAA was linked with locus q1B-4 (tag SNP: Ex_c29452_302) found on chromosome 1B (tag SNP: Table 2.2, Figure 2.6, Figure 2.7, Figure 2.8).

Photosynthetic efficiency (fv/fm) at heading was associated with locus q2B-3 (tag SNP: Ra_c6728_590) found on chromosome 2B. Photosynthetic efficiency (fv/fm) at 21 DAA was associated with locus q5A-1 (tag SNP: Excalibur_c5398_695) located on chromosome 5A (Table 2.2).

NDVI at heading was associated with loci q1D-1, q2B-2, and q6B-2 [RAC875_c2070_566 (1D), Ku_c57425_413 (2B), and BS00074947_51 (6B)]. NDVI at anthesis was associated with loci q1D-1, q3A-4, q5A-4, q6A-1, q6A-2, q6B-1, q7A-2,

Table 2.2. Identification of target loci based on the significant SNPs from the GWAS results.

Locus	Locus ID	Chr	Tag SNP	Tag SNP Pos	Locus Start	Locus End	Tag SNP LOG10(p)	Method	Trait
1	q1A-1	1A	Ku_c6979_182	346446236	346146236	346746236	4.6615532	FarmCPU	NDVI_14DAA
2	q1A-2	1A	wsnp_Ex_c750_1474184	592090936	591790936	592390936	4.3296625	FarmCPU	NDVI_14DAA
3	q1B-1	1B	BS00110900_51	10361155	9561155	11161155	4.8127826	FarmCPU	TN
4	q1B-2	1B	Tdurum_contig44219_318	15169586	14369586	15969586	4.8400309	GLM, FarmCPU	CN
5	q1B-3	1B	RAC875_c42275_224, BobWhite_c36862_84	631832802, 631999928	631032802	632632802	4.8529549, 4.8529549	GLM, FarmCPU	CSFL
6	q1B-4	1B	Ex_c29452_302	678432525	677632525	679232525	4.7973436	GLM, FarmCPU	CHL_20DAA
7	q1D-1	1D	RAC875_c2070_566	417149	0	917149	4.5226502	FarmCPU	NDVI_A, NDVI_H
8	q1D-2	1D	Excalibur_c56999_109	459837951	459337951	460337951	4.8529549	GLM, FarmCPU	CSFL
9	q2A-1	2A	Tdurum_contig12761_125	727243449	726943449	727543449	4.4888447	GLM	PH
10	q2B-1	2B	BS00023221_51	94199616	93399616	94999616	4.5211195	GLM	NDVI_21DAA
11	q2B-2	2B	Ku_c57425_413	108905283	108105283	109705283	4.8114226	GLM, FarmCPU	RDN, NDVI_H
12	q2B-3	2B	Ra_c6728_590	134090399	133290399	134890399	4.4831116	GLM, FarmCPU	fv/fm_H
13	q2B-4	2B	BS00046164_51, BS00046165_51, Excalibur_c36280_764	697510323, 697510334, 697512054	696710323	698310323	5.4476698, 5.0887964, 4.6584825	GLM, FarmCPU	NDVI_21DAA
14	q2B-5	2B	wsnp_Ex_c22271_31463467, BobWhite_c2244_259, wsnp_Ex_c22271_31463382	700456564, 700456873, 700457023	699656564	701256564	4.5425788, 4.3835976 4.3835976	FarmCPU	NDVI_21DAA
15	q2B-6	2B	wsnp_Ex_c26818_36041748	710281768	709481768	711081768	4.6008498	FarmCPU	PH
16	q2B-7	2B	Ra_c13298_434	732344105	731544105	733144105	5.9407979	GLM, FarmCPU	PH
17	q2B-8	2B	Ra_c5004_2033 Ra_c5004_1902	733713735 733713866	732913735	734513735	5.9407979, 4.5704379	GLM, FarmCPU	PH
18	q2B-9	2B	Ku_c2936_1987, wsnp_CAP11_c1820_985143, Ku_c16249_315	782154304, 782533975, 782534125	781354304	782954304	4.5774803	FarmCPU	PH
19	q3A-1	3A	Excalibur_c11079_749	32201535	31901535	32501535	4.689403	GLM, FarmCPU	PH
20	q3A-2	3A	wsnp_Ex_c28310_37444843	487458132	487158132	487758132	4.5334271	FarmCPU	ADSFL, RDSFL

21	q3A-3	3A	RAC875_c4641_773	686766027	686466027	687066027	4.5774803	FarmCPU	PH
22	q3A-4	3A	Ku_c10817_611	708546032	708246032	708846032	5.1869237	GLM, FarmCPU	NDVI_A
23	q3B-1	3B	BS00085434_51	750357865	749557865	751157865	4.6029506	GLM, FarmCPU	CHL_A
24	q4A-1	4A	RFL_Contig1053_65	68470332	68170332	68770332	4.5693493	FarmCPU	NDVI_14DAA
25	q4A-2	4A	Excalibur_c55561_127	450883765	450583765	451183765	5.0346628	GLM, FarmCPU	CHL_A
26	q4D-1	4D	BobWhite_c4264_325	121181547	120681547	121681547	4.7034595	GLM, FarmCPU	CHL_A
27	q5A-1	5A	Excalibur_c5398_695	30027274	29727274	30327274	4.780595	GLM, FarmCPU	fv/fm_21 DAA
28	q5A-2	5A	BS00078076_51	409323859	409023859	409623859	4.3679229	FarmCPU	CHL_H
29	q5A-3	5A	BS00066127_51	414048579	413748579	414348579	4.3679229	FarmCPU	CHL_H
30	q5A-4	5A	wsnp_Ex_c17268_25935536	479908679	479608679	480208679	4.3885867	GLM	NDVI_A
31	q5B-1	5B	BS00110064_51	397838250	397038250	398638250	4.4430683	GLM, FarmCPU	CHL_10DAA
32	q6A-1	6A	BS00058159_51	3311136	3011136	3611136	4.6203969	FarmCPU	NDVI_A
33	q6A-2	6A	Tdurum_contig55193_296	6596817	6296817	6896817	4.991918	GLM, FarmCPU	NDVI_A
34	q6A-3	6A	BS00011010_51	18713239	18413239	19013239	4.6003131	FarmCPU	RDN
35	q6B-1	6B	BS00092845_51	11298715	10498715	12098715	5.1869237	GLM, FarmCPU	NDVI_A
36	q6B-2	6B	BS00074947_51	191538469	190738469	192338469	4.3348886	FarmCPU	NDVI_H
37	q6B-3	6B	RFL_Contig2387_1410	661464161	660664161	662264161	4.5774803	FarmCPU	PH
38	q6D-1	6D	Tdurum_contig10194_765	402494662	401994662	402994662	4.3001121	GLM	TN
39	q7A-1	7A	BS00109911_51	653957	353957	953957	4.3618275	GLM	CHL_T
40	q7A-2	7A	BobWhite_rep_c65070_369	452754928	452454928	453054928	5.5074067	FarmCPU	NDVI_A
41	q7A-3	7A	CAP12_c2355_239	458711102	458411102	459011102	5.5074067	FarmCPU	NDVI_A
42	q7A-4	7A	BS00091168_51	521952104	521652104	522252104	4.4451173	FarmCPU	NDVI_A
43	q7A-5	7A	wsnp_Ex_rep_c104560_89241494	531193028	530893028	531493028	4.4451173	FarmCPU	NDVI_A
44	q7A-6	7A	Excalibur_c27658_264	536152491	535852491	536452491	6.1895179	FarmCPU	NDVI_A
45	q7A-7	7A	CAP8_c4980_112	719571317	719271317	719871317	5.7785869	GLM, FarmCPU	NDVI_A
46	q7A-8	7A	BS00002510_51, Tdurum_contig42487_1555	721000126, 721224332	720700126	721300126	4.942484, 4.829763	GLM, FarmCPU	NDVI_A
47	q7B-1	7B	Kukri_c24422_423	400418416	399618416	401218416	5.5074067	FarmCPU	NDVI_A
48	q7B-2	7B	Kukri_c32807_579	401552201	400752201	402352201	5.5074067	FarmCPU	NDVI_A

q7A-3, q7A-4, q7A-5, q7A-6, q7A-7, q7A-8, q7B-1, and q7B-2 [RAC875_c2070_566 (1D), Ku_c10817_611 (3A), wsnp_Ex _c17268_25935536 (5A), Tdurum_contig55193_296 and BS00058159_51 (6A), BS00092845_51 (6B), Excalibur_c27658_264, CAP8_c4980_112, BobWhite_rep_ c65070_369, CAP12_c2355_239, BS00002510_51, Tdurum_contig42487_1555, BS00091168_51, and wsnp_Ex_rep_c104560_89241494 (7A) and Kukri_c24422_423 and Kukri_c32807_579 (7B]. NDVI at 14 DAA was associated with loci q1A-1, q1A-2, and q4A-1 [Ku_c6979_182 (1A), wsnp_Ex_c750_1474184 (1A), and RFL_Contig1053_65 (4A)]. NDVI at 21DAA was associated with q2B-1, q2B-4, and q2B-5 [BS00046164_51, BS00046165_51, Excalibur_c36280_764, wsnp_Ex_c22271_31463467, BS00023221 _51, BobWhite_c2244_259, wsnp_Ex_ c22271_31463382] located on chromosome 2B (Table 2.2, Figure 2.9, Figure 2.10, Figure 2.11).

ADSF and RDSF were associated with q3A-2 (wsnp_Ex_c28310_37444843) located on chromosome 3A. CSF was associated with q1B-3 and q1D-2 [RAC875_c42275_224 (1B), BobWhite_c36862_84 (1B), and Excalibur_c56999_109 (1D)]. RDN was associated with q2B-2 and q6A-3 (Ku_c57425_413 and BS00011010_51) found on chromosome 2B and 6A, respectively. CN was associated with q1B-2 (Tdurum_contig44219_318) found on chromosome 1B (Table 2.2, Figure 2.12, Figure 2.13, Figure 2.14).

Plant height was associated with q2A-1 (Tdurum_contig12761_125) found on chromosome 2A, q2B-6, q2B-7, q2B-8, and q2B-9 (Ra_c13298_434, Ra_c5004_2033, wsnp_Ex_c26818_36041748, Ku_c2936_1987, wsnp_CAP11_c1820_985143, Ku_c16249_315, and Ra_c5004_1902) present on chromosome 2B, q3A-1 and q3A-3 (Excalibur_c11079_749 and RAC875_c4641_773) found on chromosome 3A, and q6B-3 (RFL_Contig2387_1410) located on chromosome 6B (Table 2.2, Figure 2.15). TN was associated two loci, q1B-1 and q6D-1 (BS00110900_51 and Tdurum_contig10194_765) found on chromosome 1B and 6D, respectively (Table 2.2, Figure 2.16).

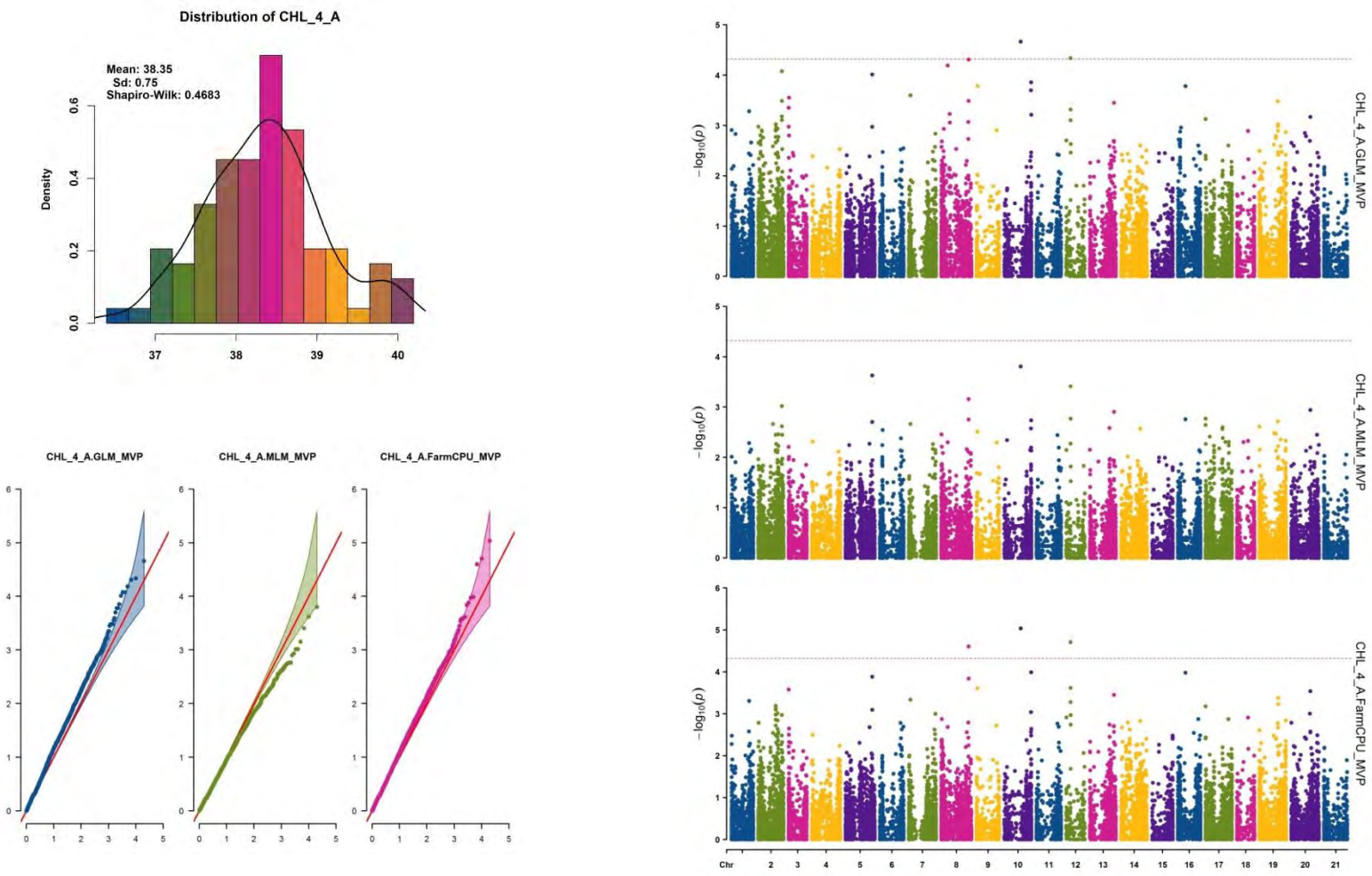

Figure 2.6. The Density Distribution plot, QQ-plot, and Manhattan plot for chlorophyll content at anthesis (CHL_4_A). (a) The density plot is showing the distribution of chlorophyll content at anthesis, (b) QQ-plot is representing deviation of the obtained p values from the expected values in GLM, MLM, and FarmCPU of chlorophyll content at anthesis, and Manhattan plot is showing the* P *values of the entire GLM, MLM, and FarmCPU analysis of chlorophyll content at anthesis.

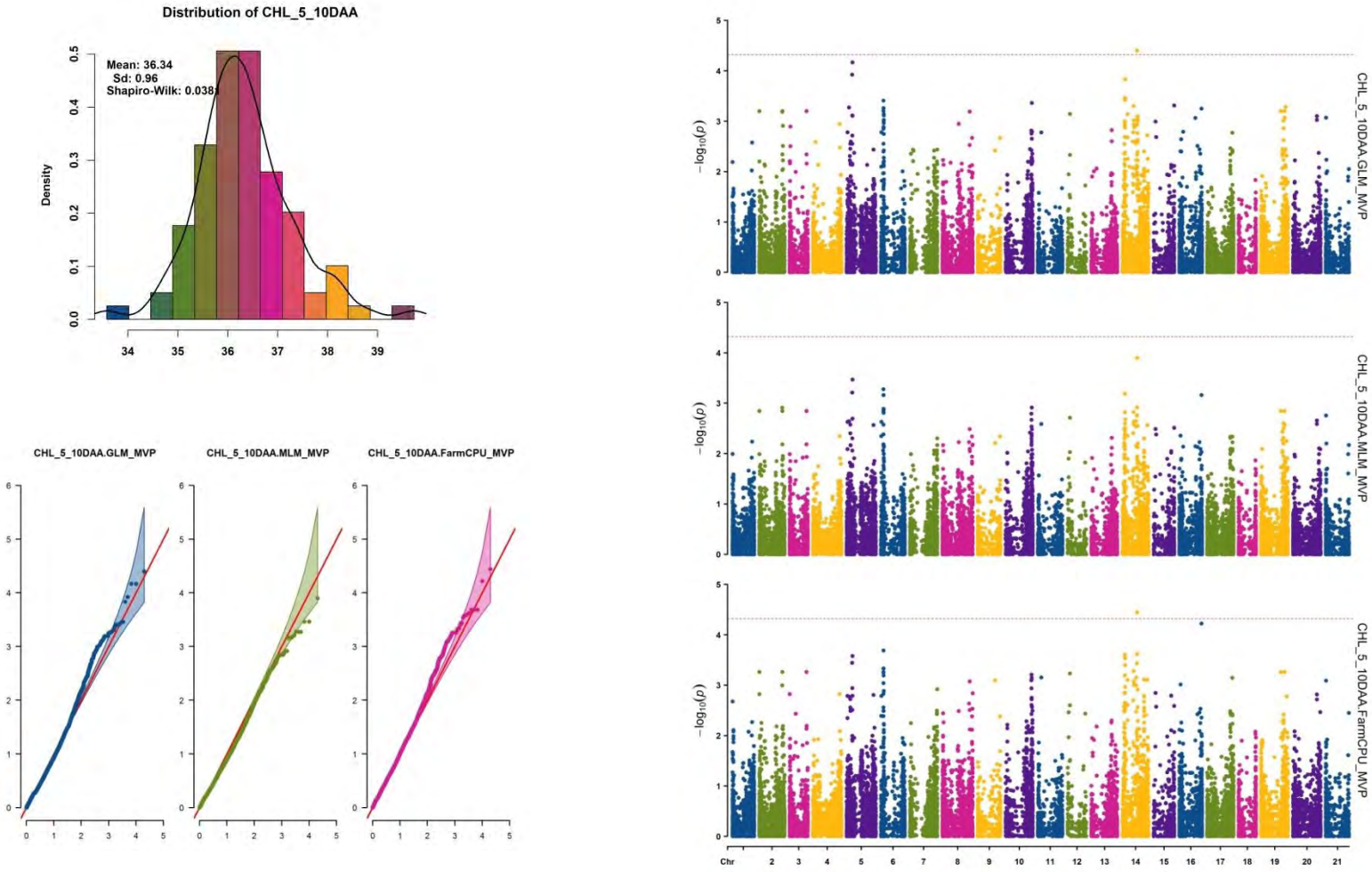

Figure 2.7. The Density Distribution plot, QQ-plot, and Manhattan plot for chlorophyll content at 10 days after anthesis (CHL_5_10 DAA). (a) The density plot is showing the distribution of chlorophyll content at 10 DAA, (b) QQ-plot is representing deviation of the obtained p values from the expected values in GLM, MLM, and FarmCPU, and Manhattan plot is showing the* P *values of the entire GLM, MLM, and FarmCPU analysis of chlorophyll content at 10 DAA.

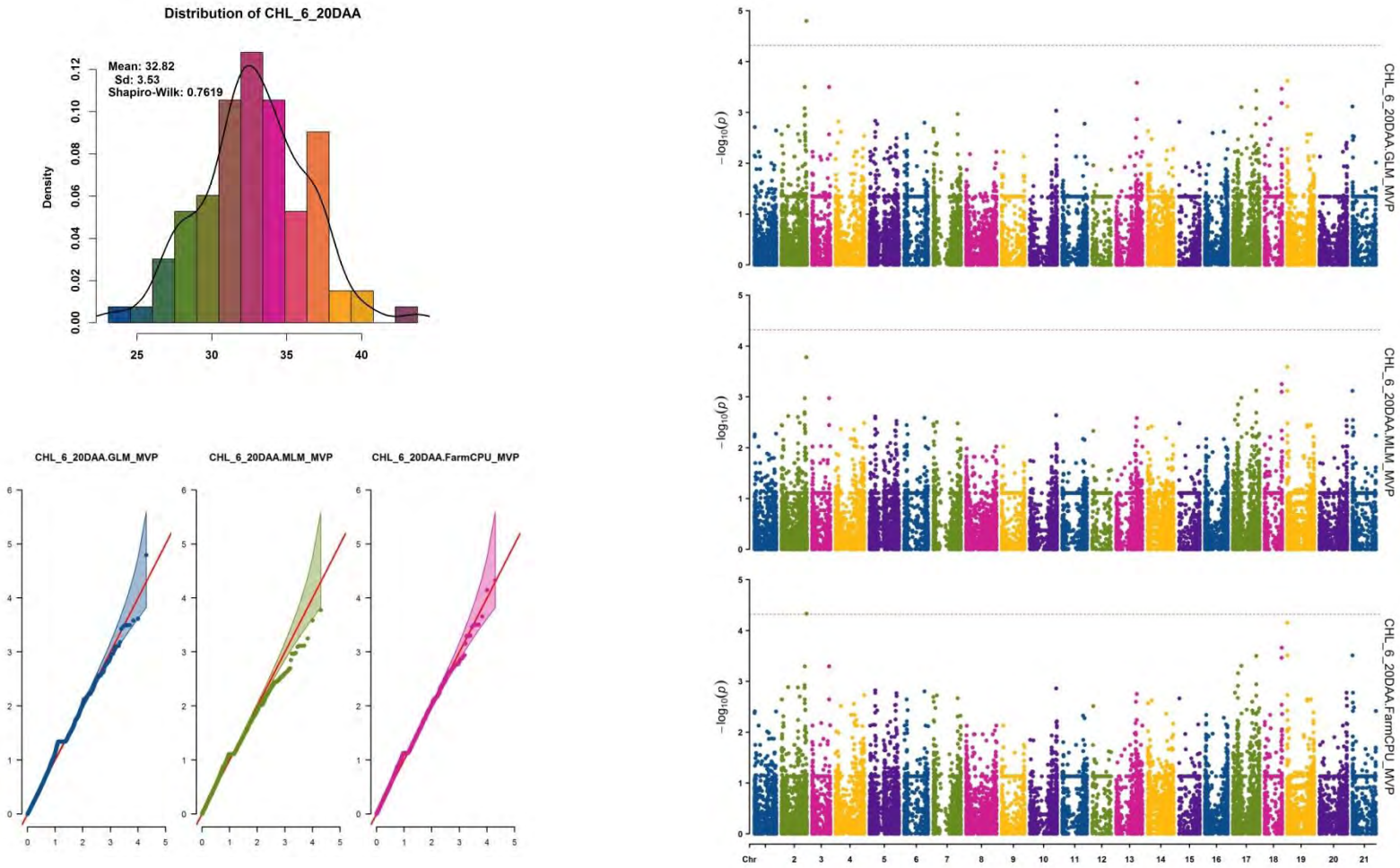

Figure 2.8. The Density Distribution plot, QQ-plot, and Manhattan plot for chlorophyll content at 20 days after anthesis (CHL_6_20 DAA). (a) The density plot is showing the distribution of chlorophyll content at 20 DAA, (b) QQ-plot is representing deviation of the obtained p values from the expected values in GLM, MLM, and FarmCPU for chlorophyll content at 20 DAA, and Manhattan plot is showing the* P *values of the entire GLM, MLM, and FarmCPU analysis for chlorophyll content at 20 DAA.

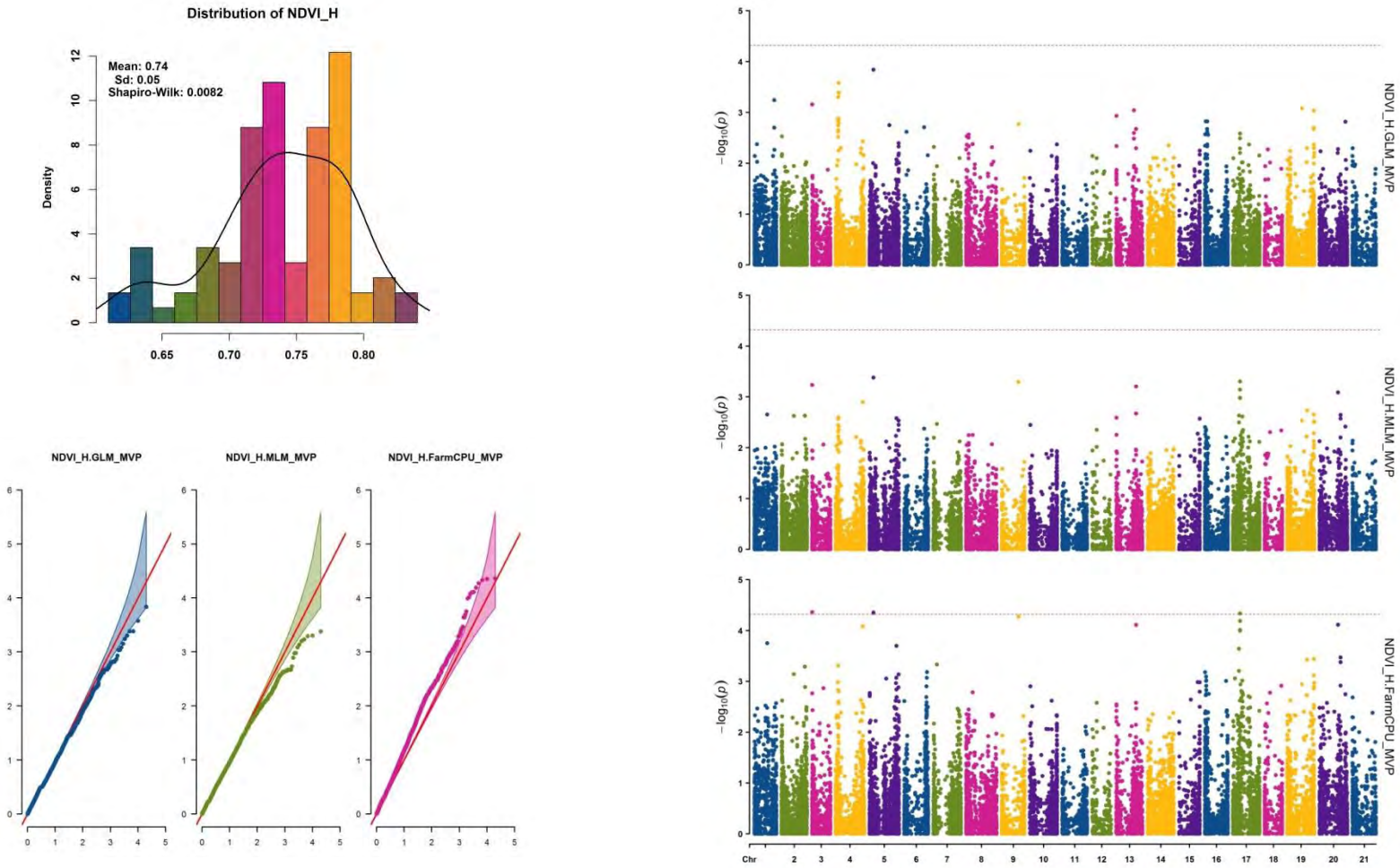

Figure 2.9. The Density Distribution plot, QQ-plot, and Manhattan plot for Normalized Difference Vegetative Index at Heading (NDVI_H). (a) The density plot is showing the distribution of NDVI_H, (b) QQ-plot is representing deviation of the obtained p values from the expected values in GLM, MLM, and FarmCPU for NDVI_H, and Manhattan plot is showing the* P *values of the entire GLM, MLM, and FarmCPU analysis for NDVI_H.

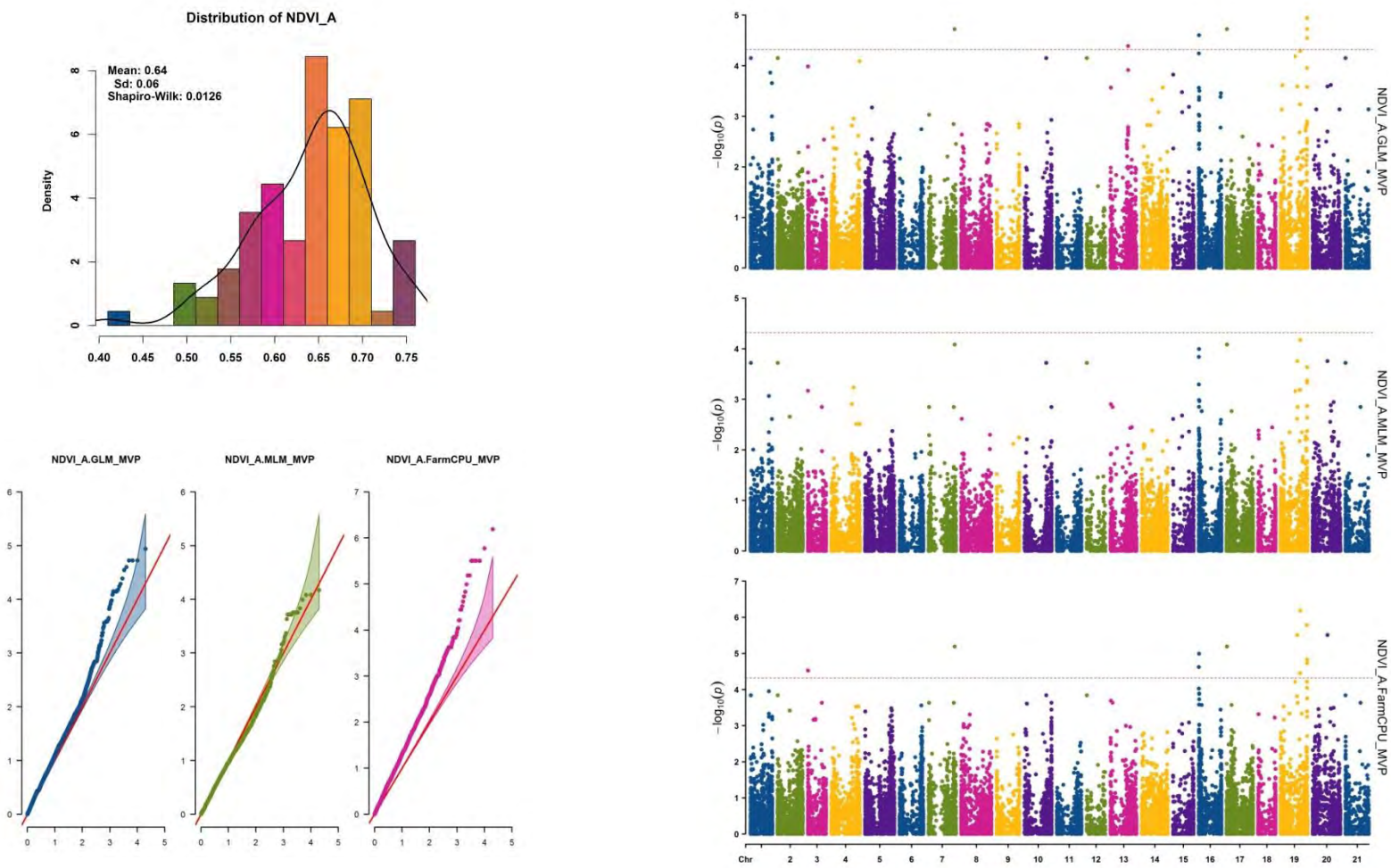

Figure 2.10. The Density Distribution plot, QQ-plot, and Manhattan plot for normalized difference vegetative index at anthesis (NDVI_A). (a) The density plot is showing the distribution of NDVI_A, (b) QQ-plot is representing deviation of the obtained p values from the expected values in GLM, MLM, and FarmCPU for NDVI_A, and Manhattan plot is showing the* P *values of the entire GLM, MLM, and FarmCPU analysis for NDVI_A.

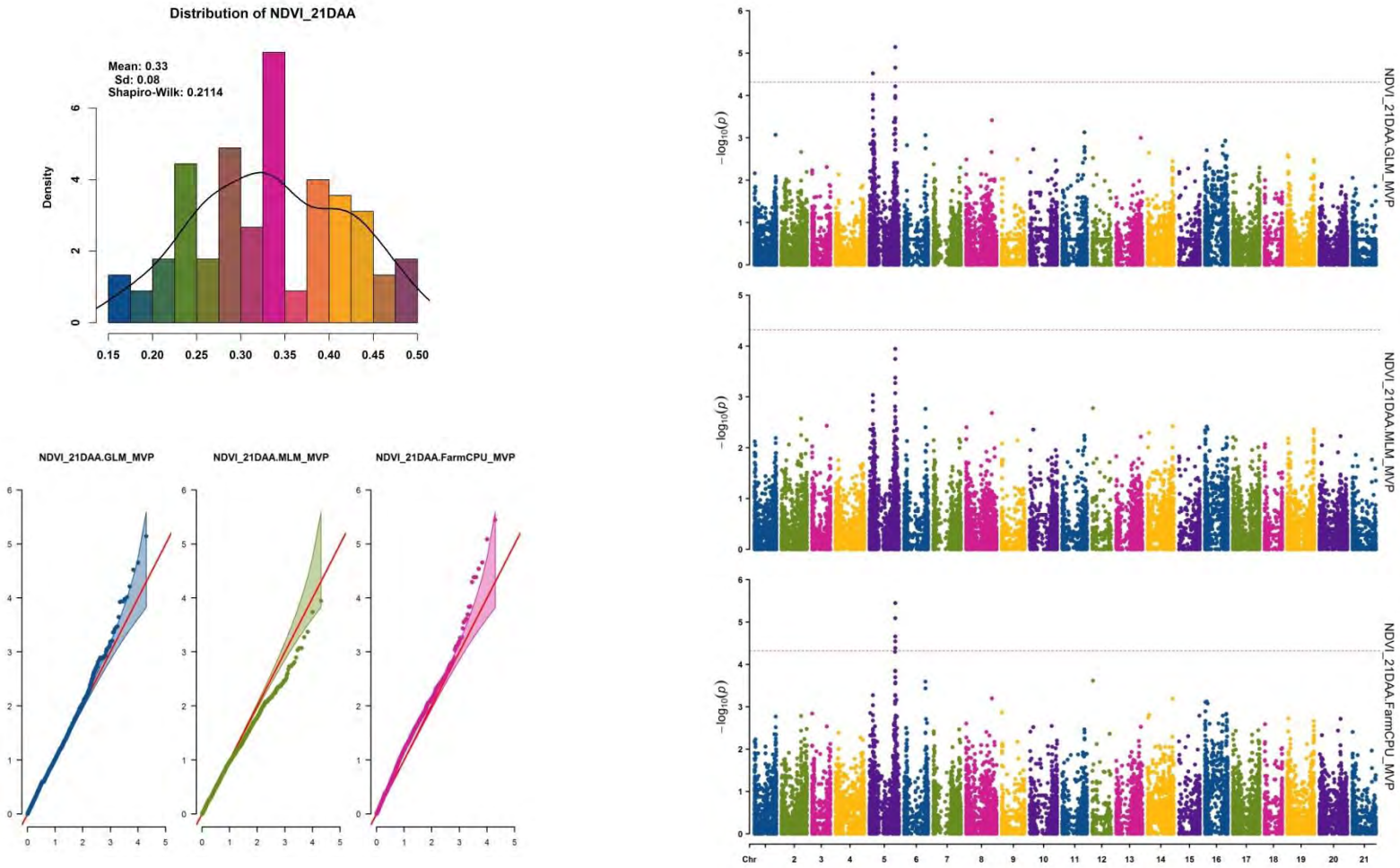

Figure 2.11. The Density Distribution plot, QQ-plot, and Manhattan plot for normalized difference vegetative index at 21 days after anthesis (NDVI_21DAA). (a) The density plot is showing the distribution of NDVI_21DAA, (b) QQ-plot is representing deviation of the obtained p values from the expected values in GLM, MLM, and FarmCPU for NDVI_21DAA, and Manhattan plot is showing the* P *values of the entire GLM, MLM, and FarmCPU analysis for NDVI_21DAA.

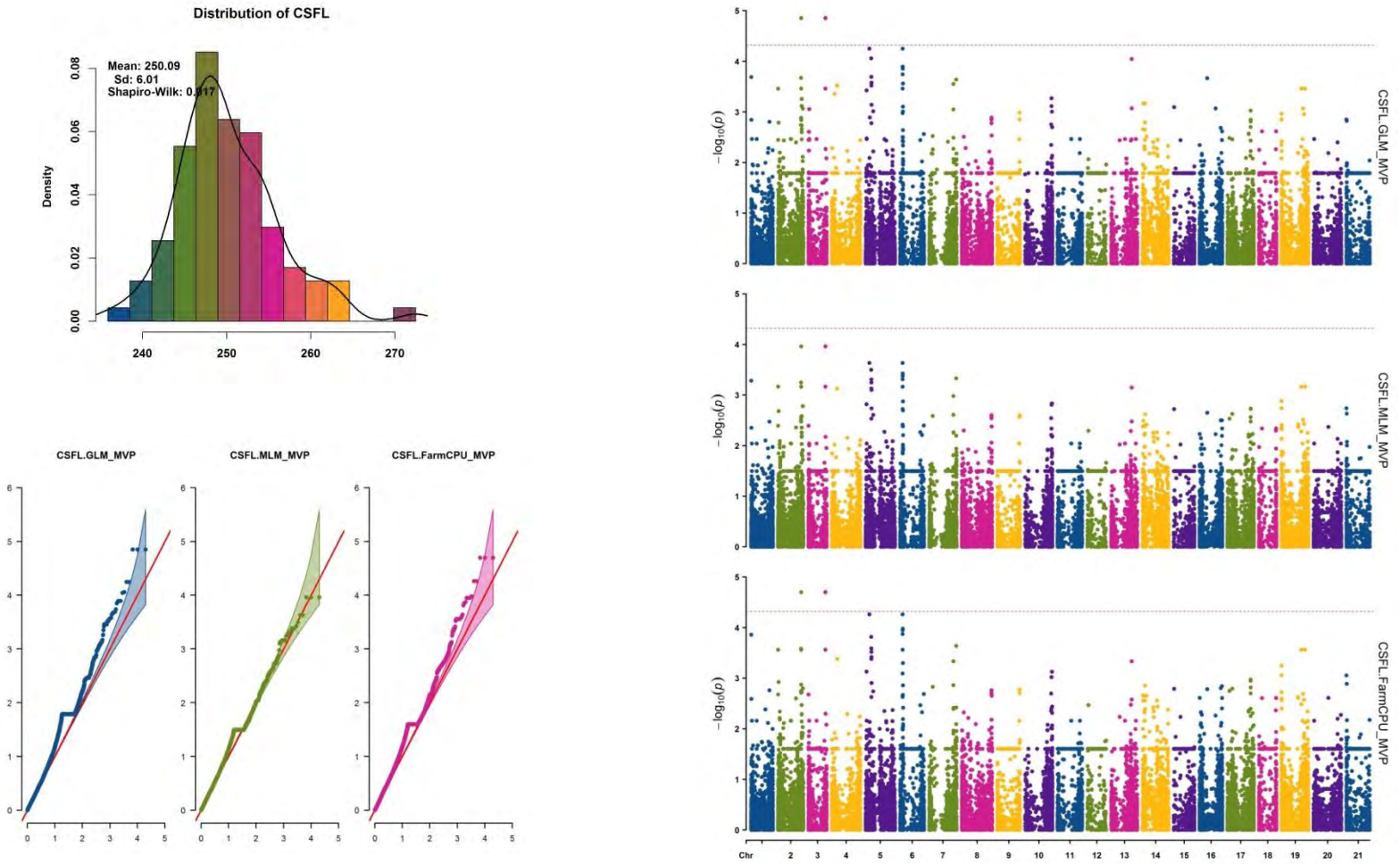

Figure 2.12. The Density Distribution plot, QQ-plot, and Manhattan plot for cumulative chlorophyll content (CSFL). (a) The density plot is showing the distribution of CSFL, (b) QQ-plot is representing deviation of the obtained p values from the expected values in GLM, MLM, and FarmCPU for CSFL, and Manhattan plot is showing the* P *values of the entire GLM, MLM, and FarmCPU analysis for CSFL.

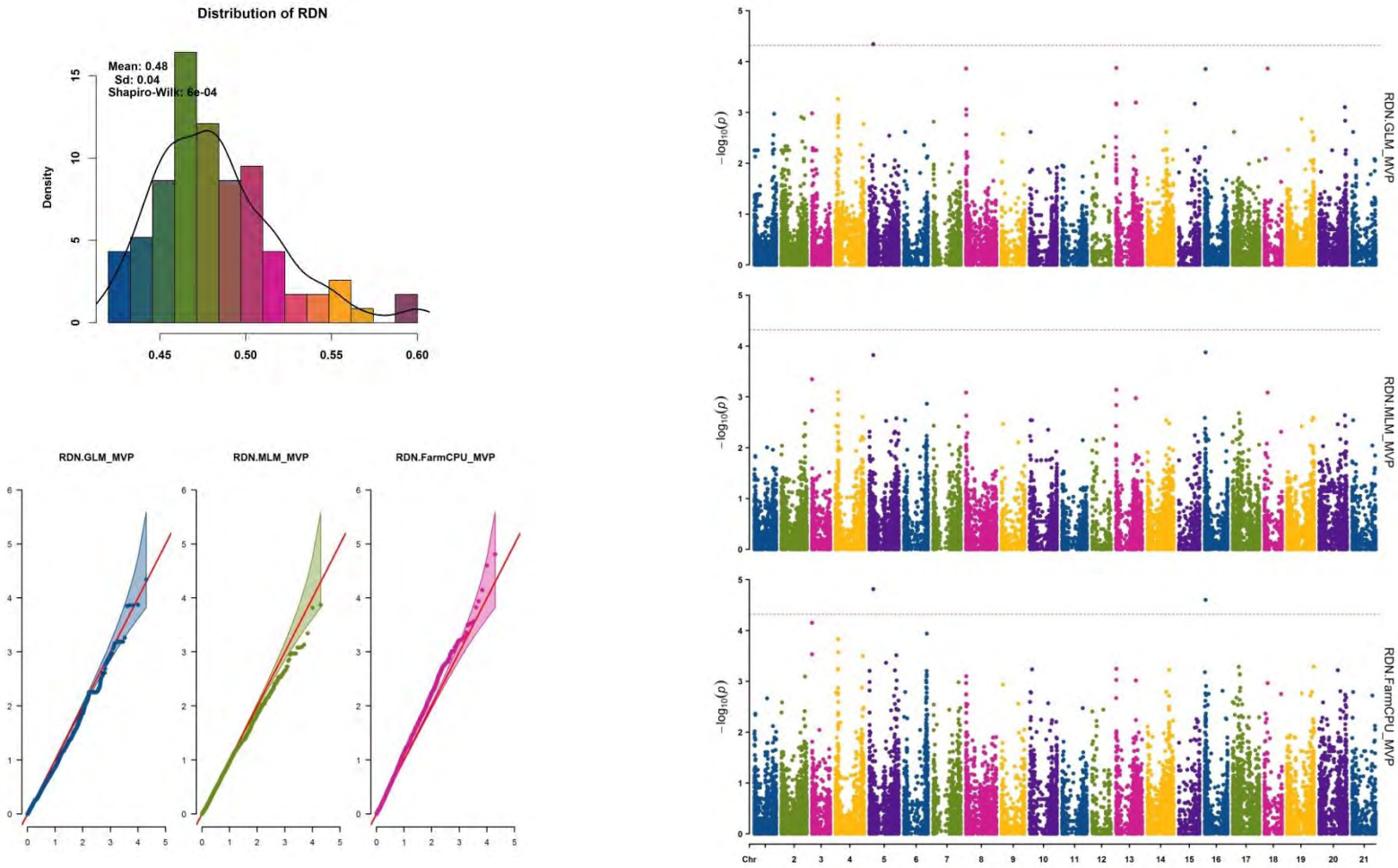

Figure 2.13. The Density Distribution plot, QQ-plot, and Manhattan plot for relative difference in the normalized difference vegetative index (RDN). (a) The density plot is showing the distribution of RDN, (b) QQ-plot is representing deviation of the obtained p values from the expected values in GLM, MLM, and FarmCPU for RDN, and Manhattan plot is showing the* P *values of the entire GLM, MLM, and FarmCPU analysis for RDN.

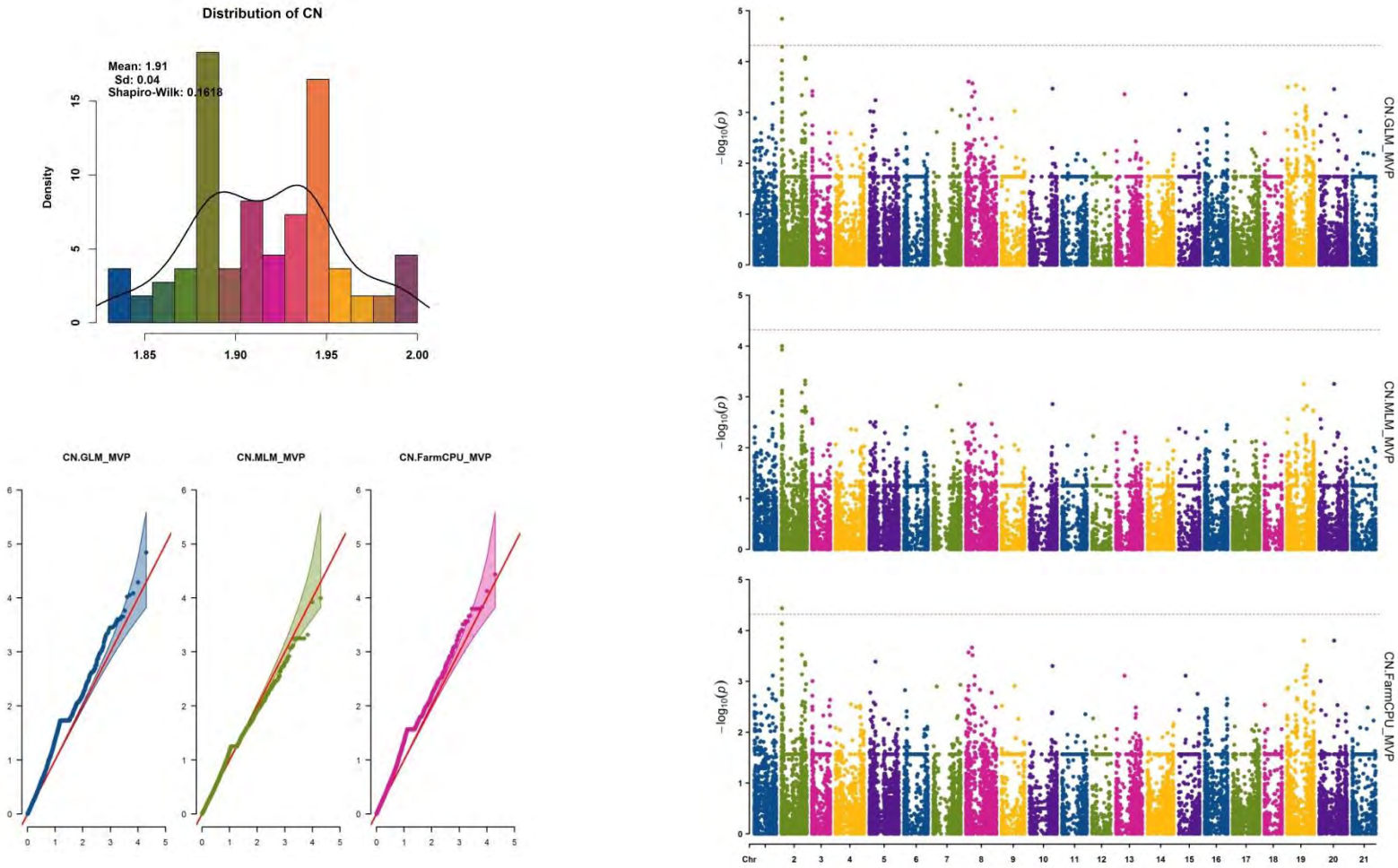

Figure 2.14. The Density Distribution plot, QQ-plot, and Manhattan plot for cumulative normalized difference vegetative index (CN). (a) The density plot is showing the distribution of CN, (b) QQ-plot is representing deviation of the obtained p values from the expected values in GLM, MLM, and FarmCPU for CN, and Manhattan plot is showing the* P *values of the entire GLM, MLM, and FarmCPU analysis for CN.

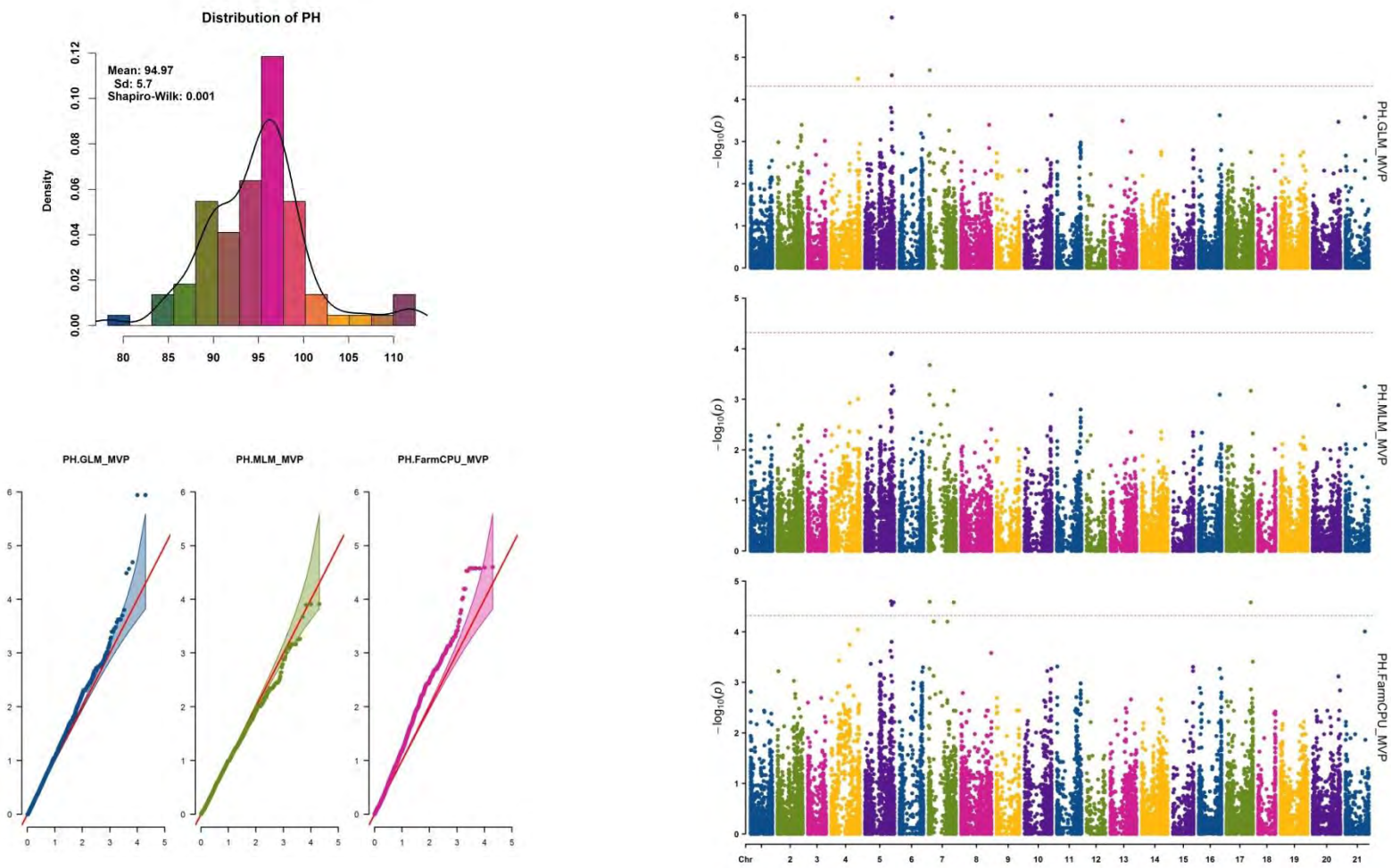

Figure 2.15. The Density Distribution plot, QQ-plot, and Manhattan plot for plant height (PH). (a) The density plot is showing the distribution of PH, (b) QQ-plot is representing deviation of the obtained p values from the expected values in GLM, MLM, and FarmCPU for PH, and Manhattan plot is showing the* P *values of the entire GLM, MLM, and FarmCPU analysis for PH.

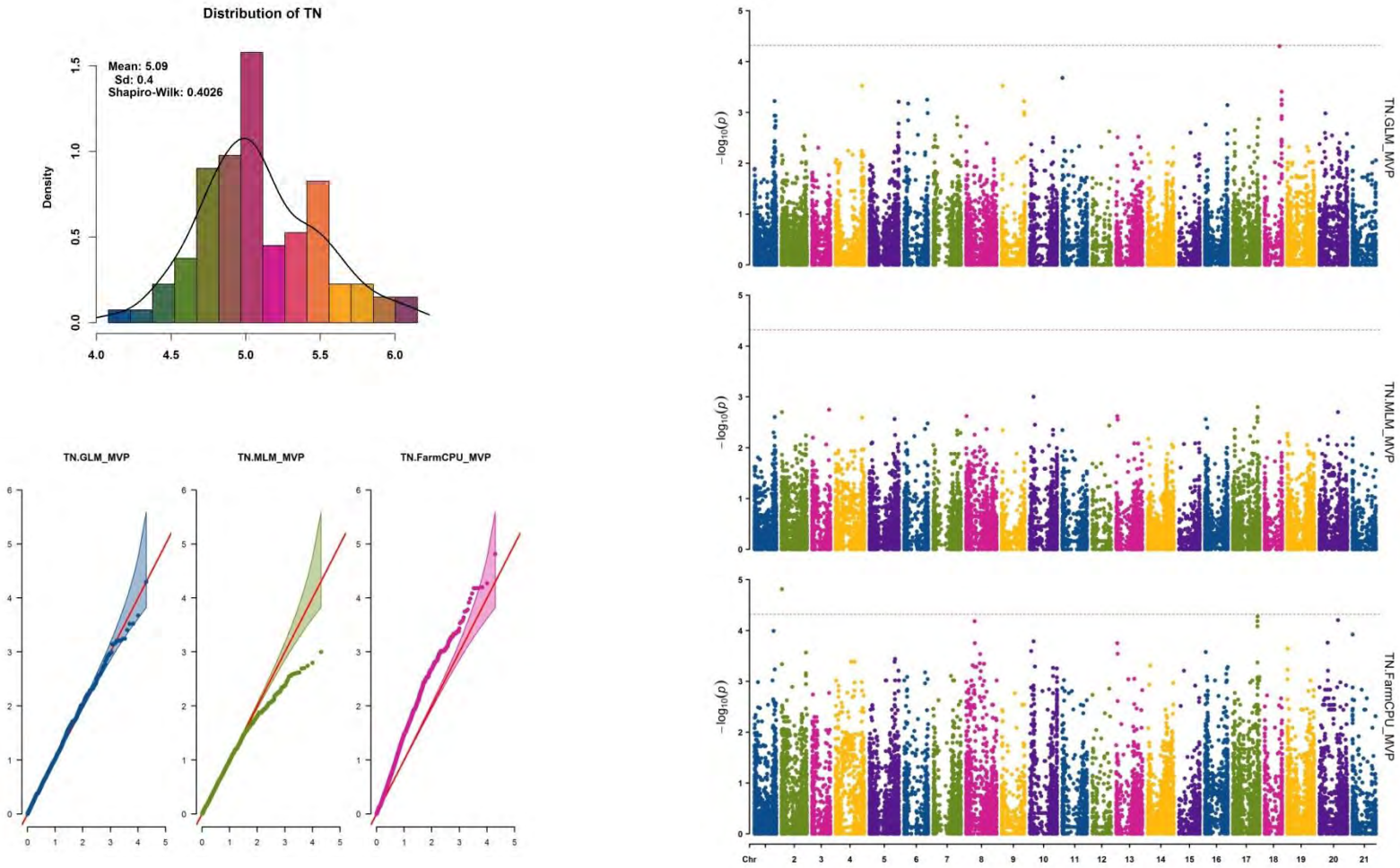

Figure 2.16. The Density Distribution plot, QQ-plot, and Manhattan plot for tiller number (TN). (a) The density plot is showing the distribution of TN in selected panel, (b) QQ-plot is representing deviation of the obtained p values from the expected values in GLM, MLM, and FarmCPU, and Manhattan plot is showing the* P *values of the entire GLM, MLM, and FarmCPU analysis.

2.4.5. Genes of interest

Of the 48 loci, 20 loci (each identified by two models, FarmCPU and GLM) were used to extract genes from Ensembl Plants database for wheat genes using BioMart function.

Table 2.3. Loci identified by multiple GWAS methods selected for candidate gene analysis.

Locus ID	Chr	Tag SNP	Locus Start	Locus End	Tag SNP LOG10(p)	Trait
q1B-2	1B	Tdurum_contig44219_318	14369586	15969586	4.840030902	CN
q1B-3	1B	RAC875_c42275_224	631032802	632632802	4.8529549	CSFL
q1B-4	1B	Ex_c29452_302	677632525	679232525	4.797343561	CHL_20DAA
q1D-2	1D	Excalibur_c56999_109	459337951	460337951	4.8529549	CSFL
q2B-2	2B	Ku_c57425_413	108105283	109705283	4.81142255	RDN, NDVI_H
q2B-3	2B	Ra_c6728_590	133290399	134890399	4.483111594	fv/fm_H
q2B-4	2B	BS00046164_51	696710323	698310323	5.447669843	NDVI_21DAA
q2B-7	2B	Ra_c13298_434	731544105	733144105	5.940797889	PH
q2B-8	2B	Ra_c5004_2033	732913735	734513735	5.940797889	PH
q3A-1	3A	Excalibur_c11079_749	31901535	32501535	4.689402959	PH
q3A-4	3A	Ku_c10817_611	708246032	708846032	5.186923741	NDVI_A
q3B-1	3B	BS00085434_51	749557865	751157865	4.60295062	CHL_A
q4A-2	4A	Excalibur_c55561_127	450583765	451183765	5.034662751	CHL_A
q4D-1	4D	BobWhite_c4264_325	120681547	121681547	4.703459538	CHL_A
q5A-1	5A	Excalibur_c5398_695	29727274	30327274	4.780595038	fv/fm_21 DAA
q5B-1	5B	BS00110064_51	397038250	398638250	4.443068306	CHL_10DAA
q6A-2	6A	Tdurum_contig55193_296	6296817	6896817	4.991917958	NDVI_A
q6B-1	6B	BS00092845_51	10498715	12098715	5.186923741	NDVI_A
q7A-7	7A	CAP8_c4980_112	719271317	719871317	5.778586875	NDVI_A
q7A-8	7A	BS00002510_51	720700126	721300126	4.942483964	NDVI_A

A total of 826 genes at 20 multi-method GWAS loci were extracted from wheat reference assembly RefSeq v1.1. Of 826 genes, 342 were high confidence protein coding genes and only 36 had description available at IWGSC assembly. The known high confidence protein coding genes encode Beta-galactosidase, serine/threonine-protein kinase WNK3, Fatty acyl-CoA reductase, Beta-amylase, Cysteine proteinase inhibitor,

Glycosyltransferase, Phosphatidylinositol 4-phosphate 5-kinase, Cyclin-U1-1, Peroxidase, Protein COFACTOR ASSEMBLY OF COMPLEX C SUBUNIT B CCB4, chloroplastic, Eukaryotic translation initiation factor 3 subunit I, Protein DAMAGED DNA-BINDING 2, zinc metalloprotease EGY2, chloroplastic, Similar to 14-3-3 protein 6, Protein detoxification, GID2 protein isoform 1, ATP-dependent DNA helicase, Laccase, Kinesin-like protein, phospholipase D, RBR-type E3 ubiquitin transferase, non-specific serine/threonine protein kinase, P-loop containing nucleoside triphosphate hydrolases superfamily protein, and putative RNA-binding protein (Annexure 2.3).

2.5. Discussion

The functional stay-green trait enables plant to maintain its chlorophyll content, and photosynthetic activity for longer duration during terminal phase of plant life cycle, consequently improves plant productivity (Thomas and Ougham, 2014; Zhang *et al*., 2019; Kamal *et al*., 2019). The stay-green trait has been associated with better performance under non-stress and stress environments (Christopher *et al*., 2008; Pinto *et al*., 2010; Bogard *et al*., 2011; Lopes and Reynolds, 2012; Pinto *et al*., 2016) the negative impact of stay-green trait on yield has been rarely reported (Derkx, *et al*., 2012). Therefore, elucidation of morpho-physiological and genetic mechanisms associated with the stay-green trait may contribute towards yield sustainability under changing environment. In the present study, a positive correlation between chlorophyll content (tillering, booting, heading, anthesis, 10DAA, and 20DAA, and 30DAA), thousand grain weight, grain yield and biological yield was observed. Photosynthetic efficiency (fv/fm) at heading, anthesis, 14DAA, and 21DAA also displayed significant positive correlation with thousand kernel weight and grain yield. The NDVI at heading, anthesis, 14DAA, and 21DAA showed significant positive correlation with grain yield. Our results are in alignment with previous studies that reported positive correlation of the chlorophyll content and fv/fm with grain yield (Talukder *et al*., 2014, Azam *et al*., 2015; Pinto *et al*., 2016). Chlorophyll content and photosynthetic efficiency can be used as selection criteria for grain yield improvement in breeding programs (Vijayalakshmi *et al*., 2010 and Azam *et al*., 2015; Pinto *et al*., 2016). In the present study, the stay-green indices, CSF and CN showed significant positive correlation with thousand grain weight, grain yield and

biological yield, whereas RDSF displayed a significant negative correlation with grain yield and biological yield. Our results are in alignment with find by Pinto *et al*., (2016). Pinto *et al*., (2016) reported significant positive correlation of stay-green trait with thousand kernel weight, kernel number, and grain filling duration. The yield advantages associated with the stay-green can be attributed to higher antioxidant activities, lower malondialdehyde concentration, delayed chlorophyll degradation, extended photosynthesis, and higher carotenes and xanthophylls that dissipate the excessive radiation energy (Zhao and Tan, 2005; Suzuki and Mittler, 2006; Luo *et al*., 2006; Luo *et al*., 2013).

Grain yield improvement under non-stress and stress environment is the ultimate aim of the plant breeding programs. Identification of loci for the stay-green trait can be useful in enabling marker assisted selection to achieve the goal of yield sustainability under varying environments. In the present study, GLM, MLM, and Farm CPU based genome wide association mapping enabled detection of 48 loci on chromosome 1A, 1B, 1D, 2A, 2B, 3A, 3B, 4A, 4D, 5A, 5B, 6A, 6B, 6D, 7A and 7B for chlorophyll content, photosynthetic efficiency, NDVI, stay-green indices, plant height, and tiller number. Of the 48 loci, 5 were detected by GLM, 23 were identified by FarmCPU, and 20 loci were explored by both GLM and FarmCPU. Chlorophyll content was associated with q1B-4, q3B-1, q4A-2, q4D-1, q5A-2, q5A-3, q5B-1, and q7A-1 on chromosome 1B, 3B, 4A, 4D, 5A, 5B, and 7A. Previous study by Hassan *et al*., 2018 detected six quantitative trait loci (QTLs) for chlorophyll content on chromosome 2D, 3B, 4A, 6A, 6B, and 7D. Huang *et al*., (2018) detected 59 marker trait associations for chlorophyll content on chromosome 1A, 1B, 2A, 2B, 3A, 4A, 4B, 5A, 5B, 6A, 6B, 7A, and 7B in durum wheat. Pinto *et al*., 2016 detected 9 QTLs for chlorophyll content on chromosome 1B, 2B, 2D, 3B, 4B, 5B, and 6A. Photosynthetic efficiency was linked with q2B-3 and q5A-1 found on chromosome 2B and 5A, respectively. Hassan *et al*., (2018) identified three QTLs for fv/fm; QFv/Fm-1D, QFv/Fm-3B, and QFv/Fm-6A on chromosome 1D, 3B, and 6A. In the present study, loci for NDVI were detected on chromosome 1A, 1D, 2B, 3A, 4A, 5A, 6A, 6B, 7A, and 7B. Pinto *et al*., (2016) identified QTLs for NDVI on 1B, 1D, 2A, 2B, 3A, 3B, 4A, 4B, 4D, 5B, 6A, 7A, and 7B. The QTLs for stay-green indices, CN detected on chromosome 1B, CSF found on chromosomes 1B and 1D, and RDN associated with

chromosomes 2B and 6A. A study by Pinto et al., (2016) identified QTLs for stay-green trait on chromosome 2A, 4B, 4D, 6A, and 7D. Kumar *et al*., (2010) detected three QTLs for stay-green trait on chromosome 1A, 3B, and 7D.

Gene annotation for 20 loci identified by two methods revealed the presence of 342 high confidence genes in these regions, only 36 were known genes. Locus q4A-2 (tag SNP: Excalibur_c55561_127, -log10(p)= 5.03) associated with chlorophyll content was linked with TraesCS4A02G178600 gene encoding ATP-dependent DNA helicase. The ATP-dependent DNA helicases are associated with stability of chromosomes, and normal growth and development in rice (Hong *et al*., 2010). TraesCS4D02G133800 gene encoding Laccase linked with q4D-1 (tag SNP: BobWhite_c4264_325, -log10(p)= 4.7) associated with chlorophyll content is involved in plant defense responses and regeneration of damage tissues under stress (Berthet *et al*., 2012; Wang *et al*., 2015; Janusz *et al*., 2020). Loci q5B-1 (tag SNP: BS00110064_51, -log10(p) = 4.44) associated with chlorophyll content are linked with TraesCS5B02G222500, TraesCS5B02G223200, and TraesCS5B02G223800 genes encoding Phospholipase-D, RBR-type E3 ubiquitin transferase, and Non-specific serine/threonine protein kinase. The phospholipase-D plays an imperative role in regulating the cellular physiological mechanisms involved in plant growth, development, and stress responses (Hong *et al*., 2016; Ji *et al*., 2018; Wang *et al*., 2019a; Lu *et al*., 2019). RBR-type E3 ubiquitin transferase plays key role in germination of seedlings, control plants flowering time, development of chloroplast, and stresses response (Shu and Yang, 2017). RBR-type E3 ubiquitin transferase has been linked with width and weight of rice grain (Song *et al*., 2007). Non-specific serine/threonine protein kinase has been associated with plant stresses response and programmed cell death. Serine/threonine protein kinase acts as the central processing unit that receives signal from environment/ hormone/ other external factor receptors and converts the input into output via modification in gene expression, cell metabolism, growth, and development (Hardie, 1999; Afzal *et al*., 2008). Non-specific serine/threonine protein kinase has been associated with potassium use efficiency in wheat (Safdar *et al*., 2020). Locus q5A-1 (tag SNP: Excalibur_c5398_695, -log10(p)= 4.78) associated with chlorophyll fluorescence is linked with TraesCS5A02G032500 genes encoding Kinesin like protein. Kinesin like protein involves in movement of chloroplast through chloroplast-actin-filament, cell

division, and cell growth (Geelen and Inzé, 2001; Vanstraelen *et al*., 2004; Suetsugu *et al*., 2010; Li *et al*., 2012). In rice, Kinesin like protein has been associated with seed length (Kitagawa *et al*., 2010). Locus q2B-2 (Ku_c57425_413, -log10(p)= 4.8) associated with NDVI is linked with TraesCS2B02G141700, TraesCS2B02G501700, TraesCS2B02 G501800, TraesCS2B02G502100, TraesCS2B02G502300, TraesCS2B02G502600, TraesCS2B02G502800, TraesCS2B02G503100, TraesCS2B02G503400, and TraesCS2B02G503500 encoding beta-amylase, cysteine proteinase inhibitor, glycosyltransferase, phosphatidylinositol 4-phosphate 5-kinase, and cyclin-U1-1. Beta-amylase stimulation results in maltose accumulation, which acts as a compatible solute in the stroma of chloroplast under temperature stress. Beta-amylase protects membranes and electron transport chain (Kaplan and Guy, 2004). Cysteine proteinase inhibitor is a key molecule involved in development and regulation of defense responses under heat, cold, drought, salinity, and oxidative stress (Zhang *et al*., 2008; Huang *et al*., 2012; Sun *et al*., 2014). Transgenic plants with higher expression of cysteine proteinase inhibitor exhibited better growth, higher antioxidase activity, lower malondialdehyde content, and greater cell viability (Li *et al*., 2015). The cysteine proteinase inhibitor improves abiotic stress tolerance by acting against cysteine proteinase activated that accumulates under stress and leads to hastened programmed cell death (Solomon *et al*., 1999; Belenghi *et al*., 2003). Glycosyltransferase is associated with detoxification of harmful molecules produced under abiotic and biotic stresses (Bowles *et al*., 2005; Shi *et al*., 2020). Glycosyltransferase catalyzes the biosynthesis of anthocyanins and flavonoids, which are involved in scavenging reactive oxygen species (Shi and Xie, 2014). Phosphatidylinositol 4-phosphate 5-kinase is associated with flowering time. The suppression of phosphatidylinositol 4-phosphate 5-kinase gene in transgenic rice results in earlier heading (Ma *et al*., 2004). Locus q1B-2 [Tdurum_contig44219_318, -log10(p)= 4.84] associated with cumulative NDVI is linked with TraesCS1B02G030400 and TraesCS1B02G032500 encodes for Beta-galactosidase and Probable serine/threonine-protein kinase WNK3, respectively. Beta-galactosidase is involved in polysaccharides degradation of cell wall under stress. Beta-galactosidase has been reported in germinating seeds and ripening fruit (Ali *et al*., 1995; Edwards *et al*., 1998, Balasubramaniam *et al*., 2005). During senescence, β-glucosidase activity enhances with lose of photosynthesis in

plants (Mohapatra *et al*., 2010). Probable serine/threonine-protein kinase WNK3 modulates photoperiod pathway and regulates flowing time (Wang *et al*., 2008). Locus q1B-3 [RAC875_c42275_224, -log10(p)= 4.85] associated with CSF was linked with TraesCS1B02G402600 gene encoding Fatty acyl-CoA reductase. The fatty acyl-CoA reductases are associated with biosynthesis of long chain alcohols and are also involved in heat, cold, drought, and powdery mildew stress responses in wheat (Chai *et al*., 2018). For further information on genes which have not been studied in wheat, it may be useful to look at the close grass relatives such as rice which is now potentially used as a reference for grasses. Future gene expression experiments on these 342 genes will help for in-depth analysis and more accurate information on candidate gene(s) for stay-green trait in wheat.

2.6. Conclusion

The stay-green attribute can be used in breeding programs for yield stability under changing environment. Present study demonstrated significant difference for chlorophyll content, chlorophyll fluorescence, plant height, tiller number, spike length, spikelet per spike, grain yield, and biological yield in the selected diversity panel. Heritability of the chlorophyll content at 20DAA and 30DAA, chlorophyll fluorescence at 14DAA, and cumulative chlorophyll content was relatively high, thus can be considered as potential traits that can be used in the evaluation of the stay-green trait. Chlorophyll content, chlorophyll fluorescence, NDVI, and stay-green indices showed positive correlation with thousand kernel weight, grain yield, and biological yield. Forty eight loci were detected for chlorophyll content, chlorophyll fluorescence, NDVI, stay-green indices, plant height, and tiller number. The identified loci were associated with thirty six putative genes which are involved in plant development, defense responses under stress, flowering time control, chloroplast development, and damage tissues regeneration. Further, exploration of these loci by expression profiling of the underlining genes may contribute towards our understanding of the stay-green trait and can be used as potential markers in marker assisted selection to develop superior stay-green cultivars that yield high under environmental stresses.

Chapter #3

Deciphering the Role of the Stay-Green Trait to Mitigate Terminal Heat Stress in Bread Wheat

Chapter #3

Deciphering the Role of the Stay-Green Trait to Mitigate Terminal Heat Stress in Bread Wheat

3.1. Abstract

The present study aimed to reveal the impact of the stay-green trait in bread wheat under terminal heat stress. Field experiments (early and late sowing; for two consecutive years) were conducted to investigate the influence of terminal heat stress on the morpho-physiological traits in different stay-green types that included non-stay-green, moderately non-stay-green, moderately stay-green, and stay-green. In addition, the greenhouse experiment was performed to dissect the stay-green trait in functional stay-green, non-functional stay-green, and non-stay-green genotypes. The results of the field experiments confirmed that genotypes exhibiting the stay-green trait have significantly high chlorophyll content, normalized difference vegetative index, grain yield, biological yield, kernel weight, and low canopy temperature under control and heat stress conditions. In the greenhouse experiment, functional stay-green and non-functional stay-green genotypes showed a high chlorophyll content and photochemical efficiency, whereas biological yield and grain yield showed a significant relation with the functional stay-green genotype under control and terminal heat stress treatments. The sequencing and expression analysis of chlorophyllide a oxygenase (CaO), light-harvesting complex (Cab), stay-green (SGR), and red chlorophyll catabolite reductase (RCCR) in functional stay-green, non-functional stay-green, and non-stay-green genotypes revealed variations in the exons of CaO and RCCR; and significant difference in the regulation of CaO and Cab at 7 days after anthesis under terminal heat stress. This study confirms that genotypes displaying the stay-green trait can aid wheat breeders to cope with increasing temperature in the impending decades.

3.2. Introduction

Agriculture and climate change are internally correlated, as climate change is the main cause of biotic and abiotic stresses. Agriculture is being affected by climate changes

in different ways e.g., variations in global atmospheric CO_2 levels, changes in average temperature, heat waves, annual rainfall, and modifications in microbes, pest, or weeds (IPCC, 2014; Arunanondchai *et al*., 2018; Noya *et al*., 2018; Raza *et al*., 2019). Escalating global temperature together with intense and frequent heat episodes is of rising concern to global food security (Fontana *et al*., 2015; Mueller *et al*., 2015). High temperature adversely affects the yield potential of crops by influencing its metabolic pathways and yield losses may reach up to 40% under severe heat stress during the grain filling duration (Wollenweber *et al*., 2003; Hays *et al*., 2007). Increasing crop productivity together with the reduction in the environmental footprint is a daunting task if we want to achieve the ―Zero hunger sustainable developmental goal" (Siebert *et al*., 2014). Cereal crops are considered as the ultimate custodian of global food security. Among cereals, the golden ears of bread wheat have been considered as a symbol of global food security since the dawn of civilization. Wheat production, with decreasing land and water resources in variable climatic conditions, needs to be increased by 60% to reach the required ~840 million tonnes by 2050 (Sharma *et al*., 2015).

High temperature stress during the grain-filling period of the plant life cycle is termed as terminal heat stress. During the grain-filling duration, a 1°C rise in temperature above 15°C is estimated to reduce the wheat yield by 6% (Challinor *et al*., 2014; Akter and Islam, 2017). Heat stress causes oxidative damage which induces lipid peroxidation, protein degradation, enzyme inactivation, instability of thylakoid membranes, decrease in chlorophyll content, and reduced rubisco activity (Sairam *et al*., 2000; Dias and Lidon, 2009). It also elevates transpiration rate, pH of leaf sap, and abscissic acid production that leads to premature leaf senescence (Wilkinson and Davies, 2002). These changes in the plant physiological mechanism result in reduced starch accumulation, days to maturity, thousand kernel weight, altered grain starch lipid composition, and shriveled grains (Balla *et al*., 2012). Plants have evolved different mechanisms to cope with heat stress such as escape, avoidance, and stay-green (Sharma *et al*., 2019). The stay-green trait has been considered as an indicator of high temperature stress tolerance by decelerating plant growth cycle and increasing plant productivity (Kumari *et al*., 2007; Pinto *et al*., 2016).

Stay-green, referred to as ―heritable delayed foliar senescence", is broadly classified into functional and non-functional stay-green. In the functional stay-green, retention of chlorophyll is coupled with increased photosynthetic capacity and yield potential of plants in contrast to the non-functional stay-green type. Functional stay-green is divided into type A (senescence is initiated late) and type B (progression of senescence is slow), whereas non-functional stay-green is further classified into type C (cosmetic type), type D (pseudo stay-green), and type E (hyper green) (Hortensteiner, 2009; Thomas and Ougham, 2014). The stay-green trait has been documented in maize, oat, rice, arabidopsis, soyabean, sorghum, wheat, and other plants species (Grbić and Bleecker, 1995; Cha *et al*., 2002; Duvick *et al*., 2004; Armstead *et al*., 2006; Rampino *et al*., 2006; Barry *et al*., 2008; Wei *et al*., 2011; Fang *et al*., 2014). The genetic basis behind stay-green is complex and varies in different plant species. Various studies indicated the involvement of a multi-protein complex comprising of chlorophyll catabolic enzymes, stay-green protein, and light-harvesting complex protein (Sakuraba *et al*., 2012). The first two components of the multi-protein complex i.e., chlorophyll catabolic enzymes and stay-green protein, are linked with the chlorophyll degradation pathway. Chlorophyll catabolism is a multistep process that initiates with the conversion of chlorophyll b to 7-hydroxymethyl chlorophyll a in the presence of chlorophyll b reductase. The 7-hydroxymethyl chlorophyll a is converted into chlorophyll a and the reaction is catalyzed by 7-hydroxymethyl chlorophyll a reductase (Takamiya *et al*., 2000). Chlorophyll a degrades to pheophorbide a using magnesium dechelatase and pheophytinase, which removes the central magnesium atom and breaks the phytol side chain (Suzuki *et al*., 2002; Christ and Hörtensteiner, 2014; Shimoda *et al*., 2016). Then, pheophorbide a is catalyzed into primary fluorescent chlorophyll catabolite by the action of pheophorbide a oxygenase and red chlorophyll catabolite reductase (Hortensteiner *et al*., 1995). Primary fluorescent chlorophyll catabolite is transferred from chloroplast to vacuole where it is converted into non-fluorescent chlorophyll catabolite (Hortensteiner and Krautler, 2011). Mutations in the chlorophyll catabolic enzyme genes can result in a stay-green phenotype by delaying the foliar senescence (Thomas and Ougham, 2014; Kuai *et al*., 2018). The light-harvesting complex protein, the third element of the multi-protein complex, accounts for approximately half of the total chlorophyll involved in

photosynthesis (Niyogi *et al*., 2005; Bellafiore *et al*., 2005; Szabó *et al*., 2005; Paulsen *et al*., 2010). The current study focused on the chlorophyllide a oxygenase (CaO), light-harvesting chlorophyll a/b binding protein (Cab), stay-green (SGR), and red chlorophyll catabolite reductase (RCCR) genes.

The CaO gene is involved in the synthesis of chlorophyll b from chlorophyll a by the oxidation of a methyl group to a formyl group (Tanaka *et al*., 1998; Espineda *et al*., 1999; Oster *et al*., 2000; Nagata *et al*., 2004). The over expression of the CaO gene results in an enhanced chlorophyll b content, changed chlorophyll a/b ratio, increased light-harvesting chlorophyll protein, boosted light capture, and the electron transport of photosystem I and II (Biswal *et al*., 2012). The Cab harvests photons that are converted into biochemical energy and biomass during photosynthesis. The Cab genes are down-regulated under abiotic and biotic stresses (Seki *et al*., 2002; Hazen *et al*., 2005; Guo *et al*., 2009; Manickavelu *et al*., 2010). However, a high expression level has been observed in the tolerant genotypes (Hazen *et al*., 2005; Guo *et al*., 2009). The SGR also called the non-yellowing (NYE1) gene encodes for magnesium dechelatase, which catalyzes the conversion of chlorophyll a into pheophytin a *(*Christ and Hörtensteiner, 2014; Shimoda *et al*., 2016). The up-regulation of SGR results in chlorophyll degradation by reducing the number of lamellae in the grana thylakoids (Jiang *et al*., 2007). The RCCR, also known as accelerated cell death 2 (ACD2), catalyzes red chlorophyll catabolite to primary fluorescence chlorophyll catabolite (Hörtensteiner, 2006; Sugishima *et al*., 2009). The RCCR mutants accumulate red chlorophyll catabolite, which induces the production of reactive oxygen species and causes cell death (Mach *et al*., 2001; Pruzinska *et al*., 2007). The up-regulation of the RCCR gene is connected with defense responses under abiotic and biotic stresses (Mach *et al*., 2001; Yao and Greenberg, 2006; Pruzinska *et al*., 2007; Tang *at al*., 2011; Zhang *et al*., 2011; Cheng *et al*., 2012).

The stay-green trait seems to improve grain yield under high temperature stress by retaining chlorophyll content, improving photosynthetic capacity, and extending the grain-filling period (Reynolds *et al*., 2000; Kumari *et al*., 2013; Pinto *et al*., 2016). The precise mechanism behind the stay-green trait as an adaptive trait to heat stress still needs to be explored. The present study aimed to examine the association of the stay-green trait

with the chlorophyll content, photochemical efficiency, normalized difference vegetative index (NDVI), canopy temperature, grain yield, biological yield, kernel weight, the expression profile of chlorophyll catabolism pathway genes (CaO, SGR, and RCCR), and the photosynthetic responsive gene (Cab) in bread wheat under terminal heat stress. Furthermore, it is the pioneer study that unraveled the CaO, SGR, and RCCR gene expression in relation to the stay-green trait in *Triticum aestivum* under high temperature stress.

3.3. Materials and methods

3.3.1. Phenotyping

3.3.1.1. Field experiment

The diversity panel consisting of 123 bread wheat genotypes including landraces, green revolution cultivars, post-green revolution cultivars, elite genotypes, and synthetic derivatives was subjected to field trials (Annexure 3.1). The field experiments were performed for two consecutive years (2014–2015 and 2015 –2016) with early and late sowing to investigate the impact of heat stress. Planting was done on November 15 and December 31 each year in alpha lattice design at the National Agricultural Research Centre, Islamabad, located between 33.6701° N latitude and 73.1261° E longitude. The average temperature ranged between 2.8-34.6 °C and 3.7-37.2 °C at the experimental site during November 2014-May 2015 and November 2015-May 2016, respectively. The daily maximum and minimum temperature is given in Annexure 3.2. The field experiments consisted of four rows of 1 m per plot for each genotype, with a sowing density of 20 seeds per row. The fertilizers were applied during land preparation using standard agricultural procedures and the irrigation regime was practiced to ensure the crop growth without water limitation. The evaluated traits were chlorophyll content, normalized difference vegetative index (NDVI), canopy temperature (CT), plant height (PH), tiller number (Til No), spike length (SL), spikelet per spike (SpS), days to maturity (DM), biological yield (BY), grain yield (GY), and thousand kernel weight (TKW). All the morpho-physiological traits were determined using standard protocols as described by Pask *et al*., (2012).

The chlorophyll content was measured at booting, heading, anthesis, seven days after anthesis (7DAA), 14 days after anthesis (14DAA), and 21 days after anthesis (21DAA) in the flag leaves using the Chlorophyll Meter (SPAD-502). The normalized difference vegetative index (NDVI) was recorded at heading, anthesis, 14DAA, and 21DAA using the Trimble handheld Green-seeker. An Infrared Thermometer (Telatemp AG-42) was used to record canopy temperature at heading, anthesis, 14DAA, and 21DAA. The chlorophyll content and NDVI were measured between 11:30 a.m. and 2:00 p.m. and the canopy temperature was recorded between 1:00 p.m. and 2: 00 p.m. on windless and cloudless day. PH (cm) was determined at maturity by measuring individual culms from the soil surface to the tip of the spike excluding awn, using a meter rod. Fertile tillers per plant were recorded at the flowering stage. SL (cm) was measured from the base of the rachis to the tip of the terminal spikelet excluding awn using a meter rod. SpS was recorded by counting the total number of spikelets from the base to the tip of the spike. Chlorophyll content, PH, Til No, SL, and SpS were measured in three replicates. DM was recorded when more than 50% of the plants per plot exhibited a loss of complete greenness. All the above-ground biomass excluding borders was harvested, dried, and weighed to determine the BY (g). The harvested above-ground biomass was threshed and weighed to obtain the GY (g). The thousand kernel weight was determined by weighing 200 seeds and multiplying the obtained weight with 5.

3.3.1.2. Greenhouse experiment

The greenhouse experiment was conducted to dissect the stay-green trait in functional stay-green (Nepal-38), non-functional stay-green (SG-30), and non-stay-green (Sonalika) genotypes under controlled greenhouse conditions at South Dakota State University, USA (Annexure 3.3). The genotypes were selected on the basis of morpho-physiological traits evaluated during the field experiments (Nepal-38 and SG-30 showed maximum values for chlorophyll content, NDVI, and days to maturity compared to Sonalika whereas, SG-30 showed shriveled grains under control conditions). The sterilized seeds of the selected genotypes were grown in the pots filled with Metro-mix®360 soil mixture and each pot contained four plants. The experiment was laid out in a completely randomized design with six biological replicates. During the experiment,

the greenhouse conditions were maintained at 24/18 °C day/night temperatures with a photoperiod of 12 h. Half plants of each genotype at anthesis were transferred to a growth chamber for heat stress treatment at 36/28 °C day/night temperatures. The pots were well watered throughout the experiment and a teaspoon of Osmocote (15N-9P-12K) was applied at tillering and booting.

The leaf chlorophyll content and photosynthetic efficiency of photosystem II (ØII) were determined using the Chlorophyll Meter (SPAD-502) and the handheld MutispeQ, respectively. Both the chlorophyll content and ØII were measured at anthesis, 7DAA, and 14DAA from the flag leaf between 12 p.m. and 2 p.m. using six replicates. The chlorophyll content for each sample was determined from three parts of the same flag leaf and the average was recorded. The ØII was measured using the photosynQ application via a global plant census project according to the manufacturer‘s protocol. The biological yield and grain yield per plant were determined using three biological replicates. The plant above ground biomass was harvested, dried, and weighed to obtain the biological yield per plant. After threshing, the grain harvest per plant was weighed to obtain the grain yield per plant.

3.3.2. Genotyping

3.3.2.1. Sample preparation

The leaf samples were harvested at anthesis, 7DAA, and 14DAA from both the control and heat-treated samples in triplicate. The samples were washed with distilled water, incised with a sharp blade, immediately shifted to liquid nitrogen, and stored at −80 °C to prevent any degradation. Leaf tissues were freeze dried for 48 h using FreeZone Freeze Dryer System by Labconco. The lyophilized leaf tissues were ground into fine powder using tissuelyser. The sequencing and expression analysis were performed at the Plant Molecular and Cellular Biology Laboratory, University of Florida, USA.

3.3.2.2. DNA extraction and gel electrophoresis

Total genomic DNA was isolated from 20 mg of the lyophilized leaf tissues using MagJET Plant Genomic DNA Kit by Thermo Scientific, following the manufacturer‘s

protocol. To confirm the presence of DNA, the isolated DNA (4 µL) was mixed with 6X loading dye (2 µL) and resolved on 1% agarose gel. The gel was viewed using a gel documentation system (Bio-Rad).

3.3.2.3. Identification of CaO, Cab, SGR, and RCCR genes in the wheat genome

For sequence accession in *Triticum aestivum*, the gene, cDNA, and protein sequences of the orthologous and phylogenetically closely related species that included *Brachypodium distachyon*, *Hordeum vulgare*, *Sorghum bicolor*, *Oryza sativa,* and *Zea mays* were used. The gene, cDNA, and protein sequences of CaO, Cab, SGR, and RCCR in reference species were obtained from the National Center for Biotechnology Information (NCBI). The complete coding sequence of each gene from the reference species was blasted in Ensembl Plants against *Triticum aestivum* to obtain the genes, cDNA, and protein sequences in *Triticum aestivum* (Annexure 3.4). Sequence homologies between the cDNA and the protein sequences of *Triticum aestivum, Brachypodium distachyon*, *Hordeum vulgare*, *Sorghum bicolor*, *Oryza sativa,* and *Zea mays* were determined by multiple sequence alignment using the Clustal Omega tool.

3.3.2.4. Phylogenetic analysis

Molecular evolutionary genetics analysis (Mega 6.06) was used for phylogenetic analysis (Tamura *et al*., 2013). The neighbor-joining method employing the p-distance and boot-strap with 1,000 replicates was used to compute the phylogenetic tree using amino acid sequences (Nei and Kumar, 2000).

3.3.2.5. Primer designing

The primers were designed using Primer3 plus (Annexure 3.5). The primers were checked for hairpin structure, self or heterodimer formation using Integrated DNA Technology.

3.3.2.6. Amplification and sequencing

The CaO, Cab, SGR, and RCCR genes were amplified in functional stay-green, non-functional stay-green, and non-stay-green genotypes using the primers listed in Annexure 3.5. The reaction cocktail was prepared using 10 µL of Go TAQ Master Mix, 1

µL of primer forward, 1 µL of primer reverse, 1.5 µL of DNA template, and 6.5 µL of PCR water. The PCR profile used was; 95 °C for 4 min, followed by 40 cycles of 95 °C for 45 sec, 56–62 °C for 30 sec, 72 °C for 1 min, and the final extension at 72 °C for 10 min. The amplified PCR products were sent for sequencing to the Genomic Centre, University of Florida. The sequences were subjected to multiple sequences alignment using CLUSTALW to reveal variations.

3.3.2.7. RNA extraction, gel electrophoresis, and qubit assay

Total RNA was extracted from the lyophilized leaf samples (200 mg) using the plant RNA reagent (Trizol by Ambion, Life Technologies) followed by treatment with Qiagen on column DNaseI (RNeasay Mini Kit, Part 2, QIAGEN) according to the manufacturer‘s protocol. RNA integrity was confirmed using 1.5% formaldehyde agarose, gel stained with ethidium bromide. The quantification of RNA was done using a Qubit RNA assay following the Qubit RNA BR Assay kit protocol.

3.3.2.8. cDNA synthesis and quantification

First strand cDNA was synthesized by the reverse transcription of 3 µg of the RNA template in the presence of a random hexamer primer (50 ng), deoxyribonucleotide triphosphates dNTPs (10 mM), 10X reverse transcriptase buffer (2 µL), $MgCl_2$ (100 mM), dithiothreitol DDT (0.2 M), RNase (40 U), and superscript III reverse transcriptase (200 U). The total reaction volume for each sample was 20 µL. The standard reaction conditions as described in Superscript III First Strand Synthesis System for RT-PCR were followed (Invitrogen, Life Technologies). The cDNA was quantified by a Qubit 2.0 Fluorometer using the DsDNA feature.

3.3.2.9. Transcript abundance by reverse transcription quantitative PCR

Real-time quantitative PCR was performed in a total reaction volume of 25 µL for each sample, containing 12.5 µL SYBR Green PCR Master Mix (Applied Biosystems, 4309155), 1 µL of cDNA (5 ng/µL), 1.25 µL each primer forward and reverse, and 9 µL PCR water using the BIO-RAD CFX Connect Real time PCR system. The standard real time PCR profile by SYBR Green PCR Master Mix, Applied Biosystems, was used, which included polymerase activation at 95 °C for 10 min followed by 40 cycles of

denaturation at 95 °C for 30 sec and annealing at 60 °C for 1 min. The melt curve temperature was from 65 °C to 95 °C.

Amplification efficiency was determined for each primer pair using ten-fold cDNA dilution series in triplicate (n = 3). The threshold cycle (CT) values of ten-fold cDNA dilution series were plotted to obtain the slope using linear regression. The efficiency was calculated using the following formulas:

$$\text{Efficiency}=10^{-(1/\text{slope})} \quad (1)$$

$$\text{Percentage Efficiency}= (E - 1) \times 100 \quad (2)$$

For expression profiling, the CT values were normalized using the ACTIN2 gene (Buchner *et al*., 2015) expression as:

$$\Delta\text{CT(Control)} = \text{CT(Control)} - \text{CT(Reference gene)} \quad (3)$$

$$\Delta\text{CT(Treated)} = \text{CT(Treated)} - \text{CT(Reference gene)} \quad (4)$$

In the second step, the value of the ΔCT control was subtracted from the ΔCT stress and the relative expression levels were determined using 2-ΔΔCT Livak‘s method (Livak and Schmittgen, 2001). The log2 fold change was determined to demonstrate the up-regulation or down-regulation of the gene transcript.

3.3.3. Statistical analysis

Heatmap for NDVI was developed by ClustalVis, a tool to visualize the clusters of multivariate data. The analysis of variance (ANOVA) for the phenotypic and expression profiling data was performed using XLSTAT Version 2014.5.03 by Tukey‘s honest significant difference (HSD) test to determine the effect of treatments on groups.

3.4. Results

3.4.1. Phenotyping

3.4.1.1. Field experiment

The germplasm was categorized into non-stay-green, moderately non-stay-green, moderately stay-green and stay-green groups on the basis of the NDVI. This rating scale

was developed considering the mean NDVI values at heading, anthesis, 14DAA, and 21DAA together with a time point at which the NDVI decline was initiated. The genotypes showing a mean NDVI of 0.40->0.495, 0.495->0.55, 0.55->0.605, and 0.605-0.66 were classified into non-stay-green, moderately non-stay-green, moderately stay-green, and stay-green groups, respectively. The majority of the genotypes were classified as moderately non-stay-green (30.9%) followed by moderately stay-green (27.6%), stay-green (26.8%), and non-stay-green groups (14.7%) (Figure 3.1).

Physiological traits

The chlorophyll content measured at booting, heading, anthesis, 7DAA, 14DAA, and 21DAA showed a significant decline among all the groups under heat stress treatment. The chlorophyll content greatly varied between the groups at day 14 and day 21 after anthesis under control; and at day 7, day 14, and day 21 after anthesis under high temperature stress (Figure 3.2, Annexure 3.6).

The NDVI at heading, anthesis, 14DAA, and 21DAA declined among all the groups under terminal heat stress. Significant variation was observed between groups and treatments for the NDVI at all-time points. The stay-green group showed maximum values for the NDVI at all-time points under control and heat stress conditions (Figure 3.3, Annexure 3.6).

The CT was recorded at heading, anthesis, 14DAA, and 21DAA. CT increased under heat stress conditions among all the groups, except for the non-stay-green and moderately non-stay-green groups at 14DAA. CT revealed significant variations among the groups and treatments at all-time points. The stay-green group and non-stay-green group showed minimum and maximum mean values, respectively, at all the time points (Figure 3.4, Annexure 3.6).

Morphological traits

The PH, Til No, SL, SpS, DM, GY, BY, and the TKW significantly declined under heat stress conditions among all the groups. The Til No, SpS, GY, BY, and the TKW depicted significant difference among the groups. The maximum mean values for

the Til No, SL, SpS, BY, GY, and the TKW were observed in the stay-green group under control and heat stress conditions (Figure 3.5, Annexure 3.6).

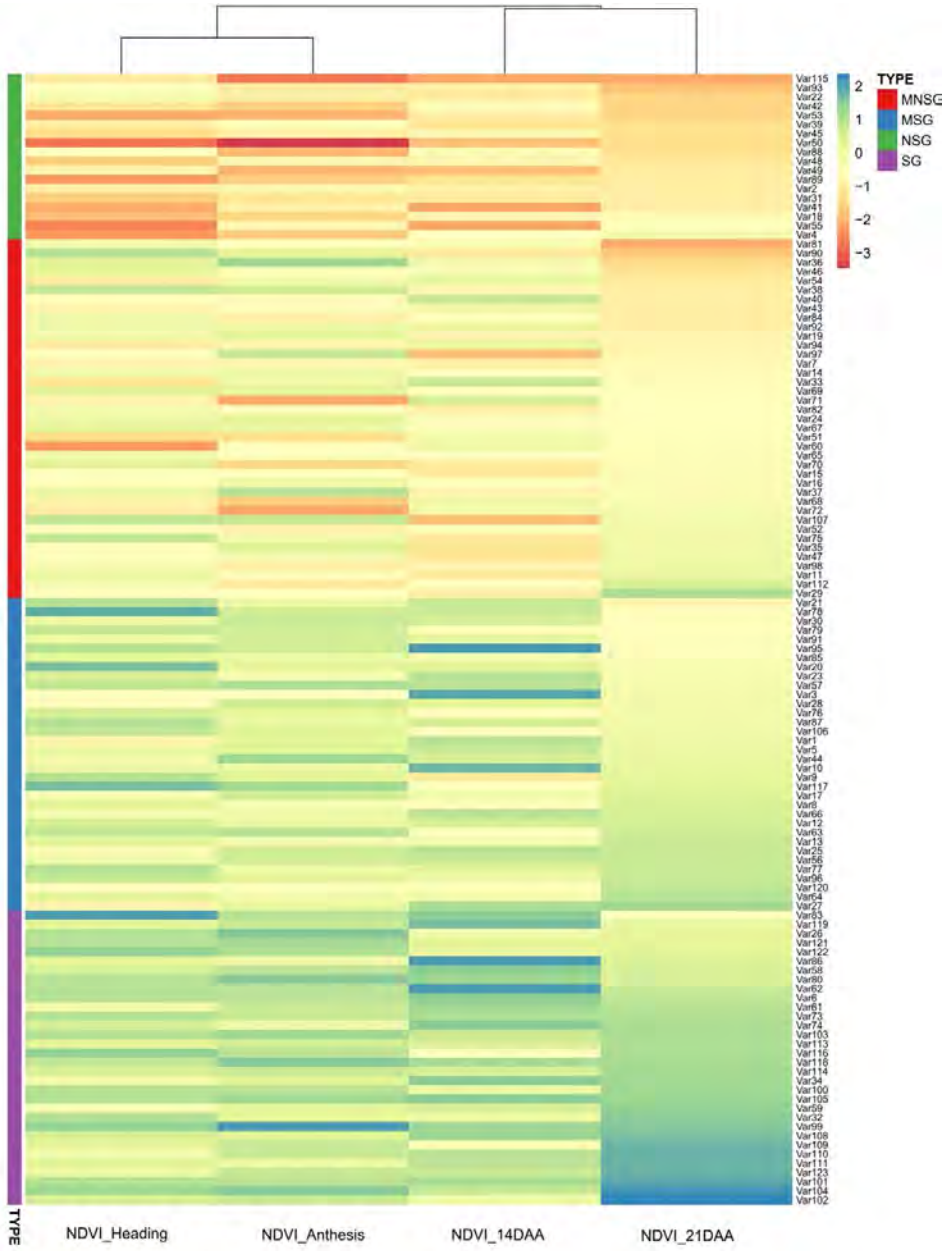

Figure 3.1. Heatmap depicting the normalized difference vegetative index (NDVI) in the non-stay-green (NSG), moderately non-stay-green (MNSG), moderately stay-green (MSG), and stay-green (SG) genotypes at different developmental stages under control condition. The blue color represents the maximum value for the NDVI and the red color indicates the minimum value for the NDVI.

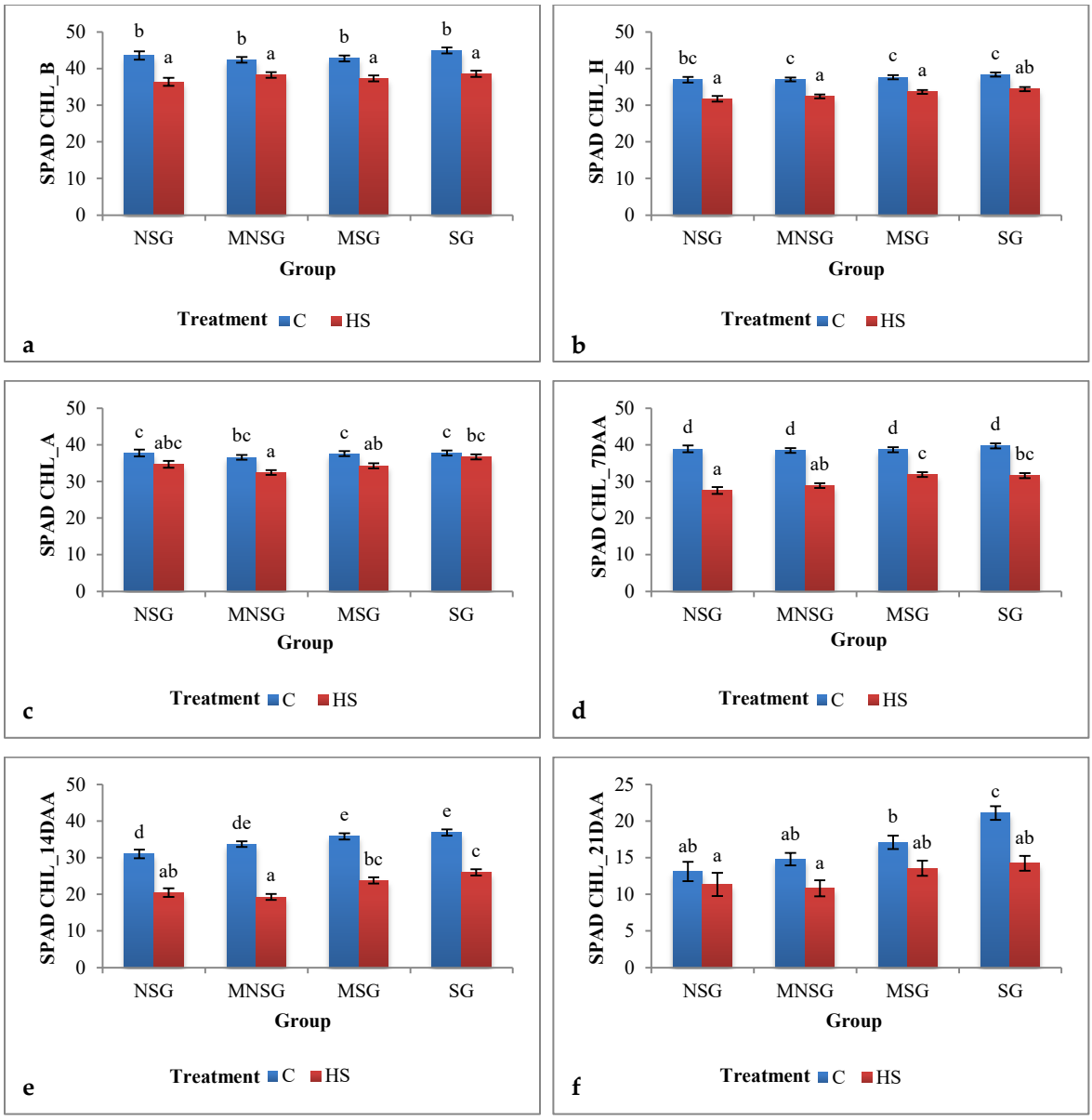

Figure 3.2. Chlorophyll content (CHL) in the non-stay-green (NSG), moderately non-stay-green (MNSG), moderately stay-green (MSG), and stay-green (SG) groups under control (C) and heat stress (HS) conditions. (a) Chlorophyll content at booting; (b) chlorophyll content at heading; (c) chlorophyll content at anthesis; (d) chlorophyll content at seven days after anthesis (7DAA); (e) chlorophyll content at 14 days after anthesis (14DAA); and (f) chlorophyll content at 21 days after anthesis (21DAA). Bars represent the least square means from the 2014–2015 and 2015–2016 field trails. Error bars depict the standard errors and different lowercase letters denote the significant differences among the groups and treatments at p < 0.05.

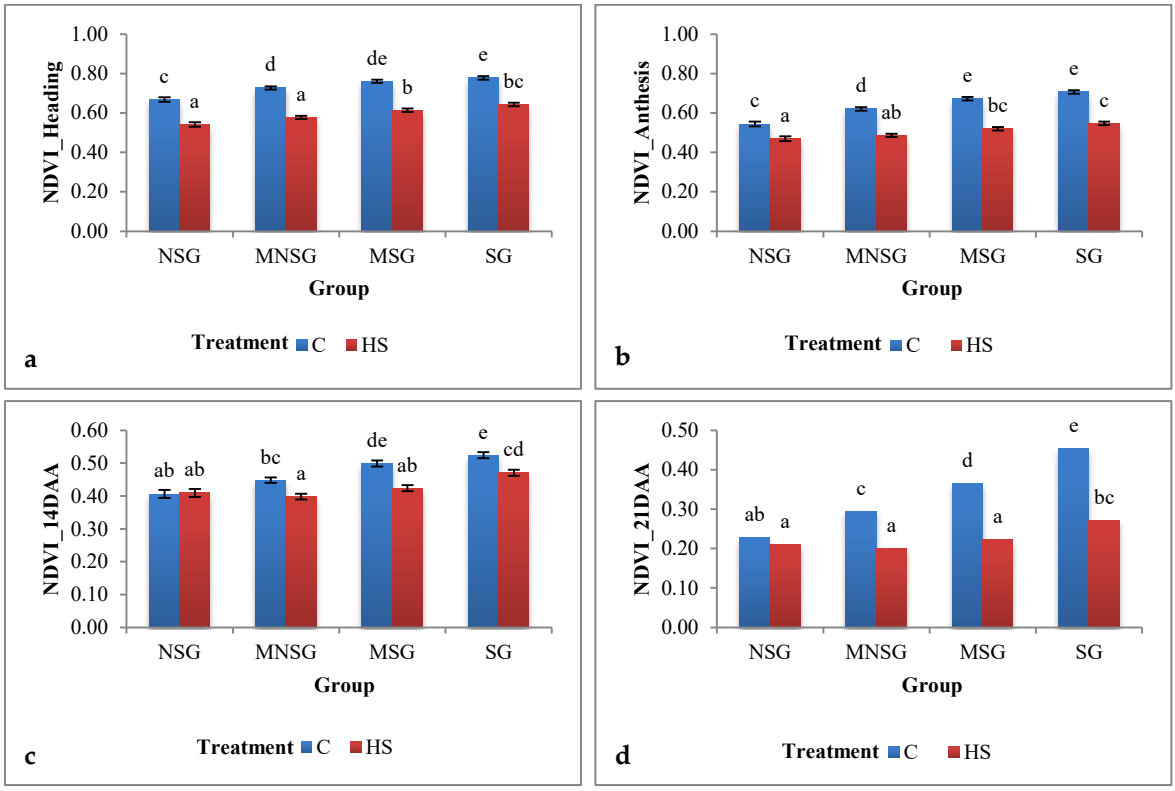

Figure 3.3. Variation in the normalized difference vegetative index (NDVI) between the non-stay-green (NSG), moderately non-stay-green (MNSG), moderately stay-green (MSG), and stay-green (SG) groups under control (C) and heat stress (HS) conditions. (a) NDVI at heading; (b) NDVI at anthesis; (c) NDVI after 14 days of anthesis; and (d) NDVI after 21 days of anthesis. Bars represent the least square means. Error bars correspond to the standard errors and the different lowercase letters signify the significant differences among the types and treatments at $p < 0.05$.

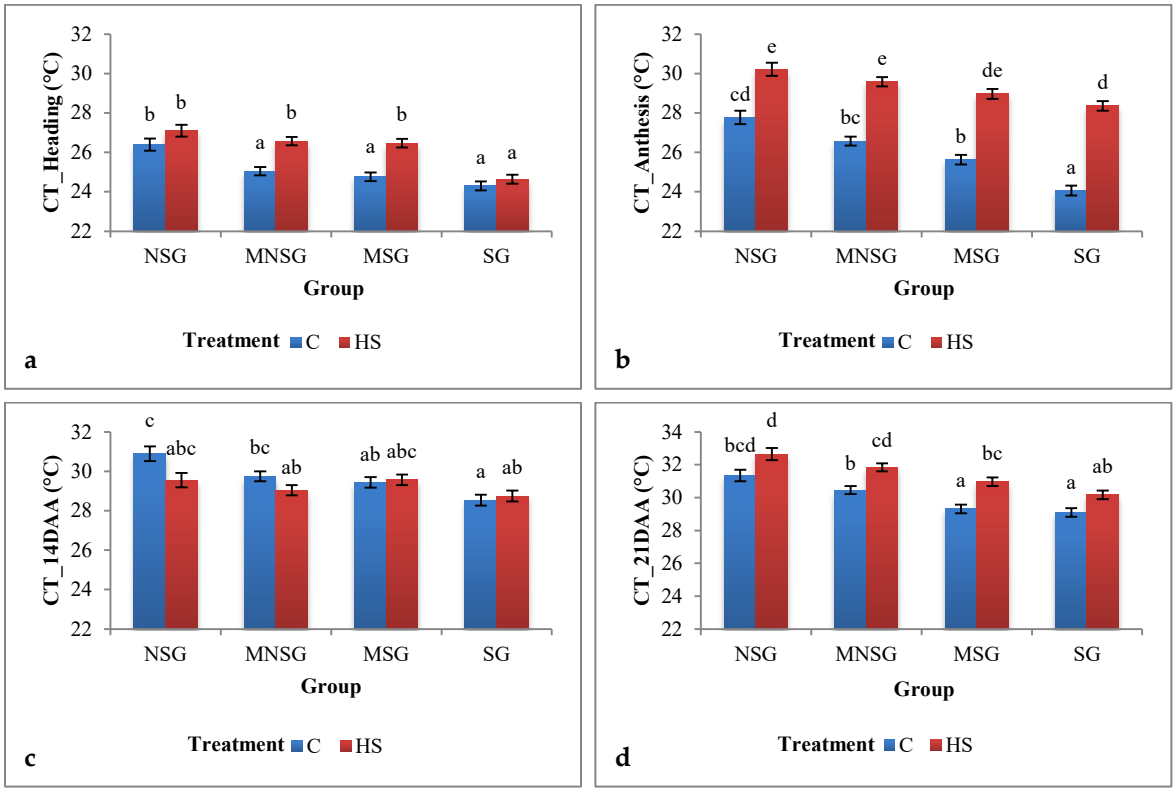

Figure 3.4. Variation in the canopy temperature (CT) among the non-stay-green (NSG), moderately non-stay-green (MNSG), moderately stay-green (MSG), and stay-green (SG) groups under control (C) and heat stress (HS) conditions. (a) Canopy temperature at heading; (b) canopy temperature at anthesis; (c) canopy temperature after 14 days of anthesis; and (d) canopy temperature after 21 days of anthesis. Bars represent the least square means. Error bars signify the standard errors and the different lowercase letters represent the significant differences among the groups and treatments at $p < 0.05$.

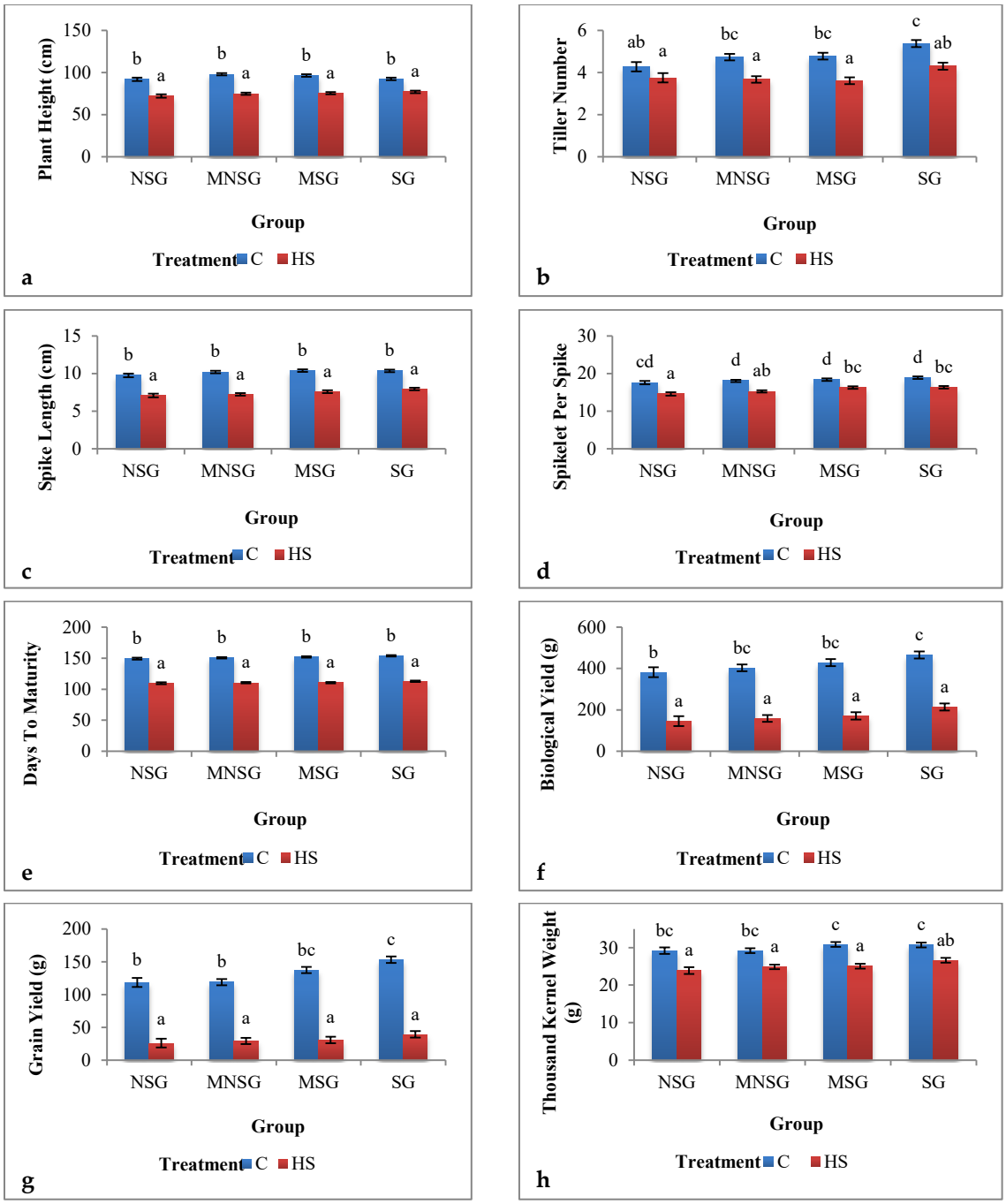

Figure 3.5. Variation in the morphological traits between the non-stay-green (NSG), moderately non-stay-green (MNSG), moderately stay-green (MSG), and stay-green (SG) groups under control (C) and heat stress (HS) conditions. (a) Plant height; (b) tiller number; (c) spike length; (d) spikelet per spike; (e) days to maturity; (f) biological yield; (g) grain yield; and (h) thousand kernel weight. Bars represent the least square means from the 2014–2015 and 2015–2016 field experiments. Error bars depict the standard errors and different lowercase letters representing significant differences among the groups and treatments at $p < 0.05$.

3.4.1.2. Greenhouse experiment

Physiological traits

The chlorophyll content decreased in the non-stay-green genotype after seven days from anthesis and the value declined with an increase in duration under high temperature stress. In the non-stay-green genotype, the decline in chlorophyll content was 25% and 85% after seven and fourteen days from anthesis, respectively, whereas the functional and non-functional stay-green genotypes maintained the chlorophyll content during high temperature stress (Figure 3.6a, Annexure 3.7).

The ØII decreased in the non-stay-green and functional stay-green genotypes under heat stress treatment compared to the control. The percentage decrease observed in the non-stay-green genotype was 32% and 79% after seven and fourteen days from anthesis under high temperature stress. Whereas the functional stay-green genotype showed 6% and 15% decline in the ØII compared to the control after seven and fourteen days of heat stress (Figure 3.6b, Annexure 3.7).

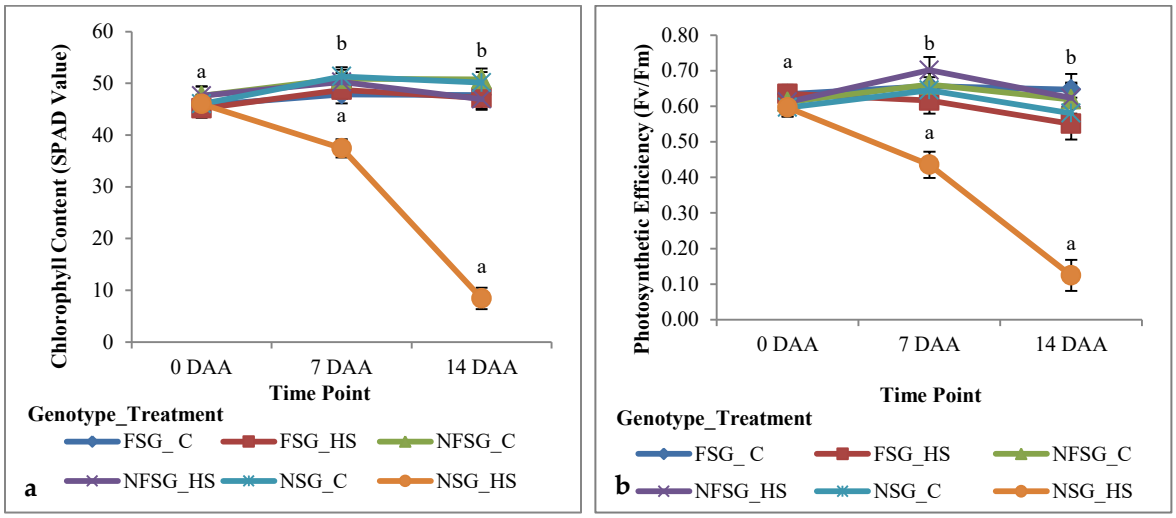

Figure 3.6. Chlorophyll content and photosynthetic efficiency in the functional stay-green (FSG), non-functional stay-green (NFSG), and non-stay-green (NSG) genotypes at 0, 7, and 14 days after anthesis under control (C) and high temperature stress (HS). (a) Chlorophyll content; and (b) photosynthetic efficiency. Line graphs represent the least square means. Error bars represent standard errors and different lowercase letters indicate the significant differences among genotypes and treatments at p < 0.05.

Biological yield and grain yield

The BY varied greatly among functional stay-green, non-functional stay-green, and non-stay-green genotypes. The BY significantly declined under terminal heat stress conditions in the non-stay-green genotype. The functional stay-green genotype showed a maximum yield under the control and stress conditions. The functional stay-green, non-functional stay-green, and non-stay-green genotypes showed 6.7%, 7%, and 52% decline in the biomass, compared to the control (Figure 3.7a, Annexure 3.7).

The GY varied significantly among all the genotypes. The functional stay-green genotype showed a maximum yield under the control and stress conditions. The percentage reduction in the GY was 4%, 5%, and 59% in the functional stay-green, non-functional stay-green, and non-stay-green genotypes, respectively, under high temperature stress (Figure 3.7b, Annexure 3.7).

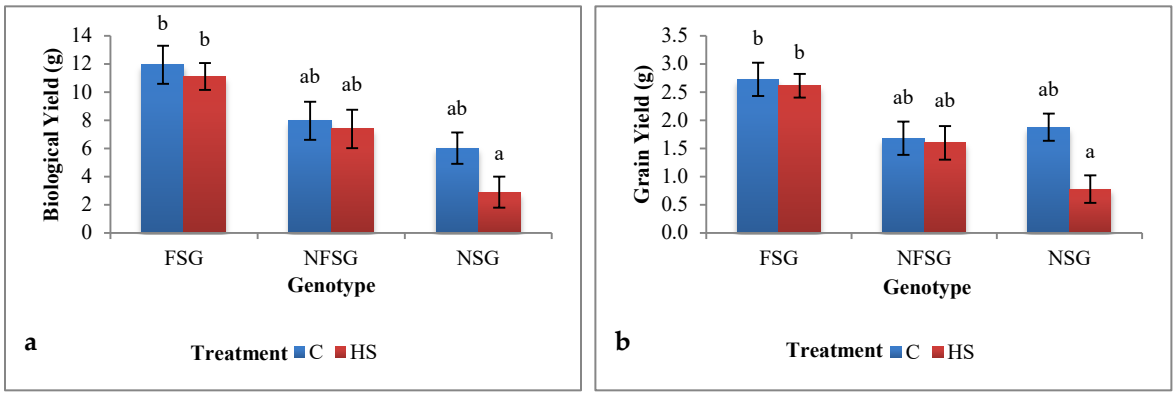

Figure 3.7. Biological yield and grain yield of the functional stay-green (FSG), non-functional stay-green (NFSG), and non-stay-green genotypes (NSG) under control (C) and terminal heat stress (HS) conditions. (a) Biological yield; and (b) grain yield. Bars represent the least square means and the error bars refer to the standard errors. Different lowercase letters represent significant difference among the genotypes and treatments at p < 0.05.

3.4.2. Genotyping

3.4.2.1. Identification of CaO, Cab, SGR, and RCCR in the wheat genome

The CaO, Cab, SGR, and RCCR in *Triticum aestivum* consisted of nine exons of 1653 bp, a single exon of 800 bp, three exons of 843 bp, and two exons of 1002 bp, respectively, as coding regions. The coding regions and protein sequences of CaO, Cab,

SGR, and RCCR in *Triticum aestivum*, *Brachypodium distachyon*, *Hordeum vulgare*, *Oryza sativa*, *Sorghum bicolor,* and *Zea mays* showed a high degree of homology (Table 3.1).

Table 3.1. Homology in the coding regions and amino acid sequences of chlorophyllide a oxygenase (CaO), light-harvesting complex (Cab), stay-green (SGR), and red chlorophyll catabolite reductase (RCCR) in Triticum aestium, Brachypodium distachyon, Hordeum vulgare, Oryza sativa, Sorghum bicolor, and Zea mays.

Gene	Plant	*Triticum aestivum*		*Brachypodium distachyon*		*Hordeum vulgare*		*Oryza sativa*		*Sorghum bicolor*		*Zea mays*	
		cDNA	Protein	*cDNA*	Protein	*cDNA*	Protein	*cDNA*	Protein	*cDNA*	Protein	*cDNA*	Protein
CaO	*Triticum aestivum*	100	100	89.53	94.73	96.98	99.45	82.24	86.85	81.67	85.4	81.3	85.03
	Brachypodium distachyon	89.53	94.73	100	100	89.66	94.55	84.65	88.15	82.35	87.06	81.92	86.32
	Hordeum vulgare	96.98	99.45	89.66	94.55	100	100	82.31	87.04	81.55	85.58	81.06	85.21
	Oryza sativa	82.24	86.85	84.65	88.15	82.31	87.04	100	100	84.98	90.74	84.31	90.74
	Sorghum bicolor	81.67	85.4	82.35	87.06	81.55	85.58	84.98	90.74	100	100	93.49	95.57
	Zea mays	81.3	85.03	81.92	86.32	81.06	85.21	84.31	90.74	93.49	95.57	100	100
Cab	*Triticum aestivum*	100	100	92.04	95.82	94.88	98.87	90.18	90.15	91.81	91.29	90.93	91.67
	Brachypodium distachyon	92.04	95.82	100	100	91.16	96.2	86.51	91.19	88.04	91.95	87.28	91.95
	Hordeum vulgare	94.88	98.87	91.16	96.2	100	100	87.3	90.53	89.56	91.67	87.92	92.05
	Oryza sativa	90.18	90.15	86.51	91.19	87.3	90.53	100	100	90.15	92.83	89.14	92.08
	Sorghum bicolor	91.81	91.29	88.04	91.95	89.56	91.67	90.15	92.83	100	100	95.61	98.49
	Zea mays	90.93	91.67	87.28	91.95	87.92	92.05	89.14	92.08	95.61	98.49	100	100
SGR	*Triticum aestivum*	100	100	82.21	76.43	94.55	93.07	80.54	77.69	77.96	74.62	79.49	73.83
	Brachypodium distachyon	82.21	76.43	100	100	83.21	77.42	80.58	77.82	76	75	77.72	76.52
	Hordeum vulgare	94.55	93.07	83.21	77.42	100	100	81.68	77.01	78.47	73.31	79.1	72.41
	Oryza sativa	80.54	77.69	80.58	77.82	81.68	77.01	100	100	80.1	77.44	78.97	75.29
	Sorghum bicolor	77.96	74.62	76	75	78.47	73.31	80.1	77.44	100	100	87.61	82.97
	Zea mays	79.49	73.83	77.72	76.52	79.1	72.41	78.97	75.29	87.61	82.97	100	100
RCCR	*Triticum aestivum*	100	100	79.61	73.93	91.75	92.68	79.9	79.92	73.29	69.6	72.71	67.38
	Brachypodium distachyon	79.61	73.93	100	100	80.23	77.83	78.3	76.19	74.64	69.44	73.31	68.83
	Hordeum vulgare	91.75	92.68	80.23	77.83	100	100	79.45	79.51	75.73	73.17	74.92	73.66
	Oryza sativa	79.9	79.92	78.3	76.19	79.45	79.51	100	100	74.32	74.41	73.67	73.23
	Sorghum bicolor	73.29	69.6	74.64	69.44	75.73	73.17	74.32	74.41	100	100	90.59	90.66
	Zea mays	72.71	67.38	73.31	68.83	74.92	73.66	73.67	73.23	90.59	90.66	100	100

3.4.2.2. Phylogenetics of CaO, Cab, SGR, and RCCR

Phylogenetic analysis was performed using the amino acid sequences for the targeted genes from *Triticum aestivum*, *Brachypodium distachyon*, *Hordeum vulgare*, *Sorghum bicolor*, *Oryza sative,* and *Zea mays*. Phylogenetic analysis revealed a close relationship of *Triticum aestivum* and *Hordeum vulgare* for the CaO, Cab, and SGR,

whereas the maximum similarity was observed between *Triticum aestivum* and *Oryza sative* for the RCCR gene (Figure 3.8).

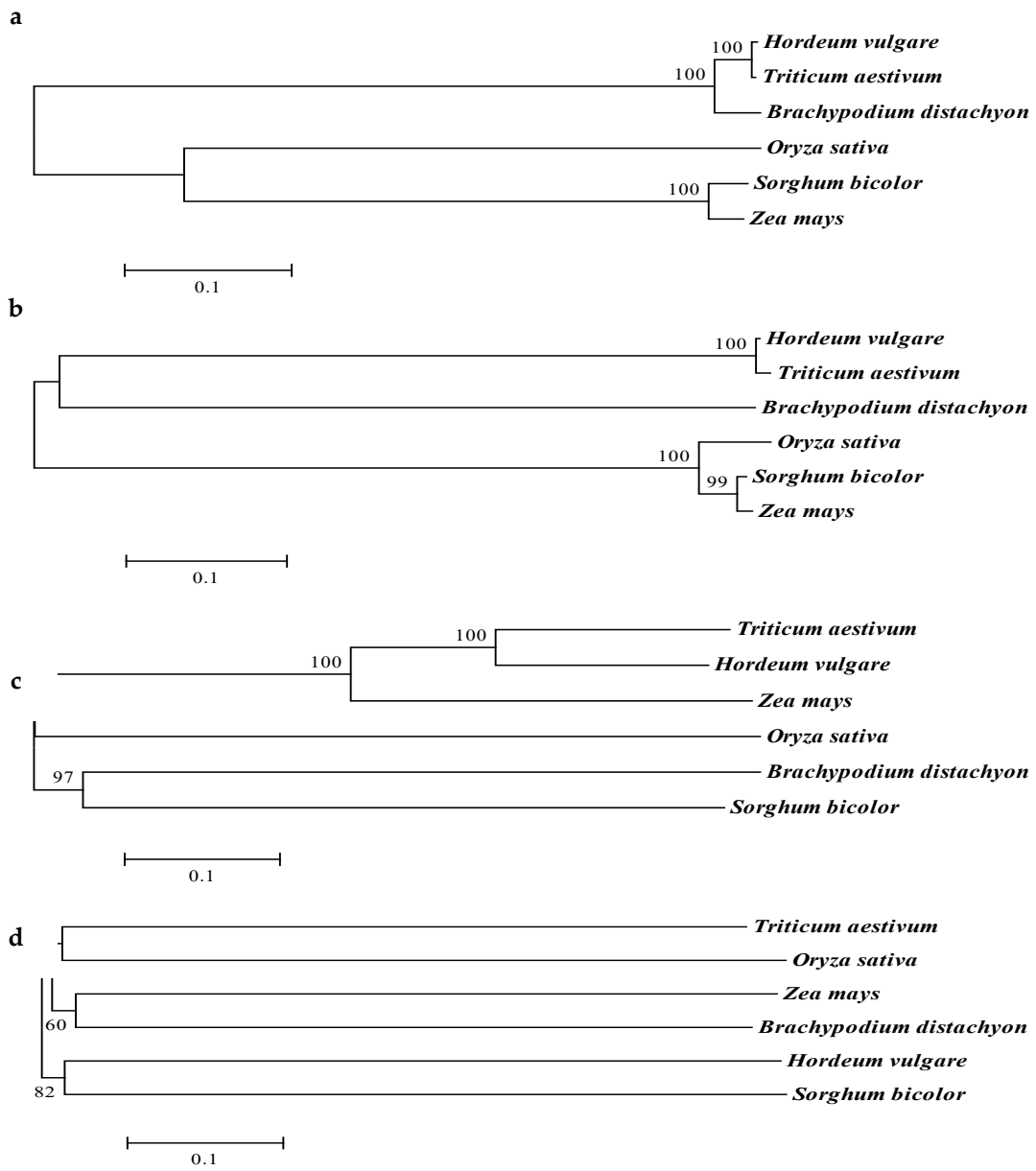

Figure 3.8. Phylogenetic analysis of the CaO, Cab, SGR, and RCCR using protein sequences from Triticum aestivum, Brachypodium distachyon, Hordeum vulgare, Sorghum bicolor, Oryza sative, and Zea mays. (a) CaO; (b) Cab; (c) SGR; (d) RCCR.

3.4.2.3. Amplification and sequencing of CaO, Cab, SGR, and RCCR

The CaO, Cab, SGR, and RCCR genes were amplified in functional stay-green, non-functional stay-green, and non-stay-green genotypes. The amplified regions were

sequenced to explore the variations in the gene sequences among functional stay-green, non-functional stay-green, and non-stay-green genotypes (Annexure 3.8, Annexure 3.9).

The partial sequences of Cab and SGR genes showed no variation between functional stay-green, non-functional stay-green, and non-stay-green genotypes. The CaO gene revealed a single nucleotide variation in the non-stay-green genotype where cytosine was replaced by guanine at the position 292 of exon 8. This resulted in a change in amino acid sequence at the position 489 where glutamic acid was replaced by aspartic acid in the non-stay-green genotype. The partial RCCR gene sequence revealed great variation. The amino acid sequence of RCCR showed variations at position 204 (valine is replaced by alanine), 264 (alanine is replaced by glycine), 275 (valine is replaced by glycine), and 290 (lysine is replaced by arginine) in the functional stay-green and non-stay-green genotypes.

3.4.2.4. Expression analysis of CaO, Cab, SGR, and RCCR under terminal heat stress

Expression profiling in relation to the stay-green trait was performed using functional stay-green, non-functional stay-green, and non-stay-green genotypes. Expression profiling was done at anthesis, 7DAA, and 14DAA in the control and heat-treated samples with three biological replicates and three technical replicates. The amplification efficiency for the Actin2, CaO, Cab, SGR, and RCCR genes primers were found between 91 and 103.9%.

The expression pattern of the CaO gene revealed a significant relation with the stay-green trait. In the functional stay-green genotype, an up-regulation of the CaO gene was observed at 7DAA. However, the relative abundance of the gene transcript was reduced till 14DAA. In the non-functional stay-green genotype, the gene transcript slightly increased at 14DAA. The non-stay-green genotype showed a significant decrease in the log2 fold change of the CaO gene at 7DAA under terminal heat stress condition (Figure 3.9a).

The expression pattern of the Cab gene also showed significant relation with the stay-green trait. The log2 fold change of the Cab gene revealed a decrease in the relative abundance of the gene transcript among all the genotypes. However, the decrease was more pronounced in the non-stay-green genotype at 7DAA (Figure 3.9b).

The expression analysis of the SGR gene revealed an increase in the gene transcript among all the genotypes under heat stress treatment. There was a constant increase in the SGR gene transcript in the functional stay-green and non-stay-green genotypes, whereas an increase in the expression of the SGR gene in non-functional stay-green was more obvious after 7 days of anthesis (Figure 3.9c).

Expression analysis depicted an up-regulation of the RCCR gene in functional stay-green, non-functional stay-green, and non-stay-green genotypes. The relative abundance of the gene transcript increased consistently after day 7 and 14 of anthesis in the functional stay-green genotype. In non-functional stay-green and non-stay-green genotypes, an increase in the expression of RCCR gene was more evident at 7DAA (Figure 3.9d).

3.5. Discussion

Global temperature is predicted to increase by 3 °C to 5 °C by the end of the 21st century (Mile and Liffey, 2018). The increasing global temperature is of major concern to sustainable agriculture. High temperature stress adversely affects plant productivity, particularly when it occurs during reproductive and grain filling period of the plant life cycle (Wollenweber *et al*., 2003; Farooq *et al*., 2011). The stay-green trait has been considered as a mechanism of tolerance to terminal heat stress. Since crop productivity is related to the duration and rate of senescence, it is expected that stay-green genotypes with longer grain-filling duration and a faster grain filling rate can sustain productivity under stress (Kumari *et al*., 2013). Studies have reported the association of the stay-green trait with better performance in wheat under terminal heat stress (Reynolds *et al*., 2000; Kumari *et al*., 2013; Pinto *et al*., 2016). In the present study, the germplasm consisting of land races, green revolution, post green revolution, elite genotypes, and synthetic derivatives was categorized into non-stay-green, moderately non-stay-green, moderately stay-green, and stay-green groups on the basis of the NDVI. The use of the Green-seeker to measure the NDVI is a high throughput approach that has been used for the precise quantification of the stay-green trait in recent years. It offers an integrated measure of the

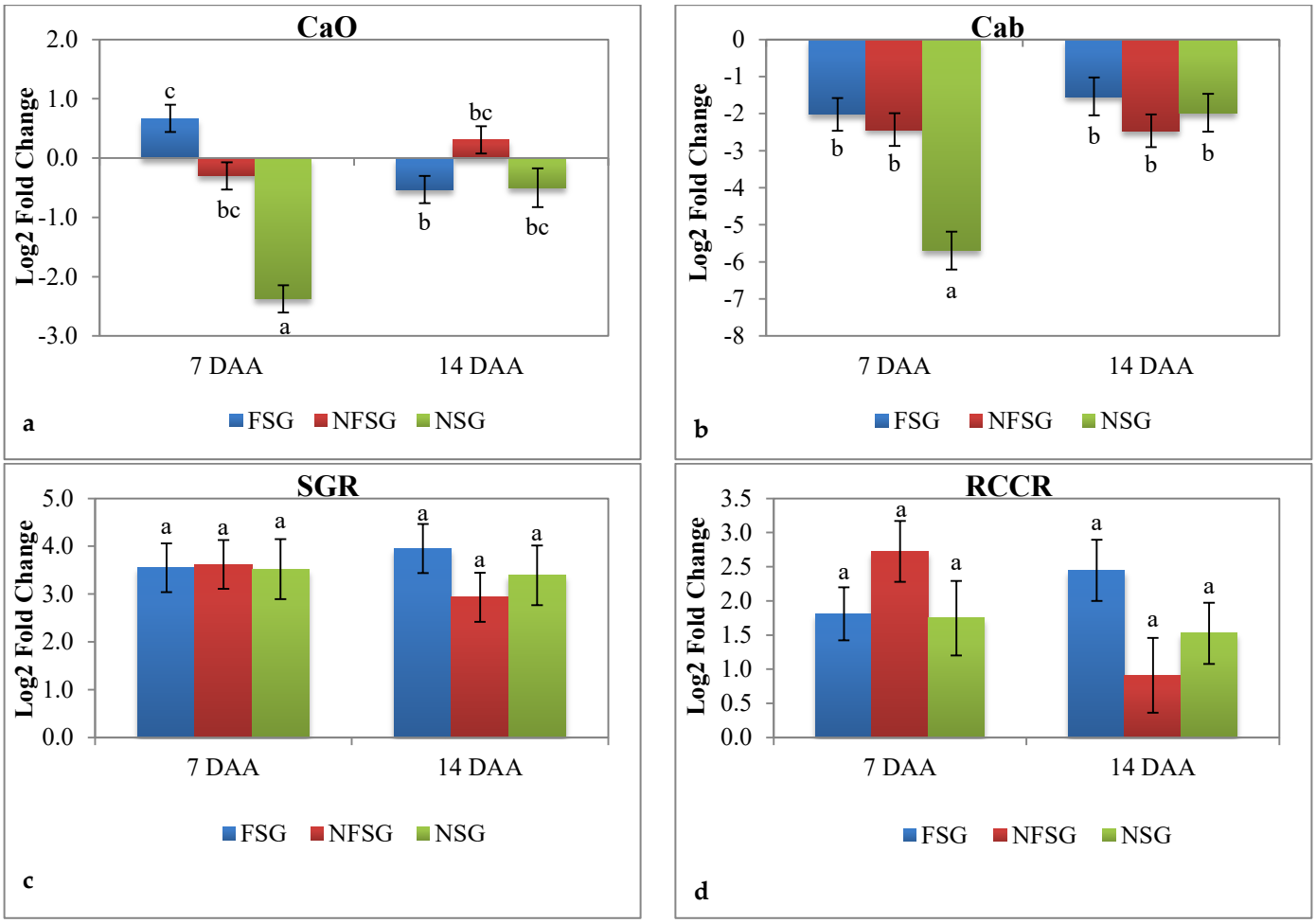

Figure 3.9. Fold change in the relative abundance of the CaO, Cab, SGR, and RCCR gene transcripts among functional stay-green (FSG), non-functional stay-green (NFSG), and non-stay-green (NSG) genotypes under terminal heat stress. FSG: functional stay-green (Nepal-38), NFSG: non-functional stay-green (SG-30), and NSG: non-stay-green (Sonalika). (a) Expression pattern of CaO; (b) expression pattern of Cab; (c) expression pattern of SGR; and (d) expression pattern of RCCR. Bar represents the least square mean of the log2 fold change using three biological and three technical replicates. The error bars refer to the standard errors and the different lowercase letters represent significant difference among the genotypes at p < 0.05.

total canopy greenness including leaves, stems, and spikes (Lopes and Reynolds, 2012; Pinto *et al*., 2016; Christopher *et al*., 2018a). The Chlorophyll meter and visual scoring were also used to measure the stay-green trait (Harris *et al*., 2007; Kumar *et al*., 2010), but these approaches are more subjective. The current study demonstrated the response of non-stay-green, moderately non-stay-green, moderately stay-green, and stay-green genotypes to the terminal heat stress under field conditions. The PH, Til No, SL, SpS,

chlorophyll content, NDVI, GY, BY, and TKW significantly declined, whereas CT increased under high temperature stress among all the groups, several previous studies also reported a reduction in chlorophyll content, Til No, kernel weight, shoot, and grain mass under high temperature stress (Viswanathan and Khanna-Chopra, 2001; Mohammadi *et al*., 2004; Shah *et al*., 2005). However, genotypes depicting the stay-green trait showed significantly high chlorophyll content, NDVI, GY, BY, TKW, and low CT under control and terminal heat stress treatments. A study by Pinto and coworkers also revealed a positive association of the stay-green trait with yield, TKW, and low CT in wheat under terminal heat stress (Pinto *et al*., 2016). The association of the stay-green trait with low canopy temperature confirms a link between stay-green expression, roots, and gas exchange, whereas a high value of canopy temperature in non-stay-green genotypes is an indicator of low evaporative cooling that is linked with low stomatal conductance and gas exchange. Christopher *et al*., (2018b) proposed that stay-green genotypes can extract extra moisture late in the season which confers a yield advantage.

The greenhouse experiment was conducted to elucidate the stay-green trait in functional stay-green, non-functional stay-green, and non-stay-green genotypes under terminal heat stress. Chlorophyll content and photosynthetic efficiency significantly declined in the non-stay-green genotype after seven days from the anthesis, whereas the functional stay-green and non-functional stay-green genotypes showed negligible variations. Thomas and Ougham, (2014) attributed the retention of greenness and photosynthetic efficiency in the functional stay-green genotypes to yield improvement. In the present study, the maintenance of the chlorophyll content and photosynthetic efficiency resulted in increased BY and GY in the functional stay-green genotype under the control and heat stress treatments. Despite the increased chlorophyll content and photochemical efficiency in the non-functional stay-green genotype, the low BY and GY can be presumed to be due to the disruption in nutrient assimilation or yield improvement locus on the chromosome seven of wheat that was not linked with the stay-green phenotype (Pinto *et al*., 2016). Whereas the functional stay-green trait may be controlled by quantitative trait loci (QTLs) that are common for stay-green, yield, and yield components (Pinto *et al*., 2016). The present study also confirmed that the reduction in

photosynthetic efficiency was proportional to the yield reduction in the functional stay-green, non-functional stay-green, and non-stay-green genotypes under terminal heat stress.

The genetic basis behind the stay-green trait is complex and varies in different plant species. The multi-protein complex that includes chlorophyll catabolic enzymes, stay-green protein, and the light-harvesting complex protein is considered to be associated with the stay-green trait (Sakuraba *et al*., 2012). In the present study, selected chlorophyll catabolism and photosynthetic responsive genes were analyzed. The cDNA and protein sequences of CaO, Cab, SGR, and RCCR obtained from *Triticum aestivum*, *Brachypodium distachyon*, *Hordeum vulgare*, *Oryza sativa*, *Sorghum bicolor,* and *Zea mays* showed a high degree of percentage similarity. A previous study by Mueller and coworkers showed great percentage similarity in the amino acid sequences of CaO in *Hordeum vulgare*, *Arabidopsis thaliana*, *Brachypodium distachyon,* and *Oryza sativa* (OsCaO 1, OsCaO2) (Mueller *et al*., 2012). Xiao and coworkers showed high sequence homology between the RCCR gene sequences from *Solanum lycopersicum*, *Nicotiana tabacum*, *Vitis vinifera*, *Ricinus communis*, *Fragaria vesca* subsp vesca, *Brassica napus,* and *Arabidopsis thaliana* (Xiao *et al*., 2015). High sequence homology suggests that the genes are highly conserved during evolution *(*Park *et al*., 2007). The present study also revealed the partial gene sequences and amino acid sequences of CaO, Cab, SGR, and RCCR in functional stay-green, non-functional stay-green, and non-stay-green genotypes. The CaO and RCCR sequences showed few variations. These sequence variations need to be explored in the complete germplasm to be used as potential biomarkers for the marker-assisted selection for the stay-green trait in wheat. The expression pattern of CaO, Cab, SGR, and RCCR at 0DAA, 7DAA and 14DAA was determined in functional stay-green, non-functional stay-green, and non-stay-green genotypes. The expression profiling of the CaO gene showed significant relation with the stay-green trait. The CaO gene was up-regulated in the functional stay-green genotype and down-regulated in the non-stay-green genotype at 7DAA. It is assumed that the increased abundance of the CaO gene transcript in the stay-green genotype was associated with delayed senescence. Sakuraba *et al*., (2012) and Kusaba *et al*., (2007) previously reported that an over expression of the CaO gene transcript can cause increased chlorophyll b accumulation and delayed senescence.

The over expression of the CaO gene in *Arabidopsis* resulted in reduced chlorophyll a:b ratio and an increased light-harvesting complex apoprotein (Tanaka *et al*., 2001). Biswal *et al*., (2012) reported the controlled up-regulation of the CaO gene that resulted in increased chlorophyll b biosynthesis and modulated the expression of several thylakoid proteins, which increased the antenna size, rate of electron transport, carbon dioxide assimilation, and dry matter accumulation. The CaO mutant pale green leaf (pgl) in rice with chlorophyll b deficiency exhibited early senescence under terminal heat stress due to the accumulation of reactive oxygen species (Yang *et al*., 2016). Expression profiling of photosynthetic responsive Cab gene depicted a reduction in gene transcript among all the genotypes under terminal heat stress. However, the decline in the expression of the Cab gene in the non-stay-green genotype was far greater compared to the functional stay-green and non-functional stay-green genotypes at 7DAA. The expression pattern of the Cab gene intriguingly correlates to the stay-green trait. The down-regulation of the LHCP genes under biotic and abiotic stresses has been reported in several studies (Seki *et al*., 2002; Hazen *et al*., 2005; Guo *et al*., 2009; Manickavelu *et al*., 2010; Wang *et al*., 2011). The up-regulation of the Cab gene is associated with increased photosynthetic capacity (Fan *et al*., 2017). In the present study, the expression analysis of SGR showed non-significant variation between the genotypes. However, the up-regulation of the SGR gene was observed among all the genotypes under terminal heat stress. The expression profiling before day seven of heat stress may illustrate the role of the SGR gene in functional stay-green, non-functional stay-green, and non-stay-green genotypes. Park *et al*., (2007) revealed an increase in chlorophyll degradation with the increase in SGR expression. Moreover, it has been reported previously that the number of SGR genes varies among species and homologous SGR genes are not always associated with yellowing. In *Arabidopsis*, SGR1 over expression promoted leaf yellowing, whereas SGR2 over expression caused the stay-green phenotype (Sakuraba *et al*., 2015). The current study revealed an up-regulation of the RCCR gene among all the genotypes under heat stress, whereas no significant variation was observed between the genotypes. The increase in the relative abundance of the gene transcript was more pronounced in the non-functional stay-green type at 7DAA and in the functional stay-green genotype at 14DAA. CaRCCR gene up-regulation under biotic and abiotic stresses had been previously

reported by Xiao *et al*., (2015). The up-regulation of the RCCR gene is associated with the defense responses in plants under stress conditions (Xiao *et al*., 2015). The present study demonstrated that the expression pattern of CaO and Cab at 7DAA is proportional to the increase/decrease in the chlorophyll content and photosynthetic capacity in functional stay-green, non-functional stay-green, and non-stay-green genotypes under terminal heat stress.

3.6. Conclusion

The present study proposed an integrated way to classify a large set of genotypes into non-stay-green, moderately non-stay-green, moderately stay-green, and stay-green types on the basis of the NDVI values recorded between heading and maturity. All the morpho-physiological traits showed significant variations among non-stay-green, moderately non-stay-green, moderately stay-green, and stay-green types under control and heat stress treatments. The genotypes characterized into the stay-green type depicted high chlorophyll content, NDVI, GY, BY, and TKW and low CT under control and heat stress conditions. The study also revealed the response of functional stay-green, non-functional stay-green, and non-stay-green genotypes to terminal heat stress. Chlorophyll content and photochemical efficiency was retained for a longer duration under control and heat stress treatments in both functional stay-green and non-functional stay-green, however non-functional stay-green genotype showed shriveled grains. Thus, unraveling a non-functional stay-green type in which chlorophyll content and photosynthetic efficiency was maintained but nutrient assimilation was considered to be disrupted. The percentage reduction in biological yield and grain yield under stress corresponded to the decline in chlorophyll content and photosynthetic efficiency. The partial gene sequences of CaO and RCCR; and the expression profiling of CaO and Cab revealed significant variations between functional stay-green, non-functional stay-green, and non-stay-green genotypes. Collectively, results indicate that the stay-green phenotype can significantly mitigate the harmful aspects of the terminal heat stress by sustaining grain yield and biological yield.

Chapter #4

Ultra-High-Performance Liquid Chromatography-High Resolution Mass Spectrometry based Untargeted Global Metabolic Profiling for Stay-Green Trait in Triticum aestivum L. under Terminal Heat Stress

Chapter #4

Ultra-High-Performance Liquid Chromatography-High Resolution Mass Spectrometry Based Untargeted Global Metabolic Profiling for Stay-green Trait in *Triticum aestivum* L. under Terminal Heat Stress

4.1. Abstract

Genetic improvement for heat tolerance required elucidation of biochemical processes associated with different stress tolerance mechanisms. During the recent decade, the stay-green trait has received substantial attention from crop breeders owing to the potential of increasing crop productivity under rapid warming scenario. The present study aimed to demonstrate the metabolic regulation of the secondary stay-green trait using stay-green and non-stay-green genotypes under control and heat stress treatments by employing Ultra-High-Performance Liquid Chromatography High-Resolution Mass Spectrometry (UHPLC-HRMS). Plants grown under control greenhouse conditions (24/18 ºC day/night temperature) were exposed to heat stress (36/28 ºC day/night temperature) at anthesis, morpho-physiological traits that included chlorophyll content, chlorophyll fluorescence, membrane stability index, biological yield, and grain yield were evaluated, and flag leaves tissues were harvested at day seven and day fourteen after imposition of heat stress for metabolic profiling. Chlorophyll fluorescence, membrane stability index, and biological yield significantly declined under heat stress; however decline was more pronounced in the non-stay-green genotype. Untargeted metabolic profiling detected 6,945 features from positive ion mode and 5,586 features from negative ion mode. Of the total detected features, 166 significant known metabolites were identified by Analysis of Variance, Partial Least Squares Discriminant Analysis, and Significant Analysis of Metabolites. The predominant metabolites that showed significant high accumulation in non-stay-green genotype were deoxyuridine, deoxycytidine, 5'-deoxyadenosine, glycyl-L-leucine, leucyl-proline, cytidine, uridine, isocytosine and adenine, whereas the dominant metabolites that showed high accumulation in stay-green genotype were ADP, phosphocholine, glutathione, 2-phosphoglyceric acid, cADPR, allantoin, trigonelline, syringic acid, spermine, and hexanesulfonic acid sulfate under control and heat stress treatments. Both non-stay-green and stay-green genotypes showed increase in

accumulation of 5-hydroxy-L-tryptophan, L-kynurenine, and L-pipecolic acid and decrease in accumulation of 2-phosphoglyceric acid, shikimate, and spermidine under heat stress, however the levels varied between genotypes. Fifty five metabolic pathways have been identified where significant known metabolites were involved. The variation in the levels of myriad of metabolites in non-stay-green and stay-green genotypes under control and heat stress conditions highlighted variable metabolic adjustment in stay-green genotype that reduce heat impacts.

4.2. Introduction

Hexaploid bread wheat (*Triticum aestivum* L.) is the third most important cereal crop after maize and rice with 745.26 million tonnes of average annual global production from an average cultivated area of 219.008 million hectares from 2014 to 2018 (www.fao.org/faostat/ en/#data/QC/visualize). Hexaploid bread wheat contributes to global food security by supplying carbohydrates, proteins, vitamins, dietary fibers, and phytochemicals to 21% of the world population (Shewry and Hey, 2015; FAO, 2015; Enghiad *et al*., 2017). The drastic climate change is haunting global food security by limiting sustainable agriculture (Campbell *et al*., 2016; Lesk *et al*., 2016; Daryanto *et al*., 2016). Approximately 40% of the irrigated areas under wheat cultivation is being affected by heat stress (Reynolds *et al*., 2001) and it is projected that yield losses can reach to 63 to 83% under rapid warming scenario till the end of 21st century (Schlenker and Roberts, 2009). High temperature stress induces oxidative damage that leads to lipid peroxidation, protein degradation, and enzyme inactivation in turn influencing the stability of thylakoid membrane by increasing membrane fluidity, decrease chlorophyll content by disruption of chlorophyll structure, reduce photosynthesis by diminishing rubisco activity, and decrease leaf relative water content by increasing transpiration rate, pH of leaf sap, and abscisic acid production (Sairam *et al*., 2000; Wilkinson and Davies, 2002; Dias and Lidon, 2009). These changes in the notably complex physiological processes of plant causes reduce germination rate, lessen days to anthesis and maturity, fewer spikelets/spike, slower pollen growth, reduced pollen fertility, sterile grains, abnormal ovary development, reduce seed setting, decrease in thousand kernel weight, shriveled grains, reduce starch accumulation, and alter starch lipid composition in grains

(Balla *et al*., 2012; Balla *et al*., 2019). The genetic improvement for heat tolerance required mining and breeding of superior germplasm that can adapt to future changing climate (Stratonovitch and Semenov, 2015). During the recent decade, the stay-green trait has received substantial attention from crop breeders owing to the potential of increasing crop productivity together with a dramatically shrunken environmental footprint.

Stay-green refers to mutants, transgenic plants, or cultivars with the trait of heritable impeded foliar senescence compared with wild type or reference genotype (Thomas and Stoddart, 1975; Thomas and Howarth, 2000; Thomas and Ougham, 2014). The stay-green genotypes are broadly classified into functional stay-green (Type-A and Type-B) and non-functional stay-green (Type-C, Type-D, and Type-E) depending on the performance of photosynthesis (Thomas and Howarth, 2000; Jiang *et al*., 2004; Park *et al*., 2007; Ho¨rtensteiner, 2009; Thomas and Ougham, 2014). The former is the target of plant breeders (Pinto *et al.*, 2016), as the functional stay-green genotypes have the potential to retain chlorophyll content and photosynthetic capacity, delay canopy development phase from carbon capture to nitrogen remobilization, and improve plant productivity (Thomas and Ougham, 2014). A functional type stay-green in sorghum (Borrell and Hammer, 2000), rice (Yoo *et al*., 2007; Fu and Lee, 2008), maize (Echarte *et al*., 2008) and wheat (Spano *et al*., 2003) revealed a direct relationship of stay-green trait with grain yield. Stay-green trait has been associated with better performance under abiotic and biotic stresses such as water deficit (Borrell *et al*., 2014; Christopher *et al*., 2016; George-Jaeggli *et al*., 2017; Kamal *et al*., 2018), high temperature (Kumari *et al*., 2007; Pinto *et al*., 2016), stem lodging (Rosenow *et al*., 1983a), and spot blotch infection (Josh *et al*., 2007). Little is known of the biochemical regulation of the complex stay-green trait. The core biochemical profiling of the stay-green genotypes might deepen our understanding of the stay-green trait.

The term metabolomics coined in late 1990s (Fiehn, 2002), refers to the study of unique chemical fingerprints that includes primary and secondary metabolites in a complex sample matrix associated with cellular processes (Weston *et al*., 2015). Currently, the foremost approaches used in metabolomics are targeted analysis, metabolic

fingerprinting, and metabolite profiling (Fiehn, 2002; Halket *et al*., 2005; Shulaev, 2006). With the advent of metabolite profiling, a complete set of metabolites can be measured simultaneously using multiply analytical techniques that includes Nuclear Magnetic Resonance Spectroscopy, Gas Chromatography-Mass Spectrometry, Liquid Chromatography-Mass Spectrometry, Capillary Electrophoresis-Mass Spectrometry and Fourier Transform Infrared Spectroscopy (Sumner *et al*., 2003; Shulaev, 2006; Roessner and Bacic, 2009; Sawada and Hirai, 2013). The application of highly sensitive and selective high throughput Liquid Chromatography-Mass Spectrometry in metabolomics is increasing with the adoption of the Ultra-High-Performance Liquid Chromatography technology that has spectacularly increased the separation efficiency and decreased the analysis time (Granger *et al*., 2007). Indubitably the untargeted high throughput metabolic analysis with advanced biochemical detection techniques have made possible to study the global view of metabolism bridging the major knowledge gaps in understanding the dynamic interactions in plant stress associated metabolism (Weckwerth 2003; Kaplan *et al*., 2004).

Plant kingdom thought to contain between 2,00,000 to 10,00,000 metabolites, with an array of approximately 5,000 metabolites in a single species (Dixon and Strack, 2003; Rai *et al*., 2017; Fang *et al*., 2019; Wang *et al*., 2019b). The myriad of structurally and functionally diverse plant metabolites play a significant role in growth, development, and stress responses in plants (Wang *et al*., 2019b). The plant physiology modifies with metabolic changes under stress to adapt to a particular ecological niche (Weckwerth, 2003). Untargeted global metabolic profiling under post anthesis heat stress in wheat revealed a considerable increase in the levels of L-tryptophan, pipecolate, alpha-aminoadipate, L-arginine, L-histidine, and piperidine, whereas decline in drummondol, anthranilate, dimethylmaleate, galactoglycerol, guanine, and glycerone (Thomason *et al*., 2018). Soybean showed a significant decrease in the amount of glycolysis, pentose phosphate pathway, and tricarboxylic acid cycle metabolites under heat stress (Das *et al*., 2017). A study in maize found an increase in phenylalanine, alanine, gamma aminobutyric acid, threonate, xylose, galactinol, and isoleucine, whereas a decrease in glycerol, malate, glycerate, and phosphate under heat stress (Obata *et al*., 2015). So far the knowledge of metabolic regulation for the stay-green trait as a

mechanism of tolerance to terminal heat stress is lacking. Thus, comprehensive metabolic analysis of stress associate metabolism in relation to stay-green can pave the way towards understanding and successful breeding of the stress tolerant stay-green crops.

The foremost advances in the perspective of the stay-green trait expedited with the growing knowledge of leaf senescence, chlorophyll degradation, photosynthesis, and nitrogen remobilization (Hörtensteiner and Kräutler, 2011; Gregersen, 2011; Breeze *et al*., 2011; Guo and Gan, 2012; Guo, 2013). The functional stay-green type improves grain yield by adjourning senescence that is delaying chlorophyll degradation, carbon capture, and nitrogen remobilization and increasing photosynthesis (Thomas and Ougham, 2014). Functional stay-green trait has been associated with post-anthesis heat stress tolerance in *Triticum aestivum* (Reynold *et al*., 2000; Kumari *et al*., 2013; Pinto *et al*., 2016). However, metabolic regulation for the trait has not been explored. The objective of the current study is to demonstrate the differential accumulation of metabolites in the leaf tissues of non-stay-green and stay-green genotypes in control and heat stressed *Triticum aestivum* plants during grain filling duration to unveil the mechanism behind stay-green trait in relation to heat stress tolerance. The UHPLC-HRMS based untargeted global metabolomics was deployed to identify the novel metabolites and pathways varying in non-stay-green and stay-green genotypes at different time points after anthesis under control and heat stress treatments. To our knowledge, this is the first report that unraveled inclusive metabolic profiles of non-stay-green and stay-green genotypes under control and heat stress treatments to determine the metabolic regulation underlying the stay-green trait.

4.3. Materials and methods

4.3.1. Plant materials, growth conditions, and treatments

The experiment was conducted under controlled greenhouse conditions at the Department of Agronomy, University of Florida, Gainesville, Florida. *Triticum aestivum* L. stay-green variety Nepal-38 (CHIRYA7/ANB) and non-stay-green variety Sonalika (SASONO KOMOGI/NORIN//BOB'S') were used for the present study (Latif *et al*.,

2020). The seeds of the selected varieties were obtained from National Agricultural Research Centre, Islamabad, Pakistan. The seeds were surface sterilized using 95% ethanol for 2-3 minutes followed by soaking in 10% Clorox for 30 minutes and subsequent washes for 3 to 4 times with autoclaved distilled water (Khan *et al*., 2019a). The sterilized seeds were sown in pots filled with 2,000 g of the Metro-mix® 360 soil mixture with the sowing density of five seeds per pot and thinned to four plants per pot after germination. The experiment was laid out in a completely randomized design with six biological replicates. During the experiment, the greenhouse conditions were maintained at 24/18 ºC day/night temperature with a photoperiod of 12 hours. Heat stress was imposed at anthesis by shifting half of the plants to a growth chamber where the temperature was maintained at 36/28 ºC day/night temperature with a photoperiod of 12 hours. The set of plants in the greenhouse grown at 24/18 ºC day/night temperature served as a control. The pots were well watered throughout the experiment and a teaspoon of Osmocote (15N 9P 12K) was applied after germination and booting. Chlorophyll content, chlorophyll fluorescence (Fv/Fm ratio and performance index), membrane stability index, biological yield, and grain yield were estimated under control and heat stress conditions. For global metabolic profiling, the leaf tissues were harvested at 7 and 14 days of the heat stress treatment.

4.3.2 Physiological characterization

The data was collected for physiological traits used to measure stay-green trait and known to be affected by heat stress. Chlorophyll content and chlorophyll fluorescence (the maximum quantum yield of photosystem II, Fv/Fm=$(F_m–F_o)/F_m$ and the effective quantum yield of photosystem II, $\Phi_{PSII} = (F_m'–F')/F_m'$) were used as an indirect method to measure the damage caused to chlorophyll due to heat stress and the efficiency of photosystem II under control and heat stress treatments. The traits were measured from 0 to 14 days regularly after imposition of heat stress following the methods described by Yuan *et al*., (2016), Kuhlgert *et al*., (2016) and Prinzenberg *et al*., (2018). Leaf Chlorophyll content was determined using SPAD chlorophyll meter (Model 502, Spectrum Technologies, Plainfield, IL, USA) in both control and heat stressed flag leaves from six biological replicates. Leaf chlorophyll fluorescence [Fv/Fm (mid-night) and Phi

II (mid-day)] was measured from the flag leaves using the handheld MultispeQ beta version (www.photosynq.org) in both control and heat stressed samples. The chlorophyll content and chlorophyll fluorescence were measured from the flag leaf at three parts: 1/3 of the distance from base, 1/2 of the distance from the base, and 2/3 of the distance from base), four plants per pot (a total of 12 readings) and averaged. The average value of 12 readings is considered as single replicate, six replicates per variety were used for statistical analysis. The membrane stability index (MSI) was determined from flag leaves at 0, 7 and 14 days after imposition of heat stress according to protocol described by Sairam *et al*., (1994). Leaf samples (six leaf discs of uniform size) were placed in 25 mL of double-distilled water in two sets using six replicates for each variety. One set was kept at 40°C for 30 minutes and its conductivity (C1) was recorded using a conductivity meter. The second set was placed in a boiling water bath (100°C) for 15 minutes and conductivity (C2) was recorded using a conductivity meter. The MSI was calculated as [1-(C1/C2)] x 100.

4.3.3. Biological yield and grain yield

The plant above ground biomass (shoot and spike) was harvested, dried for 72 hours, and weighed using an electronics balance to determine the biological yield per plant. The spikes of the same plant were cut from the collar, threshed, and grain harvest obtained was weighed using an electronics balance to determine the grain yield per plant. Biological yield and grain yield were determined from six biological replicates (Pask *et al*., 2012).

4.3.4. Sample collection and preparation for metabolic profiling

Flag leaf tissues were collected during mid-day at 7 and 14 days of heat stress from both control and heat treated plants. The leaf tissues were collected from six biological replicates (six individual pots) for each variety and treatment. For sample collection, the leaf blade was washed with distilled water, incised with a sharp blade, immediately shifted to liquid nitrogen, and stored at -80ºC to prevent any degradation. The leaf tissues were lyophilized for 72 hours using FreeZone Freeze Dryer System

(Labconco) and grinded to fine powder using Qiagen TissueLyser II. The finely powdered freeze dried leaf tissues were subjected to cellular extraction procedure to obtain extract used for untargeted global metabolic profiling. For extraction, 30 mg of the lyophilized leaf samples were taken in the clean eppendorf tubes followed by addition of 20 µL of the daily internal standard mix, 750 µL of methanol, and 750 µL of 10 mM ammonium acetate to each sample. All the samples were subjected to vortex mixing for one minute which was followed by ultrasonication (20 minutes) at room temperature (20-25 ºC) and centrifugation at 17,000 g (10 minutes). The supernatant (200 µL) was transferred to a clean eppendorf tube and dried down. The dried samples were constituted in 50 µL of the internal standard solution. The samples were vortex for 30 seconds, incubated at 4 ºC (10 minutes), and centrifuged at 20,000 rpm (10 minutes). The supernatant obtained was transferred to LC vials for metabolic profiling.

4.3.5. Untargeted global metabolomic profiling using ultra-high-performance liquid chromatography-high resolution mass spectrometry

The untargeted global metabolic profiling was performed using Dionex UltiMate 3000 ultrahigh performance liquid chromatography system with thermo Q-Exactive Orbitrap mass spectrometer and an autosampler. The chromatographic separation was achieved on an ACE 18-pfp 100 x 2.1 mm, 2 µm column with 0.1% formic acid in water as mobile phase A and acetonitrile as mobile phase B at a flow rate of 350 µL/min. The column temperature was maintained at 25 ºC. All the samples were analyzed in both positive and negative heated electrospray ionization with a mass resolution of 35,000 at m/z 200 as separate injections, HESI probe temperature of 350 ºC, spray voltage of 3,500 V and capillary temperature of 320 ºC. The injection volume was 2 µL for positive ion mode and 4 µL for negative ions mode.

4.3.6. Data analysis

The raw files for both positive and negative ion modes were converted to .mzXML using MS converter ProteoWizard version 3.0. MZmine 2.15 (freeware) was used for identifying features, aligning features, deisotoping peaks to remove duplicates,

and gap filling to fill in any feature that may have been missed in the first alignment algorithm. All adducts and complexes from the data set were identified and removed. The data was searched against an internal retention time metabolite library developed by Southeast Center for Integrated Metabolomics, University of Florida. The mzMine data was exported in comma-separated values (CSV) format for statistical analysis. The data from both positive and negative ion modes were subjected to statistical analyses using MetaboAnalyst 4.0 server (https://www.metaboanalyst.ca/; Chong *et al*., 2018; Chong *et al*., 2019). To minimize the possible variance and improve statistical analysis, the data was checked for data integrity, filtered by interquartile range (IQR) and normalized to the sum of metabolites for each sample by selecting normalization by sum, log transformation, and autoscaling. Univariate analysis was performed by Analysis of Variance (ANOVA) using Tukey‘s HSD (Honestly Significant Difference) post-hoc analysis with adjusted p-value cutoff 0.05 to identify the significant metabolites and fold change analysis to unravel variations in the levels of metabolites between groups [SG_C1/NSG_C1, SG_T1/NSG_T1, SG_C2/NSG_C2, SG_T2/NSG_T2, NSG_T1/NSG_C1, NSG_T2/NSG_C2, SG_T1/SG_C1, and SG_T2/SG_C2 (where SG= Stay-green, NSG= Non-stay-green, C= Control, T= Heat stress treatment, 1= day 7 of heat stress, 2= day 14 of heat stress)]. Multivariate analysis was performed using a supervised method Partial Least Squares Discriminant Analysis (PLS-DA) and an unsupervised method hierarchical clustering by heatmap. The PLS-DA identified the important metabolites on the basis of variable importance in projection scores using five component model. A heat map was generated by Pearson distance measure and Ward clustering algorithm for the top 30 features selected by PLS-DA. The Significant Analysis of Metabolites (SAM) plot with delta value 0.8 and false discovery rate (FDR) 0.000431 was used to identify the most significant features. Collectively, the important metabolites were identified by ANOVA, PLS-DA, and SAM.

The pathway analysis was performed for the significant metabolites using *Oryza sativa* japonica (Japanese rice) (KEGG) library by Metaboanalyst 4.0. Kyoto Encyclopedia of Genes and Genomes (KEGG) pathway database (http://www.genome.ad.jp/kegg/pathway.html) was used to generate pathways.

Phenotypic data was analyzed using XLSTAT 2014.5.03. ANOVA was performed using Tukey Honest Significant difference to determine the level of statistical significance between groups (varieties and treatments).

4.4. Results

4.4.1. Physiological response

Chlorophyll content and chlorophyll fluorescence were determined from the flag leaves of non-stay-green and stay-green genotypes between 0 to 14 days of heat stress in control and heat stress plants. Chlorophyll content significantly declined ($p<0.0001$) in the non-stay-green genotype under heat stress and the percentage decline in the chlorophyll content augmented with increase in duration of heat stress. The decrease in the chlorophyll content was evident on day 7 of heat stress in the non-stay-green genotype. The observed decline in chlorophyll content of non-stay-green genotype at 7, 8, 9, 10, 11, 12, 13, and 14 days of heat stress was 11%, 26%, 34%, 52%, 64%, 70%, 77%, and 85%, respectively. On the other hand, the stay-green genotype maintained the chlorophyll content in the flag leaves under heat stress treatment (Figure 4.1). The fv/fm and Phi II showed significant differences *($p<0.0001$)* between genotypes and treatments. The fv/fm and Phi II declined in both the genotypes under heat stress conditions. However, the decline in fv/fm and Phi II was more pronounced in non-stay-green genotype. The percentage decline in fv/fm ratio in non-stay-green genotype at 7, 8, 9, 10, 11, 12, 13, and 14 days of heat stress was 5%, 13%, 16%, 25%, 43%, 58%, 71%, and 89%, respectively. The percentage decrease of Phi II in non-stay-green genotype was 17%, 18%, 28%, 47%, 60%, 77%, 80%, and 83% at 7, 8, 9, 10, 11, 12, 13, and 14 days of heat stress (Figure 4.2). The MSI was determined at 0, 7, and 14 days of heat stress in non-stay-green and stay-green genotypes. Heat stress caused significant decline *($p<0.0001$)* in the MSI of both non-stay-green and stay-green genotypes. The percentage decline in the MSI of non-stay-green genotype at 7 and 14 days of heat stress was 19% and 84%, whereas the MSI of stay-green genotype declined by 7% and 15% under heat stress conditions as compared to control (Figure 4.3).

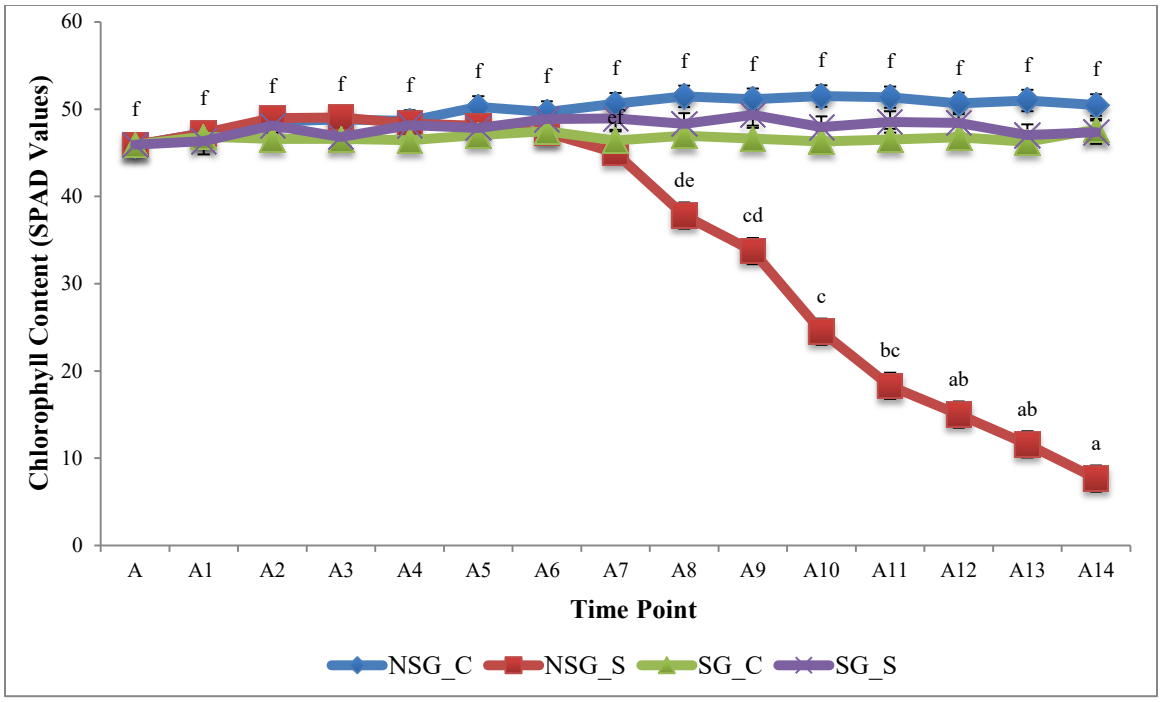

Figure 4.1. Chlorophyll content in the flag leaves of non-stay-green (NSG) and stay-green (SG) genotypes under control (C) and heat stress (S) between 0 days after anthesis (A) to 14 days after anthesis (A14). Error bars represent standard error and different lowercase letters represents significant difference between genotypes and treatments at p<0.05.

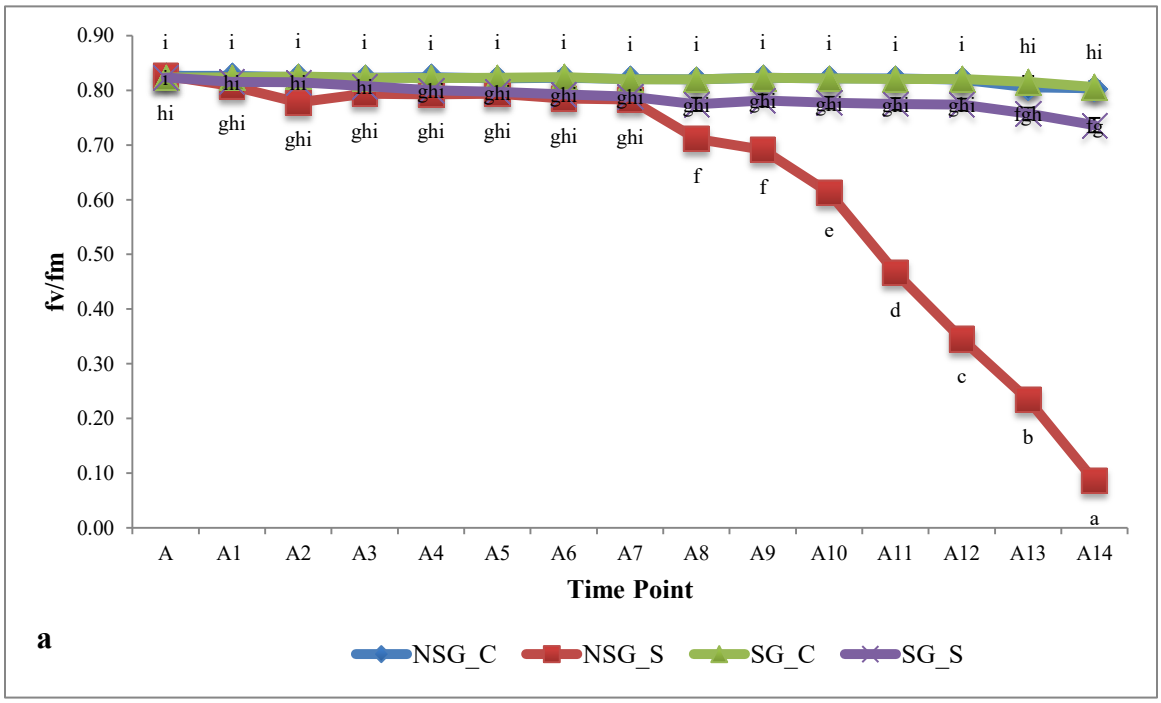

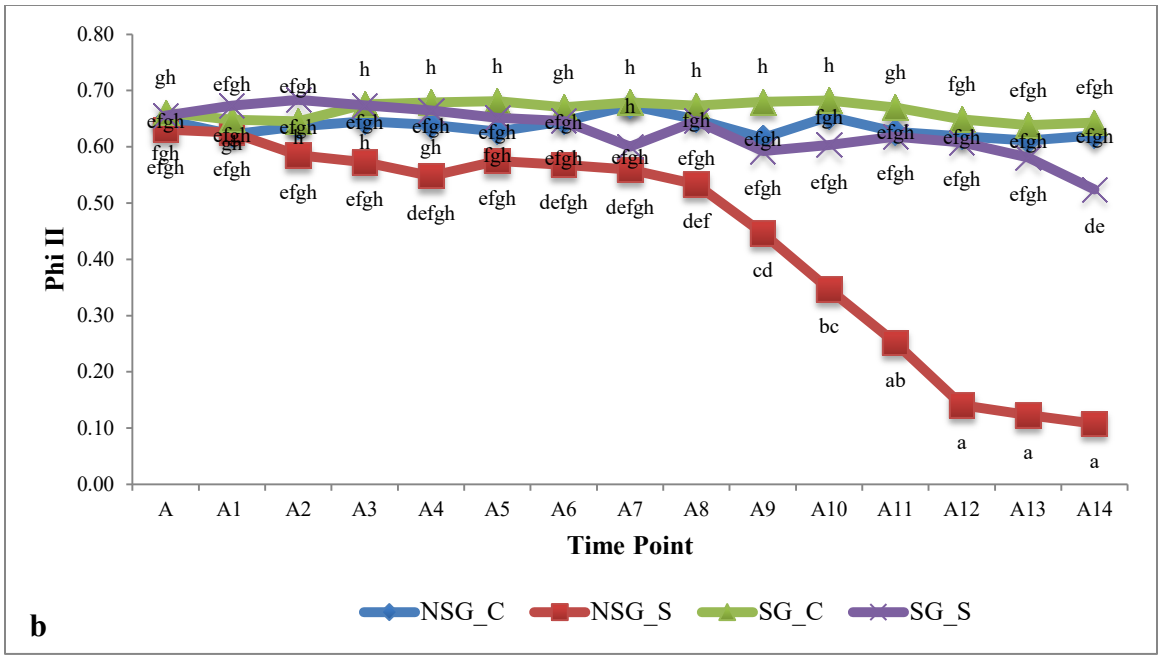

Figure 4.2. Photosynthetic efficiency of photosystem II (fv/fm and Phi II) of non-stay-green (NSG) and stay-green (SG) genotypes under control (C) and heat stress (S) treatment between 0 days after anthesis (A) to 14 days after anthesis (14A). Error bars represent standard error and different lowercase letters represent significant difference between genotypes and treatments at p<0.05.

4.4.2. Biological yield and grain yield

Biological yield and grain yield showed significant differences *(p<0.0001)* between genotypes and treatments. The biological yield was reduced significantly in both the genotypes under heat stress treatment. The percentage reduction in the biological yield was 54% and 19% in non-stay-green and stay-green genotypes, respectively (Figure 4.4a). Heat stress also significantly reduced (60%) the grain yield in the non-stay-green genotype (Figure 4.4b).

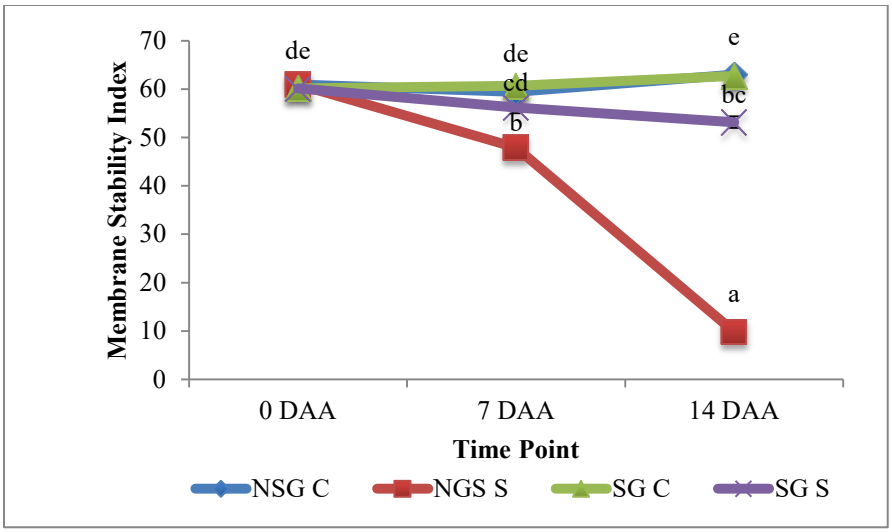

Figure 4.3. The membrane stability index of non-stay-green (NSG) and stay-green (SG) genotypes under control (C) and heat stress (S) treatments. Error bars represent standard error and different lowercase letters represent significant difference between genotypes and treatments at p<0.05.

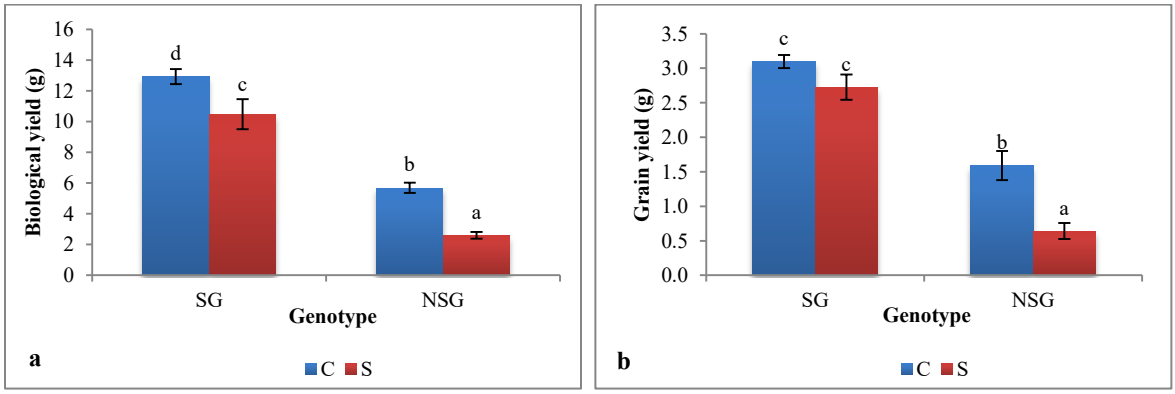

Figure 4.4. Biological yield and grain yield of non-stay-green (NSG) and stay green (SG) genotypes under control (C) and heat stress (S) treatments. Error bars represent standard errors and different lowercase letters represent significant difference between genotypes and treatments at p<0.05.

4.4.3. Metabolomics for stay-green trait in Triticum aestivum under terminal heat stress

4.4.3.1. Global metabolic profiling

All the samples were subjected to positive and negative heated electrospray ionization via UHPLC-HRMS to identify the core metabolites accumulated in non-stay-

green and stay-green genotypes under control and heat stress treatments at day 7 (time point 1) and day 14 (time point 2) of heat stress. The UHPLC-HRMS based non-targeted global metabolomic profiling detected a total of 6,945 features from the positive ion mode and 5,586 features from the negative ion mode. Of the total, 185 metabolites from positive ion mode and 123 metabolites from negative ion mode were identified as known metabolites. The metabolites were highly reproducible among the six biological replicates. The identified metabolites included amino acids, acetylated amino acids, amines, polyamines, amino sugars, dipeptides, modified amino acids, alcohols and polyols, alkaloids, carbohydrates, lipids, nucleic acids, nucleobases, nucleosides, plant growth regulators, vitamins, organic acids, and organic compounds.

The PLS-DA was performed using all known metabolites in non-stay-green and stay-green genotypes under control and heat stress treatments at both the time points. The top five Partial Least Squares (PLS) components described a total of 74.2% variance. The first PLS component explained 38.7% of the total variance and the second PLS component explained 18.9% of the total variance (Figure 4.5a). The 2D scores plot between component 1 and component 2 revealed unambiguous differences between the metabolites accumulation in non-stay-green and stay-green genotypes (Figure 4.5b).

The top 30 significant known metabolites found in non-stay-green and stay-green genotypes under control and heat stress conditions were evident from heatmap. The hierarchical clustering of samples revealed two major clusters with cluster 1 including non-stay-green control and heat treated samples at different time points and cluster 2 including stay-green control and heat treated samples at different time points. The hierarchical clustering of features revealed two major clusters with different patterns of metabolite abundance. The metabolites that were highly accumulated in the stay-green genotype forming cluster 1 included 4-aminobenzoate, L-glutamic acid, taurine, L-lactic acid, cyclic ADP-ribose, cytidine monophosphate (CMP), spermine, phosphocholine, glutathione, trigonelline, syringic acid, and starch acetate. The set of metabolites highly accumulated in the non-stay-green genotype forming cluster 2 included picolinic acid, nicotinate, adenine, choline, 4-aminobutanoate, glucose/fructose, LL-2,6-diaminoheptanedioate, deoxyuridine, leu pro, glycyl-L-leucine, methionine sulfoxide,

guanosine, uridine, cytidine, isocytosine, 3-ureidopropionate, 5´-deoxyadenosine, and deoxycytidine (Figure 4.6).

Of the total 308 metabolites, 166 (269 with duplication) were identified as significant metabolites by ANOVA, PLS-DA, and SAM. The significant metabolites identified were amino acids, nucleic acids, nucleosides, nucleobases, vitamins and cofactors, sugars, amines organic acids, and organic compounds (Table 4.1, Figure 4.7). The variations in the levels of metabolites accumulated in the leaves of non-stay-green and stay-green genotypes grown under control and heat stress treatments at different time points were revealed by fold change analysis. The variation between genotypes was elucidated by determining the fold change among stay-green/non-stay-green genotypes under control and heat stress treatments at different time points. The fold change was determined for heat stress treated/control samples in non-stay-green and stay-green genotypes at two different time points to unravel variation in the levels of metabolites under heat stress (Table 4.1, Figure 4.8).

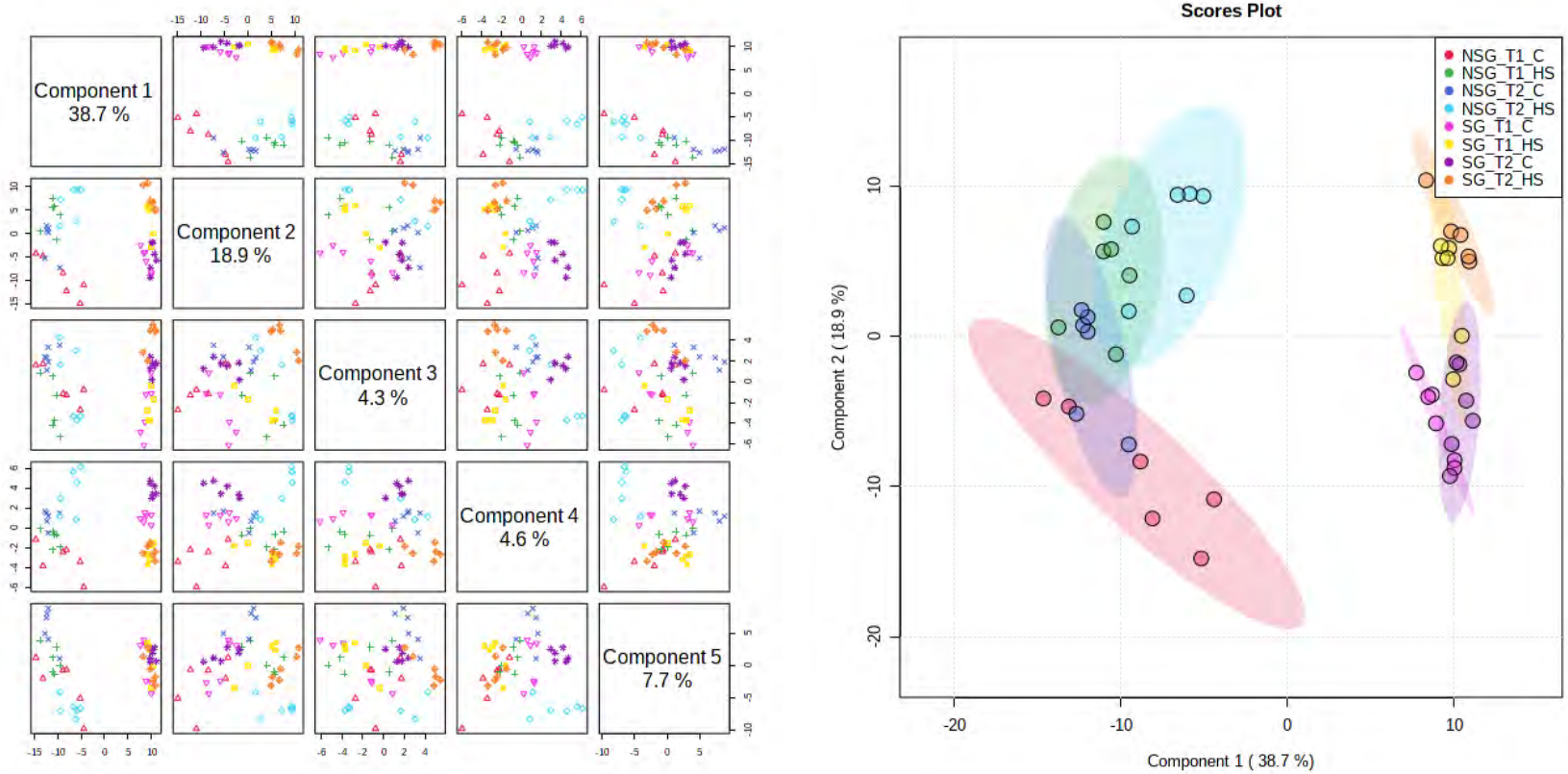

a **b**

Figure 4.5. The PLS-DA and 2D Scores plot for non-stay-green (NSG) and stay-green (SG) genotypes under control (C) and heat stress (HS) treatments at day 7 and day 14 of heat stress. The samples of two genotypes didn't overlap with each other, indicating an altered state of metabolite levels in two genotypes (T1: Day 7 of heat stress/7 Days after anthesis and T2: day 14 of heat stress/14 Days after anthesis)

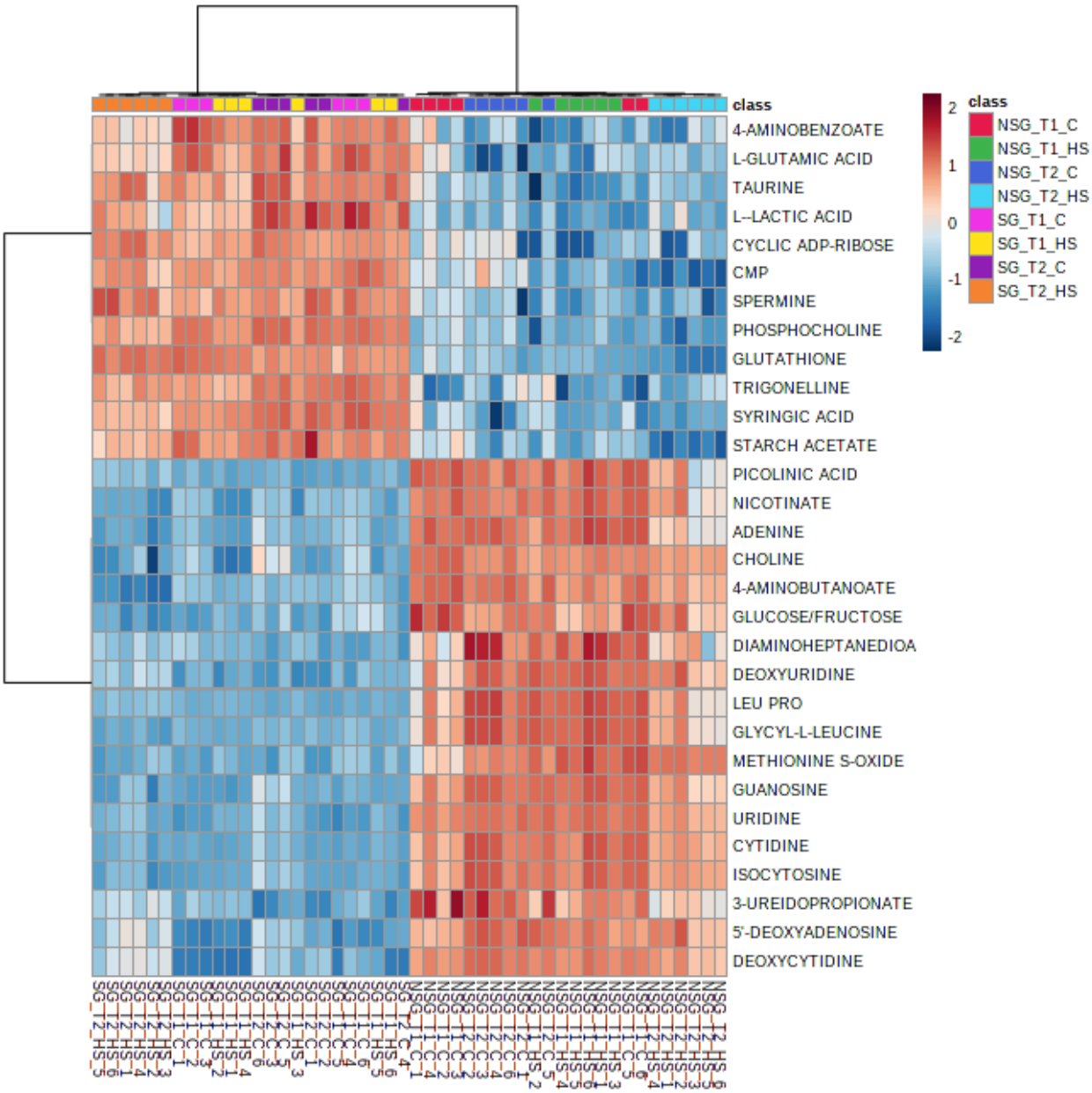

Figure 4.6. Heatmap illustrating the top 30 metabolites in the flag leaves of non-stay-green (NSG) and stay-green (SG) genotypes under control (C) and heat stress (HS) treatment at day 7 (T1) and day 14 days (T2) of heat stress according to the partial least square discriminant analysis variable importance in projection score.

Table 4.1. The significant know metabolites with their compound ID, molecular formula identified by ANOVA, SAM and PLSDA in non-stay green (NSG) and stay green (SG) genotypes under control (C) and heat stress (HS) treatments at day 7 (T1) and day 14 (T2) of heat stress

Metabolite	Compound ID	Molecular formula	Compound type	ANOVA		SAM		PLSDA	log2(FC)							
				p value	FDR	d value	STD. DEV.	Comp 1	SG/NSG_T1		SG/NSG _T2		NSG_HS/C		SG_HS/C	
									C	HS	C	HS	T1	T2	T1	T2
4-Aminobutanoate	C00334	C4H9NO2	Amino Acid	1.42E-32	3.93E-30	6.18	0.02	1.76	-4.49	-4.22	-4.8	-5.17	-	-1.09	-	-1.45
Uridine	C00299	C9H12N2O6	Nucleosides	8.46E-31	1.17E-28	6.12	0.03	1.6	-7.35	-6.69	-6.29	-5.2	-	-1.34	-	-
Cytidine	C02961	C9H13N3O5	Nucleosides	6.97E-28	3.86E-26	6.01	0.04	1.6	-6.6	-6.96	-6.68	-5.48	-	-1.6	-	-
Adenine	C00147	C5H5N5	Nucleobase	1.78E-27	8.20E-26	5.99	0.04	1.72	-5.62	-6.67	-5.31	-3.93	-	-2.73	-1.02	-1.35
Isocytosine	-	C4H5N3O	Nucleic acid	1.41E-26	5.57E-25	5.94	0.04	1.59	-6.5	-6.69	-6.28	-5.65	-	-1.49	-	-
Glutathione	C00051	C10H17N3O6S	Vitamins and Cofactors	3.14E-26	1.09E-24	5.92	0.05	1.5	3.94	4.57	4.07	6.13	-	-1.53	-	-
Nicotinate	C00253	C6H5NO2	Vitamins and Cofactors	1.12E-25	3.44E-24	5.89	0.05	1.7	-4.62	-5.82	-4.43	-4.32	-	-1.05	-1.23	-
Guanosine	C00387	C10H13N5O5	Nucleosides	1.55E-24	4.28E-23	5.82	0.06	1.6	-5.02	-5.69	-4.38	-4.05	-	-1.39	-	-1.05
Glycyl-L-leucine	-	C8H16N2O3	Dipeptide	3.29E-24	7.07E-23	5.8	0.06	1.62	-7.06	-8.61	-8.13	-6.2	1.04	-2.57	-	-
Picolinic Acid	C10164	C6H5NO2	Organic Acid	3.32E-24	7.07E-23	5.8	0.06	1.65	-4.15	-3.87	-3.85	-2.15	-	-1.28	-	-
5'-Deoxyadenosine	C05198	C10H13N5O3	Deoxyribonucleoside	1.73E-23	3.42E-22	5.74	0.06	1.3	-8.58	-9.01	-7.66	-4.85	1.52	-1.16	1.09	1.66
Deoxycytidine	C00881	C9H13N3O4	Deoxyribonucleosides	3.13E-23	5.78E-22	5.73	0.06	1.33	-9.74	-10.55	-8.13	-4.36	-	-1.89	-	1.88
Leucylproline	-	C11H20N2O3	Dipeptide	1.25E-22	2.16E-21	5.68	0.07	1.56	-6.68	-7.55	-7.94	-4.7	1.1	-2.47	-	-
Phosphocholine	C00588	C5H14NO4P	Organic Compound	1.36E-22	2.22E-21	5.67	0.07	1.45	4.73	5.05	4.99	5.02	-	-1.33	-	-1.3
5-Aminolevulinic Acid	C00430	C5H9NO3	Endogenous Non-Proteinogenic Amino Acid	1.60E-21	2.47E-20	5.58	0.08	1.66	-1.56	-1.54	-1.78	-2.28	-	-	-	-
5-Hydroxyindoleacetate	C05635	C10H9NO3	Organic Acid	2.56E-21	3.73E-20	5.56	0.08	1.62	-4.1	-4.21	-4.19	-2.79	-	-2.58	-	-
Methionine sulfoxide	C02989	C5H11NO3S	Organic Compound	3.10E-21	4.29E-20	5.56	0.08	1.51	-3.73	-4.71	-4.39	-4.39	-	-	-	-
Starch Acetate	-	-	Sugar	5.89E-21	7.78E-20	5.53	0.08	1.24	1.68	2.34	2.37	2.73	-	-	-	-
Deoxyuridine	C00526	$C_9H_{12}N_2O_5$	nucleoside	8.78E-21	1.11E-19	5.51	0.09	1.45	-8.02	-10.08	-9.86	-6.5	1.52	-1.02	-	-
3-Ureidopropionate	C02642	C4H8N2O3	Organic Acid	9.98E-21	1.20E-19	5.51	0.09	1.52	-2.17	-1.76	-2.66	-	-	-1.15	-	-
Glucose	C00031	C6H12O6	Sugar	1.25E-20	1.44E-19	5.5	0.09	1.69	-5	-3.73	-4.41	-4.93	-1.63	-	-	-
Glyceric acid	C00258	C3H6O4	Organic Acid	1.16E-19	1.12E-18	5.4	0.10	1.49	-3.88	-2.36	-2.81	-2.84	-2.14	-	-	-
Choline	C00114	C5H13NO	Organic Compound	2.67E-19	2.39E-18	5.36	0.10	1.62	-3.31	-4.25	-2.54	-3.79	-	-	-1.34	-1.53
Taurine	C00245	C2H7NO3S	Amino sulfonic acid	8.39E-19	7.04E-18	5.3	0.11	1.51	1.45	2.37	2.05	1.7	-1.03	-	-	-
Thiamine	C00378	C12H16N4OS	Vitamin	9.57E-19	7.80E-18	5.29	0.11	1.24	-4.52	-2.87	-4.46	-	-	-1.62	1.2	2.66
CMP	C00055	C9H14N3O8P	Nucleotide	1.16E-18	9.22E-18	5.28	0.11	1.31	2.28	2.59	1.41	3.37	-	-2.19	-	-

Syringic Acid	C10833	C9H10O5	Organic compound (Phenols)	3.95E-18	3.04E-17	5.21	0.12	1.36	2.86	3.76	4.29	3.29	-1.07	-	-	-1.27
L-Glutamine	C00064	C5H10N2O3	Amino Acid	7.45E-18	5.58E-17	5.18	0.12	1.27	-1.02	-1.18	-1.33	-	-	-	-	1.22
Tyramine	C00483	C8H11NO	Amine/Alkaloid	2.96E-17	2.10E-16	5.1	0.13	1.39	1.04	3.14	-	3.34	-	-	2.73	2.6
L-Glutamic Acid	C00025	C5H9NO4	Amino Acid	5.33E-17	3.69E-16	5.06	0.13	1.17	2.17	2.48	4.05	1.54	-1.12	1.17	-	-1.34
Pyridoxal	C00250	C8H9NO3	Vitamin	6.36E-17	4.29E-16	5.05	0.13	1.61	-3.76	-3.77	-3.94	-2.35	-	-2.31	-1	-
Riboflavin	C00255	C17H20N4O6	Vitamin	1.08E-16	7.15E-16	5.02	0.14	1.62	-3.9	-4	-4.01	-2.19	-	-2.14	-	-
Pyridoxine	C00314	C8H11NO3	Vitamin	1.52E-16	9.78E-16	5	0.14	1.63	-3.3	-4.92	-5.17	-3.33	-	-2.47	-2.59	-
LL-2,6-Diaminoheptanedioate	C00666	C7H14N2O4	Amine	3.53E-16	2.22E-15	4.94	0.15	1.46	-2.21	-3.22	-3.49	-1.49	-	-1.47	-	-
Spermine	C00750	C10H26N4	Polyamine	8.43E-16	5.19E-15	4.88	0.15	1.49	2.68	3.7	3.52	4.15	-1.05	-	-	-
2-Phosphoglyceric acid	-	C3H7O7P	Organic Acid	9.93E-16	5.98E-15	4.87	0.15	0.94	1.79	5.14	4.57	5.56	-4.42	-2.66	-1.07	-1.67
L-Lactic Acid	C00256	C3H6O3	Organic Acid	2.71E-15	1.60E-14	4.8	0.16	1.46	2.71	2.86	3.15	1.64	-	-	-	-1.23
Trigonelline	C01004	C7H7NO2	Alkaloid	4.85E-15	2.74E-14	4.76	0.17	1.57	4.25	3.8	2.97	3.2	-	-	-	-
L-Kynurenine	C00328	C10H12N2O3	Organic Compound (alkyl-phenylketones)	1.19E-14	6.33E-14	4.69	0.17	0.26	-	-	-	-1.49	2.24	3.52	1.4	2.44
Homogentisate	C00544	C8H8O4	Organic Compound (Phenolic Acid))	1.94E-14	1.01E-13	4.65	0.18	1.01	1.41	1.22	2.14	2.53	-	-	-	-
Alanine	C00041	C3H7NO2	Amino acid	2.36E-14	1.21E-13	4.64	0.18	1.38	-2.03	-1.82	-1.71	-1.64	-	-	-	-
L-Histidine	C00135	C6H9N3O2	Amino Acid	2.73E-14	1.36E-13	4.63	0.18	1.5	2.75	2.37	1.63	4.25	1.57	-1.52	1.19	1.1
Tartaric Acid	C00898	C4H6O6	Organic Acid	2.75E-14	1.36E-13	4.63	0.18	1.33	-2.18	-1.03	-1.34	-1.64	-1.24	-	-	-
Guanine	C00242	C5H5N5O	Nucleobase	3.13E-14	1.52E-13	4.62	0.18	1.52	-2.43	-4.2	-2.95	-1.82	-	-1.7	-1.03	-
Shikimate	C00493	C7H10O5	Organic Acid	3.74E-14	1.78E-13	4.6	0.18	0.35	-2.03	-	1.73	1.18	-3.7	-2.35	-1.57	-2.9
Spermidine	C00315	C7H19N3	Polyamine	4.08E-14	1.92E-13	4.6	0.19	0.74	1.15	1.72	2.03	2.65	-1.86	-1.71	-1.28	-1.09
cADPR	-	C15H21N5O13P2	Purine Nucleotide Sugars	5.05E-14	2.29E-13	4.58	0.19	1.43	2.76	5.5	3.13	4.41	-	-	-	-
Allantoin	C01551	C4H6N4O3	Organic Compound (Imidazoles)	5.86E-14	2.62E-13	4.57	0.19	1.63	3.97	3.27	3.68	3.99	-	-	-	-
Nicotinamide Ribotide	C00455	C11H15N2O8P	Organic Compounds (Nicotinamide Nucleotides)	6.64E-14	2.92E-13	4.56	0.19	1.05	-	1.73	1.67	1.48	-1.24	-1.03	-	-1.22
Anthranilate	C00108	C7H7NO2	Organic Compounds (Aminobenzoic Acid)	1.15E-13	4.90E-13	4.51	0.20	1.23	2.08	2.59	2.68	1.41	-	-	-	-1.06
Propionylcarnitine	C03017	C10H19NO4	Lipids and lipid-like molecules	2.82E-13	1.16E-12	4.44	0.20	1.17	-4.13	-2.01	-5.31	-2.3	-1.44	-1.86	-	1.15
D-Raffinose	C00492	C18H32O16	Sugar (Oligosaccharide)	3.24E-13	1.32E-12	4.43	0.21	1.28	1.87	2.51	4.29	-	-1	2.63	-	-
2-alpha-D-Glucosyl-D-Glucose	C19632	C12H22O11	Sugar (Disaccharide)	3.28E-13	1.32E-12	4.42	0.21	1.32	1.36	2.45	3.37	-	-1.19	1.97	-	-
4-Guanidinobutanoate	C01035	C5H11N3O2	Gamma Amino Acid and Derivative	4.49E-13	1.75E-12	4.4	0.21	1.5	1.49	1.96	1.96	1.7	-	-	-	-
Creatine	C00300	C4H9N3O2	Alpha Amino Acid and Derivative	5.45E-13	2.10E-12	4.38	0.21	1.02	1.27	1.14	1.45	-	-	-	-1.01	-

Xanthine	C00385	C5H4N4O2	Organic Compound (Xanthines)	7.10E-13	2.69E-12	4.36	0.21	0.49	-	-1.34	-	-	1.95	2.17	-	1.49
Homocysteine	C05330	C4H9NO2S	Amino Acid, Peptide and Derivatives	1.34E-12	4.96E-12	4.3	0.22	1.36	1.95	2.03	-	-	-	1.44	1.06	-
Hexane-1-sulfonic Acid	-	C6H14O3S	Organosulfur	2.76E-12	1.01E-11	4.23	0.23	1.44	-	-1.41	-	-2.16	-	-	-	-1.64
4-Imidazoleacetic Acid	C02835	C5H6N2O2	Organic Compound (Imidazolyl Carboxylic Acid and Derivative)	5.02E-12	1.80E-11	4.18	0.24	1.48	2.17	1.63	2.65	1.39	1.21	1.46	-	-
Cytosine	C00380	$C_4H_5N_3O$	Pyrimidine Nucleotide	6.14E-12	2.18E-11	4.16	0.24	1.18	1.33	-	1.47	-	-	-	-	-
3-(4-Hydroxyphenyl)lactate	C03672	C9H10O4	Organic Compound (Phenylpropanoic Acid)	8.74E-12	3.03E-11	4.13	0.24	1.48	-	-1.87	-1.31	-1.9	-	-	-	-1.24
Disaccharide	-	C12H22O11	Sugar (Disaccharide)	1.13E-11	3.85E-11	4.1	0.25	1.28	1.39	2.35	3.54	-	-	2.68	-	-
3-Hydroxykynurenine	C02794	C10H12N2O4	Organic Compound (Alkyl-phenylketone)	1.21E-11	4.05E-11	4.09	0.25	1.25	-2.15	-3.18	-3.21	-	1.07	-1.43	-	1.45
Betaine	C00719	C5H11NO2	Alpha Amino Acid	1.47E-11	4.83E-11	4.08	0.25	1.25	-	1.17	-	-	-	-	-	-
N-Methyl-D-Aspartic Acid	C12269	C5H9NO4	Amino Acid, Peptide and Derivatives	1.52E-11	4.94E-11	4.07	0.25	1.02	1.5	1.88	2.89	1.07	-1.26	-	-	-1.35
5-Methylcytosine	C02376	C5H7N3O	Organic Compound (Hydroxypyrimidine)	1.82E-11	5.85E-11	4.05	0.25	1.06	-	1.09	1.59	1.3	-1.02	-	-	-
5-Hydroxymethyl-2-furancarboxaldehyde	C11101	C6H6O3	Organic Compound (Aryl-aldehyde)	2.28E-11	7.25E-11	4.03	0.26	1.33	-	1.64	1.95	1.53	-	-	-	-
Alpha-Aminoadipate	C00956	C6H11NO4	Alpha Amino Acid	2.32E-11	7.29E-11	4.03	0.26	0.15	-	-4.09	1.4	-3.17	4.09	5.34	-	-
Pantothenic Acid	C00864	C9H17NO5	Vitamin	2.46E-11	7.57E-11	4.02	0.26	0.57	-	-	-	-1.03	-	-	-1.38	-1.48
4-Coumarate	C00811	C9H8O3	Phenylpropanoid (Hydroxycinnamic acid and derivative)	2.49E-11	7.57E-11	4.02	0.26	1.41	1.94	1.92	1.47	1.22	-	-	-	-
L-Serine	C00065	C3H7NO3	Amino Acid	2.51E-11	7.57E-11	4.02	0.26	0.03	-	1.02	-	1.03	-	-1.86	-	-
Proline	C00148	C5H9NO2	Amino Acid	2.61E-11	7.77E-11	4.02	0.26	0.62	-	-3.31	-1.47	-4	3.3	3.86	-	1.34
Xanthurenic Acid	C02470	C10H7NO4	Quinoline Carboxylic Acid	3.32E-11	9.69E-11	3.99	0.26	1.09	-1.38	-2.86	-1.63	-	-	-2.83	-2.31	-1.14
D-Glucuronic Acid	C00191	C6H10O7	Carbohydrate and carbohydrate conjugate	3.63E-11	1.05E-10	3.99	0.26	1.55	-3.49	-3.83	-4.44	-4.88	-	-1.56	-1.32	-
Carnosine	C00386	C9H14N4O3	Organic acid (Hybrid peptide)	4.26E-11	1.22E-10	3.97	0.27	1.39	-7.6	-5.53	-8.67	-	-	-3.54	-	-
3-Hydroxyphenylacetate	C05593	C8H8O3	Phenols	4.71E-11	1.33E-10	3.96	0.27	1.21	-	-1.12	-1.18	-1.92	-	-	-	-
Source Fragment TRP	-	-	-	6.05E-11	1.69E-10	3.93	0.27	0.65	-	-	-	2.75	3.17	-	2.19	2.82
N-a-Acetyl-L-arginine	-	C8H16N4O3	Amino acid, peptide and analogue	6.16E-11	1.71E-10	3.93	0.27	0.76	-	-1.73	-	-	1.13	-	-	-1.53
Kynurenic Acid	C01717	C10H7NO3	Quinoline Carboxylic Acid	7.98E-11	2.19E-10	3.9	0.27	0.15	-	-	-	-	1.52	2.13	-	2.81
Glycine	C00037	C2H5NO2	Amino Acid	8.20E-11	2.23E-10	3.9	0.27	1.28	-1.44	-1.1	-2.5	-	-	-2.14	-	-
Glycerol	C00116	C3H8O3	Sugar alcohol	1.40E-10	3.74E-10	3.85	0.28	1.19	-	-	1.02	1.47	-	-	-	-
N-Butoxycarbonyl-L-aspartic acid	-	C9H15NO6	Organic Compound	1.47E-10	3.87E-10	3.84	0.28	1.27	-	1.74	1.04	1.68	-1.06	-	-	-

Formylkynurenine	C02406	C11H12N2O4	Amino Acid	1.90E-10	4.93E-10	3.81	0.29	0.23	-	-	-	-	-	-	-	-1.28
Urate	C00366	C5H4N4O3	Purines and purine derivatives	3.26E-10	8.30E-10	3.76	0.29	1.29	1.63	2.25	-	4.11	-	-	-	2.31
Erythritol	C16884	C4H10O4	Sugar alcohols	4.23E-10	1.06E-09	3.73	0.30	1.1	-	1.2	1.42	1.64	-	-	-	-
Allopurinol	-	C5H4N4O	Organoheterocyclic compound (pyrazolo[3,4-d]pyrimidine)	4.36E-10	1.08E-09	3.72	0.30	0.66	-1.01	-2.12	-	-1.24	-	-	-	-
Asparagine	C00152	C4H8N2O3	Amino Acid	4.47E-10	1.10E-09	3.72	0.30	0.71	3.06	1.38	-	-	1.15	-	-	-
Trans-Cinnamate	C00423	C9H8O2	Phenylpropanoid	4.79E-10	1.16E-09	3.71	0.30	1.48	-1.99	-2.18	-5.48	-4	-	-1.91	-	-
2-Hydroxyhippuric Acid	C07588	C9H9NO4	Benzoic acid and derivative	5.87E-10	1.40E-09	3.69	0.30	1.36	-2.01	-2.23	-2.84	-	-1.21	-1.65	-1.43	-
N6-(delta2-Isopentenyl)-adenine	C04083	C10H13N5	Plant Growth Regulator (Phytohormone)	6.45E-10	1.53E-09	3.68	0.31	1.33	1.17	-	2.39	-	-	2	-	-
Adenosine	C00212	C10H13N5O4	Nucleoside	7.94E-10	1.85E-09	3.66	0.31	0.96	-4.02	-3.46	-2.01	-2.97	-	-	-	-
Hexose-Disaccharide	-	C12H22O11	Sugar	8.69E-10	2.01E-09	3.65	0.31	1.08	-	1.18	2.01	-	-	-	-	-
Threonine	C00188	C4H9NO3	Amino Acid	9.47E-10	2.15E-09	3.64	0.31	0.88	-	-	-1.16	-	-	-1.82	-	-
L-4-Hydroxyphenylglycine	C12323	C8H9NO3	Amino acid, peptide and analogue	1.06E-09	2.39E-09	3.62	0.31	1.5	1.46	1.72	2.01	1.28	-	-	-	-
Hexanesulfonic Acid-Sulfate	-	-	-	1.11E-09	2.48E-09	3.62	0.31	1.1	1.2	2.89	1.59	5.75	-2.04	-3.8	-	-
Glycerophosphocholine	C00670	C8H20NO6P	Lipids and lipid-like molecules	1.41E-09	3.08E-09	3.59	0.32	1.41	2.41	3.11	3.35	1.97	-	1.34	-	-
ADP	C00008	C10H15N5O10P2	Nucleotide	1.57E-09	3.36E-09	3.58	0.32	1.37	4.37	6.91	4.66	4.31	-2.21	-	-	-
Hydroquinone	C00530	C6H6O2	Benzenoids (Phenol)	1.69E-09	3.60E-09	3.57	0.32	0.99	-	3.18	1.92	2.47	-2.73	-	-	-1.14
Tryptophan	C00078	C11H12N2O2	Amino Acid	1.94E-09	4.09E-09	3.56	0.32	0.45	-	-	-1.4	2.76	3.23	-	2.61	3.31
Ascorbate	C00072	C6H8O6	Organoheterocyclic compound (Vitamin)	2.97E-09	6.19E-09	3.51	0.33	1.13	-	1.75	1.47	2.1	-1.22	-1.2	-	-
N-Alpha-Acetyl-L-Lysine	C12989	C8H16N2O3	Amino acid, peptide and analogue	3.35E-09	6.88E-09	3.49	0.33	1.09	-1.33	-1.04	-1.92	-	1.14	-	1.43	-
Quinate	C00296	C7H12O6	Alcohols and polyols	4.20E-09	8.55E-09	3.47	0.34	0.69	-2.5	-	-	-	-4.43	-	-1.79	-1.99
1-Methyladenosine	C02494	C11H15N5O4	Nucleosides, nucleotides and analogues	4.49E-09	9.08E-09	3.46	0.34	1.13	-	-4.14	-3.54	-	-	-2.57	-	-
Diethyl oxalpropionate	C04067	C9H14O5	Organic Acid	7.00E-09	1.37E-08	3.41	0.35	0.22	-	-	-	1.92	-1.79	-2.36	-	-
L-Methionine	C00073	C5H11NO2S	Amino Acid	8.35E-09	1.61E-08	3.39	0.35	0.75	-2.69	-2.77	-3.83	1.36	-	-4.1	-	1.09
Nicotinamide	C00153	C6H6N2O	Vitamin	8.43E-09	1.61E-08	3.38	0.35	1.04	1.03	2.05	3.27	-	-1.48	2.83	-	-1.08
Malonate	C00383	C3H4O4	Organic Acid	1.02E-08	1.93E-08	3.36	0.35	0.22	-	-	-	-	-	1.15	-	-
d-Camphor	-	C10H16O	Lipid	1.14E-08	2.14E-08	3.35	0.36	0.17	-	-	-	-	-	-1.56	-1.14	-1.39
Glucosamine	C00329	C6H13NO5	Amino Sugar	1.24E-08	2.27E-08	3.34	0.36	1.37	-1.66	-	-	-	-	-	-	-
Isocitric Acid	C00311	C6H8O7	Organic Acid	2.52E-08	4.45E-08	3.25	0.37	0.02	-	-	-	-	-2.12	-1.11	-1.16	-1.33
Valerylcarnitine	-	C12H23NO4	Lipids and lipid-like molecules	2.61E-08	4.55E-08	3.25	0.37	0.77	-	-1.45	-	-3.41	-	2.25	-	-

(S)-Dihydroorotate	C00337	C5H6N2O4	Amino acids, peptides, and analogues	5.88E-08	9.93E-08	3.14	0.39	0.48	-	-1.47	-	-1	-	1.28	-	-
Anthranilate-Water	-	C7H6NO	Organic Compound (Aminobenzoic Acid)	7.51E-08	1.25E-07	3.11	0.39	0.23	-	-	1.57	1.81	-1.48	-	-	-1.14
5-Hydroxy-L-Tryptophan	C00643	C11H12N2O3	Organic Compounds	8.85E-08	1.46E-07	3.09	0.40	0.29	-	-	-	-	3.32	1.17	2.17	1.75
4-Oxoproline	C01877	C5H7NO3	Alpha Amino Acids and Derivatives	9.82E-08	1.61E-07	3.08	0.40	0.02	-	-	-	-2.43	1.07	3.48	-	-
D-Saccharic Acid	C00818	C6H10O8	Organic Acid	1.58E-07	2.52E-07	3.02	0.41	1.2	-1.17	-	-	-	-1.26	-	-	-
L-Valine	C00183	C5H11NO2	Amino Acid	2.86E-07	4.38E-07	2.94	0.42	0.21	1.06	-	-1.84	-	1.23	-	-	-
2,5-Dihydroxybenzoate	C00628	C7H6O4	Organic Compounds (Hydroxybenzoic Acid Derivatives)	3.67E-07	5.52E-07	2.91	0.43	0.01	-	1.76	-	-	-2.77	-	-	-1.2
Hexose	C00984	C6H12O6	Sugar Alcohol	4.17E-07	6.25E-07	2.89	0.43	1.01	-1.15	-	-	-	-1.23	-	-	-
Aspartate	C00049	C4H7NO4	Amino Acid	6.34E-07	9.40E-07	2.83	0.44	0.04	-	-	-	1.54	-1.87	-2.5	-	-1.35
Caffeate	C01197	C9H8O4	Phenylpropanoids	7.84E-07	1.15E-06	2.8	0.44	0.75	-	1.55	1.63	1.39	-2.2	-1	-	-1.24
L-Lysine	C00047	C6H14N2O2	Amino Acid	7.97E-07	1.16E-06	2.8	0.44	0.35	-	1.18	-1.6	3.34	-	-2.96	1.86	1.97
L-Arginine	C00062	C6H14N4O2	Amino Acid	8.91E-07	1.29E-06	2.79	0.45	0.87	-	1.7	-	3.95	-	-2.29	1.48	1.51
Dopamine	C03758	C8H11NO2	Phenol	9.84E-07	1.41E-06	2.77	0.45	0.9	-	-	-1.47	-	-	-1.26	-	-
Serotonin-NH3	-	C10H9NO	Organic Compound	1.69E-06	2.39E-06	2.7	0.46	1.15	1.47	-	3.69	-	-	4.69	-	1.58
Putrescine	C02896	C4H12N2	Amine	2.02E-06	2.85E-06	2.67	0.47	0.32	-1.07	2.72	-	2.13	-3.05	-1.45	-	-
L-Isoleucine	C00407	C6H13NO2	Amino Acid	3.27E-06	4.55E-06	2.6	0.48	0.27	1.61	-	-1.34	-	1.51	-	-	1.13
4-Hydroxybenzenesulfonic Acid	-	C6H6O4S	Organosulfur	3.61E-06	4.98E-06	2.59	0.48	1.33	-1.53	-2.4	-1.57	-1.67	-	-	-	-
Agmatine	C00179	C5H16N4O4S	Amine	4.28E-06	5.87E-06	2.57	0.49	0.45	-2.57	-	-3.1	1.18	-	-1	1.93	3.28
Orthophosphate	C00009	H3O4P	Organic Acid	4.80E-06	6.55E-06	2.55	0.49	0.9	1.15	2.49	1.26	2.82	-1.6	-2.32	-	-
Ibuprofen	C01588	C13H18O2	Organic Acid	5.195E-06	7.05E-06	2.54	0.49	1.01	-2.47	-2.3	-1.63	-1.55	-	-	-	-
Ornithine	C00077	C5H12N2O2	Amino Acid (Peptide)	1.755E-05	2.34E-05	2.36	0.53	0.84	-	1.53	-	2.84	-1.09	-1.06	-	1.97
Inosine	C00294	C10H12N4O5	Nucleoside	2.586E-05	3.41E-05	2.3	0.54	1	-	-	-1.08	-	-	-	-	-
Vanilloloside	-	C14H20O8	Organic compound	4.939E-05	6.45E-05	2.2	0.56	0.62	-	-	-	-	-	1.3	-	-
L-Leucine	C00123	C6H13NO2	Amino Acid	5.708E-05	7.42E-05	2.18	0.56	0.34	-	-	-1.76	-	-	-	-	1.03
6-Hydroxycaproic Acid	C06103	C6H12O3	Lipids	6.194E-05	7.98E-05	2.17	0.56	1.2	-2.75	-1.91	-2.39	-2.04	-1.09	-	-	-
Indolepyruvate	C00331	C11H9NO3	Organic acid	7.002E-05	8.98E-05	2.15	0.57	0.35	-	-	-	1.57	-	-	-	-
N-Acetylputrescine	C02714	C6H14N2O	Organic acid	8.895E-05	1.14E-04	2.11	0.58	0.56	-	-	-	1.7	-1.37	-	-	1.11
Triethanolamine	C06771	C6H15NO3	Amine	9.965E-05	1.27E-04	2.09	0.58	0.28	-	-1.88	-	-1.46	-	-	-1.35	-1
Pipecolate	C00408	C6H11NO2	Alkaloids	0.0001102	1.39E-04	2.08	0.58	0.2	-1.06	-2.01	-	-1.13	2.13	2.18	1.18	1.06

O-Acetyl-L-Serine	C00979	C5H9NO4	Alpha Amino Acid	0.0001271	1.60E-04	2.06	0.59	0.07	-	-	1.55	-1.01	-1.84	-	-	-2.39
Beta-Alanine	C00099	C3H7NO2	Amino Acid	0.0001352	1.69E-04	2.05	0.59	0	-	-	-	1.25	-1.9	-1.95	-	-1.12
3'-CMP	C05822	C9H14N3O8P	-	0.0001705	2.12E-04	2.01	0.60	0.79	-1.15	-	-2.41	-	-	-1.68	-	-
2-Hydroxyphenylalanine	-	C9H11NO3	Amino Acid (Peptide)	0.000189	2.33E-04	1.99	0.60	0.52	-	-	-2.07	-	1.2	-1.12	-	-
Ferulic Acid Sulfate	-	C10H10O7S	Organic compound (hydroxycinnamic acid)	0.0002707	3.29E-04	1.93	0.61	1.02	-	-	-	-1.51	-	-	-1.14	-1.66
Phenylalanine	C00079	C9H11NO2	Amino Acid (Peptide)	0.0003263	3.95E-04	1.9	0.62	0.36	-	-	-1.03	-	1.38	-	-	-
Glycolate	C00160	C2H4O3	Organic Acid	0.0003346	4.03E-04	1.9	0.62	0.03	-	-	-	-	-1.04	-	-1.52	-1.22
Glutathione Disulfide	C00127	C20H32N6O12S2	Amino Acid (Peptide)	0.0004369	5.22E-04	1.86	0.63	0.67	-	1.25	-	-	-1.06	-	-	-
3-Methoxy-L-Tyrosine	-	C10H13NO4	Organic Compound	0.0004387	5.22E-04	1.86	0.63	0.77	-	-	-1.96	-	-	-	-	1.33
N(pi)-Methyl-L-histidine	C01152	C7H11N3O2	Organic Compound	0.0004895	5.75E-04	1.84	0.63	1.03	-	-	1.12	1.75	-	-	-	-
N-Acetyl-DL-Glutamic Acid	C00624	C7H11NO5	Acetylated Amino Acid	0.0006111	7.08E-04	1.8	0.64	0.51	-1.1	-	-	1.01	-1.57	-1.63	-	-
L-Tyrosine	C00082	C9H11NO3	Amino Acid	0.0006287	7.26E-04	1.8	0.64	0.49	-	-	-1.91	-	1.15	-1.09	-	-
Norephedrine	C02343	C9H13NO	Amine	0.000873	1.00E-03	1.74	0.66	0.56	1.52	-	-	1.94	-	-1.46	-1.26	1.14
S-Carboxymethyl-L-Cysteine	-	C5H9NO4S	Organic Compound (Amino Acid)	0.001457	1.67E-03	1.66	0.68	0.16	-	-1.95	-	-	2.42	-	-	-
(R)-Malate	C00497	C4H6O5	Organic Acid	0.0015088	1.72E-03	1.65	0.68	0.35	-	-	-	-	-1.09	-	-	-
6-Phosphogluconic Acid	C00345	C6H13O10P	Organic Compound	0.0046952	5.18E-03	1.45	0.73	0.84	-4.12	-	-4.32	-1.31	-5.2	-	-1.27	-
Mannitol	C00392	C6H14O6	Sugar Alcohol	0.0058995	6.43E-03	1.41	0.74	0.45	1.29	-	-	-	-	-	-	-
Alpha-Ketoglutaric Acid	C00026	C5H6O5	Organic Acid	0.0063986	6.90E-03	1.4	0.74	0.56	-	1.44	3.2	3.32	-	-	1.26	-
Xylitol	C00379	C5H12O5	Sugar Alcohol	0.0074512	8.00E-03	1.37	0.75	0.77	1.58	1.08	-	2.85	1.15	-2.14	-	1.2
3-(2-Hydroxyphenyl)propanoic acid	C01198	C9H10O3	Organic Acid	0.0094585	1.01E-02	1.33	0.76	0.81	-2.7	-	-1.51	-1.94	-1.79	-	-	-
Oxaloacetate	C00036	C4H4O5	Organic Acid	0.010901	1.16E-02	1.3	0.76	0.33	-	-	-	-1.09	-1.09	-	-	-
D-Ribose	C00121	C5H10O5	Sugar	0.012657	1.33E-02	1.27	0.77	0.19	1.08	-	-	-	-	-	-1.61	-
O-Acetyl-L-serine	C00979	C5H9NO4	Amino Acid	0.01524	1.60E-02	1.24	0.78	0.65	-	-	1.91	-	-	-	-	-
3,4-Dihydroxy-L-Phenylalanine	C00355	C9H11NO4	Amino Acid	0.028753	3.01E-02	1.11	0.81	0.6	-	-	-1.23	-2.06	-1.18	-	-1.61	-
L-Carnitine	C00318	C7H15NO3	Organic Acid	0.034909	3.62E-02	1.08	0.82	0.65	-	2.76	-	2.27	-3.25	-2.35	-	-
3-Amino-4-hydroxybenzoate	-	C7H7NO3	Organic Acid	0.039478	4.08E-02	1.05	0.83	0.2	-	-1.08	-	1.33	-	-	-1.39	-

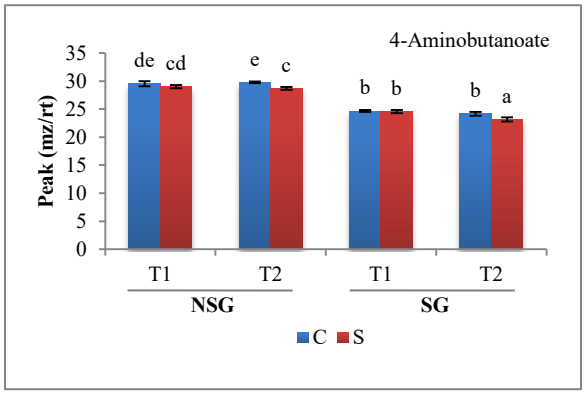
4-Aminobutanoate
Peak (mz/rt)
35
30
25
20
15
10
5
0
de cd
e c
b b
b a
T1 T2 T1 T2
NSG
SG
C S

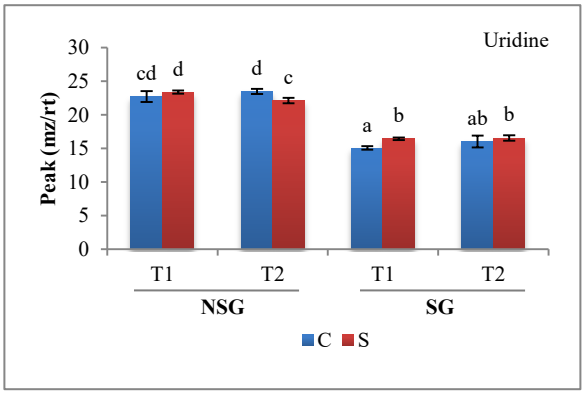
Uridine
Peak (mz/rt)
30
25
20
15
10
5
0
cd d
d c
a b
ab b
T1 T2 T1 T2
NSG
SG
C S

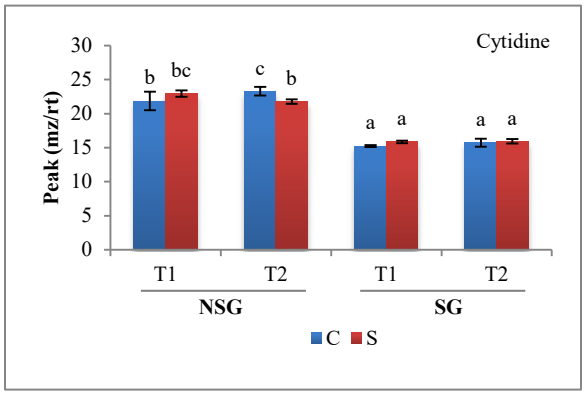
Cytidine
Peak (mz/rt)
30
25
20
15
10
5
0
b bc
c b
a a
a a
T1 T2 T1 T2
NSG
SG
C S

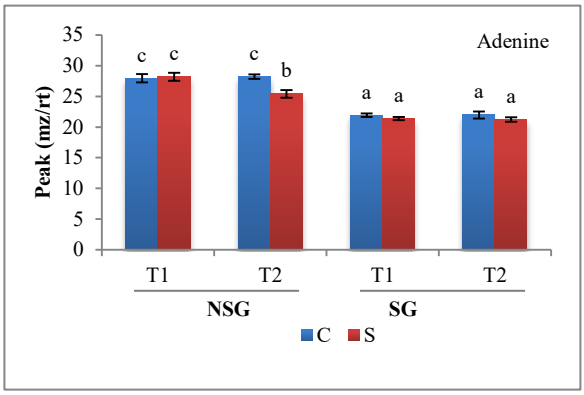
Adenine
Peak (mz/rt)
35
30
25
20
15
10
5
0
c c
c b
a a
a a
T1 T2 T1 T2
NSG
SG
C S

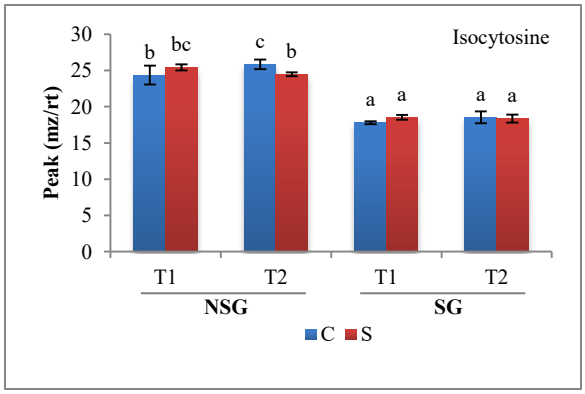
Isocytosine
Peak (mz/rt)
30
25
20
15
10
5
0
b bc
c b
a a
a a
T1 T2 T1 T2
NSG
SG
C S

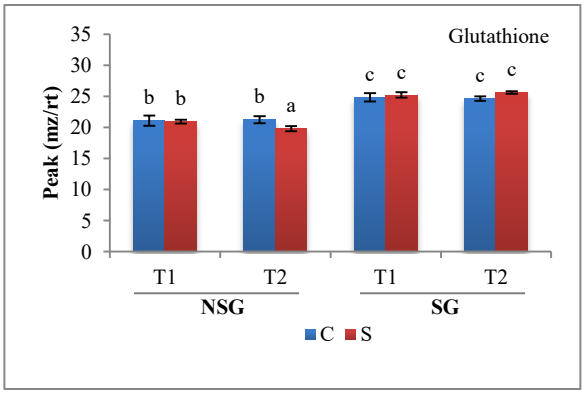
Glutathione
Peak (mz/rt)
35
30
25
20
15
10
5
0
b b
b a
c c
c c
T1 T2 T1 T2
NSG
SG
C S

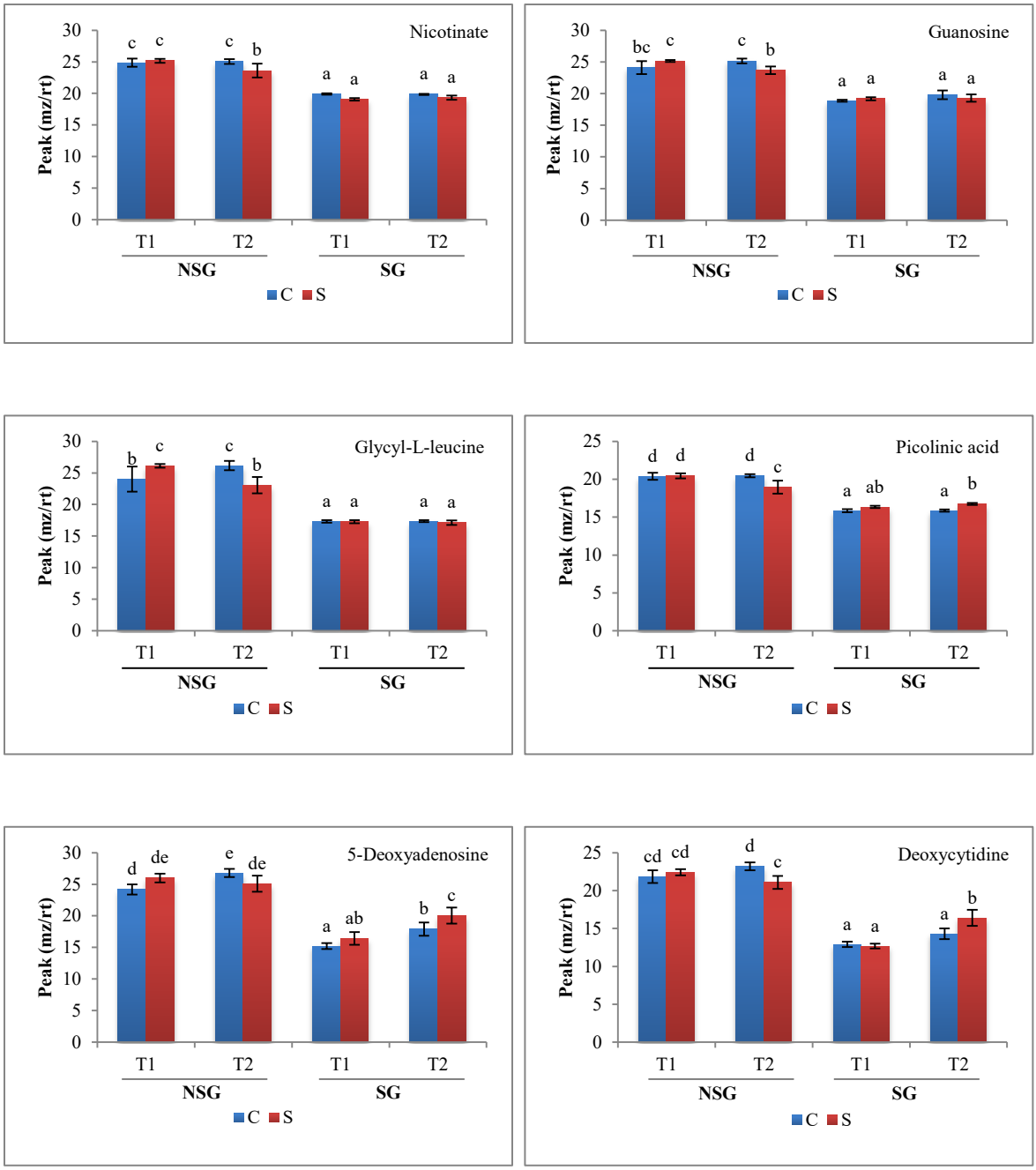

Figure 4.7. The predominant metabolites that significantly varied between non-stay-green (NSG) and stay-green (SG) genotypes under control (C) and heat stress (S) treatments at 7 days after anthesis (T1) and 14 days after anthesis (T2) (Tukey's HSD; p <0.05). Error bars represent standard deviation (n=6) and different lowercase letters represent significant difference among genotypes and treatments.

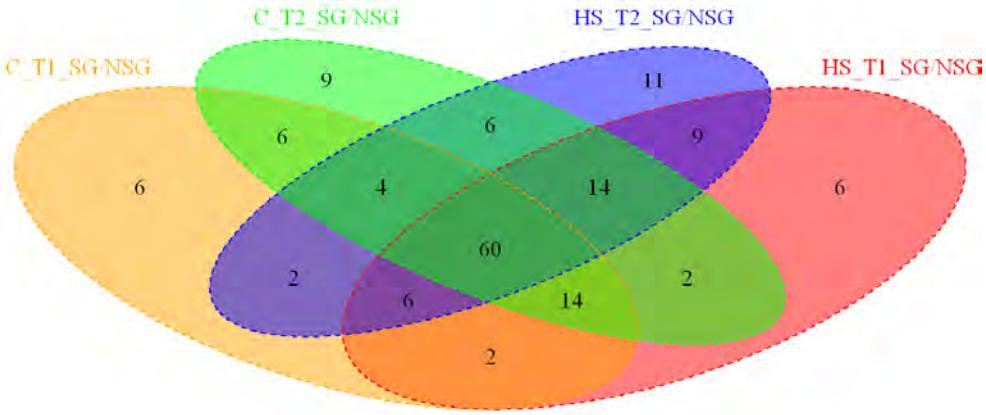

a

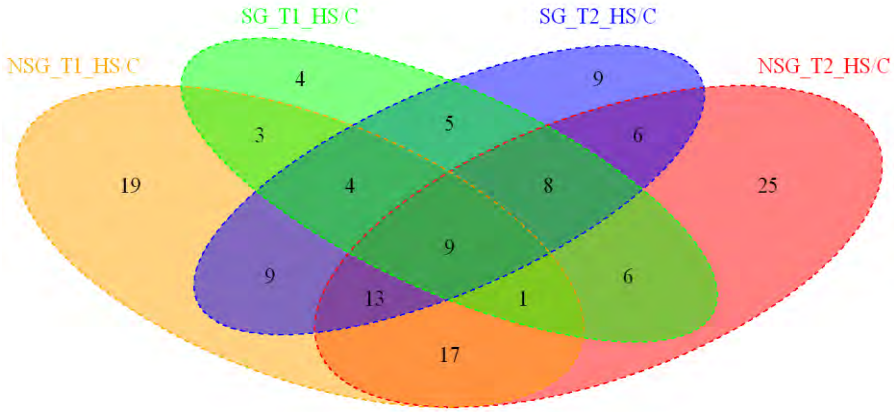

b

Figure 4.8. The number of metabolites showing significant variation in non-stay-green (NSG) and stay-green (SG) genotype under control (C) and heat stress (HS) treatment at different time points. (a) Venn plot depicting the number of metabolites that are significantly different in stay-green genotype compared to non-stay-green genotype under control and heat stress treatment at 7 days after anthesis (T1) and 14 days after anthesis (T2), (b) Venn plot showing the number of metabolites significantly regulated in non-stay-green and stay-green genotype under heat stress compare to control at 7 days after anthesis (T1) and 14 days after anthesis (T2).

Of 100 metabolites that varied between stay-green genotype and non-stay-green genotype under control at time point 1, 56 were significantly higher in the non-stay-green genotype and 44 exhibited dramatically high content in the stay-green genotype, whereas of 115 total metabolites that varied between stay-green genotype and non-stay-green

genotype under control at time point 2, 64 were considerably higher in the non-stay-green genotype and 51 were highly accumulated in the stay-green genotype. The predominant metabolites in the non-stay-green genotype compared to the stay-green genotype under control at both time points were deoxyuridine, deoxycytidine, carnosine, 5'-deoxyadenosine, glycyl-L-leucine, leucylproline, uridine, cytidine, isocytosine, and adenine. On the contrary, phosphocholine, ADP, trigonelline, allantoin, glutathione, asparagine, syringic acid, cyclic ADP-ribose, L-histidine, and L-lactic acid were highly accumulated in the stay-green genotype under control at time point 1 and phosphocholine, ADP, L-2-phosphoglyceric acid, D-raffinose, syringic acid, glutathione, L-glutamic acid, serotonin-NH3, allantoin, and disaccharide-6C/6C GLC-GLC/GLC-FRC/GAL-GLC were highly accumulated in the stay-green genotype under control at time point 2. Of 113 metabolites that varied between stay-green genotype and non-stay-green genotype under heat stress treatment at time point 1, 58 were significantly higher in the non-stay-green genotype and 55 showed high accumulation in the stay-green genotype, whereas of 112 metabolites that varied between stay-green genotype and non-stay-green genotype under heat stress at time point 2, 52 showed high accumulation in the non-stay-green genotype and 60 were highly accumulated in the stay-green genotype. The dominant metabolites in the non-stay-green genotype compare to the stay-green genotype under heat stress treatment at time point 1 were deoxycytidine, deoxyuridine, 5'-deoxyadenosine, glycyl-L-leucine, leucylproline, cytidine, uridine, isocytosine, adenine, and nicotinate, whereas the dominant metabolites in the non-stay-green genotype compare to the stay-green genotype under heat stress treatment at time point 2 were deoxyuridine, glycyl-L-leucine, isocytosine, cytidine, uridine, 4-aminobutanoate, glucose/fructose, D-glucuronic acid/D-glucuronolactone/D-galacturonic acid, 5'-deoxyadenosine, and leucylproline. The prominent metabolites in the stay-green genotype compared to the non-stay-green genotype under heat stress treatment were ADP, cyclic ADP-ribose, L-2-phosphoglyceric acid, phosphocholine, glutathione, trigonelline, syringic acid, spermine, allantoin, and hydroquinone at time point 1; and glutathione, hexanesulfonic acid-sulfate, L-2-phosphoglyceric acid, phosphocholine, cyclic ADP-ribose, ADP, L-histidine, spermine, urate, and allantoin at time point 2 (Table 4.1, Figure 4.9).

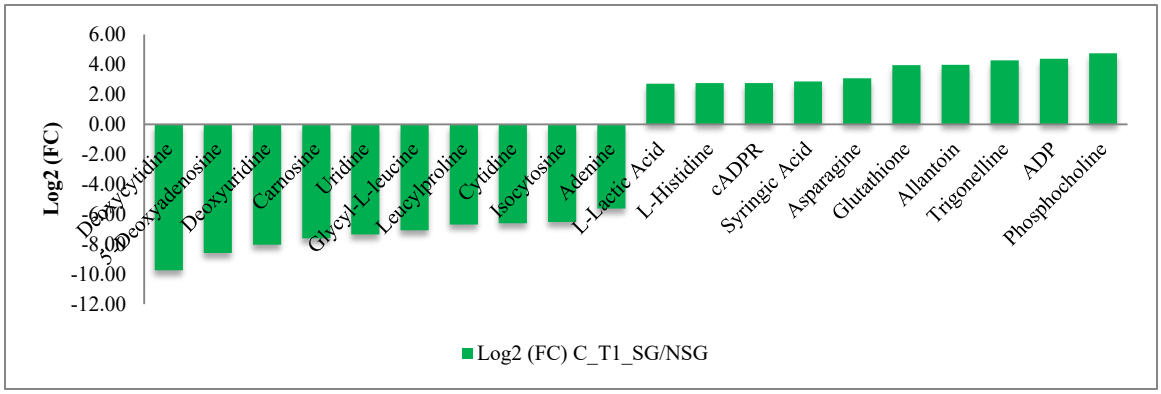
6.00
4.00
2.00
0.00
-2.00
-4.00
-6.00
-8.00
-10.00
-12.00
Log2 (FC)
Deoxycytidine
Deoxyadenosine
Deoxyuridine
Carnosine
Uridine
Glycyl-L-leucine
Leucylproline
Cytidine
Isocytosine
Adenine
L-Lactic Acid
L-Histidine
cADPR
Syringic Acid
Asparagine
Glutathione
Allantoin
Trigonelline
ADP
Phosphocholine
Log2 (FC) C_T1_SG/NSG

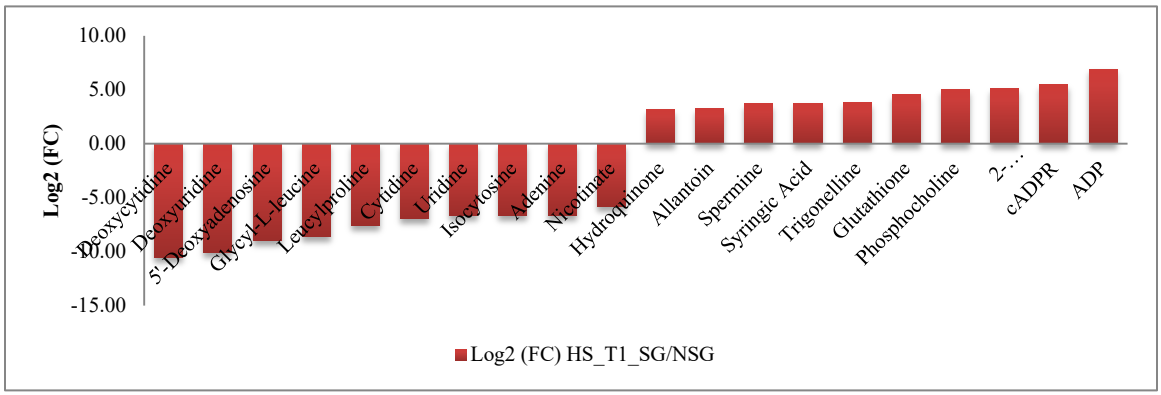
10.00
5.00
0.00
-5.00
-10.00
-15.00
Log2 (FC)
Deoxycytidine
Deoxyuridine
5'-Deoxyadenosine
Glycyl-L-leucine
Leucylproline
Cytidine
Uridine
Isocytosine
Adenine
Nicotinate
Hydroquinone
Allantoin
Spermine
Syringic Acid
Trigonelline
Glutathione
Phosphocholine
2-…
cADPR
ADP
Log2 (FC) HS_T1_SG/NSG

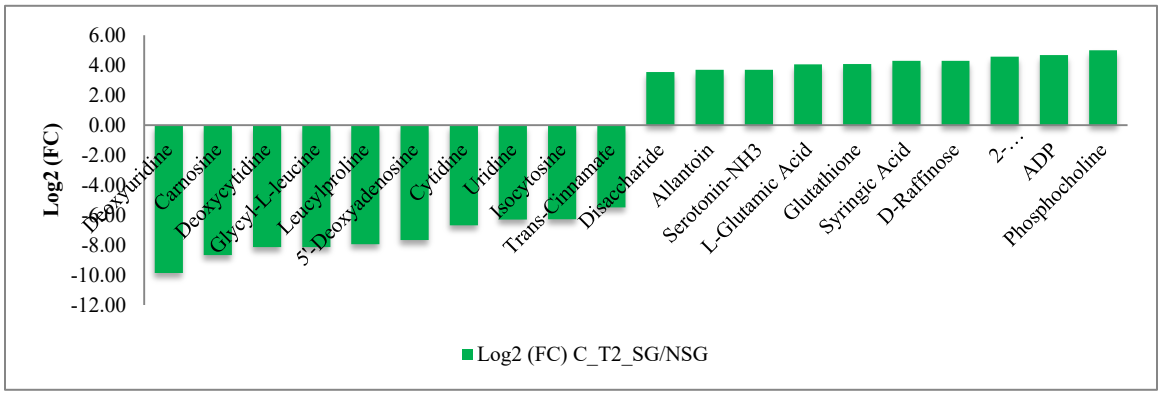
6.00
4.00
2.00
0.00
-2.00
-4.00
-6.00
-8.00
-10.00
-12.00
Log2 (FC)
Deoxyuridine
Carnosine
Deoxycytidine
Glycyl-L-leucine
Leucylproline
5'-Deoxyadenosine
Cytidine
Uridine
Isocytosine
Trans-Cinnamate
Disaccharide
Allantoin
Serotonin-NH3
L-Glutamic Acid
Glutathione
Syringic Acid
D-Raffinose
2-…
ADP
Phosphocholine
Log2 (FC) C_T2_SG/NSG

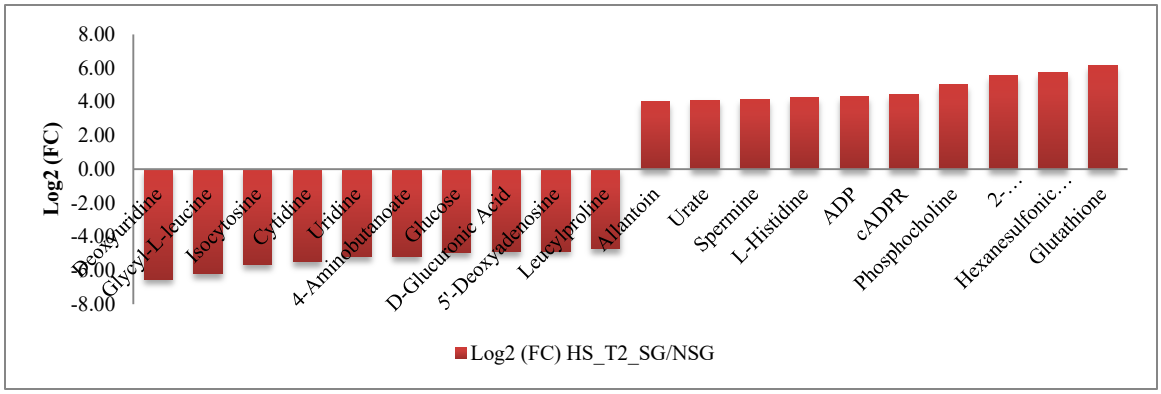

Figure 4.9. The variations in the levels of metabolites accumulated in the leaves of stay-green (SG) compare to non-stay-green (NSG) genotype grown under control (C) and heat stress (HS) treatments at different time points (T1: Day 7 of heat stress and T2: day 14 of heat stress).

The fold change analysis between the non-stay-green heat treated samples and the non-stay-green controlled samples revealed a variation in the accumulation of 75 and 85 metabolites at time point 1 and time point 2, respectively. The metabolites that increased in the non-stay-green genotype under heat stress treatment at time point 1 with log2 fold change greater than 2 included N-methyl-L-glutamate, 5-hydroxy-L-tryptophan, proline, tryptophan, source fragment TRP, S-carboxymethyl-L-cysteine, L-kynurenine, and L-pipecolic acid. The metabolites that showed a significant decline with log2 fold change less than -2 in the non-stay-green genotype under heat stress treatment at time point 1 were 6-phosphogluconic acid, quinate, L-2-phosphoglyceric acid, shikimate, L-carnitine, putrescine, 2,5-dihydroxybenzoate, hydroquinone, ADP, caffeate, glyceric acid, isocitric acid, and hexanesulfonic acid-sulfate. The metabolites accumulated in the non-stay-green genotype in heat stress treated sample at time point 2 with log2 fold change greater than 2 were N-methyl-L-glutamate, serotonin-NH3, proline, L-kynurenine, 4-oxoproline, nicotinamide, disaccharide-GLC-GLC/GLC-FRC/GAL-GLC, D-raffinose, valerylcarniti--ne, L-pipecolic acid, xanthine, kynurenic acid, and N6-delta2-isopentenyl-adenine; whereas the metabolites that showed significant decline were L-methionine, hexanesulfonic acid-sulfate, carnosine, L-lysine, xanthurenic acid, adenine, L-2-phosphoglyceric acid, 5-hydroxyindoleacetate, glycyl-L-leucine, 1-methyladenosine, aspartate, Leu Pro, pyridoxine, diethyl 2-methyl-3-oxosuccinate, L-carnitine, shikimate,

orthophosphate, pyridoxal, L-arginine, CMP, glycine, C5-sugar alcohol, and riboflavin. The fold change analysis between the stay-green heat treated plants and stay-green controlled plants unraveled variable accumulation of 40 and 63 metabolites at time point 1 and time point 2, respectively. Tyramine, Tryptophan, Source Fragment TRP, and 5-Hydroxy-L-Tryptophan were accumulated in the stay-green genotype with log2 fold change greater than 2 under heat stress treatment at time point 1, whereas the levels of pyridoxine and xanthurenic acid reduced in the stay-green genotype under heat stress at time point 1. The metabolites that increased with log2 fold change greater than 2 in the stay-green genotype under heat stress treatment at time point 2 included tryptophan, agmatine sulfate, source fragment TRP, kynurenic acid, thiamine, tyramine, L-kynurenine, and urate; and the metabolites that declined in the stay-green genotype under heat stress treatment at time point 2 were shikimate and O-acetyl-L-serine (Table 4.1, Figure 4.10).

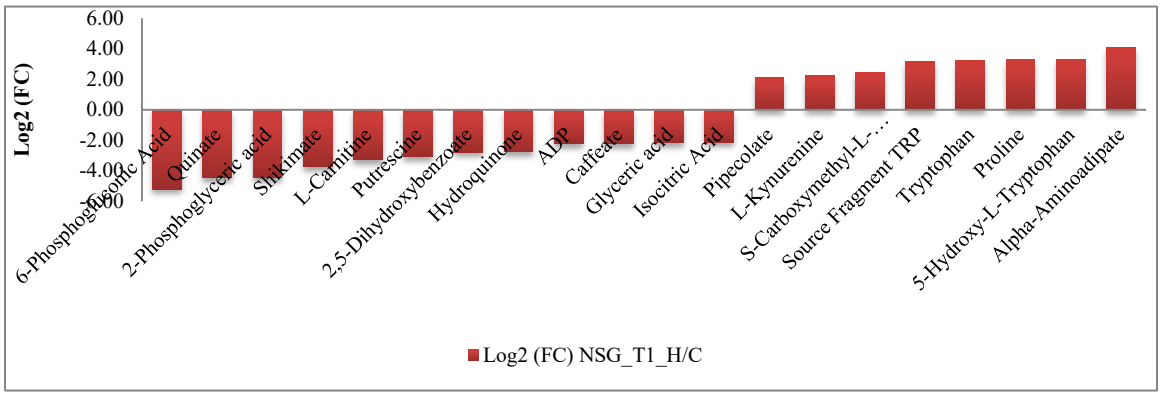

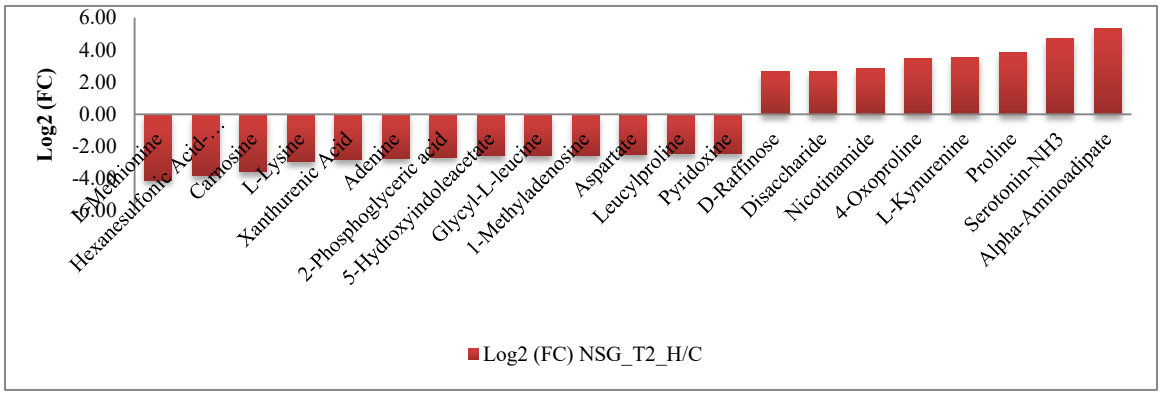

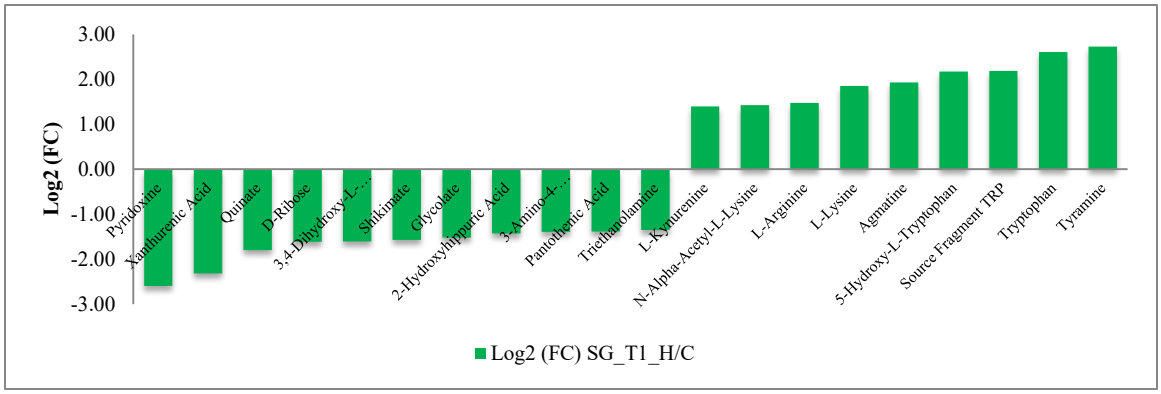

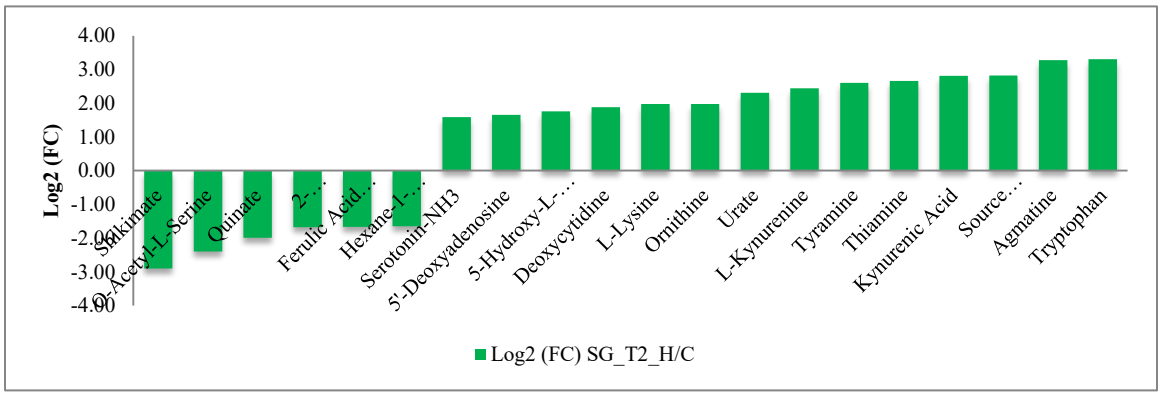

Figure 4.10. The variations in the levels of metabolites accumulated in the leaves of non-stay-green (NSG) and stay-green (SG) genotype grown under heat stress at different time points (T1: Day 7 of heat stress and T2: day 14 of heat stress).

5-Hydroxy-L-tryptophan, tryptophan, source fragment TRP, L-kynurenine, L-pipecolic acid, L-histidine, 5'-deoxyadenosine, and N-alpha-acetyl-L-lysine were highly accumulated in both non-stay-green and stay-green heat stress treated samples at time point 1 and serotonin-NH3, proline, L-kynurenine, L-pipecolic acid, xanthine, kynurenic acid, and 5-hydroxy-L-tryptophan showed increase abundance in both the genotypes under heat stress at time point 2. The metabolites that declined in both non-stay-green and stay-green genotypes under heat stress were 6-phosphogluconic acid, quinate, L-2-phosphoglyceric acid, shikimate, isocitric acid, spermidine, 2-hydroxyhippuric acid, 3,4-dihydroxy-L-phenylalanine, and glycolate at time point 1, whereas xanthurenic acid, adenine, L-2-phosphoglyceric acid, aspartate, shikimate, sarcosine/beta-alanine,

spermidine, camphor, guanosine, phosphocholine, isocitric acid, 4-aminobutanoate, nicotinamide ribotide, and caffeate at time point 2 (Table 4.1, Figure 4.11).

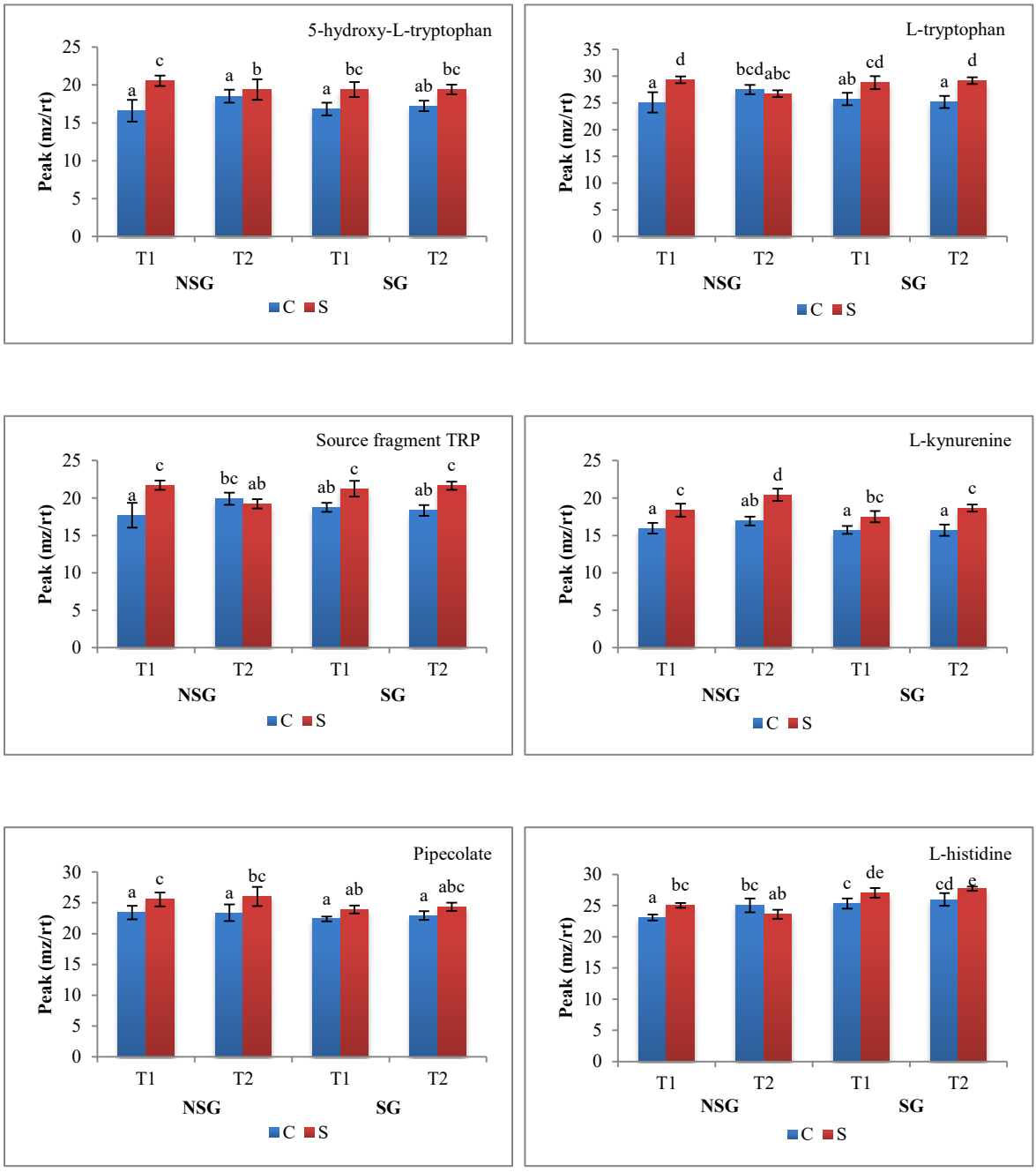

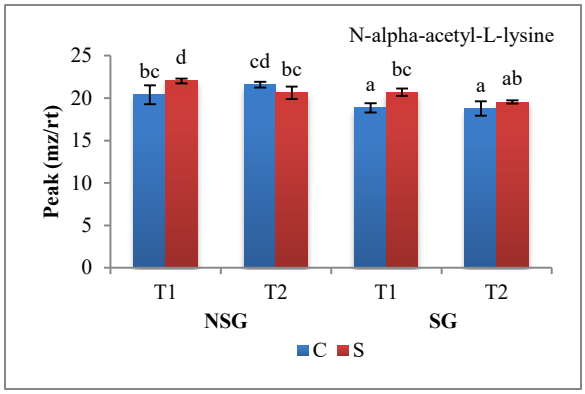
N-alpha-acetyl-L-lysine
Peak (mz/rt)
25
20
15
10
5
0
bc
d
cd
bc
bc
a
a
ab
T1
T2
T1
T2
NSG
SG
C
S

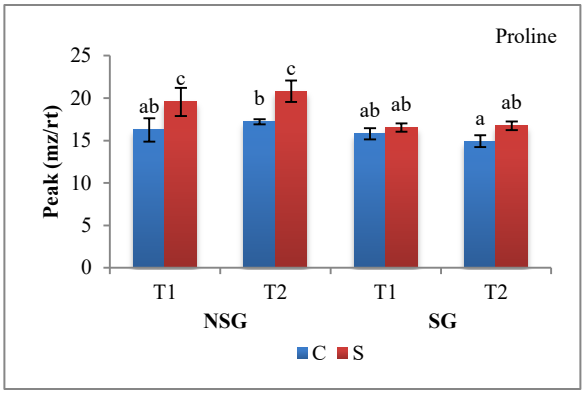
Proline
Peak (mz/rt)
25
20
15
10
5
0
ab
c
b
c
ab
ab
a
ab
T1
T2
T1
T2
NSG
SG
C
S

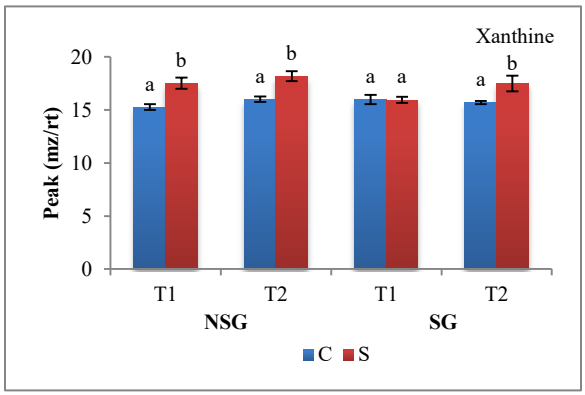
Xanthine
Peak (mz/rt)
20
15
10
5
0
a
b
a
b
a
a
a
b
T1
T2
T1
T2
NSG
SG
C
S

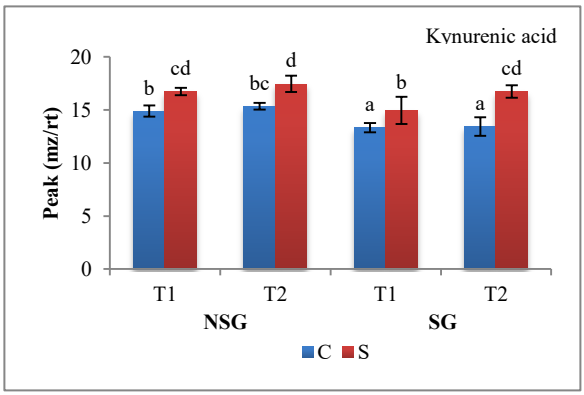
Kynurenic acid
Peak (mz/rt)
20
15
10
5
0
b
cd
bc
d
a
b
a
cd
T1
T2
T1
T2
NSG
SG
C
S

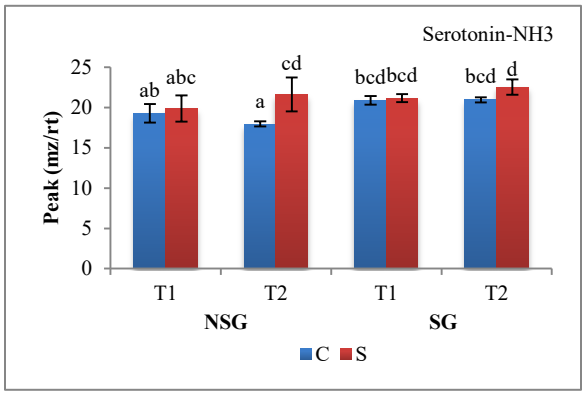
Serotonin-NH3
Peak (mz/rt)
25
20
15
10
5
0
ab
abc
a
cd
bcd
bcd
bcd
d
T1
T2
T1
T2
NSG
SG
C
S

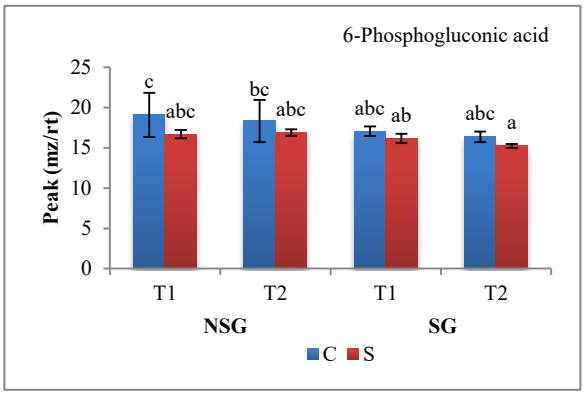
6-Phosphogluconic acid
Peak (mz/rt)
25
20
15
10
5
0
c
abc
bc
abc
abc
ab
abc
a
T1
T2
T1
T2
NSG
SG
C
S

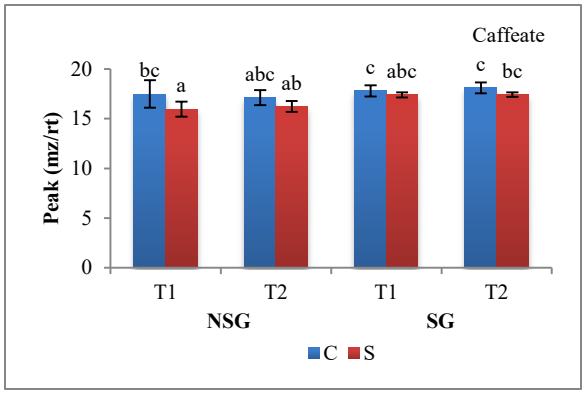
Caffeate
Peak (mz/rt)
20
15
10
5
0
bc
a
abc
ab
c
abc
c
bc
T1
T2
T1
T2
NSG
SG
C
S

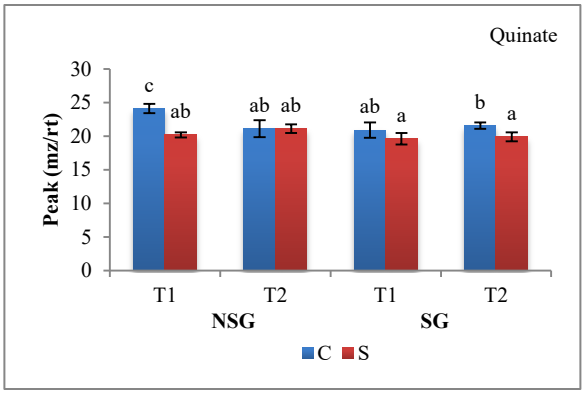
Quinate
Peak (mz/rt)
30
25
20
15
10
5
0
c
ab
ab
ab
ab
a
b
a
T1
T2
T1
T2
NSG
SG
C
S

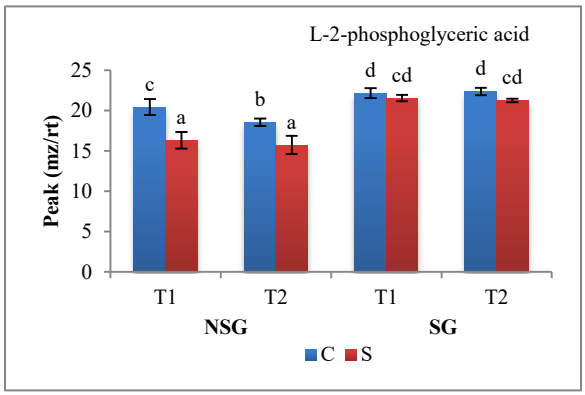
L-2-phosphoglyceric acid
Peak (mz/rt)
25
20
15
10
5
0
c
a
b
a
d
cd
d
cd
T1
T2
T1
T2
NSG
SG
C
S

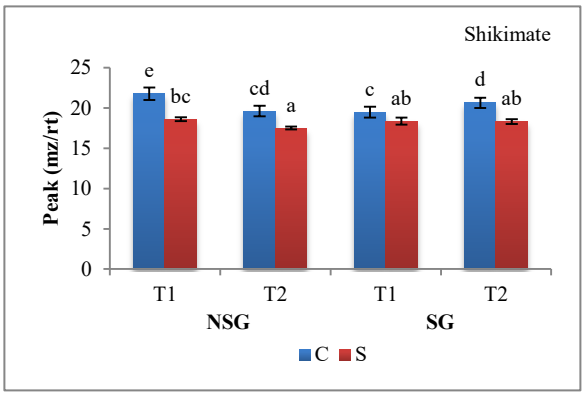
Shikimate
Peak (mz/rt)
25
20
15
10
5
0
e
bc
cd
a
c
ab
d
ab
T1
T2
T1
T2
NSG
SG
C
S

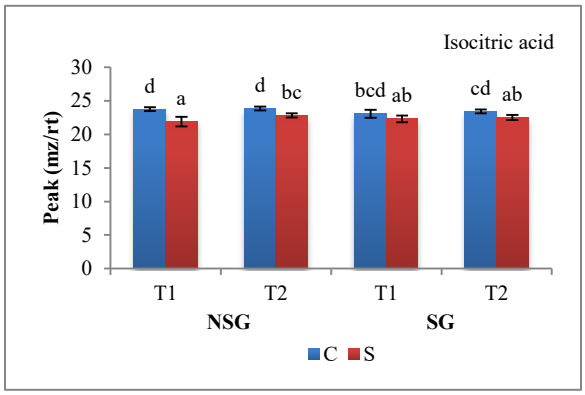
Isocitric acid
Peak (mz/rt)
30
25
20
15
10
5
0
d
a
d
bc
bcd
ab
cd
ab
T1
T2
T1
T2
NSG
SG
C
S

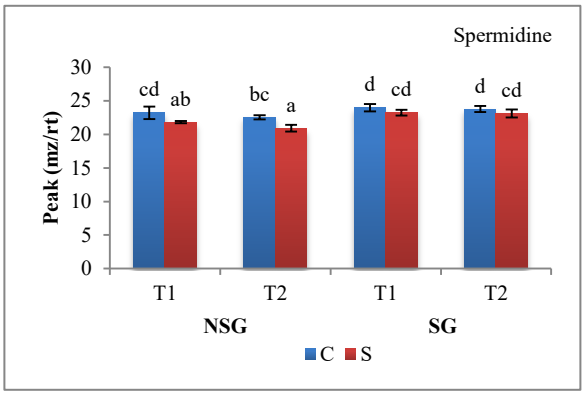
Spermidine
Peak (mz/rt)
30
25
20
15
10
5
0
cd
ab
bc
a
d
cd
d
cd
T1
T2
T1
T2
NSG
SG
C
S

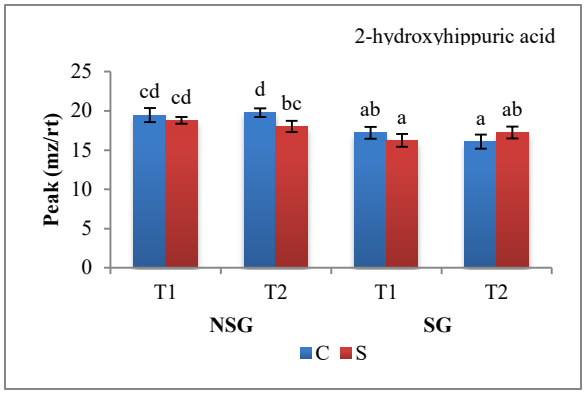
2-hydroxyhippuric acid
Peak (mz/rt)
25
20
15
10
5
0
cd cd
d bc
ab a
a ab
T1 T2 T1 T2
NSG
SG
C S

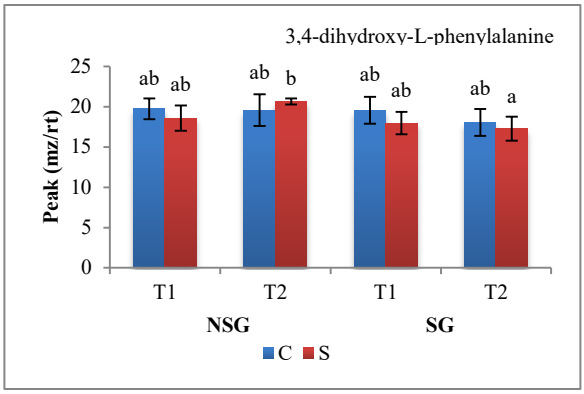
3,4-dihydroxy-L-phenylalanine
Peak (mz/rt)
25
20
15
10
5
0
ab ab
ab b
ab ab
ab a
T1 T2 T1 T2
NSG
SG
C S

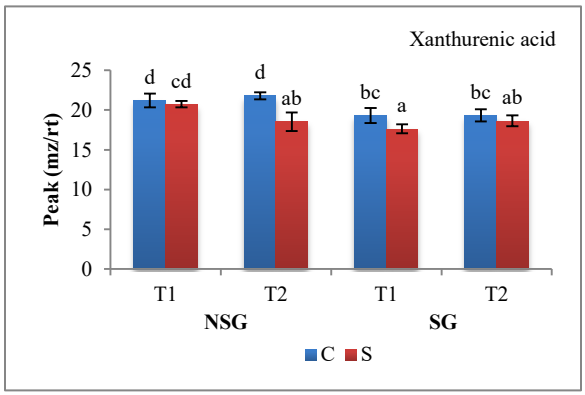
Xanthurenic acid
Peak (mz/rt)
25
20
15
10
5
0
d cd
d ab
bc a
bc ab
T1 T2 T1 T2
NSG
SG
C S

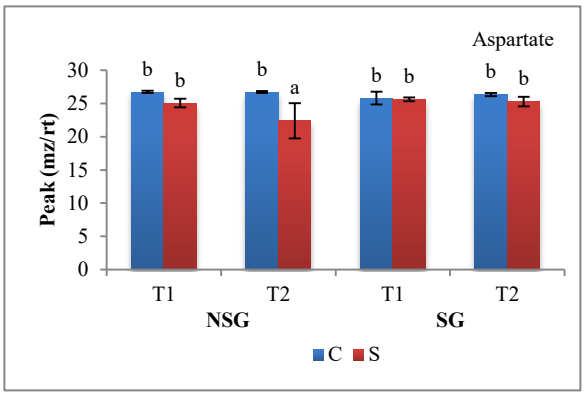
Aspartate
Peak (mz/rt)
30
25
20
15
10
5
0
b b
b a
b b
b b
T1 T2 T1 T2
NSG
SG
C S

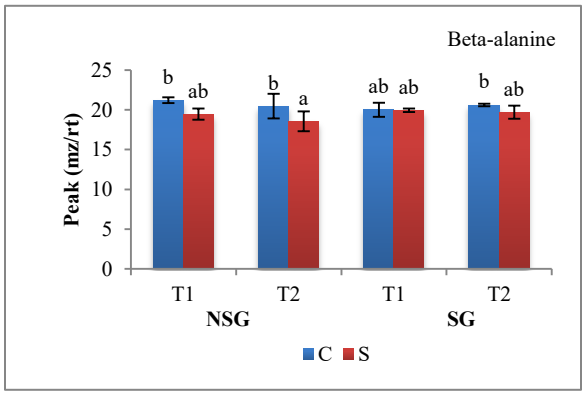
Beta-alanine
Peak (mz/rt)
25
20
15
10
5
0
b ab
b a
ab ab
b ab
T1 T2 T1 T2
NSG
SG
C S

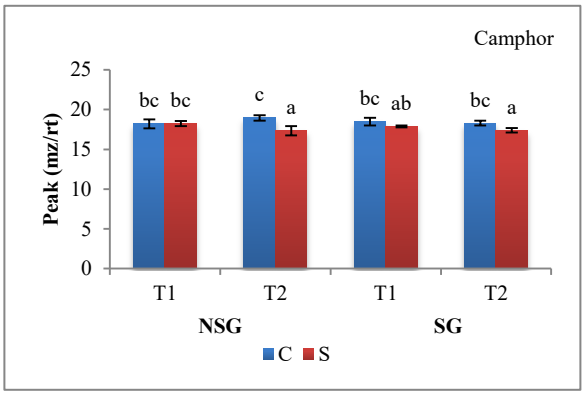
Camphor
Peak (mz/rt)
25
20
15
10
5
0
bc bc
c a
bc ab
bc a
T1 T2 T1 T2
NSG
SG
C S

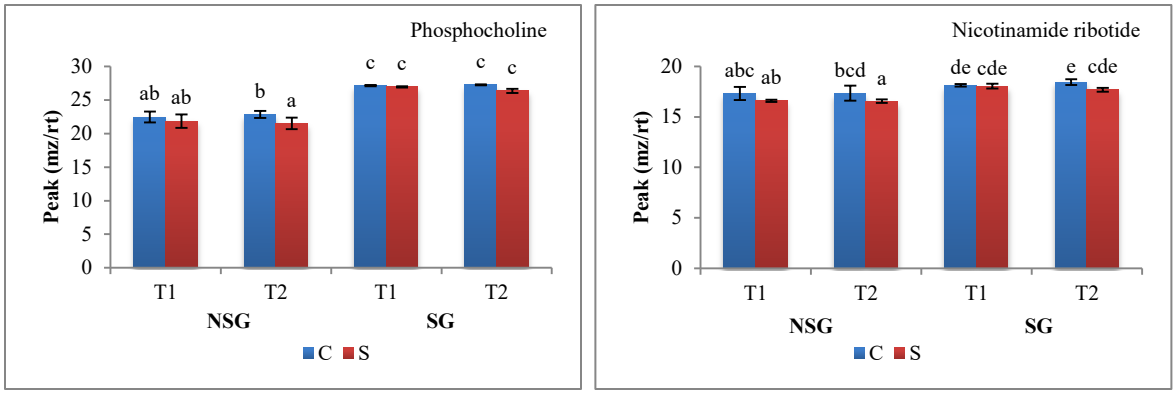

Figure 4.11. The metabolites that showed significant variation under heat stress treatment at day 7 (T1) and day 14 (T2) of heat stress (Tukey's HSD; p <0.05). NSG: Non-stay-green, SG: Stay-green, C: Control, S: Stress. Error bars represent standard deviation (n=6) and different lowercase letters represent significant difference among genotypes and treatments.

4.4.3.1. Metabolic pathway analysis

Metabolic pathway analysis was performed in *Metaboanalyst 4.0* using *Oryza sativa* japonica (Japanese rice) (KEGG) library. Fifty five metabolic pathways were identified where the significant known metabolites were involved in different steps. Fifteen biosynthesis pathways identified were aminoacyl-tRNA biosynthesis, arginine biosynthesis, isoquinoline alkaloid biosynthesis, betalain biosynthesis, lysine biosynthesis, phenylalanine, tyrosine and tryptophan biosynthesis, biosynthesis of secondary metabolites – unclassified, valine, leucine and isoleucine biosynthesis, pantothenate and CoA biosynthesis, phenylpropanoid biosynthesis, zeatin biosynthesis, ubiquinone and other terpenoid-quinone biosynthesis, monobactam biosynthesis, tropane, piperidine and pyridine alkaloid biosynthesis, and fatty acid biosynthesis. Two degradation pathways detected were lysine degradation and valine, leucine, and isoleucine degradation. Other important metabolic pathways included porphyrin and chlorophyll metabolism, citrate cycle (TCA cycle), glyoxylate and dicarboxylate metabolism, carbon fixation in photosynthetic organisms, glycolysis/gluconeogenesis, and pyruvate metabolism (Table 4.2, Figure 4.12).

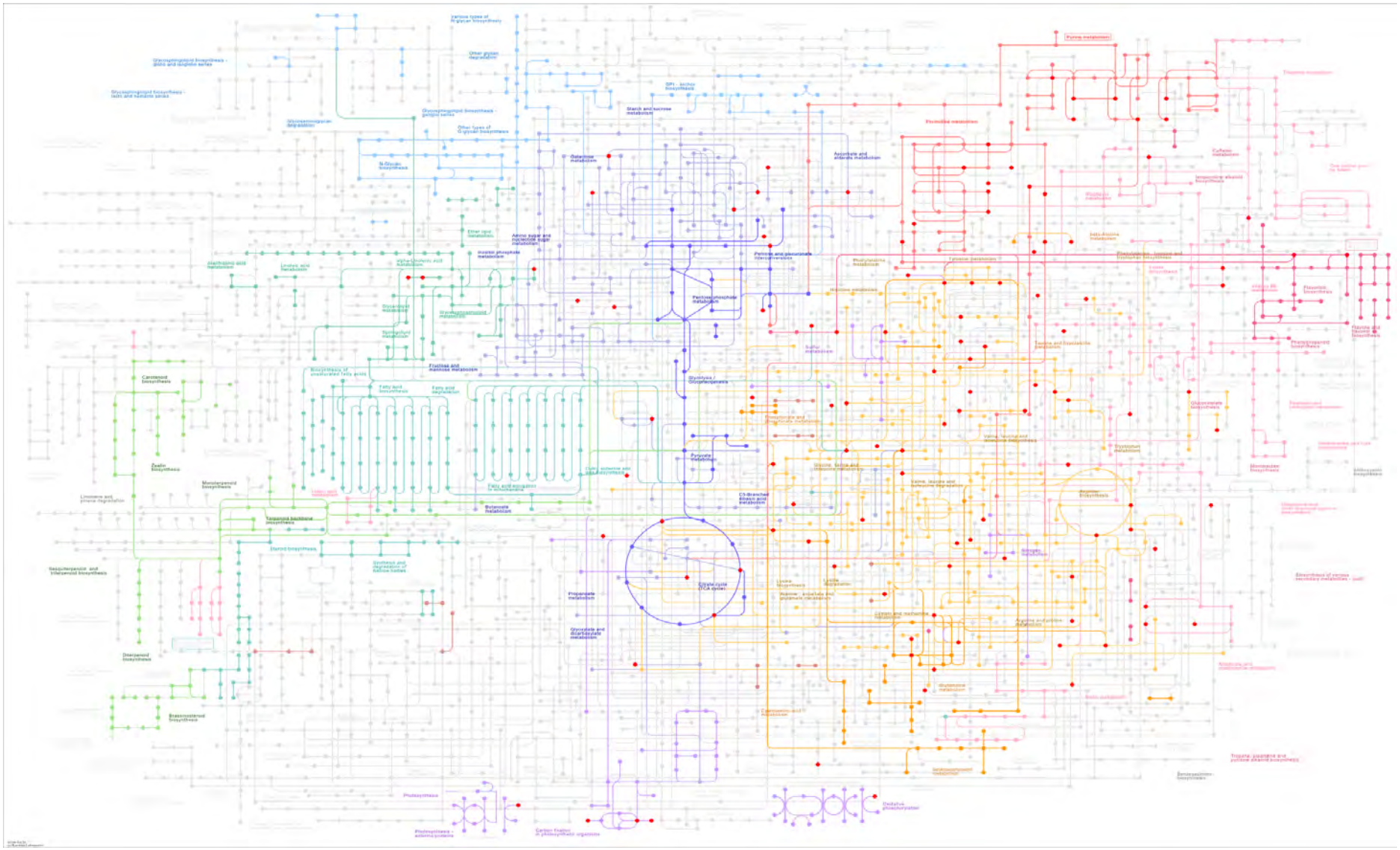

Figure 4.12. The metabolic pathways that varied in the non-stay-green and stay-green genotypes at different time points under heat stress treatment at day 7 and day 14 of heat stress. The red circle represents the metabolites that varied between genotypes at different time points under control and heat stress treatments.

Table 4.2. Metabolic pathway analysis using Oryza sativa japonica (Japanese rice) (KEGG) library

Pathway	Total	Hits	Metabolites
Aminoacyl-tRNA biosynthesis	46	19	L-Asparagine; L-Histidine; L-Phenylalanine; L-Arginine; L-Glutamine; Glycine; L-Aspartate; L-Serine; L-Methionine; L-Valine; L-Alanine; L-Lysine; L-Isoleucine; L-Leucine; L-Threonine; L-Tryptophan; L-Tyrosine; L-Proline; L-Glutamate
Alanine, aspartate and glutamate metabolism	22	8	L-Aspartate; L-Asparagine; L-Alanine; 2-Oxoglutarate; L-Glutamine; L-Glutamate; 4-Aminobutanoate; Oxaloacetate
Arginine and proline metabolism	28	9	L-Arginine; Agmatine; Spermidine; Spermine; L-Proline; L-Glutamate; L-Ornithine; 4-Guanidinobutanoate; 4-Aminobutanoate
Arginine biosynthesis	18	7	L-Glutamate; L-Arginine; N-Acetyl-L-glutamate; L-Aspartate; L-Ornithine; 2-Oxoglutarate; L-Glutamine
Isoquinoline alkaloid biosynthesis	6	4	L-Tyrosine; 3,4-Dihydroxy-L-phenylalanine; Dopamine; Tyramine
Glyoxylate and dicarboxylate metabolism	29	9	Isocitrate; Glycolate; D-Glycerate; L-Serine; Glycine; L-Glutamate; L-Glutamine; 2-Oxoglutarate; Oxaloacetate
beta-Alanine metabolism	18	6	beta-Alanine; L-Aspartate; 3-Ureidopropionate; Spermine; Spermidine; Pantothenate
Glycine, serine and threonine metabolism	33	8	L-Serine; Choline; D-Glycerate; Glycine; L-Aspartate; L-Threonine; Betaine; L-Tryptophan
Glutathione metabolism	27	7	Glutathione; Glutathione disulfide; Glycine; L-Glutamate; L-Ornithine; Ascorbate; Spermidine
Tyrosine metabolism	18	5	3,4-Dihydroxy-L-phenylalanine; Homogentisate; L-Tyrosine; Tyramine; Dopamine
Betalain biosynthesis	3	2	3,4-Dihydroxy-L-phenylalanine; Dopamine
Pyrimidine metabolism	38	8	L-Glutamine; (S)-Dihydroorotate; Uridine; 3-Ureidopropionate; CMP; Deoxyuridine; Deoxycytidine; beta-Alanine
Nicotinate and nicotinamide metabolism	13	4	L-Aspartate; Nicotinamide D-ribonucleotide; Nicotinate; Nicotinamide
Lysine biosynthesis	9	3	LL-2,6-Diaminoheptanedioate; L-Aspartate; L-Lysine
Phenylalanine, tyrosine and tryptophan biosynthesis	22	5	L-Tyrosine; Shikimate; L-Tryptophan; Anthranilate; L-Phenylalanine
Biosynthesis of secondary metabolites - unclassified	5	2	trans-Cinnamate; 4-Coumarate
Valine, leucine and isoleucine biosynthesis	22	4	L-Threonine; L-Leucine; L-Isoleucine; L-Valine
Purine metabolism	63	9	Xanthine; L-Glutamine; ADP; Adenosine; Guanine; Urate; Adenine; Inosine; Guanosine
Pantothenate and CoA biosynthesis	23	4	Pantothenate; 3-Ureidopropionate; beta-Alanine; L-Valine
Tryptophan metabolism	23	4	5-Hydroxy-L-tryptophan; L-Tryptophan; Indolepyruvate; 5-Hydroxyindoleacetate
Histidine metabolism	17	3	Carnosine; L-Histidine; Imidazole-4-acetate
Butanoate metabolism	17	3	L-Glutamate; 2-Oxoglutarate; 4-Aminobutanoate
Cyanoamino acid metabolism	26	4	L-Asparagine; Glycine; L-Aspartate; L-Serine
Lysine degradation	18	3	L-Lysine; L-Pipecolate; L-2-Aminoadipate
Ascorbate and aldarate metabolism	18	3	D-Glucuronate; Ascorbate; D-Glucarate
Phenylpropanoid biosynthesis	35	5	L-Tyrosine; L-Phenylalanine; Caffeate; 4-Coumarate; trans-Cinnamate
Galactose metabolism	27	4	Raffinose; D-Glucose; Glycerol; alpha-D-Galactose
Vitamin B6 metabolism	11	2	Pyridoxine; Pyridoxal

Citrate cycle (TCA cycle)	20	3	2-Oxoglutarate; Isocitrate; Oxaloacetate
Nitrogen metabolism	12	2	L-Glutamine; L-Glutamate
Phenylalanine metabolism	12	2	L-Phenylalanine; trans-Cinnamate
Zeatin biosynthesis	21	3	ADP; N6-(Delta2-Isopentenyl)-adenine; Adenine
Carbon fixation in photosynthetic organisms	21	3	Oxaloacetate; L-Aspartate; L-Alanine
Sulfur metabolism	15	2	O-Acetyl-L-serine; L-Serine
Taurine and hypotaurine metabolism	6	1	Taurine
Ubiquinone and other terpenoid-quinone biosynthesis	35	4	L-Tyrosine; 4-Coumarate; Homogentisate; trans-Cinnamate
Cysteine and methionine metabolism	46	5	L-Cystathionine; L-Methionine; O-Acetyl-L-serine; L-Serine; L-Aspartate
Pentose and glucuronate interconversions	17	2	D-Glucuronate; Xylitol
Monobactam biosynthesis	8	1	L-Aspartate
Tropane, piperidine and pyridine alkaloid biosynthesis	8	1	L-Phenylalanine
Pentose phosphate pathway	19	2	D-Ribose; 6-Phospho-D-gluconate
Glycerolipid metabolism	21	2	Glycerol; D-Glycerate
Thiamine metabolism	22	2	Thiamine; Glycine
Pyruvate metabolism	22	2	Oxaloacetate; (R)-Lactate
Riboflavin metabolism	11	1	Riboflavin
Valine, leucine and isoleucine degradation	37	3	L-Valine; L-Isoleucine; L-Leucine
Glycerophospholipid metabolism	37	3	Choline phosphate; Choline; sn-Glycero-3-phosphocholine
Selenocompound metabolism	13	1	L-Alanine
Sphingolipid metabolism	17	1	L-Serine
Starch and sucrose metabolism	22	1	D-Glucose
Glycolysis / Gluconeogenesis	26	1	Oxaloacetate
Inositol phosphate metabolism	28	1	D-Glucuronate
Porphyrin and chlorophyll metabolism	47	2	5-Aminolevulinate; L-Glutamate
Amino sugar and nucleotide sugar metabolism	50	2	D-Glucuronate; D-Glucosamine
Fatty acid biosynthesis	56	1	Malonate

4.5. Discussion

Heat stress adversely affects plant growth, development, and productivity by alternating an array of biochemical, morpho-physiological, and anatomical processes (Akter and Islam, 2017). Terminal heat stress accelerates the deterioration of chlorophyll content, which results in decrease in photosynthetic activity and biological yield (Liu *et al*., 2017). The effects of heat stress can be managed by development of superior genotypes with specific tolerance mechanisms. Plants have evolved distinct tolerance mechanisms such as avoidance, escape, and stay-green to maintain productivity by acclimation to heat stress (Sharma *et al*., 2019). Of these mechanisms, a secondary stay-green trait enables plants to maintain chlorophyll content and photosynthetic capacity during the grain filling duration, which in turn results in maximum mass per grain. Stay-green genotypes retain its leaf photosynthetic activity for longer duration even under abiotic and biotic stresses. Thus, the stay-green trait can be used as a principal selection strategy for yield sustainability under rapid warming scenario (Kamal *et al*., 2019). The present study was conducted to unravel the variation in morpho-physiology responses and metabolic regulation among non-stay-green and stay-green genotypes under terminal heat stress.

Heat stress affects the notable complex physiological mechanisms, which eventually influences plant‘s green biomass and photosynthetic activity (Liu *et al*., 2017; Djanaguiraman *et al*., 2018). Photosynthesis is one of the most sensitive metabolic processes, having direct impact on cereal yields (Ristic *et al*., 2007). The estimation of chlorophyll content and chlorophyll fluorescence used to detect the damage cause to photosystem II, is an indirect measure of photosynthesis (Guidi *et al*., 2019). The current study demonstrated a significant decline in chlorophyll content in the non-stay-green genotype under heat stress treatment, whereas the stay-green genotype retained chlorophyll content under heat stress treatment. The photosynthetic efficiency (fv/fm and Phi II) showed significant decrease under heat stress in both non-stay-green and stay-green genotypes. However, the reduction in photosynthetic efficiency was more pronounced in non-stay-green genotype. Our results are in alignment with previous studies that reported a significant decline in chlorophyll content and photosynthetic

efficiency under heat stress, percentage decline in chlorophyll content and photosynthetic efficiency varied among genotypes, and stay-green genotypes retain chlorophyll content and photosynthetic efficiency for longer duration under stress (Talukder *et al*., 2014; Azam *et al*., 2015; Pinto *et al*., 2016; Bhusal *et al*., 2018; Sattar *et al*., 2020; Latif *et al*., 2020). The stay-green genotypes seems to protect the chloroplast and reduce damage cause to the photosynthetic apparatus by dissipating excess of the radiation energy through high levels of carotenes and xanthophylls in their leaves and vegetative parts (Zhao and Tan, 2005; Suzuki and Mittler, 2006). Carotenes and xanthophylls are the structural components of the photosynthetic machinery and contribute to the protection of the photosystems against oxidative stress generated by light, heat, chilling, drought, salinity, or senescence (Latowski *et al*., 2011; Pinto *et al*., 2017). The strong antioxidant defense system that includes increased superoxide dismutase and catalase activities may also protects the chlorophyll and maintains the photosynthetic efficiency (Luo *et al*., 2006).

The MSI commonly estimated by measuring the ion leakage from plants is an indicator of heat stress tolerance. Positive correlation between MSI and thousand kernel weight has been reported in wheat under heat stress treatment (Rehman *et al*., 2016). Wheat genotypes showing high MSI tend to yield high under abiotic stress conditions (Blum *et al*., 2001). In the present study, a decline was noted in the MSI of both the genotypes, but the decline was significantly higher in the non-stay-green genotype than in the stay-green genotype which is in agreement with previous findings by ElBasyoni *et al*., (2017) that reported an overall decline in MSI under heat stress treatment. The cultivar specific antioxidant defense mechanism explains its tolerance to oxidative stresses (Abid *et al*., 2018). The stay-green genotypes may protect membranes from oxidative damage by minimizing the accumulation of reactive oxygen species and preventing lipid peroxidation through enhanced antioxidant enzymes activities.

Heat stress induced reduction in yield has been studied extensively in cereal crops (Ferris *et al*., 1998; Rahman *et al*., 2009; Shah *et al*., 2011; Liu et al., 2014; Fahad *et al*., 2016; Schittenhelm *et al*., 2020). For instance, wheat production declined by 6% with one-degree celsius increase in temperature (Asseng *et al*., 2015). In the current study,

biological yield and grain yield declined in both non-stay green and stay-green genotypes under heat stress conditions, however the percentage decline was significantly higher in the non-stay-green genotype. Several previous studies revealed significant decline in biological yield and grain yield in wheat under heat stress conditions (Stone *et al*., 1995; Modarresi *et al*., 2010; Prasad and Djanaguiraman *et al*., 2014; Balla *et al*., 2019). The superior performance of stay-green genotype under heat stress is an indicator of higher assimilation of photosynthate; the potential reason can be extended or higher rate of photosynthesis (Haris *et al*., 2007).

The stay-green genotype showed less damage to chlorophyll content, photosynthetic efficiency, membrane stability index, biological yield, and grain yield under heat stress treatment, which is in agreement with previous findings by Reynolds *et al*., 2000; Kumari *et al*., 2013; Pinto *et al*., 2016). Luo *et al*., (2006) and Luo *et al*., (2013) reported that functional stay-green Chuannong17 wheat genotype yield 25.7% higher than the non-stay-green Minyan11 by delaying chlorophyll degradation by 14 days; they attributed the yield advantage of the stay-green genotype to greater superoxide dismutase and catalase activity, lower malondialdehyde content, higher soluble protein content, unsaturated to saturated fatty acids ratio, and chlorophyll content, extended and enhanced photosynthetic competence, retention of shape and arrangement of chlorophyll structure, and regeneration of the chloroplast structure during the grain filling stage. The stay-green trait has been found valuable under different abiotic and biotic stresses (Duncan *et al.*, 1981; Rosenow, 1983b; Evangelista and Tangonan, 1990; Joshi *et al*., 2007; Borrell *et al*., 2014; Cerrudo *et al*., 2017); however, biochemical, physiological, and genetic basis of the stay-green trait are not yet clear. The current study demonstrated the comprehensive metabolic network underlying the stay-green trait.

To understand the metabolic regulation behind the stay-green trait under control and heat stress treatments the global metabolic profiling was carried out in the two contrasting genotypes (stay-green genotype and non-stay-green genotype) at different time points by UHPLC-HRMS. The differential accumulation of metabolites in stay-green genotype and non-stay-green genotype can provide precise information of the regulation of complex traits. The study revealed significant differences in the metabolic

phenotypes of the two selected genotypes. Approximately, 87% of the known metabolites showed variable accumulation between different groups (stay-green/non-stay-green under control, stay-green/non-stay-green under heat stress, non-stay-green under heat stress/non-stay-green under control, and stay-green under heat stress/stay-green under control).

The dominant metabolites that showed high accumulation in non-stay-green genotype were deoxyuridine, deoxycytidine, carnosine, 5'-deoxyadenosine, glycyl-L-leucine, leucyl proline, uridine, cytidine, isocytosine, adenine, nicotinate, 4-aminobutanoate, glucose/fructose, D-glucuronic acid/D-glucuronolactone/D-galacturonic acid, picolinic acid, choline, LL-2,6-diaminoheptanedioate, methionine sulfoxide, guanosine, and 3-ureidopropionate. The high levels of nucleotides and nucleobases after anthesis can be the indication of programmed cell death in non-stay-green genotype. Programmed cell death leads to cessation of nucleic acids into nucleotides and nucleobases (pyrimidines and purines), which are mobilized and transported from source to sink organs. These nucleotides and nucleobases serve as a source of nitrogen and phosphorus. However, little is known of the nucleic acid degradation in plants (Sakamoto and Takami, 2014). The role of carnosine, glycyl-L-leucine, and leucyl proline have not been identified in plants, in the present study the high accumulation of these metabolites in the non-stay-green genotype showed its association with early senescence. High accumulation of leucyl proline has been reported previously in drought tolerant genotype under control conditions (Khan *et al*., 2019b). Nicotinate over-accumulation has been reported to cause toxicity in plants (Zheng *et al*., 2005; Li *et al*., 2017). Nicotinate high accumulation can trigger premature leaf senescence by DNA fragmentation, hydrogen peroxide accumulation, increase histone H3K9 acetylation, disruption of NAD salvage pathway, and up-regulation of senescence associated genes (Wu *et al*., 2016). 4-Aminobutanoate (GABA) is a non-protein amino acid exhibiting several physiological roles. It is involved in stress tolerance by maintaining cytoplasmic pH and osmoregulation (Barbosa *et al*., 2010; Li *et al*., 2016a). GABA has also been reported to have positive correlation with plant senescence (Masclaux *et al*., 2000; Diaz *et al*., 2005). Leaf senescence induced by sugar starvation or sugar accumulation is still under debate. Some experiments supported the sugar starvation hypothesis and other studies reported

high sugar level induced senescence. Few studies demonstrated that exogenous supply of sugar induces leaf senescence; however the role of sugar during senescence is not clear (van Doorn, 2008). During senescence, the accumulation of glucose and fructose has been reported in *Arabidopsis*, barley, and tobacco (Krapp *et al.*, 1991; Parrott *et al.*, 2005; Pourtau *et al*., 2006; Li *et al*., 2016b). It has also been conceived that sugar accumulation may not be the cause but result of leaf senescence (van Doorn, 2008). Metabolic analysis of tobacco mid leaves at S5 developmental stage (when the lower leaves turned yellow) using liquid chromatography, capillary electrophoresis, and gas chromatography coupled with mass spectrometry revealed an increase accumulation of glucose and fructose during early senescence (Li *et al*., 2016b). Glucuronic acid involved in the biosynthesis of arabinose, xylose, galacturonic acid, and apiose (Reboul *et al*., 2011), has been reported to increase under heat, drought, and combined heat and drought conditions (Safronov *et al*., 2017). The role of glucuronic acid has not been investigated under environmental stresses. In the present study, high levels of glucuronic acid in non-stay-green genotype under control and heat stress treatments also need to be explored to unravel its relation with early senescence. Picolinic acid, a catabolite of tryptophan via kynurenine pathway, is a non-host specific toxin used for disease control. The spray of picolinic acid on rice leaves can inhibit growth of *P. oryzae* by the production of reactive oxygen species (Pasechnik *et al*., 1993; Zhang *et al*., 2004). The concentration of picolinic acid greater than 0.1 mg/L has been reported to cause foliar lesion, dramatic decrease in photosynthetic performance, and increase accumulation of hydrogen peroxide and superoxide anion radical in wheat (Aucique-Pérez *et al*., 2019). High accumulation of picolinic acid in non-stay-genotype might attribute to early senescence. Choline is a precursor of glycine betaine; an osmo-protectant confers tolerance to drought, salinity, and other environmental stresses (Rhodes and Hanson, 1993; Kent, 1995; Sakamoto and Murata, 2000). The role of choline in relation to stay-green trait has not been reported previously. In the present study, high accumulation of choline in non-stay-green genotype compared to stay-green genotype under control and heat stress treatments suggests its role in early senescence. Methionine is highly susceptible to oxidation by reactive oxygen species and reactive nitrogen species (Vogt, 1995; Chao *et al*., 1997; Tien *et al*., 1999). The major product of methionine oxidation is methionine sulfoxide. Methionine

sulfoxide accumulation is a common form of damage during aging that has been observed in all organisms (Châtelain *et al*., 2013). Methionine oxidation to methionine sulfoxide alters confirmation and function of protein (Dos Santos *et al*., 2005). Among the metabolites that highly accumulated in non-stay-green genotype nicotinate, methionine sulfoxide, and picolinic acid are probably the key contributors to early senescence, GABA and choline seems to be associated with defense responses, and high levels of nucleotides, nucleobases, and sugars (glucose and fructose) are possibly the senescence indicator.

Stay-green genotype showed significantly high accumulation of phosphocholine, ADP, trigonelline, allantoin, glutathione, asparagine, syringic acid, cyclic ADP-ribose, L-histidine, L-lactic acid, L-2-phosphoglyceric acid, D-raffinose, L-glutamic acid, disaccharide-6C/6C GLC-GLC/GLC-FRC/GAL-GLC, spermine, and hydroquinone. Phosphocholine, the most abundant primary organic phosphate is an intermediate in synthesis of phosphotidylcholine and choline. Both phosphotidylcholine and choline are involved in defense response under stress (Gout *et al*., 1990; Pical *et al*., 1999; Sakamoto and Murata, 2000; Tasseva *et al*., 2004; Zhang *et al*., 2015). Trigonelline serves as an inducer of defense metabolism by signal transmission under oxidative stress and accumulation of secondary compounds associated with defense mechanisms like glutathione metabolism (Berglund, 1994; Minorsky, 2002). Trigonelline like proline and glycinebetaine accumulates as compatible solute under salt and water stress (Tramontano and Jouve, 1997; Minorsky, 2002; Ashihara, 2008). Trigonelline increases the thermal stability of pyruvate kinase (Shomerilan *et al*., 1991). It has also been associated with detoxification of excessive nicotinic acid and nicotinamide produced in the pyridine nucleotide cycle (Nishitani *et al*., 1995; Zheng *et al*., 2005; Ashihara, 2008). Allantoin is a major intermediate in purine metabolism (Takagi *et al*., 2016). Allantoin has been studied in *Arabidopsis*, rice, and other species under drought, high salinity, cold, nutrient constraint, extended darkness, and pathogen invasion (Montalbini, 1991; Kaplan *et al.*, 2004; Brychkova *et al.*, 2008; Kanani *et al.*, 2010; Yobi *et al.*, 2013; Coneva *et al.*, 2014; Wang *et al.*, 2016). Allantoin involvement in stress protection has been suggested after the study of Xanthine dehydrogenase knockout mutants of *Arabidopsis*. The knockout mutants have defected xanthine oxidation, resulted in diminished stress tolerance and

early senescence (Nakagawa *et al.*, 2007; Brychkova *et al.*, 2008; Watanabe *et al.*, 2014). Allantoin plays a significant role in metabolism, signaling, and bioenergetics in plants. It functions in stress tolerance by reducing reactive oxygen species (Brychkova *et al*., 2008). Glutathione is one of a robust antioxidant system, which protects plants from oxidative damages caused by reactive oxygen species (Gill and Tuteja, 2010a; Das and Roychoudhury, 2014; Hasanuzzaman *et al*., 2017). Glutathione acts as an active electron donor during detoxification of reactive oxygen species (Asada, 1994). It is an integral part of the glutathione-ascorbate cycle that scavenges hydrogen peroxide. It has been reported previously that an inhibition of glutathione biosynthesis under stress resulted in overproduction of reactive oxygen species (Jin *et al*., 2008). Several studies reported that glutathione exogenous application provides protection against oxidative stress (Asada, 1994). Glutathione is also involved in the methylglyoxal detoxification; an organic cytotoxic α-oxoaldehyde compound that develops oxidative stress and disrupts the activities of antioxidant enzymes (Wang *et al*., 2009; Desai *et al*., 2010). Methylglyoxal detoxification is an important stress tolerance strategy under abiotic stress conditions. Glutathione is not only associated with defense responses but also modulates other antioxidant enzymes (Yadav *et al*., 2008). Lactic acid augments growth and production (quality and quantity) of plants by increasing net leaf area and plastid pigment, improving nutrient availability and assimilation, and alleviating abiotic and biotic stresses. The plant with high lactic acid levels displayed better tolerance to temperature, pH, and disease (Böhme *et al*., 1998; Lamont *et al*., 2017). Histidine reduces the oxidative damage caused by abiotic and biotic stresses. The 10 fold higher histidine accumulation was observed in the tolerant genotype of *Arabidopsis* under cadmium stress. Histidine metabolism is integrated with numerous metabolic pathways including tryptophan metabolism. Tryptophan also plays a major role in development and defense responses in plants (Zemanová *et al*., 2014). ADP-ribose free molecules maintain NAD and ATP levels by recycling nucleotides under oxidative stress, thus enhancing plant tolerance (Ogawa *et al.*, 2009). Syringic acid is a phenolic compound, which attenuates the growth defects induced by stresses (Adams *et al*., 2020). Syringic acid application alleviates oxidative stress by increasing antioxidant levels and preventing lipid and protein peroxidation (Cotoras *et al*., 2014). L-2-phosphoglyceric acid, an intermediate of

glycolysis, has been reported to significantly increase in the tolerant genotype under stress treatment (Matsunami *et al*., 2020). In the current study, the high accumulation of L-2-phosphoglyceric acid can be an attribute of stay-green trait and stress tolerance. Raffinose belonging to raffinose family oligosaccharide has been reported as an osmoprotectant under abiotic stresses (ElSayed *et al*., 2014; Sengupta *et al*., 2015). Raffinose accumulation showed positive correlation with drought stress tolerance (Downie *et al*., 2003; Egert *et al*., 2015). Raffinose acts as a protective agent by scavenging reactive oxygen species (Nishizawa *et al*., 2008). It is involved in membrane stability by preventing cellular contents leakage during dehydration and membrane infusion after rehydration (Cacela and Hincha, 2006). Raffinose is transported to chloroplast, where it protects thylakoids and photosystem II (Schneider and Keller, 2009). Raffinose plays many other significant roles in plant that included protection of embryo during maturity, prevention of seed desiccation, long-distance sugar transport, carbon storage, mRNA export, act as signaling molecule during wound and pathogen infection, stabilizing sensitive macromolecules under stress, and source of energy during germination and recovery from abiotic stresses (Vinson *et al*., 2020; Nishizawa *et al*., 2008; Hernandez-Marin and Martínez *et al*., 2012). Glutamic acid takes part in root architecture, seed germination, pollen germination, pollen tube growth, response and adaptation to abiotic (salt, cold, heat, and drought) and biotic stresses, and signal transduction (Qiu *et al*., 2020). Application of glutamic acid elevates percentage survival of maize seedlings under heat stress. Glutamic acid enhances heat stress tolerance by activating glutamate receptors calcium signaling. However, the detail mechanism needs to be explored (Li *et al*., 2019). Metabolic profiling of creeping bentgrass plants sprayed with carbonyldiamide (Nitrogen source), aminoethoxyvinylglycine (ethylene inhibitor), and zeatin riboside (cytokinin) to suppress heat induced senescence revealed an increase accumulation of disaccharides (sucrose) and decrease accumulation of monosaccharides (glucose and fructose). Increased disaccharides levels represent active supply of carbohydrates by photosynthesis, which could protect plants during prolonged heat stress (Jespersen *et al*., 2015). Spermine has been reported to increase linearly under heat stress (Sagor *et al*., 2013). Spermine application significantly increases thiol-containing compounds like glutathione under control and heat stress conditions, which are involved

in defense responses (Todorova *et al*., 2016). Spermine application can alleviate the adverse effects of heat stress by decreasing lipid peroxidation, stabilizing cell bio-membranes, delaying leaf pigment damage, and maintaining photosynthesis and antioxidant activities (Groppa and Benavides, 2008; Gill and Tuteja, 2010b; Amooaghaie and Moghym, 2011; Tian *et al*., 2012; Todorova *et al*., 2016). Spermine may protect plants from heat stress by activating various heat shock transcription factors (Kuzmin *et al*., 2004). High spermine level promotes grain filling and increases grain weight (Yang *et al*., 2008). Exogenous application of spermine in wheat has been reported to increase grain yield of heat tolerant genotype by 19% and heat sensitive genotype by 31% (Jing *et al*., 2020). Hydroquinone improves plant growth at lower concentration (Kamran *et al*., 2017). The application of hydroquinone (20mM) not only enhances seed germination but inhibits growth of seed borne fungi (Elwakil, 2003). Hydroquinone application has been reported to increase wheat seedling growth (Li *et al*., 2009). In the present study, the high levels of trigonelline, glutathione, L-histidine, L-lactic acid, D-raffinose, L-glutamic acid, and spermine in stay-green genotype compare to non-stay-green genotype suggests association of these metabolites with the stay-green trait. The stay-green genotype seems to maintain cellular homeostasis under heat stress by attenuating the damage caused by reactive oxygen species through its strong antioxidant system.

In the present study, both non-stay-green and stay-green genotypes showed high accumulation of 5-hydroxy-L-tryptophan, L-kynurenine, and L-pipecolic acid at both the time points under heat stress. 5-hydroxy-L-tryptophan is an intermediate of *N*-acetyl-5-methoxytryptamine biosynthesis (Kang *et al*., 2011). *N*-acetyl-5-methoxytryptamine is a multi-regulatory molecule involved in seed growth, root development, circadian rhythm, senescence, fruit ripening, yield, and response to abiotic and biotic stresses (Hernández *et al*., 2015; Sun *et al*., 2015; Hardeland, 2016). *N*-acetyl-5-methoxytryptamine scavenges the ROS generated during abiotic and biotic stresses (Manchester *et al*., 2015; Reiter *et al*., 2018). L-kynurenine is an end product of tryptophan oxidation (Ronsein *et al*., 2008). Pipecolate, a non-proteinaceous product of lysine catabolism (Wang *et al*., 2018), had negative correlation with yield. High accumulation of pipecolate has been previously reported in wheat under heat stress (Thomason *et al*., 2018). Though, L-kynurenine and pipecolate accumulated in both the genotypes but their levels were relatively higher in

non-stay-green genotype at both the time points. The levels of L-2-phosphoglyceric acid, shikimate, isocitric acid, and spermidine dropped in both the genotypes under heat stress; however the decline was more evident in the non-stay-green genotype. Several previous studies reported decline in the levels of phosphoglyceric acid (Weis 1981; Law and Crafts-Brandner 1999; Schrader *et al*., 2004), shikimate (Singh *et al*., 2016) and spermidine (Upadhyay *et al*., 2020) during heat stress.

4.6. Conclusion

The Ultra-High-Performance Liquid Chromatography High-Resolution Mass Spectrometry based untargeted global metabolic profiling of leaf tissues of the control and heat treated plants at two different time points unraveled variable accumulation of metabolites in stay-green and non-stay-green genotypes. The dominant metabolites that showed significant high accumulation in non-stay-green genotype were deoxyuridine, deoxycytidine, carnosine, 5'-deoxyadenosine, glycyl-L-leucine, leucyl proline, uridine, cytidine, isocytosine, adenine, nicotinate, 4-aminobutanoate, glucose/fructose, D-glucuronic acid/D-glucuronolactone/D-galacturonic acid, picolinic acid, choline, LL-2,6-diaminoheptanedioate, methionine sulfoxide, guanosine, and 3-ureidopropionate. Among the metabolites that showed high accumulation in non-stay-green genotype nicotinate, methionine sulfoxide, and picolinic acid can be considered as key contributor to early senescence by producing reactive oxygen species and 4-aminobutanoate and choline seems to be associated with defense responses. Stay-green genotype showed significantly high accumulation of phosphocholine, ADP, trigonelline, allantoin, glutathione, asparagine, syringic acid, cyclic ADP-ribose, L-histidine, L-lactic acid, L-2-phosphoglyceric acid, D-raffinose, L-glutamic acid, disaccharide-6C/6C GLC-GLC/GLC-FRC/GAL-GLC, spermine, and hydroquinone. The high levels of trigonelline, glutathione, L-histidine, L-lactic acid, D-raffinose, L-glutamic acid, and spermine in stay-green genotype compare to non-stay-green genotype suggests association of these metabolites with the stay-green trait and may be used as metabolic markers for screening of climate resilient stay-green genotypes.

Chapter #5

Conclusion

Chapter #5

Conclusion

Advances in plant-omics in the last two decades have demonstrated an unprecedent power to dissect the genetic basis of important agronomic traits. Advent of next generation sequencing platforms and their utilization in breeding have helped breeders to jump from QTL mapping to association mapping, from marker trait selection to genomic selection, from years to days, small region sequencing to complete genome sequencing and most importantly from millions of dollars to hundreds of dollars. Transcriptomics of plants using next generation platforms have also helped to understand not only complete transcriptional responses of plant but also post transcriptional responses. Proteomics and metabolomics using advance mass spectrophotometry have also enabled to unravel the mysteries of plant metabolisms and responses to both abiotic and biotic stresses. With escalating temperature, intense and frequent heat waves, water scarcity, and salinity together on top soaring population rates, breeders needs to utilize plant-omics tools to tailor cultivars to ensure future food security and safety.

Geographic historians have documented constant change in climate of planet earth since its inception. Evolution of life on planet earth has been driven by these climatic changes. However, recent fluctuation is unprecedented with extreme high temperature and disrupted rainfall. It is quite evident that we ~~the~~ humans" cause these changes by burning fossil fuels, cutting forest trees, and utilizing nonrenewable resources. These causes have helped in accumulation of heat trapping gasses (Greenhouse gasses) in planet's atmosphere. Since the creation of planet earth, ~800,000 years ago green-house gasses concentration is at the highest. These gasses and their swift increase are changing our climate at a rapid rate too fast for proper adaptation of life. Safety and prosperity are the key elements of every human civilization. We must act now, as the impact of climate changes are leaving unrepairable damages.

Agriculture is the most affected by climate change. Pre- and post-harvest losses are increasing due to climate changes. To cope with yield losses due to climatic extremes and to meet future food demand of increasing population, there is an urgent need for

exploring sustainable strategies for yield improvement. Terminal heat, prolong drought, and rainfall during grain filling are significantly reducing crop yields. Stay-green trait has received considerable attention from breeders owing to the potential of increasing and stabilizing productivity under altering environment. Stay-green trait needs to be explored at greater depth to be employed in future breeding programs.

- ✓ The present study demonstrated significant positive association of the stay-green attribute with crop yield and detected forty eight quantitative trait loci for stay-green and related traits. The identified loci were associated with putative genes involved in flowering time control, chloroplast development, and damage tissues regeneration. The genes identified can be subjected to expression profiling in future to validate their role in the appearance of the stay-green trait. Further, exploration of these loci will contribute towards our understanding of the stay-green trait and can be effectively utilized to develop high yielding stress tolerant stay-green cultivars.
- ✓ Current study also suggested an integrated way to classify a large set of genotypes into different stay-green types. The genotypes characterized into the stay-green type displayed high yield under control and heat stress conditions. Gene sequencing and expression profiling of selected chlorophyll related and photosynthetic responsive genes revealed significant variations between functional stay-green, non-functional stay-green, and non-stay-green genotypes. Collectively, it is concluded that the stay-green phenotype can significantly mitigate the harmful aspects of the terminal heat stress by sustaining grain yield and biological yield. Moreover, the stay-green trait is a complex trait that needs to be explored at greater depth using high throughput phenomics and genomics tools.
- ✓ The untargeted global metabolic profiling detected a variable accumulation of metabolites in stay-green and non-stay-green genotypes. Among the metabolites that showed high accumulated in non-stay-green genotype nicotinate, methionine sulfoxide, and picolinic acid can be considered as key contributor to early senescence by producing reactive oxygen species and 4-aminobutanoate and choline seems to be associated with defense responses. The high levels of trigonelline, glutathione, L-histidine, L-lactic acid, D-raffinose, L-glutamic acid, and spermine in stay-green genotype compare to non-stay-green genotype suggests association of these metabolites with the stay-green trait and may be used as metabolic markers for screening of climate resilient stay-green genotypes.

Since, only approximately 3% of the metabolites are known metabolites, poses a major challenge towards thorough understanding of the biochemical mechanisms linked with the stay-green trait. Further investigation using nuclear magnetic resonance to identify approximately 97% of the unknown metabolites will help to understand the comprehensive array of biochemical pathways underlying the stay-green trait as a mechanism of tolerance to heat stress.

The current thesis reports fundamental knowledge of molecular basis of stay-green trait in bread wheat. Moreover, we demonstrated that utilization of multiple plant-omics approaches will allow the identification of robust candidates for agronomical quantitative traits in bread wheat. The identified genes/loci can be functionally validated using transgenic as well as non-transgenic approaches and can be consider as molecular markers for genomics/marker selection breeding programs.

REFERENCES

References

Abdelrahman, M., El-Sayed, M., Jogaiah, S., Burritt, D. J., & Tran, L. S. P. (2017). The "STAY-GREEN" trait and phytohormone signaling networks in plants under heat stress. *Plant Cell Reports*, *36*(7), 1009-1025.

Abhinandan, K., Skori, L., Stanic, M., Hickerson, N., Jamshed, M., & Samuel, M. A. (2018). Abiotic stress signaling in wheat–an inclusive overview of hormonal interactions during abiotic stress responses in wheat. *Frontiers in plant science*, *9*, 734.

Abid, M., Ali, S., Qi, L. K., Zahoor, R., Tian, Z., Jiang, D., Snider, J.L., & Dai, T. (2018). Physiological and biochemical changes during drought and recovery periods at tillering and jointing stages in wheat (*Triticum aestivum* L.). *Scientific reports*, *8*(1), 1-15.

Abreu, M. E., & Munne-Bosch, S. (2009). Salicylic acid deficiency in NahG transgenic lines and sid2 mutants increases seed yield in the annual plant *Arabidopsis* thaliana. *Journal of experimental botany*, *60*(4), 1261-1271, doi:10.1093/jxb/ern363.

Adams, E., Miyazaki, T., Moon, J. Y., Sawada, Y., Sato, M., Toyooka, K., Hirai, M. Y., & Shin, R. (2020). Syringic Acid Alleviates Cesium-Induced Growth Defect in *Arabidopsis*. *International journal of molecular sciences*, *21*(23), 9116.

Adams, M. L., Lombi, E., Zhao, F. J., & McGrath, S. P. (2002). Evidence of low selenium concentrations in UK bread-making wheat grain. *Journal of the Science of Food and Agriculture*, *82*(10), 1160-1165.

Adeyanju, A., Yu, J., Little, C., Rooney, W., Klein, P., Burke, J., & Tesso, T. (2016). Sorghum RILs Segregating for Stay-Green QTL and Leaf Dhurrin Content Show Differential Reaction to Stalk Rot Diseases. *Crop Science*, *56*(6), 2895-2903.

Afzal, A. J., Wood, A. J., & Lightfoot, D. A. (2008). Plant receptor-like serine threonine kinases: roles in signaling and plant defense. *Molecular Plant-Microbe Interactions*, *21*(5), 507-517.

Akhunov, E., Nicolet, C., & Dvorak, J. (2009). Single nucleotide polymorphism genotyping in polyploid wheat with the Illumina GoldenGate assay. *Theoretical and Applied Genetics*, *119*(3), 507-517.

Akter, N., & Islam, M. R. (2017). Heat stress effects and management in wheat. A review. *Agronomy for sustainable development*, *37*(5), 1-17.

Akula, R., & Ravishankar, G. A. (2011). Influence of abiotic stress signals on secondary metabolites in plants. *Plant signaling & behavior*, *6*(11), 1720-1731.

Alaux, M., Rogers, J., Letellier, T., Flores, R., Alfama, F., Pommier, C., & Quesneville, H. (2018). Linking the International Wheat Genome Sequencing Consortium bread wheat reference genome sequence to wheat genetic and phenomic data. *Genome biology*, *19*(1), 1-10.

Ali, Z. M., Armugam, S., & Lazan, H. (1995). β-Galactosidase and its significance in ripening mango fruit. *Phytochemistry*, *38*(5), 1109-1114.

Amooaghaie, R., & Moghym, S. (2011). Effect of polyamines on thermotolerance and membrane stability of soybean seedling. *African Journal of Biotechnology*, *10*(47), 9677-9682.

Armstead, I., Donnison, I., Aubry, S., Harper, J., Hörtensteiner, S., James, C., Mani, J., Moffet, M., Ougham, H., Roberts, L., & King, I. (2006). From crop to model to crop: identifying the genetic basis of the staygreen mutation in the Lolium/Festuca forage and amenity grasses. *New Phytologist*, *172*(4), 592-597.

Arunanondchai, P., Fei, C., Fisher, A., McCarl, B.A., Wang, W., & Yang, Y. (2018). How does climate change affect agriculture? In *The Routledge Handbook of Agricultural Economics*, 1st ed.; Cramer, G.L., Paudel, K.P., Schmitz, A., Eds.; Routledge: Abingdon-on-Thames, UK, pp. 191–210.

Asada, K. (1994). Production and action of active oxygen species in photosynthetic tissues. Causes of photooxidative stress and amelioration of defense systems in plants, 77-104.

Ashihara, H. (2008). Trigonelline (N-methylnicotinic acid) biosynthesis and its biological role in plants. *Natural Product Communications*, *3*(9), 1934578X0800300906.

Asseng, S., Ewert, F., Martre, P., Rötter, R. P., Lobell, D. B., Cammarano, D., Kimball, B. A., Ottman, M. J., Wall, G. W., White, J. W., Reynolds, M. P., & Zhu, Y. (2015). Rising temperatures reduce global wheat production. *Nature climate change*, *5*(2), 143-147.

Asseng, S., Ewert, F., Rosenzweig, C., Jones, J. W., Hatfield, J. L., Ruane, A. C., Boote, K. J., Thorburn, P. J., Rötter, R. P., Cammarano, D., & Wolf, J. (2013).

Uncertainty in simulating wheat yields under climate change. *Nature climate change*, *3*(9), 827-832.

Aucique-Pérez, C. E., Resende, R. S., Neto, L. B. C., Dornelas, F., DaMatta, F. M., & Rodrigues, F. Á. (2019). Picolinic acid spray stimulates the antioxidative metabolism and minimizes impairments on photosynthesis on wheat leaves infected by Pyricularia oryzae. *Physiologia plantarum*, *167*(4), 628-644.

Aulchenko, Y. S., Ripke, S., Isaacs, A., & Van Duijn, C. M. (2007). GenABEL: an R library for genome-wide association analysis. *Bioinformatics*, *23*(10), 1294-1296.

Azam, F., Chang, X., & Jing, R. (2015). Mapping QTL for chlorophyll fluorescence kinetics parameters at seedling stage as indicators of heat tolerance in wheat. Euphytica, *202*(2), 245-258.

Balasubramaniam, S., Lee, H. C., Lazan, H., Othman, R., & Ali, Z. M. (2005). Purification and properties of a β-galactosidase from carambola fruit with significant activity towards cell wall polysaccharides. *Phytochemistry*, *66*(2), 153-163.

Balazadeh, S., Kwasniewski, M., Caldana, C., Mehrnia, M., Zanor, M. I., Xue, G. P., & Mueller-Roeber, B. (2011). ORS1, an H2O2-responsive NAC transcription factor, controls senescence in *Arabidopsis thaliana*. *Molecular plant*, *4*(2), 346-360.

Balla, K., Karsai, I., Bencze, S., & Veisz, O. (2012). Germination ability and seedling vigour in the progeny of heat-stressed wheat plants. *Acta Agronomica Hungarica*, *60*(4), 299-308.

Balla, K., Karsai, I., Bónis, P., Kiss, T., Berki, Z., Horváth, Á., Mayer, M., Bencze, S., & Veisz, O. (2019). Heat stress responses in a large set of winter wheat cultivars (*Triticum aestivum* L.) depend on the timing and duration of stress. *PloS one*, *14*(9), e0222639.

Barbosa, J. M., Singh, N. K., Cherry, J. H., & Locy, R. D. (2010). Nitrate uptake and utilization is modulated by exogenous γ-aminobutyric acid in *Arabidopsis thaliana* seedlings. *Plant Physiology and Biochemistry*, *48*(6), 443-450.

Barry, C. S., McQuinn, R. P., Chung, M. Y., Besuden, A., & Giovannoni, J. J. (2008). Amino acid substitutions in homologs of the STAY-GREEN protein are responsible for the green-flesh and chlorophyll retainer mutations of tomato and pepper. *Plant Physiology*, *147*(1), 179-187.

Bate, N. J., Rothstein, S. J., & Thompson, J. E. (1991). Expression of nuclear and chloroplast photosynthesis-specific genes during leaf senescence. *Journal of experimental botany*, *42*(6), 801-811.

Bates, D., Maechler, M., Bolker, B., & Walker, S. (2015). lme4: Linear mixed-effects models using Eigen and S4. R package version 1.1–7. 2014.

Bauerle, W. L., Oren, R., Way, D. A., Qian, S. S., Stoy, P. C., Thornton, P. E., Bowden J. D., Hoffman F. M., & Reynolds, R. F. (2012). Photoperiodic regulation of the seasonal pattern of photosynthetic capacity and the implications for carbon cycling. *Proceedings of the National Academy of Sciences*, *109*(22), 8612-8617.

Belenghi, B., Acconcia, F., Trovato, M., Perazzolli, M., Bocedi, A., Polticelli, F., Ascenzi, P., & Delledonne, M. (2003). AtCYS1, a cystatin from *Arabidopsis thaliana*, suppresses hypersensitive cell death. *European Journal of Biochemistry*, *270*(12), 2593-2604.

Bellafiore, S., Barneche, F., Peltier, G., & Rochaix, J. D. (2005). State transitions and light adaptation require chloroplast thylakoid protein kinase STN7. *Nature*, *433*(7028), 892-895, doi:10.1038/nature03286.

Berglund, T. (1994). Nicotinamide, a missing link in the early stress response in eukaryotic cells: a hypothesis with special reference to oxidative stress in plants. *FEBS letters*, *351*(2), 145-149.

Berthet, S., Thevenin, J., Baratiny, D., Demont-Caulet, N., Debeaujon, I., Bidzinski, P., Leple, J. C., Huis, R., Hawkins, S., Gomez, L.D., & Jouanin, L. (2012). Role of plant laccases in lignin polymerization. *Advances in Botanical Research*, *61*, 145-172.

Besseau, S., Li, J., & Palva, E. T. (2012). WRKY54 and WRKY70 co-operate as negative regulators of leaf senescence in *Arabidopsis thaliana*. *Journal of experimental botany*, *63*(7), 2667-2679.

Bhusal, N., Sharma, P., Sareen, S., & Sarial, A. K. (2018). Mapping QTLs for chlorophyll content and chlorophyll fluorescence in wheat under heat stress. *Biologia plantarum*, *62*(4), 721-731.

Biswal, A. K., Pattanayak, G. K., Pandey, S. S., Leelavathi, S., Reddy, V. S., & Tripathy, B. C. (2012). Light intensity-dependent modulation of chlorophyll b biosynthesis and photosynthesis by overexpression of chlorophyllide a oxygenase in tobacco. *Plant Physiology*, *159*(1), 433-449.

Blum, A., Klueva, N., & Nguyen, H. T. (2001). Wheat cellular thermotolerance is related to yield under heat stress. *Euphytica*, *117*(2), 117-123.

Bogard, M., Jourdan, M., Allard, V., Martre, P., Perretant, M. R., Ravel, C., Heumez, E., Orford, S., Snape, J., Griffiths, S., & Le Gouis, J. (2011). Anthesis date mainly explained correlations between post-anthesis leaf senescence, grain yield, and grain protein concentration in a winter wheat population segregating for flowering time QTLs. *Journal of experimental botany*, *62*(10), 3621-3636.

Böhme, M., Ouahid, A., & Shaban, N. (1998, August). Reaction of some vegetable crops to treatments with lactate as bioregulator and fertilizer. In XXV International Horticultural Congress, Part 4: Culture Techniques with Special Emphasis on Environmental Implications 514 (pp. 33-40).

Bolot, S., Abrouk, M., Masood-Quraishi, U., Stein, N., Messing, J., Feuillet, C., & Salse, J. (2009). The _inner circle‘of the cereal genomes. *Current opinion in plant biology*, *12*(2), 119-125.

Borrell, A. K., & Hammer, G. L. (2000). Nitrogen dynamics and the physiological basis of stay-green in sorghum. *Crop science*, *40*(5), 1295-1307.

Borrell, A. K., Hammer, G. L., & Douglas, A. C. (2000). Does maintaining green leaf area in sorghum improve yield under drought? I. Leaf growth and senescence. *Crop science*, *40*(4), 1026-1037.

Borrell, A. K., Mullet, J. E., George-Jaeggli, B., van Oosterom, E. J., Hammer, G. L., Klein, P. E., & Jordan, D. R. (2014). Drought adaptation of stay-green sorghum is associated with canopy development, leaf anatomy, root growth, and water uptake. *Journal of experimental botany*, *65*(21), 6251-6263.

Borrell, A., Hammer, G., & Van Oosterom, E. R. I. K. (2001). Stay-green: A consequence of the balance between supply and demand for nitrogen during grain filling?. *Annals of Applied Biology*, *138*(1), 91-95.

Bowles, D., Isayenkova, J., Lim, E. K., & Poppenberger, B. (2005). Glycosyltransferases: managers of small molecules. *Current opinion in plant biology*, *8*(3), 254-263.

Bradbury, P. J., Zhang, Z., Kroon, D. E., Casstevens, T. M., Ramdoss, Y., & Buckler, E. S. (2007). TASSEL: software for association mapping of complex traits in diverse samples. *Bioinformatics*, *23*(19), 2633-2635.

Breeze, E., Harrison, E., McHattie, S., Hughes, L., Hickman, R., Hill, C., Kiddle, S., Kim, Y.S., Penfold, C.A., Jenkins, D., & Buchanan-Wollaston, V. (2011). High-

resolution temporal profiling of transcripts during *Arabidopsis* leaf senescence reveals a distinct chronology of processes and regulation. *The Plant Cell*, *23*(3), 873-894.

Brown, A. H. (2010). Variation under domestication in plants: 1859 and today. *Philosophical Transactions of the Royal Society B: Biological Sciences*, *365*(1552), 2523-2530.

Brychkova, G., Alikulov, Z., Fluhr, R., & Sagi, M. (2008). A critical role for ureides in dark and senescence-induced purine remobilization is unmasked in the Atxdh1 *Arabidopsis* mutant. *The Plant Journal*, *54*(3), 496-509.

Buchanan-Wollaston, V., Earl, S., Harrison, E., Mathas, E., Navabpour, S., Page, T., & Pink, D. (2003). The molecular analysis of leaf senescence–a genomics approach. *Plant biotechnology journal*, *1*(1), 3-22.

Buchanan-Wollaston, V., Page, T., Harrison, E., Breeze, E., Lim, P. O., Nam, H. G., Lin J. F., Wu S. H., Swidzinski J., Ishizaki K.,& Leaver, C. J. (2005). Comparative transcriptome analysis reveals significant differences in gene expression and signalling pathways between developmental and dark/starvation-induced senescence in *Arabidopsis*. *The Plant Journal*, *42*(4), 567-585, doi: 10.1111/j.1365-313X. 2005. 02399.x.

Buchner, P., Tausz, M., Ford, R., Leo, A., Fitzgerald, G. J., Hawkesford, M. J., & Tausz-Posch, S. (2015). Expression patterns of C-and N-metabolism related genes in wheat are changed during senescence under elevated CO2 in dry-land agriculture. *Plant Science*, *236*, 239-249, doi:10.1016/j.plantsci.2015.04.006.

Buckler IV, E. S., & Thornsberry, J. M. (2002). Plant molecular diversity and applications to genomics. *Current opinion in plant biology*, *5*(2), 107-111.

Cacela, C., & Hincha, D. K. (2006). Monosaccharide composition, chain length and linkage type influence the interactions of oligosaccharides with dry phosphatidylcholine membranes. *Biochimica et Biophysica Acta (BBA)-Biomembranes*, *1758*(5), 680-691.

Campbell B.M., Vermeulen S.J., Aggarwal P.K., Corner-Dolloff C., Girvetz E., Loboguerrero A.M., Ramirez-Villegas J., Rosenstock T., Sebastian L., Thornton P.K., & Wollenberg E. (2016). Reducing risks to food security from climate change. *Global Food Security*, *11*, 34-43.

Cerrudo, D., González Pérez, L., Mendoza Lugo, J. A., & Trachsel, S. (2017). Stay-green and associated vegetative indices to breed maize adapted to heat and combined heat-drought stresses. *Remote Sensing*, *9*(3), 235.

Cha, K. W., Lee, Y. J., Koh, H. J., Lee, B. M., Nam, Y. W., & Paek, N. C. (2002). Isolation, characterization, and mapping of the stay green mutant in rice. *Theoretical and Applied Genetics*, *104*(4), 526-532.

Chai, G., Li, C., Xu, F., Li, Y., Shi, X., Wang, Y., & Wang, Z. (2018). Three endoplasmic reticulum-associated fatty acyl-coenzyme a reductases were involved in the production of primary alcohols in hexaploid wheat (*Triticum aestivum* L.). *BMC plant biology*, *18*(1), 1-16.

Chen, M., Maodzeka, A., Zhou, L., Ali, E., Wang, Z., & Jiang, L. (2014). Removal of DELLA repression promotes leaf senescence in *Arabidopsis*. *Plant Science*, *219*, 26-34.

Challinor, A. J., Watson, J., Lobell, D. B., Howden, S. M., Smith, D. R., & Chhetri, N. (2014). A meta-analysis of crop yield under climate change and adaptation. *Nature Climate Change*, *4*(4), 287-291, doi:10.1038/nclimate2153.

Chao, C. C., Ma, Y. S., & Stadtman, E. R. (1997). Modification of protein surface hydrophobicity and methionine oxidation by oxidative systems. *Proceedings of the National Academy of Sciences*, *94*(7), 2969-2974.

Charmet, G. (2011). Wheat domestication: lessons for the future. *Comptes rendus biologies*, *334*(3), 212-220.

Châtelain, E., Satour, P., Laugier, E., Vu, B. L., Payet, N., Rey, P., & Montrichard, F. (2013). Evidence for participation of the methionine sulfoxide reductase repair system in plant seed longevity. *Proceedings of the National Academy of Sciences*, *110*(9), 3633-3638.

Chen, J., Liang, Y., Hu, X., Wang, X., Tan, F., Zhang, H., Ren Z., & Luo, P. (2010). Physiological characterization of _stay green‘wheat cultivars during the grain filling stage under field growing conditions. *Acta physiologiae plantarum*, *32*(5), 875-882, doi: 10.1007/s11738-010-0475-0.

Chen, M. K., Hsu, W. H., Lee, P. F., Thiruvengadam, M., Chen, H. I., & Yang, C. H. (2011). The MADS box gene, FOREVER YOUNG FLOWER, acts as a repressor controlling floral organ senescence and abscission in *Arabidopsis*. *The Plant Journal*, *68*(1), 168-185.

Cheng, Y., Dong, Y., Yan, H., Ge, W., Shen, C., Guan, J., Liu, L., & Zhang, Y. (2012). Effects of 1-MCP on chlorophyll degradation pathway-associated genes expression and chloroplast ultrastructure during the peel yellowing of Chinese pear fruits in storage. *Food Chemistry*, *135*(2), 415-422, doi:10.1016/j.foodchem.2012.05.017.

Chinnusamy, V., Schumaker, K., & Zhu, J. K. (2004). Molecular genetic perspectives on cross-talk and specificity in abiotic stress signalling in plants. *Journal of experimental botany*, *55*(395), 225-236.

Chong, J., Soufan, O., Li, C., Caraus, I., Li, S., Bourque, G., Wishart, D.S., & Xia, J. (2018). MetaboAnalyst 4.0: towards more transparent and integrative metabolomics analysis. *Nucleic acids research*, *46*(W1), W486-W494.

Chong, J., Wishart, D. S., & Xia, J. (2019). Using MetaboAnalyst 4.0 for comprehensive and integrative metabolomics data analysis. *Current protocols in bioinformatics*, *68*(1), e86.

Christ, B., & Hörtensteiner, S. (2014). Mechanism and significance of chlorophyll breakdown. *Journal of plant growth regulation*, *33*(1), 4-20, doi:10.1007/s00344-013-9392-y.

Christiansen, M. N. (1978). The physiology of plant tolerance to temperature extremes. *Crop tolerance to suboptimal land conditions*, *32*, 173-191.

Christopher, J. T., Christopher, M. J., Borrell, A. K., Fletcher, S., & Chenu, K. (2016). Stay-green traits to improve wheat adaptation in well-watered and water-limited environments. *Journal of Experimental Botany*, *67*(17), 5159-5172.

Christopher, J. T., Manschadi, A. M., Hammer, G. L., & Borrell, A. K. (2008). Developmental and physiological traits associated with high yield and stay-green phenotype in wheat. *Australian Journal of Agricultural Research*, *59*(4), 354-364.

Christopher, J. T., Manschadi, A. M., Hammer, G. L., & Borrell, A. K. (2008b). Stay-green wheat for Australia‘s changing, dry environment. In *11th International Wheat Genetics Symposium 2008 Proceedings* (p. 119).

Christopher, J. T., Veyradier, M., Borrell, A. K., Harvey, G., Fletcher, S., & Chenu, K. (2014). Phenotyping novel stay-green traits to capture genetic variation in senescence dynamics. *Functional Plant Biology*, *41*(11), 1035-1048.

Christopher, M., Chenu, K., Jennings, R., Fletcher, S., Butler, D., Borrell, A., & Christopher, J. (2018a). QTL for stay-green traits in wheat in well-watered and water-limited environments. *Field crops research*, *217*, 32-44.

Coneva, V., Simopoulos, C., Casaretto, J. A., El-Kereamy, A., Guevara, D. R., Cohn, J., Guo, L., Alexander, D. C., Bi, Y. M., McNicholas, P. D., & Rothstein, S. J. (2014). Metabolic and co-expression network-based analyses associated with nitrate response in rice. *BMC genomics*, *15*(1), 1-14.

Cotoras, M., Vivanco, H., Melo, R., Aguirre, M., Silva, E., & Mendoza, L. (2014). In vitro and in vivo evaluation of the antioxidant and prooxidant activity of phenolic compounds obtained from grape (Vitis vinifera) pomace. *Molecules*, *19*(12), 21154-21167.

Cramer, G. R., Urano, K., Delrot, S., Pezzotti, M., & Shinozaki, K. (2011). Effects of abiotic stress on plants: a systems biology perspective. *BMC plant biology*, *11*(1), 1-14.

Curtis, B. C., Rajaram, S., & Gómez Macpherson, H. (2002). *Bread wheat: improvement and production*. Food and Agriculture Organization of the United Nations (FAO).

Curtis, B.C. Wheat in the World. Available online: http://www.fao.org/3/ y4011e /y4011e04.htm (accessed on 28 March 2019).

Danisman, S., Van der Wal, F., Dhondt, S., Waites, R., de Folter, S., Bimbo, A., & Immink, R. G. (2012). *Arabidopsis* class I and class II TCP transcription factors regulate jasmonic acid metabolism and leaf development antagonistically. *Plant physiology*, *159*(4), 1511-1523.

Darwin, C. (1905). *Journal of researches*. PF Collier.

Daryanto, S., Wang, L., & Jacinthe, P. A. (2016). Global synthesis of drought effects on maize and wheat production. *PloS one*, *11*(5), e0156362.

Das, A., Rushton, P. J., & Rohila, J. S. (2017). Metabolomic profiling of soybeans (Glycine max L.) reveals the importance of sugar and nitrogen metabolism under drought and heat stress. *Plants*, *6*(2), 21.

Das, K., & Roychoudhury, A. (2014). Reactive oxygen species (ROS) and response of antioxidants as ROS-scavengers during environmental stress in plants. *Frontiers in environmental science*, *2*, 53.

Debernardi, J. M., Mecchia, M. A., Vercruyssen, L., Smaczniak, C., Kaufmann, K., Inze, D., Rodriguez, R. E., & Palatnik, J. F. (2014). Post-transcriptional control of GRF transcription factors by micro RNA miR396 and GIF co-activator affects leaf size and longevity. *The Plant Journal*, *79*(3), 413-426.

Deery, D., Jimenez-Berni, J., Jones, H., Sirault, X., & Furbank, R. (2014). Proximal remote sensing buggies and potential applications for field-based phenotyping. *Agronomy*, *4*(3), 349-379.

Del Blanco, I. A., Rajaram, S., Kronstad, W. E., & Reynolds, M. P. (2000). Physiological performance of synthetic hexaploid wheat-derived populations. *Crop Science*, *40*(5), 1257-1263.

Demirevska, K., Zasheva, D., Dimitrov, R., Simova-Stoilova, L., Stamenova, M., & Feller, U. (2009). Drought stress effects on Rubisco in wheat: changes in the Rubisco large subunit. *Acta Physiologiae Plantarum*, *31*(6), 1129.

Derkx, A. P., Orford, S., Griffiths, S., Foulkes, M. J., & Hawkesford, M. J. (2012). Identification of Differentially Senescing Mutants of Wheat and Impacts on Yield, Biomass and Nitrogen Partitioning F. *Journal of integrative plant biology*, *54*(8), 555-566.

Desai, K. M., Chang, T., Wang, H., Banigesh, A., Dhar, A., Liu, J., Untereiner, A., & Wu, L. (2010). Oxidative stress and aging: is methylglyoxal the hidden enemy?. *Canadian journal of physiology and pharmacology*, *88*(3), 273-284.

Dias, A. S., & Lidon, F. C. (2009). Evaluation of grain filling rate and duration in bread and durum wheat, under heat stress after anthesis. *Journal of Agronomy and Crop Science*, *195*(2), 137-147.

Diaz, C., Purdy, S., Christ, A., Morot-Gaudry, J. F., Wingler, A., & Masclaux-Daubresse, C. (2005). Characterization of markers to determine the extent and variability of leaf senescence in *Arabidopsis*. A metabolic profiling approach. *Plant Physiology*, *138*(2), 898-908.

Dixon, R. A. (2003). Phytochemistry meets genome analysis, and beyond. *Phytochemistry*, *62*, 815-816.

Djanaguiraman, M., Boyle, D. L., Welti, R., Jagadish, S. V. K., & Prasad, P. V. V. (2018). Decreased photosynthetic rate under high temperature in wheat is due to lipid desaturation, oxidation, acylation, and damage of organelles. *BMC plant biology*, *18*(1), 1-17.

Dos Reis, S. P., Lima, A. M., & De Souza, C. R. B. (2012). Recent molecular advances on downstream plant responses to abiotic stress. *International Journal of Molecular Sciences*, *13*(7), 8628-8647.

Dos Santos, C. V., Cuiné, S., Rouhier, N., & Rey, P. (2005). The *Arabidopsis* plastidic methionine sulfoxide reductase B proteins. Sequence and activity characteristics, comparison of the expression with plastidic methionine sulfoxide reductase A, and induction by photooxidative stress. *Plant Physiology*, *138*(2), 909-922.

Doust, A. N., Lukens, L., Olsen, K. M., Mauro-Herrera, M., Meyer, A., & Rogers, K. (2014). Beyond the single gene: How epistasis and gene-by-environment effects influence crop domestication. *Proceedings of the National Academy of Sciences*, *111*(17), 6178-6183.

Downie, B., Gurusinghe, S., Dahal, P., Thacker, R. R., Snyder, J. C., Nonogaki, H., Yim, K., Fukanaga, K., Alvarado, V. & Bradford, K. J. (2003). Expression of a GALACTINOL SYNTHASE gene in tomato seeds is up-regulated before maturation desiccation and again after imbibition whenever radicle protrusion is prevented. *Plant Physiology*, *131*(3), 1347-1359.

Dreisigacker, S., Shewayrga, H., Crossa, J., Arief, V. N., DeLacy, I. H., Singh, R. P., Dieters, M.J., & Braun, H. J. (2012). Genetic structures of the CIMMYT international yield trial targeted to irrigated environments. *Molecular breeding*, *29*(2), 529-541.

Duncan, R. R., Bockholt, A. J., & Miller, F. R. (1981). Descriptive Comparison of Senescent and Nonsenescent Sorghum Genotypes 1. *Agronomy Journal*, *73*(5), 849-853.

Duvick, D. N., Smith, J. S. C., & Cooper, M. (2004). Long-term selection in a commercial hybrid maize breeding program. *Plant breeding reviews*, *24*(2), 109-152.

Echarte, L., Rothstein, S., & Tollenaar, M. (2008). The response of leaf photosynthesis and dry matter accumulation to nitrogen supply in an older and a newer maize hybrid. *Crop Science*, *48*(2), 656-665.

Eckardt, N. A. (2010). Evolution of domesticated bread wheat.

Economic Survey 2017-2018. Government of Pakistan, Finance Division, Economic Advisory Wing, Islamabad.

Edwards, M., Bowman, Y. J., Dea, I. C., & Reid, J. S. (1988). A beta-D-galactosidase from nasturtium (Tropaeolum majus L.) cotyledons. Purification, properties, and demonstration that xyloglucan is the natural substrate. *Journal of Biological Chemistry*, *263*(9), 4333-4337.

Egert, A., Eicher, B., Keller, F., & Peters, S. (2015). Evidence for water deficit-induced mass increases of raffinose family oligosaccharides (RFOs) in the leaves of three Craterostigma resurrection plant species. *Frontiers in physiology*, *6*, 206.

ElBasyoni, I., Saadalla, M., Baenziger, S., Bockelman, H., & Morsy, S. (2017). Cell membrane stability and association mapping for drought and heat tolerance in a worldwide wheat collection. *Sustainability*, *9*(9), 1606.

Ellis, C. M., Nagpal, P., Young, J. C., Hagen, G., Guilfoyle, T. J., & Reed, J. W. (2005). AUXIN RESPONSE FACTOR1 and AUXIN RESPONSE FACTOR2 regulate senescence and floral organ abscission in *Arabidopsis* thaliana. *Development*, *132*(20), 4563-4574, doi: 10.1242/dev.02012.

ElSayed, A. I., Rafudeen, M. S., & Golldack, D. (2014). Physiological aspects of raffinose family oligosaccharides in plants: protection against abiotic stress. *Plant Biology*, *16*(1), 1-8.

Elwakil, M. A. (2003). Use of antioxidant hydroquinone in the control of seed-borne fungi of peanut with special reference to the production of good quality seed. Pakistan Journal of Plant Pathology, *2*, 75-79.

Enghiad, A., Ufer, D., Countryman, A. M., & Thilmany, D. D. (2017). An overview of global wheat market fundamentals in an era of climate concerns. *International Journal of Agronomy*, 2017.

Espineda, C. E., Linford, A. S., Devine, D., & Brusslan, J. A. (1999). The AtCAO gene, encoding chlorophyll a oxygenase, is required for chlorophyll b synthesis in *Arabidopsis thaliana*. *Proceedings of the National Academy of Sciences*, *96*(18), 10507-10511, doi:10.1073/pnas.96.18.10507.

Evangelista, C. C., & Tangonan, N. G. (1990). Reaction of 31 non-senescent sorghum genotypes to stalk rot complex in southern Philippines. *International Journal of Pest Management*, *36*(3), 214-215.

Evanno, G., Regnaut, S., & Goudet, J. (2005). Detecting the number of clusters of individuals using the software STRUCTURE: a simulation study. *Molecular ecology*, *14*(8), 2611-2620.

Fahad, S., Hussain, S., Saud, S., Hassan, S., Ihsan, Z., Shah, A. N., Wu, C., Yousaf, M., Nasim, W., Alharby, H., & Huang, J. (2016). Exogenously applied plant growth regulators enhance the morpho-physiological growth and yield of rice under high temperature. *Frontiers in Plant Science*, *7*, 1250.

Fan, Y., Tian, Z., Yan, Y., Hu, C., Abid, M., Jiang, D., Ma, C., Huang, Z., & Dai, T. (2017). Winter night-warming improves post-anthesis physiological activities and sink strength in relation to grain filling in winter wheat (*Triticum aestivum* L.). *Frontiers in plant science*, *8*, 992, doi:10.3389/fpls.2017.00992.

Fang, C., Fernie, A. R., & Luo, J. (2019). Exploring the diversity of plant metabolism. *Trends in plant science*, *24*(1), 83-98.

Fang, C., Li, C., Li, W., Wang, Z., Zhou, Z., Shen, Y., Wu, M., Wu, Y., Li, G., Kong, L.A., & Tian, Z. (2014). Concerted evolution of D1 and D2 to regulate chlorophyll degradation in soybean. *The Plant Journal*, *77*(5), 700-712, doi:10.1111/tpj.12419.

FAO (2011). Global Food Losses and Food Waste - extent, causes and prevention. Rome, Food and Agriculture Organization of the United Nations.

FAO, Unicef, & World Health Organization. (2017). The state of food security and nutrition in the world 2017: Building resilience for peace and food security.

FAOSTAT, Food and Agriculture Organization of the United Nations, 2018 Available online: *http://www. fao. org/faostat/en/*

Farooq, M., Bramley, H., Palta, J. A., & Siddique, K. H. (2011). Heat stress in wheat during reproductive and grain-filling phases. *Critical Reviews in Plant Sciences*, *30*(6), 491-507, doi:10.1080/07352689.2011.615687.

Farooq, M., Wahid, A., Kobayashi, N. S. M. A., Fujita, D. B. S. M. A., & Basra, S. M. A. (2009). Plant drought stress: effects, mechanisms and management. *Sustainable agriculture*, 153-188.

Ferris, R., Ellis, R. H., Wheeler, T. R., & Hadley, P. (1998). Effect of high temperature stress at anthesis on grain yield and biomass of field-grown crops of wheat. *Annals of Botany*, *82*(5), 631-639.

Fiehn, O. (2002). Metabolomics the link between genotypes and phenotypes. *Functional genomics*, 155-171.

Flexas, J., Bota, J., Loreto, F., Cornic, G., & Sharkey, T. D. (2004). Diffusive and metabolic limitations to photosynthesis under drought and salinity in C3 plants. *Plant biology*, *6*(3), 269-279, doi: 10.1055/s-2004-820867.

Flint-Garcia, S. A., Thornsberry, J. M., & Buckler IV, E. S. (2003). Structure of linkage disequilibrium in plants. *Annual review of plant biology*, *54*(1), 357-374.

Fokar, M., Blum, A., & Nguyen, H. T. (1998). Heat tolerance in spring wheat. II. Grain filling. *Euphytica*, *104*(1), 9-15.

Fontana, G., Toreti, A., Ceglar, A., & De Sanctis, G. (2015). Early heat waves over Italy and their impacts on durum wheat yields. *Natural Hazards and Earth System Sciences*, 15(7), 1631-1637.

Food and Agriculture Organization of the United Nations (2014-18) http://www.fao.org/faostat/en/#data/QC/visualize

Food And Agriculture Organization of The United Nations Statistics (2014-15) http://faostat3.fao.org/browse/T/*/E.

Fu, J. D., & Lee, B. W. (2008). Changes in Photosynthetic Characteristics during Grain Filling of a Functional Stay-Green Rice SNUSTAY-GREEN1 and its $ F_1 $ Hybrids. *Journal of Crop Science and Biotechnology*, *11*(1), 75-82.

Fu, J. D., Yan, Y. F., Kim, M. Y., Lee, S. H., & Lee, B. W. (2011). Population-specific quantitative trait loci mapping for functional stay-green trait in rice (Oryza sativa L.). *Genome*, *54*(3), 235-243.

Fujita, M., Fujita, Y., Noutoshi, Y., Takahashi, F., Narusaka, Y., Yamaguchi-Shinozaki, K., & Shinozaki, K. (2006). Crosstalk between abiotic and biotic stress responses: a current view from the points of convergence in the stress signaling networks. *Current opinion in plant biology*, *9*(4), 436-442.

Fukao, T., Yeung, E., & Bailey-Serres, J. (2012). The submergence tolerance gene SUB1A delays leaf senescence under prolonged darkness through hormonal regulation in rice. *Plant Physiology*, *160*(4), 1795-1807.

Gan, S., & Amasino, R. M. (1995). Inhibition of leaf senescence by autoregulated production of cytokinin. *Science*, *270*(5244), 1986-1988.

Geelen, D. N., & Inzé, D. G. (2001). A bright future for the bright yellow-2 cell culture. *Plant Physiology*, *127*(4), 1375-1379.

George-Jaeggli, B., Mortlock, M. Y., & Borrell, A. K. (2017). Bigger is not always better: Reducing leaf area helps stay-green sorghum use soil water more slowly. *Environmental and Experimental Botany*, *138*, 119-129.

Gepstein, S., Sabehi, G., Carp, M. J., Hajouj, T., Nesher, M. F. O., Yariv, I., Dor, C., & Bassani, M. (2003). Large-scale identification of leaf senescence-associated genes. *The Plant Journal*, *36*(5), 629-642.

Gill, S. S., & Tuteja, N. (2010a). Reactive oxygen species and antioxidant machinery in abiotic stress tolerance in crop plants. *Plant physiology and biochemistry*, *48*(12), 909-930.

Gill, S. S., & Tuteja, N. (2010b). Polyamines and abiotic stress tolerance in plants. *Plant signaling & behavior*, *5*(1), 26-33.

Giraldo, P., Benavente, E., Manzano-Agugliaro, F., & Gimenez, E. (2019). Worldwide research trends on wheat and barley: A bibliometric comparative analysis. *Agronomy*, *9*(7), 352.

Gong, Y. H., Zhang, J., Gao, J. F., Lu, J. Y., & Wang, J. R. (2005). Slow export of photoassimilate from stay-green leaves during late grain-filling stage in hybrid winter wheat (*Triticum aestivum* L.). *Journal of Agronomy and Crop Science*, *191*(4), 292-299.

Gout, E., Bligny, R., Roby, C., & Douce, R. (1990). Transport of phosphocholine in higher plant cells: 31P nuclear magnetic resonance studies. *Proceedings of the National Academy of Sciences*, *87*(11), 4280-4283.

Granger, J. H., Williams, R., Lenz, E. M., Plumb, R. S., Stumpf, C. L., & Wilson, I. D. (2007). A metabonomic study of strain-and age-related differences in the Zucker rat. *Rapid Communications in Mass Spectrometry: An International Journal Devoted to the Rapid Dissemination of Up-to-the-Minute Research in Mass Spectrometry*, *21*(13), 2039-2045.

Grbić, V., & Bleecker, A. B. (1995). Ethylene regulates the timing of leaf senescence in *Arabidopsis*. *The Plant Journal*, *8*(4), 595-602, doi:10.1046/j.1365-313X.1995.8040595.x.

Gregersen, P. L. (2011). Senescence and nutrient remobilization in crop plants. *The molecular and physiological basis of nutrient use efficiency in crops*, 83-102.

Groppa, M. D., & Benavides, M. P. (2008). Polyamines and abiotic stress: recent advances. *Amino acids*, *34*(1), 35.

Guiamet, J. J., & Giannibelli, M. C. (1996). Nuclear and cytoplasmic –stay-green" mutations of soybean alter the loss of leaf soluble proteins during senescence. *Physiologia Plantarum*, *96*(4), 655-661.

Guiamét, J. J., Schwartz, E., Pichersky, E., & Noodén, L. D. (1991). Characterization of cytoplasmic and nuclear mutations affecting chlorophyll and chlorophyll-binding proteins during senescence in soybean. *Plant Physiology*, *96*(1), 227-231.

Guiamét, J. J., Teeri, J. A., & Nooden, L. D. (1990). Effects of nuclear and cytoplasmic genes altering chlorophyll loss on gas exchange during monocarpic senescence in soybean. *Plant and cell physiology*, *31*(8), 1123-1130.

Guidi, L., Lo Piccolo, E., & Landi, M. (2019). Chlorophyll fluorescence, photoinhibition and abiotic stress: does it make any difference the fact to be a C3 or C4 species?. *Frontiers in plant science*, *10*, 174.

Guo, P., Baum, M., Grando, S., Ceccarelli, S., Bai, G., Li, R., Von Korff, M., Varshney, R.K., Graner, A., & Valkoun, J. (2009). Differentially expressed genes between drought-tolerant and drought-sensitive barley genotypes in response to drought stress during the reproductive stage. *Journal of experimental botany*, *60*(12), 3531-3544, doi:10.1093/jxb/erp194.

Guo, Y. (2013). Towards systems biological understanding of leaf senescence. *Plant Molecular Biology*, *82*(6), 519-528.

Guo, Y., & Gan, S. (2006). AtNAP, a NAC family transcription factor, has an important role in leaf senescence. *The Plant Journal*, *46*(4), 601-612.

Guo, Y., & GAN, S. S. (2012). Convergence and divergence in gene expression profiles induced by leaf senescence and 27 senescence-promoting hormonal, pathological and environmental stress treatments. *Plant, Cell & Environment*, *35*(3), 644-655.

Guo, Y., Cai, Z., & Gan, S. (2004). Transcriptome of *Arabidopsis* leaf senescence. *Plant, cell & environment*, *27*(5), 521-549.

Gupta, P. K., Mir, R. R., Mohan, A., & Kumar, J. (2008). Wheat genomics: present status and future prospects. *International journal of plant genomics*, *2008*.

Halket, J. M., Waterman, D., Przyborowska, A. M., Patel, R. K., Fraser, P. D., & Bramley, P. M. (2005). Chemical derivatization and mass spectral libraries in metabolic profiling by GC/MS and LC/MS/MS. *Journal of experimental botany*, *56*(410), 219-243.

Hamant, O., Nogué, F., Belles-Boix, E., Jublot, D., Grandjean, O., Traas, J., & Pautot, V. (2002). The KNAT2 homeodomain protein interacts with ethylene and cytokinin signaling. *Plant Physiology*, *130*(2), 657-665.

Hanft, J. M., & Wych, R. D. (1982). Visual Indicators of Physiological Maturity of Hard Red Spring Wheat 1. *Crop Science, 22*(3), 584-588.

Hanson, H., Borlaug, N. E., & Anderson, R. G. (1982). *Wheat in the third world*. Westview press.

Hardeland, R. (2016). Melatonin in plants–diversity of levels and multiplicity of functions. *Frontiers in Plant Science*, *7*, 198.

Hardie, D. G. (1999). Plant protein serine/threonine kinases: classification and functions. *Annual review of plant biology*, *50*(1), 97-131.

Harris, K., Subudhi, P. K., Borrell, A., Jordan, D., Rosenow, D., Nguyen, H., Klein, P., Klein, R., & Mullet, J. (2007). Sorghum stay-green QTL individually reduce post-flowering drought-induced leaf senescence. *Journal of experimental botany*, *58*(2), 327-338.

Hasanuzzaman, M., Nahar, K., Anee, T. I., & Fujita, M. (2017). Glutathione in plants: biosynthesis and physiological role in environmental stress tolerance. *Physiology and Molecular Biology of Plants*, *23*(2), 249-268.

Hassan, F. S. C., Solouki, M., Fakheri, B. A., Nezhad, N. M., & Masoudi, B. (2018). Mapping QTLs for physiological and biochemical traits related to grain yield under control and terminal heat stress conditions in bread wheat (*Triticum aestivum* L.). *Physiology and Molecular Biology of Plants*, *24*(6), 1231-1243.

Hays, D., Mason, E., Do, J. H., Menz, M., & Reynolds, M. (2007). Expression Quantitative Trait Loci Mapping Heat Tolerance During Reproductive Development in Wheat (*Triticum Aestivum*). In *Wheat Production in Stressed Environments, Proceedings of the 7th International Wheat Conference, Mar del Plata, Argentina, 27 November–2 December 2005*; Buck, H.T., Nisi, J.E., Salomon, N., Eds.; Springer: Dordrecht, The Netherlands, pp. 373–382.

Hazen, S. P., Pathan, M. S., Sanchez, A., Baxter, I., Dunn, M., Estes, B., Chang, H.S., Zhu, T., Kreps, J.A., & Nguyen, H. T. (2005). Expression profiling of rice segregating for drought tolerance QTLs using a rice genome array. *Functional & Integrative Genomics*, *5*(2), 104-116.

Hernández, I. G., Gomez, F. J. V., Cerutti, S., Arana, M. V., & Silva, M. F. (2015). Melatonin in *Arabidopsis thaliana* acts as plant growth regulator at low concentrations and preserves seed viability at high concentrations. *Plant physiology and biochemistry*, *94*, 191-196.

Hickman, R., Hill, C., Penfold, C. A., Breeze, E., Bowden, L., Moore, J. D., Zhang, P., Jackson, A., Cooke, E., Bewicke-Copley, F., & Buchanan-Wollaston, V. (2013). A local regulatory network around three NAC transcription factors in stress responses and senescence in A rabidopsis leaves. *The Plant Journal*, *75*(1), 26-39.

Hichri, I., Muhovski, Y., Žižková, E., Dobrev, P. I., Franco-Zorrilla, J. M., Solano, R., & Lutts, S. (2014). The Solanum lycopersicum Zinc Finger2 cysteine-2/histidine-2 repressor-like transcription factor regulates development and tolerance to salinity in tomato and *Arabidopsis*. *Plant Physiology*, *164*(4), 1967-1990.

Hong, J. P., Byun, M. Y., An, K., Yang, S. J., An, G., & Kim, W. T. (2010). OsKu70 is associated with developmental growth and genome stability in rice. *Plant physiology*, *152*(1), 374-387.

Hong, Y., Zhao, J., Guo, L., Kim, S. C., Deng, X., Wang, G., Zhang, G., Li, M., & Wang, X. (2016). Plant phospholipases D and C and their diverse functions in stress responses. *Progress in Lipid Research*, *62*, 55-74.

Hörtensteiner, S. (2006). Chlorophyll degradation during senescence. *Annual Review of Plant Biology*, *57*, 55-77, doi:10.1146/annurev.arplant.57.032905.105212.

Hörtensteiner, S. (2009). Stay-green regulates chlorophyll and chlorophyll-binding protein degradation during senescence. *Trends in plant science*, *14*(3), 155-162.

Hörtensteiner, S., & Feller, U. (2002). Nitrogen metabolism and remobilization during senescence. *Journal of experimental botany*, *53*(370), 927-937.

Hörtensteiner, S., & Kräutler, B. (2011). Chlorophyll breakdown in higher plants. *Biochimica et Biophysica Acta (BBA)-Bioenergetics*, *1807*(8), 977-988.

Hörtensteiner, S., Vicentini, F., & Matile, P. (1995). Chlorophyll breakdown in senescent cotyledons of rape, Brassica napus L.: enzymatic cleavage of phaeophorbide a in vitro. *New Phytologist*, *129*(2), 237-246, doi:10.1111/j.1469-8137.1995.tb04293.x.

Huang, H., Møller, I. M., & Song, S. Q. (2012). Proteomics of desiccation tolerance during development and germination of maize embryos. *Journal of proteomics*, *75*(4), 1247-1262.

Huang, S., Sun, L., Hu, X., Wang, Y., Zhang, Y., Nevo, E., Peng, J., & Sun, D. (2018). Associations of canopy leaf traits with SNP markers in durum wheat (*Triticum turgidum* L. durum (Desf.)). *PloS one*, *13*(10), e0206226.

Huang, X. Q., Kempf, H., Ganal, M. W., & Röder, M. S. (2004). Advanced backcross QTL analysis in progenies derived from a cross between a German elite winter wheat variety and a synthetic wheat (*Triticum aestivum*L.). *Theoretical and Applied Genetics*, *109*(5), 933-943.

Ibrahim, A. K., Zhang, L., Niyitanga, S., Afzal, M. Z., Xu, Y., Zhang, L., Zhang, L., & Qi, J. (2020). Principles and approaches of association mapping in plant breeding. *Tropical Plant Biology*, *13*, 212-224.

IPCC (2014) Summary of Policymakers. In: Field, C. B., Barros, V. R., Dokken, D. J., Mach, K. J., Mastrandrea, M. D., Bilir, T. E., Chatterjee, M., Ebi, K. L., Estrada, Y. O., Genova, R. C., Girma, B., Kissl, E. S., Levy, A. N., MacCracken, S., Mastrandrea, S., White, L. L. (eds) Climate Change 2014: Impacts, Adaptation, and Vulnerability. Part A: Global and Sectoral Aspects. *Contribution of working group II to the Fifth Assessment Report of the Intergovernmental Panel on Climate Change*. Cambridg University Press, Cambridge, pp 1-32.

Janusz, G., Pawlik, A., Świderska-Burek, U., Polak, J., Sulej, J., Jarosz-Wilkołazka, A., & Paszczyński, A. (2020). Laccase properties, physiological functions, and evolution. *International journal of molecular sciences*, *21*(3), 966.

Jaradat, M. R., Feurtado, J. A., Huang, D., Lu, Y., & Cutler, A. J. (2013). Multiple roles of the transcription factor AtMYBR1/AtMYB44 in ABA signaling, stress responses, and leaf senescence. *BMC Plant Biology*, *13*(1), 1-19.

Jespersen, D., Yu, J., & Huang, B. (2015). Metabolite responses to exogenous application of nitrogen, cytokinin, and ethylene inhibitors in relation to heat-induced senescence in creeping bentgrass. *PloS one*, *10*(3), e0123744.

Ji, T., Li, S., Li, L., Huang, M., Wang, X., Wei, M., Shi, Q., Li, Y., Gong, B., & Yang, F. (2018). Cucumber Phospholipase D alpha gene overexpression in tobacco enhanced drought stress tolerance by regulating stomatal closure and lipid peroxidation. *BMC plant biology*, *18*(1), 1-14.

Ji, X., Shiran, B., Wan, J., Lewis, D. C., Jenkins, C. L., Condon, A. G., Richards R. A., & Dolferus, R. (2010). Importance of pre-anthesis anther sink strength for maintenance of grain number during reproductive stage water stress in wheat. *Plant, Cell & Environment*, *33*(6), 926-942.

Jiang, G. H., He, Y. Q., Xu, C. G., Li, X. H., & Zhang, Q. (2004). The genetic basis of stay-green in rice analyzed in a population of doubled haploid lines derived from an indica by japonica cross. *Theoretical and Applied Genetics*, *108*(4), 688-698.

Jiang, Y., Liang, G., Yang, S., & Yu, D. (2014). *Arabidopsis* WRKY57 functions as a node of convergence for jasmonic acid–and auxin-mediated signaling in jasmonic acid–induced leaf senescence. *The Plant Cell*, *26*(1), 230-245.

Jiang, H., Li, M., Liang, N., Yan, H., Wei, Y., Xu, X., Liu, J., Xu, Z., Chen, F., & Wu, G. (2007). Molecular cloning and function analysis of the stay green gene in rice. *The Plant Journal*, *52*(2), 197-209.

Jin, X., Yang, X., Islam, E., Liu, D., & Mahmood, Q. (2008). Effects of cadmium on ultrastructure and antioxidative defense system in hyperaccumulator and non-hyperaccumulator ecotypes of Sedum alfredii Hance. *Journal of hazardous materials*, *156*(1-3), 387-397.

Jing, J., Guo, S., Li, Y., & Li, W. (2020). The alleviating effect of exogenous polyamines on heat stress susceptibility of different heat resistant wheat (*Triticum aestivum* L.) varieties. *Scientific reports*, *10*(1), 1-12.

Jones, R. J., Roessler, J., & Ouattar, S. (1985). Thermal Environment During Endosperm Cell Division in Maize: Effects on Number of Endosperm Cells and Starch Granules 1. *Crop Science*, *25*(5), 830-834.

Jørgensen, K., Rasmussen, A. V., Morant, M., Nielsen, A. H., Bjarnholt, N., Zagrobelny, M., Bak, S., & Møller, B. L. (2005). Metabolon formation and metabolic channeling in the biosynthesis of plant natural products. *Current opinion in plant biology*, *8*(3), 280-291.

Joshi, A. K., Kumari, M., Singh, V. P., Reddy, C. M., Kumar, S., Rane, J., & Chand, R. (2007). Stay green trait: variation, inheritance and its association with spot blotch resistance in spring wheat (*Triticum aestivum* L.). *Euphytica*, *153*(1), 59-71.

Kamal, N. M., Gorafi, Y. S. A., Abdelrahman, M., Abdellatef, E., & Tsujimoto, H. (2019). Stay-green trait: A prospective approach for yield potential, and drought and heat stress adaptation in globally important cereals. *International journal of molecular sciences*, *20*(23), 5837.

Kamal, N. M., Gorafi, Y. S. A., Tsujimoto, H., & Ghanim, A. M. A. (2018). Stay-green QTLs response in adaptation to post-flowering drought depends on the drought severity. *BioMed research international*, *2018*.

Kamran, M., Khan, A. L., Ali, L., Hussain, J., Waqas, M., Al-Harrasi, A., Imran, Q. M., Kim, Y. H., Kang, S. M., Yun, B. W., & Lee, I. J. (2017). Hydroquinone; a novel bioactive compound from plant-derived smoke can cue seed germination of lettuce. *Frontiers in chemistry*, *5*, 30.

Kanani, H., Dutta, B., & Klapa, M. I. (2010). Individual vs. combinatorial effect of elevated CO 2 conditions and salinity stress on *Arabidopsis thaliana* liquid cultures: comparing the early molecular response using time-series transcriptomic and metabolomic analyses. *BMC Systems Biology*, *4*(1), 1-15.

Kang, H. M., Sul, J. H., Service, S. K., Zaitlen, N. A., Kong, S. Y., Freimer, N. B., Sabatti, C., & Eskin, E. (2010). Variance component model to account for sample structure in genome-wide association studies. *Nature genetics*, *42*(4), 348-354.

Kang, K., Kong, K., Park, S., Natsagdorj, U., Kim, Y. S., & Back, K. (2011). Molecular cloning of a plant N-acetylserotonin methyltransferase and its expression characteristics in rice. *Journal of Pineal Research*, *50*(3), 304-309.

Kaplan, F., & Guy, C. L. (2004). β-Amylase induction and the protective role of maltose during temperature shock. *Plant physiology*, *135*(3), 1674-1684.

Kaplan, F., Kopka, J., Haskell, D. W., Zhao, W., Schiller, K. C., Gatzke, N., Sung, D. Y., & Guy, C. L. (2004). Exploring the temperature-stress metabolome of *Arabidopsis*. *Plant physiology*, *136*(4), 4159-4168.

Kassahun, B., Bidinger, F. R., Hash, C. T., & Kuruvinashetti, M. S. (2010). Stay-green expression in early generation sorghum [Sorghum bicolor (L.) Moench] QTL introgression lines. *Euphytica*, *172*(3), 351-362.

Kaur, V., & Behl, R. K. (2010). Grain yield in wheat as affected by short periods of high temperature, drought and their interaction during pre-and post-anthesis stages. *Cereal Research Communications*, *38*(4), 514-520.

Kent, C. (1995). Eukaryotic phospholipid biosynthesis. *Annual review of biochemistry*, *64*(1), 315-343.

Khadka, K., Earl, H. J., Raizada, M. N., & Navabi, A. (2020). A physio-morphological trait-based approach for breeding drought tolerant wheat. *Frontiers in plant science*, *11*, 715.

Khan, N., Bano, A., Rahman, M. A., Guo, J., Kang, Z., & Babar, M. A. (2019b). Comparative physiological and metabolic analysis reveals a complex mechanism

involved in drought tolerance in chickpea (*Cicer arietinum* L.) induced by PGPR and PGRs. *Scientific reports*, *9*(1), 1-19.

Khan, N., Bano, A., Rahman, M. A., Rathinasabapathi, B., & Babar, M. A. (2019a). UPLC-HRMS-based untargeted metabolic profiling reveals changes in chickpea (*Cicer arietinum*) metabolome following long-term drought stress. *Plant, cell & environment*, *42*(1), 115-132.

Kihara, H. (1919). Über Cytologische Studien bei einigen Getreidearten. MITTEILUNG I Spezies-Bastarde des Weizens und Weizenroggen-Bastard. *Shokubutsugaku zasshi*, *33*(386), 17-38.

Kihara H (1924) Cytologische und genetische Studien bei wichtigen Getreidearten mit besonderer Rucksicht auf das verhalten der Chromosomen und die Sterilitat in den Bastarden. Mem Coll Sci Kyoto Imp Univ B 1:1–200.

Kim, H. J., Hong, S. H., Kim, Y. W., Lee, I. H., Jun, J. H., Phee, B. K., & Lim, P. O. (2014). Gene regulatory cascade of senescence-associated NAC transcription factors activated by ETHYLENE-INSENSITIVE2-mediated leaf senescence signalling in *Arabidopsis*. *Journal of experimental botany*, *65*(14), 4023-4036.

Kim, J. H., Woo, H. R., Kim, J., Lim, P. O., Lee, I. C., Choi, S. H., Hwang, D., & Nam, H. G. (2009). Trifurcate feed-forward regulation of age-dependent cell death involving miR164 in *Arabidopsis*. *Science*, *323*(5917), 1053-1057.

Kitagawa, K., Kurinami, S., Oki, K., Abe, Y., Ando, T., Kono, I., Yano, M., Kitano, H., & Iwasaki, Y. (2010). A novel kinesin 13 protein regulating rice seed length. *Plant and Cell Physiology*, *51*(8), 1315-1329.

Kong, Z., Li, M., Yang, W., Xu, W., & Xue, Y. (2006). A novel nuclear-localized CCCH-type zinc finger protein, OsDOS, is involved in delaying leaf senescence in rice. *Plant physiology*, *141*(4), 1376-1388.

Koyama, T., Nii, H., Mitsuda, N., Ohta, M., Kitajima, S., Ohme-Takagi, M., & Sato, F. (2013). A regulatory cascade involving class II ETHYLENE RESPONSE FACTOR transcriptional repressors operates in the progression of leaf senescence. *Plant Physiology*, *162*(2), 991-1005.

Krapp, A., Quick, W. P., & Stitt, M. (1991). Ribulose-1, 5-bisphosphate carboxylase-oxygenase, other Calvin-cycle enzymes, and chlorophyll decrease when glucose is supplied to mature spinach leaves via the transpiration stream. *Planta*, *186*(1), 58-69.

Kuai, B., Chen, J., & Hörtensteiner, S. (2018). The biochemistry and molecular biology of chlorophyll breakdown. *Journal of Experimental Botany*, *69*(4), 751-767, doi:10.1093/jxb/erx322.

Kuhlgert, S., Austic, G., Zegarac, R., Osei-Bonsu, I., Hoh, D., Chilvers, M. I., Roth, M.G., Bi, K., TerAvest, D., Weebadde, P., & Kramer, D. M. (2016). MultispeQ Beta: a tool for large-scale plant phenotyping connected to the open PhotosynQ network. *Royal Society open science*, *3*(10), 160592.

Kulcheski, F. R., Côrrea, R., Gomes, I. A., de Lima, J. C., & Margis, R. (2015). NPK macronutrients and microRNA homeostasis. *Frontiers in plant science*, *6*, 451.

Kumar, U., Joshi, A. K., Kumari, M., Paliwal, R., Kumar, S., & Röder, M. S. (2010). Identification of QTLs for stay green trait in wheat (*Triticum aestivum* L.) in the _Chirya 3'×_Sonalika'population. *Euphytica*, *174*(3), 437-445.

Kumari, M., Pudake, R. N., Singh, V. P., & Joshi, A. K. (2013). Association of staygreen trait with canopy temperature depression and yield traits under terminal heat stress in wheat (*Triticum aestivum* L.). *Euphytica*, *190*(1), 87-97.

Kumari, M., Singh, V. P., Tripathi, R., & Joshi, A. K. (2007). Variation for staygreen trait and its association with canopy temperature depression and yield traits under terminal heat stress in wheat. In *Wheat production in stressed environments* (pp. 357-363). Springer, Dordrecht.

Kusaba, M., Ito, H., Morita, R., Iida, S., Sato, Y., Fujimoto, M., Kawasaki, S., Tanaka, R., Hirochika, H., Nishimura, M., & Tanaka, A. (2007). Rice NON-YELLOW COLORING1 is involved in light-harvesting complex II and grana degradation during leaf senescence. *The Plant Cell*, *19*(4), 1362-1375.

Kuzmin, E. V., Karpova, O. V., Elthon, T. E., & Newton, K. J. (2004). Mitochondrial respiratory deficiencies signal up-regulation of genes for heat shock proteins. *Journal of Biological Chemistry*, *279*(20), 20672-20677.

Langridge, P., & Reynolds, M. P. (2015). Genomic tools to assist breeding for drought tolerance. *Current opinion in biotechnology*, *32*, 130-135.

Lara, M. E. B., Garcia, M. C. G., Fatima, T., Ehneß, R., Lee, T. K., Proels, R., Tanner, W., & Roitsch, T. (2004). Extracellular invertase is an essential component of cytokinin-mediated delay of senescence. *The Plant Cell*, *16*(5), 1276-1287.

Latif, S., Wang, L., Khan, J., Ali, Z., Sehgal, S. K., Babar, M. A., Wang, J., & Quraishi, U. M. (2020). Deciphering the Role of Stay-Green Trait to Mitigate Terminal Heat Stress in Bread Wheat. *Agronomy*, *10*(7), 1001.

Latowski, D., Kuczyńska, P., & Strzałka, K. (2011). Xanthophyll cycle–a mechanism protecting plants against oxidative stress. *Redox Report*, *16*(2), 78-90.

Law, R. D., & Crafts-Brandner, S. J. (1999). Inhibition and acclimation of photosynthesis to heat stress is closely correlated with activation of ribulose-1, 5-bisphosphate carboxylase/oxygenase. *Plant physiology*, *120*(1), 173-182.

Lechner, E., Achard, P., Vansiri, A., Potuschak, T., & Genschik, P. (2006). F-box proteins everywhere. *Current opinion in plant biology*, *9*(6), 631-638.

Lee, I. C., Hong, S. W., Whang, S. S., Lim, P. O., Nam, H. G., & Koo, J. C. (2011). Age-dependent action of an ABA-inducible receptor kinase, RPK1, as a positive regulator of senescence in *Arabidopsis* leaves. *Plant and Cell physiology*, *52*(4), 651-662, doi: 10.1093/pcp/pcr026.

Lesk, C., Rowhani, P., & Ramankutty, N. (2016). Influence of extreme weather disasters on global crop production. *Nature*, *529*(7584), 84-87.

Li, J., Xu, Y., & Chong, K. (2012). The novel functions of kinesin motor proteins in plants. *Protoplasma*, *249*(2), 95-100.

Li, L., Zhao, J., Zhao, Y., Lu, X., Zhou, Z., Zhao, C., & Xu, G. (2016b). Comprehensive investigation of tobacco leaves during natural early senescence via multi-platform metabolomics analyses. *Scientific reports*, *6*(1), 1-10.

Li, M. F., Li, W., Yang, D. L., & Sun, P. (2009). The dormancy mechanism and bioactivity of hydroquinone extracted from Podophyllum hexandrum Royle seed. *Electronic Journal of Biology*, *5*, 11-16.

Li, R., Wang, W., Wang, W., Li, F., Wang, Q., Xu, Y., & Wang, S. (2015). Overexpression of a cysteine proteinase inhibitor gene from Jatropha curcas confers enhanced tolerance to salinity stress. *Electronic Journal of Biotechnology*, *18*(5), 368-375.

Li, W., Zhang, F., Wu, R., Jia, L., Li, G., Guo, Y., Liu, C., & Wang, G. (2017). A novel N-methyltransferase in *Arabidopsis* appears to feed a conserved pathway for nicotinate detoxification among land plants and is associated with lignin biosynthesis. *Plant Physiology*, *174*(3), 1492-1504.

Li, Z. G., Ye, X. Y., & Qiu, X. M. (2019). Glutamate signaling enhances the heat tolerance of maize seedlings by plant glutamate receptor-like channels-mediated calcium signaling. *Protoplasma*, *256*(4), 1165-1169.

Li, Z., Peng, J., Wen, X., & Guo, H. (2013). Ethylene-insensitive3 is a senescence-associated gene that accelerates age-dependent leaf senescence by directly repressing miR164 transcription in *Arabidopsis*. *The Plant Cell*, *25*(9), 3311-3328.

Li, Z., Yu, J., Peng, Y., & Huang, B. (2016a). Metabolic pathways regulated by γ-aminobutyric acid (GABA) contributing to heat tolerance in creeping bentgrass (Agrostis stolonifera). *Scientific Reports*, *6*(1), 1-16.

Li, Z., Zhao, Y., Liu, X., Peng, J., Guo, H., & Luo, J. (2014). LSD 2.0: an update of the leaf senescence database. *Nucleic Acids Research*, *42*(D1), D1200-D1205.

Liang, C., Wang, Y., Zhu, Y., Tang, J., Hu, B., Liu, L., Ou, S., Wu, H., Sun, X., Chu, J., & Chu, C. (2014). OsNAP connects abscisic acid and leaf senescence by fine-tuning abscisic acid biosynthesis and directly targeting senescence-associated genes in rice. *Proceedings of the National Academy of Sciences*, *111*(27), 10013-10018.

Lim, P. O., Lee, I. C., Kim, J., Kim, H. J., Ryu, J. S., Woo, H. R., & Nam, H. G. (2010). Auxin response factor 2 (ARF2) plays a major role in regulating auxin-mediated leaf longevity. *Journal of Experimental Botany*, *61*(5), 1419-1430.

Lim, P. O., Woo, H. R., & Nam, H. G. (2003). Molecular genetics of leaf senescence in *Arabidopsis*. *Trends in plant science*, *8*(6), 272-278.

Lipiec, J., Doussan, C., Nosalewicz, A., & Kondracka, K. (2013). Effect of drought and heat stresses on plant growth and yield: a review. *International Agrophysics*, *27*(4), 463-477. doi: 10.2478/intag-2013-0017.

Lipka, A. E., Tian, F., Wang, Q., Peiffer, J., Li, M., Bradbury, P. J., Gore, M. A., Buckler, E. S., & Zhang, Z. (2012). GAPIT: genome association and prediction integrated tool. *Bioinformatics*, *28*(18), 2397-2399.

Liu, B., Asseng, S., Wang, A., Wang, S., Tang, L., Cao, W., Zhu, Y., & Liu, L. (2017). Modelling the effects of post-heading heat stress on biomass growth of winter wheat. *Agricultural and Forest Meteorology*, *247*, 476-490.

Liu, B., Liu, L., Tian, L., Cao, W., Zhu, Y., & Asseng, S. (2014). Post-heading heat stress and yield impact in winter wheat of China. *Global change biology*, *20*(2), 372-381.

Liu, X., Li, Z., Jiang, Z., Zhao, Y., Peng, J., Jin, J., Guo H., & Luo, J. (2010). LSD: a leaf senescence database. *Nucleic Acids Research*, *39*(suppl_1), D1103-D1107.

Liu, Z. H., Anderson, J. A., Hu, J., Friesen, T. L., Rasmussen, J. B., & Faris, J. D. (2005). A wheat intervarietal genetic linkage map based on microsatellite and target region amplified polymorphism markers and its utility for detecting quantitative trait loci. *Theoretical and Applied Genetics*, *111*(4), 782-794.

Livak, K. J., & Schmittgen, T. D. (2001). Analysis of relative gene expression data using real-time quantitative PCR and the 2−ΔΔCT method. *Methods*, *25*, 402–408, doi:10.1006/meth.2001.1262.

Lopes, M. S., & Reynolds, M. P. (2012). Stay-green in spring wheat can be determined by spectral reflectance measurements (normalized difference vegetation index) independently from phenology. *Journal of experimental botany*, *63*(10), 3789-3798.

Lu, S., Fadlalla, T., Tang, S., Li, L., Ali, U., Li, Q., & Guo, L. (2019). Genome-wide analysis of Phospholipase D gene family and profiling of phospholipids under abiotic stresses in Brassica napus. *Plant and Cell Physiology*, *60*(7), 1556-1566.

Luche, H., da Silva, J. A. G., Nornberg, R., Zimmer, C. M., Arenhardt, E. G., da Rosa Caetano, V., & de Oliveira, A. C. (2015). Stay-green effects on adaptability and stability in wheat. *African Journal of Agricultural Research*, *10*(11), 1142-1149.

Luo, P. G., Deng, K. J., Hu, X. Y., Li, L. Q., Li, X., Chen, J. B., Zhang, H. Y., Tang, Z. X., Zhang, Y., Sun, Q. X., & Ren, Z. L. (2013). Chloroplast ultrastructure regeneration with protection of photosystem II is responsible for the functional _stay-green‘trait in wheat. *Plant, cell & environment*, *36*(3), 683-696.

Luo, P., Ren, Z., Wu, X., Zhang, H., Zhang, H., & Feng, J. (2006). Structural and biochemical mechanism responsible for the stay-green phenotype in common wheat. *Chinese Science Bulletin*, *51*(21), 2595-2603.

Ma, H., Xu, S. P., Luo, D., Xu, Z. H., & Xue, H. W. (2004). OsPIPK 1, a rice phosphatidylinositol monophosphate kinase, regulates rice heading by modifying the expression of floral induction genes. *Plant molecular biology*, *54*(2), 295-310.

Mach, J. M., Castillo, A. R., Hoogstraten, R., & Greenberg, J. T. (2001). The *Arabidopsis*-accelerated cell death gene ACD2 encodes red chlorophyll catabolite reductase and suppresses the spread of disease symptoms. *Proceedings of the National Academy of Sciences*, *98*(2), 771-776, doi:10.1073/pnas.98.2.771.

Maggio, A., Bressan, R. A., Zhao, Y., Park, J., & Yun, D. J. (2018). It‘s hard to avoid avoidance: Uncoupling the evolutionary connection between plant growth, productivity and stress ~~-t~~olerance”. *International journal of molecular sciences*, *19*(11), 3671.

Manchester, L. C., Coto-Montes, A., Boga, J. A., Andersen, L. P. H., Zhou, Z., Galano, A., Vriend, J., Tan, D. X., & Reiter, R. J. (2015). Melatonin: an ancient molecule that makes oxygen metabolically tolerable. *Journal of pineal research*, *59*(4), 403-419.

Manickavelu, A., Kawaura, K., Oishi, K., Shin-I, T., Kohara, Y., Yahiaoui, N., Keller, B., Suzuki, A., Yano, K., & Ogihara, Y. (2010). Comparative gene expression analysis of susceptible and resistant near-isogenic lines in common wheat infected by Puccinia triticina. *DNA research*, *17*(4), 211-222, doi:10.1093/dnares/dsq009.

Masclaux, C., Valadier, M. H., Brugière, N., Morot-Gaudry, J. F., & Hirel, B. (2000). Characterization of the sink/source transition in tobacco (Nicotiana tabacum L.) shoots in relation to nitrogen management and leaf senescence. *Planta*, *211*(4), 510-518.

Masferrer, A., Arró, M., Manzano, D., Schaller, H., Fernández-Busquets, X., Moncaleán, P., Fernández B., Cunillera N., Boronat A., & Ferrer, A. (2002). Overexpression of *Arabidopsis thaliana* farnesyl diphosphate synthase (FPS1S) in transgenic *Arabidopsis* induces a cell death/senescence-like response and reduced cytokinin levels. *The Plant Journal*, *30*(2), 123-132.

Mason, K. E., Hilmer, J. K., Maaty, W. S., Reeves, B. D., Grieco, P. A., Bothner, B., & Fischer, A. M. (2016). Proteomic comparison of near-isogenic barley (Hordeum vulgare L.) germplasm differing in the allelic state of a major senescence QTL identifies numerous proteins involved in plant pathogen defense. *Plant Physiology and Biochemistry*, *109*, 114-127.

Matsunami, M., Toyofuku, K., Kimura, N., & Ogawa, A. (2020). Osmotic Stress Leads to Significant Changes in Rice Root Metabolic Profiles between Tolerant and Sensitive Genotypes. *Plants*, *9*(11), 1503.

Mayer, K. F., Rogers, J., Doleˇzel, J., Pozniak, C., Eversole, K., Feuillet, C., ... & Lukaszewski, A. J. International Wheat Genome Sequencing Consortium (IWGSC)(2014) A chromosome-based draft sequence of the hexaploid bread wheat (*Triticum aestivum*) genome. *Science*, *345*, 1251788.

McDonald, A. E., & Vanlerberghe, G. C. (2004). Branched mitochondrial electron transport in the Animalia: presence of alternative oxidase in several animal phyla. *IUBMB life*, *56*(6), 333-341.

Meng, Y., Li, H., Wang, Q., Liu, B., & Lin, C. (2013). Blue light–dependent interaction between cryptochrome2 and CIB1 regulates transcription and leaf senescence in soybean. *The Plant Cell*, *25*(11), 4405-4420.

Mi, G. H., Chen, F. J., Chun, L., Guo, Y. F., Tian, Q. Y., & Zhang, F. S. (2007). Biological characteristics of nitrogen efficient maize genotypes. *Plant Nutrition and Fertilizer Science*, *1*.

Mi, X., Wegenast, T., Utz, H. F., Dhillon, B. S., & Melchinger, A. E. (2011). Best linear unbiased prediction and optimum allocation of test resources in maize breeding with doubled haploids. *Theoretical and applied genetics*, *123*(1), 1-10.

Miao, Y., Laun, T., Zimmermann, P., & Zentgraf, U. (2004). Targets of the WRKY53 transcription factor and its role during leaf senescence in *Arabidopsis*. *Plant molecular biology*, *55*(6), 853-867.

Mickelbart, M. V., Hasegawa, P. M., & Bailey-Serres, J. (2015). Genetic mechanisms of abiotic stress tolerance that translate to crop yield stability. *Nature Reviews Genetics*, *16*(4), 237-251.

Miles, T., & Liffey, K. (2018). Global temperatures on track for 3–5 degree rise by 2100: UN. *Geneva, Switzerland, 29 November 2018*, *Reuters*, 2018, Available online: https://www.reuters.com/article/us-climate-change-un/global-temperatures-on-track-for-3-5-degree-rise-by-2100-u-n-idUSKCN1NY186.

Minorsky, P. V. (2002). The hot and the classic: Trigonelline: A diverse regulator in plants. *Plant physiology*, *128*(1), 7.

Mochizuki, N., Tanaka, R., Grimm, B., Masuda, T., Moulin, M., Smith, A. G., Tanaka A., & Terry, M. J. (2010). The cell biology of tetrapyrroles: a life and death struggle. *Trends in plant science*, *15*(9), 488-498.

Modarresi, M., Mohammadi, V., Zali, A., & Mardi, M. (2010). Response of wheat yield and yield related traits to high temperature. *Cereal Research Communications*, *38*(1), 23-31.

Mohammadi, V., Qannadha, M. R., Zali, A. A., & Yazdi-Samadi, B. (2004). Effect of post anthesis heat stress on head traits of wheat. *International Journal of Agriculture and Biology*, *6*(1), 42-44.

Mohapatra, P. K., Patro, L., Raval, M. K., Ramaswamy, N. K., Biswal, U. C., & Biswal, B. (2010). Senescence-induced loss in photosynthesis enhances cell wall β-glucosidase activity. *Physiologia plantarum*, *138*(3), 346-355.

Montalbini, P. (1991). Effect of rust infection on levels of uricase, allantoinase and ureides in susceptible and hypersensitive bean leaves. *Physiological and molecular plant pathology*, *39*(3), 173-188.

Morita, R., Sato, Y., Masuda, Y., Nishimura, M., & Kusaba, M. (2009). Defect in non-yellow coloring 3, an α/β hydrolase-fold family protein, causes a stay-green phenotype during leaf senescence in rice. *The Plant Journal*, *59*(6), 940-952.

Mueller, A. H., Dockter, C., Gough, S. P., Lundqvist, U., von Wettstein, D., & Hansson, M. (2012). Characterization of mutations in barley fch2 encoding chlorophyllide a oxygenase. *Plant and Cell Physiology*, *53*(7), 1232-1246, doi:10.1093/pcp/pcs062.

Mueller, B., Hauser, M., Iles, C., Rimi, R. H., Zwiers, F. W., & Wan, H. (2015). Lengthening of the growing season in wheat and maize producing regions, Weather Clim. Extrem., 9, 47–56, doi:10.1016/j.wace.2015.04.001.

Nagata, N., Satoh, S., Tanaka, R., & Tanaka, A. (2004). Domain structures of chlorophyllide a oxygenase of green plants and Prochlorothrix hollandica in relation to catalytic functions. *Planta*, *218*(6), 1019-1025, doi:10.1007/s00425-003-1181-6.

Nakagawa, A., Sakamoto, S., Takahashi, M., Morikawa, H., & Sakamoto, A. (2007). The RNAi-mediated silencing of xanthine dehydrogenase impairs growth and fertility and accelerates leaf senescence in transgenic *Arabidopsis* plants. *Plant and Cell Physiology*, *48*(10), 1484-1495.

Nei, M., & Kumar, S. (2000). *Molecular evolution and phylogenetics*. Oxford university press, UK, 2000.

Nishitani, H., Yamada, Y., Ohshima, N., Okumura, K., & Taguchi, H. (1995). Identification of N-(beta-D-glucopyranosyl) nicotinic acid as a major metabolite from niacin in cultured tobacco cells. *Bioscience, biotechnology, and biochemistry*, *59*(7), 1336-1338.

Nishizawa, A., Yabuta, Y., & Shigeoka, S. (2008). Galactinol and raffinose constitute a novel function to protect plants from oxidative damage. *Plant physiology*, *147*(3), 1251-1263.

Niyogi, K. K., Li, X. P., Rosenberg, V., & Jung, H. S. (2005). Is PsbS the site of non-photochemical quenching in photosynthesis?. *Journal of experimental botany*, *56*(411), 375-382, doi:10.1093/jxb/eri056.

Noya, I., González-García, S., Bacenetti, J., Fiala, M., & Moreira, M. T. (2018). Environmental impacts of the cultivation-phase associated with agricultural crops for feed production. *Journal of Cleaner Production*, 172, 3721-3733, doi:10.1016/j.jclepro.2017.07.132.

Obata, T., Witt, S., Lisec, J., Palacios-Rojas, N., Florez-Sarasa, I., Yousfi, S., Araus, J.L., Cairns, J.E., & Fernie, A. R. (2015). Metabolite profiles of maize leaves in drought, heat, and combined stress field trials reveal the relationship between metabolism and grain yield. *Plant Physiology*, *169*(4), 2665-2683.

Ogawa, T., Ishikawa, K., Harada, K., Fukusaki, E., Yoshimura, K., & Shigeoka, S. (2009). Overexpression of an ADP-ribose pyrophosphatase, AtNUDX2, confers enhanced tolerance to oxidative stress in *Arabidopsis* plants. *The Plant Journal*, *57*(2), 289-301.

Oka, M., Shimoda, Y., Sato, N., Inoue, J., Yamazaki, T., Shimomura, N., & Fujiyama, H. (2012). Abscisic acid substantially inhibits senescence of cucumber plants (Cucumis sativus) grown under low nitrogen conditions. *Journal of plant physiology*, *169*(8), 789-796.

Onaga, G., & Wydra, K. (2016). Advances in plant tolerance to abiotic stresses. *Plant genomics*, *2*, 1-12.

Ori, N., Juarez, M. T., Jackson, D., Yamaguchi, J., Banowetz, G. M., & Hake, S. (1999). Leaf senescence is delayed in tobacco plants expressing the maize homeobox gene knotted1 under the control of a senescence-activated promoter. *The Plant Cell*, *11*(6), 1073-1080.

Oster, U., Tanaka, R., Tanaka, A., & Rüdiger, W. (2000). Cloning and functional expression of the gene encoding the key enzyme for chlorophyll b biosynthesis

(CAO) from *Arabidopsis thaliana*. *The Plant Journal*, *21*(3), 305-310, doi:10.1046/j.1365-313x.2000.00672.x.

Park, S. Y., Yu, J. W., Park, J. S., Li, J., Yoo, S. C., Lee, N. Y., Lee S. K., Jeong S. W., Seo H. S., Koh H. J., Jeon J. S., Park Y. I., & Paek, N. C. (2007). The senescence-induced staygreen protein regulates chlorophyll degradation. *The Plant Cell*, *19*(5), 1649-1664.

Parrott, D., Yang, L., Shama, L., & Fischer, A. M. (2005). Senescence is accelerated, and several proteases are induced by carbon ―feast" conditions in barley (Hordeum vulgare L.) leaves. *Planta*, *222*(6), 989-1000.

Pasechnik, T. D., Sviridov, S. I., Aver'yanov, A. A., & Lapikova, V. P. (1993). Picolinic acid toxicity for Pyricularia oryzae Cav. spores and self-inhibition of their germination. *Mikol Fitopatol*, *27*, 38-42.

Pask, A. J. D., Pietragalla, J., Mullan, D. M., & Reynolds, M. P. (2012). *Physiological breeding II: a field guide to wheat phenotyping*. Cimmyt: *Mexico City*, Mexico, 2012.

Paulsen, H., Dockter, C., Volkov, A., & Jeschke, G. (2010). Folding and pigment binding of light-harvesting chlorophyll a/b protein (LHCIIb). In *The Chloroplast*; Rebeiz, C.A., Benning, C., Bohnert, H. J., Daniell, H., Hoober, J. K., Lichtenthaler, H. K., Portis, A. R., & Tripathy, B.C., Eds.; Springer: Dordrecht, The Netherlands, Volume 31, pp. 231–244, doi:10.1007/978-90-481-8531-3_16.

Peleg, Z., & Blumwald, E. (2011). Hormone balance and abiotic stress tolerance in crop plants. *Current opinion in plant biology*, *14*(3), 290-295.

Peña, R. J. Wheat for Bread and Other Foods. Available online: http://www.fao.org/3/y4011e/y4011e0w.htm (accessed on 28 March 2019).

Peng, M., Hannam, C., Gu, H., Bi, Y. M., & Rothstein, S. J. (2007). A mutation in NLA, which encodes a RING-type ubiquitin ligase, disrupts the adaptability of *Arabidopsis* to nitrogen limitation. *The Plant Journal*, *50*(2), 320-337.

Pical, C., Westergren, T., Dove, S. K., Larsson, C., & Sommarin, M. (1999). Salinity and hyperosmotic stress induce rapid increases in phosphatidylinositol 4, 5-bisphosphate, diacylglycerol pyrophosphate, and phosphatidylcholine in *Arabidopsis thaliana* cells. *Journal of Biological Chemistry*, *274*(53), 38232-38240.

Pinto, R. S., Lopes, M. S., Collins, N. C., & Reynolds, M. P. (2016). Modelling and genetic dissection of staygreen under heat stress. *Theoretical and Applied Genetics*, *129*(11), 2055-2074.

Pinto, R. S., Molero, G., & Reynolds, M. P. (2017). Identification of heat tolerant wheat lines showing genetic variation in leaf respiration and other physiological traits. *Euphytica*, *213*(3), 76.

Pinto, R. S., Reynolds, M. P., Mathews, K. L., McIntyre, C. L., Olivares-Villegas, J. J., & Chapman, S. C. (2010). Heat and drought adaptive QTL in a wheat population designed to minimize confounding agronomic effects. *Theoretical and applied genetics*, *121*(6), 1001-1021.

Pourtau, N., Jennings, R., Pelzer, E., Pallas, J., & Wingler, A. (2006). Effect of sugar-induced senescence on gene expression and implications for the regulation of senescence in *Arabidopsis*. *Planta*, *224*(3), 556-568.

Praba, M. L., Cairns, J. E., Babu, R. C., & Lafitte, H. R. (2009). Identification of physiological traits underlying cultivar differences in drought tolerance in rice and wheat. *Journal of Agronomy and Crop Science*, *195*(1), 30-46.

Prasad, P. V., & Djanaguiraman, M. (2014). Response of floret fertility and individual grain weight of wheat to high temperature stress: sensitive stages and thresholds for temperature and duration. *Functional Plant Biology*, *41*(12), 1261-1269.

Prinzenberg, A. E., Víquez-Zamora, M., Harbinson, J., Lindhout, P., & van Heusden, S. (2018). Chlorophyll fluorescence imaging reveals genetic variation and loci for a photosynthetic trait in diploid potato. *Physiologia plantarum*, *164*(2), 163-175.

Pritchard, J. K., Stephens, M., Rosenberg, N. A., & Donnelly, P. (2000). Association mapping in structured populations. *The American Journal of Human Genetics*, *67*(1), 170-181.

Pružinská, A., Anders, I., Aubry, S., Schenk, N., Tapernoux-Lüthi, E., Müller, T., Kräutler, B., & Hörtensteiner, S. (2007). In vivo participation of red chlorophyll catabolite reductase in chlorophyll breakdown. *The Plant Cell*, *19*(1), 369-387, doi:10.1105/tpc.106.044404.

Purcell, S., Neale, B., Todd-Brown, K., Thomas, L., Ferreira, M. A., Bender, D., Maller, J., Sklar, P., De Bakker, P. I., Daly, M. J., & Sham, P. C. (2007). PLINK: a tool set for whole-genome association and population-based linkage analyses. *The American journal of human genetics*, *81*(3), 559-575.

Qiu, X. M., Sun, Y. Y., Ye, X. Y., & Li, Z. G. (2020). Signaling role of glutamate in plants. *Frontiers in plant science*, *10*, 1743.

Quraishi, U. M., Murat, F., Abrouk, M., Pont, C., Confolent, C., Oury, F. X., Ward, J., Boros, D., Gebruers, K., Delcour, J. A., Courtin, C. M., & Salse, J. (2011). Combined meta-genomics analyses unravel candidate genes for the grain dietary fiber content in bread wheat (*Triticum aestivum* L.). *Functional & integrative genomics*, *11*(1), 71-83.

Raab, S., Drechsel, G., Zarepour, M., Hartung, W., Koshiba, T., Bittner, F., & Hoth, S. (2009). Identification of a novel E3 ubiquitin ligase that is required for suppression of premature senescence in *Arabidopsis*. *The Plant Journal*, *59*(1), 39-51. doi: 10.1111/j.1365-313X.2009.03846.x.

Rad, R. N., Kadir, M. A., Jaafar, H. Z., & Gement, D. C. (2012). Physiological and biochemical relationship under drought stress in wheat (*Triticum aestivum*). *African Journal of Biotechnology*, *11*(7), 1574-1578.

Rahman, M. A., Chikushi, J., Yoshida, S., & Karim, A. J. M. S. (2009). Growth and yield components of wheat genotypes exposed to high temperature stress under control environment. *Bangladesh Journal of Agricultural Research*, *34*(3), 360-372.

Rahman, S., Islam, S., Yu, Z., She, M., Nevo, E., & Ma, W. (2020). Current progress in understanding and recovering the wheat genes lost in evolution and domestication. *International Journal of Molecular Sciences*, *21*(16), 5836.

Rai, A., Saito, K., & Yamazaki, M. (2017). Integrated omics analysis of specialized metabolism in medicinal plants.

Rampino, P., Spano, G., Pataleo, S., Mita, G., Napier, J. A., Di Fonzo, N., Shewry P. R., & Perrotta, C. (2006). Molecular analysis of a durum wheat _stay green‘mutant: expression pattern of photosynthesis-related genes. *Journal of Cereal Science*, *43*(2), 160-168.

Rauf, M., Arif, M., Dortay, H., Matallana-Ramírez, L. P., Waters, M. T., Gil Nam, H., Lim, P.O., Mueller-Roeber, B., & Balazadeh, S. (2013). ORE1 balances leaf senescence against maintenance by antagonizing G2-like-mediated transcription. *EMBO reports*, *14*(4), 382-388.

Raza, A., Razzaq, A., Mehmood, S. S., Zou, X., Zhang, X., Lv, Y., & Xu, J. (2019). Impact of climate change on crops adaptation and strategies to tackle its outcome: A review. *Plants*, 8(2), 34.

Reboul, R., Geserick, C., Pabst, M., Frey, B., Wittmann, D., Lütz-Meindl, U., Léonard, R., & Tenhaken, R. (2011). Down-regulation of UDP-glucuronic acid biosynthesis leads to swollen plant cell walls and severe developmental defects associated with changes in pectic polysaccharides. *Journal of Biological Chemistry*, *286*(46), 39982-39992.

Reddy, B. V., Ramaiah, B., Ashok Kumar, A., & Reddy, P. S. (2007). Evaluation of sorghum genotypes for the stay-green trait and grain yield. *Journal of SAT Agricultural Research*, *3*(1), 1-4.

Rehman, S. U., Bilal, M., Rana, R. M., Tahir, M. N., Shah, M. K. N., Ayalew, H., & Yan, G. (2016). Cell membrane stability and chlorophyll content variation in wheat (*Triticum aestivum*) genotypes under conditions of heat and drought. *Crop and Pasture Science*, *67*(7), 712-718.

Reiter, R. J., Tan, D. X., Rosales-Corral, S., Galano, A., Zhou, X. J., & Xu, B. (2018). Mitochondria: central organelles for melatonin′ s antioxidant and anti-aging actions. *Molecules*, *23*(2), 509.

Reynolds, M. P., Guti rrez-Rodr guez, M., & Larqu -Saavedra, A. (2000). Photosynthesis of wheat in a warm, irrigated environment: I: genetic diversity and crop productivity. *Field Crops Research*, *66*(1), 37-50.

Reynolds, M. P., Nagarajan, S., Razzaque, M. A., & Ageeb, O. A. A. (2001). Heat tolerance. Application of physiology in wheat breeding, 124-135.

Rhodes, D., & Hanson, A. D. (1993). Quaternary ammonium and tertiary sulfonium compounds in higher plants. *Annual review of plant biology*, *44*(1), 357-384.

Riefler, M., Novak, O., Strnad, M., & Schmülling, T. (2006). *Arabidopsis* cytokinin receptor mutants reveal functions in shoot growth, leaf senescence, seed size, germination, root development, and cytokinin metabolism. *The Plant Cell*, *18*(1), 40-54. doi: 10.1105/tpc.105.037796.

Ristic, Z., Bukovnik, U., & Prasad, P. V. (2007). Correlation between heat stability of thylakoid membranes and loss of chlorophyll in winter wheat under heat stress. *Crop Science*, *47*(5), 2067-2073.

Rivero, R. M., Kojima, M., Gepstein, A., Sakakibara, H., Mittler, R., Gepstein, S., & Blumwald, E. (2007). Delayed leaf senescence induces extreme drought tolerance in a flowering plant. *Proceedings of the National Academy of Sciences*, *104*(49), 19631-19636.

Robatzek, S., & Somssich, I. E. (2002). Targets of AtWRKY6 regulation during plant senescence and pathogen defense. *Genes & development*, *16*(9), 1139-1149.

Robinson, G. K. (1991). That BLUP is a good thing: the estimation of random effects. *Statistical science*, *6*(1), 15-32.

Roessner, U., & Bacic, A. (2009). Metabolomics in plant research. *Australian Biochemist*, *40*, 9-20.

Roessner, U., Wagner, C., Kopka, J., Trethewey, R. N., & Willmitzer, L. (2000). Simultaneous analysis of metabolites in potato tuber by gas chromatography–mass spectrometry. *The Plant Journal*, *23*(1), 131-142.

Ronsein, G. E., Oliveira, M. C., Miyamoto, S., Medeiros, M. H., & Di Mascio, P. (2008). Tryptophan oxidation by singlet molecular oxygen [O2 (1Δg)]: mechanistic studies using 18O-labeled hydroperoxides, mass spectrometry, and light emission measurements. *Chemical research in toxicology*, *21*(6), 1271-1283.

Rosenow, D. T. (1983b). Breeding for resistance to root and stalk rots in Texas. Sorghum root and stalk rots, a critical review. Patancheru, AP, India: ICRISTAT, 209-217.

Rosenow, D. T., Quisenberry, J. E., Wendt, C. W., & Clark, L. E. (1983a). Drought tolerant sorghum and cotton germplasm. *Agricultural Water Management*, *7*(1-3), 207-222.

Safdar, L. B., Andleeb, T., Latif, S., Umer, M. J., Tang, M., Li, X., Liu, S., & Quraishi, U. M. (2020). Genome-wide association study and QTL meta-analysis identified novel genomic loci controlling potassium use efficiency and agronomic traits in bread wheat. *Frontiers in plant science*, *11*, 70.

Safronov, O., Kreuzwieser, J., Haberer, G., Alyousif, M. S., Schulze, W., Al-Harbi, N., Arab, L., Ache, P., Stempfl, T., Kruse, J., & Kangasjärvi, J. (2017). Detecting early signs of heat and drought stress in Phoenix dactylifera (date palm). *PLoS One*, *12*(6), e0177883.

Sagor, G. H. M., Berberich, T., Takahashi, Y., Niitsu, M., & Kusano, T. (2013). The polyamine spermine protects *Arabidopsis* from heat stress-induced damage by increasing expression of heat shock-related genes. *Transgenic research*, *22*(3), 595-605.

Sairam, R. K. (1994). Effects of homobrassinolide application on plant metabolism and grain yield under irrigated and moisture-stress conditions of two wheat varieties. *Plant Growth Regulation*, *14*(2), 173-181.

Sairam, R. K., Srivastava, G. C., & Saxena, D. C. (2000). Increased antioxidant activity under elevated temperatures: a mechanism of heat stress tolerance in wheat genotypes. *Biologia Plantarum*, *43*(2), 245-251.

Sakamoto, A., & Murata, N. (2000). Genetic engineering of glycinebetaine synthesis in plants: current status and implications for enhancement of stress tolerance. *Journal of Experimental Botany*, *51*(342), 81-88.

Sakamoto, T., Sakakibara, H., Kojima, M., Yamamoto, Y., Nagasaki, H., Inukai, Y., Sato, Y., & Matsuoka, M. (2006). Ectopic expression of KNOTTED1-like homeobox protein induces expression of cytokinin biosynthesis genes in rice. *Plant Physiology*, *142*(1), 54-62.

Sakamoto, W., & Takami, T. (2014). Nucleases in higher plants and their possible involvement in DNA degradation during leaf senescence. *Journal of experimental botany*, *65*(14), 3835-3843.

Sakamura, T. (1918). Kurze Mitteilung ueber die Chromosomenzahlen und die Verwandtschaftsverhältnisse der Triticum-arten. *Shokubutsugaku Zasshi*, *32*(379), 150-153.

Sakuraba, Y., Park, S. Y., & Paek, N. C. (2015). The divergent roles of STAYGREEN (SGR) homologs in chlorophyll degradation. *Molecules and cells*, *38*(5), 390.

Sakuraba, Y., Schelbert, S., Park, S. Y., Han, S. H., Lee, B. D., Andrès, C. B., Kessler, F., Hörtensteiner, S., & Paek, N. C. (2012). STAY-GREEN and chlorophyll catabolic enzymes interact at light-harvesting complex II for chlorophyll detoxification during leaf senescence in *Arabidopsis*. *The Plant Cell*, *24*(2), 507-518.

Salamini, F., Özkan, H., Brandolini, A., Schäfer-Pregl, R., & Martin, W. (2002). Genetics and geography of wild cereal domestication in the near east. *Nature Reviews Genetics*, *3*(6), 429-441.

Sarto, M. V. M., Sarto, J. R. W., Rampim, L., Rosset, J. S., Bassegio, D., da Costa, P. F., & Inagaki, A. M. (2017). Wheat phenology and yield under drought: a review. *Australian Journal of Crop Science*, *11*(8), 941.

Sato, Y., Morita, R., Katsuma, S., Nishimura, M., Tanaka, A., & Kusaba, M. (2009). Two short-chain dehydrogenase/reductases, NON-YELLOW COLORING 1 and NYC1-LIKE, are required for chlorophyll b and light-harvesting complex II degradation during senescence in rice. *The Plant Journal*, *57*(1), 120-131.

Sattar, A., Sher, A., Ijaz, M., Ul-Allah, S., Rizwan, M. S., Hussain, M., Jabran, K., & Cheema, M. A. (2020). Terminal drought and heat stress alter physiological and biochemical attributes in flag leaf of bread wheat. *Plos one*, *15*(5), e0232974.

Sawada, Y., & Hirai, M. Y. (2013). Integrated LC-MS/MS system for plant metabolomics. *Computational and structural biotechnology journal*, *4*(5), e201301011.

Sax, K. (1922). Sterility in wheat hybrids. II. Chromosome behavior in partially sterile hybrids. *Genetics*, *7*(6), 513.

Schelbert, S., Aubry, S., Burla, B., Agne, B., Kessler, F., Krupinska, K., & Hörtensteiner, S. (2009). Pheophytin pheophorbide hydrolase (pheophytinase) is involved in chlorophyll breakdown during leaf senescence in *Arabidopsis*. *The Plant Cell*, *21*(3), 767-785.

Schittenhelm, S., Langkamp-Wedde, T., Kraft, M., Kottmann, L., & Matschiner, K. (2020). Effect of two-week heat stress during grain filling on stem reserves, senescence, and grain yield of European winter wheat cultivars. *Journal of Agronomy and Crop Science*, *206*(6), 722-733.

Schlenker, W., & Roberts, M. J. (2009). Nonlinear temperature effects indicate severe damages to US crop yields under climate change. *Proceedings of the National Academy of sciences*, *106*(37), 15594-15598.

Schneider, T., & Keller, F. (2009). Raffinose in chloroplasts is synthesized in the cytosol and transported across the chloroplast envelope. *Plant and Cell Physiology*, *50*(12), 2174-2182.

Schrader, S. M., Wise, R. R., Wacholtz, W. F., Ort, D. R., & Sharkey, T. D. (2004). Thylakoid membrane responses to moderately high leaf temperature in Pima cotton. *Plant, Cell & Environment*, *27*(6), 725-735.

Schommer, C., Palatnik, J. F., Aggarwal, P., Chételat, A., Cubas, P., Farmer, E. E., & Weigel, D. (2008). Control of jasmonate biosynthesis and senescence by miR319 targets. *PLoS Biol*, *6*(9), e230.

Sears, E. R. (1952). *Homoeologous chromosomes in Triticum aestivum* (No. REP-585. CIMMYT.).

Seki, M., Narusaka, M., Ishida, J., Nanjo, T., Fujita, M., Oono, Y., Kamiya, A., Nakajima, M., Enju, A., Sakurai, T., Satou, M., & Shinozaki, K. (2002). Monitoring the expression profiles of 7000 *Arabidopsis* genes under drought, cold

and high-salinity stresses using a full-length cDNA microarray. *The Plant Journal*, *31*(3), 279-292, doi:10.1046/j.1365-313X.2002.01359.x.

Sengupta, S., Mukherjee, S., Basak, P., & Majumder, A. L. (2015). Significance of galactinol and raffinose family oligosaccharide synthesis in plants. *Frontiers in plant science*, *6*, 656.

Shah, F., Huang, J., Cui, K., Nie, L., Shah, T., Chen, C., & Wang, K. (2011). Impact of high-temperature stress on rice plant and its traits related to tolerance. *The Journal of Agricultural Science*, *149*(5), 545.

Shah, N. H., & Paulsen, G. M. (2005). Injury to photosynthesis and productivity from interaction between high temperature and drought during maturation of wheat. *Asian Journal of Plant Sciences*, doi:10.3923/ajps.2005.67.74.

Shan, X., Wang, J., Chua, L., Jiang, D., Peng, W., & Xie, D. (2011). The role of *Arabidopsis* Rubisco activase in jasmonate-induced leaf senescence. *Plant physiology*, *155*(2), 751-764, doi: 10.1104/pp.110.166595.

Shao, H. B., Chu, L. Y., Jaleel, C. A., Manivannan, P., Panneerselvam, R., & Shao, M. A. (2009). Understanding water deficit stress-induced changes in the basic metabolism of higher plants–biotechnologically and sustainably improving agriculture and the ecoenvironment in arid regions of the globe. *Critical reviews in biotechnology*, *29*(2), 131-151.

Sharabi-Schwager, M., Lers, A., Samach, A., Guy, C. L., & Porat, R. (2010). Overexpression of the CBF2 transcriptional activator in *Arabidopsis* delays leaf senescence and extends plant longevity. *Journal of experimental botany*, *61*(1), 261-273.

Sharma, D., Singh, R., Tiwari, R., Kumar, R., & Gupta, V. K. (2019). Wheat Responses and Tolerance to Terminal Heat Stress: A Review. In *Wheat Production in Changing Environments*; Hasanuzzaman, M., Nahar, K., Hossain, M., Eds.; Springer: Singapore, pp. 149–173.

Sharma, I., Tyagi, B. S., Singh, G., Venkatesh, K., & Gupta, O. P. (2015). Enhancing wheat production-A global perspective. *Indian Journal of Agricultural Sciences*, 85(1), 3-13.

Shewry, P. R., & Hey, S. J. (2015). The contribution of wheat to human diet and health. *Food and energy security*, *4*(3), 178-202.

Shi, M. Z., & Xie, D. Y. (2014). Biosynthesis and metabolic engineering of anthocyanins in *Arabidopsis thaliana*. *Recent patents on biotechnology*, *8*(1), 47-60.

Shi, S., Azam, F. I., Li, H., Chang, X., Li, B., & Jing, R. (2017). Mapping QTL for stay-green and agronomic traits in wheat under diverse water regimes. *Euphytica*, *213*(11), 1-19.

Shi, Y., Phan, H., Liu, Y., Cao, S., Zhang, Z., Chu, C., & Schläppi, M. R. (2020). Glycosyltransferase OsUGT90A1 helps protect the plasma membrane during chilling stress in rice. *Journal of experimental botany*, *71*(9), 2723-2739.

Shimoda, Y., Ito, H., & Tanaka, A. (2016). *Arabidopsis* STAY-GREEN, Mendel‘s green cotyledon gene, encodes magnesium-dechelatase. *The Plant Cell*, *28*(9), 2147-2160.

Shomerilan, A., Jones, G. P., & Paleg, L. G. (1991). In vitro thermal and salt stability of pyruvate kinase are increased by proline analogues and trigonelline. *Functional Plant Biology*, *18*(3), 279-286.

Shrivastava, P., & Kumar, R. (2015). Soil salinity: A serious environmental issue and plant growth promoting bacteria as one of the tools for its alleviation. *Saudi journal of biological sciences*, *22*(2), 123-131.

Shu, K., & Yang, W. (2017). E3 ubiquitin ligases: ubiquitous actors in plant development and abiotic stress responses. *Plant and Cell Physiology*, *58*(9), 1461-1476.

Shulaev, V. (2006). Metabolomics technology and bioinformatics. *Briefings in bioinformatics*, *7*(2), 128-139.

Siebert, S., Ewert, F., Rezaei, E. E., Kage, H., & Graß, R. (2014). Impact of heat stress on crop yield—on the importance of considering canopy temperature. *Environmental Research Letters*, 9(4), 044012.

Silva, S. A., de Carvalho, F. I., da R. Caetano, V., de Oliveira, A. C., de Coimbra, J. L., de Vasconcellos, N. J. S., & Lorencetti, C. (2001). Genetic basis of stay-green trait in bread wheat. *Journal of New Seeds*, *2*(2), 55-68.

Singh, D., Balota, M., Collakova, E., Isleib, T. G., Welbaum, G. E., & Tallury, S. P. (2016). Heat stress related physiological and metabolic traits in peanut seedlings. *Peanut Science*, *43*(1), 24-35.

Smýkal, P., Varshney, R. K., Singh, V. K., Coyne, C. J., Domoney, C., Kejnovský, E., & Warkentin, T. (2016). From Mendel‘s discovery on pea to today‘s plant genetics and breeding. *Theoretical and Applied Genetics*, *129*(12), 2267-2280.

Solomon, M., Belenghi, B., Delledonne, M., Menachem, E., & Levine, A. (1999). The involvement of cysteine proteases and protease inhibitor genes in the regulation of programmed cell death in plants. *The Plant Cell*, *11*(3), 431-443.

Song, X. J., Huang, W., Shi, M., Zhu, M. Z., & Lin, H. X. (2007). A QTL for rice grain width and weight encodes a previously unknown RING-type E3 ubiquitin ligase. *Nature genetics*, *39*(5), 623-630.

Spano, G., Di Fonzo, N., Perrotta, C., Platani, C., Ronga, G., Lawlor, D. W., Napier, J. A., & Shewry, P. R. (2003). Physiological characterization of _stay green‘mutants in durum wheat. *Journal of experimental botany*, *54*(386), 1415-1420.

Stirnberg, P., Furner, I. J., & Ottoline Leyser, H. M. (2007). MAX2 participates in an SCF complex which acts locally at the node to suppress shoot branching. *The Plant Journal*, *50*(1), 80-94. doi: 10.1111/j.1365-313X.2007.03032.x.

Stone, P. J., & Nicolas, M. E. (1995). Comparison of sudden heat stress with gradual exposure to high temperature during grain filling in two wheat varieties differing in heat tolerance. I. Grain growth. *Functional Plant Biology*, *22*(6), 935-944.

Stratonovitch, P., & Semenov, M. A. (2015). Heat tolerance around flowering in wheat identified as a key trait for increased yield potential in Europe under climate change. *Journal of experimental botany*, *66*(12), 3599-3609.

Suetsugu, N., Yamada, N., Kagawa, T., Yonekura, H., Uyeda, T. Q., Kadota, A., & Wada, M. (2010). Two kinesin-like proteins mediate actin-based chloroplast movement in *Arabidopsis thaliana*. *Proceedings of the National Academy of Sciences*, *107*(19), 8860-8865.

Sugishima, M., Kitamori, Y., Noguchi, M., Kohchi, T., & Fukuyama, K. (2009). Crystal structure of red chlorophyll catabolite reductase: enlargement of the ferredoxin-dependent bilin reductase family. *Journal of molecular biology*, *389*(2), 376-387, doi:10.1016/j.jmb.2009.04.017.

Sumner, L. W., Mendes, P., & Dixon, R. A. (2003). Plant metabolomics: large-scale phytochemistry in the functional genomics era. *Phytochemistry*, *62*(6), 817-836.

Sun, Q., Zhang, N., Wang, J., Zhang, H., Li, D., Shi, J., Li, R., Weeda, S., Zhao, B., Ren, S., & Guo, Y. D. (2015). Melatonin promotes ripening and improves quality of

tomato fruit during postharvest life. *Journal of Experimental Botany*, *66*(3), 657-668.

Sun, X., Yang, S., Sun, M., Wang, S., Ding, X., Zhu, D., Ji, W., Cai, H., Zhao, C., Wang, X., & Zhu, Y. (2014). A novel Glycine soja cysteine proteinase inhibitor GsCPI14, interacting with the calcium/calmodulin-binding receptor-like kinase GsCBRLK, regulated plant tolerance to alkali stress. *Plant molecular biology*, *85*(1-2), 33-48.

Suzuki, N., & Mittler, R. (2006). Reactive oxygen species and temperature stresses: a delicate balance between signaling and destruction. *Physiologia plantarum*, *126*(1), 45-51.

Suzuki, Y., Doi, M., & Shioi, Y. (2002). Two enzymatic reaction pathways in the formation of pyropheophorbide a. *Photosynthesis research*, *74*(2), 225-233, doi:10.1023/A:1020919929608.

Sýkorová, B., Kurešová, G., Daskalova, S., Trčková, M., Hoyerová, K., Raimanová, I., ... & Kamínek, M. (2008). Senescence-induced ectopic expression of the A. tumefaciens ipt gene in wheat delays leaf senescence, increases cytokinin content, nitrate influx, and nitrate reductase activity, but does not affect grain yield. *Journal of Experimental Botany*, *59*(2), 377-387. doi: 10.1093/jxb/erm319.

Szabó, I., Bergantino, E., & Giacometti, G. M. (2005). Light and oxygenic photosynthesis: energy dissipation as a protection mechanism against photo-oxidation. *EMBO reports*, *6*(7), 629-634, doi:10.1038/sj.embor.7400460.

Szegletes, Z. S., Erdei, L., Tari, I., & Cseuz, L. (2000). Accumulation of osmoprotectants in wheat cultivars of different drought tolerance. *Cereal Research Communications*, *28*(4), 403-410.

Takagi, H., Ishiga, Y., Watanabe, S., Konishi, T., Egusa, M., Akiyoshi, N., Matsuura, T., Mori, I.C., Hirayama, T., Kaminaka, H., & Sakamoto, A. (2016). Allantoin, a stress-related purine metabolite, can activate jasmonate signaling in a MYC2-regulated and abscisic acid-dependent manner. *Journal of Experimental Botany*, *67*(8), 2519-2532.

Takamiya, K. I., Tsuchiya, T., & Ohta, H. (2000). Degradation pathway (s) of chlorophyll: what has gene cloning revealed?. *Trends in plant science*, *5*(10), 426-431, doi:10.1016/S1360-1385(00)01735-0.

Talukder, A. S. M. H. M., McDonald, G. K., & Gill, G. S. (2014). Effect of short-term heat stress prior to flowering and early grain set on the grain yield of wheat. Field Crops Research, *160*, 54-63.

Tamura, K., Stecher, G., Peterson, D., Filipski, A., & Kumar, S. (2013). MEGA6: molecular evolutionary genetics analysis version 6.0. *Molecular biology and evolution*, *30*(12), 2725-2729, doi:10.1093/molbev/mst197.

Tanaka, A., Ito, H., Tanaka, R., Tanaka, N. K., Yoshida, K., & Okada, K. (1998). Chlorophyll a oxygenase (CAO) is involved in chlorophyll b formation from chlorophyll a. *Proceedings of the National Academy of Sciences*, *95*(21), 12719-12723, doi:10.1073/pnas.95.21.12719.

Tanaka, R., & Tanaka, A. (2007). Tetrapyrrole biosynthesis in higher plants. *Annu. Rev. Plant Biol.*, *58*, 321-346.

Tanaka, R., Hirashima, M., Satoh, S., & Tanaka, A. (2003). The *Arabidopsis*-accelerated cell death gene ACD1 is involved in oxygenation of pheophorbide a: inhibition of the pheophorbide a oxygenase activity does not lead to the ―stay-green" phenotype in *Arabidopsis*. *Plant and Cell Physiology*, *44*(12), 1266-1274.

Tanaka, R., Koshino, Y., Sawa, S., Ishiguro, S., Okada, K., & Tanaka, A. (2001). Overexpression of chlorophyllide a oxygenase (CAO) enlarges the antenna size of photosystem II in *Arabidopsis thaliana*. *The Plant Journal*, *26*(4), 365-373, doi:10.1046/j.1365-313X.2001.2641034.x.

Tang, Y., Li, M., Chen, Y., Wu, P., Wu, G., & Jiang, H. (2011). Knockdown of OsPAO and OsRCCR1 cause different plant death phenotypes in rice. *Journal of plant physiology*, *168*(16), 1952-1959, doi:10.1016/j.jplph.2011.05.026.

Tang, Y., Liu, X., Wang, J., Li, M., Wang, Q., Tian, F., Su, Z., Pan, Y., Liu, D., Lipka, A.E., & Zhang, Z. (2016). GAPIT version 2: an enhanced integrated tool for genomic association and prediction. *The plant genome*, *9*(2), plantgenome2015-11.

Tasseva, G., Richard, L., & Zachowski, A. (2004). Regulation of phosphatidylcholine biosynthesis under salt stress involves choline kinases in *Arabidopsis thaliana*. *FEBS letters*, *566*(1-3), 115-120.

Thomas, H. (1987). Sid: a Mendelian locus controlling thylakoid membrane disassembly in senescing leaves of Festuca pratensis. *Theoretical and Applied Genetics*, *73*(4), 551-555. doi: 10.1007/bf00289193.

Thomas, H., & Howarth, C. J. (2000). Five ways to stay green. *Journal of experimental botany*, *51*(suppl_1), 329-337.

Thomas, H., & Ougham, H. (2014). The stay-green trait. *Journal of Experimental Botany*, *65*(14), 3889-3900.

Thomas, H., & SMART, C. M. (1993). Crops that stay green 1. *Annals of applied Biology*, *123*(1), 193-219.

Thomas, H., & Stoddart, J. L. (1975). Separation of chlorophyll degradation from other senescence processes in leaves of a mutant genotype of meadow fescue (Festuca pratensis L.). *Plant Physiology*, *56*(3), 438-441.

Thomas, H., Evans, C., Thomas, H. M., Humphreys, M. W., Morgan, G., Hauck, B., & Donnison, I. (1997). Introgression, tagging and expression of a leaf senescence gene in Festulolium. *New Phytologist*, *137*(1), 29-34.

Thomason, K., Babar, M. A., Erickson, J. E., Mulvaney, M., Beecher, C., & MacDonald, G. (2018). Comparative physiological and metabolomics analysis of wheat (*Triticum aestivum* L.) following post-anthesis heat stress. *PLoS One*, *13*(6), e0197919.

Tian, J., Wang, L. P., Yang, Y. J., Sun, J., & Guo, S. R. (2012). Exogenous spermidine alleviates the oxidative damage in cucumber seedlings subjected to high temperatures. *Journal of the American Society for Horticultural Science*, *137*(1), 11-19.

Tien, M., Berlett, B. S., Levine, R. L., Chock, P. B., & Stadtman, E. R. (1999). Peroxynitrite-mediated modification of proteins at physiological carbon dioxide concentration: pH dependence of carbonyl formation, tyrosine nitration, and methionine oxidation. *Proceedings of the National Academy of Sciences*, *96*(14), 7809-7814.

Tilman, D., Balzer, C., Hill, J., & Befort, B. L. (2011). Global food demand and the sustainable intensification of agriculture. *Proceedings of the national academy of sciences*, *108*(50), 20260-20264.

Todorova, D., Katerova, Z., Shopova, E., Jodinskienė, M., Jurkonienė, S., & Sergiev, I. (2016). Responses of pea plants to heat stress and spermine treatment *Karščio ir apdorojimo sperminu įtaka žirniams. Žemdirbystė*, *103*(1), 99-106.

Tramontano, W. A., & Jouve, D. (1997). Trigonelline accumulation in salt-stressed legumes and the role of other osmoregulators as cell cycle control agents. *Phytochemistry*, *44*(6), 1037-1040.

Uauy, C., Distelfeld, A., Fahima, T., Blechl, A., & Dubcovsky, J. (2006). A NAC gene regulating senescence improves grain protein, zinc, and iron content in wheat. *Science*, *314*(5803), 1298-1301.

Upadhyay, R. K., Fatima, T., Handa, A. K., & Mattoo, A. K. (2020). Polyamines and their biosynthesis/catabolism genes are differentially modulated in response to heat versus cold stress in tomato leaves (Solanum lycopersicum L.). *Cells*, *9*(8), 1749.

Upadhyay, R. K., Soni, D. K., Singh, R., Dwivedi, U. N., Pathre, U. V., Nath, P., & Sane, A. P. (2013). SlERF36, an EAR-motif-containing ERF gene from tomato, alters stomatal density and modulates photosynthesis and growth. *Journal of experimental botany*, *64*(11), 3237-3247.

Vadez, V., Krishnamurthy, L., Kashiwagi, J., Kholova, J., Devi, J. M., Sharma, K. K., Bhatnagar-Mathur P., Hoisington D., Hash C., Bidinger F & Keatinge, J. D. H. (2007). Exploiting the functionality of root systems for dry, saline, and nutrient deficient environments in a changing climate. *Journal of SAT Agricultural Research*, *4*(1), 1-61.

van der Graaff, E., Schwacke, R., Schneider, A., Desimone, M., Flügge, U. I., & Kunze, R. (2006). Transcription analysis of *Arabidopsis* membrane transporters and hormone pathways during developmental and induced leaf senescence. *Plant physiology*, *141*(2), 776-792.

van Doorn, W. G. (2008). Is the onset of senescence in leaf cells of intact plants due to low or high sugar levels?. *Journal of experimental botany*, *59*(8), 1963-1972.

Vanstraelen, M., Acosta, J. A. T., De Veylder, L., Inzé, D., & Geelen, D. (2004). A plant-specific subclass of C-terminal kinesins contains a conserved a-type cyclin-dependent kinase site implicated in folding and dimerization. *Plant Physiology*, *135*(3), 1417-1429.

Varshney, R. K., Hoisington, D. A., & Tyagi, A. K. (2006). Advances in cereal genomics and applications in crop breeding. *Trends in biotechnology*, *24*(11), 490-499.

Viana, J. M. S., de Almeida, Í. F., de Resende, M. D. V., Faria, V. R., & e Silva, F. F. (2010). BLUP for genetic evaluation of plants in non-inbred families of annual crops. *Euphytica*, *174*(1), 31-39.

Vicentini, F., Hörtensteiner, S., Schellenberg, M., Thomas, H., & Matile, P. (1995). Chlorophyll breakdown in senescent leaves identification of the biochemical lesion in a stay-green genotype of Festuca pratensis Huds. *New Phytologist*, *129*(2), 247-252.

Vijayalakshmi, K., Fritz, A. K., Paulsen, G. M., Bai, G., Pandravada, S., & Gill, B. S. (2010). Modeling and mapping QTL for senescence-related traits in winter wheat under high temperature. *Molecular Breeding*, *26*(2), 163-175.

Vinson, C. C., Mota, A. P., Porto, B. N., Oliveira, T. N., Sampaio, I., Lacerda, A. L., Danchin, E. G., Guimaraes, P. M., Williams, T. C., & Brasileiro, A. C. (2020). Characterization of raffinose metabolism genes uncovers a wild Arachis galactinol synthase conferring tolerance to abiotic stresses. *Scientific reports*, *10*(1), 1-19.

Viswanathan, C., & Khanna-Chopra, R. (2001). Effect of heat stress on grain growth, starch synthesis and protein synthesis in grains of wheat (*Triticum aestivum* L.) varieties differing in grain weight stability. *Journal of Agronomy and Crop Science*, *186*(1), 1-7.

Vogt, W. (1995). Oxidation of methionyl residues in proteins: tools, targets, and reversal. Free Radical Biology and Medicine, 18(1), 93-105.

Wagstaff, C., Yang, T. J., Stead, A. D., Buchanan-Wollaston, V., & Roberts, J. A. (2009). A molecular and structural characterization of senescing *Arabidopsis* siliques and comparison of transcriptional profiles with senescing petals and leaves. *The Plant Journal*, *57*(4), 690-705.

Wang, C., Liu, R., Lim, G. H., de Lorenzo, L., Yu, K., Zhang, K., Hunt, A. G., Kachroo, A., & Kachroo, P. (2018). Pipecolic acid confers systemic immunity by regulating free radicals. *Science advances*, *4*(5), eaar4509.

Wang, H., Liu, J., & Wu, L. (2009). Methylglyoxal-induced mitochondrial dysfunction in vascular smooth muscle cells. *Biochemical pharmacology*, *77*(11), 1709-1716.

Wang, J., Feng, J., Jia, W., Chang, S., Li, S., & Li, Y. (2015). Lignin engineering through laccase modification: a promising field for energy plant improvement. *Biotechnology for biofuels*, *8*(1), 1-11.

Wang, P., Shen, L., Guo, J., Jing, W., Qu, Y., Li, W., Bi, R., Xuan, W., Zhang, Q., & Zhang, W. (2019a). Phosphatidic acid directly regulates PINOID-dependent phosphorylation and activation of the PIN-FORMED2 auxin efflux transporter in response to salt stress. *The Plant Cell*, *31*(1), 250-271.

Wang, S., Alseekh, S., Fernie, A. R., & Luo, J. (2019b). The structure and function of major plant metabolite modifications. *Molecular plant*, *12*(7), 899-919.

Wang, S., Wong, D., Forrest, K., Allen, A., Chao, S., Huang, B. E., Maccaferri, M., Salvi, S., Milner, S. G., Cattivelli, L., & Akhunov, E. (2014). Characterization of polyploid wheat genomic diversity using a high-density 90 000 single nucleotide polymorphism array. *Plant biotechnology journal*, *12*(6), 787-796.

Wang, W. S., Zhao, X. Q., Li, M., Huang, L. Y., Xu, J. L., Zhang, F., Cui, Y. R., Fu, B. Y., Cui, Y.R., Fu, B.Y., & Li, Z. K. (2016). Complex molecular mechanisms underlying seedling salt tolerance in rice revealed by comparative transcriptome and metabolomic profiling. *Journal of experimental botany*, *67*(1), 405-419.

Wang, X., Cai, J., Jiang, D., Liu, F., Dai, T., & Cao, W. (2011). Pre-anthesis high-temperature acclimation alleviates damage to the flag leaf caused by post-anthesis heat stress in wheat. *Journal of plant physiology*, *168*(6), 585-593, doi:10.1016/j.jplph.2010.09.016.

Wang, Y., Liu, K., Liao, H., Zhuang, C., Ma, H., & Yan, X. (2008). The plant WNK gene family and regulation of flowering time in *Arabidopsis*. *Plant Biology*, *10*(5), 548-562.

Watanabe, S., Kounosu, Y., Shimada, H., & Sakamoto, A. (2014). *Arabidopsis* xanthine dehydrogenase mutants defective in purine degradation show a compromised protective response to drought and oxidative stress. *Plant Biotechnology*, 14-0117.

Weaver, L. M., Gan, S., Quirino, B., & Amasino, R. M. (1998). A comparison of the expression patterns of several senescence-associated genes in response to stress and hormone treatment. *Plant molecular biology*, *37*(3), 455-469.

Weckwerth, W. (2003). Metabolomics in systems biology. *Annual review of plant biology*, *54*(1), 669-689.

Wei, Q., Guo, Y., & Kuai, B. (2011). Isolation and characterization of a chlorophyll degradation regulatory gene from tall fescue. *Plant cell reports*, *30*(7), 1201-1207, doi:10.1007/s00299-011-1028-8.

Weis, E. (1981). Reversible effects of high, sublethal temperatures on light-induced light scattering changes and electrochromic pigment absorption shift in spinach leaves. *Zeitschrift für Pflanzenphysiologie*, *101*(2), 169-178.

Weston, L. A., Skoneczny, D., Weston, P. A., & Weidenhamer, J. D. (2015). Metabolic profiling: An overview—New approaches for the detection and functional analysis of biologically active secondary plant products. *Journal of Allelochemical Interactions*, *1*, 15-27.

Wilkinson, S., & Davies, W. J. (2002). ABA-based chemical signalling: the co-ordination of responses to stress in plants. *Plant, cell & environment*, *25*(2), 195-210.

Willey, N. (2015). *Environmental plant physiology*. Garland Science.

Wollenweber, B., Porter, J. R., & Schellberg, J. (2003). Lack of interaction between extreme high-temperature events at vegetative and reproductive growth stages in wheat. *Journal of Agronomy and Crop Science*, *189*(3), 142-150.

Woo, H. R., Chung, K. M., Park, J. H., Oh, S. A., Ahn, T., Hong, S. H., Jang S.K & Nam, H. G. (2001). ORE9, an F-box protein that regulates leaf senescence in *Arabidopsis*. *The Plant Cell*, *13*(8), 1779-1790.

Wu, A., Allu, A. D., Garapati, P., Siddiqui, H., Dortay, H., Zanor, M. I., Asensi-Fabado, M.A., Munné-Bosch, S., Antonio, C., Tohge, T., & Balazadeh, S. (2012). JUNGBRUNNEN1, a reactive oxygen species–responsive NAC transcription factor, regulates longevity in *Arabidopsis*. *The Plant Cell*, *24*(2), 482-506.

Wu, K., Zhang, L., Zhou, C., Yu, C. W., & Chaikam, V. (2008). HDA6 is required for jasmonate response, senescence and flowering in *Arabidopsis*. *Journal of experimental botany*, *59*(2), 225-234. doi: 10.1093/jxb/erm300

Wu, L., Ren, D., Hu, S., Li, G., Dong, G., Jiang, L., Hu, X., Ye, W., Cui, Y., Zhu, L., & Guo, L. (2016). Down-regulation of a nicotinate phosphoribosyltransferase gene, OsNaPRT1, leads to withered leaf tips. *Plant physiology*, *171*(2), 1085-1098.

Wüthrich, K. L., Bovet, L., Hunziker, P. E., Donnison, I. S., & Hörtensteiner, S. (2000). Molecular cloning, functional expression and characterisation of RCC reductase involved in chlorophyll catabolism. *The Plant Journal*, *21*(2), 189-198.

Xiao, H. J., Jin, J. H., Chai, W. G., & Gong, Z. H. (2015). Cloning and expression analysis of pepper chlorophyll catabolite reductase gene CaRCCR. *Genetics and Molecular Research*, *14*(1), 368-379.

Xu, W., Subudhi, P. K., Crasta, O. R., Rosenow, D. T., Mullet, J. E., & Nguyen, H. T. (2000). Molecular mapping of QTLs conferring stay-green in grain sorghum (Sorghum bicolor L. Moench). *Genome*, *43*(3), 461-469.

Yadav, S. K., Singla-Pareek, S. L., & Sopory, S. K. (2008). An overview on the role of methylglyoxal and glyoxalases in plants. *Drug Metabolism and Drug Interactions*, *23*(1-2), 51-68.

Yan, H., Saika, H., Maekawa, M., Takamure, I., Tsutsumi, N., Kyozuka, J., & Nakazono, M. (2007). Rice tillering dwarf mutant dwarf3 has increased leaf longevity during darkness-induced senescence or hydrogen peroxide-induced cell death. *Genes & genetic systems*, *82*(4), 361-366.

Yang, J., Lee, S. H., Goddard, M. E., & Visscher, P. M. (2011). GCTA: a tool for genome-wide complex trait analysis. *The American Journal of Human Genetics*, *88*(1), 76-82.

Yang, J., Yunying, C., Zhang, H., Liu, L., & Zhang, J. (2008). Involvement of polyamines in the post-anthesis development of inferior and superior spikelets in rice. *Planta*, *228*(1), 137-149.

Yang, Y., Xu, J., Huang, L., Leng, Y., Dai, L., Rao, Y., Chen, L., Wang, Y., Tu, Z., Hu, J., & Zeng, D. (2016). PGL, encoding chlorophyllide a oxygenase 1, impacts leaf senescence and indirectly affects grain yield and quality in rice. *Journal of experimental botany*, *67*(5), 1297-1310.

Yao, N., & Greenberg, J. T. (2006). *Arabidopsis* ACCELERATED CELL DEATH2 modulates programmed cell death. *The Plant Cell*, *18*(2), 397-411.

Yin, L., Zhang, H., Tang, Z., Xu, J., Yin, D., Zhang, Z., Yuan, X., Zhu, M., Zhao, S., Li, X., & Liu, X. (2021). rmvp: A memory-efficient, visualization-enhanced, and parallel-accelerated tool for genome-wide association study. *Genomics, Proteomics & Bioinformatics*.

Yin, Y., Wang, Z. Y., Mora-Garcia, S., Li, J., Yoshida, S., Asami, T., & Chory, J. (2002). BES1 accumulates in the nucleus in response to brassinosteroids to regulate gene expression and promote stem elongation. *Cell*, *109*(2), 181-191.

Yobi, A., Wone, B. W., Xu, W., Alexander, D. C., Guo, L., Ryals, J. A., Oliver, M. J., & Cushman, J. C. (2013). Metabolomic profiling in Selaginella lepidophylla at various hydration states provides new insights into the mechanistic basis of desiccation tolerance. *Molecular Plant*, *6*(2), 369-385.

Yoo, S. C., Cho, S. H., Zhang, H., Paik, H. C., Lee, C. H., Li, J., Yoo, J. H., Koh, H. J., Seo, H. S., & Paek, N. C. (2007). Quantitative trait loci associated with functional stay-green SNU-SG1 in rice. *Molecules & Cells* (Springer Science & Business Media BV), *24*(1).

Yoshida, S. (2003). Molecular regulation of leaf senescence. *Current opinion in plant biology*, *6*(1), 79-84.

Yoshida, S., Ito, M., Callis, J., Nishida, I., & Watanabe, A. (2002). A delayed leaf senescence mutant is defective in arginyl-tRNA: protein arginyltransferase, a component of the N-end rule pathway in *Arabidopsis*. *The Plant Journal*, *32*(1), 129-137.

Yang, S. D., Seo, P. J., Yoon, H. K., & Park, C. M. (2011). The *Arabidopsis* NAC transcription factor VNI2 integrates abscisic acid signals into leaf senescence via the COR/RD genes. *The Plant Cell*, *23*(6), 2155-2168.

Yu, J., & Buckler, E. S. (2006). Genetic association mapping and genome organization of maize. *Current opinion in biotechnology*, *17*(2), 155-160.

Yuan, Z., Cao, Q., Zhang, K., Ata-Ul-Karim, S. T., Tian, Y., Zhu, Y., Cao, W., & Liu, X. (2016). Optimal leaf positions for SPAD meter measurement in rice. *Frontiers in plant science*, *7*, 719.

Zavaleta-Mancera, H. A., Thomas, B. J., Thomas, H., & Scott, I. M. (1999). Regreening of senescent Nicotiana leaves: II. Redifferentiation of plastids. *Journal of Experimental Botany*, *50*(340), 1683-1689.

Zemanová, V., Pavlík, M., Pavlíková, D., & Tlustoš, P. (2014). The significance of methionine, histidine and tryptophan in plant responses and adaptation to cadmium stress. *Plant, Soil and Environment*, *60*(9), 426-432.

Zhang, H. K., Zhang, X., Mao, B. Z., Qun, L. I., & Zu Hua, H. E. (2004). Alpha-picolinic acid, a fungal toxin and mammal apoptosis-inducing agent, elicits hypersensitive-like response and enhances disease resistance in rice. *Cell research*, *14*(1), 27-33.

Zhang, H., Murzello, C., Sun, Y., Kim, M. S., Xie, X., Jeter, R. M., Zak, J. C., Dowd, S. E., & Paré, P. W. (2010). Choline and osmotic-stress tolerance induced in *Arabidopsis* by the soil microbe Bacillus subtilis (GB03). *Molecular plant-microbe interactions*, *23*(8), 1097-1104.

Zhang, J., Fengler, K. A., Van Hemert, J. L., Gupta, R., Mongar, N., Sun, J., Mongar, N., Sun, J., Allen, W. B., Wang, Y., Weers, B., Mo, H., & Shen, B. (2019). Identification and characterization of a novel stay-green QTL that increases yield in maize. *Plant biotechnology journal*, *17*(12), 2272-2285.

Zhang, X., Liu, S., & Takano, T. (2008). Two cysteine proteinase inhibitors from *Arabidopsis thaliana*, AtCYSa and AtCYSb, increasing the salt, drought, oxidation and cold tolerance. *Plant molecular biology*, *68*(1-2), 131-143.

Zhang, X., Zhang, Z., Li, J., Wu, L., Guo, J., Ouyang, L., Xia, Y., Huang, X., & Pang, X. (2011). Correlation of leaf senescence and gene expression/activities of chlorophyll degradation enzymes in harvested Chinese flowering cabbage (Brassica rapa var. parachinensis). *Journal of plant physiology*, *168*(17), 2081-2087.

Zhao, H. J., & Tan, J. F. (2005). Role of calcium ion in protection against heat and high irradiance stress-induced oxidative damage to photosynthesis of wheat leaves. *Photosynthetica*, *43*(3), 473-476.

Zhao, Y., Qiang, C., Wang, X., Chen, Y., Deng, J., Jiang, C., Sun, X., Chen, H., Li, J., Piao, W., & Li, J. (2019). New alleles for chlorophyll content and stay-green traits revealed by a genome wide association study in rice (Oryza sativa). *Scientific reports*, *9*(1), 1-11.

Zheng, X. Q., Hayashibe, E., & Ashihara, H. (2005). Changes in trigonelline (N-methylnicotinic acid) content and nicotinic acid metabolism during germination of mungbean (Phaseolus aureus) seeds. *Journal of experimental botany*, *56*(416), 1615-1623.

Zhou, C., Cai, Z., Guo, Y., & Gan, S. (2009). An *Arabidopsis* mitogen-activated protein kinase cascade, MKK9-MPK6, plays a role in leaf senescence. *Plant physiology*, *150*(1), 167-177.

Zhou, X., & Stephens, M. (2012). Genome-wide efficient mixed-model analysis for association studies. *Nature genetics*, *44*(7), 821.

Zhou, Y., Huang, W., Liu, L., Chen, T., Zhou, F., & Lin, Y. (2013). Identification and functional characterization of a rice NAC gene involved in the regulation of leaf senescence. *BMC Plant Biology*, *13*(1), 1-13.

Zwack, P. J., Robinson, B. R., Risley, M. G., & Rashotte, A. M. (2013). Cytokinin response factor 6 negatively regulates leaf senescence and is induced in response to cytokinin and numerous abiotic stresses. *Plant and Cell Physiology*, *54*(6), 971-981.

ANNEXURE

Annexure

Annexure 2.1. Pedigree of the association panel used for phenotyping

SR. NO.	VARIETY NAME	PEDIGREE
1	KOHSAR-95	PSN/BOW
2	SHAHKAR-95	CNO67//SN64/KLRE/3/8156
3	BAKHTAWAR-94	BB/NOR67
4	KAGHAN-93	CMH-77A917/PKV 1600//RL6010/6*SKA
5	SAIRAB-92	CHENAB2000/INQ-91
6	ANMOL-91	LUAN/KOH-97
7	PARWAZ-94	OASIS/SKAUZ//4*BCN/3/2*PASTOR
8	PASBAN-90	BLS/KHUSHAL
9	MARGHALA-99	OPATA/BOW'S'
10	DERA	F12-71/COC/CNO 79
11	DAMAN	BOWS/3/CAR853/COC//VEES
12	D-97	FORD//DUNDEE/BOBIN or FORD/DONDEE (I)
13	KOHISTAN-97	KVZ/3/TOB/CTFN/BB/4/BLO/5/VEE#5/6/BOW/3/YD//BB/CHA
14	MH-97	KAUZ/PASTOR
15	NARC-2009	INQALAB 91*2/TUKURU
16	SULEMAN -96	BUC/FLK//MYNA/VUL
17	NOWSHERA-96	C516/C591
18	ROHTAS-9O	INIA F 66/TH.DISTICHUM//INIA F 66/3/GENARO T 81 or INIA F 66/ A.DISTCHUM//INIA66/3/GEN
19	SOGHAT-90	PSN/BOW
20	BWP-97	NORD-DESPREZ(ND)/VG-9144//KALYANSONA/BLUEBIRD/3/YACO/4/VEERY-5
21	DWR-97; DRAWAR 97	SASONO KOMOGI/NORIN//BOB'S'
22	SHALIMAR-88	WL 711/CROW"S"
23	KHYBER-87	21931-CHAPINGO53/ANDES SIB/3/Y50/4/C271
24	RAWAL-87	MAYA/MON//KVZ/TRM
25	SUTLAJ-86	ULC/PVN//TAN/3/BUC
26	PUNJAB-85	BURGUS/SORT 12-13//KAL/BB/3/PAK 81
27	FSD-85	CHIL/2*STAR
28	FSD-83	MAYA/MON//KVZ/TRM
29	KOHINOOR-83	PT'S'/3/TOB/LFN//BB/4/BB/HD-832-5//ON/5/G-V/ALD'S'//HPO
30	SARHAD-82	JUP/ALD'S'//KLT'S'/3/VEE'S'/6/BEZ//TOB/8156/4/ON/3/6*TH/KF//6*LEE/KF/5
31	PUNJAB-81	PBW65/2*Pastor
32	PAK-81	FURY//KAL/BB
33	ZARDANA	PJ/GB55 or PJ62/GB55
34	ZARGHOON-79	CC/INIA/3/TOB/CTFN//BB/4/7C
35	BWP-79	CNO/LR64A*2//SN64/SN63 or CNO/LR64*2/SON64/SON

36	DIRIK	PIT/GB//C271
37	TARNAB-73	T9/8D or T9 X 8A
38	LYP-73	BB/NOR67
39	PARI-73	FORLANI/ACC//ANA or Fln/ACS//ANA
40	SA-72	C-271/WILLET-DWARF//SONORA-64
41	B-SILVER	C 230 X IP 165
42	CHENAB-70	HARD FEDERATION X 9D
43	YECORA-70	BUC'S'/FCT'S'
44	NURI-70	HARD FED/9D
45	UP-262	land races
46	LOCAL-WHITE	BB/GLL/3/GTO/7C//BB/CNO67
47	POTHOWAR	ATTILA/3/HUI/CARC//CHEN/CHTO/4/ATTILA
48	SA—75	CHUM18/BAU
49	SA-42	C 209 X C 591
50	KHUSHALL-69	II53-388/AN//YT54/N10B/3/LR64/4/B4946.A.4.18.2.IY/Y53//3*Y50
51	WL-711	S308/CHRIS//KAL
52	MEXIPAK	PJ/GB55 or PJ62/GB55
53	SONALIKA	SASONO KOMOGI/NORIN//BOB'S'
54	SANDAL	T9 X 8A
55	LU-26	BLS/KHUSHAL
56	PUNJAB-76	NAI60/CB151//S949/3/MEXIPAK
57	BARANI-70	CNO/LR64A*2//SN64/SN63 or CNO/LR64*2/SON64/SON
58	CHAKWAL-86	KVZ/TRM//PTM/ANA
59	PIRSBK-91	KAUZ//ALTAR84/AOS
60	INQILAB-91	V-1562//CHRC'S'/HORK/3/KUFRA-I/4/CARP'S'/BJY'S'
61	CHAKWAL-97	INIA F66/TH.DISTICHUM//INIAF66/3/GENARO T81 or INIA F66/A.DISTCHUM//INIA66/3/GEN
62	BARANI-83	DWL5023/SNB//SNB
63	CHAKWAL-50	F6.74/BUN//SIS/3/VEE#7 or F6-74/BUN//SIS/3/VEE#7
64	C-217	KHP/D31708//CM74A370/3/CNO79/4/RL6043/4*NAC or KHP/D31708//CM74A370/3/CIANO79/4/RL6043/*4NAC
65	C-228	KVZ/TRM//PTM/ANA
66	C-271	C-230/IP-165;
67	C-273	C-591/C-209; C-209/C-591
68	C-250	CROW'S'/NAC//BOW'S'
69	C-306	AU/UP301//GLL/Sx/3/PEW S/4/MAI S/MAY A S//PEWS
70	C-518	SH-88/90A-204//MH97
71	T-8	land races
72	SKD-1	LU 26/HD 21790/ 2*INQALAB 91
73	TD-1	BY/MAYA/4/BB//HD832.5.5/ON/3/CNO67/PJ62 or PITIC-62/FROND//MEXIPAK/3/PITIC-62/MAZOE-79-75-76 [wheatpedigree.net] or PI/FRND//MXP/3/PI/M20/79
74	RASKOH	Kauz/Yaco//Kauz
75	SARSABZ	TTR/JUN

76	SASSUI	HD-2329
77	WAFAQ	Kauz/Yaco//Kauz
78	AS-2002	CHAM6//KITE/PGO
79	T-9	land races
80	GA-2002	NAI60/CB151//S949/3/MEXIPAK
81	UFAQ	NAI60/CB151/S949/3/MEXIPAK
82	BAKHAR-2002	URES/BOW`S
83	MOOMAL-2003	CNO67//SN64/KLRE/3/8156
84	SH-2003	AU//KAL/BB/3/WOP
85	PIRSBK-04	KAUZ/STAR
86	IMDAD-05	CHILL/2* STAR/4/BOW//BUC/PVN/3/2*VEE#10
87	PIRSBK-05	MUNIA/CHTO//AMSEL
88	SEHER-2006	WL711//F371/TRM
89	SHAFAQ-2006	PB81/HD2182//PB81
90	LASANI-2008	PAVON MUTANT-3
91	PIRSBK-08	JUP/ALD'S'//KLT'S'
92	FSD-08	PBW65/2*Pastor
93	MAIRAJ-08	WT(E)/SON64
94	NARC-09	INQALAB 91*2/TUKURU
95	NARC-11	CNO67/8156//TOB66/CNO67/4/NO/3/12300//LR64A/8156/5/PVN or CNO67/8156//TOB 66/CNO67/4/NOROESTE F66/3/12300//LR64A/8156/5/PVN
96	AARI-11	OPATA/RAYON//KAUZ
97	AAS-11	LU26/HD 2179
98	PUNB-11	CNO67//SON64/KLRE/3/8156
99	FAREED-2006	INQALAB-91/FINK'S'
100	IQBAL-2000	BURT/KENYA//QUETA(L)/3/NAD63
101	FK.SARHAD	MUNIA/CHTO//AMSEL
102	KHIRMAN-2006	ULC/PVN//TAN/3/BUC
103	MANTHAR-2003	KAUZ//ALTAR84/AOS
104	SALEEM-2002	C271//LR64/SN64
105	TATARA-96	CNO//SN64/KLRE/3/8156
106	CHENAB-2000	AMSEL/ATTILA//INQ-91/PEW'S'
107	BWP-2000	NAI60/CB151/S949/3/MEXIPAK
108	AUQAB-2000	INIA/3/SN64/P4160(E)//SN64 or INIA/3/SON64/P4160(E)//SON64
109	BARS-2009	MAI'S'/NORTENO65/H68
110	SH-2002	INQALAB-91/FINK'S'
111	SALEEM-2000	KVZ/TRM//PTM/ANA
112	MILLAT-2011	NOR67/7C
113	MARVI-2000	PB85/NKT'S'
114	SOKOLL	Synthetic Derivative Variety
115	AUR-809	
116	TAX 8A	

117	UAF-9452	Advance line
118	V-070 96	
119	PAVON	VCM//CNO/7C/3/KAL/BB
120	HAIDER-2000	CHIL/WUH3
121	ZARLASHTA-99	URES/BOW'S'
122	PAKISTAN-13	CMH84.3379/CMH78.578//MILAN
123	SHAKAR-13	CMH84.3379/CMH78.578//MILAN
124	PUNJAB-85	KVZ/TRM//PTM/ANA
125	C-591	PRL/PASTOR//2236(V6550/SUTLEH-86)
126	STAY GREEN; NEPAL-38	CHIRYA7/ANB
127	STAY GREEN; NEPAL-49	CHIRYA1
128	STAY GREEN; NEPAL-50	CHIRYA7
129	STAY GREEN; NEPAL-51	CHIRYA3
130	STAY GREEN; NEPAL-268	DUCULA//HUI/TUB/3/CAZO/4/CROC-1/AE.SQ(224)//OPATA
131	STAY GREEN; SG-30	SABUF//ALTAR84/AE.SQ(205)
132	STAY GREEN; SG-33	SABUF//ALTAR84/AE.SQ(205)
133	STAY GREEN; SG-73	SABUF//ALTAR84/AE.SQ(205)
134	STAY GREEN; ITMI-35	ALTAR84/AE.SQ//OPATA
135	STAY GREEN; PROGENATOR-2	PASTOR
136	STAY GREEN; SL OPATA	
137	STAY GREEN; SG LINE (12x2)	
138	STAY GREEN; 3(9x1)	CHIRYA-1//CROC/AE.SQ(224)
139	STAY GREEN; 5(9x1)	CHIRYA-1//CROC/AE.SQ(224)
140	STAY GREEN; 90(9x1)	CHIRYA-1//CROC/AE.SQ(224)
141	STAY GREEN; 130(12x2)	PAPGO//LARU/AE.SQ(347)
142	STAY GREEN, SD(MK)-23	
143	STAY GREEN, SD(MK)-24	MAYOOR//TKSN1081/AE.SQUARROSA(222)/3/OPATA/4/
144	STAY GREEN, SD(MK)-25	TURACO/5/CHIR3/4/SIREN//ALTAR
145	STAY GREEN, SD(MK)-28	OPATA//DOY1/AE.SQUARROSA(372)
146	STAY GREEN, SD(MK)-30	D67.2/P66.270//AE.SQUARROSA(223)3/ARLIN_1/T.MONOCOCCUM(95) 34
147	STAY GREEN, SD(MK)-34	MAYOOR//TKSN1081/AE.SQUARROSA(222)3/OPATA/6/68.111/RGB-U//WARD/3/FGO/4/RABI/5/AE.SQUARROSA(878)
148	STAY GREEN, SD(MK)-36	URES/PRL//BAV92/3/YAV_2/TEZ//AE.SQUARROSA(249)
149	STAY GREEN, SD(MK)-37	GAN/AE.SQUARROSA(897)//OPATA/3/D67.2/P66.270//AE.SQUARROSA(223)
150	STAY GREEN, SD(MK)-39	OPATA//DOY1/AE.SQUARROSA(255)

Annexure 2.2. Genome-wide association mapping showing marker trait association at – log10(p) ≥ 3

Trait	Method	Marker	Chrom	Position	Effect	p Value	-log10(p)
PI_21DAA	FarmCPU	RAC875_rep_c110533_92	1A	1339580	0.0182	0.00099	3
CSFL	FarmCPU	tplb0025b13_2687	1A	3386986	4.4836	0.00014	3.86
CSFL	GLM	tplb0025b13_2687	1A	3386986	4.6581	0.00021	3.69
PI_21DAA	FarmCPU	tplb0025b13_2687	1A	3386986	0.0303	0.00093	3.03
CSFL	MLM	tplb0025b13_2687	1A	3386986	4.5585	0.00052	3.28
NDVI_A	FarmCPU	Tdurum_contig11679_319	1A	6570191	0.116	0.00014	3.84
NDVI_A	GLM	Tdurum_contig11679_319	1A	6570191	0.114	7.11E-05	4.15
NDVI_A	MLM	Tdurum_contig11679_319	1A	6570191	0.1181	0.00019	3.72
SPS	FarmCPU	wsnp_Ex_c29914_38896441	1A	76031015	1.1701	0.00092	3.04
SPS	GLM	wsnp_Ex_c14733_22819350	1A	100292629	0.5381	0.00077	3.11
SPS	GLM	IAAV7414	1A	100292829	0.5381	0.00077	3.11
SL	FarmCPU	wsnp_Ex_c14733_22819625	1A	100292904	0.4048	0.00029	3.54
SL	GLM	wsnp_Ex_c14733_22819625	1A	100292904	0.419	0.00019	3.72
SPS	FarmCPU	wsnp_Ex_c14733_22819625	1A	100292904	0.5467	0.00063	3.2
SPS	GLM	wsnp_Ex_c14733_22819625	1A	100292904	0.5829	0.00026	3.59
SL	MLM	wsnp_Ex_c14733_22819625	1A	100292904	0.4048	0.0007	3.16
SL	GLM	wsnp_Ex_c49829_54319220	1A	101764563	0.3612	0.00079	3.1
SPS	GLM	wsnp_Ex_c49829_54319220	1A	101764563	0.5384	0.0004	3.4
SL	GLM	wsnp_RFL_Contig1736_858448	1A	101764713	0.3612	0.00079	3.1
SPS	GLM	wsnp_RFL_Contig1736_858448	1A	101764713	0.5384	0.0004	3.4
SL	FarmCPU	wsnp_Ex_c26098_35349418	1A	107227745	0.5039	0.00063	3.2
SL	GLM	wsnp_Ex_c26098_35349418	1A	107227745	0.5259	0.00042	3.38
SL	FarmCPU	Kukri_rep_c101218_200	1A	108760658	0.418	0.00069	3.16
SL	GLM	Kukri_rep_c101218_200	1A	108760658	0.4344	0.00048	3.32
SPS	GLM	Kukri_rep_c101218_200	1A	108760658	0.5948	0.00077	3.12
SL	FarmCPU	BS00028874_51	1A	117808227	0.418	0.00069	3.16
SL	GLM	BS00028874_51	1A	117808227	0.4344	0.00048	3.32
SPS	GLM	BS00028874_51	1A	117808227	0.5948	0.00077	3.12
SL	FarmCPU	BS00066308_51	1A	147908325	0.418	0.00069	3.16
SL	GLM	BS00066308_51	1A	147908325	0.4344	0.00048	3.32
SPS	GLM	BS00066308_51	1A	147908325	0.5948	0.00077	3.12
SL	FarmCPU	wsnp_Ex_c2389_4479047	1A	155080158	0.418	0.00069	3.16
SL	GLM	wsnp_Ex_c2389_4479047	1A	155080158	0.4344	0.00048	3.32
SPS	GLM	wsnp_Ex_c2389_4479047	1A	155080158	0.5948	0.00077	3.12
SL	GLM	wsnp_Ex_c2389_4477880	1A	155081443	0.4514	0.0008	3.1
SL	FarmCPU	BS00033760_51	1A	157831818	0.418	0.00069	3.16
SL	GLM	BS00033760_51	1A	157831818	0.4344	0.00048	3.32
SPS	GLM	BS00033760_51	1A	157831818	0.5948	0.00077	3.12
SL	FarmCPU	wsnp_Ex_c41237_48104282	1A	176457891	0.418	0.00069	3.16

SL	GLM	wsnp_Ex_c41237_48104282	1A	176457891	0.4344	0.00048	3.32
SPS	GLM	wsnp_Ex_c41237_48104282	1A	176457891	0.5948	0.00077	3.12
SL	FarmCPU	Kukri_c23382_1431	1A	176458041	0.4704	0.00043	3.37
SL	GLM	Kukri_c23382_1431	1A	176458041	0.4896	0.00029	3.53
SL	MLM	Kukri_c23382_1431	1A	176458041	0.4704	0.00094	3.03
SPS	GLM	Ku_c2898_1284	1A	182069500	0.6652	0.00055	3.26
SL	FarmCPU	wsnp_Ex_rep_c66875_65276404	1A	208209736	0.418	0.00069	3.16
SL	GLM	wsnp_Ex_rep_c66875_65276404	1A	208209736	0.4344	0.00048	3.32
SPS	GLM	wsnp_Ex_rep_c66875_65276404	1A	208209736	0.5948	0.00077	3.12
NDVI_14DAA	FarmCPU	RAC875_c18539_1159	1A	344294391	-0.0415	0.00021	3.67
NDVI_14DAA	FarmCPU	wsnp_Ex_c34260_42602746	1A	344483035	-0.0415	0.00021	3.67
NDVI_A	FarmCPU	wsnp_Ex_c34260_42602649	1A	344483036	-0.0473	0.00095	3.02
NDVI_14DAA	FarmCPU	Ex_c5759_663	1A	345108277	-0.0327	0.00088	3.06
NDVI_A	FarmCPU	RAC875_c15998_53	1A	345308642	-0.0473	0.00095	3.02
NDVI_A	FarmCPU	wsnp_Ex_c33831_42253707	1A	345308792	-0.0473	0.00095	3.02
NDVI_14DAA	FarmCPU	Excalibur_c102582_360	1A	345786652	-0.0415	0.00021	3.67
NDVI_H	FarmCPU	Ku_c6979_182	1A	346446236	-0.0372	0.00018	3.75
NDVI_14DAA	FarmCPU	Ku_c6979_182	1A	346446236	-0.0499	2.18E-05	4.66
NDVI_14DAA	FarmCPU	wsnp_Ex_c13564_21327699	1A	350753736	-0.037	0.00069	3.16
NDVI_14DAA	FarmCPU	wsnp_Ex_c1374_2630879	1A	352137757	-0.0415	0.00021	3.67
NDVI_14DAA	FarmCPU	wsnp_Ra_c18045_27024765	1A	353253752	-0.0415	0.00021	3.67
NDVI_14DAA	FarmCPU	wsnp_Ex_c21592_30743815	1A	353255562	-0.0415	0.00021	3.67
NDVI_14DAA	FarmCPU	CAP12_c6266_339	1A	354823522	-0.0367	0.00069	3.16
NDVI_14DAA	FarmCPU	Excalibur_c17872_137	1A	355335949	-0.0415	0.00021	3.67
NDVI_14DAA	FarmCPU	Excalibur_c14943_695	1A	361511937	-0.0415	0.00021	3.67
CHL_A	FarmCPU	BS00040968_51	1A	480755333	0.3013	0.0005	3.3
CHL_A	GLM	BS00040968_51	1A	480755333	0.3167	0.00053	3.28
TN	FarmCPU	wsnp_Ex_c9345_15516291	1A	488661702	0.4941	0.00097	3.01
PI_H	FarmCPU	BS00021714_51	1A	490087945	0.0546	0.00034	3.47
PI_H	GLM	BS00021714_51	1A	490087945	0.0593	0.00019	3.73
FV/FM_H	FarmCPU	BS00021714_51	1A	490087945	0.0056	0.00058	3.24
FV/FM_H	GLM	BS00021714_51	1A	490087945	0.006	0.0004	3.4
PI_H	MLM	BS00021714_51	1A	490087945	0.055	0.00084	3.08
PI_H	FarmCPU	Ra_c4159_2716	1A	490520958	0.0537	0.00063	3.2
PI_H	GLM	Ra_c4159_2716	1A	490520958	0.0583	0.00037	3.43
FV/FM_H	GLM	Ra_c4159_2716	1A	490520958	0.0059	0.00078	3.11
PI_H	FarmCPU	RAC875_c23081_141	1A	491130234	0.0537	0.00063	3.2
PI_H	GLM	RAC875_c23081_141	1A	491130234	0.0583	0.00037	3.43
FV/FM_H	GLM	RAC875_c23081_141	1A	491130234	0.0059	0.00078	3.11
PI_H	GLM	BS00032112_51	1A	494446871	0.0591	0.00093	3.03
PI_H	GLM	Ex_c105443_895	1A	494450006	0.0591	0.00093	3.03
NDVI_A	FarmCPU	wsnp_Ex_c55986_58282517	1A	497520528	0.0858	0.00047	3.33
NDVI_A	FarmCPU	Ra_c105707_788	1A	497520605	0.0748	0.00057	3.24

NDVI_14DAA	FarmCPU	Ra_c105707_788	1A	497520605	0.0737	0.00043	3.36
NDVI_A	FarmCPU	Kukri_c24715_175	1A	498049972	0.0711	0.00011	3.95
NDVI_A	MLM	Kukri_c24715_175	1A	498049972	0.0728	0.00086	3.06
CN	FarmCPU	Tdurum_contig42490_1315	1A	499797489	0.0314	0.00078	3.11
CN	GLM	Tdurum_contig42490_1315	1A	499797489	0.0322	0.00067	3.17
TN	FarmCPU	Excalibur_c14911_546	1A	515551602	0.3878	0.0001	3.99
PI_H	FarmCPU	wsnp_CAP7_c3472_1623955	1A	534265650	0.0568	0.0006	3.22
PI_H	GLM	wsnp_CAP7_c3472_1623955	1A	534265650	0.057	0.00067	3.18
FV/FM_H	FarmCPU	wsnp_CAP7_c3472_1623955	1A	534265650	0.0061	0.00057	3.25
FV/FM_H	GLM	wsnp_CAP7_c3472_1623955	1A	534265650	0.0061	0.00065	3.18
ADN	FarmCPU	wsnp_CAP7_c3472_1623955	1A	534265650	0.0063	0.00045	3.35
ADN	GLM	wsnp_CAP7_c3472_1623955	1A	534265650	0.0063	0.00052	3.28
NDVI_H	GLM	BS00020241_51	1A	537352861	-0.053	0.00057	3.24
NDVI_A	GLM	BS00020241_51	1A	537352861	-0.0712	0.00014	3.86
NDVI_14DAA	GLM	BS00020241_51	1A	537352861	-0.0658	0.00041	3.39
ADN	GLM	GENE-0033_233	1A	542003186	0.0075	0.00099	3.01
ADSFL	FarmCPU	IACX14	1A	544605206	0.5474	0.00012	3.93
ADSFL	GLM	IACX14	1A	544605206	0.5556	0.00039	3.41
ADSFL	MLM	IACX14	1A	544605206	0.5537	0.00049	3.31
TN	GLM	JD_c13024_360	1A	546037054	0.1789	0.0006	3.22
ADSFL	FarmCPU	wsnp_CAP11_c29_68486	1A	548563957	0.4341	0.00098	3.01
ADSFL	FarmCPU	BS00034899_51	1A	548941277	0.4914	0.0006	3.23
TN	FarmCPU	wsnp_Ex_c13955_21833712	1A	549704401	0.1744	0.00059	3.23
NDVI_21DAA	GLM	Excalibur_c88792_93	1A	574338358	-0.0329	0.00086	3.07
NDVI_A	GLM	Tdurum_contig84252_155	1A	580496917	-0.0304	0.00022	3.65
NDVI_14DAA	FarmCPU	tplb0049h18_765	1A	584683017	-0.0354	0.00069	3.16
NDVI_A	FarmCPU	IAAV1301	1A	589874399	0.0242	0.00068	3.17
CHL_30DAA	FarmCPU	BS00022797_51	1A	590342457	0.3849	0.00096	3.02
NDVI_A	FarmCPU	wsnp_Ex_c412_814247	1A	590344598	-0.0334	0.00057	3.25
NDVI_14DAA	FarmCPU	wsnp_Ex_c412_814247	1A	590344598	-0.0311	0.0009	3.05
NDVI_14DAA	FarmCPU	wsnp_Ex_c750_1474184	1A	592090936	-0.0387	4.68E-05	4.33
NDVI_14DAA	GLM	wsnp_Ex_c750_1474184	1A	592090936	-0.0351	0.00022	3.66
NDVI_14DAA	MLM	wsnp_Ex_c750_1474184	1A	592090936	-0.0372	0.00047	3.32
CSFL	MLM	BS00075116_51	1B	1848277	10.662	0.00069	3.16
CHL_10DAA	FarmCPU	BS00075116_51	1B	1848277	1.648	0.00055	3.26
CHL_10DAA	GLM	BS00075116_51	1B	1848277	1.6077	0.00064	3.2
CSFL	FarmCPU	BS00075116_51	1B	1848277	10.708	0.00028	3.56
CSFL	GLM	BS00075116_51	1B	1848277	10.565	0.00035	3.46
NDVI_A	MLM	GENE-1118_1049	1B	8222519	-0.2362	0.00019	3.72
NDVI_A	FarmCPU	GENE-1118_1049	1B	8222519	-0.2319	0.00014	3.84
NDVI_A	GLM	GENE-1118_1049	1B	8222519	-0.2279	7.11E-05	4.15
TN	FarmCPU	Tdurum_contig10767_538	1B	9690544	0.2509	0.00046	3.34
TN	FarmCPU	BS00110900_51	1B	10361155	0.4061	1.54E-05	4.81

CN	FarmCPU	RAC875_c113582_346	1B	11697033	-0.0182	0.0009	3.05
CN	GLM	RAC875_c113582_346	1B	11697033	-0.0224	0.00017	3.77
CN	MLM	Tdurum_contig44219_318	1B	15169586	-0.0248	0.0001	4
PI_14DAA	FarmCPU	Tdurum_contig44219_318	1B	15169586	-0.1361	0.00063	3.2
PI_14DAA	GLM	Tdurum_contig44219_318	1B	15169586	-0.147	0.00059	3.23
FV/FM_14DAA	FarmCPU	Tdurum_contig44219_318	1B	15169586	-0.0135	0.0007	3.16
FV/FM_14DAA	GLM	Tdurum_contig44219_318	1B	15169586	-0.0148	0.00059	3.23
CN	FarmCPU	Tdurum_contig44219_318	1B	15169586	-0.0218	3.67E-05	4.44
CN	GLM	Tdurum_contig44219_318	1B	15169586	-0.0246	1.45E-05	4.84
CN	FarmCPU	wsnp_Ex_rep_c67198_65702998	1B	15169706	-0.0179	0.00058	3.24
CN	GLM	wsnp_Ex_rep_c67198_65702998	1B	15169706	-0.0199	0.00036	3.45
CN	FarmCPU	wsnp_Ku_c28164_38103270	1B	15171154	-0.0186	0.00039	3.41
CN	GLM	wsnp_Ku_c28164_38103270	1B	15171154	-0.0207	0.00022	3.65
CN	GLM	Kukri_c38845_821	1B	15449332	-0.0212	0.00053	3.27
PI_14DAA	FarmCPU	BS00074962_51	1B	15658734	-0.1732	0.00097	3.02
CN	MLM	RAC875_c5243_479	1B	15745770	-0.0287	0.00076	3.12
CN	FarmCPU	RAC875_c5243_479	1B	15745770	-0.0283	0.00015	3.83
CN	GLM	RAC875_c5243_479	1B	15745770	-0.0281	0.00033	3.48
PI_14DAA	MLM	Excalibur_c16851_835	1B	17383825	-0.1558	0.0003	3.52
FV/FM_14DAA	MLM	Excalibur_c16851_835	1B	17383825	-0.0152	0.00041	3.39
CN	MLM	Excalibur_c16851_835	1B	17383825	-0.0231	0.00012	3.93
PI_14DAA	FarmCPU	Excalibur_c16851_835	1B	17383825	-0.1526	7.73E-05	4.11
PI_14DAA	GLM	Excalibur_c16851_835	1B	17383825	-0.153	0.00017	3.77
FV/FM_14DAA	FarmCPU	Excalibur_c16851_835	1B	17383825	-0.0149	0.00012	3.9
FV/FM_14DAA	GLM	Excalibur_c16851_835	1B	17383825	-0.0151	0.00024	3.63
FV/FM_21DAA	FarmCPU	Excalibur_c16851_835	1B	17383825	-0.002	0.00088	3.05
CN	FarmCPU	Excalibur_c16851_835	1B	17383825	-0.0206	7.39E-05	4.13
CN	GLM	Excalibur_c16851_835	1B	17383825	-0.0214	9.55E-05	4.02
CN	MLM	IAAV6001	1B	17623269	-0.0213	0.00086	3.07
CN	FarmCPU	IAAV6001	1B	17623269	-0.0198	0.00021	3.67
CN	GLM	IAAV6001	1B	17623269	-0.0233	5.14E-05	4.29
CN	GLM	RFL_Contig4104_670	1B	20174583	-0.0196	0.00061	3.21
CN	GLM	Tdurum_contig403_290	1B	22206040	-0.0179	0.00099	3
PH	FarmCPU	wsnp_Ex_c5780_10154132	1B	26186618	-3.409	0.00061	3.22
NDVI_14DAA	MLM	RFL_Contig2160_617	1B	46884361	-0.0333	0.00054	3.27
NDVI_14DAA	FarmCPU	RFL_Contig2160_617	1B	46884361	-0.0307	0.00024	3.63
NDVI_14DAA	GLM	RFL_Contig2160_617	1B	46884361	-0.0344	0.00012	3.92
TKW	FarmCPU	GENE-4608_280	1B	144274227	1.0441	0.00084	3.08
TKW	GLM	GENE-4608_280	1B	144274227	1.0461	0.00098	3.01
CHL_30DAA	FarmCPU	BS00063574_51	1B	144879114	0.6925	0.00088	3.06
CHL_30DAA	MLM	BS00022218_51	1B	156565298	0.7659	0.00052	3.29
CHL_30DAA	FarmCPU	BS00022218_51	1B	156565298	0.7591	0.00015	3.82
CHL_30DAA	GLM	BS00022218_51	1B	156565298	0.7867	0.00032	3.49

CHL_30DAA	MLM	BS00073935_51	1B	157274715	0.7659	0.00052	3.29
CHL_30DAA	FarmCPU	BS00073935_51	1B	157274715	0.7591	0.00015	3.82
CHL_30DAA	GLM	BS00073935_51	1B	157274715	0.7867	0.00032	3.49
NDVI_H	FarmCPU	BobWhite_c4126_442	1B	333602726	0.0443	0.00072	3.14
NDVI_A	FarmCPU	BobWhite_c4126_442	1B	333602726	0.0574	0.00039	3.41
NDVI_14DAA	FarmCPU	BobWhite_c4126_442	1B	333602726	0.0551	0.00042	3.38
PH	FarmCPU	wsnp_Ex_c22006_31181239	1B	451077232	-2.3866	0.00094	3.03
CHL_A	FarmCPU	Excalibur_s102212_259	1B	474447966	0.2916	0.00076	3.12
CHL_A	FarmCPU	CAP7_s12849_67	1B	474449387	0.3077	0.0008	3.1
CHL_A	FarmCPU	wsnp_JD_c4641_5774711	1B	474449537	0.3132	0.00065	3.19
CHL_A	GLM	wsnp_JD_c4641_5774711	1B	474449537	0.3108	0.00095	3.02
CHL_A	FarmCPU	wsnp_Ex_c1495_2864718	1B	527001676	0.3313	0.00098	3.01
CN	MLM	Tdurum_contig42755_1086	1B	553143757	0.0206	0.00083	3.08
CN	FarmCPU	Tdurum_contig42755_1086	1B	553143757	0.0197	0.0003	3.52
CN	GLM	Tdurum_contig42755_1086	1B	553143757	0.0198	0.00046	3.34
CN	MLM	BobWhite_c48550_198	1B	553143857	0.0206	0.00083	3.08
CN	FarmCPU	BobWhite_c48550_198	1B	553143857	0.0197	0.0003	3.52
CN	GLM	BobWhite_c48550_198	1B	553143857	0.0198	0.00046	3.34
CN	FarmCPU	BS00089563_51	1B	560252448	0.019	0.00073	3.14
CHL_30DAA	FarmCPU	BS00055866_51	1B	577186800	0.3557	0.00039	3.41
CHL_30DAA	GLM	BS00055866_51	1B	577186800	0.3451	0.00072	3.14
CHL_30DAA	FarmCPU	BS00055864_51	1B	577186958	0.3557	0.00039	3.41
CHL_30DAA	GLM	BS00055864_51	1B	577186958	0.3451	0.00072	3.14
NDVI_14DAA	FarmCPU	Kukri_c11389_59	1B	619683676	-0.0558	0.00077	3.11
NDVI_14DAA	FarmCPU	IAAV8459	1B	619686619	-0.0265	0.00099	3
NDVI_14DAA	FarmCPU	wsnp_Ex_c18384_27213023	1B	619691671	-0.0279	0.00077	3.11
NDVI_14DAA	FarmCPU	BS00110231_51	1B	623989423	-0.0317	0.00087	3.06
CSFL	MLM	wsnp_BF200640B_Ta_2_1	1B	627946628	7.715	0.00057	3.25
CHL_10DAA	GLM	wsnp_BF200640B_Ta_2_1	1B	627946628	1.1236	0.00065	3.18
CHL_20DAA	GLM	wsnp_BF200640B_Ta_2_1	1B	627946628	4.0934	0.00083	3.08
CSFL	FarmCPU	wsnp_BF200640B_Ta_2_1	1B	627946628	7.511	0.00026	3.58
CSFL	GLM	wsnp_BF200640B_Ta_2_1	1B	627946628	7.6379	0.00021	3.67
CSFL	MLM	RAC875_c15190_1089	1B	630063122	10.662	0.00069	3.16
CHL_10DAA	FarmCPU	RAC875_c15190_1089	1B	630063122	1.648	0.00055	3.26
CHL_10DAA	GLM	RAC875_c15190_1089	1B	630063122	1.6077	0.00064	3.2
CSFL	FarmCPU	RAC875_c15190_1089	1B	630063122	10.708	0.00028	3.56
CSFL	GLM	RAC875_c15190_1089	1B	630063122	10.565	0.00035	3.46
CSFL	MLM	RAC875_c42275_224	1B	631832802	8.839	0.00011	3.96
CHL_20DAA	FarmCPU	RAC875_c42275_224	1B	631832802	4.2872	0.00051	3.29
CHL_20DAA	GLM	RAC875_c42275_224	1B	631832802	4.4112	0.00032	3.5
CSFL	FarmCPU	RAC875_c42275_224	1B	631832802	8.706	2.02E-05	4.7
CSFL	GLM	RAC875_c42275_224	1B	631832802	8.8726	1.40E-05	4.85
CSFL	MLM	BobWhite_c36862_84	1B	631999928	8.839	0.00011	3.96

CHL_20DAA	FarmCPU	BobWhite_c36862_84	1B	631999928	4.2872	0.00051	3.29
CHL_20DAA	GLM	BobWhite_c36862_84	1B	631999928	4.4112	0.00032	3.5
CSFL	FarmCPU	BobWhite_c36862_84	1B	631999928	8.706	2.02E-05	4.7
CSFL	GLM	BobWhite_c36862_84	1B	631999928	8.8726	1.40E-05	4.85
NDVI_H	FarmCPU	Tdurum_contig16606_648	1B	633333178	-0.0365	0.00052	3.29
SL	FarmCPU	Excalibur_c63243_361	1B	634150615	0.446	0.00066	3.18
SL	GLM	Excalibur_c63243_361	1B	634150615	0.4646	0.00044	3.35
SPS	GLM	Excalibur_c63243_361	1B	634150615	0.6218	0.00095	3.02
NDVI_H	FarmCPU	Kukri_c18109_475	1B	636264003	-0.0365	0.00052	3.29
PH	GLM	tplb0043a07_1411	1B	637622146	1.7495	0.00071	3.15
PH	GLM	tplb0043a07_880	1B	637622677	-1.7318	0.00097	3.01
RDN	FarmCPU	Excalibur_c13879_930	1B	642195806	0.0276	0.00081	3.09
CN	MLM	RAC875_c818_1185	1B	642677903	0.0165	0.00057	3.25
PI_A	FarmCPU	RAC875_c818_1185	1B	642677903	0.0398	0.00063	3.2
PI_A	GLM	RAC875_c818_1185	1B	642677903	0.041	0.00074	3.13
CN	FarmCPU	RAC875_c818_1185	1B	642677903	0.0145	0.00048	3.32
CN	GLM	RAC875_c818_1185	1B	642677903	0.0168	8.22E-05	4.08
CN	MLM	wsnp_Ku_rep_c107952_93214466	1B	642678714	0.0169	0.00048	3.32
CN	FarmCPU	wsnp_Ku_rep_c107952_93214466	1B	642678714	0.0147	0.00043	3.37
CN	GLM	wsnp_Ku_rep_c107952_93214466	1B	642678714	0.0167	8.87E-05	4.05
PH	GLM	BS00084895_51	1B	643101677	1.7532	0.00079	3.1
CHL_A	GLM	BS00109244_51	1B	645571247	0.3656	0.00033	3.48
CHL_A	MLM	Excalibur_c8585_701	1B	645571368	0.3752	0.00096	3.02
CHL_A	GLM	Excalibur_c8585_701	1B	645571368	0.4078	8.37E-05	4.08
CSFL	GLM	Excalibur_c8585_701	1B	645571368	2.9626	0.00077	3.11
PI_14DAA	GLM	Excalibur_c8585_701	1B	645571368	0.1372	0.00078	3.11
FV/FM_14DAA	GLM	Excalibur_c8585_701	1B	645571368	0.0136	0.00096	3.02
CHL_A	MLM	BobWhite_c23617_167	1B	645571427	0.3752	0.00096	3.02
CHL_A	GLM	BobWhite_c23617_167	1B	645571427	0.4078	8.37E-05	4.08
CSFL	GLM	BobWhite_c23617_167	1B	645571427	2.9626	0.00077	3.11
PI_14DAA	GLM	BobWhite_c23617_167	1B	645571427	0.1372	0.00078	3.11
FV/FM_14DAA	GLM	BobWhite_c23617_167	1B	645571427	0.0136	0.00096	3.02
CHL_A	GLM	Tdurum_contig11216_942	1B	645571983	0.3734	0.00066	3.18
CHL_A	GLM	Jagger_c3757_131	1B	645572022	-0.7312	0.00033	3.48
CHL_A	GLM	BS00099794_51	1B	645708030	0.4022	0.00079	3.1
CSFL	GLM	BS00099794_51	1B	645708030	3.4629	0.00056	3.25
PI_14DAA	MLM	wsnp_CAP11_c1902_1022408	1B	646167376	-0.1234	0.0004	3.4
FV/FM_14DAA	MLM	wsnp_CAP11_c1902_1022408	1B	646167376	-0.0127	0.00029	3.54
PI_14DAA	FarmCPU	wsnp_CAP11_c1902_1022408	1B	646167376	-0.1166	0.00021	3.68
PI_14DAA	GLM	wsnp_CAP11_c1902_1022408	1B	646167376	-0.1201	0.0002	3.71
FV/FM_14DAA	FarmCPU	wsnp_CAP11_c1902_1022408	1B	646167376	-0.012	0.00013	3.9
FV/FM_14DAA	GLM	wsnp_CAP11_c1902_1022408	1B	646167376	-0.0124	0.00012	3.92
FV/FM_14DAA	MLM	RAC875_c15625_520	1B	646167526	-0.0113	0.00096	3.02

PI_14DAA	FarmCPU	RAC875_c15625_520	1B	646167526	-0.1026	0.00093	3.03
FV/FM_14DAA	FarmCPU	RAC875_c15625_520	1B	646167526	-0.0106	0.0006	3.22
FV/FM_14DAA	GLM	RAC875_c15625_520	1B	646167526	-0.0108	0.00068	3.17
PH	GLM	Ex_c74049_545	1B	659661094	4.4269	0.0004	3.4
TN	FarmCPU	wsnp_BE591290B_Ta_2_7	1B	661896651	-0.5154	0.0007	3.16
TN	FarmCPU	BS00078414_51	1B	662718672	-0.2669	0.00027	3.56
TN	FarmCPU	IACX2234	1B	664302415	-0.2385	0.00078	3.11
TN	FarmCPU	Tdurum_contig55429_147	1B	664302525	-0.2385	0.00078	3.11
TN	FarmCPU	Tdurum_contig55429_116	1B	664302556	-0.2385	0.00078	3.11
CN	GLM	Kukri_c56333_178	1B	670176203	-0.0221	0.00022	3.66
CHL_B	FarmCPU	Excalibur_c14706_421	1B	671505564	1.2813	0.00042	3.38
CHL_B	GLM	Excalibur_c14706_421	1B	671505564	1.2855	0.00046	3.34
CHL_B	MLM	Excalibur_c14706_421	1B	671505564	1.2813	0.00093	3.03
NDVI_14DAA	FarmCPU	IAAV4884	1B	676262821	-0.0352	0.00041	3.39
SPS	FarmCPU	BobWhite_c11756_79	1B	676776429	0.4547	0.00098	3.01
SPS	GLM	BobWhite_c11756_79	1B	676776429	0.4637	0.00073	3.13
FV/FM_21DAA	MLM	RAC875_c13829_224	1B	677867931	-0.0033	0.00085	3.07
FV/FM_21DAA	FarmCPU	RAC875_c13829_224	1B	677867931	-0.0033	0.00032	3.5
FV/FM_21DAA	GLM	RAC875_c13829_224	1B	677867931	-0.0033	0.00064	3.2
NDVI_14DAA	FarmCPU	Tdurum_contig52086_264	1B	678263256	-0.0354	0.00069	3.16
CHL_20DAA	MLM	Ex_c29452_302	1B	678432525	-2.3323	0.00017	3.78
CHL_20DAA	FarmCPU	Ex_c29452_302	1B	678432525	-2.3052	4.68E-05	4.33
CHL_20DAA	GLM	Ex_c29452_302	1B	678432525	-2.4417	1.59E-05	4.8
CSFL	GLM	Ex_c29452_302	1B	678432525	-3.2698	0.00086	3.06
FV/FM_21DAA	MLM	RAC875_rep_c111730_97	1B	685723919	0.0043	0.00073	3.14
FV/FM_21DAA	FarmCPU	RAC875_rep_c111730_97	1B	685723919	0.0043	0.00029	3.53
FV/FM_21DAA	GLM	RAC875_rep_c111730_97	1B	685723919	0.0044	0.00023	3.63
NDVI_14DAA	FarmCPU	Tdurum_contig1631_240	1B	686840546	-0.028	0.00066	3.18
NDVI_14DAA	FarmCPU	wsnp_Ex_c750_1474300	1B	686843834	-0.034	0.00024	3.63
NDVI_14DAA	GLM	wsnp_Ex_c750_1474300	1B	686843834	-0.0321	0.00037	3.43
NDVI_14DAA	FarmCPU	wsnp_BE446672B_Ta_2_1	1B	687718613	-0.0304	9.53E-05	4.02
NDVI_14DAA	GLM	wsnp_BE446672B_Ta_2_1	1B	687718613	-0.0272	0.00051	3.29
NDVI_14DAA	FarmCPU	Tdurum_contig9144_222	1B	687719783	-0.0337	8.44E-05	4.07
NDVI_14DAA	GLM	Tdurum_contig9144_222	1B	687719783	-0.0293	0.001	3
NDVI_14DAA	FarmCPU	wsnp_Ex_c24777_34031473	1B	687799049	-0.0269	0.00057	3.25
NDVI_14DAA	FarmCPU	wsnp_Ex_c955_1827719	1B	688768195	-0.0298	0.00043	3.37
NDVI_14DAA	FarmCPU	Ku_c11537_539	1B	688769204	-0.0265	0.00044	3.36
CHL_A	FarmCPU	BS00000744_51	1D	216812	0.4468	0.00027	3.58
CHL_A	GLM	BS00000744_51	1D	216812	0.4362	0.00044	3.35
CHL_30DAA	GLM	BS00000744_51	1D	216812	0.3608	0.00068	3.17
CHL_A	FarmCPU	wsnp_Ex_c41048_47969948	1D	216962	0.4468	0.00027	3.58
CHL_A	GLM	wsnp_Ex_c41048_47969948	1D	216962	0.4362	0.00044	3.35
CHL_30DAA	GLM	wsnp_Ex_c41048_47969948	1D	216962	0.3608	0.00068	3.17

NDVI_H	MLM	RAC875_c2070_566	1D	417149	-0.0231	0.00059	3.23
NDVI_A	MLM	RAC875_c2070_566	1D	417149	-0.028	0.00068	3.17
RDN	MLM	RAC875_c2070_566	1D	417149	0.0172	0.00045	3.35
NDVI_H	FarmCPU	RAC875_c2070_566	1D	417149	-0.0246	4.37E-05	4.36
NDVI_H	GLM	RAC875_c2070_566	1D	417149	-0.0212	0.0007	3.15
NDVI_A	FarmCPU	RAC875_c2070_566	1D	417149	-0.0311	3.00E-05	4.52
NDVI_A	GLM	RAC875_c2070_566	1D	417149	-0.0294	0.0001	3.98
RDN	FarmCPU	RAC875_c2070_566	1D	417149	0.0176	7.08E-05	4.15
RDN	FarmCPU	RAC875_c2070_893	1D	417476	0.0169	0.00029	3.53
RDN	FarmCPU	wsnp_Ex_c278_538285	1D	417712	0.0169	0.00029	3.53
PI_21DAA	MLM	BS00065168_51	1D	2486045	0.0603	0.00051	3.29
PI_21DAA	FarmCPU	BS00065168_51	1D	2486045	0.0603	0.00019	3.72
PI_21DAA	GLM	BS00065168_51	1D	2486045	0.0591	0.00032	3.49
CN	FarmCPU	RAC875_c63624_1040	1D	8714487	-0.0257	0.001	3
CHL_A	GLM	D_contig50935_198	1D	11457893	0.2997	0.00028	3.55
CN	GLM	D_contig50935_198	1D	11457893	0.0154	0.00038	3.42
CN	GLM	Excalibur_c55959_710	1D	12313575	-0.022	0.00047	3.33
CSFL	GLM	D_contig17787_645	1D	18679079	3.5558	0.00088	3.05
NDVI_A	FarmCPU	IAAV4500	1D	153777053	-0.0414	0.0007	3.16
NDVI_A	FarmCPU	wsnp_Ex_c3372_6195001	1D	203318230	-0.0414	0.0007	3.16
NDVI_A	FarmCPU	BobWhite_c28341_51	1D	204295610	-0.0441	0.00065	3.18
NDVI_A	FarmCPU	Excalibur_c54508_64	1D	378867321	-0.1717	0.00023	3.63
CHL_20DAA	FarmCPU	Excalibur_c56999_109	1D	459837951	4.2872	0.00051	3.29
CHL_20DAA	GLM	Excalibur_c56999_109	1D	459837951	4.4112	0.00032	3.5
CSFL	MLM	Excalibur_c56999_109	1D	459837951	8.839	0.00011	3.96
CSFL	FarmCPU	Excalibur_c56999_109	1D	459837951	8.706	2.02E-05	4.7
CSFL	GLM	Excalibur_c56999_109	1D	459837951	8.8726	1.40E-05	4.85
CHL_10DAA	FarmCPU	Excalibur_c46797_317	1D	460143564	1.648	0.00055	3.26
CHL_10DAA	GLM	Excalibur_c46797_317	1D	460143564	1.6077	0.00064	3.2
CSFL	MLM	Excalibur_c46797_317	1D	460143564	10.662	0.00069	3.16
CSFL	FarmCPU	Excalibur_c46797_317	1D	460143564	10.708	0.00028	3.56
CSFL	GLM	Excalibur_c46797_317	1D	460143564	10.565	0.00035	3.46
PH	GLM	Ra_c7324_1464	1D	462488065	-1.7318	0.00097	3.01
TN	FarmCPU	BS00048108_51	2A	17040555	-0.9882	0.00097	3.01
NDVI_H	GLM	JG_c936_115	2A	71421116	0.0202	0.0005	3.3
RDN	FarmCPU	wsnp_Ex_c2887_5330426	2A	71623182	-0.0158	0.00057	3.24
RDN	MLM	Kukri_rep_c73477_888	2A	71623332	-0.0166	0.00081	3.09
NDVI_H	FarmCPU	Kukri_rep_c73477_888	2A	71623332	0.0214	0.00049	3.31
RDN	FarmCPU	Kukri_rep_c73477_888	2A	71623332	-0.017	0.00015	3.83
RDN	GLM	Kukri_rep_c73477_888	2A	71623332	-0.0152	0.00054	3.26
RDN	FarmCPU	Kukri_rep_c83485_398	2A	74136401	-0.0162	0.00059	3.23
CSFL	GLM	RAC875_c13116_1162	2A	74960438	4.3331	0.00044	3.35
RDN	FarmCPU	BS00062843_51	2A	77335035	-0.0167	0.00027	3.57

NDVI_H	GLM	IACX6028	2A	83829207	0.0204	0.00041	3.39
NDVI_H	GLM	IAAV2376	2A	83928687	0.0212	0.00026	3.58
NDVI_H	GLM	Excalibur_c50934_159	2A	85289048	0.0203	0.00041	3.38
PI_H	FarmCPU	IAAV3789	2A	87881112	0.0878	0.00088	3.06
FV/FM_H	FarmCPU	IAAV3789	2A	87881112	0.0094	0.00084	3.08
FV/FM_H	MLM	BS00065418_51	2A	90576790	0.0154	0.00053	3.28
PI_H	FarmCPU	BS00065418_51	2A	90576790	0.1341	0.00059	3.23
PI_H	GLM	BS00065418_51	2A	90576790	0.1343	0.00072	3.14
FV/FM_H	FarmCPU	BS00065418_51	2A	90576790	0.0154	0.0002	3.7
FV/FM_H	GLM	BS00065418_51	2A	90576790	0.0155	0.00023	3.64
ADN	FarmCPU	BS00065418_51	2A	90576790	0.0145	0.00059	3.23
ADN	GLM	BS00065418_51	2A	90576790	0.0146	0.0007	3.15
CHL_30DAA	FarmCPU	BS00008805_51	2A	111457271	0.7776	0.00022	3.66
CHL_30DAA	GLM	BS00008805_51	2A	111457271	0.7787	0.00028	3.56
CHL_30DAA	MLM	BS00008805_51	2A	111457271	0.78	0.00064	3.19
PI_21DAA	MLM	BS00008805_51	2A	111457271	0.0633	0.00023	3.64
PI_21DAA	FarmCPU	BS00008805_51	2A	111457271	0.0633	6.31E-05	4.2
PI_21DAA	GLM	BS00008805_51	2A	111457271	0.0652	5.05E-05	4.3
CSFL	MLM	GENE-1181_231	2A	151263891	4.5074	0.00075	3.13
CSFL	FarmCPU	GENE-1181_231	2A	151263891	4.3572	0.00042	3.38
CSFL	GLM	GENE-1181_231	2A	151263891	4.5172	0.0003	3.52
PI_A	GLM	GENE-1181_231	2A	151263891	0.0748	0.00072	3.14
PH	FarmCPU	BS00065413_51	2A	209936056	-2.242	0.00037	3.43
TN	FarmCPU	CAP8_c533_120	2A	423206400	0.3908	0.00041	3.38
PH	FarmCPU	CAP8_c607_659	2A	504710995	4.4009	0.00018	3.74
TN	FarmCPU	RAC875_rep_c72609_652	2A	515956944	0.3908	0.00041	3.38
TN	FarmCPU	BS00061867_51	2A	517399143	0.3908	0.00041	3.38
CHL_30DAA	FarmCPU	RAC875_c6156_428	2A	549678785	0.7776	0.00022	3.66
CHL_30DAA	GLM	RAC875_c6156_428	2A	549678785	0.7787	0.00028	3.56
CHL_30DAA	MLM	RAC875_c6156_428	2A	549678785	0.78	0.00064	3.19
PI_21DAA	MLM	RAC875_c6156_428	2A	549678785	0.0633	0.00023	3.64
PI_21DAA	FarmCPU	RAC875_c6156_428	2A	549678785	0.0633	6.31E-05	4.2
PI_21DAA	GLM	RAC875_c6156_428	2A	549678785	0.0652	5.05E-05	4.3
FV/FM_14DAA	MLM	BS00085765_51	2A	558529515	-0.0152	0.0008	3.1
PI_14DAA	FarmCPU	BS00085765_51	2A	558529515	-0.1482	0.00037	3.43
PI_14DAA	GLM	BS00085765_51	2A	558529515	-0.1416	0.00077	3.12
FV/FM_14DAA	FarmCPU	BS00085765_51	2A	558529515	-0.0152	0.00028	3.55
FV/FM_14DAA	GLM	BS00085765_51	2A	558529515	-0.0146	0.00055	3.26
NDVI_A	FarmCPU	BS00085765_51	2A	558529515	-0.0324	0.00061	3.21
NDVI_A	MLM	tplb0052b22_504	2A	607841361	-0.0837	0.00059	3.23
NDVI_A	FarmCPU	tplb0052b22_504	2A	607841361	-0.073	0.00091	3.04
NDVI_A	FarmCPU	Excalibur_c34964_326	2A	677486375	0.0581	0.0003	3.53
NDVI_14DAA	FarmCPU	RAC875_c81899_216	2A	714207590	0.0595	0.00071	3.15

NDVI_14DAA	FarmCPU	BobWhite_rep_c64440_83	2A	714331732	0.0595	0.00071	3.15
SPS	GLM	wsnp_Ex_c5856_10276064	2A	714339001	0.9677	0.00087	3.06
TN	GLM	BS00110386_51	2A	718838996	0.2728	0.0003	3.52
PH	MLM	Tdurum_contig12761_125	2A	727243449	-2.2131	0.00098	3.01
PH	FarmCPU	Tdurum_contig12761_125	2A	727243449	-2.429	9.28E-05	4.03
PH	GLM	Tdurum_contig12761_125	2A	727243449	-2.4798	3.24E-05	4.49
CHL_30DAA	GLM	BobWhite_c12767_148	2A	734346331	-0.3035	0.00021	3.69
TKW	MLM	wsnp_JD_c2578_3489735	2A	735564461	-0.4992	0.00062	3.21
TKW	FarmCPU	wsnp_JD_c2578_3489735	2A	735564461	-0.4992	0.00025	3.6
TKW	GLM	wsnp_JD_c2578_3489735	2A	735564461	-0.5069	0.00027	3.57
NDVI_H	FarmCPU	Tdurum_contig60205_644	2A	739712795	-0.0216	8.34E-05	4.08
NDVI_A	FarmCPU	Tdurum_contig60205_644	2A	739712795	-0.0248	0.0003	3.53
RDN	FarmCPU	Tdurum_contig60205_644	2A	739712795	0.0146	0.00032	3.49
CHL_30DAA	FarmCPU	BS00071350_51	2A	757918495	0.2342	0.00093	3.03
FV/FM_21DAA	FarmCPU	BS00071350_51	2A	757918495	0.0017	0.00067	3.17
PI_14DAA	FarmCPU	Kukri_c1947_70	2A	763046823	0.1742	0.00072	3.14
ADSFL	FarmCPU	BS00060594_51	2A	766393921	0.3937	0.00065	3.19
ADSFL	GLM	BS00060594_51	2A	766393921	0.4089	0.00034	3.47
RDSFL	FarmCPU	BS00060594_51	2A	766393921	0.007	0.00062	3.21
RDSFL	GLM	BS00060594_51	2A	766393921	0.0072	0.00041	3.39
NDVI_A	GLM	Excalibur_c40335_198	2A	779881502	-0.0564	8.19E-05	4.09
CHL_30DAA	FarmCPU	Excalibur_c34937_710	2B	4988254	0.7776	0.00022	3.66
CHL_30DAA	GLM	Excalibur_c34937_710	2B	4988254	0.7787	0.00028	3.56
CHL_30DAA	MLM	Excalibur_c34937_710	2B	4988254	0.78	0.00064	3.19
PI_21DAA	MLM	Excalibur_c34937_710	2B	4988254	0.0633	0.00023	3.64
PI_21DAA	FarmCPU	Excalibur_c34937_710	2B	4988254	0.0633	6.31E-05	4.2
PI_21DAA	GLM	Excalibur_c34937_710	2B	4988254	0.0652	5.05E-05	4.3
NDVI_14DAA	FarmCPU	Kukri_rep_c108293_98	2B	7443056	-0.0288	0.00057	3.25
NDVI_A	FarmCPU	BS00083768_51	2B	7443104	-0.0314	0.00041	3.39
NDVI_14DAA	FarmCPU	BS00083768_51	2B	7443104	-0.0285	0.00094	3.03
RDN	FarmCPU	BS00083768_51	2B	7443104	0.018	0.00063	3.2
CSFL	FarmCPU	Kukri_c63748_1453	2B	25021466	6.9782	0.00074	3.13
CSFL	GLM	Kukri_c63748_1453	2B	25021466	7.3837	0.00038	3.42
CN	GLM	Kukri_c63748_1453	2B	25021466	0.0432	0.00095	3.02
SPS	FarmCPU	RAC875_c6358_1091	2B	47839760	1.0196	0.00062	3.21
SPS	GLM	RAC875_c6358_1091	2B	47839760	1.0517	0.0004	3.4
CHL_10DAA	GLM	Excalibur_c36070_300	2B	65466219	0.4572	0.00053	3.27
PI_A	FarmCPU	Excalibur_c36070_300	2B	65466219	0.0465	0.00092	3.03
NDVI_21DAA	GLM	Ku_c68678_924	2B	91837000	0.0473	0.00065	3.18
NDVI_21DAA	GLM	IAAV1101	2B	91837150	0.0489	0.00023	3.65
NDVI_21DAA	GLM	RFL_Contig996_818	2B	93688548	0.0729	0.00012	3.92
NDVI_21DAA	FarmCPU	Tdurum_contig45350_605	2B	94190817	0.0446	0.00093	3.03
NDVI_21DAA	GLM	Tdurum_contig45350_605	2B	94190817	0.0515	9.63E-05	4.02

NDVI_21DAA	GLM	Tdurum_contig60978_352	2B	94192833	0.0475	0.00034	3.47
NDVI_21DAA	MLM	BS00023221_51	2B	94199616	0.0477	0.00092	3.04
NDVI_21DAA	FarmCPU	BS00023221_51	2B	94199616	0.0447	0.00054	3.27
NDVI_21DAA	GLM	BS00023221_51	2B	94199616	0.0528	3.01E-05	4.52
CSFL	MLM	Excalibur_c4303_184	2B	101236701	5.7421	0.00023	3.63
CSFL	FarmCPU	Excalibur_c4303_184	2B	101236701	5.6997	5.49E-05	4.26
CSFL	GLM	Excalibur_c4303_184	2B	101236701	5.733	5.66E-05	4.25
NDVI_21DAA	GLM	Tdurum_contig81917_141	2B	105912910	0.0533	0.0009	3.05
NDVI_21DAA	GLM	Kukri_c4790_154	2B	105913070	0.0533	0.0009	3.05
NDVI_H	MLM	Ku_c57425_413	2B	108905283	0.024	0.00042	3.38
RDN	MLM	Ku_c57425_413	2B	108905283	-0.0188	0.00015	3.82
NDVI_H	FarmCPU	Ku_c57425_413	2B	108905283	0.0246	4.45E-05	4.35
NDVI_H	GLM	Ku_c57425_413	2B	108905283	0.0226	0.00015	3.84
RDN	FarmCPU	Ku_c57425_413	2B	108905283	-0.0189	1.54E-05	4.81
RDN	GLM	Ku_c57425_413	2B	108905283	-0.0176	4.57E-05	4.34
CN	GLM	wsnp_Ku_c4042_7375890	2B	118285404	0.0226	0.00097	3.01
SPS	GLM	wsnp_Ex_c7738_13195349	2B	129662454	0.3442	0.00088	3.06
SPS	GLM	Kukri_c4632_115	2B	129662604	0.3442	0.00088	3.06
NDVI_21DAA	GLM	BS00083078_51	2B	131130420	0.0502	0.00084	3.08
PI_21DAA	GLM	BS00022657_51	2B	132340683	0.0187	0.00081	3.09
PI_H	MLM	Ra_c6728_590	2B	134090399	0.1179	0.00037	3.43
FV/FM_H	MLM	Ra_c6728_590	2B	134090399	0.0132	0.00014	3.85
ADN	MLM	Ra_c6728_590	2B	134090399	0.0122	0.00066	3.18
PI_H	FarmCPU	Ra_c6728_590	2B	134090399	0.1172	9.34E-05	4.03
PI_H	GLM	Ra_c6728_590	2B	134090399	0.117	0.00013	3.89
FV/FM_H	FarmCPU	Ra_c6728_590	2B	134090399	0.0132	3.29E-05	4.48
FV/FM_H	GLM	Ra_c6728_590	2B	134090399	0.0132	4.20E-05	4.38
ADN	FarmCPU	Ra_c6728_590	2B	134090399	0.0122	0.0002	3.7
ADN	GLM	Ra_c6728_590	2B	134090399	0.0121	0.00028	3.56
FV/FM_H	MLM	wsnp_Ku_c28266_38201643	2B	139814904	0.0136	0.0004	3.4
PI_H	FarmCPU	wsnp_Ku_c28266_38201643	2B	139814904	0.1171	0.00052	3.28
PI_H	GLM	wsnp_Ku_c28266_38201643	2B	139814904	0.1167	0.00068	3.17
FV/FM_H	FarmCPU	wsnp_Ku_c28266_38201643	2B	139814904	0.0136	0.00014	3.87
FV/FM_H	GLM	wsnp_Ku_c28266_38201643	2B	139814904	0.0137	0.00017	3.78
PI_H	FarmCPU	Kukri_c53318_204	2B	140772627	0.0878	0.00088	3.06
FV/FM_H	FarmCPU	Kukri_c53318_204	2B	140772627	0.0094	0.00084	3.08
PI_H	FarmCPU	BS00099097_51	2B	140775210	0.0878	0.00088	3.06
FV/FM_H	FarmCPU	BS00099097_51	2B	140775210	0.0094	0.00084	3.08
PI_H	FarmCPU	Kukri_c67546_342	2B	140777133	0.0878	0.00088	3.06
FV/FM_H	FarmCPU	Kukri_c67546_342	2B	140777133	0.0094	0.00084	3.08
PI_H	FarmCPU	Kukri_c39968_221	2B	140845943	0.0878	0.00088	3.06
FV/FM_H	FarmCPU	Kukri_c39968_221	2B	140845943	0.0094	0.00084	3.08
PI_H	FarmCPU	RFL_Contig1385_326	2B	141559346	0.0878	0.00088	3.06

FV/FM_H	FarmCPU	RFL_Contig1385_326	2B	141559346	0.0094	0.00084	3.08
PI_H	FarmCPU	RFL_Contig1385_1575	2B	141564669	0.0878	0.00088	3.06
FV/FM_H	FarmCPU	RFL_Contig1385_1575	2B	141564669	0.0094	0.00084	3.08
FV/FM_H	FarmCPU	Tdurum_contig18197_86	2B	152712590	0.008	0.00075	3.12
FV/FM_H	GLM	Tdurum_contig18197_86	2B	152712590	0.008	0.00089	3.05
CHL_10DAA	FarmCPU	RAC875_c43790_242	2B	154909766	0.6528	0.00036	3.44
CHL_10DAA	GLM	RAC875_c43790_242	2B	154909766	0.702	0.00012	3.92
CHL_10DAA	MLM	RAC875_c43790_242	2B	154909766	0.705	0.00062	3.21
CSFL	MLM	RAC875_c43790_242	2B	154909766	4.475	0.00032	3.5
CSFL	FarmCPU	RAC875_c43790_242	2B	154909766	4.273	0.00015	3.81
CSFL	GLM	RAC875_c43790_242	2B	154909766	4.5	8.74E-05	4.06
CSFL	MLM	GENE-1147_486	2B	157640041	4.5074	0.00075	3.13
CSFL	FarmCPU	GENE-1147_486	2B	157640041	4.3572	0.00042	3.38
CSFL	GLM	GENE-1147_486	2B	157640041	4.5172	0.0003	3.52
PI_A	GLM	GENE-1147_486	2B	157640041	0.0748	0.00072	3.14
CSFL	FarmCPU	GENE-1147_394	2B	157640129	4.3572	0.00042	3.38
CSFL	GLM	GENE-1147_394	2B	157640129	4.5172	0.0003	3.52
CSFL	MLM	GENE-1147_394	2B	157640129	4.5074	0.00075	3.13
PI_A	GLM	GENE-1147_394	2B	157640129	0.0748	0.00072	3.14
CHL_B	FarmCPU	Excalibur_c5079_170	2B	157640887	0.9854	0.00049	3.31
CHL_B	GLM	Excalibur_c5079_170	2B	157640887	1.0325	0.00035	3.46
CHL_10DAA	GLM	Excalibur_c5079_170	2B	157640887	0.6252	0.00077	3.11
CSFL	MLM	Excalibur_c5079_170	2B	157640887	4.2898	0.00057	3.25
CSFL	FarmCPU	Excalibur_c5079_170	2B	157640887	4.1434	0.0003	3.52
CSFL	GLM	Excalibur_c5079_170	2B	157640887	4.2435	0.00027	3.58
PI_A	FarmCPU	Excalibur_c5079_170	2B	157640887	0.0681	0.00073	3.14
PI_A	GLM	Excalibur_c5079_170	2B	157640887	0.0727	0.0004	3.4
FV/FM_A	GLM	Excalibur_c5079_170	2B	157640887	0.0069	0.00073	3.14
CHL_B	FarmCPU	Ra_c4397_542	2B	157694697	1.0201	0.00065	3.18
CHL_B	GLM	Ra_c4397_542	2B	157694697	1.0706	0.00047	3.33
CSFL	MLM	Ra_c4397_542	2B	157694697	4.5963	0.0005	3.3
CSFL	FarmCPU	Ra_c4397_542	2B	157694697	4.4282	0.00026	3.59
CSFL	GLM	Ra_c4397_542	2B	157694697	4.5653	0.0002	3.69
PI_A	FarmCPU	Ra_c4397_542	2B	157694697	0.0722	0.00071	3.15
PI_A	GLM	Ra_c4397_542	2B	157694697	0.077	0.00039	3.4
FV/FM_A	GLM	Ra_c4397_542	2B	157694697	0.0073	0.00076	3.12
PH	FarmCPU	Excalibur_c9248_771	2B	158618802	3.7747	0.00043	3.36
CHL_B	FarmCPU	Excalibur_c23723_141	2B	161409209	1.1169	0.0008	3.09
CHL_B	GLM	Excalibur_c23723_141	2B	161409209	1.1714	0.00058	3.24
CHL_10DAA	FarmCPU	Excalibur_c23723_141	2B	161409209	0.7938	0.00026	3.58
CHL_10DAA	GLM	Excalibur_c23723_141	2B	161409209	0.8583	6.82E-05	4.17
CHL_10DAA	MLM	Excalibur_c23723_141	2B	161409209	0.8692	0.00034	3.47
CSFL	GLM	Excalibur_c23723_141	2B	161409209	4.6461	0.00073	3.14

GY	FarmCPU	Excalibur_c23723_141	2B	161409209	10.745	0.00091	3.04
GY	GLM	Excalibur_c23723_141	2B	161409209	11.464	0.00039	3.41
CHL_B	FarmCPU	RAC875_c7827_218	2B	161468654	1.1169	0.0008	3.09
CHL_B	GLM	RAC875_c7827_218	2B	161468654	1.1714	0.00058	3.24
CHL_10DAA	FarmCPU	RAC875_c7827_218	2B	161468654	0.7938	0.00026	3.58
CHL_10DAA	GLM	RAC875_c7827_218	2B	161468654	0.8583	6.82E-05	4.17
CHL_10DAA	MLM	RAC875_c7827_218	2B	161468654	0.8692	0.00034	3.47
CSFL	GLM	RAC875_c7827_218	2B	161468654	4.6461	0.00073	3.14
GY	FarmCPU	RAC875_c7827_218	2B	161468654	10.745	0.00091	3.04
GY	GLM	RAC875_c7827_218	2B	161468654	11.464	0.00039	3.41
FV/FM_H	FarmCPU	BS00070091_51	2B	163714291	0.0088	0.00074	3.13
FV/FM_H	GLM	BS00070091_51	2B	163714291	0.0088	0.00089	3.05
CHL_10DAA	GLM	BS00035894_51	2B	164107384	0.9118	0.00079	3.1
CSFL	FarmCPU	BS00035894_51	2B	164107384	6.0263	0.00038	3.42
CSFL	GLM	BS00035894_51	2B	164107384	6.1976	0.00027	3.58
CSFL	MLM	BS00035894_51	2B	164107384	6.1298	0.00079	3.1
CN	FarmCPU	tplb0024p13_611	2B	164938789	0.0165	0.00041	3.39
CN	GLM	tplb0024p13_611	2B	164938789	0.0165	0.00058	3.24
CN	FarmCPU	wsnp_Ku_c15336_23908130	2B	164938939	0.0165	0.00041	3.39
CN	GLM	wsnp_Ku_c15336_23908130	2B	164938939	0.0165	0.00058	3.24
CHL_T	GLM	BobWhite_c647_668	2B	184331490	-0.6088	0.00052	3.28
NDVI_A	GLM	BS00034315_51	2B	189603633	0.0277	0.00067	3.17
CSFL	GLM	RAC875_c5080_915	2B	206113266	3.391	0.00097	3.01
BY	GLM	IAAV3528	2B	212579562	-18.052	0.0009	3.05
BY	FarmCPU	Ra_c2527_1124	2B	314764061	15.821	0.00087	3.06
BY	GLM	Ra_c2527_1124	2B	314764061	15.554	0.00099	3
PH	FarmCPU	CAP8_c621_57	2B	403693312	-2.2869	0.00075	3.13
PH	FarmCPU	wsnp_Ex_c52458_56049703	2B	403698856	-2.2869	0.00075	3.13
PH	FarmCPU	wsnp_Ex_c6295_10967631	2B	404414062	-2.2869	0.00075	3.13
PH	FarmCPU	wsnp_Ex_c43212_49594902	2B	406091057	-2.2499	0.00069	3.16
PH	FarmCPU	RAC875_c20950_461	2B	406110798	-2.2499	0.00069	3.16
PH	FarmCPU	wsnp_Ex_rep_c69340_68274022	2B	423836995	-2.3116	0.00039	3.41
PH	GLM	wsnp_Ex_rep_c69340_68274022	2B	423836995	-2.2403	0.00091	3.04
PH	FarmCPU	Tdurum_contig42226_2355	2B	429140546	-2.5448	0.00074	3.13
PH	FarmCPU	wsnp_Ex_c19819_28827344	2B	429145584	-2.2869	0.00075	3.13
PH	FarmCPU	Kukri_rep_c107732_99	2B	429487778	-2.2499	0.00069	3.16
TN	FarmCPU	Ra_c6266_140	2B	440214959	0.4941	0.00097	3.01
TN	FarmCPU	Ra_c6266_136	2B	440214963	0.4941	0.00097	3.01
NDVI_H	FarmCPU	Excalibur_c11409_1166	2B	454741011	-0.0291	0.00089	3.05
RDN	FarmCPU	Excalibur_c11409_1166	2B	454741011	0.0225	0.00043	3.36
TN	FarmCPU	RAC875_c65251_683	2B	458622284	0.4941	0.00097	3.01
PH	FarmCPU	wsnp_Ex_rep_c105129_89641882	2B	523085296	-1.9288	0.00084	3.08
NDVI_14DAA	GLM	wsnp_JD_c47318_32176833	2B	632920983	0.0358	0.00083	3.08

NDVI_A	FarmCPU	wsnp_Ex_c10796_17575074	2B	660461088	0.0232	0.00098	3.01
NDVI_21DAA	GLM	BobWhite_c22106_204	2B	665189342	0.0472	0.00083	3.08
NDVI_21DAA	GLM	Tdurum_contig59522_420	2B	665189442	0.0473	0.00043	3.37
CHL_30DAA	FarmCPU	RAC875_c28108_400	2B	681540402	0.3233	0.00043	3.37
CHL_30DAA	GLM	RAC875_c28108_400	2B	681540402	0.3265	0.0004	3.4
CHL_30DAA	MLM	RAC875_c28108_400	2B	681540402	0.3259	0.00093	3.03
PI_21DAA	MLM	RAC875_c28108_400	2B	681540402	0.0261	0.00045	3.34
PI_21DAA	FarmCPU	RAC875_c28108_400	2B	681540402	0.0261	0.00016	3.79
PI_21DAA	GLM	RAC875_c28108_400	2B	681540402	0.026	0.00019	3.73
TN	FarmCPU	Tdurum_contig55699_246	2B	683028910	-0.1762	0.00042	3.38
NDVI_A	FarmCPU	Excalibur_c7449_587	2B	694051030	0.0244	0.00056	3.25
NDVI_21DAA	FarmCPU	Excalibur_c7449_587	2B	694051030	0.0315	0.00085	3.07
RDN	FarmCPU	Ku_c9369_1965	2B	695374866	0.0171	0.00061	3.21
TN	FarmCPU	wsnp_Ex_rep_c110284_92725051	2B	696357428	0.4941	0.00097	3.01
NDVI_21DAA	FarmCPU	BS00092869_51	2B	696677237	0.0388	5.06E-05	4.3
NDVI_21DAA	GLM	BS00092869_51	2B	696677237	0.0354	0.00043	3.36
TN	FarmCPU	BS00092869_51	2B	696677237	0.1631	0.00037	3.44
NDVI_21DAA	FarmCPU	wsnp_Ex_c5123_9088111	2B	696677468	0.0361	0.00075	3.13
PH	FarmCPU	CAP11_c1716_97	2B	697435638	-4.4033	0.00024	3.62
NDVI_21DAA	MLM	BS00046164_51	2B	697510323	0.0431	0.00011	3.94
SPS	MLM	BS00046164_51	2B	697510323	0.3784	0.00039	3.4
NDVI_21DAA	FarmCPU	BS00046164_51	2B	697510323	0.0439	3.57E-06	5.45
NDVI_21DAA	GLM	BS00046164_51	2B	697510323	0.0418	7.19E-06	5.14
SPS	FarmCPU	BS00046164_51	2B	697510323	0.3781	0.0001	3.99
SPS	GLM	BS00046164_51	2B	697510323	0.3704	0.00015	3.82
NDVI_21DAA	MLM	BS00046165_51	2B	697510334	0.0419	0.00018	3.74
SPS	MLM	BS00046165_51	2B	697510334	0.3695	0.0006	3.22
NDVI_21DAA	FarmCPU	BS00046165_51	2B	697510334	0.043	8.15E-06	5.09
NDVI_21DAA	GLM	BS00046165_51	2B	697510334	0.0404	2.22E-05	4.65
SPS	FarmCPU	BS00046165_51	2B	697510334	0.3694	0.00019	3.72
SPS	GLM	BS00046165_51	2B	697510334	0.3613	0.00029	3.54
NDVI_21DAA	MLM	Excalibur_c36280_764	2B	697512054	0.0392	0.00042	3.37
NDVI_21DAA	FarmCPU	Excalibur_c36280_764	2B	697512054	0.0413	2.20E-05	4.66
NDVI_21DAA	GLM	Excalibur_c36280_764	2B	697512054	0.0386	6.12E-05	4.21
SPS	FarmCPU	Excalibur_c36280_764	2B	697512054	0.3442	0.00057	3.25
SPS	GLM	Excalibur_c36280_764	2B	697512054	0.3421	0.00066	3.18
NDVI_21DAA	FarmCPU	BS00021713_51	2B	698208660	0.0348	0.00053	3.27
NDVI_21DAA	FarmCPU	wsnp_Ex_c11748_18884081	2B	698213070	0.0363	0.0002	3.69
NDVI_21DAA	GLM	wsnp_Ex_c11748_18884081	2B	698213070	0.0333	0.00062	3.21
NDVI_21DAA	FarmCPU	RAC875_c103094_120	2B	698303784	0.0324	0.00078	3.11
NDVI_21DAA	FarmCPU	BobWhite_c2521_117	2B	699106259	-0.0615	0.00055	3.26
NDVI_21DAA	GLM	BobWhite_c2521_117	2B	699106259	-0.0594	0.00063	3.2
NDVI_21DAA	FarmCPU	RAC875_c4465_549	2B	699108786	0.0368	0.00014	3.84

NDVI_21DAA	GLM	RAC875_c4465_549	2B	699108786	0.0343	0.00034	3.46
SPS	FarmCPU	RAC875_c4465_549	2B	699108786	0.3381	0.00059	3.23
NDVI_21DAA	FarmCPU	IAAV3067	2B	699173366	-0.0615	0.00055	3.26
NDVI_21DAA	GLM	IAAV3067	2B	699173366	-0.0594	0.00063	3.2
NDVI_21DAA	FarmCPU	Excalibur_rep_c66400_52	2B	700207431	-0.0724	0.00028	3.55
NDVI_21DAA	GLM	Excalibur_rep_c66400_52	2B	700207431	-0.0665	0.0008	3.1
NDVI_21DAA	MLM	wsnp_Ex_c22271_31463467	2B	700456564	0.0394	0.00053	3.27
NDVI_21DAA	FarmCPU	wsnp_Ex_c22271_31463467	2B	700456564	0.0413	2.87E-05	4.54
NDVI_21DAA	GLM	wsnp_Ex_c22271_31463467	2B	700456564	0.0382	0.0001	3.98
NDVI_21DAA	MLM	BobWhite_c2244_259	2B	700456873	0.037	0.00085	3.07
NDVI_21DAA	FarmCPU	BobWhite_c2244_259	2B	700456873	0.0398	4.13E-05	4.38
NDVI_21DAA	GLM	BobWhite_c2244_259	2B	700456873	0.037	0.00012	3.94
NDVI_21DAA	MLM	wsnp_Ex_c22271_31463382	2B	700457023	0.037	0.00085	3.07
NDVI_21DAA	FarmCPU	wsnp_Ex_c22271_31463382	2B	700457023	0.0398	4.13E-05	4.38
NDVI_21DAA	GLM	wsnp_Ex_c22271_31463382	2B	700457023	0.037	0.00012	3.94
NDVI_21DAA	FarmCPU	wsnp_Ex_c1915_3618286	2B	701097163	0.0362	0.00014	3.85
NDVI_21DAA	GLM	wsnp_Ex_c1915_3618286	2B	701097163	0.0335	0.00036	3.44
NDVI_21DAA	FarmCPU	Ku_c12447_2002	2B	703976209	0.0381	0.00027	3.57
PH	MLM	wsnp_Ex_c26818_36041748	2B	710281768	-3.7073	0.00013	3.89
PH	FarmCPU	wsnp_Ex_c26818_36041748	2B	710281768	-3.5258	2.51E-05	4.6
PH	GLM	wsnp_Ex_c26818_36041748	2B	710281768	-3.3407	0.00016	3.8
PH	FarmCPU	Excalibur_rep_c78626_295	2B	711718168	-2.8686	0.00074	3.13
NDVI_A	FarmCPU	Excalibur_c3506_610	2B	715926581	-0.0404	0.00033	3.48
NDVI_H	FarmCPU	BobWhite_c3428_233	2B	728755455	-0.0184	0.00085	3.07
PH	MLM	Kukri_c30973_414	2B	728755700	-4.9177	0.00077	3.11
PH	FarmCPU	Kukri_c30973_414	2B	728755700	-5.027	0.00016	3.8
PH	GLM	Kukri_c30973_414	2B	728755700	-4.5285	0.00051	3.29
CHL_30DAA	GLM	Excalibur_c10133_292	2B	728757405	-0.3074	0.00041	3.38
FV/FM_21DAA	FarmCPU	Tdurum_contig28113_579	2B	730189892	0.0032	0.00065	3.19
FV/FM_21DAA	GLM	Tdurum_contig28113_579	2B	730189892	0.0031	0.00092	3.04
CHL_A	FarmCPU	BS00065327_51	2B	731481845	0.3108	0.00013	3.88
CHL_A	GLM	BS00065327_51	2B	731481845	0.3191	9.78E-05	4.01
CHL_A	MLM	BS00065327_51	2B	731481845	0.3354	0.00024	3.63
NDVI_A	FarmCPU	BS00067347_51	2B	731535910	-0.0354	0.00075	3.13
NDVI_21DAA	FarmCPU	BS00067347_51	2B	731535910	-0.0475	0.00069	3.16
CHL_A	FarmCPU	BS00065471_51	2B	731536167	0.3003	0.00081	3.09
NDVI_H	FarmCPU	GENE-1236_418	2B	731605318	-0.0204	0.0002	3.7
NDVI_A	FarmCPU	GENE-1236_418	2B	731605318	-0.0237	0.00052	3.28
RDN	FarmCPU	GENE-1236_418	2B	731605318	0.0146	0.00031	3.51
PH	GLM	BobWhite_c6365_540	2B	731894827	-4.3642	0.00035	3.45
PH	MLM	Ra_c13298_434	2B	732344105	-7.4829	0.00012	3.91
PH	FarmCPU	Ra_c13298_434	2B	732344105	-7.4435	2.95E-05	4.53
PH	GLM	Ra_c13298_434	2B	732344105	-8.2527	1.15E-06	5.94

NDVI_A	FarmCPU	Excalibur_c60164_137	2B	732607436	0.0271	0.00038	3.42
PH	MLM	Ra_c5004_2033	2B	733713735	-3.7415	0.00012	3.91
PH	FarmCPU	Ra_c5004_2033	2B	733713735	-3.7217	2.95E-05	4.53
PH	GLM	Ra_c5004_2033	2B	733713735	-4.1263	1.15E-06	5.94
PH	GLM	Ra_c5004_2032	2B	733713736	-5.0077	0.0002	3.7
PH	MLM	Ra_c5004_1902	2B	733713866	-3.8445	0.00054	3.26
PH	FarmCPU	Ra_c5004_1902	2B	733713866	-3.7187	0.00032	3.5
PH	GLM	Ra_c5004_1902	2B	733713866	-4.1432	2.69E-05	4.57
CHL_30DAA	GLM	BobWhite_c32336_504	2B	736245708	-0.3074	0.00041	3.38
PH	FarmCPU	RAC875_c54391_236	2B	741124185	-1.8131	0.00097	3.01
RDN	FarmCPU	Excalibur_c13046_700	2B	742466712	0.0139	0.00096	3.02
NDVI_14DAA	FarmCPU	RAC875_c66695_560	2B	746037411	-0.0517	0.00027	3.57
NDVI_14DAA	GLM	RAC875_c66695_560	2B	746037411	-0.0472	0.00074	3.13
NDVI_14DAA	FarmCPU	Tdurum_contig9214_279	2B	746101679	0.0274	0.00024	3.63
NDVI_14DAA	GLM	Tdurum_contig9214_279	2B	746101679	0.0248	0.00076	3.12
PH	MLM	Ku_c2936_1987	2B	782154304	6.1554	0.00068	3.17
PH	FarmCPU	Ku_c2936_1987	2B	782154304	6.2551	2.65E-05	4.58
PH	MLM	wsnp_CAP11_c1820_985143	2B	782533975	6.1554	0.00068	3.17
PH	FarmCPU	wsnp_CAP11_c1820_985143	2B	782533975	6.2551	2.65E-05	4.58
PH	MLM	Ku_c16249_315	2B	782534125	6.1554	0.00068	3.17
PH	FarmCPU	Ku_c16249_315	2B	782534125	6.2551	2.65E-05	4.58
TN	FarmCPU	BS00026409_51	2B	787140854	0.4323	0.00062	3.21
NDVI_H	FarmCPU	wsnp_Ex_c29008_38081173	2B	788664700	-0.0192	0.00073	3.13
NDVI_H	FarmCPU	wsnp_Ex_c707_1391630	2B	789131651	-0.0197	0.00073	3.13
TN	GLM	RFL_Contig1115_407	2B	789601671	0.2604	0.00062	3.21
TN	GLM	BS00072839_51	2B	789605589	0.2604	0.00062	3.21
TN	FarmCPU	BobWhite_c18071_171	2B	798310139	0.4941	0.00097	3.01
TN	FarmCPU	RAC875_rep_c107312_358	2D	5763801	0.4941	0.00097	3.01
FV/FM_21DAA	FarmCPU	BS00047901_51	2D	15967348	0.0018	0.00055	3.26
SPS	GLM	Excalibur_c20196_264	2D	29879871	0.8448	0.00059	3.23
CSFL	FarmCPU	BS00067757_51	2D	65536985	4.088	0.00081	3.09
CHL_10DAA	FarmCPU	BS00022143_51	2D	66868522	0.8989	0.00021	3.69
CHL_10DAA	GLM	BS00022143_51	2D	66868522	0.8618	0.00039	3.4
CHL_10DAA	MLM	BS00022143_51	2D	66868522	0.915	0.00053	3.28
CHL_10DAA	FarmCPU	Kukri_c49522_254	2D	67225699	1.648	0.00055	3.26
CHL_10DAA	GLM	Kukri_c49522_254	2D	67225699	1.6077	0.00064	3.2
CSFL	FarmCPU	Kukri_c49522_254	2D	67225699	10.708	0.00028	3.56
CSFL	GLM	Kukri_c49522_254	2D	67225699	10.565	0.00035	3.46
CSFL	MLM	Kukri_c49522_254	2D	67225699	10.662	0.00069	3.16
CSFL	FarmCPU	wsnp_Ku_c1016_2065367	2D	67226340	11.399	5.49E-05	4.26
CSFL	GLM	wsnp_Ku_c1016_2065367	2D	67226340	11.466	5.66E-05	4.25
CSFL	MLM	wsnp_Ku_c1016_2065367	2D	67226340	11.484	0.00023	3.63
CSFL	FarmCPU	Kukri_c1016_2269	2D	67231055	4.088	0.00081	3.09

CHL_10DAA	FarmCPU	GENE-0787_85	2D	67231626	0.7631	0.00047	3.33
CHL_10DAA	GLM	GENE-0787_85	2D	67231626	0.7499	0.00055	3.26
CSFL	FarmCPU	GENE-0787_85	2D	67231626	5.1805	0.00011	3.95
CSFL	GLM	GENE-0787_85	2D	67231626	5.1925	0.00013	3.89
CHL_10DAA	MLM	GENE-0787_85	2D	67231626	0.8232	0.00069	3.16
CSFL	MLM	GENE-0787_85	2D	67231626	5.1907	0.00042	3.38
PI_21DAA	FarmCPU	GENE-0787_85	2D	67231626	0.0347	0.00088	3.06
CHL_10DAA	FarmCPU	BobWhite_c36072_272	2D	67430408	0.673	0.00092	3.04
CSFL	FarmCPU	BobWhite_c36072_272	2D	67430408	4.7534	0.00013	3.87
CSFL	GLM	BobWhite_c36072_272	2D	67430408	4.7285	0.00018	3.74
CSFL	MLM	BobWhite_c36072_272	2D	67430408	4.7525	0.00049	3.31
CHL_10DAA	FarmCPU	BS00081578_51	2D	67552871	0.7646	0.00056	3.25
CSFL	FarmCPU	BS00106937_51	2D	68733875	4.088	0.00081	3.09
CHL_10DAA	FarmCPU	BS00062865_51	2D	69251664	0.8989	0.00021	3.69
CHL_10DAA	GLM	BS00062865_51	2D	69251664	0.8618	0.00039	3.4
CHL_10DAA	MLM	BS00062865_51	2D	69251664	0.915	0.00053	3.28
CHL_10DAA	FarmCPU	BS00062864_51	2D	69251672	0.8989	0.00021	3.69
CHL_10DAA	GLM	BS00062864_51	2D	69251672	0.8618	0.00039	3.4
CHL_10DAA	MLM	BS00062864_51	2D	69251672	0.915	0.00053	3.28
CHL_10DAA	FarmCPU	BS00032252_51	2D	69504659	0.7631	0.00047	3.33
CHL_10DAA	GLM	BS00032252_51	2D	69504659	0.7499	0.00055	3.26
CSFL	FarmCPU	BS00032252_51	2D	69504659	5.1805	0.00011	3.95
CSFL	GLM	BS00032252_51	2D	69504659	5.1925	0.00013	3.89
CHL_10DAA	MLM	BS00032252_51	2D	69504659	0.8232	0.00069	3.16
CSFL	MLM	BS00032252_51	2D	69504659	5.1907	0.00042	3.38
PI_21DAA	FarmCPU	BS00032252_51	2D	69504659	0.0347	0.00088	3.06
CHL_10DAA	FarmCPU	IAAV3173	2D	71208615	0.6868	0.00064	3.19
CSFL	FarmCPU	IAAV3173	2D	71208615	4.7904	0.00011	3.98
CSFL	GLM	IAAV3173	2D	71208615	4.7799	0.00014	3.85
CSFL	MLM	IAAV3173	2D	71208615	4.8263	0.00038	3.43
CHL_10DAA	FarmCPU	Excalibur_c2887_131	2D	73019372	0.7631	0.00047	3.33
CHL_10DAA	GLM	Excalibur_c2887_131	2D	73019372	0.7499	0.00055	3.26
CSFL	FarmCPU	Excalibur_c2887_131	2D	73019372	5.1805	0.00011	3.95
CSFL	GLM	Excalibur_c2887_131	2D	73019372	5.1925	0.00013	3.89
CHL_10DAA	MLM	Excalibur_c2887_131	2D	73019372	0.8232	0.00069	3.16
CSFL	MLM	Excalibur_c2887_131	2D	73019372	5.1907	0.00042	3.38
PI_21DAA	FarmCPU	Excalibur_c2887_131	2D	73019372	0.0347	0.00088	3.06
CHL_10DAA	GLM	Excalibur_c17456_428	2D	75257714	0.7078	0.00095	3.02
CSFL	GLM	Excalibur_c17456_428	2D	75257714	4.8693	0.00028	3.56
CHL_10DAA	GLM	Excalibur_c22877_1990	2D	75396081	0.7078	0.00095	3.02
CSFL	GLM	Excalibur_c22877_1990	2D	75396081	4.8693	0.00028	3.56
CHL_10DAA	GLM	Kukri_c16557_855	2D	76007905	0.6718	0.00073	3.13
CSFL	GLM	BS00076261_51	2D	76580004	4.3171	0.00099	3.01

CHL_10DAA	GLM	RAC875_c26896_339	2D	76899697	0.6853	0.00077	3.11
CSFL	FarmCPU	Kukri_c11935_65	2D	78376919	4.0555	0.00051	3.3
CSFL	GLM	Kukri_c11935_65	2D	78376919	3.9781	0.00079	3.1
TN	FarmCPU	GENE-1353_120	2D	80730266	0.3993	0.00082	3.08
TN	GLM	Excalibur_c7110_90	2D	108922083	0.153	0.00067	3.17
TKW	GLM	Kukri_c15427_119	2D	372814464	-0.5793	0.00065	3.18
TN	FarmCPU	Excalibur_c40976_111	2D	571077855	-0.1617	0.00067	3.18
NDVI_21DAA	FarmCPU	IACX6309	2D	577149344	0.0344	0.00026	3.59
NDVI_21DAA	FarmCPU	BobWhite_c4831_490	2D	580194188	0.0345	0.00037	3.43
NDVI_21DAA	GLM	BobWhite_c4831_490	2D	580194188	0.0319	0.00087	3.06
PH	GLM	BS00036456_51	2D	592788886	-2.1568	0.00064	3.19
NDVI_A	FarmCPU	wsnp_RFL_Contig2659_2346243	2D	595545931	0.0289	0.00028	3.55
PI_A	GLM	tplb0021c10_951	2D	600131741	0.0448	0.00083	3.08
CHL_30DAA	GLM	Excalibur_c63522_172	2D	601184292	-0.3158	0.00078	3.11
RDN	FarmCPU	CAP12_rep_c5547_123	2D	601601804	0.0139	0.00096	3.02
NDVI_H	FarmCPU	Jagger_c914_72	2D	613026999	-0.0184	0.00085	3.07
RDN	FarmCPU	BobWhite_c1275_304	2D	614644389	0.0143	0.0008	3.1
RDN	FarmCPU	D_GDS7LZN02G73QS_245	2D	614751087	0.0144	0.00073	3.13
RDN	FarmCPU	BS00066527_51	2D	615715119	0.0148	0.00063	3.2
PH	FarmCPU	BS00024884_51	2D	617089389	-1.9295	0.00062	3.21
NDVI_H	FarmCPU	GENE-1388_216	2D	618152321	-0.0195	0.00066	3.18
RDN	FarmCPU	GENE-1388_216	2D	618152321	0.016	0.00012	3.94
TN	GLM	RAC875_c66820_684	2D	622919464	0.158	0.00057	3.25
TN	FarmCPU	Excalibur_c25781_232	2D	635951838	0.2777	0.0009	3.04
PH	FarmCPU	RAC875_c23815_716	2D	641963537	-2.0819	0.00051	3.29
PH	GLM	RAC875_c23815_716	2D	641963537	-2.0686	0.0008	3.1
PI_A	FarmCPU	BS00110922_51	3A	12813884	0.0396	0.00092	3.03
PI_A	GLM	BS00110922_51	3A	12813884	0.0417	0.00093	3.03
PI_A	FarmCPU	BS00022279_51	3A	12813972	0.0427	0.00077	3.12
CHL_B	FarmCPU	BS00110921_51	3A	12814092	0.6162	0.00064	3.19
CHL_B	GLM	BS00110921_51	3A	12814092	0.631	0.00077	3.11
PI_A	FarmCPU	BS00110921_51	3A	12814092	0.0464	0.00029	3.54
PI_A	GLM	BS00110921_51	3A	12814092	0.0469	0.00041	3.38
PI_A	MLM	BS00110921_51	3A	12814092	0.0464	0.0007	3.15
FV/FM_A	FarmCPU	BS00110921_51	3A	12814092	0.0044	0.00062	3.21
FV/FM_A	GLM	BS00110921_51	3A	12814092	0.0044	0.00099	3.01
PI_A	FarmCPU	Ku_c17560_162	3A	12980723	0.0427	0.00077	3.12
PI_A	FarmCPU	BS00073062_51	3A	12997772	0.045	0.00063	3.2
PI_A	GLM	BS00073062_51	3A	12997772	0.0458	0.00082	3.09
NDVI_A	FarmCPU	BS00055211_51	3A	12998761	0.0859	0.00023	3.63
PI_14DAA	FarmCPU	RAC875_c82493_67	3A	13497099	0.129	0.00011	3.94
PI_14DAA	GLM	RAC875_c82493_67	3A	13497099	0.1366	9.98E-05	4
PI_14DAA	MLM	RAC875_c82493_67	3A	13497099	0.134	0.00027	3.57

FV/FM_14DAA	MLM	RAC875_c82493_67	3A	13497099	0.0128	0.00047	3.32
FV/FM_14DAA	FarmCPU	RAC875_c82493_67	3A	13497099	0.0123	0.00026	3.59
FV/FM_14DAA	GLM	RAC875_c82493_67	3A	13497099	0.0131	0.00022	3.66
NDVI_A	FarmCPU	BobWhite_c2570_781	3A	13739562	-0.0295	0.00071	3.15
NDVI_A	GLM	BobWhite_c2570_781	3A	13739562	-0.0286	0.00094	3.03
PH	MLM	Excalibur_c63353_216	3A	28723237	-7.8655	0.00081	3.09
PH	FarmCPU	Excalibur_c63353_216	3A	28723237	-7.9339	0.00054	3.27
PH	GLM	Excalibur_c63353_216	3A	28723237	-8.0771	0.00024	3.62
PH	MLM	Excalibur_c11079_749	3A	32201535	-6.7146	0.00021	3.67
PH	FarmCPU	Excalibur_c11079_749	3A	32201535	-6.8484	2.56E-05	4.59
PH	GLM	Excalibur_c11079_749	3A	32201535	-6.683	2.04E-05	4.69
CHL_A	FarmCPU	Ku_c18096_552	3A	45598472	0.2671	0.00046	3.33
CHL_A	GLM	Ku_c18096_552	3A	45598472	0.2843	0.00025	3.6
BY	GLM	Ku_c18096_552	3A	45598472	16.481	0.00022	3.66
SPS	FarmCPU	GENE-4252_246	3A	56670697	-0.4062	0.00087	3.06
NDVI_H	FarmCPU	Kukri_c35661_63	3A	94172710	-0.0294	0.00047	3.33
ADN	FarmCPU	BS00064800_51	3A	102879813	0.0073	0.00069	3.16
ADN	GLM	BS00064800_51	3A	102879813	0.0081	0.00062	3.21
PH	FarmCPU	wsnp_Ra_c16846_25598885	3A	135989086	4.427	0.00075	3.13
PH	FarmCPU	BS00098840_51	3A	140043235	5.7612	6.36E-05	4.2
PH	FarmCPU	Kukri_c51247_322	3A	140043493	4.427	0.00075	3.13
TN	FarmCPU	IAAV5166	3A	477602530	0.3656	0.00078	3.11
CHL_30DAA	FarmCPU	Ra_c14565_1056	3A	486360289	0.2363	0.00056	3.25
CHL_30DAA	GLM	Ra_c14565_1056	3A	486360289	0.2641	0.00045	3.35
ADSFL	FarmCPU	Ra_c14565_1056	3A	486360289	-0.3992	0.00033	3.48
ADSFL	GLM	Ra_c14565_1056	3A	486360289	-0.4394	0.00028	3.56
RDSFL	FarmCPU	Ra_c14565_1056	3A	486360289	-0.0074	0.00018	3.75
RDSFL	GLM	Ra_c14565_1056	3A	486360289	-0.0082	0.00012	3.92
ADSFL	MLM	Ra_c14565_1056	3A	486360289	-0.4049	0.00092	3.04
RDSFL	MLM	Ra_c14565_1056	3A	486360289	-0.0074	0.00048	3.32
ADSFL	FarmCPU	wsnp_BE443995B_Ta_2_2	3A	487437295	-0.4121	0.00055	3.26
RDSFL	FarmCPU	wsnp_BE443995B_Ta_2_2	3A	487437295	-0.0072	0.00062	3.2
CHL_30DAA	FarmCPU	Kukri_rep_c112061_617	3A	487438216	0.2459	0.00061	3.22
ADSFL	FarmCPU	Kukri_rep_c112061_617	3A	487438216	-0.4056	0.00052	3.29
RDSFL	FarmCPU	Kukri_rep_c112061_617	3A	487438216	-0.0074	0.00032	3.5
RDSFL	GLM	Kukri_rep_c112061_617	3A	487438216	-0.0075	0.00072	3.14
RDSFL	MLM	Kukri_rep_c112061_617	3A	487438216	-0.0074	0.00075	3.13
ADSFL	FarmCPU	wsnp_Ex_c28310_37444843	3A	487458132	-0.4664	2.93E-05	4.53
ADSFL	GLM	wsnp_Ex_c28310_37444843	3A	487458132	-0.4747	7.96E-05	4.1
RDSFL	FarmCPU	wsnp_Ex_c28310_37444843	3A	487458132	-0.0081	4.24E-05	4.37
RDSFL	GLM	wsnp_Ex_c28310_37444843	3A	487458132	-0.0085	7.87E-05	4.1
ADSFL	MLM	wsnp_Ex_c28310_37444843	3A	487458132	-0.465	0.00018	3.74
RDSFL	MLM	wsnp_Ex_c28310_37444843	3A	487458132	-0.0081	0.00017	3.77

CN	GLM	BS00071823_51	3A	511755046	0.016	0.00089	3.05
PH	FarmCPU	Ra_c5515_2396	3A	514111849	5.7612	6.36E-05	4.2
TN	FarmCPU	Tdurum_contig5096_193	3A	534536551	0.4941	0.00097	3.01
TN	FarmCPU	Tdurum_contig31087_229	3A	535002765	0.4941	0.00097	3.01
TN	FarmCPU	BS00073009_51	3A	550655397	0.9882	0.00097	3.01
TN	FarmCPU	Tdurum_contig49518_1002	3A	552022535	0.4941	0.00097	3.01
PH	GLM	Ra_c38505_544	3A	558890611	2.4031	0.00055	3.26
TN	FarmCPU	Tdurum_contig70196_106	3A	558891262	0.4941	0.00097	3.01
TN	FarmCPU	Tdurum_contig41906_783	3A	562983631	0.4941	0.00097	3.01
CSFL	FarmCPU	BobWhite_c17879_519	3A	658905330	3.1088	0.00046	3.33
CSFL	GLM	BobWhite_c17879_519	3A	658905330	3.2588	0.00028	3.55
CSFL	GLM	wsnp_Ex_c14202_22144844	3A	659160811	2.9634	0.0009	3.05
NDVI_A	FarmCPU	BobWhite_c38444_238	3A	686162018	0.0859	0.00023	3.63
PH	MLM	RAC875_c4641_773	3A	686766027	6.1554	0.00068	3.17
PH	FarmCPU	RAC875_c4641_773	3A	686766027	6.2551	2.65E-05	4.58
NDVI_14DAA	FarmCPU	wsnp_Ku_c10468_17301216	3A	699858231	-0.0555	0.00029	3.54
NDVI_A	MLM	Ku_c10817_611	3A	708546032	-0.0504	8.31E-05	4.08
NDVI_A	FarmCPU	Ku_c10817_611	3A	708546032	-0.0528	6.50E-06	5.19
NDVI_A	GLM	Ku_c10817_611	3A	708546032	-0.0483	1.89E-05	4.72
SL	MLM	tplb0036i05_182	3A	714951111	0.3953	0.00024	3.62
SL	FarmCPU	tplb0036i05_182	3A	714951111	0.3953	6.87E-05	4.16
SL	GLM	tplb0036i05_182	3A	714951111	0.3906	9.04E-05	4.04
CHL_B	FarmCPU	Ku_c12191_1202	3A	737800235	1.1933	0.00045	3.35
CHL_B	GLM	Ku_c12191_1202	3A	737800235	1.1898	0.00057	3.24
CSFL	FarmCPU	Ku_c12191_1202	3A	737800235	5.0785	0.00023	3.64
CSFL	GLM	Ku_c12191_1202	3A	737800235	5.107	0.00023	3.64
PI_A	FarmCPU	Ku_c12191_1202	3A	737800235	0.0818	0.00075	3.13
CHL_B	MLM	Ku_c12191_1202	3A	737800235	1.1933	0.00098	3.01
CSFL	MLM	Ku_c12191_1202	3A	737800235	5.2337	0.00047	3.33
FV/FM_A	MLM	Ku_c12191_1202	3A	737800235	0.0086	0.00075	3.13
CN	MLM	Ku_c12191_1202	3A	737800235	0.0326	0.00058	3.24
FV/FM_A	FarmCPU	Ku_c12191_1202	3A	737800235	0.0086	0.00032	3.5
FV/FM_A	GLM	Ku_c12191_1202	3A	737800235	0.0085	0.00045	3.34
RDN	MLM	Kukri_c17082_519	3B	2487710	-0.0624	0.00083	3.08
RDN	GLM	Kukri_c17082_519	3B	2487710	-0.0657	0.00014	3.86
PI_H	GLM	BobWhite_c4864_326	3B	2511694	0.0606	0.00088	3.06
FV/FM_H	FarmCPU	BobWhite_c4864_326	3B	2511694	0.0061	0.00077	3.11
FV/FM_H	GLM	BobWhite_c4864_326	3B	2511694	0.0066	0.00063	3.2
ADN	FarmCPU	BobWhite_c4864_326	3B	2511694	0.0062	0.00091	3.04
ADN	GLM	BobWhite_c4864_326	3B	2511694	0.0065	0.00093	3.03
RDN	FarmCPU	RAC875_c30348_182	3B	7373265	-0.0159	0.0008	3.1
FV/FM_H	FarmCPU	BS00079522_51	3B	9778461	0.0136	0.00029	3.54
FV/FM_H	GLM	BS00079522_51	3B	9778461	0.0136	0.00035	3.46

FV/FM_H	MLM	BS00079522_51	3B	9778461	0.0136	0.0007	3.16
RDN	GLM	RFL_Contig5709_3312	3B	9780518	0.0171	0.00087	3.06
NDVI_14DAA	FarmCPU	wsnp_CAP11_c3742_1796552	3B	9917600	-0.0555	0.00029	3.54
NDVI_14DAA	FarmCPU	RAC875_c4389_1344	3B	11087285	0.0235	0.0004	3.39
GY	FarmCPU	BS00025792_51	3B	29776802	-10.373	0.00086	3.06
GY	GLM	BS00025792_51	3B	29776802	-11.109	0.0005	3.3
NDVI_14DAA	FarmCPU	BS00022242_51	3B	42340498	-0.0601	0.0006	3.22
SPS	FarmCPU	BobWhite_c828_329	3B	60254933	0.5343	0.00065	3.19
SPS	FarmCPU	RAC875_c20041_1062	3B	60868291	0.5399	0.00076	3.12
SPS	FarmCPU	wsnp_Ku_c33335_42844594	3B	60868441	0.5399	0.00076	3.12
NDVI_A	FarmCPU	Excalibur_c36626_228	3B	65558366	0.0448	0.00091	3.04
NDVI_14DAA	GLM	RAC875_c35355_952	3B	65561878	0.0421	0.00089	3.05
CN	FarmCPU	RAC875_c35355_952	3B	65561878	0.0268	0.00027	3.57
CN	GLM	RAC875_c35355_952	3B	65561878	0.0292	0.00025	3.6
NDVI_14DAA	GLM	Kukri_c90676_212	3B	65704307	0.0421	0.00089	3.05
CN	FarmCPU	Kukri_c90676_212	3B	65704307	0.0268	0.00027	3.57
CN	GLM	Kukri_c90676_212	3B	65704307	0.0292	0.00025	3.6
PI_H	FarmCPU	BobWhite_rep_c50834_145	3B	66180308	0.1238	0.00031	3.5
PI_H	GLM	BobWhite_rep_c50834_145	3B	66180308	0.1326	0.00019	3.73
FV/FM_H	FarmCPU	BobWhite_rep_c50834_145	3B	66180308	0.0131	0.00033	3.48
FV/FM_H	GLM	BobWhite_rep_c50834_145	3B	66180308	0.0139	0.00024	3.62
PI_H	MLM	BobWhite_rep_c50834_145	3B	66180308	0.1244	0.00075	3.13
FV/FM_H	MLM	BobWhite_rep_c50834_145	3B	66180308	0.0131	0.00077	3.11
NDVI_14DAA	FarmCPU	wsnp_Ex_c11246_18191331	3B	67942359	0.0438	0.00074	3.13
NDVI_14DAA	GLM	wsnp_Ex_c11246_18191331	3B	67942359	0.0475	0.00072	3.15
PI_14DAA	GLM	BS00102622_51	3B	68464256	0.1418	0.00086	3.06
FV/FM_14DAA	GLM	BS00102622_51	3B	68464256	0.0142	0.00095	3.02
PI_14DAA	GLM	Ku_c24126_637	3B	68465440	0.1418	0.00086	3.06
FV/FM_14DAA	GLM	Ku_c24126_637	3B	68465440	0.0142	0.00095	3.02
GY	FarmCPU	RAC875_c5913_172	3B	69604705	-6.4866	0.0006	3.22
NDVI_14DAA	GLM	wsnp_Ex_c19372_28313727	3B	69818358	0.0421	0.00089	3.05
CN	FarmCPU	wsnp_Ex_c19372_28313727	3B	69818358	0.0268	0.00027	3.57
CN	GLM	wsnp_Ex_c19372_28313727	3B	69818358	0.0292	0.00025	3.6
GY	FarmCPU	IAAV6423	3B	70301813	-6.8766	0.00049	3.31
GY	FarmCPU	Ku_c3416_572	3B	70301963	-6.6994	0.00094	3.03
NDVI_A	FarmCPU	RAC875_c86306_256	3B	71807479	0.0448	0.00091	3.04
FV/FM_21DAA	GLM	wsnp_BE498786B_Ta_2_1	3B	78397428	0.0026	0.00046	3.34
FV/FM_21DAA	GLM	wsnp_Ex_c6065_10623213	3B	79128942	0.0026	0.00046	3.34
PI_A	FarmCPU	Excalibur_c25659_609	3B	117587045	-0.0488	0.00047	3.32
PI_A	GLM	Excalibur_c25659_609	3B	117587045	-0.0522	0.00026	3.59
TN	FarmCPU	GENE-2001_150	3B	145258274	0.4941	0.00097	3.01
PI_A	GLM	Kukri_c8625_1941	3B	145958682	0.0465	0.00073	3.14
PI_A	GLM	Kukri_c35146_2094	3B	151226347	0.0475	0.00067	3.17

FV/FM_14DAA	FarmCPU	BS00045195_51	3B	160842485	-0.0116	0.00055	3.26
CN	FarmCPU	BS00045195_51	3B	160842485	-0.0166	0.00022	3.66
CN	GLM	BS00045195_51	3B	160842485	-0.0162	0.00049	3.31
GY	FarmCPU	BS00045195_51	3B	160842485	-6.0594	0.00042	3.37
CHL_A	GLM	RAC875_c37608_216	3B	175093566	0.5391	6.49E-05	4.19
PI_14DAA	FarmCPU	RAC875_c37608_216	3B	175093566	0.1684	0.00017	3.78
PI_14DAA	GLM	RAC875_c37608_216	3B	175093566	0.1992	0.00016	3.8
PI_14DAA	MLM	RAC875_c37608_216	3B	175093566	0.1722	0.00093	3.03
FV/FM_14DAA	FarmCPU	RAC875_c37608_216	3B	175093566	0.0168	0.00018	3.76
FV/FM_14DAA	GLM	RAC875_c37608_216	3B	175093566	0.0202	0.00014	3.86
FV/FM_14DAA	MLM	RAC875_c37608_216	3B	175093566	0.0172	0.00088	3.05
CN	FarmCPU	RAC875_c37608_216	3B	175093566	0.0218	0.00031	3.51
CN	GLM	RAC875_c37608_216	3B	175093566	0.0261	0.00027	3.57
TN	FarmCPU	RAC875_c37608_216	3B	175093566	0.2246	0.00049	3.31
CHL_B	FarmCPU	BobWhite_c362_1038	3B	222089727	1.8094	0.0002	3.71
CHL_B	GLM	BobWhite_c362_1038	3B	222089727	1.8165	0.00022	3.65
PI_A	FarmCPU	BobWhite_c362_1038	3B	222089727	0.1217	0.00046	3.34
PI_A	GLM	BobWhite_c362_1038	3B	222089727	0.121	0.00058	3.24
CHL_B	MLM	BobWhite_c362_1038	3B	222089727	1.8094	0.00052	3.28
FV/FM_A	FarmCPU	BobWhite_c362_1038	3B	222089727	0.0128	0.00019	3.72
FV/FM_A	GLM	BobWhite_c362_1038	3B	222089727	0.0127	0.00024	3.63
FV/FM_A	MLM	BobWhite_c362_1038	3B	222089727	0.0128	0.00051	3.29
CHL_A	GLM	Kukri_c4747_330	3B	230336598	0.4371	0.00059	3.23
FV/FM_21DAA	MLM	Kukri_c4747_330	3B	230336598	0.0022	0.00095	3.02
FV/FM_21DAA	FarmCPU	Kukri_c4747_330	3B	230336598	0.0021	0.00036	3.44
FV/FM_21DAA	GLM	Kukri_c4747_330	3B	230336598	0.0026	0.00059	3.23
NDVI_A	FarmCPU	Kukri_c4747_330	3B	230336598	0.0301	0.00096	3.02
CN	GLM	Kukri_c4747_330	3B	230336598	0.0224	0.00085	3.07
TN	FarmCPU	Kukri_c4747_330	3B	230336598	0.2265	6.58E-05	4.18
CHL_A	GLM	wsnp_Ex_c19982_29009504	3B	232634990	0.4371	0.00059	3.23
FV/FM_21DAA	MLM	wsnp_Ex_c19982_29009504	3B	232634990	0.0022	0.00095	3.02
FV/FM_21DAA	FarmCPU	wsnp_Ex_c19982_29009504	3B	232634990	0.0021	0.00036	3.44
FV/FM_21DAA	GLM	wsnp_Ex_c19982_29009504	3B	232634990	0.0026	0.00059	3.23
NDVI_A	FarmCPU	wsnp_Ex_c19982_29009504	3B	232634990	0.0301	0.00096	3.02
CN	GLM	wsnp_Ex_c19982_29009504	3B	232634990	0.0224	0.00085	3.07
TN	FarmCPU	wsnp_Ex_c19982_29009504	3B	232634990	0.2265	6.58E-05	4.18
TN	FarmCPU	wsnp_Ex_c257_491667	3B	232636140	0.1722	0.00052	3.28
TN	FarmCPU	BS00106922_51	3B	232636290	0.1722	0.00052	3.28
CHL_A	GLM	wsnp_BE497469B_Ta_2_1	3B	237107013	0.4546	0.00088	3.06
PI_21DAA	FarmCPU	wsnp_BE497469B_Ta_2_1	3B	237107013	0.0242	0.00051	3.29
PI_21DAA	GLM	wsnp_BE497469B_Ta_2_1	3B	237107013	0.0302	0.00063	3.2
FV/FM_21DAA	MLM	wsnp_BE497469B_Ta_2_1	3B	237107013	0.0024	0.00045	3.34
FV/FM_21DAA	FarmCPU	wsnp_BE497469B_Ta_2_1	3B	237107013	0.0024	0.00014	3.85

FV/FM_21DAA	GLM	wsnp_BE497469B_Ta_2_1	3B	237107013	0.003	0.00015	3.84
NDVI_A	FarmCPU	wsnp_BE497469B_Ta_2_1	3B	237107013	0.0333	0.0005	3.3
CN	FarmCPU	wsnp_BE497469B_Ta_2_1	3B	237107013	0.019	0.00079	3.1
CN	GLM	wsnp_BE497469B_Ta_2_1	3B	237107013	0.0253	0.0004	3.4
TN	FarmCPU	wsnp_BE497469B_Ta_2_1	3B	237107013	0.2247	0.00018	3.75
TN	FarmCPU	BS00069274_51	3B	278776317	0.1722	0.00052	3.28
FV/FM_21DAA	FarmCPU	JD_c15105_367	3B	279495868	0.0036	0.00059	3.23
TN	FarmCPU	Excalibur_c54388_193	3B	368904600	0.1693	0.00044	3.35
TN	FarmCPU	RFL_Contig3799_987	3B	378688217	0.1753	0.00087	3.06
TN	FarmCPU	wsnp_CAP8_c6899_3227098	3B	379343255	0.1678	0.00087	3.06
TN	FarmCPU	wsnp_Ex_rep_c69783_68742690	3B	379995120	0.1875	0.00029	3.54
TN	FarmCPU	wsnp_CAP11_c558_382875	3B	399970923	0.1665	0.00063	3.2
TN	FarmCPU	RAC875_c17884_616	3B	482994453	0.3802	0.00045	3.34
TN	FarmCPU	BS00105995_51	3B	484872389	0.3802	0.00045	3.34
TN	FarmCPU	wsnp_Ex_c123_244117	3B	485388729	0.3802	0.00045	3.34
TN	FarmCPU	wsnp_Ku_c8722_14766699	3B	485693423	0.3802	0.00045	3.34
TN	FarmCPU	RAC875_c100413_60	3B	487048885	0.3802	0.00045	3.34
TN	FarmCPU	Tdurum_contig75784_771	3B	488878740	0.3408	0.00099	3
PI_14DAA	GLM	RAC875_rep_c74125_1150	3B	691267232	-0.2478	0.00044	3.35
FV/FM_14DAA	GLM	RAC875_rep_c74125_1150	3B	691267232	-0.0244	0.0006	3.22
SPS	GLM	RAC875_rep_c74125_1150	3B	691267232	-0.7485	0.0005	3.3
PI_14DAA	GLM	RAC875_c12200_57	3B	696738694	-0.2478	0.00044	3.35
FV/FM_14DAA	GLM	RAC875_c12200_57	3B	696738694	-0.0244	0.0006	3.22
SPS	GLM	RAC875_c12200_57	3B	696738694	-0.7485	0.0005	3.3
CHL_H	FarmCPU	Ku_c12345_328	3B	702364946	-0.549	0.00031	3.51
CHL_H	GLM	Ku_c12345_328	3B	702364946	-0.5322	0.00063	3.2
NDVI_21DAA	FarmCPU	Ku_c12345_328	3B	702364946	-0.0553	0.00064	3.19
NDVI_21DAA	GLM	Ku_c12345_328	3B	702364946	-0.0569	0.00038	3.41
TKW	GLM	wsnp_Ex_c13154_20784674	3B	728910585	0.5495	0.00093	3.03
GY	MLM	CAP12_c1991_127	3B	732427484	-10.606	0.00079	3.1
GY	FarmCPU	CAP12_c1991_127	3B	732427484	-10.398	0.00025	3.59
GY	GLM	CAP12_c1991_127	3B	732427484	-10.143	0.00033	3.48
CHL_A	GLM	Tdurum_contig69073_365	3B	741467125	-0.3685	0.00086	3.07
CHL_10DAA	FarmCPU	BS00059416_51	3B	745289740	-0.3805	0.00085	3.07
CHL_10DAA	GLM	BS00059416_51	3B	745289740	-0.393	0.00065	3.19
CHL_A	FarmCPU	tplb0044b20_1610	3B	750137826	0.2969	0.00015	3.84
CHL_A	GLM	tplb0044b20_1610	3B	750137826	0.2962	0.00033	3.48
CHL_A	FarmCPU	BS00085434_51	3B	750357865	0.3337	2.49E-05	4.6
CHL_A	GLM	BS00085434_51	3B	750357865	0.3325	4.93E-05	4.31
CHL_A	MLM	BS00085434_51	3B	750357865	0.3049	0.0007	3.15
PH	GLM	Kukri_c3243_1065	3B	765394680	4.4269	0.0004	3.4
PH	GLM	wsnp_Ra_c67016_65144188	3B	765558499	4.4269	0.0004	3.4
TKW	FarmCPU	BS00024496_51	3B	776031854	0.4314	0.00052	3.29

TKW	GLM	BS00024496_51	3B	776031854	0.4321	0.00071	3.15
CHL_30DAA	FarmCPU	BS00057343_51	3B	811220595	0.5004	0.00023	3.63
CHL_30DAA	GLM	BS00057343_51	3B	811220595	0.504	0.00022	3.66
CHL_30DAA	MLM	BS00057343_51	3B	811220595	0.4964	0.00071	3.15
CHL_30DAA	FarmCPU	BS00044955_51	3B	811303174	0.5004	0.00023	3.63
CHL_30DAA	GLM	BS00044955_51	3B	811303174	0.504	0.00022	3.66
CHL_30DAA	MLM	BS00044955_51	3B	811303174	0.4964	0.00071	3.15
CHL_30DAA	FarmCPU	BS00044942_51	3B	811306769	0.5004	0.00023	3.63
CHL_30DAA	GLM	BS00044942_51	3B	811306769	0.504	0.00022	3.66
CHL_30DAA	MLM	BS00044942_51	3B	811306769	0.4964	0.00071	3.15
PH	FarmCPU	Kukri_c49220_167	3B	820288917	6.1607	0.00026	3.58
TN	FarmCPU	BS00024762_51	3B	829208732	0.4941	0.00097	3.01
CHL_A	FarmCPU	CAP8_c9373_277	3D	21005688	0.5152	0.00025	3.61
CHL_A	GLM	CAP8_c9373_277	3D	21005688	0.5391	0.00017	3.78
TN	GLM	Kukri_c18068_438	3D	22089269	0.3309	0.0003	3.52
CHL_B	GLM	Excalibur_c35491_788	3D	100227496	0.6179	0.00097	3.02
CHL_H	FarmCPU	wsnp_Ex_c7260_12463738	3D	160612854	0.3161	0.00098	3.01
CN	GLM	RFL_Contig5953_1298	3D	351288398	0.043	0.00095	3.02
NDVI_H	MLM	D_contig00075_218	3D	450871695	-0.0429	0.00051	3.29
NDVI_H	FarmCPU	D_contig00075_218	3D	450871695	-0.044	5.37E-05	4.27
CHL_10DAA	FarmCPU	BobWhite_c9000_114	3D	474433495	0.647	0.0008	3.1
CHL_B	FarmCPU	RAC875_c24267_258	3D	507029561	2.0112	8.74E-05	4.06
CHL_B	GLM	RAC875_c24267_258	3D	507029561	2.0255	9.78E-05	4.01
PI_A	FarmCPU	RAC875_c24267_258	3D	507029561	0.1346	0.00024	3.61
PI_A	GLM	RAC875_c24267_258	3D	507029561	0.1338	0.00032	3.5
FV/FM_A	FarmCPU	RAC875_c24267_258	3D	507029561	0.0145	6.09E-05	4.22
FV/FM_A	GLM	RAC875_c24267_258	3D	507029561	0.0144	7.84E-05	4.11
CHL_B	MLM	RAC875_c24267_258	3D	507029561	2.0111	0.00029	3.54
PI_A	MLM	RAC875_c24267_258	3D	507029561	0.1346	0.00061	3.21
FV/FM_A	MLM	RAC875_c24267_258	3D	507029561	0.0145	0.00022	3.66
NDVI_14DAA	FarmCPU	Kukri_s110037_62	3D	575526354	-0.0341	0.00016	3.79
TN	GLM	Kukri_c92813_223	3D	602274567	-0.2729	0.00061	3.21
TN	GLM	wsnp_Ra_c5433_9630495	3D	603264129	-0.2729	0.00061	3.21
CHL_B	FarmCPU	RAC875_c5433_682	3D	603264170	1.0888	0.00097	3.02
CHL_B	GLM	RAC875_c5433_682	3D	603264170	1.1024	0.00099	3
PI_21DAA	FarmCPU	RAC875_c5222_245	3D	609626385	0.0368	0.00063	3.2
FV/FM_21DAA	FarmCPU	RAC875_c5222_245	3D	609626385	0.0035	0.00032	3.49
FV/FM_21DAA	MLM	RAC875_c5222_245	3D	609626385	0.0035	0.00089	3.05
CHL_H	FarmCPU	BS00003119_51	3D	612272471	-0.3592	0.0003	3.52
CHL_H	GLM	BS00003119_51	3D	612272471	-0.3481	0.00061	3.22
CHL_H	MLM	BS00003119_51	3D	612272471	-0.3554	0.0009	3.04
CHL_B	FarmCPU	BS00024440_51	3D	613395237	0.9557	0.00061	3.21
CHL_B	GLM	BS00024440_51	3D	613395237	0.9575	0.0007	3.15

TN	FarmCPU	IAAV4754	4A	40442520	-0.1735	0.00026	3.59
ADSFL	FarmCPU	Tdurum_contig13140_69	4A	59321707	0.5983	0.00037	3.43
NDVI_14DAA	MLM	RFL_Contig1053_65	4A	68470332	-0.0356	0.00035	3.46
NDVI_A	FarmCPU	RFL_Contig1053_65	4A	68470332	-0.0327	0.00025	3.61
NDVI_14DAA	FarmCPU	RFL_Contig1053_65	4A	68470332	-0.0358	2.70E-05	4.57
NDVI_14DAA	GLM	RFL_Contig1053_65	4A	68470332	-0.0321	0.00056	3.25
RDN	FarmCPU	RFL_Contig1053_65	4A	68470332	0.0182	0.00058	3.23
TN	MLM	wsnp_RFL_Contig1073_101625	4A	104266989	-0.1925	0.001	3
TN	FarmCPU	wsnp_RFL_Contig1073_101625	4A	104266989	-0.1874	0.00016	3.78
TN	FarmCPU	GENE-2354_155	4A	138832448	-0.1751	0.00051	3.29
ADSFL	GLM	Excalibur_c42502_96	4A	281691882	0.9813	0.00079	3.1
CHL_A	FarmCPU	Excalibur_c55561_127	4A	450883765	0.3757	9.23E-06	5.03
CHL_A	GLM	Excalibur_c55561_127	4A	450883765	0.3737	2.16E-05	4.66
CHL_A	MLM	Excalibur_c55561_127	4A	450883765	0.3926	0.00016	3.8
NDVI_A	MLM	BobWhite_c20909_243	4A	598591987	-0.1181	0.00019	3.72
NDVI_A	FarmCPU	BobWhite_c20909_243	4A	598591987	-0.116	0.00014	3.84
NDVI_A	GLM	BobWhite_c20909_243	4A	598591987	-0.114	7.11E-05	4.15
PH	FarmCPU	Kukri_c20719_949	4A	622190131	-2.7798	0.0006	3.22
CN	FarmCPU	Excalibur_rep_c74900_73	4A	625076761	0.015	0.0005	3.3
CN	GLM	Excalibur_rep_c74900_73	4A	625076761	0.0155	0.00034	3.46
TN	FarmCPU	wsnp_BF474862A_Ta_2_1	4A	634736424	0.1585	0.00079	3.1
TN	FarmCPU	Kukri_rep_c109167_89	4A	634737614	0.1632	0.00055	3.26
CHL_H	GLM	wsnp_Ex_c3988_7221220	4A	666149150	0.2772	0.00092	3.03
CHL_30DAA	FarmCPU	RAC875_c59673_500	4A	681670845	0.7776	0.00022	3.66
CHL_30DAA	GLM	RAC875_c59673_500	4A	681670845	0.7787	0.00028	3.56
PI_21DAA	FarmCPU	RAC875_c59673_500	4A	681670845	0.0633	6.31E-05	4.2
PI_21DAA	GLM	RAC875_c59673_500	4A	681670845	0.0652	5.05E-05	4.3
CHL_30DAA	MLM	RAC875_c59673_500	4A	681670845	0.78	0.00064	3.19
PI_21DAA	MLM	RAC875_c59673_500	4A	681670845	0.0633	0.00023	3.64
CHL_10DAA	FarmCPU	Tdurum_contig93100_640	4A	705178811	-0.3881	0.0008	3.1
CHL_H	FarmCPU	Ra_c60252_743	4A	708567924	-0.5	0.00079	3.1
CHL_H	GLM	Ra_c60252_743	4A	708567924	-0.5259	0.00043	3.36
CHL_10DAA	FarmCPU	RFL_Contig3841_2595	4A	712864977	-0.41	0.00062	3.21
BY	FarmCPU	RFL_Contig3841_2595	4A	712864977	-17.346	0.00077	3.11
PH	FarmCPU	BS00070687_51	4A	713519029	5.3429	0.00094	3.03
PH	FarmCPU	BS00075048_51	4A	713519432	-2.6714	0.00094	3.03
PH	FarmCPU	BS00045554_51	4A	713523345	-2.5068	0.00088	3.06
CHL_10DAA	FarmCPU	Tdurum_contig10672_117	4A	717966388	0.5503	0.00072	3.14
CHL_10DAA	GLM	Tdurum_contig10672_117	4A	717966388	0.5646	0.00044	3.36
CHL_20DAA	GLM	Tdurum_contig10672_117	4A	717966388	1.9817	0.00092	3.03
CSFL	FarmCPU	Tdurum_contig10672_117	4A	717966388	3.3358	0.00096	3.02
CSFL	GLM	Tdurum_contig10672_117	4A	717966388	3.4092	0.00077	3.11
CHL_B	FarmCPU	GENE-4606_439	4A	719058868	0.613	0.00031	3.51

CHL_B	GLM	GENE-4606_439	4A	719058868	0.6917	0.00015	3.82
CSFL	GLM	GENE-4606_439	4A	719058868	2.5679	0.00054	3.27
CHL_B	MLM	GENE-4606_439	4A	719058868	0.613	0.00073	3.14
ADN	FarmCPU	Excalibur_c2023_345	4A	721383095	0.0122	0.00069	3.16
ADN	GLM	Excalibur_c2023_345	4A	721383095	0.0122	0.00078	3.11
CSFL	FarmCPU	Tdurum_contig10654_704	4A	732512147	-2.7602	0.00075	3.12
CSFL	GLM	Tdurum_contig10654_704	4A	732512147	-2.7155	0.00099	3
PH	MLM	BS00009680_51	4A	733696281	-7.8655	0.00081	3.09
PH	FarmCPU	BS00009680_51	4A	733696281	-7.9339	0.00054	3.27
PH	GLM	BS00009680_51	4A	733696281	-8.0771	0.00024	3.62
CHL_A	FarmCPU	Tdurum_contig42019_1714	4A	733912688	0.3581	0.00092	3.04
CHL_A	GLM	Tdurum_contig42019_1714	4A	733912688	0.4194	0.0002	3.7
NDVI_A	FarmCPU	Ra_c662_521	4A	735503358	0.0305	0.00094	3.03
NDVI_A	FarmCPU	Tdurum_contig10289_74	4A	737295451	0.0297	0.00094	3.03
NDVI_A	FarmCPU	BobWhite_c20558_413	4A	737340112	0.0293	0.00078	3.11
TN	FarmCPU	BobWhite_c20558_209	4A	737340406	0.209	0.00084	3.07
TN	FarmCPU	Excalibur_c12374_62	4A	737340520	0.218	0.00056	3.25
NDVI_A	FarmCPU	Tdurum_contig46583_2364	4A	738781185	0.0286	0.00036	3.44
NDVI_A	FarmCPU	Tdurum_contig46583_1275	4A	738782355	0.0859	0.00023	3.63
CHL_A	FarmCPU	Tdurum_contig47143_161	4A	739600557	0.5982	0.0001	3.99
CHL_A	GLM	Tdurum_contig47143_161	4A	739600557	0.596	0.00014	3.86
CHL_A	GLM	Kukri_c4709_53	4A	742549530	0.3743	0.00062	3.21
NDVI_A	FarmCPU	IAAV8135	4A	742552247	0.0288	0.00061	3.21
TN	GLM	RAC875_c86104_111	4B	1047091	0.2196	0.00021	3.68
PH	FarmCPU	Tdurum_contig67399_676	4B	13945650	2.088	0.00049	3.31
SL	MLM	Kukri_rep_c106598_114	4B	17043959	0.5443	0.0005	3.3
SL	FarmCPU	Kukri_rep_c106598_114	4B	17043959	0.5443	0.00019	3.73
SL	GLM	Kukri_rep_c106598_114	4B	17043959	0.5734	9.05E-05	4.04
SL	FarmCPU	Kukri_rep_c106598_51	4B	17044022	0.489	0.00088	3.06
TN	FarmCPU	Tdurum_contig6153_192	4B	43175612	0.2176	0.00095	3.02
CHL_10DAA	FarmCPU	Tdurum_contig65570_163	4B	95072178	-0.4094	0.0007	3.15
NDVI_14DAA	GLM	RAC875_c54853_88	4B	545862775	-0.052	0.00049	3.31
CHL_30DAA	FarmCPU	wsnp_Ex_c16825_25387841	4B	594872895	0.7776	0.00022	3.66
CHL_30DAA	GLM	wsnp_Ex_c16825_25387841	4B	594872895	0.7787	0.00028	3.56
PI_21DAA	FarmCPU	wsnp_Ex_c16825_25387841	4B	594872895	0.0633	6.31E-05	4.2
PI_21DAA	GLM	wsnp_Ex_c16825_25387841	4B	594872895	0.0652	5.05E-05	4.3
CHL_30DAA	MLM	wsnp_Ex_c16825_25387841	4B	594872895	0.78	0.00064	3.19
PI_21DAA	MLM	wsnp_Ex_c16825_25387841	4B	594872895	0.0633	0.00023	3.64
CHL_30DAA	FarmCPU	BS00011492_51	4B	597033042	0.7776	0.00022	3.66
CHL_30DAA	GLM	BS00011492_51	4B	597033042	0.7787	0.00028	3.56
PI_21DAA	FarmCPU	BS00011492_51	4B	597033042	0.0633	6.31E-05	4.2
PI_21DAA	GLM	BS00011492_51	4B	597033042	0.0652	5.05E-05	4.3
CHL_30DAA	MLM	BS00011492_51	4B	597033042	0.78	0.00064	3.19

PI_21DAA	MLM	BS00011492_51	4B	597033042	0.0633	0.00023	3.64
NDVI_21DAA	GLM	IAAV5572	4B	601198468	0.0533	0.00075	3.13
NDVI_14DAA	GLM	Excalibur_c106884_135	4B	611858235	0.0301	0.00025	3.6
CHL_H	FarmCPU	Ku_c2885_1277	4B	672937093	0.3119	0.00067	3.17
CHL_H	GLM	Ku_c2885_1277	4B	672937093	0.3457	0.00019	3.71
ADSFL	GLM	Ku_c2885_1277	4B	672937093	0.4171	0.00028	3.56
NDVI_A	FarmCPU	Kukri_rep_c112779_183	4D	4133349	-0.116	0.00014	3.84
NDVI_A	GLM	Kukri_rep_c112779_183	4D	4133349	-0.114	7.11E-05	4.15
NDVI_A	MLM	Kukri_rep_c112779_183	4D	4133349	-0.1181	0.00019	3.72
SL	GLM	Kukri_rep_c106598_51	4D	17044022	0.4984	0.00072	3.14
NDVI_21DAA	FarmCPU	Excalibur_c1107_577	4D	19755437	-0.0431	0.00024	3.61
CHL_10DAA	FarmCPU	wsnp_Ex_rep_c67296_65839761	4D	62469466	-0.5619	0.00059	3.23
CHL_10DAA	GLM	wsnp_Ex_rep_c67296_65839761	4D	62469466	-0.5465	0.00072	3.14
CHL_A	FarmCPU	Excalibur_c7123_667	4D	120831511	0.3088	0.00053	3.27
CHL_A	GLM	Excalibur_c7123_667	4D	120831511	0.3085	0.00079	3.1
CHL_A	FarmCPU	BobWhite_c4264_325	4D	121181547	0.3618	1.98E-05	4.7
CHL_A	GLM	BobWhite_c4264_325	4D	121181547	0.3558	4.60E-05	4.34
CHL_A	MLM	BobWhite_c4264_325	4D	121181547	0.365	0.00039	3.41
CHL_A	FarmCPU	CAP8_c9110_427	4D	121181624	0.3174	0.00024	3.61
CHL_A	GLM	CAP8_c9110_427	4D	121181624	0.3087	0.00049	3.31
CHL_30DAA	FarmCPU	Excalibur_c29496_799	4D	475027917	0.7776	0.00022	3.66
CHL_30DAA	GLM	Excalibur_c29496_799	4D	475027917	0.7787	0.00028	3.56
PI_21DAA	FarmCPU	Excalibur_c29496_799	4D	475027917	0.0633	6.31E-05	4.2
PI_21DAA	GLM	Excalibur_c29496_799	4D	475027917	0.0652	5.05E-05	4.3
CHL_30DAA	MLM	Excalibur_c29496_799	4D	475027917	0.78	0.00064	3.19
PI_21DAA	MLM	Excalibur_c29496_799	4D	475027917	0.0633	0.00023	3.64
RDN	GLM	BobWhite_c41542_354	5A	693222	-0.0156	0.00067	3.18
CHL_T	FarmCPU	Excalibur_c12644_58	5A	2423146	1.1357	0.0004	3.4
CHL_T	GLM	Excalibur_c12644_58	5A	2423146	1.117	0.00055	3.26
PI_H	FarmCPU	Excalibur_c12644_58	5A	2423146	0.1812	0.00012	3.91
PI_H	GLM	Excalibur_c12644_58	5A	2423146	0.1807	0.00016	3.8
FV/FM_H	FarmCPU	Excalibur_c12644_58	5A	2423146	0.0193	0.00012	3.9
FV/FM_H	GLM	Excalibur_c12644_58	5A	2423146	0.0193	0.00016	3.8
CHL_T	MLM	Excalibur_c12644_58	5A	2423146	1.1357	0.00089	3.05
PI_H	MLM	Excalibur_c12644_58	5A	2423146	0.18	0.00036	3.44
FV/FM_H	MLM	Excalibur_c12644_58	5A	2423146	0.0193	0.00037	3.43
ADN	MLM	Excalibur_c12644_58	5A	2423146	0.02	0.00026	3.58
ADN	FarmCPU	Excalibur_c12644_58	5A	2423146	0.0201	8.20E-05	4.09
ADN	GLM	Excalibur_c12644_58	5A	2423146	0.02	0.00011	3.95
RDN	MLM	BS00023008_51	5A	8059358	-0.0151	0.00073	3.14
RDN	FarmCPU	BS00023008_51	5A	8059358	-0.0144	0.00057	3.24
RDN	GLM	BS00023008_51	5A	8059358	-0.0157	0.00013	3.87
PI_H	FarmCPU	BS00101071_51	5A	8059402	0.0506	0.00062	3.21

PI_H	GLM	BS00101071_51	5A	8059402	0.0505	0.00075	3.12
ADN	FarmCPU	BS00101071_51	5A	8059402	0.0054	0.00086	3.06
RDN	FarmCPU	wsnp_Ku_c9559_15999945	5A	8243240	-0.0147	0.00094	3.02
RDN	GLM	wsnp_Ku_c9559_15999945	5A	8243240	-0.0144	0.0007	3.16
NDVI_A	FarmCPU	Excalibur_c36501_188	5A	9325617	-0.0481	0.00021	3.69
NDVI_A	GLM	Excalibur_c36501_188	5A	9325617	-0.0454	0.00027	3.56
CHL_H	FarmCPU	IAAV7519	5A	17840148	0.2852	0.00072	3.14
ADSFL	FarmCPU	IAAV7519	5A	17840148	0.3689	0.00043	3.36
TN	FarmCPU	RAC875_c61887_194	5A	29892474	-0.1627	0.00018	3.75
FV/FM_21DAA	FarmCPU	Excalibur_c5398_695	5A	30027274	0.0027	1.66E-05	4.78
FV/FM_21DAA	GLM	Excalibur_c5398_695	5A	30027274	0.0028	2.45E-05	4.61
FV/FM_21DAA	MLM	Excalibur_c5398_695	5A	30027274	0.0027	9.45E-05	4.02
FV/FM_21DAA	FarmCPU	Tdurum_contig14863_916	5A	32666624	0.0024	0.00011	3.96
FV/FM_21DAA	GLM	Tdurum_contig14863_916	5A	32666624	0.0024	0.00019	3.73
FV/FM_21DAA	MLM	Tdurum_contig14863_916	5A	32666624	0.0024	0.00037	3.43
TN	FarmCPU	RFL_Contig2251_434	5A	37617802	-0.292	0.00029	3.54
NDVI_A	FarmCPU	wsnp_BE444720A_Ta_2_1	5A	57376456	0.0859	0.00023	3.63
CN	FarmCPU	Ra_c9994_865	5A	229771555	0.0358	0.00078	3.11
CN	GLM	Ra_c9994_865	5A	229771555	0.0377	0.00044	3.36
PH	GLM	Excalibur_c2389_334	5A	331865767	3.8901	0.00033	3.49
TN	FarmCPU	Excalibur_c2389_334	5A	331865767	-0.2745	0.00092	3.04
NDVI_14DAA	FarmCPU	Excalibur_c17553_84	5A	375375809	-0.051	0.00022	3.65
CHL_H	FarmCPU	BS00051181_51	5A	404177285	0.671	0.00014	3.86
CHL_H	GLM	BS00051181_51	5A	404177285	0.6828	0.00043	3.37
ADSFL	FarmCPU	BS00051181_51	5A	404177285	0.7907	0.00034	3.47
CHL_H	MLM	BS00051181_51	5A	404177285	0.6731	0.00054	3.27
CHL_H	FarmCPU	wsnp_BE497368A_Ta_2_1	5A	408183358	0.671	0.00014	3.86
CHL_H	GLM	wsnp_BE497368A_Ta_2_1	5A	408183358	0.6828	0.00043	3.37
ADSFL	FarmCPU	wsnp_BE497368A_Ta_2_1	5A	408183358	0.7907	0.00034	3.47
CHL_H	MLM	wsnp_BE497368A_Ta_2_1	5A	408183358	0.6731	0.00054	3.27
CHL_H	FarmCPU	wsnp_CD453438A_Ta_2_1	5A	408183478	0.671	0.00014	3.86
CHL_H	GLM	wsnp_CD453438A_Ta_2_1	5A	408183478	0.6828	0.00043	3.37
ADSFL	FarmCPU	wsnp_CD453438A_Ta_2_1	5A	408183478	0.7907	0.00034	3.47
CHL_H	MLM	wsnp_CD453438A_Ta_2_1	5A	408183478	0.6731	0.00054	3.27
CHL_H	FarmCPU	BS00078076_51	5A	409323859	0.434	4.29E-05	4.37
CHL_H	GLM	BS00078076_51	5A	409323859	0.4264	0.00013	3.89
CHL_H	MLM	BS00078076_51	5A	409323859	0.4321	0.00024	3.63
CHL_H	FarmCPU	BS00066127_51	5A	414048579	0.434	4.29E-05	4.37
CHL_H	GLM	BS00066127_51	5A	414048579	0.4264	0.00013	3.89
CHL_H	MLM	BS00066127_51	5A	414048579	0.4321	0.00024	3.63
CHL_H	FarmCPU	BS00063823_51	5A	414048856	0.3593	0.00095	3.02
CHL_H	FarmCPU	BS00063822_51	5A	414048861	0.3658	0.00091	3.04
CHL_H	FarmCPU	RAC875_c13_1965	5A	414050215	0.3489	0.00083	3.08

CHL_H	FarmCPU	CAP12_c667_143	5A	415356067	0.3996	0.00041	3.38
CHL_H	FarmCPU	BS00034303_51	5A	422077684	0.4005	0.00014	3.84
CHL_H	GLM	BS00034303_51	5A	422077684	0.389	0.00039	3.4
CHL_H	MLM	BS00034303_51	5A	422077684	0.3968	0.00057	3.25
CHL_H	FarmCPU	BobWhite_c26540_273	5A	423251459	0.671	0.00014	3.86
CHL_H	GLM	BobWhite_c26540_273	5A	423251459	0.6828	0.00043	3.37
ADSFL	FarmCPU	BobWhite_c26540_273	5A	423251459	0.7907	0.00034	3.47
CHL_H	MLM	BobWhite_c26540_273	5A	423251459	0.6731	0.00054	3.27
CHL_H	FarmCPU	BS00076221_51	5A	450463881	0.338	0.00096	3.02
SPS	FarmCPU	BobWhite_c10901_578	5A	467381964	0.9934	0.00075	3.12
SPS	GLM	BobWhite_c10901_578	5A	467381964	0.9937	0.00071	3.15
SPS	GLM	BS00082002_51	5A	476659634	-0.5701	0.00094	3.03
NDVI_H	GLM	wsnp_Ex_c17268_25935536	5A	479908679	-0.0186	0.00091	3.04
NDVI_A	GLM	wsnp_Ex_c17268_25935536	5A	479908679	-0.0277	4.09E-05	4.39
NDVI_A	GLM	wsnp_Ex_c7383_12655410	5A	481901582	0.0263	0.00012	3.91
TN	FarmCPU	Tdurum_contig76136_404	5A	488629690	-0.2561	0.0009	3.05
CHL_B	FarmCPU	Excalibur_c12332_217	5A	524229943	1.462	9.75E-05	4.01
CHL_B	GLM	Excalibur_c12332_217	5A	524229943	1.472	0.00011	3.98
PI_A	FarmCPU	Excalibur_c12332_217	5A	524229943	0.0952	0.00041	3.39
PI_A	GLM	Excalibur_c12332_217	5A	524229943	0.0966	0.00037	3.43
CHL_B	MLM	Excalibur_c12332_217	5A	524229943	1.462	0.00031	3.51
PI_A	MLM	Excalibur_c12332_217	5A	524229943	0.0952	0.00091	3.04
CHL_B	FarmCPU	Excalibur_c4244_1624	5A	524245669	1.1903	0.00055	3.26
CHL_B	GLM	Excalibur_c4244_1624	5A	524245669	1.2055	0.00055	3.26
BY	FarmCPU	BS00066143_51	5A	533072063	-25.601	0.00099	3
RDN	FarmCPU	BS00021805_51	5A	535138119	0.0375	0.00096	3.02
RDN	GLM	BS00021805_51	5A	535138119	0.0371	0.00064	3.19
RDN	FarmCPU	wsnp_Ku_c3397_6300446	5A	536677434	0.0375	0.00096	3.02
RDN	GLM	wsnp_Ku_c3397_6300446	5A	536677434	0.0371	0.00064	3.19
GY	MLM	BobWhite_rep_c57159_360	5A	536677525	-13.635	0.00099	3
RDN	FarmCPU	BobWhite_c23972_590	5A	536772261	0.0375	0.00096	3.02
RDN	GLM	BobWhite_c23972_590	5A	536772261	0.0371	0.00064	3.19
RDN	FarmCPU	Kukri_c44685_238	5A	536817718	0.0375	0.00096	3.02
RDN	GLM	Kukri_c44685_238	5A	536817718	0.0371	0.00064	3.19
RDN	FarmCPU	RAC875_c103967_76	5A	537354458	0.0375	0.00096	3.02
RDN	GLM	RAC875_c103967_76	5A	537354458	0.0371	0.00064	3.19
GY	MLM	wsnp_Ex_c744_1463350	5A	537958029	-13.635	0.00099	3
TKW	GLM	Kukri_c75754_239	5A	539946247	-0.9244	0.00043	3.37
TKW	GLM	Kukri_s112978_54	5A	539947131	-0.9244	0.00043	3.37
TKW	GLM	BS00068178_51	5A	540052088	-0.9244	0.00043	3.37
TKW	GLM	Kukri_c14889_1086	5A	540052370	-0.8264	0.00085	3.07
NDVI_H	FarmCPU	BS00098207_51	5A	540060930	-0.0375	7.80E-05	4.11
NDVI_H	MLM	BS00098207_51	5A	540060930	-0.0372	0.00063	3.2

CSFL	GLM	BS00065551_51	5A	556531640	-2.2844	0.00085	3.07
CHL_20DAA	GLM	wsnp_BE399939A_Ta_2_1	5A	556683952	-1.4592	0.00026	3.58
CSFL	FarmCPU	wsnp_BE399939A_Ta_2_1	5A	556683952	-2.3157	0.00046	3.33
CSFL	GLM	wsnp_BE399939A_Ta_2_1	5A	556683952	-2.639	9.06E-05	4.04
CSFL	MLM	wsnp_BE399939A_Ta_2_1	5A	556683952	-2.4185	0.00071	3.15
CHL_A	FarmCPU	BS00085711_51	5A	657057593	0.3248	0.00035	3.45
CHL_A	GLM	BS00085711_51	5A	657057593	0.3425	0.00036	3.45
CHL_H	FarmCPU	BobWhite_c29857_228	5B	17979754	0.285	0.00073	3.13
ADSFL	FarmCPU	BobWhite_c29857_228	5B	17979754	0.3548	0.00074	3.13
CSFL	GLM	Kukri_c32784_2123	5B	27830588	4.4454	0.00068	3.17
CHL_B	FarmCPU	wsnp_Ku_c27243_37190781	5B	65588226	1.1982	0.00047	3.33
CHL_B	GLM	wsnp_Ku_c27243_37190781	5B	65588226	1.1938	0.00059	3.23
PI_A	FarmCPU	wsnp_Ku_c27243_37190781	5B	65588226	0.0827	0.00071	3.15
PI_A	GLM	wsnp_Ku_c27243_37190781	5B	65588226	0.0827	0.00083	3.08
FV/FM_A	FarmCPU	wsnp_Ku_c27243_37190781	5B	65588226	0.0087	0.00029	3.54
FV/FM_A	GLM	wsnp_Ku_c27243_37190781	5B	65588226	0.0087	0.00036	3.44
FV/FM_A	MLM	wsnp_Ku_c27243_37190781	5B	65588226	0.0087	0.0007	3.15
CSFL	GLM	Excalibur_c5540_1197	5B	68359590	3.2246	0.00069	3.16
CHL_10DAA	FarmCPU	Tdurum_contig28482_427	5B	68926803	0.6492	0.00025	3.6
CHL_10DAA	GLM	Tdurum_contig28482_427	5B	68926803	0.6627	0.00015	3.83
CHL_10DAA	MLM	Tdurum_contig28482_427	5B	68926803	0.6713	0.00065	3.19
CHL_10DAA	FarmCPU	wsnp_Ra_c8771_14786376	5B	69144599	0.5748	0.00064	3.19
CHL_10DAA	GLM	wsnp_Ra_c8771_14786376	5B	69144599	0.592	0.00035	3.46
CHL_10DAA	FarmCPU	RAC875_c51548_403	5B	72007967	-0.4233	0.0004	3.4
CHL_10DAA	GLM	RAC875_c51548_403	5B	72007967	-0.4209	0.00035	3.45
CHL_10DAA	FarmCPU	JD_c46002_350	5B	72018818	-0.4045	0.00029	3.53
CHL_10DAA	GLM	JD_c46002_350	5B	72018818	-0.3922	0.00038	3.42
TN	FarmCPU	tplb0035o24_635	5B	72258254	0.1518	0.00049	3.31
CHL_10DAA	FarmCPU	Kukri_c2640_1611	5B	137996974	-0.4075	0.00079	3.1
CHL_10DAA	GLM	Kukri_c2640_1611	5B	137996974	-0.4043	0.00072	3.14
NDVI_14DAA	FarmCPU	wsnp_RFL_Contig1809_946826	5B	139167711	-0.0555	0.00029	3.54
NDVI_A	GLM	BS00066628_51	5B	287624137	-0.0275	0.00047	3.33
CHL_10DAA	FarmCPU	IAAV6416	5B	305053831	0.5404	0.00053	3.28
CHL_10DAA	GLM	IAAV6416	5B	305053831	0.5355	0.0005	3.3
CHL_10DAA	FarmCPU	BobWhite_c44797_294	5B	306451726	0.5607	0.001	3
CHL_10DAA	GLM	BobWhite_c44797_294	5B	306451726	0.5547	0.00096	3.02
CHL_10DAA	FarmCPU	Kukri_c19116_170	5B	309004810	0.5597	0.00084	3.08
CHL_10DAA	FarmCPU	BS00002208_51	5B	378816485	0.4741	0.00071	3.15
CHL_10DAA	FarmCPU	RAC875_c29431_1849	5B	395633051	0.495	0.00037	3.43
CHL_10DAA	FarmCPU	BS00110064_51	5B	397838250	0.704	3.61E-05	4.44
CHL_10DAA	GLM	BS00110064_51	5B	397838250	0.6907	3.99E-05	4.4
CHL_10DAA	MLM	BS00110064_51	5B	397838250	0.7442	0.00013	3.9
CHL_10DAA	FarmCPU	BobWhite_c11365_273	5B	400523580	0.5412	0.00024	3.62

CHL_10DAA	GLM	BS00049793_51	5B	402843834	-0.4119	0.0008	3.1
CHL_10DAA	GLM	wsnp_BE497820B_Ta_2_2	5B	411930623	0.398	0.00099	3.01
CHL_10DAA	GLM	tplb0033f11_1381	5B	417438409	0.4387	0.00091	3.04
SPS	GLM	Kukri_c47057_758	5B	447840648	-0.5413	0.00028	3.55
NDVI_A	GLM	BobWhite_c47103_84	5B	457342662	0.0234	0.00083	3.08
SPS	FarmCPU	IAAV2246	5B	462144173	-0.493	0.00061	3.21
SPS	GLM	IAAV2246	5B	462144173	-0.6002	6.09E-05	4.22
SPS	GLM	RAC875_c929_170	5B	462145514	-0.5631	0.001	3
SPS	FarmCPU	RAC875_c33387_1102	5B	465995108	-0.493	0.00061	3.21
SPS	GLM	RAC875_c33387_1102	5B	465995108	-0.6002	6.09E-05	4.22
SPS	GLM	RAC875_c28078_871	5B	467513471	-0.5258	0.00069	3.16
GY	MLM	BobWhite_c6094_740	5B	511697392	-13.635	0.00099	3
NDVI_A	GLM	BS00093522_51	5B	571231310	0.032	0.00027	3.57
CHL_30DAA	FarmCPU	wsnp_Ex_c49423_54028488	5B	572358522	0.3481	0.00069	3.16
CHL_10DAA	FarmCPU	Ra_c2216_1449	5B	591145284	-0.3544	0.00078	3.11
RDN	FarmCPU	BS00021735_51	5B	593943103	0.0137	0.0006	3.22
NDVI_14DAA	FarmCPU	BobWhite_rep_c63253_215	5B	622040355	-0.0748	8.20E-05	4.09
NDVI_14DAA	GLM	BobWhite_rep_c63253_215	5B	622040355	-0.0733	0.00016	3.79
NDVI_14DAA	MLM	BobWhite_rep_c63253_215	5B	622040355	-0.0719	0.0007	3.15
NDVI_14DAA	FarmCPU	Tdurum_contig94033_717	5B	622040657	-0.0784	0.00018	3.73
NDVI_14DAA	GLM	Tdurum_contig94033_717	5B	622040657	-0.0745	0.00042	3.38
PI_21DAA	FarmCPU	BS00110293_51	5B	653655509	0.0312	0.00081	3.09
FV/FM_H	GLM	RAC875_c1148_609	5B	678338269	0.0069	0.001	3
CHL_10DAA	FarmCPU	wsnp_Ra_c38873_46699852	5B	680359041	0.3492	0.00078	3.11
NDVI_21DAA	FarmCPU	CAP11_c7700_247	5B	682183439	-0.0383	0.00065	3.19
CHL_30DAA	FarmCPU	Tdurum_contig59965_563	5B	703088788	0.4063	0.00044	3.36
CHL_30DAA	GLM	Tdurum_contig59965_563	5B	703088788	0.4115	0.00037	3.43
NDVI_A	GLM	BobWhite_c23714_130	5D	8543033	-0.041	0.00015	3.82
CSFL	GLM	Kukri_c9358_269	5D	9732395	-2.5786	0.00081	3.09
PI_21DAA	GLM	D_GA8KES402H1C3J_143	5D	18192647	0.0216	0.00069	3.16
TN	FarmCPU	Ra_c70331_779	5D	132880111	0.4323	0.00062	3.21
CN	FarmCPU	Kukri_c890_2697	5D	185190934	0.0358	0.00078	3.11
CN	GLM	Kukri_c890_2697	5D	185190934	0.0377	0.00044	3.36
NDVI_A	FarmCPU	BobWhite_c8092_726	5D	246298536	-0.0378	0.00092	3.04
NDVI_A	GLM	BobWhite_c8092_726	5D	246298536	-0.0397	0.00034	3.47
NDVI_A	GLM	wsnp_Ku_c6898_11962553	5D	252616451	-0.0395	0.00083	3.08
CHL_H	FarmCPU	D_contig09666_451	5D	311603129	0.629	0.00029	3.54
CHL_H	GLM	D_contig09666_451	5D	311603129	0.6401	0.00087	3.06
CHL_H	MLM	D_contig09666_451	5D	311603129	0.6293	0.00091	3.04
SPS	FarmCPU	GENE-3583_319	5D	341566438	-0.3923	0.00088	3.06
SPS	GLM	GENE-3583_319	5D	341566438	-0.4415	0.00069	3.16
GY	MLM	IAAV6298	5D	420874683	-27.27	0.00099	3
GY	MLM	D_GBB4FNX02HRJ2H_262	5D	423270428	-13.635	0.00099	3

RDN	GLM	BS00003879_51	5D	436951317	0.0169	0.00068	3.17
NDVI_A	FarmCPU	Excalibur_rep_c73156_287	5D	437345411	0.0268	0.00082	3.09
NDVI_A	GLM	Excalibur_rep_c73156_287	5D	437345411	0.029	0.00065	3.19
PI_14DAA	FarmCPU	tplb0035b17_2108	5D	505948315	-0.1778	0.00061	3.21
FV/FM_14DAA	FarmCPU	tplb0035b17_2108	5D	505948315	-0.018	0.00054	3.27
PI_14DAA	FarmCPU	Kukri_c24611_705	5D	522140142	-0.1938	0.00019	3.73
PI_14DAA	GLM	Kukri_c24611_705	5D	522140142	-0.1883	0.0003	3.53
FV/FM_14DAA	FarmCPU	Kukri_c24611_705	5D	522140142	-0.0196	0.00016	3.79
FV/FM_14DAA	GLM	Kukri_c24611_705	5D	522140142	-0.0191	0.00025	3.6
PI_14DAA	MLM	Kukri_c24611_705	5D	522140142	-0.1909	0.00063	3.2
FV/FM_14DAA	MLM	Kukri_c24611_705	5D	522140142	-0.0194	0.00055	3.26
PH	FarmCPU	D_GA8KES401AL4GG_122	5D	546653435	-2.9538	0.0005	3.3
PH	FarmCPU	IACX10520	5D	546689938	-2.7798	0.0006	3.22
PH	FarmCPU	Excalibur_c42190_383	5D	546906400	-2.9538	0.0005	3.3
CHL_10DAA	GLM	Kukri_c21384_1333	5D	561675637	-0.5397	0.00049	3.31
NDVI_A	FarmCPU	BS00030220_51	6A	1885966	-0.0379	9.50E-05	4.02
NDVI_A	GLM	BS00030220_51	6A	1885966	-0.0339	0.00027	3.56
NDVI_A	MLM	BS00030220_51	6A	1885966	-0.037	0.00051	3.29
NDVI_H	FarmCPU	Excalibur_c31801_752	6A	2953376	0.0283	0.00066	3.18
RDN	FarmCPU	Excalibur_c31801_752	6A	2953376	-0.0207	0.00067	3.18
NDVI_A	GLM	BS00037002_51	6A	2972633	-0.0441	0.00094	3.03
NDVI_A	FarmCPU	BS00058159_51	6A	3311136	0.0836	2.40E-05	4.62
NDVI_A	GLM	BS00058159_51	6A	3311136	0.0764	5.74E-05	4.24
NDVI_A	MLM	BS00058159_51	6A	3311136	0.0844	0.00015	3.84
NDVI_A	GLM	RAC875_c4668_771	6A	5326775	-0.0524	0.00042	3.38
NDVI_A	FarmCPU	wsnp_Ku_c39334_47795350	6A	5873055	-0.0363	0.00026	3.58
NDVI_A	GLM	wsnp_Ku_c39334_47795350	6A	5873055	-0.0331	0.00047	3.32
NDVI_A	FarmCPU	Tdurum_contig55193_296	6A	6596817	-0.0464	1.02E-05	4.99
NDVI_A	GLM	Tdurum_contig55193_296	6A	6596817	-0.0424	2.50E-05	4.6
NDVI_A	MLM	Tdurum_contig55193_296	6A	6596817	-0.0464	0.0001	3.99
NDVI_A	GLM	wsnp_Ku_c38982_47513233	6A	11115093	-0.0289	0.00098	3.01
NDVI_A	FarmCPU	Excalibur_c32710_68	6A	11414310	-0.0313	0.00019	3.73
NDVI_21DAA	FarmCPU	Excalibur_c32710_68	6A	11414310	-0.0378	0.00078	3.11
NDVI_A	FarmCPU	BS00064449_51	6A	11499458	0.0513	0.00013	3.87
NDVI_A	FarmCPU	BS00064453_51	6A	11499623	0.0549	0.00013	3.89
NDVI_A	FarmCPU	BS00098857_51	6A	11555369	-0.0278	0.00096	3.02
NDVI_14DAA	FarmCPU	Tdurum_contig29823_203	6A	12097638	-0.0407	0.00071	3.15
NDVI_A	FarmCPU	IACX8154	6A	12392896	-0.0341	0.00095	3.02
NDVI_A	GLM	BS00023192_51	6A	13806506	-0.0453	0.00032	3.5
RDN	FarmCPU	BS00011010_51	6A	18713239	-0.0279	2.51E-05	4.6
RDN	GLM	BS00011010_51	6A	18713239	-0.0248	0.00014	3.85
RDN	MLM	BS00011010_51	6A	18713239	-0.0279	0.00013	3.87
TN	FarmCPU	BS00011010_51	6A	18713239	0.2611	0.00027	3.57

NDVI_H	FarmCPU	Tdurum_contig64407_219	6A	30190292	-0.031	0.00081	3.09
CHL_10DAA	FarmCPU	BS00091666_51	6A	31354392	0.3628	0.00097	3.01
NDVI_H	FarmCPU	RAC875_c47243_145	6A	31358488	-0.0292	0.00098	3.01
NDVI_H	FarmCPU	Tdurum_contig42906_732	6A	32658889	-0.0301	0.00097	3.01
NDVI_21DAA	FarmCPU	GENE-0221_350	6A	47902336	0.0618	0.00076	3.12
TN	FarmCPU	wsnp_Ex_c15378_23639387	6A	49195242	-0.1606	0.00081	3.09
TN	FarmCPU	Kukri_c22149_276	6A	61386533	0.4941	0.00097	3.01
NDVI_14DAA	FarmCPU	Excalibur_c4483_1053	6A	62649462	-0.023	0.00089	3.05
GY	GLM	RAC875_c4632_934	6A	65556927	9.0751	0.00072	3.15
NDVI_14DAA	FarmCPU	Jagger_c8372_125	6A	71181774	-0.0445	0.00065	3.18
NDVI_21DAA	FarmCPU	Jagger_c8372_125	6A	71181774	-0.0603	0.00084	3.08
NDVI_A	FarmCPU	RAC875_rep_c114561_587	6A	77532917	-0.0297	0.00027	3.57
CHL_A	FarmCPU	Ku_c6998_485	6A	209392366	0.6793	0.00011	3.98
CHL_A	GLM	Ku_c6998_485	6A	209392366	0.7282	0.00017	3.78
CSFL	GLM	Ku_c6998_485	6A	209392366	6.0099	0.00022	3.66
TN	FarmCPU	IAAV3686	6A	272140958	0.4941	0.00097	3.01
CHL_10DAA	GLM	BS00064632_51	6A	435597031	0.6655	0.00086	3.06
CSFL	GLM	BS00064632_51	6A	435597031	4.1911	0.00086	3.06
GY	GLM	BS00064632_51	6A	435597031	9.9717	0.00078	3.11
CHL_30DAA	FarmCPU	RAC875_c21590_141	6A	440058484	0.5397	0.00046	3.34
CHL_30DAA	GLM	RAC875_c21590_141	6A	440058484	0.544	0.00044	3.36
PH	MLM	BS00040165_51	6A	572571979	-7.8655	0.00081	3.09
PH	FarmCPU	BS00040165_51	6A	572571979	-7.9339	0.00054	3.27
PH	GLM	BS00040165_51	6A	572571979	-8.0771	0.00024	3.62
NDVI_H	FarmCPU	RAC875_c26820_847	6A	573123775	-0.0292	0.00098	3.01
TN	FarmCPU	Excalibur_c32726_125	6A	574486433	0.1428	0.00071	3.15
GY	GLM	BobWhite_c17385_55	6A	581733533	-8.3757	0.00043	3.37
GY	GLM	wsnp_Ex_c965_1845676	6A	581747179	-7.9161	0.00064	3.19
NDVI_A	GLM	Tdurum_contig14676_637	6A	592686702	0.0431	0.00041	3.38
TN	FarmCPU	Tdurum_contig29357_338	6A	594753216	0.4941	0.00097	3.01
NDVI_A	FarmCPU	BS00099074_51	6A	595627657	0.0285	0.00036	3.44
TN	FarmCPU	Tdurum_contig51566_561	6A	600276012	0.2186	0.00056	3.25
PI_14DAA	FarmCPU	BobWhite_c5872_589	6A	602710419	0.1858	0.00044	3.36
PI_14DAA	GLM	BobWhite_c5872_589	6A	602710419	0.1922	0.00026	3.58
FV/FM_14DAA	FarmCPU	BobWhite_c5872_589	6A	602710419	0.0188	0.00038	3.42
FV/FM_14DAA	GLM	BobWhite_c5872_589	6A	602710419	0.0194	0.00025	3.61
NDVI_A	GLM	BobWhite_c5872_589	6A	602710419	0.0405	0.00035	3.46
PI_14DAA	MLM	BobWhite_c5872_589	6A	602710419	0.1924	0.00081	3.09
FV/FM_14DAA	MLM	BobWhite_c5872_589	6A	602710419	0.0193	0.00078	3.11
CHL_10DAA	FarmCPU	IAAV5158	6A	604886205	0.559	6.03E-05	4.22
CHL_10DAA	GLM	IAAV5158	6A	604886205	0.5425	0.00057	3.25
CHL_10DAA	MLM	IAAV5158	6A	604886205	0.5595	0.00069	3.16
TN	GLM	BS00067558_51	6A	606439838	0.2249	0.00072	3.14

NDVI_A	FarmCPU	wsnp_Ku_c1468_2912489	6A	609003257	0.0307	0.00071	3.15
NDVI_A	FarmCPU	RFL_Contig5262_1500	6A	609035856	0.0307	0.00071	3.15
PI_21DAA	FarmCPU	wsnp_Ex_c20352_29416468	6A	611714588	0.0609	0.00012	3.93
PI_21DAA	GLM	wsnp_Ex_c20352_29416468	6A	611714588	0.0609	0.00012	3.91
PI_21DAA	MLM	wsnp_Ex_c20352_29416468	6A	611714588	0.0609	0.00035	3.45
CHL_B	GLM	Excalibur_c5082_158	6A	615792025	0.8389	0.00092	3.03
PI_A	GLM	Excalibur_c5082_158	6A	615792025	0.0603	0.00079	3.1
FV/FM_A	FarmCPU	Excalibur_c5082_158	6A	615792025	0.0057	0.00074	3.13
FV/FM_A	GLM	Excalibur_c5082_158	6A	615792025	0.0064	0.00033	3.48
PH	FarmCPU	RAC875_c23338_792	6A	615792720	-2.3077	0.00082	3.09
PH	FarmCPU	Kukri_c14511_393	6A	615822151	-2.4783	0.00083	3.08
NDVI_14DAA	FarmCPU	BS00037162_51	6A	617689729	0.0525	0.00018	3.73
TN	FarmCPU	BS00037162_51	6A	617689729	0.32	0.00053	3.28
CHL_A	FarmCPU	Jagger_c10642_260	6B	1615167	0.2751	0.00067	3.17
CHL_A	GLM	Jagger_c10642_260	6B	1615167	0.2745	0.00075	3.12
NDVI_A	FarmCPU	BS00092845_51	6B	11298715	-0.0528	6.50E-06	5.19
NDVI_A	GLM	BS00092845_51	6B	11298715	-0.0483	1.89E-05	4.72
NDVI_A	MLM	BS00092845_51	6B	11298715	-0.0504	8.31E-05	4.08
BY	FarmCPU	wsnp_RFL_Contig4601_5473822	6B	38880494	-49.561	0.00092	3.04
NDVI_H	FarmCPU	BS00049779_51	6B	54662588	-0.0326	0.00088	3.06
PI_H	FarmCPU	BS00070120_51	6B	76002927	0.0878	0.00088	3.06
FV/FM_H	FarmCPU	BS00070120_51	6B	76002927	0.0094	0.00084	3.08
PI_H	FarmCPU	Excalibur_c6876_523	6B	76003212	0.0878	0.00088	3.06
FV/FM_H	FarmCPU	Excalibur_c6876_523	6B	76003212	0.0094	0.00084	3.08
CHL_20DAA	FarmCPU	BS00074041_51	6B	134808039	-1.6093	0.00069	3.16
NDVI_A	FarmCPU	Excalibur_c48499_250	6B	135118963	-0.0297	0.00027	3.57
CHL_30DAA	FarmCPU	BobWhite_rep_c65994_267	6B	156525702	0.6462	0.00019	3.72
CHL_30DAA	GLM	BobWhite_rep_c65994_267	6B	156525702	0.6366	0.0003	3.52
RDSFL	FarmCPU	BobWhite_rep_c65994_267	6B	156525702	-0.0179	0.00035	3.45
RDSFL	GLM	BobWhite_rep_c65994_267	6B	156525702	-0.0175	0.00056	3.25
PI_21DAA	FarmCPU	BobWhite_rep_c65994_267	6B	156525702	0.0512	8.67E-05	4.06
PI_21DAA	GLM	BobWhite_rep_c65994_267	6B	156525702	0.0517	9.71E-05	4.01
FV/FM_21DAA	GLM	BobWhite_rep_c65994_267	6B	156525702	0.004	0.00097	3.01
CHL_30DAA	MLM	BobWhite_rep_c65994_267	6B	156525702	0.647	0.00056	3.25
RDSFL	MLM	BobWhite_rep_c65994_267	6B	156525702	-0.0179	0.00081	3.09
PI_21DAA	MLM	BobWhite_rep_c65994_267	6B	156525702	0.0512	0.00028	3.55
NDVI_H	FarmCPU	RAC875_c22387_117	6B	164571184	-0.059	0.00023	3.64
NDVI_H	FarmCPU	BS00073259_51	6B	165561733	-0.0295	0.00023	3.64
NDVI_H	FarmCPU	IACX9279	6B	166595348	-0.0241	0.00062	3.21
RDN	FarmCPU	IACX9279	6B	166595348	0.0179	0.00052	3.28
NDVI_H	FarmCPU	BS00074947_51	6B	191538469	-0.0319	4.62E-05	4.33
RDN	FarmCPU	BS00074947_51	6B	191538469	0.0197	0.00072	3.14
NDVI_H	MLM	BS00074947_51	6B	191538469	-0.0313	0.0005	3.3

NDVI_H	FarmCPU	Jagger_c555_287	6B	191991803	-0.0304	9.78E-05	4.01
NDVI_H	FarmCPU	Kukri_c54324_1575	6B	193473655	-0.0316	6.46E-05	4.19
RDN	FarmCPU	Kukri_c54324_1575	6B	193473655	0.0198	0.00075	3.13
NDVI_H	MLM	Kukri_c54324_1575	6B	193473655	-0.0304	0.00073	3.14
NDVI_H	FarmCPU	Kukri_c36620_1336	6B	193892547	-0.0314	0.0001	3.99
CHL_20DAA	FarmCPU	RAC875_c48031_240	6B	227098077	-2.1042	0.0005	3.3
CHL_20DAA	GLM	RAC875_c48031_240	6B	227098077	-2.0312	0.00079	3.1
PI_H	FarmCPU	wsnp_Ex_c9948_16379867	6B	231466209	0.2325	0.00072	3.14
PI_H	GLM	wsnp_Ex_c9948_16379867	6B	231466209	0.2315	0.00087	3.06
FV/FM_H	FarmCPU	wsnp_Ex_c9948_16379867	6B	231466209	0.0253	0.00052	3.28
FV/FM_H	GLM	wsnp_Ex_c9948_16379867	6B	231466209	0.0253	0.00062	3.21
ADN	FarmCPU	wsnp_Ex_c9948_16379867	6B	231466209	0.0263	0.00042	3.38
ADN	GLM	wsnp_Ex_c9948_16379867	6B	231466209	0.0262	0.00051	3.3
ADN	MLM	wsnp_Ex_c9948_16379867	6B	231466209	0.026	0.00093	3.03
NDVI_H	FarmCPU	Excalibur_c83451_218	6B	257241507	0.0244	0.00097	3.01
CHL_30DAA	FarmCPU	RAC875_c47035_70	6B	465683531	0.5397	0.00046	3.34
CHL_30DAA	GLM	RAC875_c47035_70	6B	465683531	0.544	0.00044	3.36
CHL_30DAA	FarmCPU	GENE-0363_168	6B	470830381	0.5397	0.00046	3.34
CHL_30DAA	GLM	GENE-0363_168	6B	470830381	0.544	0.00044	3.36
TN	FarmCPU	IAAV4147	6B	528915536	0.4941	0.00097	3.01
SL	MLM	Ra_c5942_955	6B	577478964	0.5086	0.00041	3.38
SL	FarmCPU	Ra_c5942_955	6B	577478964	0.5086	0.00014	3.84
SL	GLM	Ra_c5942_955	6B	577478964	0.5026	0.0002	3.7
SL	MLM	Ku_c2212_411	6B	577479871	0.3615	0.00058	3.24
SL	FarmCPU	Ku_c2212_411	6B	577479871	0.3615	0.00023	3.64
SL	GLM	Ku_c2212_411	6B	577479871	0.3691	0.00019	3.73
SPS	FarmCPU	Ku_c2212_411	6B	577479871	0.4706	0.00083	3.08
SPS	GLM	Ku_c2212_411	6B	577479871	0.5009	0.00036	3.44
CHL_B	FarmCPU	Excalibur_c43557_540	6B	578100510	0.9285	0.00078	3.11
CHL_B	GLM	Excalibur_c43557_540	6B	578100510	0.9491	0.00072	3.14
FV/FM_A	FarmCPU	Excalibur_c43557_540	6B	578100510	0.0065	0.0009	3.05
FV/FM_A	GLM	Excalibur_c43557_540	6B	578100510	0.0066	0.00088	3.05
NDVI_14DAA	FarmCPU	Kukri_c29122_984	6B	618332275	0.0426	0.0009	3.04
CHL_20DAA	GLM	Kukri_rep_c104521_117	6B	634333515	1.9504	0.00084	3.08
CSFL	GLM	Kukri_rep_c104521_117	6B	634333515	3.276	0.00095	3.02
CHL_20DAA	FarmCPU	BobWhite_c28409_462	6B	635175431	1.9024	0.00032	3.5
CHL_20DAA	GLM	BobWhite_c28409_462	6B	635175431	1.8808	0.00038	3.43
CHL_20DAA	MLM	BobWhite_c28409_462	6B	635175431	1.9057	0.00076	3.12
PH	MLM	RFL_Contig2387_1410	6B	661464161	6.1554	0.00068	3.17
PH	FarmCPU	RFL_Contig2387_1410	6B	661464161	6.2551	2.65E-05	4.58
TN	FarmCPU	BS00074024_51	6B	664197646	0.1962	8.26E-05	4.08
TN	FarmCPU	BS00091306_51	6B	664217350	0.1972	6.57E-05	4.18
TN	FarmCPU	BobWhite_c12013_977	6B	664217781	0.1647	0.00089	3.05

TN	FarmCPU	RAC875_rep_c115149_377	6B	664218722	0.1647	0.00089	3.05
TN	FarmCPU	BS00062712_51	6B	664407561	0.1857	0.00043	3.37
TN	FarmCPU	Tdurum_contig45559_403	6B	664461756	0.1754	0.00092	3.04
ADSFL	FarmCPU	RAC875_c45515_65	6B	664835157	0.6263	0.00019	3.73
ADSFL	MLM	RAC875_c45515_65	6B	664835157	0.629	0.00073	3.14
TN	FarmCPU	Excalibur_c92249_102	6B	667963133	0.1769	5.34E-05	4.27
TN	FarmCPU	wsnp_Ex_c12433_19826311	6B	668429681	0.1548	0.00084	3.08
TN	FarmCPU	wsnp_Ku_c11846_19263340	6B	680541863	0.4941	0.00097	3.01
CHL_30DAA	FarmCPU	Ra_c5297_2104	6B	685978955	0.5352	0.00083	3.08
PI_21DAA	FarmCPU	Ra_c5297_2104	6B	685978955	0.0405	0.00083	3.08
CHL_30DAA	FarmCPU	BobWhite_c3514_717	6B	685982415	0.5352	0.00083	3.08
PI_21DAA	FarmCPU	BobWhite_c3514_717	6B	685982415	0.0405	0.00083	3.08
CHL_10DAA	FarmCPU	RAC875_c57095_240	6B	690303865	0.3493	0.00072	3.14
TN	FarmCPU	Tdurum_contig59339_428	6B	715751234	0.4207	0.00083	3.08
TN	FarmCPU	RAC875_c24832_252	6B	716258388	0.4941	0.00097	3.01
PH	FarmCPU	Excalibur_c78493_305	6B	717893216	3.8133	0.00039	3.41
FV/FM_21DAA	FarmCPU	Ex_c3405_203	6D	3976821	0.0017	0.00034	3.47
FV/FM_21DAA	GLM	Ex_c3405_203	6D	3976821	0.0016	0.00077	3.11
FV/FM_21DAA	MLM	Ex_c3405_203	6D	3976821	0.0017	0.00088	3.06
NDVI_A	FarmCPU	BobWhite_c11808_975	6D	7098479	-0.0454	0.00048	3.32
PI_21DAA	FarmCPU	IACX243	6D	81302142	0.0609	0.00012	3.93
PI_21DAA	GLM	IACX243	6D	81302142	0.0609	0.00012	3.91
PI_21DAA	MLM	IACX243	6D	81302142	0.0609	0.00035	3.45
RDN	GLM	Ra_c14408_576	6D	86760783	0.0657	0.00014	3.86
RDN	MLM	Ra_c14408_576	6D	86760783	0.0624	0.00083	3.08
TN	GLM	Tdurum_contig10194_765	6D	402494662	0.3097	5.01E-05	4.3
NDVI_A	FarmCPU	Excalibur_c827_883	6D	453013443	-0.0404	0.0006	3.22
TN	GLM	GENE-3988_79	6D	460568393	0.2249	0.00039	3.41
TN	GLM	wsnp_JD_c7795_8867843	6D	460570037	0.2249	0.00072	3.14
TN	GLM	BobWhite_c13504_378	6D	460573314	0.2139	0.00056	3.25
TN	GLM	Excalibur_c22599_921	6D	460700518	0.2291	0.0007	3.15
TN	GLM	GENE-3862_349	6D	460743475	0.1929	0.0007	3.16
CHL_20DAA	FarmCPU	RAC875_c2338_53	6D	462013888	2.9086	0.00034	3.46
CHL_20DAA	GLM	RAC875_c2338_53	6D	462013888	3.3586	0.00035	3.46
CHL_20DAA	MLM	RAC875_c2338_53	6D	462013888	2.9384	0.0008	3.1
PI_21DAA	FarmCPU	BobWhite_c3506_1559	6D	462631494	0.0609	0.00012	3.93
PI_21DAA	GLM	BobWhite_c3506_1559	6D	462631494	0.0609	0.00012	3.91
PI_21DAA	MLM	BobWhite_c3506_1559	6D	462631494	0.0609	0.00035	3.45
CHL_20DAA	FarmCPU	IAAV2130	6D	464345213	-1.7672	0.00022	3.66
CHL_20DAA	GLM	IAAV2130	6D	464345213	-1.7274	0.00066	3.18
CHL_20DAA	MLM	IAAV2130	6D	464345213	-1.7855	0.00056	3.25
CHL_B	GLM	CAP7_c2559_543	6D	471017889	0.9167	0.00088	3.06
NDVI_14DAA	FarmCPU	RAC875_c2666_528	6D	473083096	0.0447	0.0003	3.52

NDVI_14DAA	GLM	RAC875_c2666_528	6D	473083096	0.0438	0.00067	3.17
CHL_T	GLM	BS00109911_51	7A	653957	-0.9255	4.35E-05	4.36
ADN	GLM	BS00109911_51	7A	653957	-0.0124	0.00082	3.08
CHL_T	GLM	Ex_c13577_632	7A	762023	-0.6915	0.00088	3.06
ADN	GLM	Ex_c13577_632	7A	762023	-0.0114	0.00067	3.17
CHL_20DAA	FarmCPU	tplb0057f21_146	7A	1320120	-2.292	7.12E-05	4.15
CHL_20DAA	GLM	tplb0057f21_146	7A	1320120	-2.2671	0.00024	3.62
CSFL	FarmCPU	tplb0057f21_146	7A	1320120	-3.3913	0.00056	3.25
CHL_20DAA	MLM	tplb0057f21_146	7A	1320120	-2.2986	0.00026	3.58
CHL_20DAA	FarmCPU	Excalibur_c20311_388	7A	1371537	-2.1581	0.00031	3.51
CHL_20DAA	GLM	Excalibur_c20311_388	7A	1371537	-2.1215	0.00077	3.11
CSFL	FarmCPU	Excalibur_c20311_388	7A	1371537	-3.3718	0.00089	3.05
CHL_20DAA	MLM	Excalibur_c20311_388	7A	1371537	-2.1656	0.00076	3.12
CHL_H	FarmCPU	RAC875_c1553_129	7A	1705065	0.3272	0.00092	3.03
CHL_H	GLM	RAC875_c1553_129	7A	1705065	0.3444	0.00058	3.24
TN	FarmCPU	Excalibur_c23756_1461	7A	6485704	-0.4509	0.00023	3.64
TN	FarmCPU	GENE-4923_281	7A	6497498	-0.2178	0.00091	3.04
TN	FarmCPU	wsnp_Ex_rep_c66939_65371026	7A	7586802	-0.218	0.00059	3.23
CN	GLM	Tdurum_contig13048_89	7A	19420624	-0.0203	0.00032	3.5
CHL_H	FarmCPU	Excalibur_c7897_600	7A	27462851	0.4467	0.00048	3.32
NDVI_A	GLM	Kukri_c34887_734	7A	33364918	-0.0621	0.00073	3.14
NDVI_A	GLM	Tdurum_contig12722_779	7A	46720879	-0.0785	0.00024	3.61
NDVI_A	FarmCPU	Ex_c4463_146	7A	82193753	0.0371	0.00029	3.53
NDVI_A	FarmCPU	RAC875_c56439_58	7A	82531047	0.0336	0.00068	3.17
NDVI_14DAA	FarmCPU	wsnp_Ex_c24400_33645206	7A	84700489	-0.0601	0.0006	3.22
CHL_H	FarmCPU	Ku_c24562_206	7A	165824206	-0.6492	0.00066	3.18
CHL_H	GLM	Ku_c24562_206	7A	165824206	-0.7427	0.00043	3.36
NDVI_A	FarmCPU	BobWhite_c44628_61	7A	238589596	0.0858	0.00047	3.33
NDVI_A	FarmCPU	RAC875_rep_c107142_414	7A	239035785	0.0858	0.00047	3.33
NDVI_A	FarmCPU	Kukri_c11705_453	7A	240669581	0.0858	0.00047	3.33
PI_A	FarmCPU	BobWhite_c10229_415	7A	244469774	0.0623	0.00084	3.07
PI_A	GLM	BobWhite_c10229_415	7A	244469774	0.0653	0.00081	3.09
CN	FarmCPU	Excalibur_c200_1664	7A	244469935	0.0137	0.00099	3
CN	GLM	Excalibur_c200_1664	7A	244469935	0.0154	0.0003	3.53
NDVI_H	GLM	RAC875_c23581_105	7A	391912286	0.0227	0.00083	3.08
NDVI_A	FarmCPU	RAC875_c23581_105	7A	391912286	0.0345	6.12E-05	4.21
NDVI_A	GLM	RAC875_c23581_105	7A	391912286	0.0327	6.59E-05	4.18
NDVI_A	MLM	RAC875_c23581_105	7A	391912286	0.0336	0.00069	3.16
NDVI_A	FarmCPU	BS00068158_51	7A	448260409	0.047	0.00016	3.81
CN	FarmCPU	BS00068158_51	7A	448260409	0.0248	0.00084	3.07
PI_14DAA	FarmCPU	BobWhite_rep_c65070_369	7A	452754928	0.1891	0.00081	3.09
FV/FM_14DAA	FarmCPU	BobWhite_rep_c65070_369	7A	452754928	0.0192	0.00069	3.16
NDVI_A	FarmCPU	BobWhite_rep_c65070_369	7A	452754928	0.0579	3.11E-06	5.51

NDVI_A	GLM	BobWhite_rep_c65070_369	7A	452754928	0.0483	0.00026	3.59
CN	FarmCPU	BobWhite_rep_c65070_369	7A	452754928	0.0284	0.00016	3.8
CN	GLM	BobWhite_rep_c65070_369	7A	452754928	0.0298	0.00035	3.46
NDVI_A	MLM	BobWhite_rep_c65070_369	7A	452754928	0.0564	0.00018	3.76
CN	MLM	BobWhite_rep_c65070_369	7A	452754928	0.0304	0.00056	3.25
PI_14DAA	FarmCPU	CAP12_c2355_239	7A	458711102	0.1891	0.00081	3.09
FV/FM_14DAA	FarmCPU	CAP12_c2355_239	7A	458711102	0.0192	0.00069	3.16
NDVI_A	FarmCPU	CAP12_c2355_239	7A	458711102	0.0579	3.11E-06	5.51
NDVI_A	GLM	CAP12_c2355_239	7A	458711102	0.0483	0.00026	3.59
CN	FarmCPU	CAP12_c2355_239	7A	458711102	0.0284	0.00016	3.8
CN	GLM	CAP12_c2355_239	7A	458711102	0.0298	0.00035	3.46
NDVI_A	MLM	CAP12_c2355_239	7A	458711102	0.0564	0.00018	3.76
CN	MLM	CAP12_c2355_239	7A	458711102	0.0304	0.00056	3.25
NDVI_A	FarmCPU	CAP11_c1937_302	7A	459633196	0.0859	0.00023	3.63
NDVI_A	FarmCPU	Tdurum_contig48442_645	7A	466520181	0.0859	0.00023	3.63
CN	FarmCPU	BS00002897_51	7A	492781802	0.0144	0.00062	3.2
CN	GLM	BS00002897_51	7A	492781802	0.0144	0.0009	3.04
CHL_A	GLM	BS00054416_51	7A	501647852	0.3294	0.00033	3.48
CN	FarmCPU	wsnp_JD_c14118_13933380	7A	511931110	0.0148	0.0006	3.22
CN	GLM	wsnp_JD_c14118_13933380	7A	511931110	0.015	0.00076	3.12
PI_H	GLM	BS00034509_51	7A	512250750	0.0524	0.00089	3.05
CN	FarmCPU	BS00034509_51	7A	512250750	0.014	0.00082	3.09
CN	GLM	BS00034509_51	7A	512250750	0.0143	0.00099	3
PI_H	GLM	BS00100351_51	7A	512339108	0.0535	0.00073	3.14
CHL_A	FarmCPU	IACX11096	7A	512339191	0.3811	0.0006	3.23
PI_H	GLM	BS00099881_51	7A	512760251	0.0532	0.00078	3.11
CHL_A	FarmCPU	wsnp_JD_c15333_14824351	7A	512760456	0.3888	0.00042	3.38
CHL_A	GLM	wsnp_JD_c15333_14824351	7A	512760456	0.3907	0.00095	3.02
PI_A	GLM	wsnp_Ex_c558_1105911	7A	513991178	0.0434	0.00059	3.23
CN	FarmCPU	wsnp_Ex_c558_1105911	7A	513991178	0.0146	0.00082	3.09
CN	GLM	wsnp_Ex_c558_1105911	7A	513991178	0.0151	0.00077	3.11
NDVI_A	FarmCPU	BS00091168_51	7A	521952104	0.0487	3.59E-05	4.45
NDVI_A	GLM	BS00091168_51	7A	521952104	0.0405	0.00058	3.24
NDVI_A	MLM	BS00091168_51	7A	521952104	0.0456	0.00066	3.18
NDVI_A	FarmCPU	wsnp_Ex_rep_c104560_89241494	7A	531193028	0.0487	3.59E-05	4.45
NDVI_A	GLM	wsnp_Ex_rep_c104560_89241494	7A	531193028	0.0405	0.00058	3.24
NDVI_A	MLM	wsnp_Ex_rep_c104560_89241494	7A	531193028	0.0456	0.00066	3.18
NDVI_H	FarmCPU	Excalibur_c27658_264	7A	536152491	0.0373	0.00038	3.42
NDVI_A	FarmCPU	Excalibur_c27658_264	7A	536152491	0.0624	6.46E-07	6.19
NDVI_A	GLM	Excalibur_c27658_264	7A	536152491	0.0532	5.10E-05	4.29
NDVI_14DAA	FarmCPU	Excalibur_c27658_264	7A	536152491	0.0478	0.00012	3.9
CN	FarmCPU	Excalibur_c27658_264	7A	536152491	0.0269	0.00049	3.31
NDVI_A	MLM	Excalibur_c27658_264	7A	536152491	0.0605	6.70E-05	4.17

CHL_10DAA	FarmCPU	BS00065462_51	7A	540057016	1.648	0.00055	3.26
CHL_10DAA	GLM	BS00065462_51	7A	540057016	1.6077	0.00064	3.2
CSFL	FarmCPU	BS00065462_51	7A	540057016	10.708	0.00028	3.56
CSFL	GLM	BS00065462_51	7A	540057016	10.565	0.00035	3.46
CSFL	MLM	BS00065462_51	7A	540057016	10.662	0.00069	3.16
CHL_10DAA	FarmCPU	Kukri_c66328_222	7A	544263660	1.648	0.00055	3.26
CHL_10DAA	GLM	Kukri_c66328_222	7A	544263660	1.6077	0.00064	3.2
CSFL	FarmCPU	Kukri_c66328_222	7A	544263660	10.708	0.00028	3.56
CSFL	GLM	Kukri_c66328_222	7A	544263660	10.565	0.00035	3.46
CSFL	MLM	Kukri_c66328_222	7A	544263660	10.662	0.00069	3.16
PI_H	FarmCPU	wsnp_bq170165A_Ta_1_1	7A	553385076	-0.0724	0.00066	3.18
PI_H	GLM	wsnp_bq170165A_Ta_1_1	7A	553385076	-0.0737	0.00062	3.2
FV/FM_H	FarmCPU	wsnp_bq170165A_Ta_1_1	7A	553385076	-0.0077	0.00066	3.18
FV/FM_H	GLM	wsnp_bq170165A_Ta_1_1	7A	553385076	-0.0078	0.00066	3.18
ADN	FarmCPU	wsnp_bq170165A_Ta_1_1	7A	553385076	-0.0077	0.00084	3.08
ADN	GLM	wsnp_bq170165A_Ta_1_1	7A	553385076	-0.0079	0.00076	3.12
NDVI_A	FarmCPU	Excalibur_c2359_1511	7A	576454285	0.0858	0.00047	3.33
CSFL	GLM	RAC875_rep_c105182_460	7A	585066042	4.1502	0.00086	3.07
CHL_10DAA	GLM	Ra_c8985_557	7A	611804564	0.6591	0.00098	3.01
TN	FarmCPU	RAC875_c1265_1564	7A	635499453	0.9882	0.00097	3.01
TN	FarmCPU	Kukri_c4143_1055	7A	635500658	0.4941	0.00097	3.01
CHL_10DAA	FarmCPU	RAC875_c27696_798	7A	644611118	1.648	0.00055	3.26
CHL_10DAA	GLM	RAC875_c27696_798	7A	644611118	1.6077	0.00064	3.2
CSFL	FarmCPU	RAC875_c27696_798	7A	644611118	10.708	0.00028	3.56
CSFL	GLM	RAC875_c27696_798	7A	644611118	10.565	0.00035	3.46
CSFL	MLM	RAC875_c27696_798	7A	644611118	10.662	0.00069	3.16
SL	GLM	wsnp_Ra_c42862_49716715	7A	645028845	0.493	0.00098	3.01
SPS	GLM	wsnp_Ra_c42862_49716715	7A	645028845	0.7028	0.00091	3.04
NDVI_14DAA	FarmCPU	BS00042116_51	7A	645094419	-0.0475	0.00054	3.27
CHL_10DAA	GLM	wsnp_Ku_c1552_3060297	7A	645944949	0.4454	0.00085	3.07
CHL_10DAA	GLM	Ku_c11884_1220	7A	671466964	0.5636	0.00052	3.28
CHL_B	FarmCPU	BS00026622_51	7A	674272175	0.7579	0.00059	3.23
CHL_B	GLM	BS00026622_51	7A	674272175	0.8328	0.00033	3.48
NDVI_14DAA	FarmCPU	RAC875_c63057_601	7A	675587576	-0.0528	0.00055	3.26
SPS	FarmCPU	Kukri_c13171_474	7A	717311186	-0.7226	0.00055	3.26
SPS	GLM	Kukri_c13171_474	7A	717311186	-0.7878	0.00034	3.47
NDVI_A	FarmCPU	RAC875_c31997_103	7A	719567500	0.03	0.00058	3.24
NDVI_A	FarmCPU	RAC875_c65335_221	7A	719569211	0.0365	6.14E-05	4.21
NDVI_H	FarmCPU	CAP8_c4980_112	7A	719571317	0.0253	0.00037	3.44
NDVI_A	FarmCPU	CAP8_c4980_112	7A	719571317	0.0409	1.66E-06	5.78
NDVI_A	GLM	CAP8_c4980_112	7A	719571317	0.0354	2.85E-05	4.55
RDN	FarmCPU	CAP8_c4980_112	7A	719571317	-0.0181	0.00051	3.29
NDVI_A	MLM	CAP8_c4980_112	7A	719571317	0.0354	0.00023	3.63

NDVI_A	FarmCPU	BS00002510_51	7A	721000126	0.0356	1.87E-05	4.73
NDVI_A	GLM	BS00002510_51	7A	721000126	0.0344	1.14E-05	4.94
NDVI_A	MLM	BS00002510_51	7A	721000126	0.0322	0.00047	3.33
NDVI_A	FarmCPU	BS00067682_51	7A	721223694	0.0293	0.00041	3.39
NDVI_H	FarmCPU	Tdurum_contig42487_1555	7A	721224332	0.0227	0.00077	3.12
NDVI_H	GLM	Tdurum_contig42487_1555	7A	721224332	0.0215	0.00093	3.03
NDVI_A	FarmCPU	Tdurum_contig42487_1555	7A	721224332	0.0355	1.48E-05	4.83
NDVI_A	GLM	Tdurum_contig42487_1555	7A	721224332	0.0333	1.89E-05	4.72
NDVI_A	MLM	Tdurum_contig42487_1555	7A	721224332	0.0316	0.00042	3.37
PI_14DAA	FarmCPU	BS00068575_51	7A	721416201	0.1226	0.00086	3.06
NDVI_A	FarmCPU	BS00068575_51	7A	721416201	0.031	0.00018	3.75
NDVI_A	GLM	BS00068575_51	7A	721416201	0.0287	0.00026	3.58
NDVI_A	FarmCPU	BS00068033_51	7A	721417550	0.0334	8.97E-05	4.05
NDVI_A	GLM	BS00068033_51	7A	721417550	0.0313	0.00011	3.95
CHL_B	FarmCPU	wsnp_CAP8_c334_304253	7B	6753259	-1.5584	0.00013	3.87
CHL_B	GLM	wsnp_CAP8_c334_304253	7B	6753259	-1.5861	0.00013	3.9
PI_A	FarmCPU	wsnp_CAP8_c334_304253	7B	6753259	-0.1003	0.00062	3.21
PI_A	GLM	wsnp_CAP8_c334_304253	7B	6753259	-0.1033	0.00049	3.31
CHL_B	MLM	wsnp_CAP8_c334_304253	7B	6753259	-1.5584	0.00039	3.41
CN	FarmCPU	Excalibur_c41298_459	7B	28500711	-0.0257	0.001	3
NDVI_14DAA	FarmCPU	RAC875_c195_499	7B	64478331	-0.0499	0.00012	3.91
NDVI_14DAA	GLM	RAC875_c195_499	7B	64478331	-0.0451	0.00055	3.26
NDVI_14DAA	MLM	RAC875_c195_499	7B	64478331	-0.0503	0.00084	3.08
NDVI_14DAA	FarmCPU	Ku_c9561_699	7B	86666894	-0.035	0.00038	3.42
NDVI_A	GLM	BS00021979_51	7B	92718067	-0.0816	0.00073	3.14
CHL_H	FarmCPU	RAC875_rep_c116436_106	7B	126557715	-0.6492	0.00066	3.18
CHL_H	GLM	RAC875_rep_c116436_106	7B	126557715	-0.7427	0.00043	3.36
PI_A	FarmCPU	GENE-4867_119	7B	127022774	0.0465	0.00076	3.12
NDVI_A	FarmCPU	Kukri_c57677_355	7B	155727282	-0.0285	0.00035	3.46
NDVI_A	FarmCPU	Excalibur_rep_c67190_638	7B	165531843	-0.0275	0.00054	3.27
NDVI_A	FarmCPU	BobWhite_c45737_97	7B	185625059	-0.0264	0.00098	3.01
NDVI_14DAA	FarmCPU	RAC875_rep_c70874_1920	7B	198938722	-0.0409	0.00015	3.82
TN	FarmCPU	Excalibur_rep_c116920_300	7B	218382506	0.5996	0.00017	3.76
TN	FarmCPU	Excalibur_rep_c116278_53	7B	221262445	0.4941	0.00097	3.01
NDVI_14DAA	FarmCPU	Kukri_rep_c72585_111	7B	221262974	-0.0383	0.00041	3.38
TN	FarmCPU	Kukri_c29386_182	7B	225392979	0.4323	0.00062	3.21
PI_14DAA	FarmCPU	Kukri_c24422_423	7B	400418416	0.1891	0.00081	3.09
FV/FM_14DAA	FarmCPU	Kukri_c24422_423	7B	400418416	0.0192	0.00069	3.16
NDVI_A	FarmCPU	Kukri_c24422_423	7B	400418416	0.0579	3.11E-06	5.51
NDVI_A	GLM	Kukri_c24422_423	7B	400418416	0.0483	0.00026	3.59
CN	FarmCPU	Kukri_c24422_423	7B	400418416	0.0284	0.00016	3.8
CN	GLM	Kukri_c24422_423	7B	400418416	0.0298	0.00035	3.46
NDVI_A	MLM	Kukri_c24422_423	7B	400418416	0.0564	0.00018	3.76

CN	MLM	Kukri_c24422_423	7B	400418416	0.0304	0.00056	3.25
PI_14DAA	FarmCPU	Kukri_c32807_579	7B	401552201	0.1891	0.00081	3.09
FV/FM_14DAA	FarmCPU	Kukri_c32807_579	7B	401552201	0.0192	0.00069	3.16
NDVI_A	FarmCPU	Kukri_c32807_579	7B	401552201	0.0579	3.11E-06	5.51
NDVI_A	GLM	Kukri_c32807_579	7B	401552201	0.0483	0.00026	3.59
CN	FarmCPU	Kukri_c32807_579	7B	401552201	0.0284	0.00016	3.8
CN	GLM	Kukri_c32807_579	7B	401552201	0.0298	0.00035	3.46
NDVI_A	MLM	Kukri_c32807_579	7B	401552201	0.0564	0.00018	3.76
CN	MLM	Kukri_c32807_579	7B	401552201	0.0304	0.00056	3.25
PI_21DAA	FarmCPU	Kukri_c46962_1500	7B	403561796	0.0623	0.00093	3.03
NDVI_A	FarmCPU	IACX1743	7B	478859879	-0.0305	0.00079	3.1
NDVI_A	FarmCPU	Excalibur_c16687_207	7B	488411084	0.0557	0.00033	3.48
NDVI_A	GLM	Excalibur_c16687_207	7B	488411084	0.0537	0.00024	3.62
TN	FarmCPU	Excalibur_c15029_144	7B	497883345	0.3914	6.28E-05	4.2
NDVI_H	FarmCPU	BS00044443_51	7B	498149672	-0.0385	7.73E-05	4.11
NDVI_A	FarmCPU	BS00044443_51	7B	498149672	-0.0436	0.00034	3.47
NDVI_14DAA	FarmCPU	BS00044443_51	7B	498149672	-0.0439	0.00017	3.76
RDN	FarmCPU	BS00044443_51	7B	498149672	0.0247	0.00061	3.22
NDVI_H	MLM	BS00044443_51	7B	498149672	-0.0376	0.00082	3.09
CHL_A	FarmCPU	Tdurum_contig43589_340	7B	505939834	0.3845	0.00099	3
NDVI_14DAA	FarmCPU	RAC875_c2887_52	7B	518386618	-0.0305	0.00081	3.09
CHL_A	FarmCPU	Kukri_c22996_334	7B	518388296	-0.3574	0.00029	3.54
CHL_A	GLM	Kukri_c22996_334	7B	518388296	-0.3493	0.00068	3.17
NDVI_14DAA	FarmCPU	Ex_c54863_29	7B	561748635	-0.0566	0.00083	3.08
NDVI_H	FarmCPU	Ku_c682_187	7B	568488316	-0.0284	0.00034	3.47
NDVI_A	FarmCPU	Ku_c682_187	7B	568488316	-0.0353	0.00032	3.49
NDVI_14DAA	FarmCPU	Ku_c682_187	7B	568488316	-0.0342	0.00032	3.49
NDVI_H	FarmCPU	BS00108573_51	7B	568497112	-0.0293	0.00042	3.37
NDVI_14DAA	FarmCPU	BS00108573_51	7B	568497112	-0.0356	0.00033	3.48
NDVI_14DAA	FarmCPU	Tdurum_contig93081_162	7B	569419639	-0.0335	0.00047	3.33
NDVI_A	FarmCPU	wsnp_Ex_c421_832555	7B	572416743	-0.0245	0.00099	3
NDVI_A	FarmCPU	wsnp_Ex_c27323_36528037	7B	573923612	-0.0241	0.00098	3.01
NDVI_A	FarmCPU	Kukri_c21426_234	7B	574477210	-0.0241	0.00098	3.01
PI_21DAA	FarmCPU	Excalibur_c5700_244	7B	608907515	0.0448	0.00089	3.05
PI_21DAA	GLM	Excalibur_c5700_244	7B	608907515	0.0455	0.0009	3.05
CHL_10DAA	GLM	BS00080621_51	7B	648926278	0.8382	0.00079	3.1
NDVI_14DAA	FarmCPU	BS00014946_51	7B	648926388	-0.0286	0.00086	3.07
CHL_10DAA	GLM	wsnp_Ex_c10193_16730348	7B	648926428	0.805	0.00095	3.02
RDN	GLM	wsnp_Ex_c19_38763	7B	693338535	0.0685	0.00079	3.1
PH	FarmCPU	IAAV2580	7B	700829988	-3.5842	0.00077	3.12
PH	GLM	IAAV2580	7B	700829988	-3.6652	0.00034	3.47
PI_21DAA	FarmCPU	Tdurum_contig23273_179	7B	713859681	0.0212	0.00029	3.54
PI_21DAA	GLM	Tdurum_contig23273_179	7B	713859681	0.022	0.00018	3.73

FV/FM_21DAA	FarmCPU	Tdurum_contig23273_179	7B	713859681	0.0019	0.00027	3.58
FV/FM_21DAA	GLM	Tdurum_contig23273_179	7B	713859681	0.002	0.00022	3.65
PI_21DAA	MLM	Tdurum_contig23273_179	7B	713859681	0.0212	0.0007	3.16
FV/FM_21DAA	MLM	Tdurum_contig23273_179	7B	713859681	0.002	0.00064	3.2
PI_14DAA	GLM	Excalibur_c1070_2327	7B	720118816	-0.1472	0.00056	3.25
FV/FM_14DAA	GLM	Excalibur_c1070_2327	7B	720118816	-0.0149	0.00054	3.27
NDVI_14DAA	FarmCPU	Excalibur_c64848_1214	7B	725383266	-0.0287	0.00029	3.54
ADN	GLM	wsnp_CAP7_c172_96407	7B	727635203	-0.0059	0.00097	3.01
NDVI_A	GLM	Excalibur_c3510_159	7B	728281808	-0.0816	0.00073	3.14
NDVI_14DAA	FarmCPU	Ra_c69234_623	7B	728694490	-0.0263	0.0008	3.09
NDVI_A	GLM	Tdurum_contig44897_359	7B	728812366	-0.0816	0.00073	3.14
CHL_20DAA	FarmCPU	D_GBB4FNX02GR409_184	7D	744989	-2.1581	0.00031	3.51
CHL_20DAA	GLM	D_GBB4FNX02GR409_184	7D	744989	-2.1215	0.00077	3.11
CSFL	FarmCPU	D_GBB4FNX02GR409_184	7D	744989	-3.3718	0.00089	3.05
CHL_20DAA	MLM	D_GBB4FNX02GR409_184	7D	744989	-2.1656	0.00076	3.12
NDVI_A	FarmCPU	Ku_c4868_489	7D	2090345	-0.116	0.00014	3.84
NDVI_A	GLM	Ku_c4868_489	7D	2090345	-0.114	7.11E-05	4.15
NDVI_A	MLM	Ku_c4868_489	7D	2090345	-0.1181	0.00019	3.72
TN	FarmCPU	Excalibur_c46904_84	7D	5198912	0.3032	0.00012	3.92
CHL_10DAA	FarmCPU	wsnp_Ex_c5231_9256482	7D	9304289	0.8054	0.00081	3.09
CHL_10DAA	GLM	wsnp_Ex_c5231_9256482	7D	9304289	0.7909	0.00086	3.07
NDVI_A	FarmCPU	RAC875_rep_c112035_88	7D	411308291	0.0859	0.00023	3.63
NDVI_A	FarmCPU	Kukri_rep_c68399_107	7D	412673315	0.0859	0.00023	3.63
PH	FarmCPU	Ku_c3571_104	7D	527734576	-2.5536	9.92E-05	4
PH	GLM	Ku_c3571_104	7D	527734576	-2.3615	0.00027	3.58
PH	MLM	Ku_c3571_104	7D	527734576	-2.5504	0.00057	3.25
NDVI_A	GLM	IACX7421	7D	627323770	-0.0816	0.00073	3.14

Chromosome (CHROM), Chlorophyll content at tillering (CHL_T), Chlorophyll content at booting (CHL_B), Chlorophyll content at heading (CHL_H), Chlorophyll content at anthesis (CHL_A), Chlorophyll content at 10 days after anthesis (CHL_10DAA), Chlorophyll content at 20 days after anthesis (CHL_20DAA), Chlorophyll content at 30 days after anthesis (CHL_30DAA), photosynthetic efficiency at heading (fv/fm_H), photosynthetic efficiency at anthesis (fv/fm_A), photosynthetic efficiency at 14 days after anthesis (fv/fm_14DAA), photosynthetic efficiency at 21 days after anthesis (fv/fm_21DAA), NDVI at heading (NDVI_H), NDVI at anthesis (NDVI_A), NDVI at 14 days after anthesis (NDVI_14DAA), NDVI at 21 days after anthesis (NDVI_21DAA), Plant height (PH), Tiller number (TN), Spike length (SL), Spikelet per spike (SPS), Thousand kernel weight (TKW), Grain yield (GY), Biological yield (BY).

Annexure 2.3. High confidence protein coding genes at 20 multi-method GWAS loci.

Chr	Start	End	Strand	ID	Gene description
1B	14551564	14568041	+	TraesCS1B02G029600	
1B	14609435	14626525	+	TraesCS1B02G029700	
1B	14634788	14656402	+	TraesCS1B02G029800	
1B	14691678	14692533	-	TraesCS1B02G029900	
1B	14843598	14847648	+	TraesCS1B02G030000	
1B	14864455	14866465	+	TraesCS1B02G030100	
1B	14929251	14931368	+	TraesCS1B02G030200	
1B	14950407	14952265	-	TraesCS1B02G030300	
1B	15038439	15042452	-	TraesCS1B02G030400	Beta-galactosidase
1B	15097670	15100117	-	TraesCS1B02G030500	
1B	15107810	15112122	-	TraesCS1B02G030600	
1B	15141444	15142626	+	TraesCS1B02G030700	
1B	15165681	15176969	-	TraesCS1B02G030800	
1B	15236935	15238182	-	TraesCS1B02G030900	
1B	15288136	15290367	+	TraesCS1B02G031000	
1B	15290430	15295770	-	TraesCS1B02G031100	
1B	15339921	15340166	+	TraesCS1B02G031200	
1B	15421816	15422013	+	TraesCS1B02G031400	
1B	15438996	15441928	-	TraesCS1B02G031500	
1B	15448355	15451124	-	TraesCS1B02G031600	
1B	15517132	15519874	-	TraesCS1B02G031700	
1B	15526043	15528357	+	TraesCS1B02G031800	
1B	15530721	15530918	-	TraesCS1B02G031900	
1B	15578829	15579449	+	TraesCS1B02G032000	
1B	15638525	15641235	-	TraesCS1B02G032100	
1B	15655141	15661187	+	TraesCS1B02G032200	
1B	15707939	15713937	+	TraesCS1B02G032300	
1B	15742607	15743947	-	TraesCS1B02G032400	
1B	15744865	15751148	-	TraesCS1B02G032500	Probable serine/threonine-protein kinase WNK3
1B	15869836	15875064	+	TraesCS1B02G032600	
1B	15875847	15879684	+	TraesCS1B02G032700	
1B	15895667	15903558	-	TraesCS1B02G032800	
1B	631064445	631068250	-	TraesCS1B02G400500	
1B	631199519	631204466	-	TraesCS1B02G400600	
1B	631218083	631219195	-	TraesCS1B02G400700	
1B	631219588	631221927	-	TraesCS1B02G400800	
1B	631224329	631227033	-	TraesCS1B02G400900	
1B	631228409	631232363	-	TraesCS1B02G401000	
1B	631235094	631236013	-	TraesCS1B02G401100	

1B	631715199	631718677	+	TraesCS1B02G401200	
1B	631817925	631821586	-	TraesCS1B02G401300	
1B	631822128	631826952	-	TraesCS1B02G401400	
1B	631824771	631825835	+	TraesCS1B02G401500	
1B	631829400	631834179	+	TraesCS1B02G401600	
1B	631966428	631967910	-	TraesCS1B02G401700	
1B	631998104	632003904	+	TraesCS1B02G401800	At3g09740
1B	632003412	632007555	-	TraesCS1B02G401900	
1B	632009540	632011743	+	TraesCS1B02G402000	
1B	632014277	632018299	-	TraesCS1B02G402100	
1B	632145930	632156551	+	TraesCS1B02G402200	
1B	632165694	632166277	+	TraesCS1B02G402300	
1B	632170249	632173063	-	TraesCS1B02G402400	
1B	632217912	632218980	+	TraesCS1B02G402500	
1B	632420586	632423487	-	TraesCS1B02G402600	Fatty acyl-CoA reductase
1B	677616438	677634748	+	TraesCS1B02G468200	
1B	677815221	677816368	+	TraesCS1B02G468300	
1B	677867016	677868183	+	TraesCS1B02G468400	
1B	677907793	677909146	-	TraesCS1B02G468500	
1B	677913314	677915244	-	TraesCS1B02G468600	
1B	678046588	678050014	+	TraesCS1B02G468700	
1B	678050434	678056351	+	TraesCS1B02G468800	
1B	678064979	678070061	-	TraesCS1B02G468900	
1B	678206080	678207042	+	TraesCS1B02G469000	
1B	678218420	678219774	+	TraesCS1B02G469100	
1B	678254205	678257639	+	TraesCS1B02G469200	
1B	678259512	678261620	-	TraesCS1B02G469300	
1B	678262382	678268692	-	TraesCS1B02G469400	
1B	678310982	678319110	+	TraesCS1B02G469500	
1B	678404549	678405588	+	TraesCS1B02G469600	
1B	678431974	678445604	-	TraesCS1B02G469700	
1B	678469928	678471544	+	TraesCS1B02G469800	
1B	678500501	678501881	+	TraesCS1B02G469900	
1B	678547556	678551346	-	TraesCS1B02G470000	
1B	678551590	678553297	-	TraesCS1B02G470100	
1B	678605176	678606528	-	TraesCS1B02G470300	
1B	678752741	678753061	-	TraesCS1B02G470400	
1B	678754223	678765854	-	TraesCS1B02G470500	
1B	678779472	678790974	-	TraesCS1B02G470600	
1B	678907766	678908358	+	TraesCS1B02G470700	
1B	679030727	679033146	-	TraesCS1B02G470800	
1B	679174332	679175169	+	TraesCS1B02G470900	
1D	459519000	459523642	+	TraesCS1D02G386600	

1D	459624435	459627780	-	TraesCS1D02G386700	
1D	459816528	459817580	+	TraesCS1D02G386800	
1D	459817628	459818686	-	TraesCS1D02G386900	
1D	459831193	459838843	+	TraesCS1D02G387000	
1D	459879406	459880864	-	TraesCS1D02G387100	
1D	459886610	459890441	+	TraesCS1D02G387200	
1D	459892031	459896082	-	TraesCS1D02G387300	
1D	459903149	459903520	-	TraesCS1D02G387400	
1D	460142745	460144820	+	TraesCS1D02G387500	
1D	460147069	460151558	-	TraesCS1D02G387600	
1D	460152897	460159561	+	TraesCS1D02G387700	
1D	460166506	460169710	-	TraesCS1D02G387800	
1D	460177436	460178040	+	TraesCS1D02G387900	
1D	460190851	460193819	+	TraesCS1D02G388000	
1D	460252125	460258476	-	TraesCS1D02G388100	
1D	460301679	460304044	-	TraesCS1D02G388200	
1D	460326939	460331231	-	TraesCS1D02G388300	
2B	108229860	108231756	+	TraesCS2B02G141700	Beta-amylase
2B	108231966	108235902	-	TraesCS2B02G141800	
2B	108237682	108242312	-	TraesCS2B02G141900	
2B	108795498	108797770	+	TraesCS2B02G142000	
2B	108996951	109000649	-	TraesCS2B02G142100	
2B	109084989	109092675	-	TraesCS2B02G142200	
2B	109162176	109162791	+	TraesCS2B02G142300	
2B	109180671	109184323	-	TraesCS2B02G142400	
2B	109194110	109204305	-	TraesCS2B02G142500	
2B	109209278	109210221	-	TraesCS2B02G142600	
2B	133526561	133530232	-	TraesCS2B02G159800	
2B	133580027	133583731	-	TraesCS2B02G159900	
2B	133619552	133619929	-	TraesCS2B02G160000	
2B	133689733	133697900	-	TraesCS2B02G160100	
2B	133702290	133709007	-	TraesCS2B02G160200	
2B	133806215	133807080	-	TraesCS2B02G160300	
2B	133847166	133850677	-	TraesCS2B02G160400	
2B	134041972	134044060	-	TraesCS2B02G160500	
2B	134044319	134049353	-	TraesCS2B02G160600	
2B	134089986	134094837	-	TraesCS2B02G160700	
2B	134240300	134249722	-	TraesCS2B02G160800	
2B	134252585	134254779	-	TraesCS2B02G160900	
2B	134254823	134257772	-	TraesCS2B02G161000	
2B	134341627	134342555	+	TraesCS2B02G161100	
2B	134345388	134354965	-	TraesCS2B02G161200	
2B	134364241	134366623	-	TraesCS2B02G161300	

2B	134476861	134499133	-	TraesCS2B02G161400	
2B	134510507	134513347	-	TraesCS2B02G161500	
2B	134600303	134608690	-	TraesCS2B02G161600	
2B	134702368	134704526	+	TraesCS2B02G161700	
2B	697007136	697007654	+	TraesCS2B02G501600	
2B	697141935	697142588	-	TraesCS2B02G501700	Cysteine proteinase inhibitor
2B	697156916	697157553	-	TraesCS2B02G501800	Cysteine proteinase inhibitor
2B	697223516	697224750	+	TraesCS2B02G501900	
2B	697286600	697287211	+	TraesCS2B02G502000	
2B	697294756	697295142	-	TraesCS2B02G502100	Cysteine proteinase inhibitor
2B	697334132	697334743	+	TraesCS2B02G502200	
2B	697340985	697341371	-	TraesCS2B02G502300	Cysteine proteinase inhibitor
2B	697352450	697353061	+	TraesCS2B02G502400	
2B	697370753	697371364	+	TraesCS2B02G502500	
2B	697378406	697378986	-	TraesCS2B02G502600	Cysteine proteinase inhibitor
2B	697394210	697394821	+	TraesCS2B02G502700	
2B	697398239	697398802	-	TraesCS2B02G502800	Cysteine proteinase inhibitor
2B	697438813	697439560	+	TraesCS2B02G502900	
2B	697440940	697444611	-	TraesCS2B02G503000	
2B	697546485	697548362	+	TraesCS2B02G503100	Glycosyltransferase
2B	697571625	697587793	-	TraesCS2B02G503200	
2B	697665455	697666303	+	TraesCS2B02G503300	
2B	697707263	697714188	-	TraesCS2B02G503400	Phosphatidylinositol 4-phosphate 5-kinase
2B	697767267	697768957	+	TraesCS2B02G503500	Cyclin-U1-1
2B	697976012	697980451	+	TraesCS2B02G503600	
2B	697986239	697996332	+	TraesCS2B02G503700	
2B	698002411	698004562	+	TraesCS2B02G503800	
2B	698203732	698213036	+	TraesCS2B02G503900	
2B	698212664	698217597	-	TraesCS2B02G504000	
2B	698294968	698296747	-	TraesCS2B02G504100	
2B	698302435	698302989	-	TraesCS2B02G504200	
2B	698303626	698306747	-	TraesCS2B02G504300	
2B	731561401	731564433	-	TraesCS2B02G535800	
2B	731600447	731603049	+	TraesCS2B02G535900	
2B	731603259	731609742	+	TraesCS2B02G536000	Golgin candidate 2
2B	731889302	731896486	+	TraesCS2B02G536100	
2B	731895898	731898962	-	TraesCS2B02G536200	
2B	731933894	731935553	-	TraesCS2B02G536300	
2B	732017353	732020895	-	TraesCS2B02G536400	
2B	732038730	732042160	-	TraesCS2B02G536500	
2B	732044802	732047394	-	TraesCS2B02G536600	
2B	732222759	732224651	+	TraesCS2B02G536700	

2B	732223289	732223837	-	TraesCS2B02G536800	
2B	732342397	732344660	+	TraesCS2B02G536900	
2B	732346480	732352286	+	TraesCS2B02G537000	
2B	732567244	732570497	-	TraesCS2B02G537100	
2B	732591609	732592582	-	TraesCS2B02G537200	
2B	732597482	732606603	+	TraesCS2B02G537300	
2B	732839527	732839826	-	TraesCS2B02G537400	
2B	732893022	732894677	+	TraesCS2B02G537500	
2B	733062825	733073795	+	TraesCS2B02G537600	
2B	733076628	733078033	-	TraesCS2B02G537700	Peroxidase
2B	733178973	733186807	+	TraesCS2B02G537800	
2B	733267240	733267973	-	TraesCS2B02G537900	
2B	733470137	733475121	-	TraesCS2B02G538000	
2B	733642201	733647003	-	TraesCS2B02G538100	
2B	733713197	733716418	-	TraesCS2B02G538200	
2B	733730631	733732147	-	TraesCS2B02G538300	
2B	733732194	733732934	-	TraesCS2B02G538400	
2B	733742977	733747406	-	TraesCS2B02G538500	
2B	733889920	733892344	-	TraesCS2B02G538600	
2B	733970649	733973385	-	TraesCS2B02G538700	
2B	734050489	734050911	-	TraesCS2B02G538800	
2B	734123952	734127544	+	TraesCS2B02G538900	
2B	734185174	734185410	-	TraesCS2B02G539000	
2B	734199796	734200667	-	TraesCS2B02G539100	
2B	734397106	734398794	+	TraesCS2B02G539200	
2B	734452993	734457716	-	TraesCS2B02G539300	Protein COFACTOR ASSEMBLY OF COMPLEX C SUBUNIT B CCB4, chloroplastic
2B	734459049	734460668	+	TraesCS2B02G539400	
2B	734495024	734500006	-	TraesCS2B02G539500	Eukaryotic translation initiation factor 3 subunit I
3A	31888572	31906228	+	TraesCS3A02G054500	
3A	31926134	31930997	+	TraesCS3A02G054600	
3A	31948379	31952404	+	TraesCS3A02G054700	Protein DAMAGED DNA-BINDING 2
3A	31952535	31956959	-	TraesCS3A02G054800	
3A	32096354	32097926	-	TraesCS3A02G054900	
3A	32100094	32100573	-	TraesCS3A02G055000	
3A	32114968	32120378	+	TraesCS3A02G055100	
3A	32118364	32119341	-	TraesCS3A02G055200	
3A	32120273	32124902	-	TraesCS3A02G055300	Probable zinc metalloprotease EGY2, chloroplastic
3A	32142262	32144885	+	TraesCS3A02G055400	
3A	32145925	32149547	+	TraesCS3A02G055500	

3A	32150045	32153332	-	TraesCS3A02G055600	Similar to 14-3-3 protein 6
3A	32152342	32152995	-	TraesCS3A02G055700	
3A	32173013	32176735	-	TraesCS3A02G055800	
3A	32224350	32234406	-	TraesCS3A02G055900	Protein DETOXIFICATION
3A	32251515	32253338	-	TraesCS3A02G056000	GID2 protein isoform 1
3A	32384710	32387330	-	TraesCS3A02G056100	
3A	32412888	32413166	+	TraesCS3A02G056200	
3A	32414573	32417008	+	TraesCS3A02G056300	
3A	32425722	32428453	+	TraesCS3A02G056400	
3A	708322240	708323822	+	TraesCS3A02G476700	
3A	708672290	708673444	-	TraesCS3A02G476800	
3A	708819356	708824093	-	TraesCS3A02G476900	
3B	749651924	749652232	+	TraesCS3B02G505500	
3B	749680808	749682007	+	TraesCS3B02G505600	
3B	749686161	749686586	-	TraesCS3B02G505700	
3B	749686697	749697929	-	TraesCS3B02G505800	
3B	749725710	749727190	+	TraesCS3B02G505900	
3B	749728469	749728717	+	TraesCS3B02G506000	
3B	749859873	749861384	+	TraesCS3B02G506100	
3B	749864112	749864426	+	TraesCS3B02G506200	
3B	749979291	749980846	+	TraesCS3B02G506300	
3B	749983246	749983560	+	TraesCS3B02G506400	
3B	749986389	749986703	+	TraesCS3B02G506500	
3B	750134355	750138737	+	TraesCS3B02G506600	
3B	750138856	750142385	-	TraesCS3B02G506700	
3B	750354532	750358136	+	TraesCS3B02G506800	
3B	750361238	750361891	-	TraesCS3B02G506900	
3B	750784059	750786555	-	TraesCS3B02G507000	
3B	750860902	750863747	+	TraesCS3B02G507100	
3B	750900638	750901192	-	TraesCS3B02G507200	
3B	750901481	750901801	-	TraesCS3B02G507300	
3B	751013817	751015324	-	TraesCS3B02G507400	
3B	751104455	751109609	-	TraesCS3B02G507500	
4A	450762292	450764311	+	TraesCS4A02G178200	
4A	450764565	450765605	-	TraesCS4A02G178300	
4A	450786651	450792679	+	TraesCS4A02G178400	
4A	450793843	450794820	+	TraesCS4A02G178500	
4A	450859059	450884012	+	TraesCS4A02G178600	ATP-dependent DNA helicase
4D	120830509	120833590	-	TraesCS4D02G133800	Laccase
4D	120865261	120867462	+	TraesCS4D02G133900	
4D	120882134	120886868	-	TraesCS4D02G134000	
4D	120886025	120887130	+	TraesCS4D02G134100	
4D	121073905	121074757	+	TraesCS4D02G134200	

4D	121075082	121078671	-	TraesCS4D02G134300	
4D	121181560	121183872	-	TraesCS4D02G134400	
4D	121403700	121407432	+	TraesCS4D02G134500	
4D	121432471	121439689	+	TraesCS4D02G134600	
4D	121439747	121440713	-	TraesCS4D02G134700	
4D	121473917	121475043	+	TraesCS4D02G134800	
5A	29879623	29884709	+	TraesCS5A02G032500	Kinesin-like protein
5A	29886998	29889211	+	TraesCS5A02G032600	
5A	29892240	29896434	-	TraesCS5A02G032700	
5A	29905635	29910084	-	TraesCS5A02G032800	
5A	30008523	30009329	+	TraesCS5A02G032900	
5A	30214481	30215784	-	TraesCS5A02G033100	
5B	397434157	397435784	-	TraesCS5B02G222400	
5B	397513704	397517375	+	TraesCS5B02G222500	Phospholipase D
5B	397666372	397682035	+	TraesCS5B02G222600	
5B	397828412	397834362	+	TraesCS5B02G222700	
5B	397834328	397836261	-	TraesCS5B02G222800	
5B	397837635	397839847	-	TraesCS5B02G222900	
5B	397839941	397843405	+	TraesCS5B02G223000	
5B	397949659	397954665	+	TraesCS5B02G223100	
5B	397958680	397961920	-	TraesCS5B02G223200	RBR-type E3 ubiquitin transferase
5B	397965363	397966649	-	TraesCS5B02G223300	RBR-type E3 ubiquitin transferase
5B	398058622	398060284	-	TraesCS5B02G223400	RBR-type E3 ubiquitin transferase
5B	398063428	398067585	-	TraesCS5B02G223500	RBR-type E3 ubiquitin transferase
5B	398067521	398080415	+	TraesCS5B02G223600	
5B	398346089	398350472	+	TraesCS5B02G223700	
5B	398625257	398626600	-	TraesCS5B02G223800	Non-specific serine/threonine protein kinase
6A	6562757	6569872	+	TraesCS6A02G013300	
6A	6596738	6609077	-	TraesCS6A02G013400	
6A	6699199	6701391	+	TraesCS6A02G013500	
6A	6712593	6718806	+	TraesCS6A02G013566	
6A	6721481	6725416	+	TraesCS6A02G013600	P-loop containing nucleoside triphosphate hydrolases superfamily protein
6A	6727564	6735295	+	TraesCS6A02G013700	
6A	6739737	6740659	+	TraesCS6A02G013800	
6A	6741985	6742380	-	TraesCS6A02G013900	
6A	6804413	6805120	-	TraesCS6A02G014000	
6A	6890789	6893444	-	TraesCS6A02G014100	
6A	6895077	6896267	+	TraesCS6A02G014200	
6B	10744852	10746514	-	TraesCS6B02G016700	

6B	10747395	10751909	-	TraesCS6B02G016800	
6B	10903690	10905165	+	TraesCS6B02G016900	
6B	10926195	10928285	+	TraesCS6B02G017000	
6B	10934559	10936034	-	TraesCS6B02G017100	
6B	11110810	11111295	-	TraesCS6B02G017200	
6B	11153576	11155959	-	TraesCS6B02G017300	
6B	11173220	11174669	+	TraesCS6B02G017400	
6B	11244847	11246731	-	TraesCS6B02G017500	
6B	11257895	11261008	-	TraesCS6B02G017600	
6B	11286117	11289669	-	TraesCS6B02G017700	Putative RNA-binding protein
6B	11298628	11299302	-	TraesCS6B02G017800	
6B	11317464	11326092	-	TraesCS6B02G017900	
6B	11408601	11409227	-	TraesCS6B02G018000	
6B	11427868	11428770	-	TraesCS6B02G018100	
6B	11469680	11470453	-	TraesCS6B02G018200	
6B	11513863	11514513	-	TraesCS6B02G018300	
6B	11520311	11525880	-	TraesCS6B02G018400	
6B	11537907	11540117	+	TraesCS6B02G018500	
6B	11540333	11542012	-	TraesCS6B02G018600	
6B	11572059	11573488	-	TraesCS6B02G018700	
6B	11574704	11578183	+	TraesCS6B02G018800	
6B	11584758	11586346	-	TraesCS6B02G018900	
6B	11592859	11593605	+	TraesCS6B02G019000	
6B	11600271	11600858	+	TraesCS6B02G019200	
6B	11612841	11617152	+	TraesCS6B02G019300	
6B	11740071	11740577	-	TraesCS6B02G019400	
6B	11747529	11748290	-	TraesCS6B02G019500	
6B	11792361	11793467	+	TraesCS6B02G019600	
6B	11794155	11795264	+	TraesCS6B02G019700	
6B	11988263	11988710	-	TraesCS6B02G019800	
6B	12044935	12045747	-	TraesCS6B02G020000	
7A	719271245	719271601	-	TraesCS7A02G542400	
7A	719363122	719365762	+	TraesCS7A02G542500	
7A	719417796	719418420	+	TraesCS7A02G542600	
7A	719469821	719473122	-	TraesCS7A02G542700	
7A	719564494	719566803	+	TraesCS7A02G542800	
7A	719566911	719570377	-	TraesCS7A02G542900	
7A	719576843	719579559	-	TraesCS7A02G543000	
7A	719579684	719583858	-	TraesCS7A02G543100	
7A	719638601	719642604	-	TraesCS7A02G543200	
7A	720845804	720846541	+	TraesCS7A02G543900	
7A	720861944	720863185	-	TraesCS7A02G544000	
7A	720863187	720864341	-	TraesCS7A02G544100	

7A	720885208	720887286	+	TraesCS7A02G544200	
7A	720912280	720914524	-	TraesCS7A02G544300	
7A	720953556	720955355	+	TraesCS7A02G544400	
7A	721000102	721000395	-	TraesCS7A02G544500	
7A	721064202	721075033	+	TraesCS7A02G544600	
7A	721093026	721106211	+	TraesCS7A02G544700	
7A	721124709	721125004	+	TraesCS7A02G544800	
7A	721162987	721166033	-	TraesCS7A02G544900	Phospholipase D
7A	721172054	721176909	+	TraesCS7A02G545000	Phospholipase D
7A	721204810	721206569	+	TraesCS7A02G545100	
7A	721222769	721223586	+	TraesCS7A02G545200	

Annexure 3.1. List of genotypes, pedigree, and grouping of germplasm used in the study

Sr. No.	Germplasm	Pedigree	Grouping on the basis of year of release	Grouping on the basis of NDVI	Mean NDVI values
1	HS(YAQOOB MUJHAID) KOHSAR-95	PSN/BOW	Post Green Revolution	MSG	0.565
2	SHAHKAR-95	CNO67//SN64/KLRE/3/8156	Post Green Revolution	NSG	0.4875
3	BAKHTAWAR-94	BB/NOR67	Post Green Revolution	MSG	0.5625
4	KAGHAN-93	CMH-77A917/PKV 1600//RL6010/6*SKA	Post Green Revolution	NSG	0.4875
5	SAIRAB-92	CHENAB2000/INQ-91	Post Green Revolution	MSG	0.5775
6	ANMOL-91	LUAN/KOH-97	Post Green Revolution	SG	0.6225
7	PARWAZ-94	OASIS/SKAUZ//4*BCN/3/2*PASTOR	Post Green Revolution	MNSG	0.4975
8	PASBAN-90	BLS/KHUSHAL	Post Green Revolution	MSG	0.5575
9	MARGHALA-99	OPATA/BOW'S'	Post Green Revolution	MSG	0.5625
10	DERA	F12-71/COC/CNO 79	Post Green Revolution	MSG	0.59
11	DEMAN	BOWS/3/CAR853/COC//VEES	Post Green Revolution	MNSG	0.5325
12	D-97	FORD//DUNDEE/BOBIN or FORD/DONDEE (I)	Post Green Revolution	MSG	0.5875
13	KOHISTAN-97	KVZ/3/TOB/CTFN/BB/4/BLO/5/VEE#5/6/BOW/3/YD//BB/CHA	Post Green Revolution	MSG	0.5725
14	MH-97	KAUZ/PASTOR	Post Green Revolution	MNSG	0.53
15	PUNJ-86	INQALAB 91*2/TUKURU	Post Green Revolution	MNSG	0.515
16	SULEMAN -96	BUC/FLK//MYNA/VUL	Post Green Revolution	MNSG	0.535
17	NOWSHERA-96	C516/C591	Post Green Revolution	MSG	0.57
18	ROHTAS-9O	INIA F 66/TH.DISTICHUM//INIA F 66/3/GENARO T 81 or INIA F 66/ A.DISTCHUM//INIA66/3/GEN	Post Green Revolution	NSG	0.475
19	SOGHAT-90	PSN/BOW	Post Green Revolution	MNSG	0.5275
20	BWP-97	NORD-DESPREZ(ND)/VG-9144//KALYANSONA/BLUEBIRD/3/YACO/4/VEERY-5	Post Green Revolution	MSG	0.58
21	DWR-97	SASONO KOMOGI/NORIN//BOB'S'	Post Green Revolution	MSG	0.5575
22	SHALIMAR-88	WL 711/CROW"S"	Post Green Revolution	NSG	0.4775
23	KHYBER-87	21931-CHAPINGO53/ANDES SIB/3/Y50/4/C271	Post Green Revolution	MSG	0.565
24	RAWAL-87	MAYA/MON//KVZ/TRM	Post Green Revolution	MNSG	0.5425
25	SUTLAJ-86	ULC/PVN//TAN/3/BUC	Post Green Revolution	MSG	0.5925
26	PUNJAB-85	BURGUS/SORT 12-13//KAL/BB/3/PAK 81	Post Green Revolution	SG	0.605
27	FSD-85	CHIL/2*STAR	Post Green Revolution	MSG	0.59

28	FSD-83	MAYA/MON//KVZ/TRM	Post Green Revolution	MSG	0.56
29	KOHINOOR-83	PT'S'/3/TOB/LFN//BB/4/BB/HD-832-5//ON/5/G-V/ALD'S'//HPO	Post Green Revolution	MNSG	0.5475
30	SARHAD-82	JUP/ALD'S'//KLT'S'/3/VEE'S'/6/BEZ//TOB/8156/4/ON/3/6*TH/KF//6*LEE/KF/5	Post Green Revolution	MSG	0.565
31	PUNJAB-81	PBW65/2*Pastor	Post Green Revolution	NSG	0.47
32	PAK-81	FURY//KAL/BB	Post Green Revolution	SG	0.6075
33	ZARDANA	PJ/GB55 or PJ62/GB55	Post Green Revolution	MNSG	0.5325
34	ZARGHOON-79	CC/INIA/3/TOB/CTFN//BB/4/7C	Green Revolution	SG	0.6125
35	BWP-79	CNO/LR64A*2//SN64/SN63 or CNO/LR64*2/SON64/SON	Green Revolution	MNSG	0.535
36	DIRIK	PIT/GB//C271	Green Revolution	MNSG	0.54
37	TARNAB-73	T9/8D or T9 X 8A	Green Revolution	MNSG	0.5475
38	LYP-73	BB/NOR67	Green Revolution	MNSG	0.5375
39	PARI-73	FORLANI/ACC//ANA or Fln/ACS//ANA	Green Revolution	NSG	0.48
40	SA-72	C-271/WILLET-DWARF//SONORA-64	Elite Cultivars	MNSG	0.5225
41	B-SILVER	C 230 X IP 165	Green Revolution	NSG	0.455
42	CHENAB-70	HARD FEDERATION X 9D	Green Revolution	NSG	0.46
43	YECORA-70	BUC'S'/FCT'S'	Green Revolution	MNSG	0.5125
44	NURI-70	HARD FED/9D	Green Revolution	MSG	0.585
45	UP-262	land races	Elite Cultivars	NSG	0.4725
46	LOCAL-WHITE	BB/GLL/3/GTO/7C//BB/CNO67	Elite Cultivars	MNSG	0.515
47	POTHOWAR	ATTILA/3/HUI/CARC//CHEN/CHTO/4/ATTILA	Green Revolution	MNSG	0.5275
48	SA—75	CHUM18/BAU	Green Revolution	NSG	0.4775
49	SA-42	C 209 X C 591	Green Revolution	NSG	0.455
50	KHUSHALL-69	II53-388/AN//YT54/N10B/3/LR64/4/B4946.A.4.18.2.IY/Y53//3*Y50	Green Revolution	NSG	0.4
51	WL-711	S308/CHRIS//KAL	Green Revolution	MNSG	0.5
52	MEXIPAK	PJ/GB55 or PJ62/GB55	Green Revolution	MNSG	0.5225
53	SONALIKA	SASONO KOMOGI/NORIN//BOB'S'	Green Revolution	NSG	0.44
54	SANDAL	T9 X 8A	Green Revolution	MNSG	0.515
55	LU-26	BLS/KHUSHAL	Green Revolution	NSG	0.4625
56	PUNJAB-76	NAI60/CB151//S949/3/MEXIPAK	Green Revolution	MSG	0.5925
57	BARANI-70	CNO/LR64A*2//SN64/SN63 or CNO/LR64*2/SON64/SON	Green Revolution	MSG	0.59
58	CHAKWAL-86	KVZ/TRM//PTM/ANA	Post Green Revolution	SG	0.61

59	PIRSBK-91	KAUZ//ALTAR84/AOS	Post Green Revolution	SG	0.605
60	INQILAB-91	V-1562//CHRC'S'/HORK/3/KUFRA-I/4/CARP'S'/BJY'S'	Post Green Revolution	MNSG	0.51
61	CHAKWAL-97	INIA F66/TH.DISTICHUM//INIAF66/3/GENARO T81 or INIA F66/A.DISTCHUM//INIA66/3/GEN	Post Green Revolution	SG	0.6075
62	BARANI-83	DWL5023/SNB//SNB	Post Green Revolution	SG	0.63
63	CHAKWAL-50	F6.74/BUN//SIS/3/VEE#7 or F6-74/BUN//SIS/3/VEE#7	Elite Cultivars	MSG	0.585
64	C-217	KHP/D31708//CM74A370/3/CNO79/4/RL6043/4*NAC or KHP/D31708//CM74A370/3/CIANO79/4/RL6043/*4NAC	Land Races	MSG	0.5775
65	C-228	KVZ/TRM//PTM/ANA	Land Races	MNSG	0.5275
66	C-271	C-230/IP-165;	Land Races	MSG	0.5775
67	C-273	C-591/C-209; C-209/C-591	Land Races	MNSG	0.54
68	C-250	CROW'S'/NAC//BOW'S'	Land Races	MNSG	0.5075
69	C-306	AU/UP301//GLL/Sx/3/PEW S/4/MAI S/MAY A S//PEWS	Land Races	MNSG	0.5425
70	C-518	SH-88/90A-204//MH97	Land Races	MNSG	0.505
71	C-591	land races	Land Races	MNSG	0.5
72	SKD-1	LU 26/HD 21790/ 2*INQALAB 91	Elite Cultivars	MNSG	0.4975
73	TD-1	BY/MAYA/4/BB//HD832.5.5/ON/3/CNO67/PJ62 or PITIC-62/FROND//MEXIPAK/3/PITIC-62/MAZOE-79-75-76 [wheatpedigree.net] or PI/FRND//MXP/3/PI/M20/79	Elite Cultivars	SG	0.6175
74	RASKOH	Kauz/Yaco//Kauz	Elite Cultivars	SG	0.6075
75	SARSABZ	TTR/JUN	Post Green Revolution	MNSG	0.5425
76	SASSUI	HD-2329	Elite Cultivars	MSG	0.555
77	WAFAQ	Kauz/Yaco//Kauz	Elite Cultivars	MSG	0.59
78	AS-2002	CHAM6//KITE/PGO	Elite Cultivars	MSG	0.58
79	SALEEM-2002	land races	Elite Cultivars	MSG	0.5575
80	GA-2002	NAI60/CB151//S949/3/MEXIPAK	Elite Cultivars	SG	0.6225
81	UFAQ	NAI60/CB151/S949/3/MEXIPAK	Elite Cultivars	MNSG	0.495
82	BAKHAR-2002	URES/BOW`S	Elite Cultivars	MNSG	0.5125
83	MOOMAL-2003	CNO67//SN64/KLRE/3/8156	Elite Cultivars	SG	0.605
84	SH-2003	AU//KAL/BB/3/WOP	Elite Cultivars	MNSG	0.5025
85	PIRSBK-04	KAUZ/STAR	Elite Cultivars	MSG	0.555
86	IMDAD-05	CHILL/2* STAR/4/BOW//BUC/PVN/3/2*VEE#10	Elite Cultivars	SG	0.605
87	PIRSBK-05	MUNIA/CHTO//AMSEL	Elite Cultivars	MSG	0.575
88	SEHER-2006	WL711//F371/TRM	Elite Cultivars	NSG	0.475

89	SHAFAQ-2006	PB81/HD2182//PB81	Elite Cultivars	NSG	0.45
90	LASANI-2008	PAVON MUTANT-3	Elite Cultivars	MNSG	0.5125
91	PIRSBK-08	JUP/ALD'S'//KLT'S'	Elite Cultivars	MSG	0.5575
92	FSD-08	PBW65/2*Pastor	Elite Cultivars	MNSG	0.535
93	MAIRAJ-08	WT(E)/SON64	Elite Cultivars	NSG	0.47
94	NARC-09	INQALAB 91*2/TUKURU	Elite Cultivars	MNSG	0.51
95	NARC-11	CNO67/8156//TOB66/CNO67/4/NO/3/12300//LR64A/8156/5/PVN or CNO67/8156//TOB 66/CNO67/4/NOROESTE F66/3/12300//LR64A/8156/5/PVN	Elite Cultivars	MSG	0.595
96	AARI-11	OPATA/RAYON//KAUZ	Elite Cultivars	MSG	0.5875
97	AAS-11	LU26/HD 2179	Elite Cultivars	MNSG	0.515
98	PUNB-11	CNO67//SON64/KLRE/3/8156	Elite Cultivars	MNSG	0.5225
99	STAY GREEN; NEPAL-38	CHIRYA7/ANB	Elite Genotype_CIMMYT	SG	0.66
100	STAY GREEN; NEPAL-49	CHIRYA1	Elite Genotype_CIMMYT	SG	0.615
101	STAY GREEN; NEPAL-50	CHIRYA7	Elite Genotype_CIMMYT	SG	0.6425
102	STAY GREEN; NEPAL-51	CHIRYA3	Elite Genotype_CIMMYT	SG	0.63
103	STAY GREEN; NEPAL-268	DUCULA//HUI/TUB/3/CAZO/4/CROC-1/AE.SQ(224)//OPATA	Elite Genotype_CIMMYT	SG	0.6225
104	STAY GREEN; SG-30	SABUF//ALTAR84/AE.SQ(205)	Elite Genotype_CIMMYT	SG	0.655
105	STAY GREEN; SG-33	SABUF//ALTAR84/AE.SQ(205)	Elite Genotype_CIMMYT	SG	0.6375
106	STAY GREEN; SG-73	SABUF//ALTAR84/AE.SQ(205)	Elite Genotype_CIMMYT	MSG	0.56
107	STAY GREEN; ITMI-35	ALTAR84/AE.SQ//OPATA	Elite Genotype_CIMMYT	MNSG	0.5475
108	STAY GREEN; PROGENATOR-2	PASTOR	Elite Genotype_CIMMYT	SG	0.625
109	STAY GREEN; SL OPATA		Elite Genotype_CIMMYT	SG	0.6075
110	STAY GREEN; SG LINE (12x2)		Elite Genotype_CIMMYT	SG	0.6225
111	STAY GREEN; 3(9x1)	CHIRYA-1//CROC/AE.SQ(224)	Elite Genotype_CIMMYT	SG	0.6175
112	STAY GREEN; 5(9x1)	CHIRYA-1//CROC/AE.SQ(224)	Elite Genotype_CIMMYT	MNSG	0.5375
113	STAY GREEN; 90(9x1)	CHIRYA-1//CROC/AE.SQ(224)	Elite Genotype_CIMMYT	SG	0.605
114	STAY GREEN; 130(12x2)	PAPGO//LARU/AE.SQ(347)	Elite Genotype_CIMMYT	SG	0.61
115	STAY GREEN, SD(MK)-23		Synthetic Derivative	NSG	0.4425
116	STAY GREEN, SD(MK)-24	MAYOOR//TKSN1081/AE.SQUARROSA(222)/3/OPATA/4/	Synthetic Derivative	SG	0.605
117	STAY GREEN, SD(MK)-25	TURACO/5/CHIR3/4/SIREN//ALTAR	Synthetic Derivative	MSG	0.595
118	STAY GREEN, SD(MK)-28	OPATA//DOY1/AE.SQUARROSA(372)	Synthetic Derivative	SG	0.63
119	STAY GREEN, SD(MK)-30	D67.2/P66.270//AE.SQUARROSA(223)3/ARLIN_1/T.MONOCOCCUM(95)	Synthetic Derivative	SG	0.605

120	STAY GREEN, SD(MK)-34	34 MAYOOR//TKSN1081/AE.SQUARROSA(222)3/OPATA/6/68.111/RGB-U//WARD/3/FGO/4/RABI/5/AE.SQUARROSA(878)	Synthetic Derivative	MSG	0.555
121	STAY GREEN, SD(MK)-36	URES/PRL//BAV92/3/YAV_2/TEZ//AE.SQUARROSA(249)	Synthetic Derivative	SG	0.605
122	STAY GREEN, SD(MK)-37	GAN/AE.SQUARROSA(897)//OPATA/3/D67.2/P66.270//AE.SQUARROSA(223)	Synthetic Derivative	SG	0.605
123	STAY GREEN, SD(MK)-39	OPATA//DOY1/AE.SQUARROSA(255)	Synthetic Derivative	SG	0.6225

NSG Non-Stay Green, MNSG Moderately Non-Stay Green, MSG Moderately Stay Green, SG Stay Green (Scale: NSG 0.40->0.495, MNSG 0.495->0.55, MSG 0.55->0.605, SG 0.605-0.66)

Annexure 3.2. Daily maximum and minimum temperature during the field experiments in November, 2014- May, 2015 and November, 2015- May, 2016 (Source: Pakistan Meteorological Department)

DAY	November, 2014- May, 2015							November, 2015- May, 2016							November, 2014- May, 2015							November, 2015- May, 2016						
	Daily Maximum Temperature (°C)							Daily Maximum Temperature (°C)							Daily Minimum Temperature (°C)							Daily Minimum Temperature (°C)						
	Nov	Dec	Jan	Feb	Mar	Apr	May	Nov	Dec	Jan	Feb	Mar	Apr	May	Nov	Dec	Jan	Feb	Mar	Apr	May	Nov	Dec	Jan	Feb	Mar	Apr	May
1	27.8	25.0	21.0	19.0	21.0	24.0	27.8	27.0	23.5	21.5	19.0	26.5	28.0	37.3	9.8	6.0	2.4	2.0	6.5	14.0	14.4	11.5	6.5	3.7	4.0	10.0	14.4	16.0
2	27.2	25.5	21.2	16.0	13.7	16.5	30.5	26.5	25.0	21.0	20.0	26.5	25.0	39.0	9.0	5.5	1.6	9.0	10.5	13.0	13.5	13.0	6.0	2.5	3.5	10.0	16.0	17.0
3	24.7	25.0	22.0	14.0	13.0	22.6	32.0	26.0	23.0	21.0	20.0	26.5	25.5	40.0	10.5	5.0	2.0	9.0	8.5	14.8	15.0	15.0	4.5	3.0	3.5	13.0	16.5	17.5
4	23.0	26.0	19.5	16.0	15.5	21.2	33.6	25.5	24.5	20.8	22.0	28.0	26.5	32.5	11.0	5.0	2.0	2.5	6.0	12.0	14.5	10.0	6.4	3.5	4.0	12.4	15.0	21.5
5	23.5	25.2	19.0	21.0	19.7	26.3	35.3	18.6	23.5	19.0	19.5	28.0	29.5	29.0	10.0	5.0	2.5	2.5	7.0	13.4	18.0	11.0	7.0	3.0	3.0	13.5	13.0	17.7
6	27.5	25.2	20.0	21.5	11.2	26.2	35.2	19.9	22.0	20.7	24.0	20.5	30.0	32.3	11.5	4.2	2.5	3.5	5.7	14.0	18.5	9.5	5.5	5.0	4.5	12.5	15.0	17.2
7	25.0	24.3	20.3	20.0	20.8	26.3	37.1	24.5	22.8	18.3	19.5	22.0	24.8	34.5	14.0	3.5	3.5	4.5	8.5	15.0	19.0	9.5	7.0	5.0	9.5	9.0	12.0	18.5
8	22.5	23.8	16.7	14.0	14.0	22.0	37.0	23.5	22.5	21.0	20.2	26.0	29.0	36.2	10.5	3.5	3.5	5.0	7.5	12.5	18.0	9.6	6.5	5.0	6.5	10.0	12.5	19.5
9	25.3	22.0	18.0	19.3	14.8	27.0	38.2	23.7	20.5	20.0	20.5	27.0	29.5	39.0	10.0	3.5	3.0	3.5	5.5	13.0	24.0	10.5	8.5	3.5	5.0	11.0	15.0	16.0
10	26.0	22.0	20.8	23.3	20.2	28.4	36.2	19.0	18.5	20.0	21.5	27.5	25.3	38.0	7.0	2.5	1.5	4.0	7.0	13.5	19.8	6.0	9.0	2.5	6.0	12.0	13.0	20.0
11	27.6	21.0	19.2	23.5	23.2	30.2	37.2	19.0	14.5	20.5	17.6	27.3	28.3	38.3	7.5	1.5	1.5	5.0	8.0	14.3	21.0	8.0	5.1	3.0	4.5	13.0	17.5	21.5
12	26.5	22.5	22.8	24.0	23.7	31.0	30.8	18.5	17.0	19.5	12.0	17.0	26.0	33.5	6.0	4.3	2.5	5.0	7.5	15.5	19.0	9.5	3.0	4.0	3.2	14.0	12.5	21.5
13	26.0	22.0	18.7	24.2	25.2	32.0	24.0	19.0	19.0	11.5	18.0	15.2	30.0	35.7	5.0	4.5	4.0	6.4	8.0	15.6	18.0	11.0	3.5	3.6	3.5	12.5	13.5	21.0
14	26.0	21.0	14.0	25.0	26.0	31.0	30.0	24.5	18.2	17.5	19.5	15.0	31.5	36.0	5.5	4.0	2.5	6.5	11.0	15.8	17.5	10.5	3.5	4.0	4.0	9.5	14.0	21.5
15	26.3	17.0	17.5	26.8	26.2	31.0	31.3	25.5	20.0	17.5	21.2	21.0	34.2	35.0	4.6	3.0	6.3	6.5	12.5	20.0	15.8	9.5	2.0	4.0	4.5	7.0	16.0	18.0
16	25.7	17.5	19.0	25.5	15.3	31.0	33.5	26.2	21.0	20.0	20.5	21.8	34.5	36.0	4.5	3.5	3.8	12.5	11.5	16.5	18.0	8.0	1.4	2.5	4.0	9.5	17.0	19.5
17	26.0	17.0	21.3	17.8	15.2	26.3	35.0	26.0	18.7	19.5	21.5	22.0	36.0	38.0	5.0	1.5	3.5	9.5	9.5	16.0	22.5	6.5	3.0	3.0	5.0	13.0	18.5	20.5
18	25.6	17.5	21.2	22.0	22.5	30.0	32.5	26.5	18.6	12.0	23.0	15.0	30.0	38.5	5.5	1.5	2.0	10.0	9.0	16.3	18.5	7.0	2.0	6.5	5.5	12.0	15.0	19.5
19	26.0	19.0	20.5	21.5	25.0	30.5	34.2	26.0	19.5	16.5	25.0	23.0	30.5	41.0	5.5	1.2	2.5	11.0	9.5	17.5	19.0	6.0	1.0	5.0	7.0	13.5	15.0	20.5
20	25.5	18.8	21.0	15.0	26.5	25.8	35.5	26.0	19.0	18.0	17.0	25.0	28.5	41.4	5.5	1.0	3.5	11.2	12.0	17.0	17.0	8.0	1.5	2.5	9.2	13.5	14.5	20.5
21	25.0	17.6	19.0	14.2	27.0	30.0	36.2	25.0	19.0	16.5	23.5	21.0	32.0	41.5	5.0	1.5	5.5	9.8	11.2	15.0	16.5	7.0	1.0	2.5	7.0	8.0	17.5	23.0
22	25.0	17.2	12.0	23.0	28.2	32.0	37.2	26.0	18.5	12.0	25.2	23.8	30.0	42.3	5.0	3.0	8.0	9.5	11.5	16.5	18.2	7.3	2.0	4.0	7.0	9.0	15.5	23.5
23	24.5	13.2	16.5	26.3	30.0	33.0	38.0	24.0	16.0	14.5	25.5	27.8	29.5	42.0	5.0	4.0	8.4	11.0	11.5	15.0	19.6	8.0	4.0	3.0	6.0	10.0	12.0	22.0
24	24.0	19.0	14.5	22.8	31.0	33.7	37.8	24.0	15.8	12.0	30.5	28.0	30.3	38.0	4.0	2.0	3.0	15.0	15.0	14.8	21.0	6.5	-0.5	0.5	7.0	11.2	11.0	21.0
25	19.5	17.6	17.0	19.0	30.5	34.3	35.5	24.8	17.0	14.3	26.0	23.0	31.2	32.0	4.5	0.5	2.5	8.0	13.0	16.0	17.5	7.5	0.4	1.0	6.5	12.8	12.0	19.5

26	24.0	19.8	18.8	15.2	30.0	34.5	36.8	19.0	17.5	17.0	26.1	21.5	33.0	35.0	4.5	1.5	3.0	5.5	15.0	18.0	15.5	7.5	1.5	1.0	9.6	13.0	14.0	20.5
27	23.5	20.3	15.8	19.2	29.5	33.0	34.0	22.5	14.0	17.5	26.5	25.0	34.0	37.5	5.0	1.3	3.5	6.5	13.4	18.8	17.0	6.0	3.5	6.5	8.5	11.4	20.5	20.5
28	22.5	20.5	16.5	18.8	30.2	21.0	37.0	23.5	18.5	21.5	26.5	29.5	33.0	40.0	7.0	0.0	0.0	6.0	18.5	13.5	18.0	5.3	3.5	5.0	9.8	12.0	15.0	23.5
29	23.5	20.0	17.5	***	29.0	31.5	37.5	24.5	22.3	18.0	27.0	27.5	34.3	40.5	7.5	0.5	0.5	***	15.5	15.5	20.5	7.5	3.5	5.5	11.0	9.0	15.5	21.5
30	24.3	19.0	16.8	***	18.2	31.5	37.0	23.5	23.0	13.5	***	29.5	37.0	37.5	7.0	1.5	1.2	***	12.5	16.5	19.0	7.5	3.5	5.0	***	12.0	14.5	18.5
31	***	20.0	19.2	***	21.6	***	38.2	***	22.0	16.0	***	31.0	***	34.5	***	2.5	1.0	***	13.5	***	18.5	***	2.5	6.0	***	15.5	***	20.5
Average	25.0	20.7	18.6	20.3	22.5	28.5	34.6	23.6	19.8	17.7	22.0	24.1	30.2	37.2	7.1	2.8	3.0	7.2	10.4	15.3	18.1	8.7	3.8	3.7	5.9	11.4	14.8	20.0

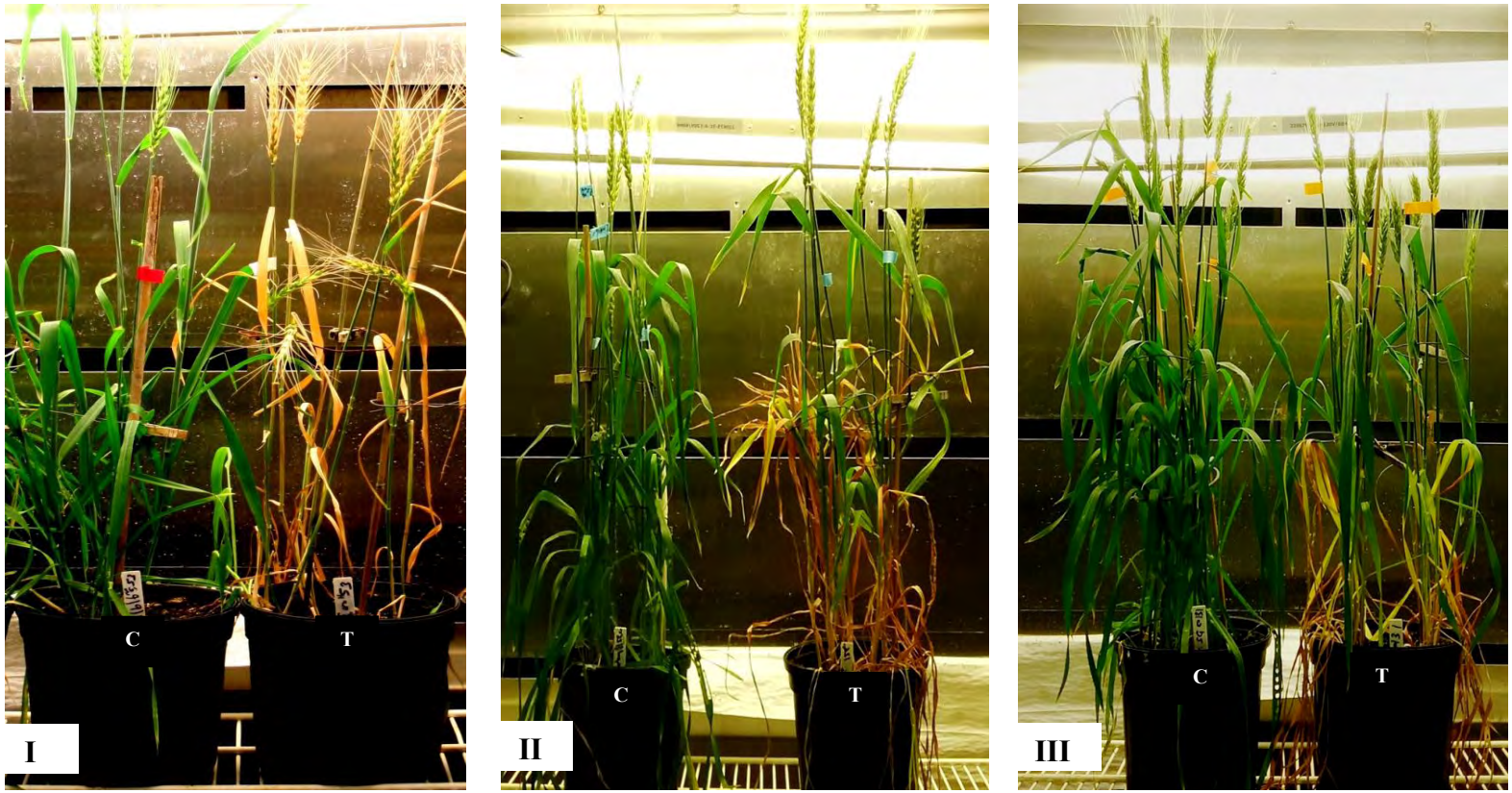

Annexure 3.3. Greenhouse experiment showing non-stay-green (I. Sonalika), functional stay-green (II. Nepal-38) and non-functional stay-green (III. SG-30) genoptyes after 14 days of heat stress treatment. C: Control and T: Heat treatment

Annexure 3.4. Coding Sequence ID and Protein ID of CaO, Cab, SGR, and RCCR in Brachypodium distachyon, Hordeum vulgare, Sorghum bicolor, Oryza sativa, Zea mays, and Gene ID of Triticum aestivum

	Brachypodium distachyon		*Hordeum vulgare*		*Oryza sativa*	
GENE	cDNA	Protein	cDNA	Protein	cDNA	Protein
CaO	XM_024459511.1	XP_024315279.1	gb_JQ627620.1	gb_AFI73229.1	XM_015758600.1	XP_015614086.1
Cab	XM_010232713.3	XP_010231015.1	AB500090.1	BAJ08392.1	XM_015756347.2	XP_015611833.1
SGR	XM_003576718.4	XP_003576766.1	AY850135.1	AAW82955.1	AY850134.1	AAW82954.1
RCCR	XM_003564293.4	XP_003564341.1	AJ243066.1	CAB77705.1	OSJNBb0061I18.21	AAK52125.1

	Sorghum bicolor		*Zea mays*	
GENE	cDNA	Protein	cDNA	Protein
CaO	XM_002459098.2	XP_002459143.1	NM_001157871.1	NP_001151343.1
Cab	XM_002440218.2	XP_002440263.1	NM_001112075.2	NP_001105545.2
SGR	AY850140.1	AAW82958.1	NM_001112301.2	NP_001105771.2
RCCR	XM_002457696.2	XP_002457741.2	NM_001147366.1	NP_001140838.1

	Triticum aestivum		
GENE	TGACv1	IWGSC	
CaO	TRIAE_CS42_3AL_TGACv1_197079_AA0664730.1	3A:727989884-727993508	TraesCS3A02G506200.1
Cab	TRIAE_CS42_1DL_TGACv1_062737_AA0219050	1D:472560850-472561762	TraesCS1D02G411300.1
SGR	TRIAE_CS42_5DL_TGACv1_433736_AA1420900.1	5D:418286170-418288613	TraesCS5D02G325900.1
RCCR	TRIAE_CS42_7BL_TGACv1_577684_AA1881030.1	7B:680170068-680171716	TraesCS7B02G692000LC.1

Annexure 3.5. List of oligonucleotide primer sequences used for the amplification and expression analysis of the CaO, Cab, SGR, and RCCR in Triticum aestivum

Gene	Primer Sequence		PRODUCT SIZE (bp)
	Forward Primer	Reverse Primer	
	Primers for Gene Amplification		
CaO	TACACCCACCATCCCTTCCT	GGCCAGTTCCAAACGTTAGC	956
Cab	GGACACGCACGAGTCTTCTT	ACCTAGCAGCTTACTTGCCG	837
SGR	ATTCCACTCGGCTGAACCTG	GAGCGAAGAAATTCGTGGCC	951
RCCR	GAAATTCACCACGGCTCGAC	TGTACCCCAAAGGCCTTACG	782
	Primers for rt-qPCR		
SGR	CACTTCCTGCTCGACCTCAT	AAGTTGGGGTTGTTGGAGTG	167
Cab	CAGAGCATCCTCGCCATCTG	CGGCCGTTCTTGATCTCCTT	191
CaO	ATCGAGAAGGGCCAGTACCT	CCGTCAAGGTCTTTCCTCAG	191
RCCR	GCGATCGACATCACGTCTCT	GAAGTTGGGCTGCCCTGTAT	92
Actin 2	GACGCACAACAGGTATCGTGTTG	AGCGAGGTCAAGACGAAGGATG	[62]

Annexure 3.6. Basic statistics for the phenotypic traits measured in stay-green, moderately stay-green, moderately non-stay-green, and non-stay-green groups under control and heat stress treatments in the field experiments

Trait	Range	Mean±SD	SG*C		SG*S		MSG*C		MSG*S	
			Least Square mean & Group	Lower bound (95%)~Upper bound (95%)	Least Square mean & Group	Lower bound (95%)~Upper bound (95%)	Least Square mean & Group	Lower bound (95%)~Upper bound (95%)	Least Square mean & Group	Lower bound (95%)~Upper bound (95%)
CHL_B	21.23~57.57	40.57±7.31	44.84B	43.18~46.5	38.58A	36.92~40.24	42.75B	41.14~44.36	37.3A	35.69~38.91
CHL_H	19.67~50.57	35.36±5.14	38.31C	37.18~39.44	34.47AB	33.34~35.6	37.63C	36.52~38.73	33.62A	32.52~34.72
CHL_A	4.3~59.7	35.88±5.91	37.74C	36.35~39.13	36.7BC	35.31~38.09	37.58C	36.24~38.93	34.3AB	32.95~35.64
CHL_7DAA	15.1~50.19	34.56±7.13	39.67D	38.3~41.04	31.49BC	30.12~32.86	38.66D	37.32~40	31.87C	30.54~33.2
CHL_14DAA	3.7~52.9	28.63±9.57	36.73E	35~38.45	25.98C	24.25~27.7	35.81E	34.13~37.48	23.79BC	22.11~25.47
CHL_21DAA	1.8~42.9	15.16±7.8	21.09C	19.27~22.9	14.25AB	12.26~16.23	17.1B	15.33~18.88	13.54AB	11.51~15.57
NDVI_Heading	0.44~0.84	0.67±0.09	0.78F	0.76~0.8	0.64CD	0.63~0.66	0.76EF	0.74~0.78	0.61BC	0.6~0.63
NDVI_Anthesis	0.39~0.79	0.58±0.1	0.71E	0.69~0.72	0.55C	0.53~0.57	0.67E	0.65~0.69	0.52BC	0.5~0.54
NDVI_14DAA	0.27~0.6	0.4514±0.07	0.53E	0.51~0.55	0.47CD	0.45~0.49	0.5DE	0.48~0.52	0.42AB	0.41~0.44
NDVI_21DAA	0.10~0.57	0.29±0.10	0.45E	0.43~0.47	0.27BC	0.25~0.29	0.36D	0.35~0.38	0.22A	0.2~0.24
CT_Heading	21.2~29.8	25.53±1.61	24.29A	23.84~24.75	24.61A	24.16~25.07	24.76A	24.32~25.21	26.47B	26.03~26.91
CT_Anthesis	20.1~33.7	27.49±2.41	24.07A	23.57~24.58	28.36C	27.85~28.86	25.64B	25.15~26.12	28.97CD	28.47~29.47
CT_14DAA	25.3~39.5	29.34±1.65	28.51A	27.97~29.06	28.67AB	28.12~29.21	29.43AB	28.91~29.96	29.56ABC	29.04~30.09
CT_21DAA	20.3~34.6	30.58±1.84	29.09A	28.56~29.62	30.17AB	29.64~30.69	29.31A	28.8~29.82	30.96BC	30.44~31.49
PH	44.5~134.83	85.20±15.71	92.69A	89.73~95.65	77.01B	74.05~79.97	96.34A	93.47~99.22	75.46B	72.59~78.33
TN	2~9	4.34±1.45	5.37D	5.04~5.7	4.32CD	3.99~4.65	4.78CD	4.46~5.09	3.61A	3.29~3.93
SL	4~14.83	8.86±1.99	10.37B	10.01~10.72	7.95A	7.6~8.3	10.4B	10.06~10.74	7.59A	7.25~7.93
SPS	8~26	17.02±2.97	18.85D	18.2~19.5	16.33BC	15.68~16.99	18.4D	17.77~19.03	16.27BC	15.65~16.9
BY	12~837.5	296.15±185.60	468.6C	435.33~501.86	200.52A	167.26~233.79	428.5BC	396~461	171.21A	138.95~203.46
GY	1.39~336.57	83.15±65.17	154.9C	145.18~164.62	39.48A	29.76~49.2	137.3BC	127.72~146.87	30.62A	20.9~40.35
TKW	9.7~44	27.69±5.79	30.8C	29.51~32.08	26.57AB	25.27~27.86	30.88C	29.6~32.15	25.05A	23.76~26.35
DTM	93~163	131.30±22.39	153.64B	151.31~155.97	112.63B	110.35~114.9	152.02B	149.77~154.26	110.44A	108.15~112.74

Trait	MNSG*C		MNSG*S		NSG*C		NSG*S		R^2	F
	Least Square mean & Group	Lower bound (95%)~Upper bound (95%)	Least Square mean & Group	Lower bound (95%)~Upper bound (95%)	Least Square mean & Group	Lower bound (95%)~Upper bound (95%)	Least Square mean & Group	Lower bound (95%)~Upper bound (95%)		
CHL_B	42.5B	41~44	38.28A	36.78~39.78	43.55B	41.34~45.76	36.38A	34.17~38.6	0.16	12.90
CHL_H	37.13C	36.1~38.16	32.41A	31.38~33.44	36.94BC	35.43~38.46	31.74A	30.22~33.25	0.20	17.73
CHL_A	36.62BC	35.36~37.87	32.57A	31.31~33.83	37.74C	35.89~39.59	34.64ABC	32.79~36.49	0.10	7.65
CHL_7DAA	38.48D	37.24~39.72	29.04AB	27.8~30.28	38.87D	37.04~40.69	27.51A	25.69~29.34	0.40	45.67
CHL_14DAA	33.91DE	32.34~35.47	19.49A	17.92~21.05	31.03D	28.72~33.33	20.48AB	18.17~22.78	0.47	60.68
CHL_21DAA	14.8AB	13.1~16.5	10.83A	8.69~12.97	13.1AB	10.51~15.69	11.34A	8.24~14.44	0.16	10.45
NDVI_Heading	0.73E	0.71~0.74	0.58AB	0.56~0.6	0.67D	0.65~0.69	0.54A	0.52~0.56	0.72	88.94
NDVI_Anthesis	0.62D	0.61~0.64	0.48AB	0.47~0.5	0.54C	0.52~0.57	0.47A	0.44~0.49	0.72	87.15
NDVI_14DAA	0.45BC	0.43~0.46	0.4A	0.38~0.42	0.41ABC	0.38~0.43	0.41AB	0.39~0.43	0.43	25.52
NDVI_21DAA	0.3C	0.28~0.31	0.2A	0.18~0.22	0.23AB	0.2~0.25	0.21A	0.18~0.24	0.68	73.06
CT_Heading	25.04A	24.63~25.45	26.54B	26.13~26.95	26.39B	25.78~27	27.1B	26.49~27.71	0.36	19.43
CT_Anthesis	26.5B	26.05~26.96	29.55D	29.09~30.01	27.77C	27.1~28.44	30.22D	29.54~30.89	0.65	63.11
CT_14DAA	29.74BC	29.24~30.23	29.1AB	28.61~29.59	30.89C	30.17~31.61	29.56ABC	28.83~30.28	0.14	5.34
CT_21DAA	30.45B	29.97~30.93	31.84CD	31.36~32.33	31.35BCD	30.64~32.05	32.65D	31.93~33.38	0.34	17.60
PH	97.66A	94.98~100.34	74.99B	72.31~77.67	92.05A	88.1~95.99	72.06B	68.12~76.01	0.42	50.05
TN	4.75CD	4.46~5.05	3.67AB	3.37~3.97	4.28ABC	3.84~4.71	3.75AB	3.31~4.19	0.17	14.34
SL	10.2B	9.88~10.52	7.25A	6.93~7.57	9.74B	9.28~10.21	7.09A	6.62~7.56	0.49	66.21
SPS	18.12D	17.54~18.71	15.29AB	14.71~15.88	17.58CD	16.72~18.45	14.6A	13.74~15.47	0.22	19.69
BY	401.36BC	371.07~431.64	158.04A	128.14~187.93	381.14B	336.51~425.77	146.08A	102.08~190.09	0.48	63.65
GY	118.2B	109.28~127.12	29.07A	19.91~38.24	118.34B	105.2~131.49	25.72A	12.57~38.86	0.64	117.10
TKW	29.17BC	27.98~30.36	24.98A	23.78~26.19	29.19BC	27.45~30.93	23.87A	22.13~25.61	0.19	16.06
DTM	150.69B	148.63~152.75	110.43A	108.35~112.5	149.17B	146.13~152.2	109.37A	106.29~112.45	0.83	332.27

Stay Green (SG), Moderately Stay Green (MSG), Moderately Non-Stay Green (MNSG) and Non-Stay Green (NSG), C Control, S Stress, PH Plant Height, TN Tiller Number, SL Spike Length, SPS SPS Spikelet per Spike,CHL Chlorophyll, NDVI Normalized Difference Vegetative index, CT Canopy Temperature, DTM Days to Maturity, BY Biological Yield, GY Grain Yield, TKW Thousand Kernel weight, B Booting, H Heading, A Anthesis, DAA Days after Anthesis

Annexure 3.7. Basic statistics for the phenotypic traits measured in the functional stay-green, non-functional stay-green, and non-stay-green genotypes under control and heat stress treatments in the greenhouse experiment

Trait	Range	Mean±SD	FSG-C		FSG-S		NFSG-C		NFSG-S	
			Least Square mean & Group	Lower bound (95%)~Upper bound (95%)	Least Square mean & Group	Lower bound (95%)~Upper bound (95%)	Least Square mean & Group	Lower bound (95%)~Upper bound (95%)	Least Square mean & Group	Lower bound (95%)~Upper bound (95%)
Chlorophyll_0DAA	39.43~49.7	46.35±2.79	45.76A	41.83~49.7	45.14A	41.21~49.07	47.59A	43.66~51.52	47.59A	43.66~51.52
Chlorophyll_7DAA	32.3~55.9	47.75±5.53	47.86B	44.02~51.69	48.75B	44.91~52.58	50.89B	47.05~54.72	50.25B	46.41~54.08
Chlorophyll_14DAA	3.6~54.1	41.87±15.75	47.75B	43.23~52.26	47.19B	42.68~51.71	50.78B	46.26~55.3	46.93B	42.42~51.45
ØII_0DAA	0.56~0.69	0.61±0.04	0.63A	0.58~0.69	0.64A	0.58~0.69	0.61A	0.56~0.67	0.61A	0.56~0.67
ØII_7DAA	0.34~0.71	0.6194±0.1	0.66B	0.58~0.74	0.62B	0.54~0.7	0.66B	0.58~0.74	0.7B	0.62~0.78
ØII_14DAA	0.027~0.68	0.52±0.2	0.65B	0.55~0.74	0.55B	0.46~0.65	0.62B	0.52~0.71	0.62B	0.53~0.72
Grain Yield	0.54~3.28	1.91±0.78	2.725B	2.06~3.39	2.61B	2.14~3.08	1.78AB	1.12~2.44	1.6AB	0.94~2.26
Biological Yield	2.23~13.88	7.85±3.62	11.9B	8.91~14.96	11.1B	8.96~13.24	7.96AB	4.93~10.99	7.38AB	4.35~10.41

Trait	NSG-C		NSG-S		R^2	F	Type * Treatement Pr > F
	Least Square mean & Group	Lower bound (95%)~Upper bound (95%)	Least Square mean & Group	Lower bound (95%)~Upper bound (95%)			
Chlorophyll_0DAA	46.02A	42.08~49.95	46.01A	42.07~49.94	0.1156	0.3137	0.8953
Chlorophyll_7DAA	51.34B	47.5~55.17	37.44A	33.61~41.28	0.7900	8.7900	0.0010
Chlorophyll_14DAA	50.13B	45.62~54.65	8.43A	3.91~12.94	0.9633	63.0244	< 0.0001
ØII_0DAA	0.6A	0.54~0.65	0.6A	0.54~0.65	0.1562	0.4443	0.8094
ØII_7DAA	0.65B	0.57~0.73	0.44A	0.36~0.52	0.7310	6.5206	0.0038
ØII_14DAA	0.58B	0.48~0.68	0.12A	0.03~0.22	0.8956	20.5989	< 0.0001
Grain Yield	1.88AB	1.34~2.41	0.78A	0.24~1.32	0.8077	8.3990	0.0024
Biological Yield	6AB	3.54~8.49	2.89A	0.42~5.36	0.8128	8.6818	0.0021

SD Standard deviation, C Control, S Stress, ØII Photosynthetic efficiency of photosystem II, FSG Functional stay green, NFSG Non-functional stay green, NSG Non-stay green

Annexure 3.8. Gene bank accession number for the CaO, Cab, SGR, and RCCR genes

GENES	Accession Numbers		
	FSG	NFSG	NSG
CaO	MN566282	MN566284	MN566286
	MN566283	MN566285	MN566287
Cab	MN566263	MN566264	MN566262
	MN566266	MN566267	MN566265
SGR	MN566274	MN566278	MN566276
	MN566275	MN566279	MN566277
RCCR	MN566272	MN566270	MN566268
	MN566273	MN566271	MN566269

Annexure 3.9. Multiple sequence alignment of CaO, Cab, SGR, and RCCR

1. Chlorophyllide a Oxygenase (CaO) Gene and Protein Sequence Alignment

Multiple Sequence Alignment of Partial Coding Sequence of CaO

```
CaO_TraesCS3A02G506200.1          ATAGTGATGGAGCTACCGGTGGAACATGGACTTCTCTTGGACAATCTACT
CaO_NEPAL38_CHIRYA7/ANB           ATAGTGATGGAGCTACCGGTGGAACATGGACTTCTCTTGGACAATCTACT
CaO_EXON7&8_SG30_SABUF//ALTAR8    ATAGTGATGGAGCTACCGGTGGAACATGGACTTCTCTTGGACAATCTACT
CaO_EXON7&8_SONALIKA              ATAGTGATGGAGCTACCGGTGGAACATGGACTTCTCTTGGACAATCTACT
                                  **************************************************

CaO_TraesCS3A02G506200.1          AGACCTCGCTCATGCCCCTTTTACTCATACATCCACCTTTGCCAAGGGCT
CaO_NEPAL38_CHIRYA7/ANB           AGACCTCGCTCATGCCCCTTTTACTCATACATCCACCTTTGCCAAGGGCT
CaO_EXON7&8_SG30_SABUF//ALTAR8    AGACCTCGCTCATGCCCCTTTTACTCATACATCCACCTTTGCCAAGGGCT
CaO_EXON7&8_SONALIKA              AGACCTCGCTCATGCCCCTTTTACTCATACATCCACCTTTGCCAAGGGCT
                                  **************************************************

CaO_TraesCS3A02G506200.1          GGAGTGTTCCAAGCTTTGTGAAGTTCTTGACACCTACATCTGGGCTCCAA
CaO_NEPAL38_CHIRYA7/ANB           GGAGTGTTCCAAGCTTTGTGAAGTTCTTGACACCTACATCTGGGCTCCAA
CaO_EXON7&8_SG30_SABUF//ALTAR8    GGAGTGTTCCAAGCTTTGTGAAGTTCTTGACACCTACATCTGGGCTCCAA
CaO_EXON7&8_SONALIKA              GGAGTGTTCCAAGCTTTGTGAAGTTCTTGACACCTACATCTGGGCTCCAA
                                  **************************************************

CaO_TraesCS3A02G506200.1          GGGTACTGGGATCCTTATCCCATCGATATGGAGTTCCGACCGCCCTGCAT
CaO_NEPAL38_CHIRYA7/ANB           GGGTACTGGGATCCTTATCCCATCGATATGGAGTTCCGACCGCCCTGCAT
CaO_EXON7&8_SG30_SABUF//ALTAR8    GGGTACTGGGATCCTTATCCCATCGATATGGAGTTCCGACCGCCCTGCAT
CaO_EXON7&8_SONALIKA              GGGTACTGGGATCCTTATCCCATCGATATGGAGTTCCGACCGCCCTGCAT
                                  **************************************************

CaO_TraesCS3A02G506200.1          GGTCTTGTCAACCATTGGCATCTCCAAGCCTGGAAAGCTAGAAGGGAAGA
CaO_NEPAL38_CHIRYA7/ANB           GGTCTTGTCAACCATTGGCATCTCCAAGCCTGGAAAGCTAGAAGGGAAGA
CaO_EXON7&8_SG30_SABUF//ALTAR8    GGTCTTGTCAACCATTGGCATCTCCAAGCCTGGAAAGCTAGAAGGGAAGA
CaO_EXON7&8_SONALIKA              GGTCTTGTCAACCATTGGCATCTCCAAGCCTGGAAAGCTAGAAGGGAAGA
                                  **************************************************

CaO_TraesCS3A02G506200.1          GCACCCAACAATGTGCAACGCATCTCCACCAGCTCCATGTATGCTTGCCC
CaO_NEPAL38_CHIRYA7/ANB           GCACCCAACAATGTGCAACGCATCTCCACCAGCTCCATGTATGCTTGCCC
CaO_EXON7&8_SG30_SABUF//ALTAR8    GCACCCAACAATGTGCAACGCATCTCCACCAGCTCCATGTATGCTTGCCC
CaO_EXON7&8_SONALIKA              GCACCCAACAATGTGCAACGCATCTCCACCAGCTCCATGTATGCTTGCCC
                                  **************************************************

CaO_TraesCS3A02G506200.1          TCATCGACGAATAAAACCAGGCTGTTGTACCGGATGTCTCTCGACTTCGC
CaO_NEPAL38_CHIRYA7/ANB           TCATCGACGAATAAAACCAGGCTGTTGTACCGGATGTCTCTCGACTTCGC
CaO_EXON7&8_SG30_SABUF//ALTAR8    TCATCGACGAATAAAACCAGGCTGTTGTACCGGATGTCTCTCGACTTCGC
CaO_EXON7&8_SONALIKA              TCATCGACGAATAAAACCAGGCTGTTGTACCGGATGTCTCTCGACTTCGC
                                  **************************************************

CaO_TraesCS3A02G506200.1          ACCCTGGATGAAGCACATGCCTTTCATGCACCTGTTGTGGTCACATTTCG
CaO_NEPAL38_CHIRYA7/ANB           ACCCTGGATGAAGCACATGCCTTTCATGCACCTGTTGTGGTCACATTTCG
CaO_EXON7&8_SG30_SABUF//ALTAR8    ACCCTGGATGAAGCACATGCCTTTCATGCACCTGTTGTGGTCACATTTCG
CaO_EXON7&8_SONALIKA              ACCCTGGATGAAGCACATGCCTTTCATGCACCTGTTGTGGTCACATTTCG
                                  **************************************************

CaO_TraesCS3A02G506200.1          CTGAGAAG
CaO_NEPAL38_CHIRYA7/ANB           CTGAGAAG
CaO_EXON7&8_SG30_SABUF//ALTAR8    CTGAGAAG
CaO_EXON7&8_SONALIKA              CTGACAAG
                                  **** ***
```

- The partial sequence of CaO revealed a single nucleotide variation in non stay green (Sonalika) where ‒C" in place of ‒G" was present at position 292 of exon 8.

Multiple Sequence Alignment of Partial Protein Sequences of CaO

```
CaO_TraesCS3A02G506200.1            IVMELPVEHGLLLDNLLDLAHAPFTHTSTFAKGWSVPSFVKFLTPTSGLQ
CaO_EXON7&8NEPAL38_CHIRYA7/ANB      IVMELPVEHGLLLDNLLDLAHAPFTHTSTFAKGWSVPSFVKFLTPTSGLQ
CaO_EXON7&8_SG30_SABUF//ALTAR8      IVMELPVEHGLLLDNLLDLAHAPFTHTSTFAKGWSVPSFVKFLTPTSGLQ
CaO_EXON7&8_SONALIKA                IVMELPVEHGLLLDNLLDLAHAPFTHTSTFAKGWSVPSFVKFLTPTSGLQ
                                    **************************************************

CaO_TraesCS3A02G506200.1            GYWDPYPIDMEFRPPCMVLSTIGISKPGKLEGKSTQQCATHLHQLHVCLP
CaO_EXON7&8NEPAL38_CHIRYA7/ANB      GYWDPYPIDMEFRPPCMVLSTIGISKPGKLEGKSTQQCATHLHQLHVCLP
CaO_EXON7&8_SG30_SABUF//ALTAR8      GYWDPYPIDMEFRPPCMVLSTIGISKPGKLEGKSTQQCATHLHQLHVCLP
CaO_EXON7&8_SONALIKA                GYWDPYPIDMEFRPPCMVLSTIGISKPGKLEGKSTQQCATHLHQLHVCLP
                                    **************************************************

CaO_TraesCS3A02G506200.1            SSTNKTRLLYRMSLDFAPWMKHMPFMHLLWSHFAEK
CaO_EXON7&8NEPAL38_CHIRYA7/ANB      SSTNKTRLLYRMSLDFAPWMKHMPFMHLLWSHFAEK
CaO_EXON7&8_SG30_SABUF//ALTAR8      SSTNKTRLLYRMSLDFAPWMKHMPFMHLLWSHFAEK
CaO_EXON7&8_SONALIKA                SSTNKTRLLYRMSLDFAPWMKHMPFMHLLWSHFADK
                                    **********************************:*
```

- Protein sequence elucidated that Glutamic acid was replaced by Aspartic acid in non-stay green genotype.

2. Light Harvesting Chlorophyll a/b Binding (Cab) Gene and Protein Sequence Alignment

Multiple Sequence Alignment of Coding Sequence of Cab

```
Cab_SG30_SABUF//ALTAR84/AE.SQ      -------------------GCTCTCCCCCTCGTCCTTCGCCGGGAAGGCG
Cab_SONALIKA                       ----------------GGCGCTCTCCCCCTCGTCCTTCGCCGGGAAGGCG
Cab_TraesCS1D02G411300.1           TGGCGACCACCGCGATGGCGCTCTCCCCCTCGTCCTTCGCCGGGAAGGCG
Cab_NEPAL38_CHIRYA7/ANB            ----------------GGCGCTCTCCCCCTCGTCCTTCGCCGGGAAGGCG
                                                      ******************************

Cab_SG30_SABUF//ALTAR84/AE.SQ      GTCAAGGACCTGCCGTCGTCGGCGCTCTTCGGGGAGGCGCGCGTCACCAT
Cab_SONALIKA                       GTCAAGGACCTGCCGTCGTCGGCGCTCTTCGGGGAGGCGCGCGTCACCAT
Cab_TraesCS1D02G411300.1           GTCAAGGACCTGCCGTCGTCGGCGCTCTTCGGGGAGGCGCGCGTCACCAT
Cab_NEPAL38_CHIRYA7/ANB            GTCAAGGACCTGCCGTCGTCGGCGCTCTTCGGGGAGGCGCGCGTCACCAT
                                   **************************************************

Cab_SG30_SABUF//ALTAR84/AE.SQ      GCGCAAGACCGCGGCCAAGGCCAAGCCGGTGTCGTCCGGCAGCCCGTGGT
Cab_SONALIKA                       GCGCAAGACCGCGGCCAAGGCCAAGCCGGTGTCGTCCGGCAGCCCGTGGT
Cab_TraesCS1D02G411300.1           GCGCAAGACCGCGGCCAAGGCCAAGCCGGTGTCGTCCGGCAGCCCGTGGT
Cab_NEPAL38_CHIRYA7/ANB            GCGCAAGACCGCGGCCAAGGCCAAGCCGGTGTCGTCCGGCAGCCCGTGGT
                                   **************************************************

Cab_SG30_SABUF//ALTAR84/AE.SQ      ACGGGTCCGACCGCGTGCTCTACCTCGGCCCGCTCTCCGGCGACCCCCCG
Cab_SONALIKA                       ACGGGTCCGACCGCGTGCTCTACCTCGGCCCGCTCTCCGGCGACCCCCCG
Cab_TraesCS1D02G411300.1           ACGGGTCCGACCGCGTGCTCTACCTCGGCCCGCTCTCCGGCGACCCCCCG
Cab_NEPAL38_CHIRYA7/ANB            ACGGGTCCGACCGCGTGCTCTACCTCGGCCCGCTCTCCGGCGACCCCCCG
```

```
                                  **************************************************

Cab_SG30_SABUF//ALTAR84/AE.SQ     AGCTACCTCACCGGCGAGTTCCCCGGCGACTACGGGTGGGACACCGCGGG
Cab_SONALIKA                      AGCTACCTCACCGGCGAGTTCCCCGGCGACTACGGGTGGGACACCGCGGG
Cab_TraesCS1D02G411300.1          AGCTACCTCACCGGCGAGTTCCCCGGCGACTACGGGTGGGACACCGCGGG
Cab_NEPAL38_CHIRYA7/ANB           AGCTACCTCACCGGCGAGTTCCCCGGCGACTACGGGTGGGACACCGCGGG
                                  **************************************************

Cab_SG30_SABUF//ALTAR84/AE.SQ     GCTGTCGGCCGACCCCGAGACCTTCGCCAAGAACCGGGAGCTGGAGGTGA
Cab_SONALIKA                      GCTGTCGGCCGACCCCGAGACCTTCGCCAAGAACCGGGAGCTGGAGGTGA
Cab_TraesCS1D02G411300.1          GCTGTCGGCCGACCCCGAGACCTTCGCCAAGAACCGGGAGCTGGAGGTGA
Cab_NEPAL38_CHIRYA7/ANB           GCTGTCGGCCGACCCCGAGACCTTCGCCAAGAACCGGGAGCTGGAGGTGA
                                  **************************************************

Cab_SG30_SABUF//ALTAR84/AE.SQ     TCCACTGCCGGTGGGCCATGCTGGGCGCGCTCGGCTGCGTCTTCCCCGAG
Cab_SONALIKA                      TCCACTGCCGGTGGGCCATGCTGGGCGCGCTCGGCTGCGTCTTCCCCGAG
Cab_TraesCS1D02G411300.1          TCCACTGCCGGTGGGCCATGCTGGGCGCGCTCGGCTGCGTCTTCCCCGAG
Cab_NEPAL38_CHIRYA7/ANB           TCCACTGCCGGTGGGCCATGCTGGGCGCGCTCGGCTGCGTCTTCCCCGAG
                                  **************************************************

Cab_SG30_SABUF//ALTAR84/AE.SQ     CTGCTCGCCCGCAACGGCGTCAAGTTCGGCGAGGCCGTGTGGTTCAAGGC
Cab_SONALIKA                      CTGCTCGCCCGCAACGGCGTCAAGTTCGGCGAGGCCGTGTGGTTCAAGGC
Cab_TraesCS1D02G411300.1          CTGCTCGCCCGCAACGGCGTCAAGTTCGGCGAGGCCGTGTGGTTCAAGGC
Cab_NEPAL38_CHIRYA7/ANB           CTGCTCGCCCGCAACGGCGTCAAGTTCGGCGAGGCCGTGTGGTTCAAGGC
                                  **************************************************

Cab_SG30_SABUF//ALTAR84/AE.SQ     CGGCTCCCAGATCTTCAGCGAGGGCGGCCTCGACTACCTCGGCAACCCCA
Cab_SONALIKA                      CGGCTCCCAGATCTTCAGCGAGGGCGGCCTCGACTACCTCGGCAACCCCA
Cab_TraesCS1D02G411300.1          CGGCTCCCAGATCTTCAGCGAGGGCGGCCTCGACTACCTCGGCAACCCCA
Cab_NEPAL38_CHIRYA7/ANB           CGGCTCCCAGATCTTCAGCGAGGGCGGCCTCGACTACCTCGGCAACCCCA
                                  **************************************************

Cab_SG30_SABUF//ALTAR84/AE.SQ     GCCTGGTCCACGCGCAGAGCATCCTCGCCATCTGGGCCTGCCAGGTCGTG
Cab_SONALIKA                      GCCTGGTCCACGCGCAGAGCATCCTCGCCATCTGGGCCTGCCAGGTCGTG
Cab_TraesCS1D02G411300.1          GCCTGGTCCACGCGCAGAGCATCCTCGCCATCTGGGCCTGCCAGGTCGTG
Cab_NEPAL38_CHIRYA7/ANB           GCCTGGTCCACGCGCAGAGCATCCTCGCCATCTGGGCCTGCCAGGTCGTG
                                  **************************************************

Cab_SG30_SABUF//ALTAR84/AE.SQ     CTCATGGGCGCCGTCGAGGGGTACCGCGTCGCCGGCGGCCCGCTCGGCGA
Cab_SONALIKA                      CTCATGGGCGCCGTCGAGGGGTACCGCGTCGCCGGCGGCCCGCTCGGCGA
Cab_TraesCS1D02G411300.1          CTCATGGGCGCCGTCGAGGGGTACCGCGTCGCCGGCGGCCCGCTCGGCGA
Cab_NEPAL38_CHIRYA7/ANB           CTCATGGGCGCCGTCGAGGGGTACCGCGTCGCCGGCGGCCCGCTCGGCGA
                                  **************************************************

Cab_SG30_SABUF//ALTAR84/AE.SQ     GATCGTCGACCCGCTCTACCCCGGCGGCAGCTTCGACCCCCTGGGCCTTG
Cab_SONALIKA                      GATCGTCGACCCGCTCTACCCCGGCGGCAGCTTCGACCCCCTGGGCCTTG
Cab_TraesCS1D02G411300.1          GATCGTCGACCCGCTCTACCCCGGCGGCAGCTTCGACCCCCTGGGCCTTG
Cab_NEPAL38_CHIRYA7/ANB           GATCGTCGACCCGCTCTACCCCGGCGGCAGCTTCGACCCCCTGGGCCTTG
                                  **************************************************

Cab_SG30_SABUF//ALTAR84/AE.SQ     CCGACGACCCTGAGGCGTTCGCGGAGCTCAAGGTGAAGGAGATCAAGAAC
Cab_SONALIKA                      CCGACGACCCTGAGGCGTTCGCGGAGCTCAAGGTGAAGGAGATCAAGAAC
Cab_TraesCS1D02G411300.1          CCGACGACCCTGAGGCGTTCGCGGAGCTCAAGGTGAAGGAGATCAAGAAC
Cab_NEPAL38_CHIRYA7/ANB           CCGACGACCCTGAGGCGTTCGCGGAGCTCAAGGTGAAGGAGATCAAGAAC
                                  **************************************************

Cab_SG30_SABUF//ALTAR84/AE.SQ     GGCCGCCTCGCCATGTTCTCCATGTTCGGCTTCTTCGTGCAGGCCATCGT
Cab_SONALIKA                      GGCCGCCTCGCCATGTTCTCCATGTTCGGCTTCTTCGTGCAGGCCATCGT
Cab_TraesCS1D02G411300.1          GGCCGCCTCGCCATGTTCTCCATGTTCGGCTTCTTCGTGCAGGCCATCGT
Cab_NEPAL38_CHIRYA7/ANB           GGCCGCCTCGCCATGTTCTCCATGTTCGGCTTCTTCGTGCAGGCCATCGT
                                  **************************************************

Cab_SG30_SABUF//ALTAR84/AE.SQ     CACCGGCAAGGGCCCCCTCGAGAACCTCGCCGACCACCTCTCCGACCCCG
```

```
Cab_SONALIKA                        CACCGGCAAGGGCCCCCTCGAGAACCTCGCCGACCACCTCTCCGACCCCG
Cab_TraesCS1D02G411300.1            CACCGGCAAGGGCCCCCTCGAGAACCTCGCCGACCACCTCTCCGACCCCG
Cab_NEPAL38_CHIRYA7/ANB             CACCGGCAAGGGCCCCCTCGAGAACCTCGCCGACCACCTCTCCGACCCCG
                                    **************************************************

Cab_SG30_SABUF//ALTAR84/AE.SQ       TCAACAACAACGCCTGGGCCTTCGCCACCAACTTCGTGCCCGGCAAGTA-
Cab_SONALIKA                        TCAACAACAACGCCTGGGCCTTCGCCACCAACTTCGTGCCCGGCAAGTA-
Cab_TraesCS1D02G411300.1            TCAACAACAACGCCTGGGCCTTCGCCACCAACTTCGTGCCCGGCAAGTAA
Cab_NEPAL38_CHIRYA7/ANB             TCAACAACAACGCCTGGGCCTTCGCCACCAACTTCGTGCCCGG-------
                                    ******************************************
```

Multiple Sequence Alignment of Protein Sequences of Cab

```
Cab_SG30_SABUF//ALTAR84/AE.SQ       -------LSPSSFAGKAVKDLPSSALFGEARVTMRKTAAKAKPVSSGSPW
Cab_SONALIKA                        ------ALSPSSFAGKAVKDLPSSALFGEARVTMRKTAAKAKPVSSGSPW
Cab_TraesCS1D02G411300.1            MATTAMALSPSSFAGKAVKDLPSSALFGEARVTMRKTAAKAKPVSSGSPW
Cab_NEPAL38_CHIRYA7/ANB             ------ALSPSSFAGKAVKDLPSSALFGEARVTMRKTAAKAKPVSSGSPW
                                           ******************************************

Cab_SG30_SABUF//ALTAR84/AE.SQ       YGSDRVLYLGPLSGDPPSYLTGEFPGDYGWDTAGLSADPETFAKNRELEV
Cab_SONALIKA                        YGSDRVLYLGPLSGDPPSYLTGEFPGDYGWDTAGLSADPETFAKNRELEV
Cab_TraesCS1D02G411300.1            YGSDRVLYLGPLSGDPPSYLTGEFPGDYGWDTAGLSADPETFAKNRELEV
Cab_NEPAL38_CHIRYA7/ANB             YGSDRVLYLGPLSGDPPSYLTGEFPGDYGWDTAGLSADPETFAKNRELEV
                                    **************************************************

Cab_SG30_SABUF//ALTAR84/AE.SQ       IHCRWAMLGALGCVFPELLARNGVKFGEAVWFKAGSQIFSEGGLDYLGNP
Cab_SONALIKA                        IHCRWAMLGALGCVFPELLARNGVKFGEAVWFKAGSQIFSEGGLDYLGNP
Cab_TraesCS1D02G411300.1            IHCRWAMLGALGCVFPELLARNGVKFGEAVWFKAGSQIFSEGGLDYLGNP
Cab_NEPAL38_CHIRYA7/ANB             IHCRWAMLGALGCVFPELLARNGVKFGEAVWFKAGSQIFSEGGLDYLGNP
                                    **************************************************

Cab_SG30_SABUF//ALTAR84/AE.SQ       SLVHAQSILAIWACQVVLMGAVEGYRVAGGPLGEIVDPLYPGGSFDPLGL
Cab_SONALIKA                        SLVHAQSILAIWACQVVLMGAVEGYRVAGGPLGEIVDPLYPGGSFDPLGL
Cab_TraesCS1D02G411300.1            SLVHAQSILAIWACQVVLMGAVEGYRVAGGPLGEIVDPLYPGGSFDPLGL
Cab_NEPAL38_CHIRYA7/ANB             SLVHAQSILAIWACQVVLMGAVEGYRVAGGPLGEIVDPLYPGGSFDPLGL
                                    **************************************************

Cab_SG30_SABUF//ALTAR84/AE.SQ       ADDPEAFAELKVKEIKNGRLAMFSMFGFFVQAIVTGKGPLENLADHLSDP
Cab_SONALIKA                        ADDPEAFAELKVKEIKNGRLAMFSMFGFFVQAIVTGKGPLENLADHLSDP
Cab_TraesCS1D02G411300.1            ADDPEAFAELKVKEIKNGRLAMFSMFGFFVQAIVTGKGPLENLADHLSDP
Cab_NEPAL38_CHIRYA7/ANB             ADDPEAFAELKVKEIKNGRLAMFSMFGFFVQAIVTGKGPLENLADHLSDP
                                    **************************************************

Cab_SG30_SABUF//ALTAR84/AE.SQ       VNNNAWAFATNFVPGK
Cab_SONALIKA                        VNNNAWAFATNFVPGK
Cab_TraesCS1D02G411300.1            VNNNAWAFATNFVPGK
Cab_NEPAL38_CHIRYA7/ANB             VNNNAWAFATNFVP--
                                    **************
```

- No Sequence variation was found for Cab Gene

3. Stay Green (SGR) Gene and Protein Sequence Alignment

Multiple Sequence Alignment of Partial Coding Sequence of SGR Gene

```
TraesCS5D02G325900.1                ATGGCCACCGCCTCCACCATGTCCCTGCTCCCCATCTCGCACCTCAAGCA
SGR_EXON1&2_NEPAL38_CHIRYA7/AN      ATGGCCACCGCCTCCACCATGTCCCTGCTCCCCATCTCGCACCTCAAGCA
SGR_EXON1&2_SONALIKA                ATGGCCACCGCCTCCACCATGTCCCTGCTCCCCATCTCGCACCTCAAGCA
SGR_EXON1&2_SABUF//ALTAR84/AE.      ATGGCCACCGCCTCCACCATGTCCCTGCTCCCCATCTCGCACCTCAAGCA
                                    **************************************************

TraesCS5D02G325900.1                GCTGCAGCAGCAGCGGCGCACGCGGCTCGCCAGCGCGCGCTCCGGGAAGG
SGR_EXON1&2_NEPAL38_CHIRYA7/AN      GCTGCAGCAGCAGCGGCGCACGCGGCTCGCCAGCGCGCGCTCCGGGAAGG
SGR_EXON1&2_SONALIKA                GCTGCAGCAGCAGCGGCGCACGCGGCTCGCCAGCGCGCGCTCCGGGAAGG
SGR_EXON1&2_SABUF//ALTAR84/AE.      GCTGCAGCAGCAGCGGCGCACGCGGCTCGCCAGCGCGCGCTCCGGGAAGG
                                    **************************************************

TraesCS5D02G325900.1                TGGTCGTGCTCGGCCGCCGGAGGCGACACGTCGTGCCGAGGGCCCGGCTG
SGR_EXON1&2_NEPAL38_CHIRYA7/AN      TGGTCGTGCTCGGCCGCCGGAGGCGACACGTCGTGCCGAGGGCCCGGCTG
SGR_EXON1&2_SONALIKA                TGGTCGTGCTCGGCCGCCGGAGGCGACACGTCGTGCCGAGGGCCCGGCTG
SGR_EXON1&2_SABUF//ALTAR84/AE.      TGGTCGTGCTCGGCCGCCGGAGGCGACACGTCGTGCCGAGGGCCCGGCTG
                                    **************************************************

TraesCS5D02G325900.1                TTCGGTCCGGCCATCTTCGAGGCGTCCAAGCTCAAGGTGCTGTTCGTGGG
SGR_EXON1&2_NEPAL38_CHIRYA7/AN      TTCGGTCCGGCCATCTTCGAGGCGTCCAAGCTCAAGGTGCTGTTCGTGGG
SGR_EXON1&2_SONALIKA                TTCGGTCCGGCCATCTTCGAGGCGTCCAAGCTCAAGGTGCTGTTCGTGGG
SGR_EXON1&2_SABUF//ALTAR84/AE.      TTCGGTCCGGCCATCTTCGAGGCGTCCAAGCTCAAGGTGCTGTTCGTGGG
                                    **************************************************

TraesCS5D02G325900.1                GGTGGACGAGGAGAAGCACCCGGGGAAGCTGCCCCGGACCTACACGCTCA
SGR_EXON1&2_NEPAL38_CHIRYA7/AN      GGTGGACGAGGAGAAGCACCCGGGGAAGCTGCCCCGGACCTACACGCTCA
SGR_EXON1&2_SONALIKA                GGTGGACGAGGAGAAGCACCCGGGGAAGCTGCCCCGGACCTACACGCTCA
SGR_EXON1&2_SABUF//ALTAR84/AE.      GGTGGACGAGGAGAAGCACCCGGGGAAGCTGCCCCGGACCTACACGCTCA
                                    **************************************************

TraesCS5D02G325900.1                CCCACAGCGACGTGACGGCGCGGCTGACGCTGGCGGTGTCGCACACCATC
SGR_EXON1&2_NEPAL38_CHIRYA7/AN      CCCACAGCGACGTGACGGCGCGGCTGACGCTGGCGGTGTCGCACACCATC
SGR_EXON1&2_SONALIKA                CCCACAGCGACGTGACGGCGCGGCTGACGCTGGCGGTGTCGCACACCATC
SGR_EXON1&2_SABUF//ALTAR84/AE.      CCCACAGCGACGTGACGGCGCGGCTGACGCTGGCGGTGTCGCACACCATC
                                    **************************************************

TraesCS5D02G325900.1                CACGCCGCGCAGCTGCAGGGCTGGTACAACCGCCTGCAGCGGGACGAGGT
SGR_EXON1&2_NEPAL38_CHIRYA7/AN      CACGCCGCGCAGCTGCAGGGCTGGTACAACCGCCTGCAGCGGGACGAGGT
SGR_EXON1&2_SONALIKA                CACGCCGCGCAGCTGCAGGGCTGGTACAACCGCCTGCAGCGGGACGAGGT
SGR_EXON1&2_SABUF//ALTAR84/AE.      CACGCCGCGCAGCTGCAGGGCTGGTACAACCGCCTGCAGCGGGACGAGGT
                                    **************************************************

TraesCS5D02G325900.1                GGTGGCCGAGTGGAAGAAGGTGCAGGGCGCCATGTCGCTGCACGTCCACT
SGR_EXON1&2_NEPAL38_CHIRYA7/AN      GGTGGCCGAGTGGAAGAAGGTGCAGGGCGCCATGTCGCTGCACGTCCACT
SGR_EXON1&2_SONALIKA                GGTGGCCGAGTGGAAGAAGGTGCAGGGCGCCATGTCGCTGCACGTCCACT
SGR_EXON1&2_SABUF//ALTAR84/AE.      GGTGGCCGAGTGGAAGAAGGTGCAGGGCGCCATGTCGCTGCACGTCCACT
                                    **************************************************

TraesCS5D02G325900.1                GCCACATCTCCGGCGGCCACTTCCTGCTCGACCTCATCGCGCCGCTCCGC
SGR_EXON1&2_NEPAL38_CHIRYA7/AN      GCCACATCTCCGGCGGCCACTTCCTGCTCGACCTCATCGCGCCGCTCCGC
SGR_EXON1&2_SONALIKA                GCCACATCTCCGGCGGCCACTTCCTGCTCGACCTCATCGCGCCGCTCCGC
SGR_EXON1&2_SABUF//ALTAR84/AE.      GCCACATCTCCGGCGGCCACTTCCTGCTCGACCTCATCGCGCCGCTCCGC
                                    **************************************************

TraesCS5D02G325900.1                TACTACATCTTCCGCAAGGAGCTCCCCGTGGT
SGR_EXON1&2_NEPAL38_CHIRYA7/AN      TACTACATCTTCCGCAAGGAGCTCCCCGTGGT
SGR_EXON1&2_SONALIKA                TACTACATCTTCCGCAAGGAGCTCCCCGTGGT
```

```
SGR_EXON1&2_SABUF//ALTAR84/AE.      TACTACATCTTCCGCAAGGAGCTCCCCGTGGT
                                    ********************************
```

Multiple Sequence Alignment of Partial Protein Sequences of SGR

```
TraesCS5D02G325900.1                MATASTMSLLPISHLKQLQQQRRTRLASARSGKVVVLGRRRRHVVPRARL
SGR_EXON1&2_NEPAL38_CHIRYA7/AN      MATASTMSLLPISHLKQLQQQRRTRLASARSGKVVVLGRRRRHVVPRARL
SGR_EXON1&2_SONALIKA                MATASTMSLLPISHLKQLQQQRRTRLASARSGKVVVLGRRRRHVVPRARL
SGR_EXON1&2_SABUF//ALTAR84/AE.      MATASTMSLLPISHLKQLQQQRRTRLASARSGKVVVLGRRRRHVVPRARL
                                    **************************************************

TraesCS5D02G325900.1                FGPAIFEASKLKVLFVGVDEEKHPGKLPRTYTLTHSDVTARLTLAVSHTI
SGR_EXON1&2_NEPAL38_CHIRYA7/AN      FGPAIFEASKLKVLFVGVDEEKHPGKLPRTYTLTHSDVTARLTLAVSHTI
SGR_EXON1&2_SONALIKA                FGPAIFEASKLKVLFVGVDEEKHPGKLPRTYTLTHSDVTARLTLAVSHTI
SGR_EXON1&2_SABUF//ALTAR84/AE.      FGPAIFEASKLKVLFVGVDEEKHPGKLPRTYTLTHSDVTARLTLAVSHTI
                                    **************************************************

TraesCS5D02G325900.1                HAAQLQGWYNRLQRDEVVAEWKKVQGAMSLHVHCHISGGHFLLDLIAPLR
SGR_EXON1&2_NEPAL38_CHIRYA7/AN      HAAQLQGWYNRLQRDEVVAEWKKVQGAMSLHVHCHISGGHFLLDLIAPLR
SGR_EXON1&2_SONALIKA                HAAQLQGWYNRLQRDEVVAEWKKVQGAMSLHVHCHISGGHFLLDLIAPLR
SGR_EXON1&2_SABUF//ALTAR84/AE.      HAAQLQGWYNRLQRDEVVAEWKKVQGAMSLHVHCHISGGHFLLDLIAPLR
                                    **************************************************

TraesCS5D02G325900.1                YYIFRKELPV
SGR_EXON1&2_NEPAL38_CHIRYA7/AN      YYIFRKELPV
SGR_EXON1&2_SONALIKA                YYIFRKELPV
SGR_EXON1&2_SABUF//ALTAR84/AE.      YYIFRKELPV
                                    **********
```

- No Sequence variation was found for SGR

4. Red Chlorophyll Catabolite Reductase (RCCR) Gene and Protein Sequence Alignment

Multiple Sequence Alignment of Partial Coding Sequence of RCCR Gene

```
RCCR_NEPAL38_CHIRYA7/ANB            ATCGATTTCATGCTGCAGTCGTCGCTTCACTGCAAAGTCCCGAATGGCGC
RCCR_SONALIKA                       ATCGATTTCATGCTGCAGTCGTCGCTTCACTGCAAAGTCCCAAATGGTGC
RCCR_TraesCS7B02G692000LC.1         ATCGATTTCATGCTGCAGTCGTCGCTTCACTGCAAAGTCCCAAATGGCGC
RCCR_SG30_SABUF//ALTAR84/AE.SQ      ATCGATTTCATGCTGCAGTCGTCGCTTCACTGCAAAGTCCCAAATGGCGC
                                    ****************************************.***** **

RCCR_NEPAL38_CHIRYA7/ANB            GATCGACATCACGTCTCTCTTCATCAACCTAAACGCCTCGACGGATGCAC
RCCR_SONALIKA                       GATCGACATCACGTCTCTCTTCATCAACCTAAACGCCTCGACGGACGCGC
RCCR_TraesCS7B02G692000LC.1         GATCGACATCACGTCTCTCTTCATCAACCTGAACGCCTCGACGGACGCGC
RCCR_SG30_SABUF//ALTAR84/AE.SQ      GATCGACATCACGTCTCTCTTCATCAACCTGAACGCCTCGACGGACGCGC
                                    ******************************.************** **.*

RCCR_NEPAL38_CHIRYA7/ANB            CGCATTTCGTCATGGAGTTCATACAGGGCAGCCCAACTTCAATGGTGGTG
RCCR_SONALIKA                       CACATTTCGTCATGGAGTTCATACAGGGCAGCCCAACTTCAATGGTCGTG
RCCR_TraesCS7B02G692000LC.1         CGCATTTCGTCATGGAGTTCATACAGGGCAGCCCAACTTCAATGGTCGTG
RCCR_SG30_SABUF//ALTAR84/AE.SQ      CGCATTTCGTCATGGAGTTCATACAGGGCAGCCCAACTTCAATGGTCGTG
                                    *.******************************************** ***

RCCR_NEPAL38_CHIRYA7/ANB            CTTCTGGACCTGCTGCCACGGAAAGACCTCGCGCTCCACCCGGAGTACAT
RCCR_SONALIKA                       CTTCTGGACCTGCTGCCACGGAAAGACCTTGCGCTCCACCCGGAGTACAT
RCCR_TraesCS7B02G692000LC.1         CTTCTGGACCTGCTGCCACGGAAAGACCTCGCGCTCCACCCGGAGTACAT
RCCR_SG30_SABUF//ALTAR84/AE.SQ      CTTCTGGACCTGCTGCCACGGAAAGACCTCGCGCTCCACCCGGAGTACAT
                                    ***************************** ********************
```

```
RCCR_NEPAL38_CHIRYA7/ANB          CGAGAAGTACTACGAAAATACTGAGGCGGACAAGCAACGCAAGATCATTG
RCCR_SONALIKA                     CGAGAAGTACTACGAAAATACTGAGGCGGACAAGCAACGCAAGATCATCG
RCCR_TraesCS7B02G692000LC.1       CGAGAAGTACTATGAAAATACTGAGGTGGACAAGCAACGCAAAATCATCG
RCCR_SG30_SABUF//ALTAR84/AE.SQ    CGAGAAGTACTATGAAAATACTGAGGTGGACAAGCAACGCAAAATCATCG
                                  ************ ************* ***************.***** *

RCCR_NEPAL38_CHIRYA7/ANB          AAGAATTGCCGCAAGCCCGCCCGTACCTTTCGCCGTCCCTCTTCGTGCGC
RCCR_SONALIKA                     AAGAATTGCCGCAAGCCCGCCCGTACCTTTCGCCGTCTCTCTTCGTGCGC
RCCR_TraesCS7B02G692000LC.1       AAGAATTGCCGCAAGCCCGCCCGTACCTTTCGCCGTCCCTCTTCGTGCGC
RCCR_SG30_SABUF//ALTAR84/AE.SQ    AAGAATTGCCGCAAGCCCGCCCGTACCTTTCGCCGTCCCTCTTCGTGCGC
                                  ************************************ ************

RCCR_NEPAL38_CHIRYA7/ANB          AGCGCGTTCTCTCCGACGGCGGTGTTCTTCACCATTGACTGTGGGCAAGG
RCCR_SONALIKA                     AGCGCGTTCTCTCCGACGGCGGTGTTCTTCACCATTGACTGTGGGCAAGG
RCCR_TraesCS7B02G692000LC.1       AGCGCGTTCTCTCCGACGGCGGTGTTCTTCACCATTGACTGTGGGCAAGG
RCCR_SG30_SABUF//ALTAR84/AE.SQ    AGCGCGTTCTCTCCGACGGCGGTGTTCTTCACCATTGACTGTGGGCAAGG
                                  **************************************************

RCCR_NEPAL38_CHIRYA7/ANB          AGGGGAGAGCGTCTTGGAGGAGATAGTGCAGGGTCATCTTGCGTCGGTTG
RCCR_SONALIKA                     AGGGGAGAGCGTCTTGGAGGAGATAGTGCAGGGTCATCTTGCGTCGGTTG
RCCR_TraesCS7B02G692000LC.1       AGGGGAGAGTGTCTTGGAGGAGATAGTGCAGGGTCATCTTGCGTCAGTTG
RCCR_SG30_SABUF//ALTAR84/AE.SQ    AGGGGAGAGTGTCTTGGAGGAGATAGTGCAGGGTCATCTTGCGTCAGTTG
                                  ********* ************************************.****

RCCR_NEPAL38_CHIRYA7/ANB          TGAAGGGGGTTCTTCAGATCTGGCTTGATACTTGCGCCGGTGGCACCTCG
RCCR_SONALIKA                     TGAAGGGGGTTCTTCAGATCTGGCTTGATACTTGCGCCGGTGGCACCTCG
RCCR_TraesCS7B02G692000LC.1       TGAAGGCGGTTCTTCAGATTTGGCTTGATACTTGCGCCGTTGGCACCTCG
RCCR_SG30_SABUF//ALTAR84/AE.SQ    TGAAGGCGGTTCTTCAGATTTGGCTTGATACTTGCGCCGTTGGCACCTCG
                                  ****** ************ ******************* **********

RCCR_NEPAL38_CHIRYA7/ANB          GAAATGGAAGAGGGCGAGAGGGAGATCATGGTTAGGAGGGACCGGACTGT
RCCR_SONALIKA                     GAAATGGAAGAGGGCGAGAGGGAGATCATGGTTAGGAGGGACCGGACTGT
RCCR_TraesCS7B02G692000LC.1       GAAATGGAAGAGGGCGAGAGGGAGATCATGGTCAAGAGGGACCGAACTGT
RCCR_SG30_SABUF//ALTAR84/AE.SQ    GAAATGGAAGAGGGCGAGAGGGAGATCATGGTCAAGAGGGACCGAACTGT
                                  ********************************* *.*********.*****

RCCR_NEPAL38_CHIRYA7/ANB          AAGATCGAAGTCGATCGAGGTCGACCTGACCGCGAATTTGCCGAGGATGT
RCCR_SONALIKA                     AAGATCGAAGTCGATCGAGGTCGACCTGACCGCGAATTTGCCGAGGATGT
RCCR_TraesCS7B02G692000LC.1       GAGATCAAAGTCGATCGAGGTCGACCTGACCGCAAATTTGCCGAGGATGT
RCCR_SG30_SABUF//ALTAR84/AE.SQ    GAGATCAAAGTCGATCGAGGTCGACCTGACCGCAAATTTGCCGAGGATGT
                                  .*****.***************************.****************

RCCR_NEPAL38_CHIRYA7/ANB          TTGGCCCGGATGTGTCCGGTCGCGTCATCGCTGAAATTCGTAA-------
RCCR_SONALIKA                     TTGGCCCGGATGTGTCCGGTCGCGTCATCGCTGAAATTCGTA--------
RCCR_TraesCS7B02G692000LC.1       TTGGCCCCGACGTGTCCGGCCGCGTCATCGCTGAAATTCGTAAGGCCTTT
RCCR_SG30_SABUF//ALTAR84/AE.SQ    TTGGCCCCGACGTGTCCGGCCGCGTCATCGCTG-----------------
                                  ******* ** ******** *************
```

Multiple Sequence Alignment of Partial Protein Sequences of RCCR

```
RCCR_NEPAL38_CHIRYA7/ANB          IDFMLQSSLHCKVPNGAIDITSLFINLNASTDAPHFVMEFIQGSPTSMVV
RCCR_SONALIKA                     IDFMLQSSLHCKVPNGAIDITSLFINLNASTDAPHFVMEFIQGSPTSMVV
RCCR_TraesCS7B02G692000LC.1       IDFMLQSSLHCKVPNGAIDITSLFINLNASTDAPHFVMEFIQGSPTSMVV
RCCR_SG30_SABUF//ALTAR84/AE.SQ    IDFMLQSSLHCKVPNGAIDITSLFINLNASTDAPHFVMEFIQGSPTSMVV
                                  **************************************************

RCCR_NEPAL38_CHIRYA7/ANB          LLDLLPRKDLALHPEYIEKYYENTEADKQRKIIEELPQARPYLSPSLFVR
RCCR_SONALIKA                     LLDLLPRKDLALHPEYIEKYYENTEADKQRKIIEELPQARPYLSPSLFVR
RCCR_TraesCS7B02G692000LC.1       LLDLLPRKDLALHPEYIEKYYENTEVDKQRKIIEELPQARPYLSPSLFVR
RCCR_SG30_SABUF//ALTAR84/AE.SQ    LLDLLPRKDLALHPEYIEKYYENTEVDKQRKIIEELPQARPYLSPSLFVR
                                  *************************.************************
```

```
RCCR_NEPAL38_CHIRYA7/ANB            SAFSPTAVFFTIDCGQGGESVLEEIVQGHLASVVKGVLQIWLDTCAGGTS
RCCR_SONALIKA                       SAFSPTAVFFTIDCGQGGESVLEEIVQGHLASVVKGVLQIWLDTCAGGTS
RCCR_TraesCS7B02G692000LC.1         SAFSPTAVFFTIDCGQGGESVLEEIVQGHLASVVKAVLQIWLDTCAVGTS
RCCR_SG30_SABUF//ALTAR84/AE.SQ      SAFSPTAVFFTIDCGQGGESVLEEIVQGHLASVVKAVLQIWLDTCAVGTS
                                    ***********************************.********** ***

RCCR_NEPAL38_CHIRYA7/ANB            EMEEGEREIMVRRDRTVRSKSIEVDLTANLPRMFGPDVSGRVIAEIR
RCCR_SONALIKA                       EMEEGEREIMVRRDRTVRSKSIEVDLTANLPRMFGPDVSGRVIAEIR
RCCR_TraesCS7B02G692000LC.1         EMEEGEREIMVKRDRTVRSKSIEVDLTANLPRMFGPDVSGRVIAEIR
RCCR_SG30_SABUF//ALTAR84/AE.SQ      EMEEGEREIMVKRDRTVRSKSIEVDLTANLPRMFGPDVSGRVIAE
                                    ***********:********************************
```

- Great variation in the Coding Sequence of Red Chlorophyll Catabolite Reductase (RCCR) was observed.
- Variation in the Amino acid Sequence of Red Chlorophyll Catabolite Reductase (RCCR): At position 204 of RCCR Protein Valine is replaced by alanine; At position 264, Alanine is replaced by Glycine; At position 275, Valine is replaced by Glycine; At position 290, Lysine is replaced by Arginine in Stay green and Non-stay Green lines

QUAID-I-AZAM UNIVERSITY, ISLAMABAD
DEPARTMENT OF PLANT SCIENCES

Dated: March 4, 2022

PUBLICATION IN W-CATEGORY JOURNAL

It is certified that **Sadia Latif**, Registration No. **03041311003,** has published an article entitled as "**Deciphering the Role of Stay-Green Trait to Mitigate Terminal Heat Stress in Bread Wheat**" in **"Agronomy Basel"** a **W-Category Journal** having an **impact factor 2.603** from her dissertation entitled as "Molecular Mechanism behind stay green trait in Bread Wheat (*Triticum aestivum* L.)".

Supervisor

Dr. Umar Masood Quraishi
Associate Professor
Department of Plant Sciences
Quaid-i-Azam University
Islamabad